The 15th General Meeting of the

INTERNATIONAL MINERALOGICAL ASSOCIATION

ABSTRACTS

Vol. 1

28 JUNE — 3 JULY 1990

BEIJING CHINA

Sponsored by Geological Society of China (GSC)
Chinese Society of Mineralogy, Petrology and Geochemistry (CSMPG)
Chinese Academy of Geological Sciences (CAGS)
China International Conference Center for Science and Technology (CICCST)

Supported by Ministry of Geology and Mineral Resources (MGMR)
National Natural Science Foundation of China (NSFC)
Mineral Resources and Geology Department, China National Nonferrous Metals Industry Corporation (CNNC)
China Association for Science and Technology (CAST)
Ministry of Metallurgical Industry (MMI)
Chinese Academy of Sciences (CAS)
China National Nuclear Industry Corporation (CNNIC)
Geology and Mine Bureau (GMB), Ministry of Chemical Industry (MCHI)
State Gold Bureau of China (SGBC)
China National Building Materials Industry Bureau (CNBMIB)
South–South Cooperation Foundation (SSCF), Chinese Academy of Sciences (CAS)
Third World Academy of Sciences (TWAS)

Copyright: 15th General Meeting of International Mineralogical Association 1990

Printed by the Printing House of Chinese Institute of Geology and Mineral Resources Information.

Copies of the volumes may be purchased from:

Geological Society of China
26 Baiwanzhuang Road
Fuchengmenwai
Beijing 100037, China

Institute of Mineral Deposits
Chinese Academy of Geological Sciences
26 Baiwanzhuang Road
Beijing 100037, China

INTERNATIONAL STEERING COMMITTEE

S.S. Hafner — Huang Yunhui
C.T. Prewitt — Xie Xiande

CHINA NATIONAL STEERING COMMITTEE

Chairman — Zhu Xun, Minister of Geology and Mineral Resources of People's Republic of China
President of Geological Society of China

Vice–Chairman — Gao Zhenning, Vice–Chairman of China Association for Science and Technology

Members	Cheng Yuqi	Tu Guangchi	Chen Yuchuan
	Jiang Rong	Yao Peihui	Liu Shanfang
	Chen Zhaobo	Wang Qingzhong	Zhang Renwei
	Wang Dezi	Zhu Lilan	Sun Honglie
	Hu Zhaosen	Zhang Bingxi	Cui Lan

ORGANIZING COMMITTEE

Chairman	Xie Xiande		
1st Vice–Chairman	Ji Kejian		
Vice–Chairmen	Yang Minzhi	Shen Jinchuan	
Secretary–General	Wang Zejiu		
Deputy Secretaries–General	Cai Wenyan	Song Xuexin	

SCIENTIFIC COMMITTEE

Chairman	Huang Yunhui		
Vice–Chairmen	Li Zhaonai	Zheng Zhi	Zhang Peishan
Secretary–General	Qin Shuying		
Deputy Secretary–General	Guo Lihe		

PREFACE

The present volumes contain 768 abstracts submitted to the 15th General Meeting of the International Mineralogical Association to be held in Beijing, China from June 28 to July 3, 1990.

Mineralogy, a fundamental science of geology, has a long history of its research. In the past decades, the rapid development of mineral physics has greatly improved the techniques and methods for studying this classic discipline, thus causing the research to be more comprehensive and deep–going and the science itself to embrace more and more branches. Considering the trend in mineralogy and the requirements of its branches, the Council of the International Mineralogical Association and the Scientific Committee of the 15th IMA General Meeting organize 28 symposia (or sessions) during the Meeting.

The abstracts included are grouped in the light of the titles of symposia (or sessions), and within each group, they are arranged in alphabetical order of the first authors, with some abstracts which arrived too late as an exception. It is to be noted that the classification of abstracts into symposia (or sessions) is based on the authors' own choice. Most of the abstracts have been reproduced directly from the camera–ready copies prepared by the authors, and a number of them had to be retyped to get into the correct format.

To view the volumes as a whole, we can see that the abstracts, with fairly high level, involve profound subjects related to mineralogy, and some of them are up to the advanced world level.

The Scientific Committee of the General Meeting is very much grateful to the Council of International Mineralogical Association, the IMA Commissions and Working Groups, the conveners of all symposia (or sessions), Chinese Academy of Geological Sciences and its Institute of Mineral Deposits and the Geological Society of China for their great support and generous efforts.

Many thanks are also extended to Zhao Donggao and Zhou Jianxiong who have done a lot of work for the publication of the two volumes.

Huang Yunhui
First Vice President of IMA

Chairman
Scientific Committee
15th IMA General Meeting

CONTENTS

Volume 1

		Page
	Genetic Mineralogy and Prospecting Mineralogy	(1)
	Applied Mineralogy	(150)
	Ore Mineralogy	(239)
	Crystal Structure and Crystal Chemistry of Minerals	(295)
	Kinetic (or Crystal Growth) Aspects in Earth and Planetary Sciences	(380)
	Mineral Physics	(420)
	Surface Analytical Methods	(473)
	Electron Microscopy Applied to Mineralogy	(483)
	Experimental and Computational Results on Mantle Mineralogy	(487)

Volume 2

	Experimental Mineralogy	(506)
	Fluid–Melt Inclusions	(552)
	Organic Mineralogy	(586)
	Minerals as Drugs	(600)
	Mineralogy of Cosmic Particles and Their Origin	(653)
	Gem Materials	(672)
	New Minerals and Mineral Names	(697)
	The Role of Minerals in Sedimentary Processes	(719)
	Origin of Granites, Petrographic and Experimental Constraints	(743)
	Geochemistry and Petrology of Subduction Zone Magmas	(774)
	Mineralization Associated with Mafic and Ultramafic Rocks	(780)
	Mineralogy, Petrology and Geochemistry of Metamorphic Rocks (Including Metamorphic Belts in China)	(834)
	Mineralogy and Geochemistry of Rare Elements	(926)
	Geochemistry, Mineralogy and Origin of Ore Deposits in Relation to Future Materials I : Applied Isotope Geochemistry	(985)
	Geochemistry, Mineralogy and Origin of Ore Deposits in Relation to Future Materials II : Minerals for Future Materials	(995)
	Geochemical Evaluation of Ore Minerals, Ore Sample and Ore Deposits	(1004)
	Open	(1006)
	Abstracts only giving the titles	(1021)
	Author Index	(1023)

GENETIC MINERALOGY AND PROSPECTING MINERALOGY

P 1.3

G. C. AMSTUTZ, Mineralogic-Petrological Institute of the University of Heidelberg.

Pseudomorphs - a revision of the terminology and of their genetic meaning in petrology and ore genesis.

The geometric and compositional steps in the formation of pseudomorphs are fairly well known, understood and pictured in figure 1. One aspect, however, is still controversial. This is the mimetic replacement of a phase A by a phase B (or C), where the final product is assumed to fill the space of A so perfectly and "crystallo-graphically" that the original presence of A is not any longer recognized. Are such cases of perfect mimicry possible (or are we "mimicking" ourselves, when introdùcing this hypothesis into genetic theories)? In other words, are such perfect pseudomorphs possible though rare and products of replacement, or are they assumptions of the impossible.

The statistical treatment of several thousands of pseudomorphs of all kinds of crystal lattices and compositions resulted in a clear minimum in the grain size distribution between the original phase A and any new (secondary) phase B or (ternary) phase C. The grain sizes of the new phases is, without known exceptions, between about 10 and 100.000 times smaller than that of the original phase A (figure 1, left side). In addition, the orientation of the new phases is different, with very few exceptions which may represent a form of epitactic growth. Consequently, the evidence is strong against the formation of optically homogenous "end-products" of infilling. -

A second problem arises from the fact that the existing definition of pseudomorphs does not include cases where the shape of the crystal is preserved and marked by an outline of remnant material, but where the phase B (or C) has grown beyond the original borders of the grain. This is shown on the right side of figure 1. These "ghost-crystals" are common and it is proposed here that their geometry corresponds in fact to both parts of the word pseudo-morphs. They are "pseudo"-crystals and their shape (greek "morphae") is visible. In a broad sense, any natural object - also fossil cells, leafs, etc. - may be pseudomorphically changed, filled and/or replaced by a phase B or C etc. -

The second topic of this abstract is intrinsically related to the first one. If the central column of Figure 1 is a "forbidden area" for pseudomorphs, various genetic theories in petrology and ore genesis must be revised. The rocks and ores in question may belong to the class of processes for which experiments (syntheses)

are still missing.

The following conclusion will be drawn: The term "mimetic replacement" is often erroneous and/or premature and should not be used when accurate and systematic observations on pseudomorphism are missing.

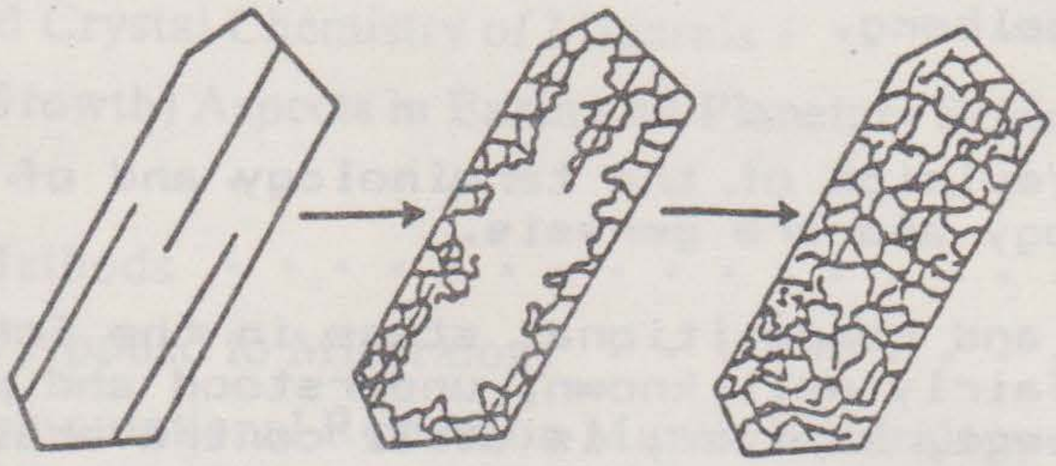

Verbreiteter Mechanismus der Pseudomorphosenbildung: das ursprüngliche Mineral A wird schrittweise in ein Gemenge B (+ C + D etc.) umgewandelt. Es resultiert in der Regel ein Gemenge (ein sogen. Mosaik), das mono- oder (häufiger) polymineralisch ist, also aus B + C + D etc. besteht.

Types of pseudomorphic replacement

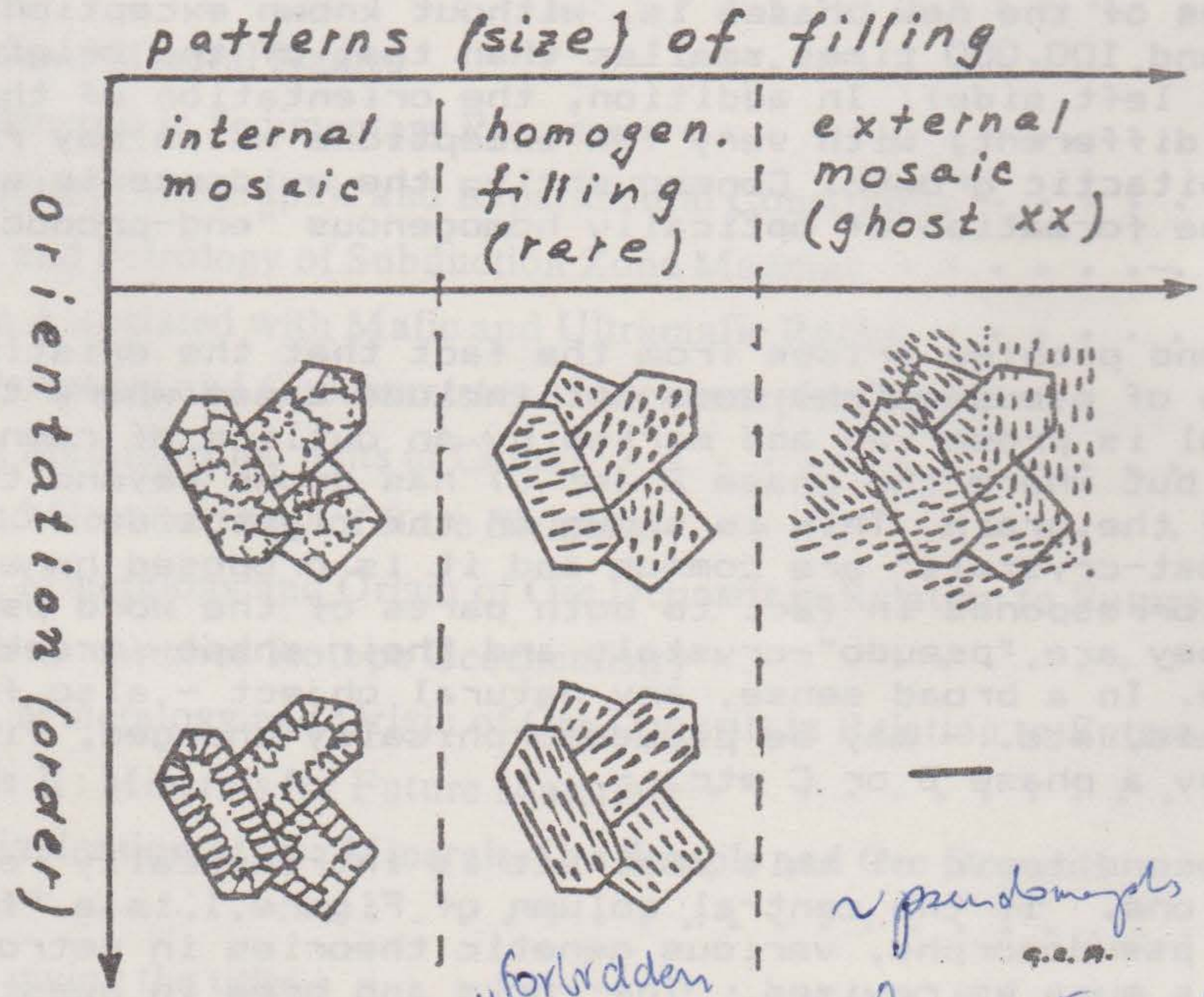

PETROGRAPHIC STUDIES AND MINERALIZATION OF SENDJ DEPOSIT, KARAJ, IRAN.

Firouz Alinia, Mining Institute, Amirkabir University of Technology, 424 Hafez Ave., Tehran, Iran.
Ahmad Khakzad, Department of Geology, Shahid Beheshti Univ. Evin, Tehran, Postal code 19834, Iran.

The Sendj ore deposit is located about 45 km. north of Karaj Iran. From petrographic view the deposit includes the following units: a) Tuffaceous series with the thickness between 200 to 250 meter, which are Tertiary in age. These rocks range in composition from andesitic type to trachyandesite, b) Porphyritic andesite which overlies the tuffs with the thickness ranging from 40 to 50 meter. The composition of these rocks ranges from trachyandesite to trachyandesite-basalt, c) The porphyritic andesite is overlain by a monzonite sill, which has a thickness of about 150 meter. The bottom part of the sill has the composition of monzodiorite and the top part is composed of quartz monzonite to alkali-monzonite.

Mineralization in Sendj deposit occurs mostly in porphyritic andesite and less so in the tuffs. The mineralization which are mainly on the form of veinlets contains chalcopyrite, molybdenite, niccolite and cobaltite. Minor ore minerals include anabergite, erithrite, Galena, Sphalerite, and pyrite.

The percentage of different metals in the samples taking from the prospect has been estimated as follows: Cu(5-14%), Mo(0.6-1.2%), Ni(0.15-1.7%), Co(0.7-2%), Au(1-2ppm).

Geochemical investigations indicated that monzonite is poor in mineralization, but the amount of Cu, Ni, Co, B, Pb, Zn, and S are high in porphyritic andesite.

Ore microscopic studies and paragenesis of the minerals indicate that the mineralization has been occurred in a hydrothermal condition and it is supposed that the area could be investigated for a possible Cu-Mo porphyry deposit.

ALTERATIONS AT THE BOTTOM OF GEOTHERMAL SYSTEMS: THE CASE STUDY OF SAINT MARTIN (LESSER ANTILLES).

D. BEAUFORT, P. PATRIER, AND A. MEUNIER, Laboratoire de pétrologie des altérations hydrothermales, U.A. 721 CNRS, Université de Poitiers, 40 Avenue du Recteur Pineau, 86022 POITIERS CEDEX, FRANCE.

The Island of Saint Martin belong to the andesitic volcanic arc of the lesser antilles along the eastern margin of the caribbean plate which is underthrust by the Atlantic ocean floor. The island of Saint Martin is composed by a sequence of Eocene sedimentary and volcanic rocks intruded by a 30 MY old quartz diorite pluton. Circulations of hydrothermal fluids characterized the subsequent thermal evolution of the system; they generated a 4 kilometers wide alteration halo in the tuffaceous rocks surrounding the pluton. The petrological characteristics of the altered rocks and the fluid inclusion data argue in the sense that the part of the geothermal system which is actually accessible corresponds to the roots the fossil system.

Fracturing pattern: The weakly fractured rocks represents the main part of the surface area of the fossil system which actually outcrops; they are characterized by massive rocks in which only small discontinuous fractures may be observed. The fracture density of weakly fractured rocks decreases with increasing distance to the pluton and desappear out of about 2.5 km from the pluton. The early regional forces controlled the emplacement of the quartz-diorite pluton of Philipsburg and the major structural breaks observed in the altered host rocks. The magmatic stresses created randomly oriented and interconnected structural breaks which are concentrated at the margin of the quartz diorite pluton. They led to several centimeters wide veins which may be continuously observed over several tens of meters.

Alteration pattern: In the overall system, alteration consists of three concentric zones locally crosscutted by fault and fracture controlled veins. With increasing distance from the intrusive body, the following secondary mineral assemblages crystallize in the weakly fractured rocks :

-epidote + actinolite + quartz + magnetite as far as 300 meters from the intrusion,

-epidote + quartz + chlorite ± haematite between 300 and 3000 meters

-mixed layer illite/smectite (R3 ordering type and 95% illite) + mixed layer chlorite/smectite (90% chlorite) + calcite + haematite between 3000 and 4000 meters.

The paleotemperatures estimated from fluid inclusions study in quartz and calcite indicate that such alteration zoning emplaced in a 350 - 200°C temperature range. In the weakly fractured rocks, the measured paleotemperatures exponentially increase toward the pluton. Chemically, these altered rocks do not seems strongly modified; the most significant compositional variation is a progressive

enrichment in volatile components, (H_2O, CO_2), toward the outest alteration zone. All the fault and fracture controlled veins result from two successive hydrothermal stages:
-During The first hydrothermal stage, toumaline + orthoclase + actinolite + quartz + apatite + magnetite and sulfides were deposited in the fractures and their adjacent wall rocks by NaCl rich brines at temperatures higher than 350°C.
-During a second stage these previous veins were largely superimposed by phengite + quartz ± pyrite alterations. This highly destructive alteration stage strongly affected the surrounding wall rock over distances which may attain 10 m on both sides of the main fractures at temperatures ranging from 350 to 250°C.

Chemically, the first vein alteration stage seems controlled by infiltration of fluids enriched in magmatic components (B, K, S, Cl, P and Cu). The second stage correspond to important dilution of the previous fluids by meoteric fluids and led to strong leaching of Na, Ca, Mg, Mn and Fe elements in the wall rocks.
As a conclusion, the alteration of the weakly fractured rocks occured near thermal metamorphic conditions (inactive flow regime in diffusive heat transfert) whereas fractures and faults were the main channelways to mass and heat transfer in active flow regime. At the bottom of this geothermal fields the phengitic veins seems to be useful guides for the prospection of productive reservoirs.

MINERAL CHEMISTRY OF TOURMALINES FROM THE BOTTINO MINING DISTRICT, APUANE ALPS (ITALY)

PO 1.17

VAS 1.24

Marco Benvenuti, Pilario Costagliola, Pierfranco Lattanzi, Dip. Scienze della Terra Universita' di Firenze, Italy
Giuseppe Tanelli, Dip. Scienze della Terra Universita' Federico II in Napoli, Italy

At Bottino (southwestern Apuane Alps), tourmaline-rich rocks (tourmalinites) occur within a low-grade, multiply deformed Paleozoic basement, in close association with Pb-Ag(Zn) mineralization. On the ground of geological, textural, and chemical features, they have been interpreted as indicators of exhalative pre-Alpine (Paleozoic?) boron and metal enrichment.
Electron probe analyses of tourmalines from both tourmalinites and metapelitic and metavolcanic country rocks reveal compositions that fall between "end-member" schorl-dravite series and a proton- and alkali-deficient end-member, $R^{1}_{1-x}R_3^{3+}R_6^{3+}(BO_3)_3Si_6O_{18}O_{3-x}(OH)_{1+x}$. There is only a loose correlation between optical zoning and chemical compositions. Tourmalines from tourmalinites show average FeO/(FeO+MgO) and $Na_2O/(Na_2O+CaO+K_2O)$ ratios of 0.56 and 0.67, respectively. Their compositions are similar to

tourmalines from exhalative tourmalinites, whereas significantly differ from granite-related tourmalines. They are slightly Fe-richer, and appear to be affected by higher degrees of proton loss- and alkali defect-type substitutions than tourmalines from host rocks. Tourmaline chemistry do not appear to have been significantly modified by metamorphism, as evidenced by absence of systematic Mg/Fe partitioning between tourmaline and metamorphic chlorite.

REFERENCE:
Benvenuti, M., Lattanzi, P., and Tanelli, G., 1989, Tourmalinite-associated Pb-Zn-Ag mineralization at Bottino, Apuane Alps, Italy : geologic setting, mineral textures, and sulfide chemistry : *Economic Geology*, v. 84, (in press).

1.8 P

MINERALOGY AND ORIGIN OF APATITE DEPOSITS IN PROCEMBRIAN STRATA ON ALDAN SCHIELD (SIBERIA, USSR)

A.G.Bulakh, Department of Mineralogy, Geological faculty, Leningrad state University, Leningrad, 199034, USSR

There are about 20 apatite mineral deposits in procembrian strata on area of Aldan schield now. They are of two main types: apatite-carbonate "ores" and apatite-silicate "ores". The best example of deposit with the first "ores" is Seligdar deposit (everage contain of P_2O_5 is about 6,3 %), the second one - Ukduska (3 %). Seligdar deposit has complicated fold structure. Here proterosoic apatite-carbonate "ores" of methasomatic hydrothermal origin occurs in archean gneises, schists and apatite-bearing marbles. Late methasomatic veins of anhydrite and (else later) gypsum generated in apatite "ores". As result apatite "ores" have such an average composition (%): apatite 18, carbonates 70, sulfates 0,2, magnetite and hematite 5, schist silicates 5, quartz 1. Apatite has very unusual brown or red-brown coloure (pigment is dispersed hematite). Formula of apatite: $(Ca_{4,92}Sr_{0,02}TR_{0,03}Na_{0,03})_5(P_3O_4)_3(F_{0,78}OH_{0,22})_1$. Ukduska deposit is an isocline fold of different methamorfic

rocks. Apatite is concentrated in a very thick stratum of diopside rocks (schists?). Apatite has blue coloure. It contains 0,60 SrO, 0,22 TR_2O_3, 1,80 % F. There are a lot of data on chemical composition, structure and properties of apatite and other minerals of apatite "ores" from both deposits. Isotopic data on C, O, Rb, Sr confirm geological data on priori sedimentogen source of phosphorus.

References:

A.G.Bulakh, A.A.Zolotarev d all. On mineralogy and origin of Seligdar apatite deposit. In: International Geol. Rev. 1985, 02.

A.G.Bulakh, V.N.Schvanov. Apatite sandstones in Seligdar river head. In: Lithology and mineral deposits 1986, 03.

A.G.Bulakh, V.N.Gulij, A.A.Zolotarev (in Russian). Phosphorous ores in procembrian strata of Aldan schield. 1990. Leningrad, Leningrad University. 190p.

GENETIC CHARACTERS OF THE GOLD MINERALS IN HONGHUAGOU GOLD FIELD, CHIFENG, INNER MONGOLIA

1.5P

CAI Aili and AI Yongde, Institute of Mineral Deposits, Chinese Academy of Geological Sciences, 26 Baiwanzhuang Road, Beijing, 100037, People's Republic of China

The Honghuagou gold field located on the margin of the North China craton includes 3 gold deposits-Honghuagou, Lianhuashan and Chaihuolanzi gold deposits. The deposits occurred in Archaean metamorphic complex-mainly amphibole-plagioclase gneiss, plagioclase amphibolite, which were migmatized in various extent. The ore bodies were controlled by the NNW-SN shear zones and fractures. The gold mineralization commonly and closely associated with the diorite porphyrite dyke. The ore bodies of the three gold deposits are mainly auriferous quartz veins with the only exception in Chaihoulanzi, where the ore bodies also occurred in altered rocks. The ore mineral assemblege is uncomplicated and dominated by a variety of sulphide and oxide minerals, including pyrite, chalcopyrite, galena and a little pyrrhotite and sphalerite. The gold mineralization is closely related to the intrusion of the granitoid in the Yan Shan Oro-

geny.

The gold mineral is mainly native gold and a little electrum, which mainly formed in four periods:

1.The early quartz period: The mineralization in the period mainly consists of gross quartz and a few native gold in filling and replacing veins. Besides, the gold also partly occurred in the both sides of the quartz veins. The native gold is micro-grained. The fineness of the native gold is 917.9-941.3. This period appeared mainly in Chaihoulanzi.

2.The quartz-magnetite-pyrite period: The mineralization in the period mainly consists of quartz,magnetite and gross pyrite. The native gold in fine-grained formed in the magnetite or micro-grained in the intercrystalline fractures of the gross pyrite and they replaced or filled the cracks in the quartz veins. The fineness of the native gold is 861.7-945.0. This period appeared typically in Lianhuashan. It is a principal period for the gold forming. The Ag-content in the native gold for 1-2nd periods is less than 10%.

3.The quartz-pyrite-sulfosalt period: The mineralization in the period mainly consists of fine-grained quartz,pyrite and a few Bi-sulfosalts. The native gold as inclusions dispersed in the fine-grained pyrite , quartz or closely associated with sulfosalt and filled the cracks or cavities of pyrite. The fineness of the native gold is 834.2-935.1. This period extensively appeared in Honghuagou. It is an important period for the gold forming. The Ag-content in the native gold is 10-20%.

4.The quartz-polymetal-sulphide period: The mineralization in the period mainly consists of quartz,pyrite , chalcopyrite and galena in the form of stringer. The native gold in fine-grained precipitated with chalcopyrite and galena at the same time or a little later and distributed in the cracks of early pyrite. The fineness of the native gold is 776.9-789.1. The mineralization of this period appeared in Honghuagou and less in Lianhuashan. The gold forming is less than 2-3rd period.The Ag-content in the native gold is more than 20%.

The fineness of the native gold formed in various periods falls down regularly from the early to the late period. The fineness is variable and the mineral assemblege,structure and texture also changed with the variety of the depth and temperature. Especially in the later period of gold forming the native gold formed the lamellar,tabular and rounded grains of tiny size in the pyrite and also in Bi-bearing minerals,i.e.,respectively with depth decreased krupkaite,aikinite and schirmerite. Both aikinite and tennantite appeared in deeper and shallower parts. It shows,that the ore forming fluids carried base metals and "granitic component"--Bi in

hydrothermal process. At the same time the fineness falls down from 918.5 to 834.2. Apparently the fineness and the other characters of the gold closely related to the forming environment. According to the cell parameter of gold-bearing pyrite, 5.414-5.417, the variety of a_0 has no distinct relation to gold content. It shows that the gold dispersed as the mechanical mixture in pyrite.

MINERALOGY STUDY ON VESUVIANITE FROM FUSHAN IRON DEPOSIT, HEBEI PROVINCE, CHINA.

Cao Zhengmin and Zhu Hong, Department of Geology, Peking University, Beijing 100871, People's Republic of China

Macrocrystals of vesuvianite were collected from contact zone of Ordovician limestone with Mesozoic diorite. The beautiful colour and huge size of the crystals are very charming.

The vesuvianites of this district are replacement product of Al-diopside, monticellite, grossularite and clintonite, formed in early Mg, Al- skarn stage and associate with blue calcite and wilkeite.

In general, they have zonal structure with brown centre and green shell and with dimensions up to 20 cm in width. The crystals are dipyramidal commonly without or with very poorly developed prismatic faces, the chief forms are e{101}, c{001} and k {112} with other eleven minor forms but {111} (Fig.1). This dipyramidal cryastal of vesuvianite is the typomorphic characteristic of high temperature. Investigation of goniometry have found that the usual crystal orientation is not correct, {111} ought to be {101}.

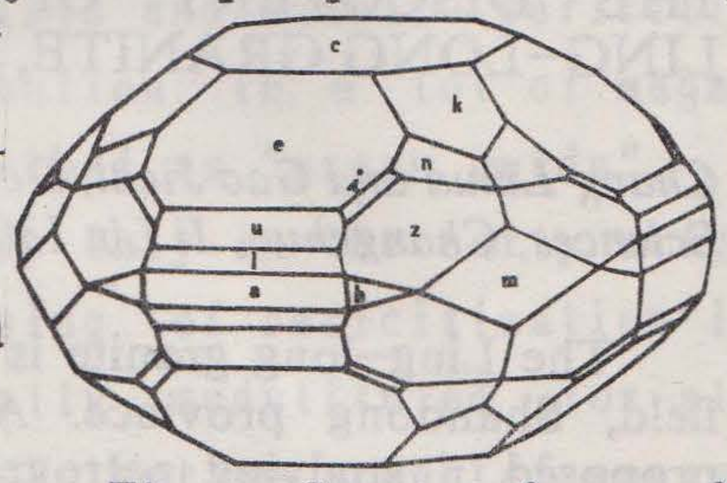

Fig.1. Crystal forms of vesuvianite

From the synthetic experiments and phase equilibrium data we know that the formation of vesuvianite is related to temperature and XCO_2 and under the circumstances of water-rach and CO_2-poor, the formation of it is essentially independent of pressure. It forms at high temperature (500—600° C) if SiO_2 is under saturation in the medium.

From the comparison study of numerous data, we find that in addition to the substitution of $Fe^{2+} \rightleftharpoons Mg^{2+}$, the replacement of $mFe^{3+}+nFe^{2+}+nTi^{4+} \rightleftharpoons (m+2n)Al$ is also exist in vasuvianite.

On the basis of 88 data of chemical compositon of vesuvianite many from the author of this paper , a new classification of vesuvianite has proposed by the author, based on ternary system Al_2O_3(A)-MgO(M)-FeO +Fe_2O_3(F) (refarence Fig.2), the vesuvianite may be classified into seven classes, normal vesuvianite (Ⅰ), Mg-Fe-vesuvianite(Ⅱ), Mg-Al-vesuvianite (Ⅲ), Fe-Al-vesuvianite (Ⅳ), Fe-rich vesuvianite (Ⅴ), Al-rich vesuvianite (Ⅵ) and Mg-rich vesuvianite (Ⅶ).

The DTA curves shows that the constitutional water of vesuvianite lose at 1040—1050° C. IR absorption band 3170 cm^{-1} of green ones in this area is due to the vibration of hydrogen- bond.

The mossbauer data prove that Fe^{3+} ions are able to occupy the 8-coordinated C sites on 4-fold axis. When the value of $Fe^{2+}/(Fe^{2+}+Fe^{3+})$

is less than 20%, Fe^{2+} ions are preferentially to occupy in the 6-coordinated A sites with a smaller distortion and shorter in bond, while about the half of Fe^{3+} ions in 8-coordinated C sites and the remaining Fe^{3+} in the 6-coordinated Al Fe sites with a more distortion. When the value of $Fe^{2+}/(Fe^{2+}+Fe^{3+})$ is over 35%, Fe^{3+} only occupy in Al Fe sites, and Fe^{2+} mainly in Al Fe sites and B sites (5-coordinated).

Both the content of total Fe and Fe^{3+} existing on C sites in brown centre are more than that in green shell of single crystal of vesuvianite.

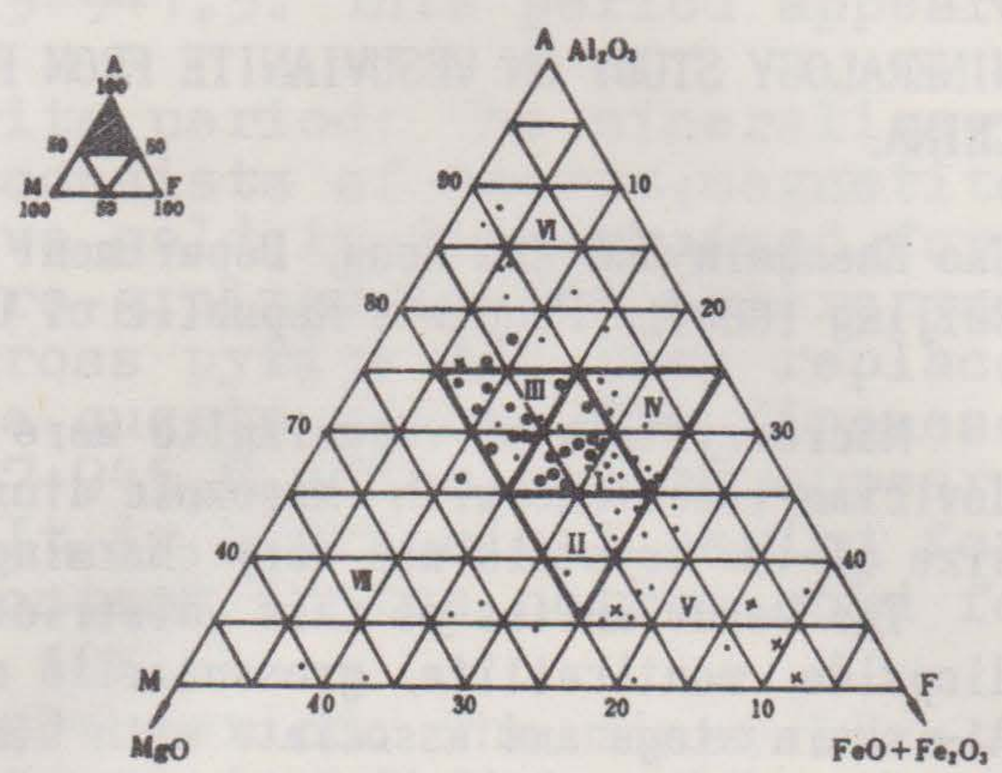

Fig. 2. The AMF diagram of classification of vesuvianite .
solid circles, this paper
dots, Deer and Dana
crosses, Crook and Himmelberg

THE DISCOVERY OF THE RESIDUAL SILLIMANITES IN LING–LONG GRANITE, SHANDONG PROVICE CHINA

Chang Lihua and Gao Jicai, Department of Geology, Changchun University of Earth Sciences, Changchun, Ji Lin 130026, People's Republic of China

The Ling–long granite is gold ore–producing intrusion in Zhao–yuan gold field, Shandong province. As for its origin, different opinions have been proposed.In studying petrography under microscope, we discoverd colourless, needle–like inclusions in some quartzs and alkali–feldspars. These very fine inclusions show medium–positive relief under the parallel polarizing microscope, are about 0.047 mm long and 0.0044 mm wide, and have cracks in the vertical direction of their extension axis. Under the orthogonal polarizing microscope their interference colours are first–order greyish–yellow, parallel extinction, length slow. It is quite evident that these characteristics are different from those of the adjacent zirkon. However, they are the same as the sillimanites in the biotite granoblastites in the Jiaodong Group (country rocks of Ling–long granite). Most of the sillimanites in the biotite granoblastites occur in form of bunch, some of them are in form of in needle and stick, and they may appear in the quartz and alkali–feldspars, which are in no defference from the above–mentioned needle–like inclusions in optical property.

The microprobe data suggest that the needle–like inclusions are sillimanites (shown in Table 1), with SiO_2 content a little higher than that of the sillimanites in the biotite granoblastites, that is accounted for by the part of SiO_2 from the circumferential quartz when punctured by electronic beam. In addition, except for SiO_2 and Al_2O_3, the content of other oxides are little indicating that it could not be confused with other aluminium–rich silicate minerals.

The above–mentioned facts show that quartz and alkali–feldspars containing sillimanites in the granite are residual minerals originally existing in the biotite

granoblastite. Their discovery further verified that the formation of Ling–long granite is closely related to the metamorphic rocks in Jiaodong Group and also give the evidence on genesis of the Ling–long granite.

Table 1 The data of microprobe analysis on sillimanite (wt%)

occurence / type / Oxides	in the granoblastites		in the granite
	bunch–like	stick–like	needle–like
SiO_2	39.53	37.17	46.09
Al_2O_3	60.09	62.65	53.70
FeO	0.25	0.05	0.00
MgO	0.00	0.00	0.03
CaO	0.00	0.05	0.03
Na_2O	0.02	0.00	0.08
K_2O	0.30	0.00	0.00
Total	100.19	99.92	99.93

A STUDY ON SERICITES IN THE GOLD ORE-FORMING GRANITES

Chang Lihua, Department of Geology, Chang Chun University of Earth Sciences, Chang Chun, Ji Lin 130026, People's Republic of China

In the study of the alteration of the gold ore–forming granites, we discovered that sericiteschists and quartz–sericitic rocks widely occur in linear distribution in a lot of magma hydrothermal gold deposits. They are described as "green guide".

Sericite substituted for plagioclase only in the early stage of the sericitization. With the increasing of sericitization in intensity sericites and quartz gradually sudstituted for all minerals in the rock. From the surface-distributing graph of energy spectrum, we understand that the gold are well–distributed and appear in dispersion in the sericite (electronic micrograph 1, omitted), which indicates that the physical chemistry condition of the formation of sericites is just suited to the activity of gold. The experimental data suggest that the temperature is 300–350℃, PH is neutral to weak acid at that time. With continuous change of the physical chemistry condition, the sericite–quartz–pyrite association appeared, quartz replaced the part of the sericited and absorbed in the dispersed gold in sericites. The appearance of the pyrites indicates that the H_2S is escaped from the solution. Much gold precipitated when much pyrites, other sulphides and quartz crystallized.

The sericites occurred in the assemblage of the scale and behaved in xenomorphic crystal, its crystal face is twist and incomplete under the electronic microscope (electronic micrograph

2, omitted) .

The analysis of energy spectrum shows that the components of the studied sericite are more close to standard metasomatic muscovite (in Table 1), but its SiO_2 content is a little higher than the standard, which results from the occurrence of a small amount of dispersed silicon in the sericite (electronic micrograph 3, omitted) .The sericite studied isn't phengite, hydromuscovite and illite, because of Si : Al = 1.4 : 1 in it, however, Si : Al = 3 : 1 in the phengite; as compared with hydromuscovite and illite, its Al_2O_3 and K_2O are higher, but MgO is lower.

Table 1 The content of the oxides of studied sample and standard mineral (w.t%)

Oxides	analytic sample			standard mineral*		
	1	2	3	metasomatic muscovite	hydro-muscovite	lillite
SiO_2	49.96	50.09	50.80	46.77	51.22	53.30
Al_2O_3	30.83	32.41	30.77	34.75	25.91	26.00
TiO_2	0.00	0.00	0.00	0.21	0.53	0.01
Fe_2O_3	—	—	—	0.71	4.59	2.50
FeO	1.69	1.67	1.50	0.77	1.70	—
MgO	0.69	0.73	0.50	0.92	2.84	4.40
CaO	0.00	0.00	0.00	0.13	0.16	0.20
N_2O	0.00	0.00	0.00	0.47	0.17	0.30
K_2O	10.06	9.91	10.61	10.19	6.09	8.30
H_2O	5.80	5.12	5.43	4.64	7.14	5.70

* Deer, W.A. 1982, Rock-forming minerals

Po 1.1. THE DISCOVERY OF LORANDITE IN CHINA AND ITS STUDY FOR THE FIRST TIME

Chen Daiyan, Department of Geology, Guizhou Institute of Technology, Guiyang, Guizhou 550003, People's Republic of China

Lorandite, a rare dispersed element mineral, was first described by Krenner (1895) who found it at Allchar, Macedonia (Yugoslavia). The lorandite, being

discovered by writer at the first time (1986), occurs in a strata-bound mercury ore deposit at Lanmuchang, Xingren county,Guizhou province in China and associated with cinnabar realgar, orpiment, pyrite, macarsite, barite,etc.

Lorandite has adamantine luster and is semitransparent.Crystals of lorandite are perfect and normally occur in the form of prisms with size ranging from 1 to 3 mm (the biggest up to 12 mm). Under refllected light it is greyish-white with light blue tint. Strongly anisotropic, internal reflection bright red. Specific gravity 5.55. Moss hardness 2.5. Reflectivity (%): Rg' 26.5—37.5, Rp' 23.9—30.1. Electron microprobe analysis (on average) gives (%): Tl 59.08, As 28.2, S 18.2, Hg 0.18, Sb 0.032, Au 0.111, Ag 0.107, Cd 0.053, In 0.072, Zn 0.022, Cu 0.012, Mn 0.016, Fe 0.016, Sn 0.066, Bi 0.031, Se 0.046, totaling 99.77,is formulated as Tl (1.02)As(1.03)S(2). DTA shows two endothermal peaks at 298—304°C and at 574—581°C. The strongest lines in X-ray powder pattern are (Å): 3.59, 2.985 and 2.890. Infrared spectrum shows four absorption peaks at 306, 330, 378 and 398 cm^{-}.

Combining these data with geological setting of ore deposit, we shed light on the origin of the lorandite, and the possibility to serve as an indicator mineral for prospecting gold deposits and its significance in utilizing rich thallium ore.

Po 1.2

A Study Of Sasaite Found In China

Chen Daiyan, Department of Geology, Guizhou Institute of Techology Guiyang, Guizhou 550003, People's Republic of China

Sasaite was found first by J.Martini (1978) in West Driefontein Cava Transvaal, South Africa. However it is first reported by writer (1986) in China. It occurs in an oxidation zone of strata–bound antimony ore deposit at Muli, Guangnan county, Yunnan province, and coexists with stibiconite, Valentinite and gypsum.

Sasaite occurs as greyish–white to green colloidal aggregates. It is possessed of earthy to glassy luster, and has specific gravity 1.87, Moss hardness 2.5–3 and refractivity 1.477. The strongest lines in X–ray diffraction pattern are (Å):11.303, 7.505, 6.937, 6.249 and 2.901. DTA shows three endothermic peaks at 152–159℃, 193℃ , and 698–704℃ . Infrared absorption spectrum shows H_2O and OH, PO_4 and SO_4 vibration zones at 3400, 1395, 1620, 1115, 600 and 520cm. Chemical analyses of sasaite gave (%): Al_2O_3 27.529, P_2O_5 21.600, SO_3 8.216, SiO_2 0.010, K_2O 0.100, Na_2O 0.200, CaO 0.001, MgO 0.001, Fe_2O_3 0.179, Zn 0.009, Sb 0.099, H_2O 41.900, summing to 100.017. Its formula is $Al_7(PO_4)_4(SO_4)(OH)_7.22H_2O$.

According to these data, the writer has discussed the genesis of sasaite and compared with sasaite found from South Africa.

1.1.P

PRINCIPLES OF MINERAL TYPOMORPHISM–ITS SIX ESSENTIAL NATURES

Chen Guangyuan, Sun Daisheng, Division of Genetic Mineralogy, China University of Geosciences, Beijing, 100083, PRC

In the investigation of a number of W, Cr, Fe, Au deposits in China from the 60′s to 80′s is summarized up the principle of six essential natures of typomorphism of minerals (Chen et al., 1986, 1987, 1989) as follows.

1. Universality of typomorphism of minerals. Typomorphism of minerals is universal in mineral kingdom since all minerals and all mineral associations are all without exception formed under definite conditions which leave on them as a rule definite marks or criteria typical of conditions of their formation. It'll be met with whenever and wherever one comes upon minerals in either natural or artificial systems.

2. Particularity of typomorphism of minerals. It helps to distinguish typomorphic minerals, typomorphic mineral associations and typomorphic characteristics of minerals because they display all of them particular marks or criteria typical of their conditions of formation in every fine detail. Ore–forming events are the most particular events in the geological process, in which minerals show always particularity in typomorphism. For example in gold mineralization the frequency of pyritohedral habit of pyrite, the total amount of trace elements in quartz and pyrite, the number of decrepitation pulses of quartz and the intensity of thermoluminescence of potash feldspar always reach its maximum while the intensity of thermoluminescence of quartz reaches its minimum (Chen et al., 1989).

3. Correspondence of typomorphism of minerals. It exists not only in crystallomorphology but also in chemical composition and crystal structure, physical properties and crystal physics as well as structure and texture of intergrown minerals etc. They provide in different respect corresponding informations of the same conditions of formation of minerals, being able to be correlated and check–up with each other and used for prediction of one from the other as in garnets and amphiboles of BIF (Chen et al., 1984).

4. Variation of typomorphism of minerals. It presents not only in crystallomorphology but also in other respects of typomorphism of minerals.

Based on further processing of quantitative data of typomorphism in time and space, gradient of variation of typomorphism of minerals plays still more important role.

Small gradient implies stable physico–chemical conditions, present in general in major or principal diagenetic and mineralization stages, epochs, periods and cycles, also in large rock bodies or ore bodies, especially in their central parts while great gradient on the contrary implies unstable physico–chemical conditions changing rapidly in a short time and space, present in general in minor or subordinate diagentic or mineralization stages, epochs, periods, and cycles, also in small rock bodies and ore bodies, especially in their marginal or swiftly thinning–out terminal parts.

5. Inheritance of typomorphism of minerals. It occurs between different generations, stages, epochs, periods, and cycles of minerals from the earlier to the later in evolution of their ontogenetic and phylogenetic history.

It is most easily recognized in chemical composition but also present in other properties related to composition. The hydrothermal replacement of almandite with almandite molecules up to 93.6% in the Archaean BIF of Gongchangling Iron Mine by Proterozoic alumino–ferruginous chlorite with f up to 94.8 and interference colour up to second bluish–green (Chen et al., 1984) is the example of inheritance of principal constituents typomorphic of rich iron deposits. Together with the inheritance of principal constituents in this example some other properties are also transmissed from the former to the latter like

deep colour, deep absorption , high refraction indices, high specific gravity etc.

Hydrothermal chrome mica with Cr_2O_3 up to 2 wt% afford the example of inheritance of subordinate constituent from Archaean metabasites assimilated by granitoids , being typomorphic of rich or large gold deposits in Jiaodong region (Chen et al., 1989).

Paramorphs and pseudomorphs are good examples of morphological inheritance with or without chemical inheritance.

6. Zonation of typomorphism of minerals. It is also not limited within crystallomorphology, since the latter is controlled not only by conditions of outer media but also by inner composition and structure of crystals, which will in turn lead certainly to variation of physical properties and crystal physics meantime.

Obvious zonation can easily be recognized with the naked eye, but hidden zonation of typomorphic characteristics like thermoluminescence of quartz in auriferous quartz veins (Chen et al., 1989) can only be detected by quantitative measurements .

Zonation displays the pattern and the direction of variation with its gradient in space and in time . It is four–dimensional , three spatial and one temporal, useful for finding out the direction of magmatic or hydrothermal activity , the structural relation, the magnitude, the degree of denudation and the extension of rock bodies and ore bodies and the location of required rock facies and rich ore sections.

All the above–mentioned six natures of typomorphism provide a sound basis for mineralogical mapping, being important for both theoretical and practical purposes.

GOLD AND PGE MINERALS IN PLACER CONCENTRATE FROM DAVAO, MINDANAO ISLAND, PHILIPPINE ISLANDS

Chen Guangyuan, Li Shuyan, Huang Shaofeng, China University of Geosciences, Beijing, 100083, PRC, Gong Runtan, Zhaoyuan Gold Conglomerate Co., Shandong, 265400, PRC

Philippine Islands are situated in the central part of the island arcs on the western Pacific rim nearby the suture line between the Pacific plate and the Eurasian plate. The deepest oceanic trough known in the world is found on the eastern margin of Philippine Islands. Therefore Mesozoic to Cenozoic tectonic and magmatic activities are well–developed, being favourable for mantle materials to reach the earth surface to form exploitable mineral deposits of chromites, titanic iron oxides, gold and PEG etc.

The investigated sample of placer gold concentrate is collected from Davao which is situated on the central eastern coast of Mindanao Island of the Philippine Islands. Its mineral constituents of noble elements are as the following.

1. Non–mercurous native gold (3) $(Au_{0.828}Ag_{0.136}Cu_{0.007}Os_{0.010}Rh_{0.009}Ru_{0.001}Fe_{0.005}Cr_{0.004})_{1.000}$
2. Mercurous native gold (6) $(Au_{0.848}Ag_{0.108}Cu_{0.004}Pt_{0.012}Rh_{0.004}Os_{0.003}Cr_{0.003}Ni_{0.002}Fe_{0.002}Co_{0.001}Hg_{0.010})_{1.002}$
3. Goldamalgam (3) $(Au_{0.602}Ag_{0.098}Ir_{0.004}Rh_{0.004}Ru_{0.003}Co_{0.001})_{0.712}Hg_{0.288}$. Au:Hg = 2.09:1.
4. γ–Goldamalgamite (12) $(Au_{0.468}Ag_{0.121}Cu_{0.004}Ru_{0.032}Pd_{0.013}Rh_{0.005}Ir_{0.005}Cr_{0.002}Fe_{0.002})_{0.692}Hg_{0.458}$. Au:Hg = 1.02:1.
5. Polyxene (6) $(Pt_{0.756}Fe_{0.175}Cu_{0.022}Ag_{0.003}Au_{0.001}Hg_{0.005}Pb_{0.004}Rh_{0.020}Pd_{0.005}Ru_{0.001}Ir_{0.001}Os_{0.001}Co_{0.003}W_{0.002})_{0.999}$
6. Osmiridium (15) $(Ir_{0.645}Os_{0.250}Pt_{0.028}Ru_{0.018}Rh_{0.007}Pd_{0.002}Cu_{0.027}Au_{0.003}Ag_{0.002}Ni_{0.003}Fe_{0.002}Co_{0.001}W_{0.009}Sb_{0.002}Hg_{0.003})_{1.002}$. Ir : Os = 72 : 28.

The total amount of PGE is up to 1.64, 2.18, 1.10 and 3.12 wt% respectively in the former four gold minerals and up to 91.44 and 97.21 wt% respectively in the latter two

PGE minerals.

The presence of remarkable PGE in gold minerals and the association of independent PEG minerals with gold indicate an ultrabasic to basic origin of the deposit.

Remarkable in association with the above–mentioned ore minerals are the following two minerals typomorphic of ultrabasic magma:

1. Chromite (4) (Mg, Fe) (Cr, Al, Fe)$_2O_4$ with Cr_2O_3 44.09, $TiO_2$0.29. $V_2O_3$0.24 in wt%.
2. Chrysolite (9) (Mg, Fe)$_2SiO_4$ with MgO / (MgO+FeO) = 77.5% f = Fe / (Fe+Mg) = 0.14, containing also NiO 0.27, V_2O_3 0.10, Cr_2O_3 0.05 , TiO_2 0.02, HgO 0.18 in wt %.

Besides, There are also a number of iron oxides mostly titanic and vanadium–bearing and typomorphic of basic magma found in placer concentrate as the following:

1. Titanium –bearing magnetic (host) (4) with MgO 1.00, TiO_2 1.52, Cr_2O_3 0.21, V_2O_3 0.05 in wt.%.
2. Titanohematite (exsolution lamellae) (3) with TiO_2 22.11, MgO 3.67, Cr_2O_3 0.08, V_2O_3 0.80 in wt.%.
3. Titanium–bearing maghemite (host) (5) with MgO 9.75, TiO_2 1.09, Cr_2O_3 0.20, V_2O_3 0.56 in wt.% .
4. Titanohematite (exsolution lamellae) (5) with TiO_2 21.89, MgO 1.48, Cr_2O_3 0.06, V_2O_3 0.84 in wt.%.
5. Titanohematite (6) with TiO_2 27.48, MgO 1.09, V_2O_3 1.05 in wt.%.
6. Titanium – bearing hematite (6) with TiO_2 0.30, MgO 0.39, V_2O_3 0.42 in wt.%.

Together with the above–mentioned opaque minerals of titanic and vanadium–bearing iron oxides present the following two related transparent accessary minerals:

1. Rutile(3) TiO_2, with TiO_2 97.72, V_2O_3 0.58, Ta_2O_5 0.38, Nb_2O_5 0.16, Ce_2O_3 0.35, Y_2O_3 0.00 in wt%, being $Ta_2O_5 > Nb_2O_5$ and $Ce_2O_3 > Y_2O_3$.
2. Zircon (12) $ZrSiO_4$, with HfO_2 1.49, MgO 0.04, Cr_2O_3 0.07, V_2O_3 0.04, TiO_2 0.04, UO_2 0.22, ThO_2 0.04 in wt% . Both contain Ti, Mg, Cr, V, U > Th, being typomorphic also of ultrabasic to basic magma with later geochemical differentiation.

Pyrite and quartz, the two common host and gangue minerals in ordinary gold deposits present also in Davao's placer with the following compositional characteristics

1. Pyrite (3) FeS_2, with Au 0.086 (0–0.17), Ag 0.150 (0.13–0.17), Se 0.030, Te 0.063, Bi 0.277 in wt%.
2. Quartz(6) SiO_2, with Au 0.00, Ag 0.14, Cr_2O_3 0.170 (max. 0.34), TiO_2 0.165 (max. 0.33), Ce_2O_3 1.335, La_2O_3 0.100, Y_2O_3 0.910 in wt%, being $Ce_2O_3+La_2O_3 > Y_2O_3$.

In Davao's placer, certain generations of pyrite may still be the host of gold as in ordinay gold deposits, but it contains Se, Te, Bi along with one another in the same pyrite, displaying altogether a low degree of differentiation. As to quartz, it contains also Cr, Ti but Ce+La > Y, displaying still the compositional inheritance form ultrabasic to basic magma with later geochemical differentiation. Rutile shows the same tendency.

From the above – mentioned points it is clear that the mineral constituents of gold placers from Davao indicate a close genetic connection with the mafic mantle materials coming from down below.

Note: Chemical compositions are determined by EPA. Number in parenthesis indicates number of analyses. Morphological study with SEM and measurements of R and VHN are also made.

SIGNICANCE OF MINERAL TYPEMORPHISM STUDY TO PROSPECT AND EVALUATION OF SOME AREAS

Po 1.3.

Cheng Minqing and Wang cunchang (Tianjin Geological Academy, Ministry of Metallurgical industry, Tianjin 300061, People's republic of china)

Abstract

Mineral typemorphism consists of paragenesis and assemblages of minerals, their typemorphic charateristics and so on.Quartz is a main mineral closely related to nonferro–metals ore deposits and gold ore deposits.Study on its typemorphism is of theoretical and practical signficance.

The Pangushan quartz–vein type w–deposit in Jiangxi Provine and some gold deposits in the East Shandong Provinceare taken as examples.

Typemorphism study of quartz from Pangushan w–deposit reveals that Vertical zoning of minerals is as follows:

1.From top to the depth W–Bi quartz veins show requlars variations in texture and structure. Quartz grows perpendicular to the vein walls with small grain size at margins of veins;in middle part of veins it becomes slim crystals. In the top part of veins is developed crystal geode at margins; in bottom part the quartz is massive.The orientations of the (100)face of the wolframite ctystals in the wolframite ore column are also different in diverse part of the orebody: in the upper part, the wolframite crystals are in random arrangement, assuming the network shape; in the funnel–like middle part, all these crystals grow perpendicular to the vein wall , with the (100)face essentially normal to the strike of the ore veins;in the lower part, however, (100)face is not wholly normal to the strike of the vein wall though the growth of the wolframite crystals is basically perpendicular to the vein wall.

2.Mineral assemblages show regular variation in space, with minerals of high temperature assemblage such as zinnwaldite, tourmaline and cassiterite in the upper part whereas those of lower temperature assemblage such as bismuth sulfosalts and tellurobismuthite group in the lower part .

3.Wolframite in the lower part contains more manganese than that in the upper part; the physical properties of wolframite also show regular variation with in creasing Mno; from the upper to the lower homogenization temperature. quartz tends to fall; the thermal luminescences curve varies regularly in space too, especially below the 585 level its shape approaches that of the bar-

ren quartz vein.

4. The spatial variations in Bi_2S_3–Pbs series and telluribiswuthite group are Characterized by downward depletion in Sulfur.

This is helpful to the comprehensive utilization of the ore.

The following discovery is made through typemorphism study of quartz of some gold deposits in the East Shandong.Province.

1. Quartz within altered–fractured–rock type Au–deposits is characterized by K+Na+Al>1% influx of xxxNc× 10^{-10}light unit in the integration range of 50～ 350℃ and single–acute peak thermoluminesence curve; quartz with in metamorphic hydrothermal gold deposits by K+Na+Al<0.5% influx of o.x Nc× 10^{-10}light unit and a–gentle–multipeaked thetmoluminescence curve in which low temperature peaks become prominent but meso–themperature peaks are reduced with the ore bodies extending to depths and pinching out; quertz within the complex deposits of alferred–fractured–rock type and quartzvein–type gold ore by K+Na+Al Value from 0.5% to 1%, influx of xNc× 10^{-10}light unit basically single–peak –thermoluminescence curve with Sub–peaks which goes gentle with depths.

2. Light density $\overline{D}_{H_2O}$ and $\overline{D}_{Co_2}$ of quartz formed in the 2nd ore–forming stage is proportional to gold grade.

3. Characteristics of quartz inclusion vary with intensities of the alteration.

4. Crystal form of pyrite changes vertically in the pattern.

Thererfore, typemorphism study of minerals not only can predict whether it is a gold–bearing vein or not,but also can determine position .of the expossure in erosion section especialy a surface expossure of a gold–bearing quartz vein,it is efficient to perdict its potential mineralization.

SPECIFIC FEATURES OF GENESIS OF SUPERGENE MINERALS IN CRIOLITH ZONE.

A.A.CHERNICOV,Institute ofgeology of ore deposits, petrography, mineralogy and geochemistry, Moscow, 109017, USSR.

1.The earlieideas and theories on the development of modern hypergenic origin ofminerals in all series of permafrost are not proved by the actual material.Under certain conditions even easily oxidized sulfides of ore bodies in outcrops do not change and are accumulated in alluvial deposits in Nordic areas. Some copper-nickel and other sulphide deposits in USSR and Northern foreign countri-

es have been discovered due to evacuation of glacial fans or some other ways of mechanical migration of minerals. Nevertheless the cryogenic phenomena significantly influence the supergenicgenesis of minerals in the cryolith zone.

2.Significant geochemical changes of rocks and ores at negative temperature take place in the upper layer of the cryolith zone in the active layer and taliks. These processes are attributed to significant change ofphysicochemical conditions and permeability of rocks during periodical freezing and frozen degradation and also to the specific features of underground waters in the permafrost areas: High concentration of dissolved O_2, CO_2, organic matter etc. and a very important role of water films under a constantly disturbed thermodynamic equilibrium.The following elements are very mobile in the upper layer of the cryolith zone: Zn, Cu,Ni, Ag,Cr,Ba,Ti,Pb,Sn,Fe,Mn and others.Under certain conditions it results in leaching of these elements out of the upper part of the infiltration zone and accumulation of the supergene minerals on the way of flow of the ground water to a dicharge area.

The hypergenic minerals,developed below the active layer at the depth of >500m below land surface (Northern granite massiff in North-West part of the Chukotka highlands) were formed during the preglacial period and interglacial stages.The absolute ages of these minerals are~300,~500, >500 thousand years. The permeability to water of the rocks and ores increased due to multiple warming or cooling while the mentioned above chang of physicochemical and thermodynamic conditions were accompanied by accumulation of typomorphic minerals. The depth of occurrence, the intensity of hypergene origin of minerals including formation of highest quality of Cu, Ag etc ore depend on a complex combination of global, regional and local factors.

3.Thypomorphic supergene minerals and mineral assemblage of permafrost - fibroferrite, melanterite,sulphur, specific brochantites, acanthite etc are formed during freezing of fissure water. A comprehensive analysis of mineral assemblages, a composition of hypergene minerals is an important criterion of evaluation of the mineral occurrences and fo-

recasting of deepseated ore deposits.

1.30 H

THE ROLE OF CALCIUM SILICOALUMINATE CARBONATE HYDRATE MINERALS IN THE FORMATION OF PALYGORSKITE

Liberto de Pablo-Galan, Instituto de Geologia, Universidad Nacional A. de Mexico, 04610 Mexico, D.F., Mexico

The formation of palygorskite in a marine environment was documented on Eocene - Pliocene deposits located in the Yucatan Peninsula, Mexico. In them, palygorskite appears to have formed from the reaction between diagenized calcite and an igneous leachate. Always associated and growing from calcite, are found calcium silicoaluminate carbonate hydrates (CSACH) of variable composition.

The dolomitized and silicated limestone that encases palygorskite contains stalactitic, acicular and subhedral calcite. Growing from calcite, appear calcium silicoaluminate carbonate hydrates in the form of elongated curved crystals in coraliferous arrangements. The chemical composition changes progressively from 5.31% to 47.17% SiO_2, 2.91 tc 11.21% Al_2O_3, 0.42 to 3.39% Fe_2O_3, 0.90 to 5.71% MgO, 46.69 to 5.68% CaO, 0 to 0.27% TiO_2, 1.21 to 0.20% Na_2O, and 0.08 to 0.96% K_2O. The total varies from 58.62% for the high-CaO compositions close to the base of the coraliferous arrangements anchored on calcite, to 70.83% for the high-SiO compositions detected on the tips of the crystals. When these compositions are plotted versus the CaO content and the analysis for calcite and palygorskite are included, smooth correlations are obtained which indicate that: (1), the difference to 100% decreases as the SiO_2 content increases, suggesting that it may correspond to H_2O for the high-SiO_2 CSACH and to CO_2 for the high-CaO ones; (2), low-CaO concentrations, below 20%, are associated to higher contents of SiO_2, Al_2O_3, Fe_2O_3, and K_2O, slightly lower MgO and Na_2O, and equal TiO_2 than high-CaO CSACH, pointing that these CSACH may have resulted

from the reaction between calcite and an igneous leachate. The CSACH somehow remember the scapolite-type minerals, eventhough these have much higher contents of Al_2O_3 (16.94 to 32.76 %). The geochemical continuity found between palygorskite, calcium silicoaluminate carbonate hydrates, and calcite does not suggest that palygorskite may have resulted from the diagenesis of smectite.

The palygorskite presents a typical feathery morphology and a chemical composition which corresponds to the formula
$(Si_{7.31}Al_{0.69})(Al_{1.33}Fe_{0.50}Mg_{0.91})_{2.74}Ca_{0.49}Na_{0.21}K_{0.15}O_{20}(OH)_2.4H_2O$. It is associated to minor occasional montmorillonite.

TYPOLOGY OF THE LEAD-ZINC DEPOSITS BASED ON MINERALOGICAL AND GEOCHEMICAL DATA.

Dobrovolskaya M.G. Institute of Geology of Ore Deposits, Petrography, Mineralogy & Geochemistry of the Academy of sciences of the USSR, Moscow 109017, USSR.

Mineralogical and geochemical investigations of the ores from lead-zinc deposits formed in different geologic situations revealed that such deposits differ by the ratio of the main ore-forming minerals, some mineral parageneses, textural and geochemical peculiarities of the ores rather than by mineralogic composition.

In the ores of the deposits located in skarns and intrusive rocks the pyrrhotite and sphalerite with Fe > 10 wt.% are the early minerals. In such deposits galena forms its own later association.

The ore in the deposits located in volcanic rocks are enriched by pyrite, chalcopyrite, hematite. Sphalerite is associated with galena, fahlore and the later generation of pyrite. The content of iron in sphalerite is under 5-6 wt.%.

There are two types of the deposits in carbonate rocks The mineral composition and textures of ores in the first one are similar to those in metasomatic and vein types in skarns and granitoids. In this group of deposits the generations of sphalerite in the early and later associations differ by the content of Fe (10-12 and 0,5-6,0 wt.% respectively). The stratiform deposits differ by the simple mineral composition, colloform, banded, cavernous textures, higher representation of marcasite and carbonate in ores. The content of Fe in sphalerite is lower than 3 wt.%.

One of the simplest and objective indicators for typology of the deposits by their genesis are the geochemical associations of trace elements in sphalerite revealed by the mathematical methods. For each type of deposits there is a specific correlation between Cd, Mn, Fe (see table).

Deposits	associations		
In skarns	Cd Fe Mn (Cu Ni Sn Mo)		Co
In granitoids	Cd (Ge Ga Ag)	Fe Mn (Cu Sn Mo)	Co (Ni As In)
In carbonates metasomatic	Cd Mn (In Ge)	Fe (Cu As)	In Sn
stratiform Mn	Cd (Sn Ge Ag)	Fe (Ni Co Cu)	

These results complement data revealed by Zhang Qian who studed trace elements in galena and sphalerite of lead-zinc deposits.

Reference:
Zhang Qian (1987). Trace elements in galena and sphalerite and their geochemical significance in distiguishing the genetic types of Pb-Zn ore deposits. Chinese journal of geochemistry, v.6, N 2.

QUARTZ — A SIGN OF EXPLORATION FOR ORE DEPOSITS

1.28H

Feng Jianliang Lu Haiya, Beijing Research Institute of Mineral Resources and Geology, Beiyuan Andingmenwai, Beijing, China

Quartz is a major component mineral in almost every metal ore deposits. It was treated as common mineral before. However, it is considered as an important sign through recent years working in the study of genesis and prospecting for ore deposits.

In some hydrothermal vein type of wolframite ore deposit in Nanling Area, South China, the higher of degree of euhedral crystal of quartz is, the more enriched of wolframite is. The colour and luster of quartz are caused by impurities. In gold vein where quartz is transparent and with strong oily luster, gold is enriched. On the contrary, there is no gold.

The variefies of content of microelements in quartz have outstanding result for prospecting vein type tungsten and gold deposits. For example, we have tested the content of microelements in quartz, the content of alkatic elements, K,Na, Ca in the quartz without tungsten is much higher than that in quartz with tungsten. The content of microelements in quartz can reveal that the composition of mineralization solution. The strongly alkaline solution is unfavourable for wolframite sediment. Especially,we have tested the content of fluorine in quartz-tungsten vein, it reaches 2.02%. Tungsten is transferred by fluorine complex compound, they have closed relation. The fluorine anomaly from 0.15% to 0.2% shows tungsten mineralization in the area. In an unknown area,it is from 0.31% to 3.19%. In table 1 we list the content of microelements in the quartz with and without tungsten, the third is in unknown area we predicted it as a well target for tungsten through our work.

The shapes, the composition of gas and fluid inclusions in quartz give us a strong evidence in looking for ore deposits. In Nanling Area, the inclusions in quartz-tungsten ore veins are smaller than 10 μ. Their homogenisation temperature is 105°C to 200°C, average 147°C, and 205°C to 365°C, average 258°C. The composition of gas inclusion is $H_2O > CO_2 > H_2$, EG = 1015, $H_2O/CO_2 < 50$. It reveals that the content of CO_2 in mineralization solution is higher and favourable for tungsten.mineralization. The composition of fluid inclusion showes the content of H_2O, CO_2, F, Cl is high. Tungsten is transferred as the form of complex compound—$WO_2F_4^{2-}$, $H_2WO_4, HWO_4^-, WO_4^{2-}$,and the more H_2O, F^-,Cl^-, the easier for tungsten and iron to be transferred and deposited. In the unknown area, the inclusions are 3 to 5 μ. Homogenisation temperature is 138°C to 200°C, average 164°C, and 201°C to 352°C, average 267°C. The composition of gas inclusion is $H_2O > CO_2 > N_2 > CH_4 > H_2 > CO.O$. The composition of fluid inclusion showes the content of Cl^- and F^- is high. The characters of inclusion are similar to those in tungsten ore veins. We get same result.

Thermoluminescence of quartz can reveal which kind quartz grows with gold and tungsten. Dr.E.K.Lazalinck, USSR, mineralogist, through detail research for thermoluminescence of quartz in auriferous and nonauriferous hydrothermal quartz vein, discovered that the strength of the thermoluminescence of quartz is observiously different at 230°C and 280°C, the thermoluminescence of auriferous quartz is strong and the nonauriferous one's is weak. We used this method to study thermoluminescence of quartz in Nanling Area, and got an ideal curve of it. The strength of thermoluminescence of quartz with tungsten is about 32 at 220°C, in quartz without tungsten is 20, and in the unknown area is 31. From the comparison, we also got same conclusion that the unknow area is a well target.

Beside these, cell dimension of quartz can also tell us some good information for prospecting gold and tungsten ore deposits.

Through our work in genetic mineralogy of quartz,we have found some target being proven by later prospecting. So, we suppose that the quartz can be used as a sign in searching for metal mineral deposits.

Table 1. Content Of Microelements In Quartz

AREA	SAMPLES	CONTENT OF MICROELEMENTS (ppm)										
		Al	Ba	Cu	Ca	K	Li	Mo	Na	Pb	Sr	Zn
tungsten	14	331.94	4.97	0.77	83.13	51.93	9.76	88.76	28.97	0.49	2.10	27.76
no tungsten	8	7308.6	25.43	9.75	180.3	1483.3	3.82	25.16	233.26	13.54	6.81	43.36
unknown	10	485.18	8.00	0.72	127.59	169.82	8.49	121.11	45.98	0.49	3.26	37.49

Ti	W	Sn	Sc	Bi	Co	Ce	Mn	Ta	Y	Yb	Cd	Be	Fe	Cr	La
21.06	51.43	79.0	0.56	56.0	2.0	5.1	9.5	45.0	2.1	1.1	5.4	0.93	108.0	4.3	4.0
159.72	—	—	—	—	—	—	—	—	—	—	—	—	—	—	—
19.76	57.0	102.0	0.62	69.0	1.9	6.4	14.0	49.0	2.5	1.2	4.2	0.86	115.0	5.4	4.6

GENETIC MINERALOGY AND PROSPECTING MINERALOGY OF BAOBAN GOLDHAINAN ISLAND

Feng Lian Shun, Guangdong Geology research institute, China national non-ferrous metals industry corporation, Guangzhou, Guangdong 510080, People's Republic of China.

The Baoban gold deposit occurs in a regional metamorphism-migmatitic complex of the late paleozic era (190-290Ma). Two types of mineralization: 1). quartz vein type. 2). structure altered rock type.

I. Typomrphic assoiation of minerals; quartz-native gold, quartz-native gold-electum, quartz-native gold-electrum-pyrite-arsenopyrte, etc.

II. Typomrphic minerals: arsenpyrite, kaolinite, azurite, Zircon (Au), Carobbiite.

III. Typomrphic features of minerals 1. Indication of Genesis: (1). Amphibole. (2). Biotite. (3). Zircon: U-Pb isotope age determination shows the Zircon-forming era is 883-1406Ma. (4). As gold content values being 873-991 in native gold and 781-811 in electrum We'll distributed composition (Ag/Au ratio 2-15), the gold was deposited in the condition of stable physical and chemcial environmen during old time. R=59-72%(548nm).

2. Typomorphism of mineralization. (1). Pyrite: The pyrite ores might be divided into poor sulfur ore (Fe/S=0.6-1) and low sulfur ore (Fe/S=0.7-0.8) coarse-granied idiomorphic pyrites contain gold (40ppm), coarsed-grained crushed allotriomorphic pyrites contain gold (160ppm), In peor sulfur quartz type, its crystal face (100), (111)

(221),crystallized completely, but (210)(100) completely altered in migmatite and (100) is rich in quartz vein type,'The fine-grain pyrite with its (210) crystal-face well grows, so the Au content is high (>100g/T). The hardness of pyrite is related to its crystal forms of (210). hardness value being 1097kg/mm^2.of (100), being 665-933kg/mm^2,and the irregular shape face being 882-946 kg/mm^2.(2).Quartz: -type which shear-tangential ductility deformation, high Al content (Al>1000ppm),large unit cell (a_o:4.915-4.932, Co 5.408-5.415) is rich in gold, but -quartz with small unit cell (a_o:4.913, Co:5.404) is poor of gold. 3. Spectroscopic features (1) reflective dispersion curve (2). IR spectra.

IV.Mineral thermometer and barometer: 1.based on liquid inclusion quartz Td 137-418°C, Th 214-252°C, Td 230-310°C 2. the temperatures based on mineral composition: native gold 250-350°C, arsenopyrite 320-450°C,quartz 220-320°C etc, gold deposit formed at 200-300°C. the pressure of the fold forming is 100-1100 bar,and it is as same as the range 0.4-4.02 kilomete depth.

V.Thermodnamic Halo: ore tenor of,the main ore reef varies(inversely as Th, directly as Im (the sttength of main wave of cracred inclusion) and free with Td,etc.

VI.Pyroelectricity typomonphism of minerals in the ore-bearing rock the types of pyrite have more P-type. Compared with other deposits in the eastern of Shandong province and western of Guangdong province, the pyro electricity of this deposit has following features: pyrite with N-type and ligh P-type (>50) is not (20-30) occurs in the wall rock near ore body and low p-type (10-20) lies in ore body. The value of the $\delta^{34}S$ of the pyrite in the ore vein varies in a range of +6.1-+9.2%. and the Rbeing 0.5-3%, with the value of the $\delta^{18}O$ and D of the wafem in the ore forming +9-15.1% and -54 -78.4%,$\delta^{18}OH_2O$0.06 +8.11%, range respectively, showing that the gold is onginated from the Baoban group and the migmatic hydrothermal process generated by the fructual-metamorphic differentiation is the major stage during the mineralization. It has been suggested that the gold in the solution probably is in the removing forms of $Au(HS)_2S^{4-}$ and the equation of the gold reaction is in the forms of $2[AuS3]^{3-} + 3Fe^{+} \rightarrow 2Au + 3FeS_2$ and

$$[Au(HS)]\,2 + e \rightleftharpoons As + 2HS^{-}$$

THE MINERALOGY AND GEOCHEMISTRY OF A LATE PRECAMBRIAN SOIL PROFILE - A POSSIBLE SOURCE OF INDUSTRIAL MINERALS. 1.7.P

Lindsay K. Ferguson, Department of Geology and Applied Geology, University of Glasgow, Glasgow, G12 8QQ, Scotland, U.K.

Weathering of the surface of Proterozoic rocks in NW Scotland is linked to the provision of constituent ions in overlying, economically important feldspar deposits. These have industrial value as a slow release fertilizer and one such horizon is currently being exploited in Scotland.

The rock of the alteration horizon in the Lewisian gneisses, pegmatites and amphibolites immediately beneath the Proterozoic/Phanerozoic unconformity in NW Scotland is named agalmatolite. The unconformity extends for more than 80km and the alteration profile is developed, to a variable extent, at most places where the unconformity is exposed. Alteration penetrates to more than 15m in places.

Na-feldspar is the most readily altered mineral, followed by biotite, microcline and quartz. Very fine grained muscovite, a form known as pinite, constitutes the initial and predominant secondary mineral formed throughout the profile, but towards the top, tourmaline rosettes and pyrophyllite are also formed. Narrow tourmaline-quartz veins penetrate the whole profile.

Although both hydrothermal and weathering processes have been suggested for the origin of the profile, the field evidence would suggest that the bulk of the alteration was caused by extensive weathering. The mineralogy is also consistent with many palaeosols and indeed, the tourmaline may reflect an addition of boron to the Precambrian surface from the Cambrian sea, due to adsorption by freshly precipitated ferric and aluminium hydroxides and incorporation into illite minerals. Erosion of this profile may have provided detrital minerals, and K and Al ions for the authigenic K-feldspar, in the extraordinarily potash rich Cambrian Fucoid Beds some 100m above the unconformity (Russell and Allison, 1985).

An $^{39}Ar/^{40}Ar$ laser probe age traverse is shown in Fig.1. The age of neoformation and growth of authigenic feldspar is given as 550-500 Ma with the detrital core showing older ages.

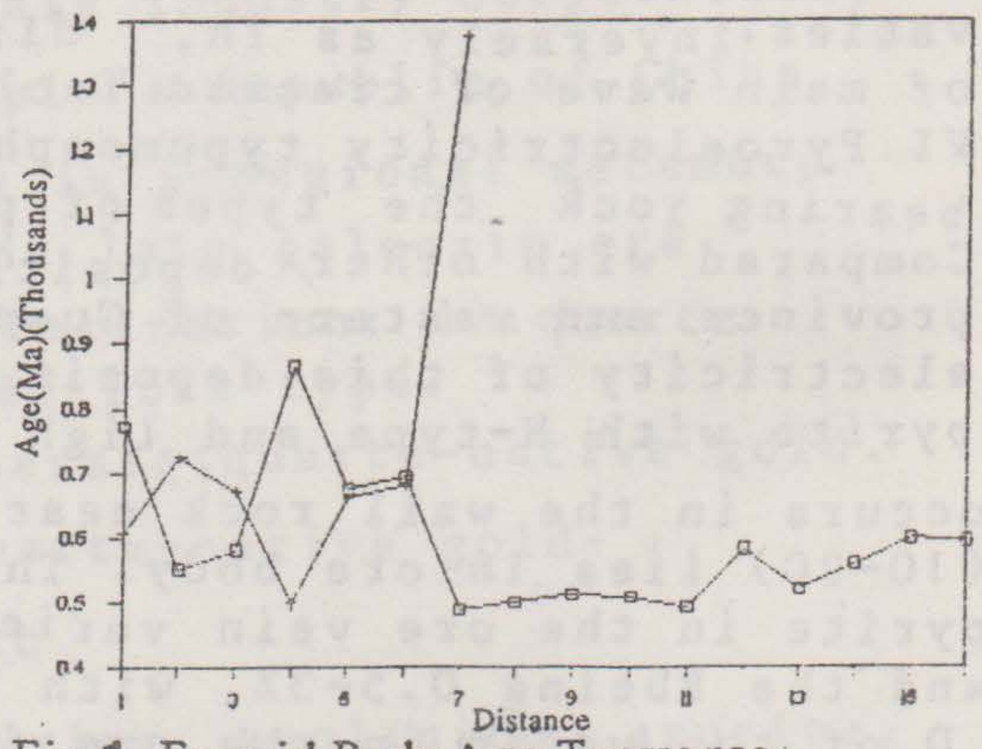

Fig.1. Fucoid Beds Age Traverse.

K/Rb ratios of agalmatolite and Fucoid Beds lie within the same field which is clearly distinct from that of other Precambrian rocks (Fig. 2). These data suggest that there is a direct link between the alteration profile and the genesis of the Fucoid Beds. Similar profiles are found across the Laurasian craton (eg.Duffin, 1989) and may therefore be developed around the margins

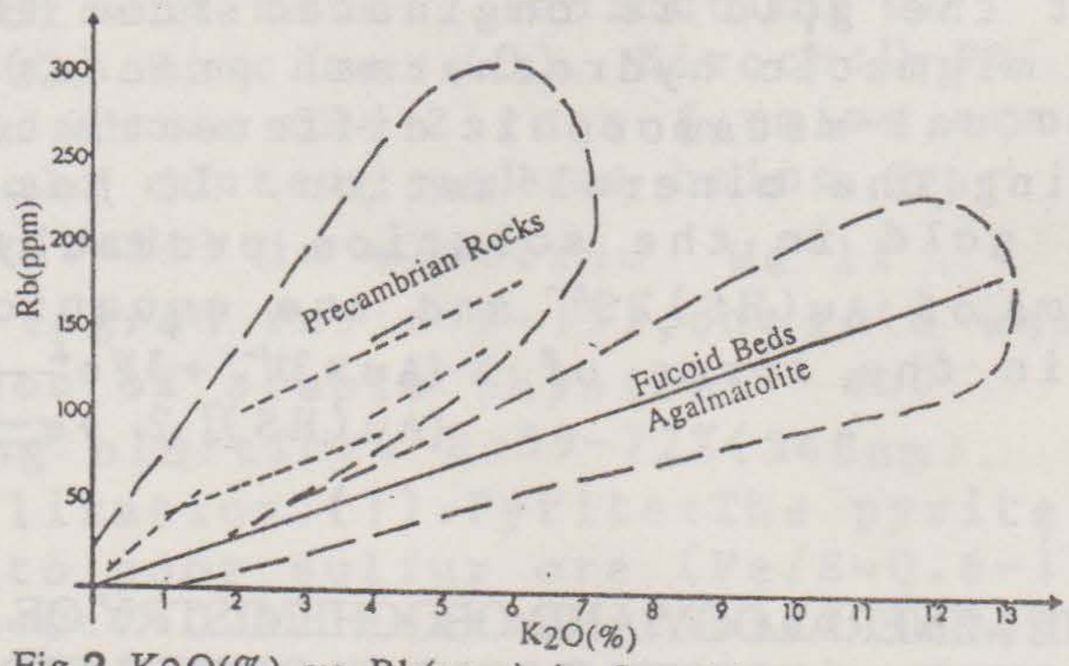

Fig.2. K2O(%) vs Rb(ppm) in Scottish Precambrian Rocks and Fucoid Beds Formation.

of the Proterozoic supercontinent elsewhere in the world. Indeed, Ronov and Migdisov (1971) pointed out that the earliest Phanerozoic rocks in North America have an extraordinarily high K content and massive developments of authigenic feldspar feature in many exhalative orebodies around the margin of the Proterozoic supercontinent (Russell, 1988).
Hence, where rocks of the Cambrian marine transgression overlie gneissic basement elsewhere throughout the world, there may also be economically important potash rich deposits nearby.

References.

DUFFIN, M.E. 1989 Nature and Origin of authigenic K-feldspar in Precambrian basement rocks of the North American Midcontinent *Geology*, v.17, 765-768.
RONOV, A.B. and MIGDISOV, A.A. 1971. Geochemical history of the crystalline basement and the sedimentary cover of the Russian and North American platforms. *Sedimentology*, v.16, 137-85.
RUSSELL, M.J. 1988. Chimneys, chemical gardens and feldspar horizons+pyrrhotine..... Proc. seventh IAGOD Symposium. Zachrisson, E. ed. Schweizerbartshe Verlagsbuch handlung, 183-190.
RUSSELL, M.J. and ALLISON, I. 1985. Agalmatolite and the maturity of sandstones of the Appin and Argyll groups and Eriboll Sandstone. *Scott. Jour. Geol*, v.21, 113-122.

BIREFRINGENT GARNETS FROM THE CALC-SILICATIC FELSES OF THE TOLFA MOUNTAINS, ITALY

1.12.P

V. Ferrini and S. Lucchesi
Dipartimento di Scienze della Terra, Universita degli Studi di Roma "La Sapienza", P.le A. Moro 5, 00185 Rome, Italy

Grandite garnet crystals, occurring in an outcrop of calc-silicatic felses in the Tolfa Mountains (Latium, Italy) are described. In this area metallogenic, metasomatic, thermo-metamorphic and hypoabyssalitic events, in close genetic relation to the local acid volcanic activities, occurred within the rocks of the Palombino flyshoid complex.

Garnets may be differentiated both optically and on a compositional basis. In fact crystals show various degrees of optical anomalous behaviour, essentially biaxial character, varying from strongly birefringent to almost totally isotropic individuals. Chemical composition ranges from a prevailing andraditic content to a more grossularitic one. Anisotropic crystals are characterized by the typical "dodecahedral twinning" of skarn garnets, with, frequently, a fine lamellar texture, showing variable birefringence. Moreover, the most birefringent garnets

are sorrounded by rims of recrystallized calcite. Such variability in garnet optical behaviour may be related to compositional zoning from andradite- (An76Gr22) to grossular-rich (An32Gr66) portions, as evidenced by electron microprobe analyses, isotropic garnets being essentially iron-rich.

In the calc-silicatic felses effects of contact thermo-metamorphism can be recognized and related to subsequent and complex petrogenetic events. The temperature range (comprised between 450 -600 °C) resulted strongly influenced by high PCO2 values. These variations of environmental conditions are closely related to the different chemical and optical typologies of the garnets.

1.18P

COMPOSITION AND PARAGENESIS OF PEGMATITIC MICAS FROM THE PIKES PEAK BATHOLITH, COLORADO, USA

Foord, Eugene E., M.S. 905, U.S. Geological Survey, Box 25046 Denver Federal Center, Denver, CO 80225 and
Černý, Petr, Dept. of Geological Sciences, University of Manitoba, Winnipeg, MB, Canada R3T 2N2

Micas (N = 29) from miarolitic pegmatites associated with granitic units of the anorogenic Pikes Peak Batholith (1.04 - 0.97 B.Y.), Colorado, range in composition from lepidomelane (N = 1) and Li-biotite (protolithionite) (N = 5) to zinnwaldite (N = 21). Locally, phlogopite (N = 1) and Fe-bearing muscovite (N = 1) are also present (Figs. 1 and 2). Pervasive late-stage hydrothermal alteration of many of these micas produced vermiculite (N = 1). Fresh micas are thus uncommon. The majority (16) are from the Lake George Intrusive Center, 12 are from the Wigwam Creek area, with one each from the Harris Park and Devils Head areas. Phlogopite and vermiculite are from tapered crystals in graphic pegmatite growing toward, and adjacent to the blocky zone; all other micas (28) are from the blocky zone and miarolitic cavities. Principal cogenetic minerals are quartz, microcline (mostly of the amazonite variety), and albite, with local topaz or fluorite, and rarely schorl-elbaite. Significant compositional as well as distinct and sharp color-zoning, resulting from primary growth fluctuations, are present in most crystals formed in miarolitic cavities. A few to more than 100 distinct zones were developed. Biotite (annite) in host granite and early graphic pegmatite is compositionally homogeneous.

Three separate crystals of zinnwaldite generally show a decrease, from core to rim (Figs. 1 and 2), in Fe_{tot} and MgO. Li_2O, F, and SiO_2 increase while MnO,

Rb_2O, Cs_2O, and Na_2O remain essentially constant. Total FeO + Fe_2O_3 ranges from 19 - 30 wt. % for lepidomelane and Li-biotite, and from 9.1 - 16.5 wt. % for zinnwaldite. The ratio FeO/Fe_2O_3 decreases from about 10.5 in early biotite to 3 or less in zinnwaldite, reflecting conditions of increasing fO_2 with continued crystallization. MnO values are between 0.53 and 2.35 wt. % for 26 Li-biotites and zinnwaldites; one additional zinnwaldite contains about 4.0 wt. % MnO, thus indicating the presence of some masutomilite component.

Trace and minor elements (in ppm) include Ba (5 - 400) , Sr (4 - 68), Tl (3 - 15) , Ga (51 - 700), Be (3 - 198), and Zn (800 - 5700). The average Sn content of three zinnwaldites is 150 ppm. The elevated Zn content is an expression of the enhanced Zn content of the Pikes Peak Granite and cogenetic pegmatites. Neutron activation analyses indicate that the chemical zonation is oscillatory and some zones of zinnwaldite crystals contain >1.1 wt. % Zn.

These micas are the products of extreme fractionation of a metaluminous granitic melt of anorogenic derivation. Strong enrichment of Li, Rb, and F is indicated. The sharp color and compositional zonation present in some crystals of zinnwaldite reflect distinct and rapid changes in the composition of the parent fluid phase.

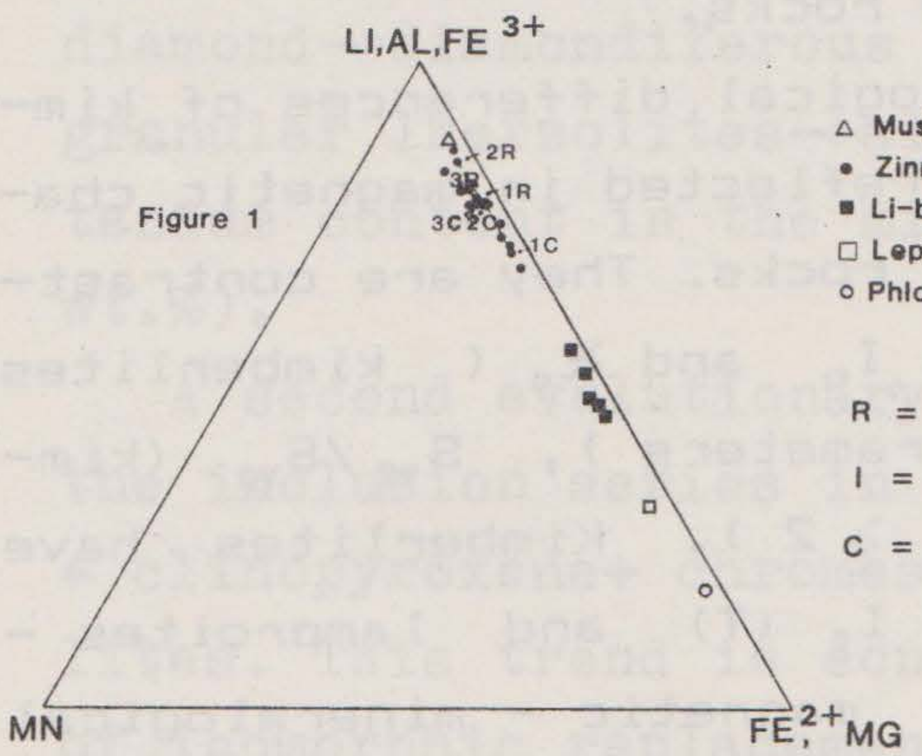

Figure 1

△ Muscovite
• Zinnwaldite
■ Li-biotite
□ Lepidomelane
○ Phlogopite

R = Rim
I = Intermediate
C = Core

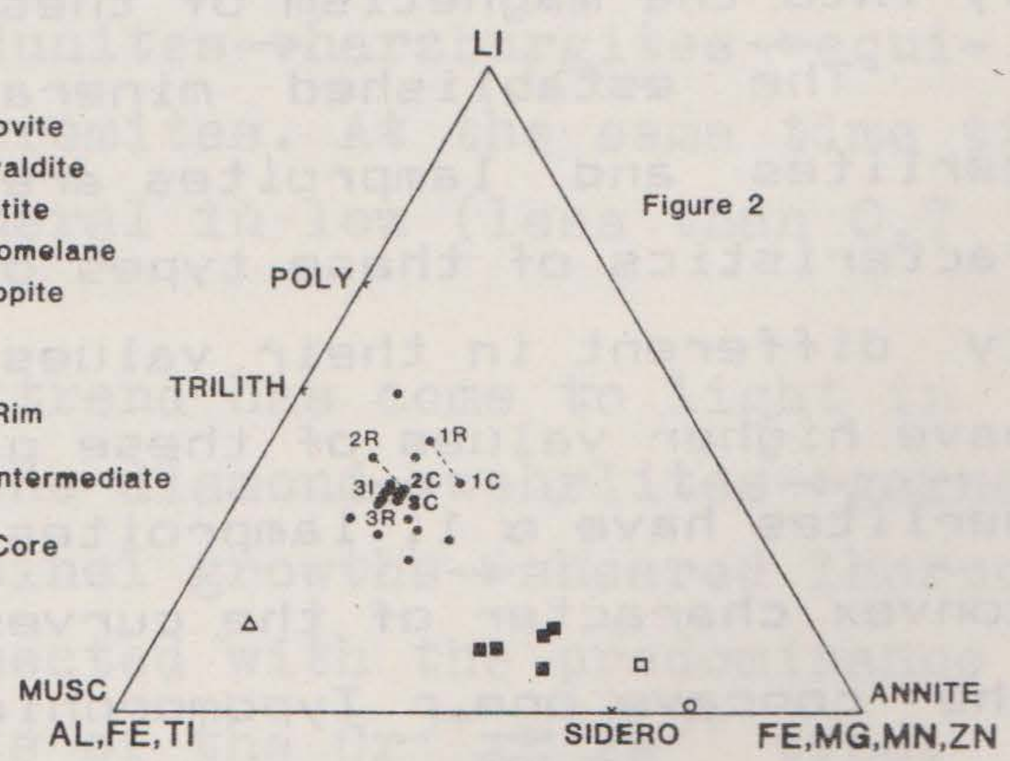

Figure 2

Dashed lines are tie lines between different zones.

MINERALOGY OF FERRIMAGNETIC OXIDES AND MAGNETIC PROPERTIES OF KIMBERLITES AND LAMPROITES

Garanin V.K. , Zhiljaeva V.A. , Kudrjavtseva G.P. ,
Mikhailichenko O.A. , Trukhin V.I.
Geological Faculty , Physical Faculty , M.S.U.,
Moscow, USSR

It has been established that the kimberlites are characterized by a wide range of similar minerals : Cr-Al-Ti - containing magnetite, Al-Ti - containing magnetite, titanomagnetite, magnomagnetite, maghemite, maghemite solid solution, magnetite, hematite.

The wide spreading of ilmenite which is ferrimagnetic under room temperature from the phenocrysts in kimberlite bodies attached to the central parts of cratons should be noted. The set of ferrimagnetic minerals in the groundmass of lamproites : magnetite, hematite, titanomagnetite. It has been discovered that the chrome-spinels from the deep rocks and Ti - containing chrome-spinels from kimberlite and lamproite rocks as well as phenocrysts of picroilmenite don't contribute essentially into the magnetism of these rocks.

The established mineralogical differences of kimberlites and lamproites are reflected in magnetic characteristics of these types of rocks. They are contrastly different in their values I_n and $\varkappa_o$ (kimberlites have higher values of these parameters), S_{ve}/S_{vo} (kimberlites have ≈ 1, lamproites $\geqslant 2$). Kimberlites have convex character of the curves I_s (T) and lamproites - the concave one. Typomorphic magnetic - mineralogical features of different types of alkali-ultrabasic rocks (kimberlites, lamproites, picrites and others) allow to sort out the bodies in accordance with their genetic characteristics and to predict ore bearing of these rocks on the basis of indirect magnetic - mineralogical investigation.

MINERALOGY OF SPINELS FROM KIMBERLITES AND LAMPROITES

V.K.Garanin, R.Kasimova, G.P.Kudryavtseva, O.A. Mikhajlichenko, Department of Geology,Moscow State University, Moscow,Lenin's Hills,II9899,USSR

On the basis of a great number of original and literary data a comparative analysis has been carried out, and the evolutionary trends of spinels from xenoliths of deep-seated rocks, from phenocrysts of these minerals and from microcrystals from the ground mass of kimberlite and lamproite rocks have been established as well. By making full use of personal computers and specially elaborated software it became possible to make the processing of analytical material highly informative and efficient.

The evolutionary trend of spinels of deep-xenoliths is connected with isomorphic replacements of isovalence character: $Cr^{3+} \rightleftarrows Al^{3+}$. The content of chromium decreases in spinels but aluminium increases when there occurs a transition in the series of inclusions in the diamond→diamondiferous dunites→harzburgites→equigranular lherzolites→alkremites. At the same time titanium content in the mineral in low (less than 0,7 wt.%).

A second evolutionary trend has come to light in the inclusion series in the diamond→wehrlites→garnet + clinopyroxene+ chromespinel growths→sheared lherzolites. This trend is connected with the predominance of isomorphic replacements of the $Cr^{3+} \rightleftarrows Fe^{3+}$ type. The peculiarity of the minerals of these rocks is a rather high to very high content of titanium.

These two trends are typical for phenocryst spinels from kimberlites and lamproites. The ratio of spinels in kimberlites and lamproites is different according to the evolutionary trends discovered. Spi-

nels with high titanium content belonging to the second evolutionary trend are widespread in lamproites.

Phase and chemical composition diversity of spinels from the ground mass of kimberlite and lamproite rocks has been established. The following trend of spinel crystallization has been discovered for kimberlites: Mg-Al-chromite with rather high content of titanium→Cr-titanomagnetite→titanomagnetite→magnosioferrite→magnetite. Spinel crystallization trend quite unlike that in kimberlites has been found for lamproite rocks but the diversity and variations of the spinel content are far less: Mg-Al-chromite with higher titanium content→Cr-titanomagnetite.

Problems concerning the genesis of spinels of the evolutionary trends found, their connection with diamond content, with the sources of deep matter and with the evolutionary conditions of kimberlite and lamproite magmas are being discussed .

1.15 R
Ro 1.55

PHASE RELATIONS IN THE PbS - Ag2S - Bi2S3 SYSTEM FROM THE Mo-W-Bi MINERALIZATION OF PERDA MAJORI, SE SARDINIA, ITALY.

C. Garbarino, G. Padalino, Istituto Giacimenti Minerari, Geofisica e Scienze Geologiche, Facoltà di Ingegneria, Piazza D'Armi - 09100 Cagliari.

M. Fiori, Centro Studi Geominerari e Mineralurgici C.N.R. Piazza D'Armi, 09100 Cagliari.

L. Maccioni, Dipartimento Scienze della Terra, Via Trentino,09100 Cagliari.

The Hercynian intrusive magmatism in Sardinia consists of a magmatic succession of basic to acid rocks. Two main intrusive phases (separated by a 10-15 m.y. time span) can be distinguished. A first phase, developed in a compressive regime,produced gabbrotonalitic to monzogranitic rocks, while the second phase was characterized by leucogranites produced in a tensive geostructural regime. These leucogranites differ from the preceding ones not only in age and chemical composition but also in the textural and structural features. These differences indicate that they derive

from a shallow level in the crust as a conseguence of the low water content of the original magmas.
Leucogranites are related to all metalliferous occurrences connected with the Hercynian batholith;molybdenite and pyrite represent the most widespread ore minerals in these occurrences.
Molybdenite may occur in quartz vein stockworks, in paints along joints, as fracture filling, in veinlets and associated disseminations, sometimes with hydrothermal alteration of the host rocks (argillic and phillic assemblages). Their major features are to be considered porphyry-style mineralization.
The mineralization of Perda Majori (Quirra, SE Sardinia, Italy) occurs in a quartz vein close to the same stock-like bodies of coarse leucogranites, that intrude a metamorphic sequence of Silurian age, made up of sandstones, black shales and limestones.
The Perda Majori vein, strictly associated to a NW - SE trending fracture system, consists of a main vein, which varies in width from a few centimetres to more than one metre. This vein was traced for almost 500 m along strike, and along several secondary veins mostly localized at the top of the main vein.
The most abundant primary ore minerals are wolframite, molybdenite, and pyrite with minor quantities of bismuthinite, native bismuth, sphalerite, galena, chalcopyrite and scheelite.
The non-metallic minerals are: quartz, feldspars, micas, calcite, fluorite and topaz. Late sericite occurs mainly as flakes on feldspar and topaz but it also fills fractures, forms veinlets, etc.
All ore minerals were investigated by means of electron microprobe (SEMQ-ARL). The analyses showed that the iron content in sphalerite is rather high (up to 5.6%), as are also the silver contents in galenas (up to 0.8%). Native bismuth and bismuthinite are usually intergrown whith molybdenite but can also be found dispersed in gangue.
Sulfbismuthides of silver and lead, in the form of solid solutions, were also observed. Moreover some phases are present in the PbS-Ag2S-Bi2S3 system: galenobismuthite and a solid solution fall in the lillianite - PbAgBi3S6 joint, close to PbAgBi3S6.
Presence of these phases are an indication of the temperature of the ore forming media, that fall into the pegmatitic to hydrothermal range.

PARAGENETIC ASSEMBLAGES OF ORE MINERALS IN AN ACID SULPHATE TYPE GOLD OCCURRENCE AT SERRENTI-FURTEI, SARDINIA, ITALY.

C. Garbarino, S.M. Grillo, F. Melis, S. Pretti, I. Uras, Istituto Giacimenti Minerari, Geofisica e Scienze Geologiche, Facoltà di

Ingegneria, Piazza D'Armi, 09100 Cagliari.
M. Fiori, Centro Studi Geominerari e Mineralurgici C.N.R. Piazza D'Armi, 09100 Cagliari.

The recently discovered gold occurrence of Serrenti-Furtei, in Sardinia, is the only acid sulphate type epithermal mineralization known in Italy so far. It occurs in Oligocene-Miocene andesites, belonging to a calc-alkaline volcanic cycle which interests wide areas in the western half of the island.
The ore occurrences are related to advanced argillic alteration phenomena which extend over an area of several square kilometres; these phenomena, in particular, originated extensive kaolin bodies which were exploited until recently.
The sulphide bodies consist of veins and lenses of chalcedonic and vuggy silica, the size of which is not yet known, even though their outcrops can easily be followed for several tens of metres.
As far as concerns the ore minerals, the samples examined up to now appear to belong to two paragenetic groups, which are also topographically separated.
The first group includes some outcrops located in the north-eastern part of the area. The paragenetic assemblage here observed includes enargite-luzonite, tennantite, pyrite, covellite and native gold. Given the disseminated distribution of the minerals, paragenetic relations among them are not well defined, as in similar occurrences in other parts of the world, except those between enargite-luzonite and tennantite.
The second group includes an outcrop located in the south-western part of the area. The paragenetic assemblage here observed, includes tetrahedrite, native tellurium, tellurides (sylvanite, hessite, stuetzite and altaite observed so far), pyrite, chalcopyrite and covellite. Here paragenetic relations are better observed, the most evident concerning those between tellurium and tellurides on one hand and tetrahedrite on the other, since they always occur in blebs, often polyphasic, inside the tetrahedrite, which, in turn, denotes high Te contents.
Thus the two groups appear well differentiated as far as concerns their mineralogical composition. However they also differ under the geochemical viewpoint. If As, Sb and Te are considered as characterizing the two paragenetic groups, one can easily see that:
- As is present in both assemblages, but is strongly enriched in the north-eastern group (enargite and tennantite), while it occurs as a minor element in tetrahedrite of the south-western group;
- Sb and Te characterize many minerals in the south-eastern group (Te bearing tetrahedrite, native tellurium and tellurides), while

they are confined to trace contents in the enargite and tennantite of the north-eastern outcrops.
The two groups show differences also as far as gold is concerned. In the north-eastern assemblage it occurs as native metal of extremely high fineness, while in the other group it appears to be confined to the tellurides.
Both the mineralogical and the geochemical characteristics of the two paragenetic groups denote differences that appear to represent various phases of ore deposition.
The north-eastern outcrops, characterized by the enargite-luzonite-tennantite association (i.e. As-dominated) might belong to a higher deposition level as compared to that of the mineralization of the south-western outcrop, where a Te-rich paragenetic assemblage predominates.
The occurrence of primary covellite in the north-eastern part might indicate a third distinct deposition phase.

HETEROELEMENTS IN CARBON MATTER FROM MINERALIZED ROCKS.

M.E.Generalov,M.I.Novgorodova, IGEM, Academy of sciences of the USSR, Moscow, Staromonetny 35,109017 USSR

Ps 1.4.

Disseminated carbon matter (CM) in mineralized terrigenous rocks from ore deposits and from eruptive breccia of pipelike bodies was investigated in connection with the problem of the role of carbon in endogenic ore formation.Structural and chemical peculiarities of CM were investigated by the complex ofdiffraction,microprobe, electron-microscopic methods,CHN-analysis.
Among the investigated CM kerite,anthraxolite varieties, differently ordered graphites were estimated.
The average thickness of graphitic packet varies from less than 10 Å for kerites,10-40 Å for anthraxolites, and more than 80 Å for graphites.
The contents of usual for natural CM heteroelements are (at.%): up to 2.5 N,12.5 O,16.5 S for kerites,up to 1.8 N, 8.0 O, 3.5 S for anthraxolites,lower 0.4 N,0.5 O, 0.1 S for graphites.
Microhardness of CM varies from 5 to 15 kG/mm^2 for graphites,10-60 for kerites,30-160 for anthraxolites.Many anthraxolites show high resilience.
Contents of main heteroelements is intimately connected with optical properties of CM: the lower contents of heteroelements (and H),the higher average reflectance coefficient,the more degree of anisotropism.CM with maximal contents of heteroelements are usually isotropic or slightly anisotropic, R is not more than 6%.
UR-spectrometric data show the presence of oxigen in

form of alcoholic,ketonic,carboxylic radicals in CM, bonds C-S,S-S are estimated too.
Increasing of anisotropism of physical properties,lowering of resilience of CM accompanied decreasing of contents of heteroelements (firstly,S) from anthraxolite to graphite point to these possible taking part in formation of 3-dimentional structure due to bridgelike bonds through S, O, N, between aromatic layers.Tearing such bonds and isolating aromatic nuclei in result of removing of heteroatomic radicals lead to additional entering of heteroatoms to mineralforming system.
Desulphurization of CM may be considered as one of the sources of S for precipitation of sulphides.

This process can be one of reasons to formation of disseminated,low ordered,sulphidizated varieties of CM.
In some CM there are also other elements ,the presence of which can not be explained by admixtures of mineral phases.
Among them there are Cl,determined in some CM from pipelike bodies of Maritime in amount up to 1 wt.%, F up to 1 wt.% in anthraxolite from Li-deposit of Uzbekistan, As,which is present in the quantity up to 0.2 wt.% (more than 1 % in microparticles)in the anthraxolite from aposcarn mica-carboniferous sulphidizated veins from the ore deposit of Maritime and P,which was observed together with Cl in CM,associated with stibnite,in veins of the gold deposit from Uzbekistan.

Po 1.5.

NATIVE METALS FROM PIPELIKE BODIES OF MARITIME.

M.E.Generalov,G.A.Tananayeva,V.V.Seredin,M.I.Novgorodova. IGEM, Academy of sciences of the USSR, Moscow, Staromonetny 35, 109017, USSR.

Within the fields of acid effusive rocks (K_2-Pg_2) of Maritime pipelike bodies of eruptive breccia with magmatic,partly recrystallized cement was investigated.
The breccia is composed from xenoliths of liparite, andesite-basalts,alevrolites,xenocrysts of quartz,feldspar.Magmatic association is partly replaced by black carboniferous quartz-mica aggregates,with mineralization which is similiar to described [1].
The most abundant metallic phases from these aggregates are iron-manganese alloys containing (wt.%) 11.8-15.2 Mn, 0.74-0.94 Si, 0.18-0.55 Cr, up to 0.2 Ni, impurities of Sn,Bi,Cu,Ti (general formula is Fe_5Mn-Fe_7Mn).
Acid treatment shows fine-fibrous, microfolded structures of metallic grains.In some of these grains disconnection in structure along microcracks was observed.
Elements of zoning were found in several comblike aggregates of metal.Around and inside the metallic grains

glassy,partly devitrificated reddish-broun material was found.The composition of glass is rather variable, it contains (wt.%): 59.7-72.2 SiO_2, 8.5-17.6 Al_2O_3, 4.7-10.0 FeO, 1.9-6.9 Na_2O, 1.3-7.2 K_2O, 0.1-0.5 CaO, impurities of Mn,Mg,Cu.
Ths grains of metal which are not preserved by glass are remarkably replaced by hydroxides,mainly by goethite, containing up to (wt.%) 3 Mn, 1 Si, 0.3 Cr. Metallic phases often contain isometric and platelike isolations of cohenite,orientated along (100) which are enriched in Mn and Cr ,contain less Fe and Si as compared with the metallic matrix.The size of metallic grains is 0.01-3 mm,grains of carbide are not more than 0.05 mm.
Connected with carboniferous quarts-mica aggregates there are also Cu-Zn alloys, metallic Cu, Pb, Sn.
Isolations of alloy with formula $Cu_{0.62}Zn_{0.38}$ were observed around the grains of quartz, in sericite aggregates, in the form of plates in the grain of biotite. Some grains form intergrows with native copper, containing up to 2.5 wt.% Zn.

Copper was found also as individual isolations with the size up to 0.5 mm.Besides Zn the copper contains impurities of Pb, Sn, Fe, Ni, Si, Al, Ca, Ba.
The counted size of an elementary cell of Cu-Zn alloy is a_o- 3.691±0.002 Å, and the one for Cu is 3.613±0.001 A,both belong to Fm3m space group.
Pb (cell Fm3m, a_o- 4.944±0.001 Å) and Sn (cell $I4_1/amd$, a_o- 5.82±0.01 Å, c_o- 3.20±0.01 Å) form fine-grained evtectoidal aggregates of platelike,spheroidal shape, which point to its melted state during precipitation.
Other minerals, connected with quartz-mica carboniferous association are oxides of Ti,for example,ilmenite, enriched in Mn (up to 14.1 wt.%),with impurities of Al, Zn,V,Sn,Cu,Cr, zircon with impurities of Hf,Mn,Bi,Ti, Al,Fe,Mg, REE-containing apatite. More rare is the association of sulphides of Fe,Zn,Cu,Pb, with native silver.
The received results can prove hypothesis of transportation of ore elements as well as alkaline and some uncoherent ones with carbon [2,3] .Mineral composition of the association of early metasomatic stage shows the transportation of ore elements in composition of high-temperature fluid, enriched in carbon, at the last stage of explosive activity.

REFERENCES

1 I.N.Tomson and oth. Graphite-ilmenite-sulphidic mineralisation in ore regions of the East of the USSR, Geol.of ore deposits, v.26, N 6, 1984
2 M.I.Novgorodova Native metals in hydrothermal ores. M.,Nauka, 1983
3 E.Y.Buslayeva,M.I.Novgorodova Elementoorganic compo-

unds in problem of migration of ore matter. M., Nauka, 1989

THE X-RAY LUMINESCENCE OF THE NATURAL FLUORITE: RECOGNISING AND ESTIMATING OF ITS CONCENTRATION IN ROCK AND VEIN MINERALS

Yu.V.Glukhov, V.P.Lutoev, T.N.Bushenyova
Institute of Geology, Komi Scientific Centre,
Ural Division, USSR Academy of Sciences,
Oplesnina 2, 167610, Syktyvkar, USSR

We have investigated fluorite from various locatypes of one of the Pai-Khoy's (behiend nothern part of Ural system) deposits. The research is made up by the X-ray luminescence method in spectra range between 230-800 nm. Nearly 400 probes are objected to analysis. After the statistic processing has been made we found that the line intensities of non-admixture fluorite Vk-center (295 nm) /1/ is approximatly constant (variation - 20%). Moreover, its radiation intensity is 2-3 range higher that others, such as Dy^{3+}, Tb^{3+}, Sm^{3+}, Eu^{3+}, Er^{3+} and Gd^{3+} lines. There is no vein mineral of this deposit which has its own luminescence in ultraviolet field.

The radiation line 295 nm has been recognised in every lithological variaty of rocks and vein minerals. Its average intensity value is equel to 1.3, 18.5 and 4733 a.u. in tuffs, limestones and ores, correspondently. Depending on the rock average meaning of vein calsites is equel to 0.9, 9.3, 108 a.u.

Thus, this method may be used for testing unvisible fluorite in rock and minerals. To estimate the quantity of fluorite it is necessary to use graduated graph for its artificial mixture with rock or mineral. The geochemical methods (for example fluorine-analysis) can be useful for determination prospects of fluorite. Our method shoud over is direct and can compete with the latter. Fluorine anomalies may be created by others minerals-concentrators (F-apatit, mica and others), the method can provide their selection. Fig. 1 demonstrates the example of application of X-ray luminescence for fluorite mapping. The distribution of fluorite in calsite probes is showed. The tendency of increasing of the fluorite concentration (intensity of the luminescence lines) toward the ore bodies is marked.

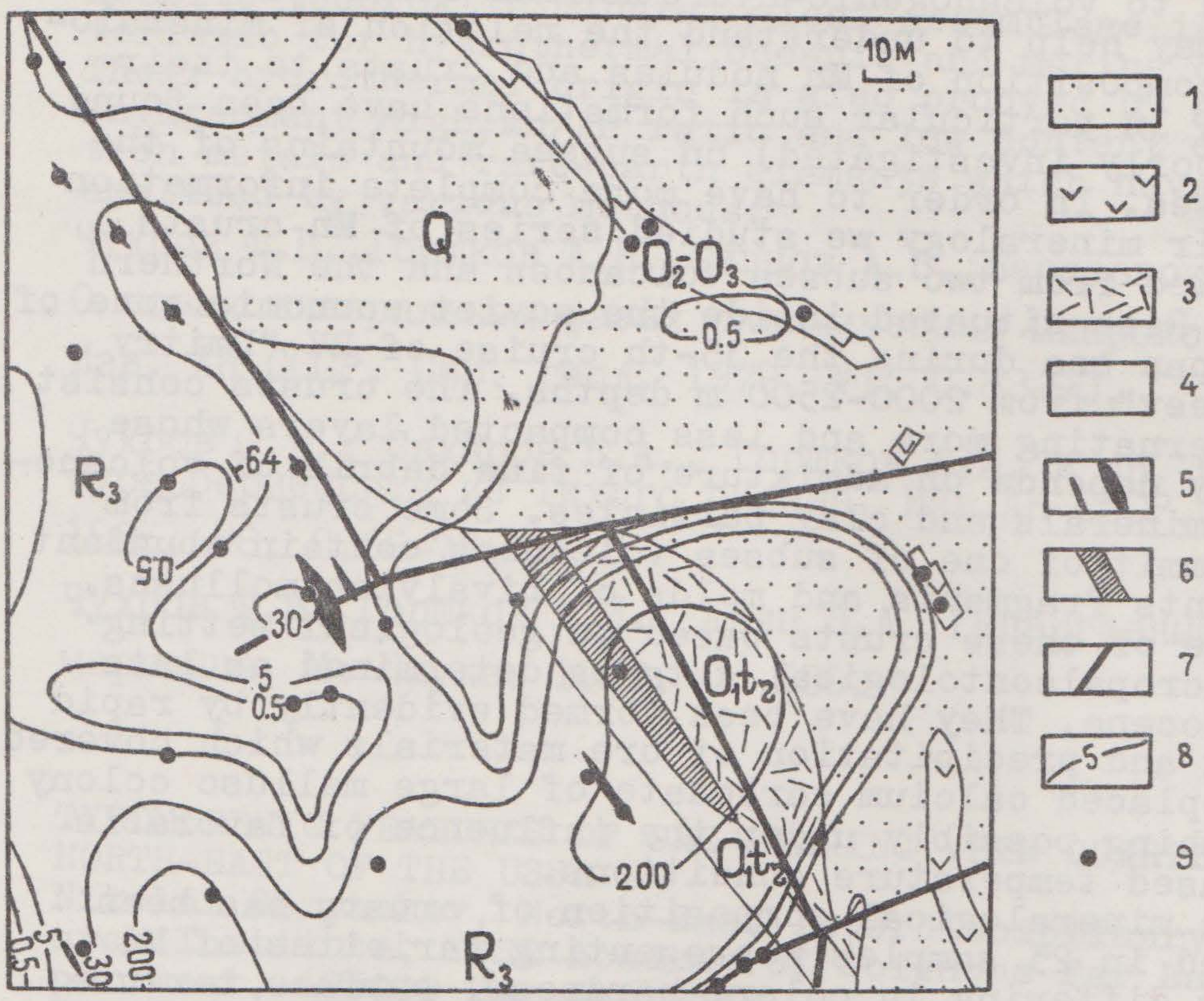

Fig.1 The distribution of X-ray luminescence intensity for calsite probes of the deposit part. The numbers of the marks: 1 - loose covers; 2 - tuffs with diabase-porfirites; 3 - tuffs; 4 - limestones; 5 - ore bodies; 6 - whethered ore zone; 7 - faults; 8 - trends of the luminescence intensity; 9 - analysed points.

Reference

1. O.A.Krasilschikova, A.N.Taraschan, A.N.Platonov. The colour and luminescence of natural fluorite. - Kiev:"Naukova Dumka", 1986, 224 p., - in Russian

MINERALOGICAL COMPOSITION AND ORIGIN OF MANGANESE CRUSTS FROM THE JAPAN SEA

Gorshkov A.I., Berezovskaya V.V., Baturin G.N., Sivtsov A.V. IGEM, Academy of Sciences of the USSR, Moscow, Staromonetny 35, 109 017, USSR

The mineralogical composition of iron-manganese formations from the sea floor appears now to be much more complex than it seemed before. In particular, a number of new mineral species has been identified in them (Chukhrov et al.,1979, 1989). Now the special attention

is paid to volcanogenic-hydrothermal formations whose study may help to understand the relation of mineralogical composition of Mn nodules and crusts to their origin. In particular such formations have been found (but poorly investigated) on subsea mountains of the Japan sea. In order to have more complete information on their mineralogy we studied series of Mn crusts collected from two subsea volcanoes and the Northern Jamato Rise situated inside the soviet economic zone of the Japan sea during the 35-th cruise of RV "Dmitry Mendeleev" from 2000-2500 m depths. The crusts consist of alternating more and less compacted layers whose density depends on admixture of fine debris of volcanogenic minerals and clay particles. Some crusts from the summit of one of subsea volcanoes contain abundant fragments fragments and molds of bivalvian molluscs. The age of these crusts based on geological setting and micropaleontological data is determined as late Pleistocene. They have been formed evidently by rapid influx and precipitation of ore materials which covered and replaced calcium carbonate of large mallusc colony florishing possibly under the influence of favorable increased temperature conditions.

The mineralogical composition of crusts has been studied in 25 samples representing varieties of Mn oxides differing in color, hardness, surface texture and structure. Under binocular these oxides look as rather monotonous loose fine-grained brounish to silver-gray mass with botryoidal texture dissicated by fissures filled with vug material.

These samples have been studied under transmission electron microscope JEM-100 equipped with energodispersive KEVEX-5100 set. All samples include assemblage of bernessite-like minerals including ordinary 7 Å-bernessite, 14 Å-Ca-bernessite, and clynobernessite. The latter is always represented by twins which are often intergrown with 14 Å-Ca-bernessite. It is known that the ordinary bernessite consists of 7 Å layers with disordered locations of vacant octahedrons and associated interlayer cations (Chukhrov et al., 1985), wheras 14 Å-Ca-bernessite and clynobernessite are characterised by ordered locations of vacant octahedrons (Chukhrov et al., 1985, 1989). It is possible that the latter two minerals are products of diffusive alteration of 7 Å-bernessite leading to ordering of cations and empty octahedroms in the layers of its structure. In some samples todorokite with a=9,75 Å was found. Occasionally bernessite includes some finely dispersed particles of vernadite which contains no iron contrast to hydrogenous crusts and nodules. It is supposed that this mineral has been developed by microbiologically induced substitution of bernessite. The described ber-

nessite-todorokite mineralogical assemblage is characteristic for hydrothermal oceanic and marine ore crusts. Their hydrothermal origin is also prooved by geologic environment high, Mn/Fe ratio and low content of transition metals and rare-earth elements which have been analized by various methods.

Чухров Ф.В., Горшков А.И., Сивцов А.В., Березовская В.В. О новых минеральных фазах океанических микроконкреций. Изв. АН СССР. Сер. геол. 1979. №1. С.83-90.

Чухров Ф.В., Сахаров Б.А., Горшков А.И. и др. О структуре бернессита из Тихого океана. Изв.АН СССР.Сер.геол. 1985. №8. С.66-73.

Чухров Ф.В., Горшков А.И., Дриц В.А. Гипергенные окислы марганца. М: Наука. 1989. С. 350.

TYPOMORPHIC FEATURES OF ORE-BEARING VEIN QUARTZ IN THE NORTH-EAST OF THE USSR

Nikolai Goryachev, North-East Interdisciplinary Research Institute, USSR Academy of Sciences Far East Department, 685000 Magadan USSR

Ps. I.G.

The occurrences of vein quartz evident from gold and tin deposits in the North-East of the USSR have been studied with mineral typomorphism in view as reflecting the genesis of minerals in their composition and properties.

Such facts as considerable admixtures of aluminium not participating in the lattice construction, non-perfect crystal structure, double-humped curves in thermoluminescence graphs, standard parameters of the lattice cell and textural-structural distinctions of quartz in gold ore deposits evidence to its crystallization in highly silica-concentrated polymer solutions at T=420° to 220° and P=0,8kbar to 1,5kbar (according to the analysis of fluid inclusion).

Quartz in near-surface deposits is characterized by high concentrations of lithium and aluminium, low sodium-to-lithium ratio, anomalous volume of the elementary cell (0,113nm and more), non-perfect crystal structure.

Different quartz thermoluminescence and grades of perfectness of the crystal structure in ore bodies and deposits reflect the cryptozonality of mineralization which is different in various types of deposits. It finds its expression in reduction of thermoluminescence intensity at depth in gold-quartz deposits and in increase of thermoluminescence intensity and perfect-

ness of the crystal structure at depth in cassiterite-quartz deposits.
Quartz from gold ore deposits is characterized by single- or double-humped thermoluminescence graphs, whereas in tin ore deposits these are double- or three-humped. There are also differences in sets of impurity elements and levels of their concentration.

MINERALOGICAL AND TYPOMORPHIC CHARACTERISTICS OF XIKUANGSHAN ANTIMONY DEPOSIT, HUNAN PROVINCE, CHINA

He Mingyue, Wang Pu, Chen Daizhang, Teaching and Research Section of Mineralogy, China University of Geosciences, Beijing 100083, People's Republic of China

Xikuangshan is the well–known antimony deposit which has the largest reserves in the world. The deposit is situated at the north of the central Hunan antimony metallogenic belt which is the most important antimony belt in China, and at the compounding of structural systems of the Neocathaysian and Qiyang Epsilon. After researching the minerals especially the quartz and stibnite occured in the antimony deposit, we have obtained several conclusions mentioned below.

The minerals occured in the antimony deposit formed in five stages, from early to late, they are (1) early silicification stage (quartz(I) and pyrite formed), (2) quartz(II)–stibnite(I) stage, (3) quartz(III)–barite–stibnite(II) stage, (4) calcite(I)– stibnite(III), (5) late residual hydrothermal stage (calcite(II), gypsum, kaolinite, gibbsite, gearksutite and creedite formed). The most important industrial ore is the quartz(II)– stibnite(I) associated type which formed in the main mineralization stage.

To contrast with the quartz(I) unconnected with mineralization, the quartz(II,III) associated with the stibnite has the below characteristics which can be considered as prospecting typomorphic characteristics: euhedral degree of crystal forms is higher; content of impurities is lower such as elements of Al,Fe,Ti, Mg,Ca,Na,Li,Pb,Zn,Sr,Ba,Cr but Cu; content of each rare elements and total content of all rare elements ($\sum$ REE) is lower; the ratio of La to Yb also is smaller; the crystal lattice constants is smaller and the crystal internal structural perfection–crystallinity index is higher; the total absorption intensities of three absorption bands near 800cm^{-1}, 695cm^{-1}, 475cm^{-1}in its infrared spectra is larger; the infrared light relative densities (D_{CO_2} ,D_{H_2O}) of $CO_2$and H_2O occured in its inclusions is smaller and so is the ratio of D_{H_2O} to D_{CO_2} ; the intensity of the thermoluminescence varies regularly with the space of its occurrence, and it increases gradually from the margin to the center of ore body. Nevertheless, the quartz(I) has no or contrary characteristics mentioned above.

The forms of pyramidal faces of the stibnite crystals are very simple,they are only the common simple forms such as rhombic dipyramid e{121} and τ{341} which their faces

wholly appear. Although the forms of prismatic faces are complex and have some of high crystal indices, yet the appeared faces are mainly common simple forms such as rhombic prism m{110}, n{210} and pinacoid b{010}, and the faces of other forms especially the high crystal indices appear in the narrow prismatic planes or disappeared. Thus, these characteristics of forms show that the growing period paralleled with c axis is longer than that paralleled a and b axes, the crystal growth tends finally to the perfect crystal forms. The main content (S and Sb) of the stibnite(I) formed in the first generation closes to the theo retical values, but the stibnite(II,III) formed in the second and third generations has a large loss value of S. The content of impurities in the stibnite such as As and Fe which affect the quality of ores increases with its formed from early to late, so the quality of quartz–stibnite(I), quartz–barite–stibnite(II) and calcite–stibnite associated types is respectively the highest, the second and the worst in this deposit. From early to late generations, the crystal lattice constants of the stibnite gradually increase, which have positive correlation with the content of As that replaces Sb atoms in the internal structure in the way of isomorphous replacement. The reflection factors R_g, $R_m$and $R_p$are very different from each other, but all of them are monotonously decreasing with the increasing of wavelength. The anisotropic rotation angle $A_{g-p}$is the maximum which monotonously decrease with the increasing of wavelength and the values of $A_{g-m}$and $A_{m-p}$are approximate similar, but the former dereases and the latter rises and falls slightly with the increasing of wavelength. Positive and negative characters belong respectively to the shortwave bands (smaller than 589nm) and longwave bands.

The pyrite connected with silicification and mineralization has the characteristic of higher contents of impurities such as Sb, As and Ba, larger crystal lattice constants and greater positive coefficients of the thermoelectricity (called "P" type). But the pyrite occured in layers of sedimentary carbonate rocks has lower content of trace elements, smaller lattice constants and smaller negative coefficients of the thermoelectricity (called "N" type).

SCANNING ELECTRON MICROSCOPE (SEM) ANALYSIS FOR THE COMPOSITION ZONING OF THE MAGNO-FERROMICAS IN PRE-CAMBRIAN REGIONAL METAMORPHIC AREAS, EAST HEBEI, CHINA. 1.19V

He Yixing, Wang Derong, Liu Fulai, Yao Jie and Cao Lin,
Electron Microscope Lab., Changchun University of Earth Sciences, People's Republic of China.

Some research workers and the author have discussed systemally the influence of metamorphism on the chemical composition (on the basis of bulk chemical analysis) of magno-ferromicas in regional

metamorphic areas, East Hebei.

This study carry into effect the observation of the micromorphological features and a lot of the microarea composition quantitative analysis in accordance with the multi-points method (the distance between points is 3μm, between lines is 10μm) on the magnoferromica grain using SEM (JEM-2000FX) with EDS (TN-5500).

The SEM analysis shows the component elements, Mg/(Mg+Fe) , Mg, Fe , Al^{IV}, k and Si , of the mica , display a complex zoning in arrangement of higher alternating and lower content from the core to margin in the grain. In a grain, there are at most eight tiny-zones. The status of the corresponding zones of the individual element don't coincide strictly, but their content variation tendency along a line of section from the core to margin of a grain correspond with each other. The content tendency is a positive relationship between Mg, Ti, K and Mg/(Mg+Fe) respectively, and a negative relationship between Fe, Si and Mg/(Mg+Fe).

According to the composition characteristic of the micas studied, we sum up two types: ①unaltered zoning mica, including a core, four higher and four lower zones in content for component elements without alteration, only observing the late-stage magno-ferromica (Fe-rich) veins cut into their host rock. It indicate that the type of mica was underwent at least four thermal events from which there is a little different temperature.They are higher mineralforming temperature and the grade of thermal events(700～800℃, belong to the granulitic facies) . e . g. Shuichang mining area. ②Altered zoning mica, meeting a core, four higher and four lower zones in content for every component element. Along some of clevages in the mica and the intergrain boundary around it's grain,there are K-feldspar veins cut into and slight replaced them,and there are also partial chloritization from the mica . This K-replacement is perhaps a evidence of the later thermal event. For this type of mica, the mineral-forming temperature and the grade of the thermal events is lower (500～650℃, belong to the amphibolitic facies) . e.g. Xingshang mining area.

Above conclusion supports the result of the times and grade of the metamorphic events from field investigation. So, SEM, a useful technique, quickly provides more and more reliable mineral genetic in-

formation which is difficult to obtain by other methods such as optical microscope, even WDS etc.

TYPOMORPHIC CHARACTERISTICS OF MAJOR MINERALS AND THEIR APPLICATIDN IN EXPLORATION OF DONGCHUANG A_u–P_b DEPOSIT, XIAOQINLING MT., WEST HENAN, CHINA

1.33H

He ZhiLi, Yang Zhenlin and Xu Jiuhua, Department of Geology, Beijing University of Science and Technology, Beijing 100083, People's Republic of China.

Located in the middle of the famous Xiaoqinling Gold Belt, Dongchuang A_u– P_b deposit was composed of a series of parallel ore–bearing quartz veins hosted in the Archean Taihua Group and controlled by E – W faults. A late Yanshanian Wenyu granitic mass is just 2.5 km north of the deposit. Alterations are dominated by Pyritization, seritization, silification, carbonatization and chloritization.

Hydrothermal mineralization was divided into 4 stages:

Ⅰ: pyrite–quartz;

Ⅱ: quartz–pyrite;

Ⅲ: carbonate–polymetallic sulphide;

Ⅳ: carbonate–quartz.

Stage Ⅱ and Ⅲ are major gold mineralization stages; stage Ⅰ and Ⅳ are minor gold mineralization stages. Native gold and electrum are main gold minerals. Many typomorphic characteristics of major gold mineralization stage minerals are different from those of minor gold mineralization minerals.Followings are major conclusions:

1.Generally, the quartz is milky or greyish massive, it contains plentiful large fluid inclusions, most of which are CO_2 inclusions. For the most part of infrared waves, stage Ⅱ and Ⅲ quartz has stronger absorbtion than stage Ⅰ and Ⅳ quartz. Fluid inclusion homogenization temperature (Th) suggest a characteristic Th range for the major gold mineralization stages with preferred values of 200℃ – 260℃. Decrepition analysis of fluid indusion indicates that the ratio ranges of CO_2 / H_2O and N_a^+ / K^+ in stage Ⅱ and Ⅲ quartz are 0.30 – 0.58 and 7.05 – 9.05 respectively, while the ratio ranges of CO_2 / H_2O and N_a^+ / K^+ in stage Ⅰ and Ⅳ quartz are 0.02 – 0.34and 5.81 respectively. Decrepition activity of gold rich quartz is stronger than that of gold poor quartz in the same stage.

2. The pyrite is dominated by semi–euhedral and euhedral cubic. The characteristics of gold rich pyrite are fine, irregular, crushed and cemented by other minerals. Analysis of minor elements shows that A_u, A_g, C_d, M_n, C_r, A_s and S_b content of stage Ⅱ and Ⅲ pyrite is higher than that of stage Ⅰ and Ⅳ pyrite, but the former's C_o / N_i ratio is lower than the latter's.

Thermal electrical study shows that the average thermal electrical coefficient ($\bar{\alpha}$) of pyrite in barren Wenyu granitic mass is −183.2μv / ℃. The $\bar{\alpha}$ of pyrite in stage Ⅱ and Ⅲ is −147.2 μv / ℃, while the $\bar{\alpha}$ of pyrite in stage Ⅰ and Ⅳ is −153.7 μv / ℃.

3. The massive apperance of chalcopyrite in quartz veins indicates the intense mineralization of stage Ⅲ, so chalcopyrite is an indirect gold indicator. Analysis of chalcopyrite shows that the S_e content is higher, while Au and Ag content is lower, $C_o / N_i = 1$.

4. The galena is dominated by semi–euhedral or euhedral. Analysis suggests that the fine crushed gelena contains more gold than the coarse eudedral one does. Gold rich galena's A_g. C_d. T_i and C_r content is higher than gold poor one's. In the same stage Ⅲ, the coarse euhedral gold–poor galena's average thermal electrical coefficient ($\bar{\alpha}$) is −294.7 μv / ℃, the fine crushed gold–rich galena's $\bar{\alpha}$ is −228.3 μv / ℃, but the $\bar{\alpha}$ in stage Ⅳ galena is only −408 μv / ℃.

The above conclusions are very useful criteria in exploration. With the help of Th thermal halo, CO_2 / H_2O, CH_4 / H_2O, CH_4 / CO_2, A_g / P_b, A_g / A_u, A_u / M_o, C_u / Z_n isoline maps and trend surface analysis of gold values, a large blind ore body was discovered by pitting.

1.25H

RESEARCH ON PROSPECTING MINERALOGY OF ARSENOPYRITE IN THE QIQIU GOLD DEPOSIT NO.1, XIJIANG, CHINA

Hu Daqian, Changchun College of Geology, Changchun, Jilin 130061, People's Republic of China

The Qiqiu gold deposit No.1 is located in the conjoining part of Anqi fault and Baobei–Qiqiu fault within the Hercynian geosynclinal folded belt, Western Junggar, XiJiang. The stratigraphy comprises the upper–middle Carboniferous Tailegula Formation and Baogutu Formation, which are characterized petralogically by lightly metamorphosed basalts, diabases,silicalites and tuffes. The ore bodies, extending along NW, NE and NNE, occur in the forms of veins and lenses, and strictly controlled by fractures. The ore minerals mainly consist of native gold, pyrite, arsenopyrite, and the gangue minerals are quartz and calcite.

Arsenopyrite is one of the major gold–bearing minerals, either euhedral or subeuhedral, and takes the form of rhombus short or slender column and transect twin of two or more short column crystals. Crystal measurement reveals that rhombus short column is the combined forms of {110} with {012}, {013} or {016}, while the slender column is only form of {110}, whose C axis is marked by fracture.

There are two kinds of arsenopyrites formed during two mineralization stage in the study area. The early generation is marked by rhombus short column or twins, and the later one by slender column. Electron microprobe analysis shows that the early generation exhibits enrichment of S. Se. Te. Sb. Pb. Zn and Ag, while the later one is relatively enriched in Fe, As, Au, W, Bi, and Mo.

Apart from the Au content in arsenopyrites, the Fe / (S+As) > 0.5(atom num-

ber), and As / Sb > 1000 are also considered as indication of Au bearing.

The microhardness of arsenopyrites with different form vary within 833–1135.5 kg / mm^2 in the study area. The first generation is Characterized by microhardness larger than 1000kg / mm^2, and the later one is usually smalier than 950 kg / mm^2. The main reason for this is the enrichment of Fe and lack of negative ions, which may result in the decrease of the covalent bonding. The large amount of Au in inclusion fractures may also contribute to such feature.

The arsenopyrite is an electronic centre type of semiconductor. This is due to that [AsS] need to catch one more electron than [S_2] to reach the stable state, which means a relatively excess of positive charge in the crystal. These extra positive charge have the tendency to absorb nearby negative charge, resulting in the electronic centre type of semiconductor. The thermoelectric coefficients (α) of the arsenopyrite show perfect zonation in the mine. For example, in the quartz veins it has α value larger than −140.00; in alteration zone it is range of −140.00 — −110.00; and within the host rocks it is usually less than −110.00. The α value of arsenopyrite, however show small variation in space within the ore bodies which shows no apparent rule.

The grain size of arsenopyrite bear some effects on a value. In general, if the grain size is increased by a factor of two, the a value could be increased by about 20% . These is also a tendency within the same size grade, that is, the larger the α value is, the higher the gold content is.

TYPOMORPHIC CHARACTERISTICS OF THE MINERALS IN ZHANG– JIAKOU–XUANHUA GOLD DEPOSITS IN CHINA

HU Xiaodie, Zhao Jianong, Li Shuangbao, Tianjin Institute of Geology and Mineral Resources, Tianjin 300170, People's Republic of China

There are more than 20 minerals in gold–bearing quartz veins in Zhangjiakou–Xuanhua gold area. The typomorphic features of pyrite, galena, chalcopyrite, quartz, potash feldspar and native gold are discussed in this paper involving typomorphism of morphology, composition, texture and physico–optical characteristics which have great geological and geochemical significances in studying gold mineralization, and genesis of gold deposits. Only some typomorphic features are mentioned as follows.

The morphology, glanularity and crushing degree of pyrite have a great influence upon the Au content in it. Pyrite with fine allotriomorphic granular structure is in company with intensive crushed pronounced enrichments of Au. The chemical composition of pyrite, especially Au, Ag, Co, Ni, Se, Te and As have typomorphic significance. The Au / Ag, Co / Ni, Se / Te, and S / Se ratios of pyrite are obviously different from those of pyrite from post magmatic hydrothermal gold deposits. Calculated unit cell parameters of gold–bearing pyrite reveal that Au does not enter its crystal lattice. Gold usually filled in cleavages and fractures of pyrite.

The deformation of quartz was very intensive. Uniaxial crystal can be changed into biaxial; the banded wavy extinction was appeared; the inclu-

sions in quartz were changed into elongated, thinner and separated each other; quartz was intensively crushed. Quartz contains difinite amounts of Al, Na, K and Li which have influence on the increasing of the Au content. The temperature, pressure, salinity and composition of inclusions in quartz indicate the characters of ore–forming fluid and the physico–chemical conditions of formation of gold deposits. Characters of hydrogen and oxygen isotopes of quartz indicate that the ore–forming medium was typical metamorphic water with some meteoric water.

On the basis of the main typomorphic features of all six species of minerals, genetic type of the gold bearing quartz veins might be inferred to the metamor phous hydrothermal ore deposits.

ON GEOLOGICAL IMPORTANCE OF THE TYPES OF SULFOSALT MINERAL ASSEMBLAGE

HUANG Minzhi, Institute of Mineral Deposits, Chinese Academy of Geological Sciences, Beijing 100037, People's Republic of China

It is proved that there is internal relation between the sulfosalt mineral assemblage (SMA) type and the mineralization condition, on the basis of the initial study of some deposits abundant in sulfosalt minerals in the Nanling arae of China. Revealing the relation is of guiding importance for the study of deposits theory and practice of seeking for deposits.

1. There is a definite evolution regularity of SMA in the process of deposits forming . In the later period of the forming of deposit, Lots of characteristic sulfosalt minerals occur in Dachang Sn–multimetal deposit(Guangxi). The minerals that deposited first from the solution are jamesonite, boulangerite and zinkenite which represent the simple Pb, Sn–SMA. Since the metasomatic reaction occurred btween the solution and the early crystalizing minerals, subsequently the franckeite, stannite, rhoclestannite and herzenbergite assemblage rich in Sn, was formed, followed successively by owyheeite, andorite, dadsonite, ramdohrite, miargyrite, Ag–tetrahedrite, freibergite, keobellite, tintinaite, lillianite, galenobismutite, matildite and pavonite assemblage which are known as Sb, Bi–minerals containing Pb, Ag, and Cu, and grecronite, heteromophite, plagionite and bournonite assemblage rich in Pb and Sb, finally benaviaisite, fuloppite and stibnite assemblage rich in Mn and Sb. It shows that the mineralizing solusion is rich in Pb, Sn, Ag, Sb and Bi showing an evolution from mineral rich in Pb to that rich in Sb at the later stage of ore formation. Furthermore, the space distribution of ores indicate that the upper part is characterized by the simple Pb, Sb–SMA, and the lower by a complex SMA resulting from metasomatic reactions.

2. SMA varies regularly relative to zonation of ore deposits both in orefield and mineralization belt. In Dachang orefield, as well as in Danchi mineralization belt where the Dachang ore deposit is located, the SMA in various deposits have distributed in zonation around the center of magmatic activity. Sideward from the rock body, the zoned mineralization is in order: (a) Sn–bearing skarn Zn, Cu–deposit where the Pb, Bi–SMA predominates; (b) high–median temprature

cassiterite sulphide deposit where predominates Sb, Bi–SMA Containing Pb, Sn, Ag; (c) median–low temprature W, Sb–multimetal deposit where predominates Pb, Sb–SMA;(d) median–low temperature Sb, As–multimetal deposit in Wuxu located on the outer side of the Danchi mineralization belt where predominates As, Sb–SMA containing Pb which is characterized by As–bearing playfairite and sterryite, Sb–strtorite, dufrenoysite, semseyite, jamesonite and boulangerite. According to the characteristics of sulfosalts devoloped and then ralative contents in varied deposits, some typical formulas of composition of the minerals are generalized showing the dostribution of the SMA from the rock body to the outside of the orefield and the mineralization belt: (a) [Pb(Ag, Cu)]x[Sb(Bi)]ySz→(b) [Pb, Sn(Ag, Cu)]x[Sb(Bi)]ySz→(C) [Pb(Ag)]xSbySz→(d) Pbx[As,Sb]ySz.

3. The SMA is different in differnt types of deposits. For example, the Dachang Sn–multimetal deposit is related to acid rocks, where the Sb, Bi–SMA containing Pb, Sn and Ag includes mainly franckeite and jamesonite, and its typical formula of composition is [Pb,Sn(Ag,Cu)]x[Sb,Bi]ySz; the Cu, Mo and Bi–multimetal deposit in Baoshan, Hunan, is related to intermediate acid rock, where Bi, Sb–SMA chara teristic of Cu, Pb includes lillianite, heyrovskyite, gladite, cosalite, bursaite, galenobismutite, wittichenite, emplectite, nuffieldiite, junoite, aikinite, jamesonite and boulangerite, and its typical formula of composition is [Pb,Cu]x[Bi,Sb]ySz.

Fact shows that there are certain evolution and distribution regularities for SMA both in time and space. The SMA can give not only information on physical–chemical conditions of deposit forming, but also important indications for dividing deposit into belts and for seeking for blind orebodies.

MINERALOGY OF ARCTIC ZONE OF WEATHERING OF PHOSPHORITE-BEARING ROCKS

Ievlev A.A., Institute of Geology, Komi Scientific Centre, Ural Division, USSR Academy of Sciences, 24 Kommunisticheskaya St., 167610, Syktyvkar, USSR

The regions of arctic climate where the periods of positive temperature are short, where the most of atmospheric precipitations falls in solid phase, where the permafrost has a broad spreading are traditionally assumed as rather inert to weathering. The role of physical destruction of rocks at the expense of frosty weathering is recognized, but it is stated that the zone of chemical remake of rocks is absent or shown very weakly.

But then, there is the information about proceeding of intensive rock-remaking processes in permafrost zone. At present the complex of physico-chemical weathering processes at freezing, melting and fluctuation of negative temperature of rocks is unified by term cryogenesis or cryohypergenesis. The characteristic features of such processes are: (i) prevalence of physical denudation, (ii) slowdown of chemical and biological

processes, (iii) primitive diageneous processes thanks to the low temperature of environment which causes the good safety of poor stable mineral products of weathering.

For the last years we study the arctic weathering zone of phosphorite-bearing black shales of Pai-Khoy mountain range (USSR). Phosphorite-bearing rocks are typical for the lower-Visean sediments of shale zone of Pai-Khoy. Such rocks contain numerous spherical-flattened concretions. The chemical study of concretion composition showed that predominate component was apatite-like three-calcium phosphate, besides that the fine-crystallized chalcedony, fine-dispersed organic matter and calcite got into their composition. X-ray study of concretions revealed the next crystalline phases: fluorapatite, quartz, feldspar and fluorite. Our study of different products of weathering allows to restore the motion of weathering processes.

Primarily the formation of altered porous rocks on black shales substratum takes place. The next processes take place: (i) pyrite, carbonate and clay material are destroyed and products of decomposition are carried out, (ii) quartz framework of rock and organic matter remain unaltered.

Then the disintegration of altered porous rock occurs with the formation of scrap material right up to fine-dispersed mass. Mineral solutions carrying out the products of black shales decomposition give rise to abundant and various sulfate mineralization which is present by both crystal and amorphous material. Leaked X-ray amorphous aggregates (stalactites, stalagmites and saline crusts) appear at slow penetration of mineral solutions through the layer of disintegrated rock and gradual deposition of dissolved matter. Rozenite and halotrichite arise thanks to the air drying of such aggregates. Crystal sulfates (jarosite, melanterite, rozenite, halotrichite, copiapite, coquimbite) form thin surface sediments (crusts, fillings of cracks and hollows in the rock). Rozenite appears as a result of natural dehydration of melanterite. The next sequence of mineral arising is discovered in copiapite-coquimbite aggregates: primarily the more water-bearing mineral (copiapite), then less water-bearing one (coquimbite). Gypsum appears as a result of interaction between sulfate solutions and calcite.

Phosphate component is registrated in chemical composition of all sulfate products of weathering. Diadochite and highly-concentrated viscous hydrosols of alumo-iron-sulfate-phosphate composition appear under the conditions of high content of phosphate in mineral solutions. The arising of crystal sulfates and formation of solid gels take place at air-dried densing of

such hydrosols. Crandallite forms under the condition of high CaO content in phosphate hydrosols. Mineral composition of zone of weathering indicates the modern proceeding of weathering processes and high degree both physical and chemical remake of material of initial rocks.

DISCUSSION ON THE GENESIS OF THE "MARBLE" IN ARCHEAN TERRAINS IN THE LIGHT OF THE GENETIC INFORMATION OF THE MINERALS CONCERNED

Jiang Yongnian, Tianjin Institute of Geology and Mineral Resources, Tianjin, 300170, People's Republic of China

In the Archean iron formation and iron ore deposit related to ultrabasic rock, there is a kind of mineral association: carbonates (calcite and dolomite) ± magnetite±actinolite±serpentine±quartz. It is named marble by some geologists when the carbonate content is rather high, and described as a kind of rock type in stratigraphic sequence. However, the so-called marble is different in some respects from a sedimento-metamorphic one.

According to the genetic information on carbonate minerals, the author considers that the main minerals, calcite and dolomite, of the so-called marble were formed by the hydrothermal alteration of Ca-pyroxene and Ca-amphibole of ultrabasic rocks (Zaoanzhuang and Naoyumen) and those of iron formations (Waitoushan and Shuichang). This has been confirmed by the genetic characteristics of carbonate minerals, such as irregular coarse-grain, short prism (pseudomorphs after Ca-pyroxene), traces of Ca-pyroxene cleavages at angles of 93° and 87° , REE distribution characteristics and relict Ca-amphibole , etc. Thus, they should be substantially considered as altered rocks rather than marbles.

Whether marbles might occur in Archean terrains has been under discussion up to now. In our country, although some geologists previously suggested that marblesdon'toccur in Archean terrains, yet they could not further put forward strong argument. Now, the conclusion of this paper supports their viewpoint.

STUDY OF GENETIC MINERALOGY OF THE OXIDIZED ZONE OF XIKUANGSHAN ANTIMONY ORE DEPOSIT, HUNAN PROVINCE

Jiang Yongnian, Tianjin Institute of Geology and Mineral Resources, Tianjin, 300170, People's Republic of China

The fundamental characteristics, genetic information and distribution in time and space, of the main secondary minerals of oxidized zone in Xikuangshan antimony ore deposit, Xinhua County, Hunan Province, such as native sulphur, kermesite, stibiconite, valentinite, limonite, carbonate, sulphate, dickite, have been studied, and the features of the oxidized zoneisdiscussed on the basis of this study.

1. Although the oxidizing process is restricted by the ore type poor in pyrite and the properties of the country rocks, the oxidizing action may take place along the fractures up to considerable depth. Thus, the oxidized zone develops imperfectly, and there usually remain the primary ores in the oxidized zone.

2. The development of the oxidized zone is probably related to the mineral species formed at certain stage, for example, kermesite forms in the initial oxidizing stage, but it may be converted to stibiconite quite soon. Valentinite and native sulphur crystallize in later stage. The carbonate may be considered as a product of the latest stage of the oxidized zone.

3. The distribution of minerals on the longitudinal profile of the oxidized zone may be given : stibiconite and limonite occur in the upper part , sulphates (gypsum, barite, etc), in the middle part, and native sulphur and valentinite, in the lower part.

In short, the author considers that the formation and regular distribution of these minerals mentioned above may depend mainly on the geochemical behavior of the elements concerned.

Jiang Yongnian, Tianjin Institute of Geology and Mineral Resources, Tianjin, 300170, People's Republic of China

ASSOCIATIONS OF Au-Ag TELLURIDES AS MINERALOGICAL INDICATORS OF GEOCHEMICAL CONDITIONS

A.I.Karapetian, Institute of Geological Sciences of the Academy of Sciences of the Armenian SSR, 375019-Yerevan, Av.Bagramian 24a, Armenian SSR, USSR

The indicator role of associations Au-Ag tellurides is established the Armenian SSR goldore and goldbearing ores investigation being an example, which are presented by petzite, calaverite, krennerite, sylvanite, hessit, nagyagite. The associations Au-Ag tollerides are mainly developed in a number of proper goldore and goldbearing deposits formations and they are less revealed in the ores of auriferous ore deposits formations.

The comparative analysis of minerals paragenetic associations revealed following peculiarities of qualitative-mineralogical composition of paragenetic associations, allowing to consider some gold tellurides as mineralogenesis geochemical conditions indicators.

I. In all minerals equilibrium paragenetic associations in which silver tellurides (hessite) take part as a rule, there are absent or are exceptionally rare sulphides and sulphosalts of bismuth i.e. bismutine, wittichonite, emplectite, aikinite, aramayoite, mutildite, cosalite, cuprobismuthite, galenobismuthite. Associated with above mentioned minerals the tellurides of bismuth take part too i.e. tellurobismuthite, pilsenite-wehrlite, tetradymite, which associate with the native gold, rarely native silver, with sulphides and sulphosalts of silver and bismuth.

2. In the equilibrium paragenetic associations the silver sulphides and sulphosalts are almost competely absent i.e. acanthite, polybasite-perseite, stephanite, pyrargyrite, miargyrit, aramayoite, stromeyerite-jalpaite etc., as well as kustetite and native silver, which have a significant development in the equilibrium paragenetic associations

3. In paragenetic associations with gold tellurides the native tellurium rarely develops only in certain mineral associations and tellurium concentrations. In ores rich in petzite and (or) hessite as well as in paragenetic associations with native silver and silver sulphides the native tellurium is absent. It is present only in very

rich in tellurium ores as microscopic segregations in association with tellurides of gold, silver, lead, sometimes bismuth, nickel, copper.

4. The sequence of tellurides segregation corresponds to the tellurides cations valence decrease. Tellurides of iron, nickel, bismuth, gold (trivalent), copper, lead, quicksilver are the earliest and tellurides of monova - lent gold and silver from later.

5. The native gold from paragenesis with petzit, as a rule, is characterized by its higher standard (900-950) in composition with paragenesis with hessite (800-850). The latter is associated with electrum or kustelite.

6. The native gold from paragenetic associations with gold tellurides is characterized its greater heterogene-

ty in composition. In the native gold by the value of trace elements content changes silver, iron, quicksilver, cobalt, platinum, copper are especially distinguished.

GENETIC MINERALOGY AND PROSPECTING FOR TIN

Radkevich Katerina, Far East Geological Institute,
Far East Branch of AS USSR, Vladivostok, 690022,USSR

When prospecting for tin, the examination of rock and ore specimens and heavy concentrates is of great importance for determination of a possible formation type of mineralization, a depth of ore formation, and prospects of ore distribution down the dip. Different methods of investigation and first of all the geochemical ones determining the composition of admixture elements are applicable, that allow to estimate a depth of erosional level and approximate temperature of ore formation and to define the under-ore, intra-ore and supra-ore level of the outeropped body. G.A. Osipova has determined some regularities of changes of admixture-element composition in cassiterite with depth - increasing In,Be,W,Fe and decreasing Sc,Nb. This is characteristic of cassiterite-sulphide deposits of the Soviet Far East. Thermobarometric method also helps to determine the depth of erosional shear of ore bodies and their erosional level by quantity and nature of gas-liquid inclusions. Thus, the field investigations must be accompanied by laboratory one. Textural and structural features of ores allow to estimate preliminarily ore concentration and choose possible technology (gravity,hydrometallurgy,alloys). Associated minerals make it possible to determine the formation type of deposits: cassiterite-quartz (greisens,quartz veins) - cassiterite and light mica aggregates; skarn - garnet-pyroxene aggregates; cassiterite-sulphide - cassiterite and sulphide, tourmaline,

and chlorite accociation. Different geological evidences are applicable to prosrect the formation types of ores of each formation, though polyformation complexes are possible, particularly when carbonate enclosing rocks (limestones) occur together with acid tin-bearing granites, which results in the occurrence of greisens and quartz veins with skarns and cassiterite-sulphide bodies.

The primary mineralogical-geochemical features predetermine the way and methods of further investigation and prospecting of deposits.

DENDRITIC PHOSPHATE MINERALS FROM GRANITIC PEGMATITES

Po 1.8

Paul Keller, Institut für Mineralogie und Kristallchemie der Universität, Pfaffenwaldring 55, 7000 Stuttgart-80, F.R.G.

Dendritic or arborescent phosphate minerals and also skeletal single crystals, mostly triphylite-lithiophilite solid solution members, but also manganaon apatite, have been observed (i) in numerous granitic pegmatites of Namibia and the Black Hills, U.S.A., (ii) in a few occurrences of Finland, Rwanda, Brasil, Sweden, and Bayrischer Wald, F.R.G. (KELLER, 1988).

The dendritic Fe-Mn phosphates are often exposed in quartz-muscovite-albite rocks, with varying amounts of each mineral. These rocks may belong to different pegmatitic units from the wall zone to the margin of the quartz core and to replacement bodies, but were preferencially seen within the outer intermediate zone and in pegmatitic units of uncertain origin (KELLER & VON KNORRING, 1989). In a number of pegmatites, the rocks with dendritic Fe-Mn phosphates are also carrying important ore minerals, e.g. beryl, columbite, cassiterite, etc.

The occurrence of dendritic phosphate minerals is, in general, an indication of crystal growth under characteristic nonequilibrium

conditions in granitic pegmatites (surprisingly!), and, in particular, an important tool in interpreting the evolution history of granitic pegmatites. Due to typical intergrowth textures between the dendritic phosphate and the silicate minerals, replacement could be excluded and paragenesis between these minerals could be corroborated (KELLER, 1988). A fact, that has been only suspected so far, but is a requirement for the determination of meaningful thermodynamic data and several other important genetic data like

- the Fe/(Fe+Mn) ratio of the Fe-Mn phosphates,
- the partition of (i) transition metal and Mg, Al, etc., and (ii) trace elements, e.g. REE, Sr, Rb, etc., between the phosphate and silicate minerals.

Some results of most recent investigations, mainly from Namibian pegmatites will be presented.

KELLER, P. (1988): Dendritic phosphate minerals and their paragenetic relation to the silicate minerals of pegmatites from Namibia and the Black Hills, South Dakota, U.S.A. - N. Jb. Miner. Abh., **159**, 249-281.

KELLER, P. & VON KNORRING, O. (1989): Pegmatites at the Okatjimukuju farm, Karibib, Namibia. Part I: Phosphate mineral associations of the Clementine II pegmatite. Eur. J. Miner., **1**, 567-593.

1.23V

DISTRIBUTION OF BENTONITE RESOURCES IN TIME AND SPACE IN IRAN

Ahmad Khakzad, Dept. of Geology, Ahahid Beheshti Univ. Evin, Tehran, Postal code 19834, Iran.
Abdolmajid Yaghubpur, Dept. of Geology, Tarviat Moalem University, Mefateh Ave., Tehran, Iran.

About 50 bentonite respects have been studied. At present time the products of bentonite mines are used in drilling mud, fuller's earth, etc.

Most bentonites in Iran are preduced from the alteration of pyrroclastic rocks (tuffs and uffited), that have been formed in marine environment. Generally the chemical composition of the tuffs are acidic, and

the way of the formation of the bentonites Cenozoic Era of the Alborz, Iran, as a typical pattern is explained in detail.

It had been suggested that the bentonites have been produced by the processes of alteration in tuffs and the tuffites and the bentonites are mostly formed in situ. It is also apparent that part of these deposits has been formed by hydrothermal processes.

In some parts of Iran as for example in the Zagros region it seems that the bentonites have sedimentary origin, but this idea is still on doubt.

The oldest bentonite deposits of Iran are found in the Cretaceous sediments, but most of them are younger in age and are usually Eocene to Olige-Miocene age.

X-ray investigations (X-ray diffractometer method) have indicated that the composition of the bentonites of Iran belohgs to the montmorillonite group minerals and are usually associated with cristobalite, quartz, and little feldspar minerals.

25 samples from bentonites have been chemically analysed and they showed to include Na-bearing bentonites, Ca bearing bentoites, Na-Ca-bearing bentonites, Mg-K-bearing vineonites and K-Na-bearing bentonites.

OCCURENCES OF SOME RARE MINERALS DERIVING FROM NEOGENE MAGMATISM IN HUNGARY

Miklos Kozak – Gyula Szoor – Peter Rozsa, University of Lajos Kossuth, H–4010 Debrecen, P.O.B. 4, Hungary

Wax opal (Telkibanya village, NE HUngary): In the Tokaj Mountains (which is the most eastern one of the Inner Carpathian Volcanic Belt in Hungary), near the eastern border of Telkibanya village, there is a shallow–extrusive perlitic mass within an area of Lower Sarmatian (Miocene) acidic volcanics. A characteristic local variety of the volatile–rich zones is the rhyolitic spherulitic perlite; in its red lithoidic rhyolitic veins, yellow wax opal and, in subordinate amount, milk opal, fire (noble) opal and other colored varieties can be found as fillings in the vesicles with tridymite on their walls.

Halloysite (Kovagoors village, W Hungary): One of the tuff cones of Pannonian basalt coming from the "final" stage of the inner carphatian magmatism can be found at the eastern border of the Kovagoors village. At the foot of the cone, lava intrusions are situated in an Upper Pannonian (Pliocene) abrasion sand–gravel bed. The material of these intrusions were converted into halloysite by the former wet environment and the subsequent supergenic processes.

Rhomboclase, copiapite (Uzsa village, W Hungary): Copiapite and rhomboclase were identified as secondary products of a strong marcasite impregnation in a lower Pannonian (Pliocene) gravel bed near Uzsa village. Their origin can be related to the one–time postvolcanic phenomena of the nearby basaltic volcanism.

Literature:

P. Gyarmati–M. Kozak–V. Szeky–Fux, 1986: Geology and genesis of the Telkibanya opal, Tokaj Mts.k, Hungary. Ann. Rep. Hung. Geol. Inst. 1984., pp. 355–376.

M. Kozak–I. Barta–Gy. Szoor, 1985: Mineralogical and geochemical investigation of the halloysite from Kovagoors (Keszthely–mountain, W Hungary) and its genetics. Bull. Geol., 115. pp. 281–292. (in Hung. with English abstract)

I. Viczian–M. Kozak–Gy. Szoor, 1986: Marcasite, copiapite and rhomboclase in lower Pannonian gravels at Uzsa (Central Transdanubia). Ann. Rep. Hung. Geol. Inst. 1984., pp. 377–387. (in Hung. with English abstract)

ORIGIN OF GARNETS WITH REGULARLY DISPOSED GYDROCARBON, SILICATE AND OXIDE INCLUSIONS FROM KIMBERLITE PIPE MIR

A.N.Krot, Vernadsky Institute of Geochem, Analyt. Chem., Kosygin Street 19, Moscow, USSR

Physical and chemical characteristics of the upper mantle rocks and minerals remain puzzling problems. Valuable insights can be gained by study of garnets with primary inclusions. Large single crystals of pink and red–violet garnets (–8 mm in diameter) have been discovered in the kimberlite pipe Mir (Yakutia). These garnets are saturated by great abundance of different silicate, oxide and fluid inclusions, disposed regularly in the garnet matrix. The garnets and inclusions were investigated by complex methods, including SEM, EPM, optical–, Raman– andIR–spectroscopy and some others. Studied garnets are characterized by low contents of FeO (4,46–8,71), TiO_2(0,03–0.15),Cr_2O_3(0,12–0,41),CaO (3,51–5,29,highcontents of MgO (18,88–23,44) and Al_2O_3(22,61–25,97), low Fe^{3+}_{VI}centers concentration and low values of colorimetric aprpmeters (P_c0,2). These compositional pecularities, optical spectroscopic and colorimetric parameters of garnets suggest their origin under very reduced conditions, which are consistent with the presence of fluid hydrocarbon inclusions in them. There are a lot of inclusions in these garnets except brown colored complex hydrocarbon inclusions. Most of them are diopside (18,38–19,87 MgO; 17,53–19,34 CaO; 0,46–1,03 Na_2O), some others are olivine (1,48–3,83 NiO; 3,53–5,05 FeO), rutile, ilmenite, sulfide (60,07 Ni; 24,07 S; 5,05 Fe; 4,05 Co; 7,37 Cu). The $\delta^{13}C$ values for carbon from fluid and bitumoid phases of the hydrocarbon inclusions are –34‰ and –29‰ respectively (data of E.M.Galimov). Estimates of equilibrium conditions for these garnets, based on garnet–olivine and garnet–clinopyroxene geothermometers are 1100℃. We can't estimate the pressure, but the presence of hydrocarbon inclusions, regularity of inclusions disposition in garnet matrix and their chemical compositions suppose these samples could have been formed by high–pressure (100 kbs) garnet–pyroxene solid–solution decomposition. These samples were uprised from the depth of about 260 kms.

DISTRIBUTION OF IMPURITY-RELATED PARAMAGNETIC CENTRES IN QUARTZ OF ALPINE VEINS

Kuznetsov S.K., Lutoev V.P., Ignatov M.I.,
Institute of Geology, Komi Scientific Centre, Ural Division, USSR Academy of Sciences, Oplesnina 2, 167610, Syktyvkar, USSR

There are many various paramagnatic centres carefully studied in quartz [1] and in rock crystal of hydrothermal veins [2]. But it is necessary to clarify the distribution of the centres in quartz veins. We have investigated the distribution of basic impurity-related centres in quartz Alpine veins of one of the Ural deposits. These are aluminum smoky colour centres $[AlO_4]^\circ$ and germanium-lithium centres $[Ge(C)Li]^\circ$, determined the number of important technical properties of quartz.

The Alpine veins of this region are the dilation one and are typical in structure and genesis. Vein quartz is white, partly transparent and consists of parallel-columnar aggregates. Rock crystal nests locate inside or in heading side of veins. Quartz crystals are present by two varieties, differed one from another by radiation-induced colours. These are smoky and smoky-citrine quartz crystals. Often the nests are surrounded by zones of transparent quartz with weak radiation-induced colour. Crystals and quartz of these zones are more late as compared with main body of vein quartz.

The investigation was made up by EPR with using powder technique. The quartz powders were annealed at 720°K and exposed to gamma-radiation by Cs-source at 300°K. Two doses of radiation were used. Dose 100 kGy was saturated dose for $[AlO4]^\circ$ and dose 5 kGy was the same for $[Ge(C)Li]^\circ$. Relative content of this centres are measured.

The statistical analysis of full set of data showed that significant positive correlation between the contents of $[AlO_4]^\circ$ and $[Ge(C)Li]^\circ$ existed. Average values of the centre contents are different in all types of quartz. Monotonous rising of the average centre contens took place in the next order: the main body of vein quartz, near-nest quartz, smoky and smoky-citrine crystals. The average content $[AlO_4]^\circ$ of extreme members of this series are differed one from another almost in four times, and their variance are no more than 30%. Besides the difference between the crystals from the nests of various locations is found. The crystals of salband nests have more high content of

impurity-related centres than the crystals of inner-veins nests.

The distributions of the centres in quartz veins have space zonning. Crystals and nearnest quartz with maximal content of $[AlO_4]^\circ$ are marked. Minor content of $[AlO_4]^\circ$ is typical for quartz of salband parts of veins, except that part where rock crystal nest is located. Such situation is typical.

Hence the rising of content of impurity-related centres from salbands towards the central parts of rock crystal-bearing veins is found. The late quartz (crystals and near-nest quartz) is rich in structure impurities. This tendencies are caused by evolution of mineral forming media as far as the filling of cavities took place and by quality new state on the stage of crystal-forming.

References:

1. Weil J.A. A review of electron spin spectroscopy and its application to the study of paramagnetic defects in crystalline quartz.- Phys. Chem.Minerals (1984), v.10, N.1, p.149-165
2. Samoilovich M.I., Tsinober L.I. Colour centres in quartz-IN: Geochemistry, Mineralogy, Petrology. Moscow:VINITI, 1969, p.118-138. - in Russian.

Bo 1.9.

MINERALS AND MINERAL PARAGENESES OF CHAROITITES AS A REFLECTION OF THEIR GENESIS CHARACTERISTICS

K.A.Lazebnic, L.V.Nikishova, Yakutsk Institute of Geosciences, Siberian Branch, Academy of Sciences, Yakutsk 677891, U.S.S.R.

Our study focuses on charoitites (Ch), peculiar rocks containing 35 to 95% charoite, an extremely rare mineral. The Ch have presently become widely known as an ornamental gem stone due to their unusual colour and peculiar structural-textural pattern. The only deposit of these rare rocks in the world is located in northern Transbaikalie and is restricted to the western slope of the Aldan Shield. The deposit is hosted by Upper Proterozoic terrigenous, quartz-carbonate series. In close vicinity to the deposit area is one of the earth's largest alcalic, potassic massifs, the Murun. That the deposit and the massif are genetically related is now recognised by all researchers. The mineralogy of the Ch is well studied by now, but their genesis - whether magmatic or metasomatic -

still remains a matter of controversy. We favour a metasomatic origin for Ch, which is supported by the following evidence:

1. Unlike magmatites, the Ch are characterized by extremely unstable composition, both mineralogical and chemical. Mineralogically, they exhibit all gradations from poly- to monomineral varieties. The Ch are also chemically unstable and have no analogues in any group of silicate magmatites from which they differ much in CaO content. In the latter parameter, they are only comparable to metasomatic rocks.

2. Unlike magmatites, the Ch are also characterized by textural inhomogeneity. They typically contain two forms of segregations: rounded, widely varying in size nodules of relict minerals (quartz, potassic feldspar) and newly-formed minerals of predominantly prismatic habit. A combination of the above forms, with size, colour and amount of deformation varying, imparts the stone its unparalleled appearance.

3. Ch are primarily composed of minerals which form a group of alcalic calcic silicates (ACS) and include eight minerals: charoite, tokkoite, miserite, pectolite, kanasite, tinaksite, fedorite, and apophyllite. These minerals differ from each other mainly in quatitative and qualitative amounts of alcalies and in H_2O amount. All the ACS, except fedorite and apophyllite, are characteristically similar in appearance and crystal structure. They present acicular to thin fibrous minerals, with elongation period of~0.7 nm, and belong to ribbon-chained silicates. Fedorite and apophyllite, like sheet silicates, are characterized by lamellar habit. The ACS often occur in regular intergrowths with each other, which is suggestive of their constitutional affinity. Such associations, which consist of minerals of similar composition and texture, are not as a rule observed in magmatites.

4. Determination of the degree of the constitutional affinity by N.Z.Evzikova's method using the concept of textural looseness leads to the conclusion that the ACS which compose the Ch may have come from a single predecessor, either wollastonite or potassic feldspar.

5. Added evidence for a solid-phase transformation of material and hence metasomatic origin of the Ch is the presence of through cavities or tunnels in the structure of ACS which permit free diffusion of alcalic cations and water along them without affecting main fragments of the crystal structure.

INVESTIGATION ON THE ORE PROSPECTING MINERALOGY OF GOLD DEPOSIT

Li Gaoshan Changchun College of Geology, Changchun, Jilin 130026The People's Republic of China

In recent years study has been carried out on prospecting mineralogy of gold deposits in TULINGSHIHU of Lingshou county, in Hebei province. Emphasis of this paper is placed on quartz and pyrite which are regarded as major gold–bearing minerals. Some guidelines for prospecting are obtained, which are described as follows: In respect of trace composition, the quartz is characterized by: (1) increase of Al_2O_3 content increasing formation temperature and depth: (2) positive correlation between the atom number of Al / (K+Na) and formation temperature of quartz, r = 0.5 (n = 7); (3) negative correlation between the value of Al / (K+Na) and depth of samples collected, r = −0.47 (n = 16): (4) positive correlation between the atom number of Al, (K+Na) and Au content of quartz, r = 0.58 (n = 12); (5) negative coherence between the logarithm of K_2O contentin quartz and altitude above sea level, r = −0.368 (n = 48). In respect of rare–earth elements, quartz is characterized by (according to 6 samples): (1) positive correlation between the value of La / Yb and Au content of quartz; (2) coherence of rare–earth fractionation to gold content, if the fractionation of light and heavy rare–earth elements is better, this quartz will be Au–bearing: if the fractionation is not good, this quartz won't be Au–bearing. The pattern of distribution of rare–earth in pyrite is similar to that of quartz. In respect of the absorption of infrared spectrum, the following conclusion can be reached. Firstly, the quartz shows a close relationship of the density ratio of absorption spectrum of H_2O and that of CO_2 in the inclusion of quartz to Au content of quartz. Given that D_1 is the relative density of absorption spectrum of H_2O and D_2 is that of CO_2, the D_2 value and Au content shows a positive coherence, r = 0.759 (n = 27). If D_2 = 0.1–0.22, the vein of quartz is Au–free; if D_2 = 0.2–0.41, it is Au–poor; and if D_2 = 0.33–0.92, it is Au–rich. The positive coherence between the value of D_2 / D and Au content of quartz indicates r = 0.78 (n = 27). If D_2 / D_1 = 0.1–0.86, the vein of quartz is Au–bearing, If D_2 / D_1 value is lower than 0.1, it will be Au–free. Secondly, the infrared spectrum of powder quartz indicates that, if the peak of absorption spectrum in 2900–3800 / cm is nonsymmetrical, this vein of quartz will be Au–bearing; if that is symmetrical and gentle, the vein of quartz will be Au–free. In respect of EPR, the positive coherence between the density of $Al–O^-$ center and Au content in quartz indicates r = 0.6 (n = 47). Finally, we have corrected Maksimowa's conclusion about the indication of pyrite thermo–electricity on prospecting for gold deposit.

STUDY ON GARNETS OF SKARN ORE DEPOSIT IN DAXINGAN RIDGE AREA

Li Henian, Changchun University of Earth Science, Changchun, Jilin 130026, Li Xuping, Nanjing Institution of Chemical Technology, Nanjing, Jiangsu,210009, People's Republic of China

In the Daxingan Ridge Hercynian Zone of fold, skarn ore deposits have been wildly discoverde. There are some large deposits: Skarn Fe deposit, Fe-Sn deposit, Fe-Sn multimetallic deposit and Pb-Zn deposit etc.In these deposits, all the skarn are consist of garnets of andradite-grossular series and monopyroxene of diopside-hedenbergite series. Garnet is main mineral facies in the deposits.The garnets of all the deposits have same character. For example, most of them are andradite. The garnets of each deposit can be divided into three generation:1),fine homogeneous garnets; 2).midcoarse nonhomogeneous garnets with fan symmetric extinction under cross crystal system; 3). coarse garnets of ring structure, Which are associated with carbonatite.Base on a great deal of chemical composition and physical properties by 69 samples that take from 7 ore deposits. There are obvious difference in different deposits.In skarn Fe deposit,the garnets are brown,specific gravity: 3.67-3.77, cell parameter: a_0 =11.98-11.99, N=1.827-1.843,VHN50=643.9-847.5kg/mm^2 , chemical composition:andradite molecular 69.5 -88.3%,on the everage 76.5%;grossular molecular 13.2-24.2%,on the everage 18.2%;almandine molecular 0.6-1.96%, on the everage 1.57%; spessartite molecular 1.56-4%, on the everage 2.6%; pyrope molecular 0.5-2.5%, on the everage 1.27%.

In skarn Fe-Sn multimetallic deposit, the garnets are mainly green and brown colour, specific gravity: 3.709-3.87, cell, parameter: a_0 =12.005-12.05, N=1.827-1.828, VHN50=643.9-723, chemical composition: andradide molecular 73.7-90.3%, on the everage 84%; grossular molecular 4.6-17.8%, on the everage 12.8%; spessartite molecular 0.6-1.99%, on the everage 1.1%; almandine molecular 0.4-2.53%, on the everage 1.9%; pyrope 6.48-3.7%, on the everage 1.95%. In skarn Pb-Zn deposit, the garnets is green, N=1.8628 -1.8266, specific gravity: 3.811-3.893,cell parameter a_0 =12.025-12.038,VHN50=847-1007,chemical composition: andradite molecular 77.5-95.9%, on the everage 89.22%; grossular molecular 1.9-13.3%, on the everage 5.3%; spessartite molecular 0.67-9.23%,on the everage 2,92%;almandine molecular 0.5-3.49%,on the everage 1.8%;pyrope molecular 0.05-7.5%,on the everage 1.8%.

As having been indicated above,the physical-chemistry properties of garnets are in relation to its chemical composition.The more iron in garnet is,the larger its cell parameter, refractive index,microscopic harden and specific gravity is . The garnets here are different from that have been reported, in those minerals there are more andradite molecular. In the garnets of skarn Fe deposit here,there are less andradite

molecular,more grossular and spessartite molecular.But in garnets of Pb-Zn deposit there are more spessartite molecular,and the most andradite molecular.

These characters depent not only on thermal liquid composition, but also on physical-chemistry condition. Higher temperature and pressuer is favourable for grossular molecular getting in crystal lattice. However, andradite molecular formed under lower temperature and pressure environment. In the same deposit, the third generation's garnets contain more andradite molecular. The composition of garnets also vary with PH and EH of thermal liquid.Base on expermental data analysis,the higher the alkali of thermal liquid is,the easier andradite molecular form.For instence,in garnets of Fe deposit: Fe^{3+}/Fe^{2+}=28.7; of Fe-Sn muiltmetallic deposit: Fe^{3+}/Fe^{2+} =34; of Pb-Zn deposit: Fe^{3+}/Fe^{2+}=150.

We can see, the composition of garnets not only on thermal liquid, but also on physical chemistry condition when ore deposit is formed. It is very important for studying why garnets are formed.(VHN50 - microscopic harden)

Po1.10.

ON THE STUDY OF GENETIC MINERALOGY FOR GANGUE MINERALS IN QINGCH–ENGZI LEAD–ZINC DEPOSIT, LIAONING PROVINCE,CHINA

Li Lee, Shenyan Institute of Gold Technology, Shenyang, Liaoning province, People's Republic of China

The Qingchengzi Lead–Zinc Deposit is located in Southeastern Liaoning province, China. It is rigidly limited by the lower Langzishan Formation and the upper Dashiqiao Formation of the Proterozic Liaohe Group which consist of metamorphic rocks, marbles and schists. The protolith of the metamorphic rocks included two parts, i.e. the upper sequence consisting of clastic rocks and carbonates and the lower sequence consisting of volcanic rocks and carbonates.

There are two types of lodes in the ore–field. One is the bandded lodes occurring mainly in the lower sequence, and the other is vein lodes prodominantly in thick carbonates of the upper sequence.

The ore mineral assemblage is composed of pyrite, sphalerite, galena, and minor chalcopyrite and arsenopyrite;while the gangue minerals mainly are quartz,calcite and dolomite.

Banded, disseminated, laminae and massive structures are found both in lodes and host rocks. Characteristically, the silicatization often occurs in host rocks close to lodes. Characteriscally, the silicatization often occurs in host rocks close to lodes. The alteration is bandded in the width of 0.1–2mm.

In this paper, the author describes the relationship between ore and gangue minerals, and features of the gangue minerals which are formed in different physi-

cal, chemical and geological conditions.

The quartz of different generations shows some differences in crystal form, cell dimension, spatial relation of microstructure, chemical composition,trace elements,contents specific gravity, fluid inclusion and ore forming temperature and pressure.

H_2O, CO_2, CH_4, N_2, Ca^{2+}, Mg^{2+}, K^+, Na^+, F^-, Cl^- has been found in the fluid inclusions of the quartz, which shows a wide temperature range, from 90℃ to 414℃, but mainly within 160℃ to 280℃.

There are abundant dolomites and calcites in the lodes. They have various forms because they are formed in different genetic types. Recently, the author has studied systematically their crystals, mineral components, isotope components of carbon and oxygen and so on, and has set up some diagnostic criteria on them. As a result of different geological agents, some of them, close to lodes have good rhombus in form, 0.1–2cm across.

Organic substances, CO^2 and daughter–minerals had been found in the fluid inclusions of calcite and dolomite. Their formation temperature varied greatly, mainly in ranges of 100–120℃, 180–200℃ and 330–360℃.

As for the source of the gangue mineral, the substances came mainly from sedimentary carbonates for dolomites and calcites, and that for quartz came mainly from submarine volcanical eruption.

The mineral substances were supplied in the process of submarine volcanic eruption and were precipitated in the Langzishan and the Dashiqiao Formations.The bedded Pb–Zn lodes were formed in process of metamorphism, and the vein–lodes were in the Indosinian when the granites intruded into the Langzishan and the Dashiqiao Series.

COVELLITE :A MINERAL INDICATIVE OF GOLD AND SILVER MINERALIZATION OF GOSSAN

Li Liping;Xu Guofeng,Department of Ore Deposits,China University of Geosciences,Wuhan,Hubei,430074,People's Republic of China

Covellite is an important ore carrier mineral in the subzone of oxidation enrichment of gossan-type gold and silver deposits.This kind of covellite is always poor in sulphur. The covellite which is rich in Fe(0.197-0.213%) and Au(910-2850 g/t) often occurs in gossan-type gold deposits,while those rich in Pb(up to 2.153%) and Ag (up to 8950g/t) may indicate the existence of gossan-type silver deposits.Researches show that,given a not very high leaching rate,covellite may stay stable in the subzone of oxidation enrichment above the phreatic surface,and covellite can deposit as well as enrich gold and silver in the leaching solution.So this kind of covellite can indicate gold and silver mineralization of gossans.

Po.1.11

SOME TYPOMORPHIC CHARACTERISTICS OF CALCITE IN PINGBAO POLYMETALLIC METALLOGENIC BELT, SOUTHERN HUNAN, CHINA

Li Rongqing, Hunan Institute of Geology, Changsha, Hunan 410007, People's Republic of China

Pingbao polymetallic metallogenic belt is located tectonically in the middle part of Nailin meridional downwarping region within the northern part of Nanling gigantic latitudinal tectonic zone. Huangshaping Pb-Zn deposit and Baoshan Cu-Mo-Pb-Zn-Ag deposit are the largest ore deposit in the metallogenic belt. Mineralization occurs as veins and bedded veins in the limestone of Shidenzi Formation of the Lower Carboniferous System. Calcites are abundant as gangue mineral in these deposits.

The calcites distributed mainly as veinlets in orebodies and in host rocks, especially abundant in the host rocks near orebodies. they wear precipitated mainly from later stage hydrothermal fluid.

The calcites occurred in cavity assume excellent crystal druse. The crystal form of calcites in Baoshan generally show ditrigonal scalenohedron or the combination of hexagonal prism and rhombohedral. Sometimes, the recrystallized dolomitic limestone yields rhombohedral calcites. In Huangshaping, the crystal form of calcites occurred in recrystallized limestone is only the combination of hexagonal prism and rhombohedron.

Analysis wear made for 30 calcite samples from Huangshaping and Baoshan areas. THe calcites related to mineralization, occurred in orebody and in hostrocks are characterized by higher Mn contents than its stratigraphic equivalent ore barren calcites far away from orebody. The Mn/Mg ratios of the former are 1.07-42.8, the latter are 0.01-0.23. The difference is distinct.

The total REE contents of 12 calcite samples range

from 1.6 to 135.9 ppm. They are decreased gradually from orebody and wall rock near orebody to limestone far away from orebody. In addition, the REE patterns of the calcites associated with mineralization in Huangshaping show obviosly negative Eu anomaly.

The intensity of thermoluminescence of the calcites decreases slightly with the nearness to orebody.

The isotopic data suggests that the calcites in and near orebody have lower $\delta^{13}C$ and $\delta^{18}O$ values, that is, $\delta^{13}C_{PDB}$(o/oo) -4.84--1.95 and $\delta^{18}O_{SMOW}$(o/oo) 10.2 --18.3; while the calcites occurred in limestone far away from the orebody have higher values, that is, $\delta^{13}C_{PDB}$(o/oo) 0.87--2.72 and $\delta^{18}O_{SMOW}$(o/oo) 15--19.8.

These characters of calcites, that the Mn/Mg ratios and the total REE contents increase and the thermoluminescence intensity, the $\delta^{13}C$ and $\delta^{18}O$ values decrease towards the orebody, can be used as indicators for exploration and prospecting.

MINERALOGY AND GEOCHEMISTRY OF THE SEDIMENT-HOSTED LEAD-ZINC ORE DEPOSITS IN EASTERN XICHENG METALLO-GENETIC PROVINCE (OREFIELD), WESTERN QINLING RANGES, CHINA

P1.12

Li Ying,Department of Geology and Exploration,Xi'an college of Geology ,Xi'an,Shaanxi 710054,People's Republic of China

In the eastern part of this province are concentrated most metals reserves in the Devonian Lead--zinc multimetallic belt of the Qinling mountains,in which exists the Super-Large ore deposit named Chang Ba.In the province there are two types of genesis,i.e. the marble-schisttype----the Lead-zinc ore (MST) of the hydrothermal-Sedmentary,and the silicalite (Shale) type----the Lead-zinc-copper ore (ST) of the hydrothermal sediment-replacement. The two ore deposits are possessed of the obvious correlatability of mineralogy and geochemistery:

1. Mineral Association:Among MST, the main ore minerals are sphalerite,pyrite

and galena; gangue is quartz (fragments),calcite,mica,feldspar(K–feldspar),etc. The characteristic minerals are pyrrhotite,arsenopyrite,magnet,barite,dolomite,etc. In schist there can be seen a few acorite,agustite,sphene,etc. Among ST,the main minerals are phalerite,galena and quartz. The characteristic minerals are binarite, ferroddomite–Sideride,tetrahe–drite–chalcopyrite and a small amounts of barium feldspar–barite.

2. Ore minerals: In the light of color,unite cell (a_0),hardness and Fe%,sphalerite can be divided into three stages:dark–brown,light–brown and yellow–brown;a_0= 5.420–5.410; its hardness 3.5–2.7;Fe%,9–0.5. In addition,all content of Cd (<0.5%), Mn(<0.05),TL,Ca,Ge,In and Bi is low.Among MST,color is darker and the TL content is comparatively higher (3––90ppm). Among ST,color is lighter and the Cd content in general is 0.1–0.2%. Hardness of galena all is 2. It contains Ag (0––500ppm),among ST,Ag is comparatively rich. Among all kinds of pyrite,the total content Pb and Zn in general is higher than 0.5%,and among MST,the Pb and Zn content is higher than that among ST,but the Cu content of the latter is comparatively higher,Cu>0.01%. The Ni / Co ratio of pyrite in marble is 3––5; in schist is 1––3,in general in ST is less 3 but sometimes it can reach up to 50. The Sb,Ni and Co content of pyrrhotine is higher than that of pyrite and the TL content is less. Ni / Co ratio of arsenopyrite is <1,Zn>1%(only two samples).

3. Altered Minerals: In anchiore wall rock and ore of MST there are feldspar (mainly K–feldspar),dolomite,barite,fluorite and tourmaline. In distant ore of ST there is albite (early stages hydrothermal passageway),in anchiore there is columnar–granalar quartz (δ^{18}_0+18––+22‰[SMOW]),ferrodolomite and a small amounts of cymrite (a_0= 5.341).

4. Typomorphic minerals: Those are sulfosalt. The results of EPMAand X–ray analyses proved that among MST there is boulangerite (Meneghinite), and among ST there is tetrahedrite (freibergite) being intergrowth with argentite.

5. Sulfide δ^{34}s‰ [CD]: Among MST,δ^{34}s in general is higher than +15‰,and only Sulfide isotopic exchange between pyrite and galena reached equilibrium. Among ST,δ^{34}s is +5––+15‰,and between sphalerite and galena was equilibrium.

6. Fluid Inclusion of Minerals: Its homogenization and decrepitation temperature are two stages. Among MST,its salinity is 15–20wt.%NaCl;the high stage of temprature hits 250℃ ––350℃ . Among ST,salinite is 5––15wt.%NaCl,and the latter hits 200℃ ––280℃ . The recrystallised inclusion belongs to a high stage,and the primary inclusion belongs to a low stage of temperature,110℃––180℃.

Although occurred obvious hysterogenic changes in minerals ,for instance, recrystallization,crash and kneaded plication,but those minerals still remained a lot of typical characteristics of hydrothermal–Sedimentary(exhalative) genese.

THE COMPOSITIONAL ZONING OF GARNET AND METAMORPHIC EVOLUTION OF KHONDALITE SERIES NEAR ZUOZI, SOUTH-EASTERN INNER MONGOLIA

Po 1.13

Liu Fulai, Jin Shiqin, Changchun College of Geology, Jilin, 130061, People's Republic of China

The Khondalite series are extensively distributed in Zuozi, Southeastern Innen Mongolia, and two metamorphic events are recognized within them. The temperature is 750-830℃ and pressure is 0.9-1.17 Gpa for the first (main) metamorphic event. The metamorphism of early stage in the second event is characterd by the similar temperature to and slightly lower pressure than the

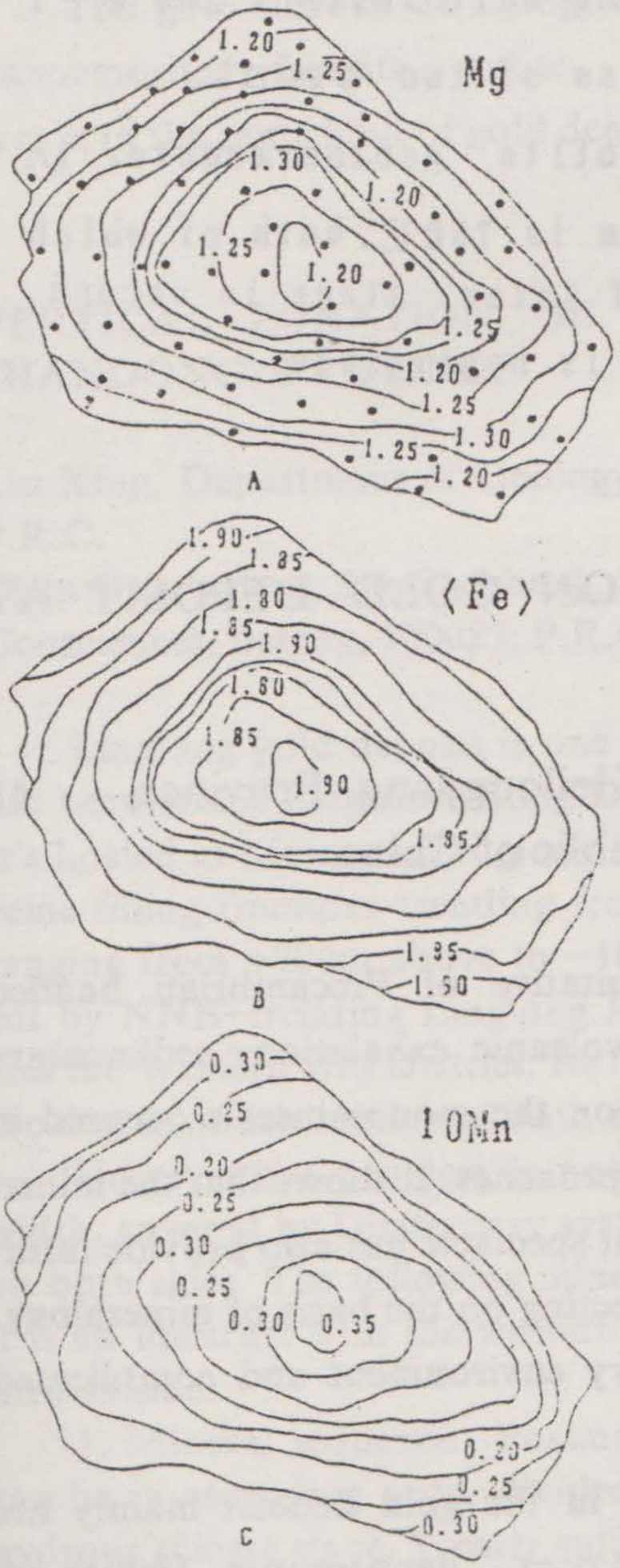

Fig. 1

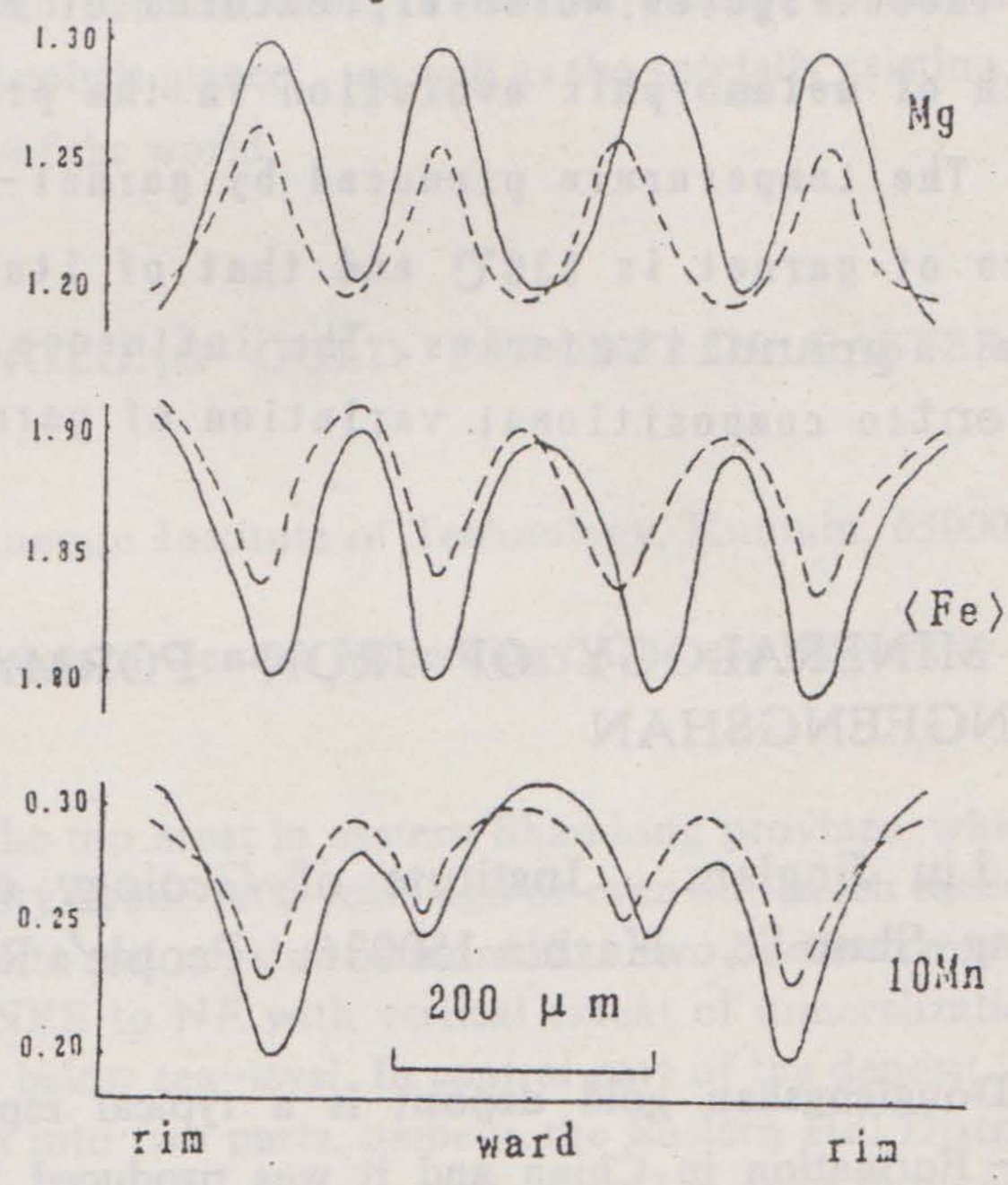

Fig. 2

Fig. 1 The compositional zoning of garnet

A. Counter line of Mg value

B. Counter line of 〈Fe〉 value

C. Counter line of 10Mn value

Fig. 2 The rim-ward compositional variation profile of garnet from two samples

first event, and the later stage is around 650℃ and 0.57-0.62 Gpa.

The widespread garnet phenoblasts in various rock types of the khondalite series show distinct compositional zoning formed by polyphase motamorphism. Regularly rim—ward compositional variation and analogous zoning pattern of Mg, 〈Fe〉 and Mn are determined in garnet from two samples of sillimanite—almandine—biotito genesis by means of energy spectrum. For example, the rim—ward compositional zoning of Mg, 〈Fe〉, Mn content in plane view and coresponding profile in sample P362—2 are illustrated in Figure 1 and 2 respectively. The negative correlation between Mg and 〈Fe〉 or Mn, and positive correlation between 〈Fe〉 and Mn are distinct in these Figures. Moreover, Features of zoning well reflect the P—T path of metamorphic evolution in the process of two event.

The temperarure produced by garnet—biotite geothermometer in core of garnet is 830℃ and that of its rim is 750℃, both of which are in granulite facies. The influence of later stage in second event to compositional variation of garnet is negligible.

A.G.P

MINERALOGY OF IRON- FORMATION GOLD DEPOSIT AT DONGFENGSHAN

Liu Jinglan, Institute of Geology of Heilongjiang Province, 48 Xiang-Shun St, Harbin 150036, People's Republic of China

Dongfengshan gold deposit is a typical representative of Precambrian banded Iron- Formation in China and it was produced by volcanic exhalation- sedimentary metamorphism. The auther has examined and studied on the monominerals occured in Dongfengshan gold deposit with various methods and approaches. It shows that the minerals and mineral associations not only afford a magnificent spectacle but also provide information about the gold evolution and the guide of prospecting on the basis of mineralogy. They are the final products of the primary sedimentary environment and complicated metamorphism.

The rock- forming minerals of ore- bearing beds in the gold deposit mainly are grunerite, cummingtonite (both occupy 5—50% of iron ore), dannemorite (which occupies 15—50% of gold ore), ferro-pargasite, fluor-arfvedsonite, fayalite (more than

80% of pure iron peridotite), eulite (sometimes 30% of iron ore), spessartine (15–55% of gold ore and closely associated with dannemorite), almanite, apartite (P_2O_5content is about 1.5% in ore), tourmaline (There are three subpecies that may form beded tourmalinite at local part.), quartz, and biotite. The metallic minerals are pyrrhotite, arsenopyrite, cobalt– arsenopyrite, cobalt glance, arsenonickel, nickelite, nicglance, pentlandite, chalcopyrite, magnetite, ilmenite and native gold.

The minerals and mineral associations mentioned above have obviously the feature of stratabound and are strictly controlled by stripped ferro– formation oxide– facies, silicate–facies, carbonate–facies, and sulfide–facies. The gold and cobalt orebodies exist strictly in Mn–bearing sulfide–facies and carbonate–facies. They exhibit like beded and lenticular orebodies. The spessartine and dannemorite are main carrying minerals of native gold and sulfide and arsenic minerals come next. The native gold always appears as irregular granular enclusions existing in the mentioned minerals or intergrowing with them. The fineness of the gold is 913.

The gold deposit as Dongfengshan deposit which is concentrated of spessartine, dannemorite, fayalite, eulite, and cobalt glance, as well as the specially existing gold is rare in the same kind of gold deposit of the world.

VERTICAL ZONATION OF LINGLONG GOLD DEPOSIT IN EASTERN SHANDONG PROVINCE

Liu Xing, Department of Geology, Kunmin Institute of Technology, Kunmin, 650000, P.R.C.
Chen Guangyuan, Sun Daisheng, Division of Genetic Mineralogy, Chinese University of Geosciences, Beijing, 100083, P.R.C.

Linglong gold deposit is one of the top most in eastern Shandong province, which has been mined long since Song Dynasty about 1000 years ago or even still much earlier. It's hosted in Mesozoic Linglong Granite and consists of more than two hundred quartz veins filling fractures trending from NEE to NE with vertical extent of mineralization ranging from +700m above to −100m below sea–level. In central part of the deposit it's cut by NNE–trending Linglong Fault into two parts, namely, the Eastern Hill District and the Western Hill District. Its future depends on the nature of the Linglong Fault and the degree of denudation of both districts on both its sides.

However the problem is not so easy to solve as the fault zone is about 200m in width, covered by Quaternary system, lying in the same granite with similar quartz veins on both sides. The following mineralogical and genetic mineralogical criteria reveal that it is an upthrust with the western side as upthrown block and the eastern side as down thrown side.

1. Mineral sequence Postmagmatic mineralization in normal vertical zoning here can be in ascending order divided into 5 stages, namely, 1. anhydrous silicate stage, 2. hydrous silicate stage, 3. early sufide stage, 4. base metal sulfide stage, 5. carbonate stage. Stages 1 & 2 (microline–quartz vein and muscovite–quartz vein) are well represented in

Western Hill District while stage 5 (calcite–quartz vein) is well represented in Eastern Hill District.

2. Vein wall alteration In Western Hill District feldspathization is strongly developed while sericitization, silicification and carbonation are weak, fading away downward already at 190 m level. In Eastern Hill District hydromuscovitization is strongly developed instead while sericitization, silicification and carbonation are also very strong in the meantime with the former two double the width at 170m level and the latter one extending even down to 10m level.

3. Vein distribution Western Hill district is full of single quartz veins with maximum length up to 5km, maximum width up to 20 m and intervening distance about 500–1000m. Further more adular–quartz vein is found at 230m level with width more than 20cm, while siderite veinlets is less than 5mm in width. Eastern Hill District is marked by composite and net–work quartz veins with interveining distance 20–100m, width of adularia–quartz veins is found to be no more than 2cm at 130m level, but that of quartz–calcite veins comes up to 5cm and even more.

4. Mineral typomorphism In Western Hill District quartz druses are less developed with length / width radio of quartz about 3–6, but growth layers on prisms and rhombohedra of quartz crystals are rather perfect. Zr, Ti, Zn are the dominant minor elements in quartz. Homogenization temperatures of fluid inclutions in quartz of stage 3 at 220m level are 310–350℃ . Crystal forms of pyrite consist mainly of {100}and {100}+{210}. Their minor elements are rich in Cr, V, Ni, Ti, Zn, Pb, Mo. N–type pyrites amount to 41.2%.

In Eastern Hill District quartz druses are much more common. Length / width ratio on prisms of quartz crystals is about 1.5–2.5. Growth islands are common on crystal faces of quartz. Al, K, Ba, Sr, Rb are dominant minor elements in quartz. Homogenization temperatures of fluid inclutions in quartz of stage 3 at 206m level is 250–300℃ . Crystal forms of pyrite consist mainly of {100} and {100}+{111}. Their minor elements are rich in Se, Te, As, Sb, Cu. N–type pyrites amount to 22.6%.

All the above –mentioned features exactly indicate that Western Hill District is the upthrown block and therefore has undergone more denudation while Eastern Hill District is the downthrown block less denuded with more ore preserved down below in depth. This conclution has already been proved by further exploration. By quantitative calculations of the variation gradient of some physical parameters of pyrite and quartz the throw of Linglong Fault is found to be 300m.

Note: The financial support is from the NSFC–4860100.

?12.3

TYPOMORPHIC CHARACTERISTICS OF APATITE IN EAST YUNNAAN PHOSPHORITES

Liu Yongxian,Ge Dingyi ,Chengdu college of Geology, Chengdu,Sichuan,610059,People's Republic of China

East yunnan is famous for its phosphrus deposits. phosphorites exist in the Lower Cambrian.Since 1987,the research group headed by Professor Zeng Yunfu have carried out a research into the East Yunnan Phosphorites. It is suggested that the phosphrites in the area are of microbial genesis and are classfied into three gen-

etic types (Table 1).therefore,it is very important to find the typomorphic features of apatite in phosphorites of various genetic types.

The chemical analysis of apatites in 25 specimens shows that theseapatites are of a isomorphous series, in which the $[PO_4]^{3-}$ is substituted by $[CO\cdot F]^{3-}$ or $[CO_3\cdot OH]^{3-}$ and F by $[OH]^-$ in less or more degree. Based on atom number of $\left[\frac{OH}{OH+F}\right]$ and [C] in their formula,apatites in this area can be classified into four subspecies(table 1).Between apatites in phosphorites of various genetic types there are obvious differences in anions,subspecies as well as a. and $\bar{N}$ (Table 1).

The formation and concentration of apatites in this area can be devided into three stages and three generations (Table 2).We have studied the microcrystals formed in each generation,with SEM,energy spectra TEM and electran diffraction and consequently found that the

Table 1. Main characteristics of apatites

*	Main composition (in wt%)					Number of atom		a.	c.	$\bar{N}$
	P_2O_5	CaO	F	CO_2	H_2O^+	$\frac{OH}{OH+F}$	C			
I	36.70	49.87	2.78	1.40	1.20	0.46	0.32	9.367	6.890	1.623
	37.14	52.93	3.59	1.51	0.91	0.33	0.35	9.360	6.894	1.619
II	35.14	50.01	3.63	1.77	0.53	0.20	0.41	9.342	6.890	1.614
	37.06	49.87	2.93	0.83	0.75	0.17	0.20	9.359	6.889	1.625
III	38.06	52.26	3.40	0.48	0.45	0.18	0.12	9.367	6.894	1.631
	36.71	47.31	3.82	0.69	0.73	0.07	0.18	9.370	6.889	1.630

Table 2. the characteristics of apatites in microforms

Formation stages	Seclimentation	Diagenesis	Secondary leaching
microforms	coccus spindle	fibrous radiating	botryoidal comb
diameter length (μm)	0.5 — 3.1 0.4 — 3.4	0.05 — 0.51 4.0 — 10.5	5.0 — 15.1 8.2 — 18.2
*	I	II	III

* .Algae-bacterial phosphorites, hydroxy-carbo-fluorapatite
.Intraclastic phosphorites,carbo-fluorapatite, lowcarbo-fluorapatite.
.Weathering or secondary leaching phosphorites, fluorapatite.

micirforms of apatites formed in various generations are obviously different and these differences are the best typomorphic features of apatites (Table 2)

In brief,1) the apatites in Algae-bacterial phosphorites from this area are all rich in hydroxyl,and the existance of hydroxy-fluor-apatite is an evidence for biogenesis of phosphorites;2)form sedimentation through diagenesis to secondary leaching or weathering, the $[OH]^-$ and $[CO_3]$ are progressively drived out from apatite,and the apatite becomes step by step fluorapatite with a more stable crystalstructure;3)among various genetic types and at various formation stages,there are obvious differences in microforms,grinsizes compositions as well as main subspecies,and these differences are valuable typomorphic features.

1.20V

PROSPECTING MINERALOGY OF CHROME MICAS FROM GOLD DEPOSITS IN JIAODONG, PRC

Lu Anhuai, Chen Guangyuan, Division of Genetic Mineralogy, Chinese University of Geosciences, Beijing, 100083, PRC

The tentative classification of chrome micas with reference to the related members of the muscovite–phengite series is given below in Tab.1.

Tab.1 Tentative classification of chrome micas

Classification	Grain size	SiO_2%	Cr_2O_3%	Si
Muscovite	>0.1mm	41.37–48.42	–	2.96–3.30
Fuchsite	>0.1mm	42.21–47.24	0.27–14.59	2.76–3.11
Sericite	<0.1mm	46.69–50.09	–	3.09–3.27
Chrome sericite	<0.1mm	47.24–50.97	0.25–2.00	3.05–3.30
Phengite	>0.1mm	50.18–52.29	–	3.33–3.53
Mariposite	>0.1mm	51.39–56.00	0.18–0.81	3.39–3.71

There are two principal genetic types of primary gold deposits known in Jiaodong gold fields, Shandong province, PRC. One belongs to auriferous quartz veins filling tension fissures in Mesozoic granites and Archaean metamorphics of the Jiaodong Group. However there is another type of filling deposit found occasionally in parallel with the quartz vein. It is represented by auriferous specularite–pyrite–fuchsite vein in which the principal gangue mineral is fuchiste instead of quartz while pyrite is thickly impregnated in fuchsite and specularite rosettes occur only sparsely in its geodes (Chen et al., 1989).

The other belongs to the replacement type, caused by hydrothermal replacement along cracks in shear zones developed in Mesozoic granitoids upthrusted by metamorphics of the Archaean Jiaodong Group from the crystalline basement. In this type ordinary sericites are by far the most common while the additional chrome sericites occur only in large deposits of this genetic type in the principal mineralization stage associated with sericite, quartz, ankerite, pyrite and electrum.

Crystallochemical formulae of the above–mentioned two types of chrome micas are

as the following.

1. $[K_{0.59}(H_3O)^+_{0.28}Na_{0.06}Ca_{0.07}]_{1.00}[Al_{1.69}(Fe^{3+}_{0.20}Cr_{0.05}Ti_{0.05}Fe^{2+}_{0.04}Mg_{0.01})_{0.35}]_{2.04}(Si_{3.13}Al_{0.87})_4O_{10}[(OH)_{1.28}O_{0.48}F_{0.09}]_{1.85}$
2. $[K_{0.61}(H_3O)^+_{0.39}]_{1.00}[Al_{1.37}(Cr_{0.10}Mg_{0.09}Fe_{0.08}Ti_{0.02})_{0.29}]_{1.66}(Si_{3.10}Al_{0.90})_4O_{10}(OH)_{2.29}$
3. $[K_{0.68}(H_3O)^+_{0.32}]_{1.00}[Al_{1.31}(Mg_{0.18}Fe_{0.10}Cr_{0.05}Ti_{0.02})_{0.29}]_{1.66}(Si_{3.11}Al_{0.89})_4O_{10}(OH)_{2.46}$
4. $[K_{0.60}(H_3O)^+_{0.40}]_{1.00}[Al_{1.65}(Fe_{0.15}Mg_{0.15}Mg_{0.07}Cr_{0.03})_{0.25}]_{1.90}(Si_{3.30}Al_{0.70})_4O_{10}[(OH)_{1.40}O_{0.19}]_{1.59}$
5. $[K_{0.69}(H_3O)^+_{0.27}Na_{0.02}Ca_{0.02}]_{1.00}[Al_{1.53}(Fe_{0.15}Mg_{0.08}Cr_{0.03})_{0.26}]_{1.79}(Si_{3.05}Al_{0.95})_4O_{10}(OH)_{2.16}$
6. $[K_{0.70}(H_3O)^+_{0.29}Ca_{0.01}]_{1.00}[Al_{1.61}(Fe_{0.17}Mg_{0.04}Cr_{0.02}Ti_{0.01})_{0.24}]_{1.85}(Si_{3.09}Al_{0.91})_4O_{10}(OH)_{2.02}$
7. $[K_{0.60}(H_3O)^+_{0.36}Na_{0.02}Ca_{0.02}]_{1.00}[Al_{1.48}(Mg_{0.11}Fe_{0.06}Cr_{0.05}Ni_{0.01})_{0.24}]_{1.72}(Si_{3.13}Al_{0.87})_4O_{10}(OH)_{2.15}$
8. $[K_{0.91}(H_3O)^+_{0.06}Na_{0.02}Ca_{0.01}]_{1.00}[Al_{1.59}(Fe_{0.15}Mg_{0.10}Cr_{0.02}Ti_{0.02})_{0.29}]_{1.88}(Si_{3.21}Al_{0.79})_4O_{10}(OH)_{2.28}$
9. $[K_{0.91}(H_3O)^+_{0.08}Na_{0.01}]_{1.00}[Al_{1.81}Fe_{0.08}Mg_{0.05}Cr_{0.02}Ti_{0.01}Ni_{0.01}Mn_{0.01})_{0.18}]_{1.99}(Si_{3.24}Al_{0.76})_4O_{10}[(OH)_{2.03}O_{0.02}]_{2.05}$
10. $[K_{0.92}Na_{0.05}(H_3O)^+_{0.02}Ca_{0.01}]_{1.00}[Al_{1.63}(Fe_{0.20}Mg_{0.16}Cr_{0.02}Ti_{0.01})_{0.39}]_{2.02}(Si_{3.25}Al_{0.75})_4O_{10}(OH)_{2.02}$
11. $[K_{0.94}(H_3O)^+_{0.05}Ca_{0.01}]_{1.00}[Al_{1.50}(Fe_{0.22}Mg_{0.14}Ti_{0.02}Ni_{0.02}Cr_{0.01})_{0.41}]_{1.91}(Si_{3.17}Al_{0.83})_4O_{10}(OH)_{2.37}$
12. $[K_{0.87}(H_3O)^+_{0.07}Na_{0.04}Ca_{0.02}]_{1.00}[Al_{1.81}(Fe_{0.15}Mg_{0.13}Cr_{0.02}Ti_{0.02})_{0.32}]_{2.13}(Si_{3.28}Al_{0.72})_4O_{10}[(OH)_{1.44}O_{0.53}]_{1.97}$

Note: No. 1 from the filling vein type, fuchsite and No. 2–12 from the hydrothermal replacement type, chrome sericite.

The presence of Mg, Cr, Ti, Ni in M(Ⅵ) together with Al(Ⅵ) reveals that part of their material is derived from the original dark constituents like biotite and hornblende in the amphibolites of the Archaean Jiaodong Group nearby which is the source rock of gold in the region.

As to K in chrome micas from Jiaodong gold fields, it is less than 1 in consequence of the isomorphic replacement of K by H_3O^+ indicating that they are fromed under a condition rich in mineralizers.

Their typomorphic features are given in Tab.3. They are good indicators for tenor and extent of the gold deposits.

Tab.3 Typomorphic features of chrome micas from gold deposits in Jiaodong

Genetic type of deposit	Filling vein	Hydrothermal replacement	
Mineral	Fuchsite	Chrome sericite	
Colour	Emerald green	Emerald green	to green
Grain size(mm)	0.50	0.1	to 0.002
a_o(Å)	5.206	5.139	to 5.204
b_o(Å)	9.050	8.796	to 9.018
c_o(Å)	20.250	19.981	to 20.126
Polymorphy	$2M_1$	$2M_1$	to $2M_1$
Loss of H_2O in TGA(%)		7.50	to 2.93
Cr_2O_3(%)	0.99	2.00	to 0.25
K	0.59	0.60	to 0.94
H_3O^+	0.28	0.40	to 0.02
M(Ⅵ)	2.04	1.66	to 2.13
Tenor of gold (g / t)	n × 100–n × 10	n × 10	to n
Typomorphic gradients of horizontal variation for chrome sericite (per meter)	Deposit	Sanshandao	Jiaojia
	Cr_2O_3(% / m)	0.05	0.02
	K(1 / m)	0.03	0.01
	H_3O^+(1 / m)	0.02	0.01
	M(Ⅵ) (1 / m)	0.02	0.003
	Extent	Large	Large

Note: The financial support is from the NSFC–4860100

THE ABRASION CHARACTERISTICS OF DIASPORES IN BAUXITE AND THEIR REGULAR ENRICHMENT PATTERN

Lü Xia, Henan Institute of Non-Ferrous Mineral Resources and Geology, Zhengzhou Henan 450052, China

Bauxite in China is mainly in diasporic type. In the paper, the regular enrichment pattern of diaspores of sand and soil bauxite has been studied from mineralogical side.

The sand and soil bauxite is the richest ore in various bauxite. It is known, they only occured in karst dolines, In vertical, they are always the lower parts of bauxite bodies. Because most of their bodies are very thick, they possess uniform texture and massive structure and not have bedding, some experts have considered that this type bauxite was formed by leaching and losing Si and autochthonous Al residures accumulated.

Bauxite in Henan, Guizhou and Shanxi provinces has been studied in detail with scanning electron microscope. Abraded diaspores were discovered in different texture bauxites, especially in the sand and soil bauxite.

In the electron microscope photographs, you can see it clear that sand bauxite is made of column crystals of diaspores that they are more uniform size from 0.02 to 0.1mm; soil bauxite is made of needle and long board column crystals of diaspores. Irregularly piled up together with a few heavy minerals, it forms the typical grain-supported. It is steady flow deposition.

The most of crystals of diaspores in the bauxite were abraded. The abrasion traces of diaspores are clear. Some crystal faces were dameged, some edges and corners were abraded away. Surfaces of diaspores changed rough. Some of diaspores are subrounded and rounded.

These abraded and collided traces of diaspores show that they were carried from land to karst depositional basin and prove that the sand and soil bauxite was allogenically clastogene deposit. Through study on mineralo-

gical characteristic of the bauxite,the concentration of diaspores in the sand and soil bauxite dues to gravity separation of minerals in water.

According to above facts, I infer origin of the sand and soil bauxite below:Primary clay or lean bauxite distributed in palaeoresiduum was weathered, diaspores and clay minerils were carried by water from higher to lower. When they went into karst basin,the water speed would be slow down. First, in water diaspores with heavier specific gravity sinked to the bottom of karst basin or doline and made up sand or soil bauxite. Then some smaller diasporic grains and some clay minerals went down on the sand or soil bauxite and formed lean bauxite. Finally, clay minerals would slowly deposit. If a karst basin or doline was very deep and the water mixed diaspores and clay minerals went continuously through above it, the heavier diaspores sinked constantly down. With diasporic concentration, the sand or soil bauxite body would get thicker, but lighter minerals were drifed away by water.

THE DISTRIBUTION OF THE SERIES OF Au–Ag MINERALS AND THE CHARACTERISTICS OF Au/Ag IN GIAPIGOU GOLD DEPOSIT ON HUADIAN, JILIN PROVINCE IN CHINA

LUO Hui, SHEN Baofeng, PENG Xiaoliang, WANG Wenying Tianjin Institute of Geology and Mineral Resources. CAGS, Tianjin, 300170, People's Republic of China

Giapigou gold deposit in Huadian, Jilin province, being distributed in the Archean granitoid–greenstone terrians of the northern margin of the North China Platform, a large one, belongs to the type of the gold–bearing guartz veins. The host rock is mainly the mafic volcanic rock with ultramafic rock band. The ore bodies are controlled by the NW trending ductile shear zone. The mineralization epoch is the early proterozoic era.

The main gold–bearing minerals in the deposit are the series of Au–Ag ones which consist of 91% native gold and 9% electrum. The native gold occurs in three types: 1)occurred in the crack of pyrite and quartz. 2)included in pyrite and quartz, or being absorbed in the adge of the minerals. 3) ultramicro gold in pyrite and quartz. The particle of gold that the size varies from 0.1 to 0.5 μm are distributed in the crystal face of the mineral. Among the three types the first is important.

The shapes of the native gold are obviously controlled by the spatial form of the distribution of gold. The composition of the native gold of 43 samples were determined by electron microprobe analysis. The results are summarized as follows: Au, 75.44 to 99.11%, with a average of 91.3%; Ag, 0.59 to 24. 13% (most < 10%), with a average of 8.01%. The distribution of Au and Ag in a single native gold from the centre to margin is homogenous and the ratio of Au / Ag is relatively constant, indicating the stable condition of the mineralization. However , the Au / Ag ratio of the native gold varies obviously in spatially. There are two kinds of trend for the Au / Ag ratio to vary: 1) discontinuous variation. On the whole, the Au / Ag ratio can be divided into four regions: the first, 3.13–5.69; the second, 8.93–20.31; the third, 29.98–49.98 and the fourth, 65.92–86.93. The samples of 60% are fallen in the second region. The discontinuity of the ratio of Au / Ag is the result of superposition of multiple mineralization. 2) The Au / Ag ratio of the native gold increase gradually from the top to the bottom of the deposit. The increasing trend of the Au / Ag ratio may be the effect of temperature. It is remarkable that the native gold from the different depth is of the multilayer texture of the Au / Ag ratio. Statistical treatment of the data of the mine reveals that the variations of the ore tenor and the thickness of the ore body in depth are similar to that of the Au / Ag ratio. As a result, the variations of the Au / Ag ratio in the native gold are important for the exploration.

MINERALOGICAL AND GEOCHEMICAL CHARACTERISTICS OF THE BAUXITE AND IRON ORES FORMATION IN THE WEATHERING CRUST ON CENOZOIC BAZALTS OF VIETNAM

Dr. Mai Trong Nhuan , Department of Geochemistry, Hanoi State University, Vietnam

In Vietnam there are three geochemical types of weathering crust on cenozoic basalts – ferite, feralite and ferosialite. The profile of the ferite and feralite weathering crusts composes of 3 zones – ferite (feralite), ferosialite and sialite (saprolite). The ferosialite weathering crust profile losses the upper (ferite of feralite) zone. The ferite and feralite weathering process (WP) could follow 3 stages – saprolitization, ferosialitization, feritization (or feralitization). The ferosialite WP consists of two stages – saproliization and ferosialitization. Each of the weathering stages is characterized by the formation of definite mineral association and element removal.

In the course of the WP of the bazalts, the chemical composition of minerals in the weathering crust is simplied, quantity of silicate minerals (pyroxene, fendspars, kaolinite ...) decreases, number of oxide, hydroxide minerals (goethite, hydrogoethite, gibbsite, boehmite...) encreases. Gibbsite, boehmite and alumogoethite are formed only during the feralite weathering process of the bazalts, manganit – only during the ferite WP.

In the course of the WP of the bazalts, the quality and quantity of removed material, the degree of removal and mobility of Na, K, Ca, Mg, Mn, Ni, Co, Pb, Zn, Cu .... increase and have the maximum value in the ferosialite stage, then decrease in the final (feralite) stage. At the same time quantity and degree of bringing and concentration of Al, Fe, Zr,

Cr, Ga ... increase and have the maximum value in the feralite stage; The correlation, geochemical association and differentiation of chemical lements, geochemical structure and formula of the weathering products are more and more complex.

The Na, K, Ca, Mg and Si removal, the Al bringing in the feralite WP and the Fe bringing in the ferite WP are the most intensive. So the feralite WP leads to the formation of bauxite, the ferite WP to the formation of brown iron ore.

MORPHOLOG' FEACHURES OF LONSDELEITE-CONTAINING DIAMONDS

Written by Ann V.Menner.

Copyright (C) 1990 IGEM,
Academy of Sciences of USSR,
Moscow, Staromonetny 35, 109017, USSR.

Printed and edited by A.Haser.
Wed 10 Jan 1990.

The investigations of morphology of lousdaleite-containing diamond grains were carried out with using optical photomicroscope of Opton firm and JEM-100C scanning electron microscope of Jeol firm.

Using X-rays methods (Laue method: RKOP-A camera, Mo-radiation, 12-14 hours exposition; and Debay method: RKD-57 camera, Fe-radiation, 8 hours exposition) polycrystalline and polyphase structures of grains were found. The cubic diamond phase prevails in all specimans; the content of lonsdaleite phase may reach 40% of light-coloured grains.

.- Graphite phase was discovered along with lonsdaleite and diamond both in dark-coloured grains and in light-coloured ones containing black inclusions.

The diamons show optical anysotrophy with wave, or block extinction. The light-coloured samples have orange-red colours of luminiscence. The grains sizes vary from 0.1 to 1.5 mm (the predominating sizes are 0.3-0.4 mm).

Basing on morphology features of investigated diamonds they (i.e. diamonds) may be referred to so-called "shale-like" diamond type, encounded in clastic

deposits in USSR. They look like peaces of flattened grains composed of parallel intergrown plates. The X-rays data obtained during our research show that the flat surfaces og grains are formed by (111) planes of diamonds crystallines. It was noticed that the single blocks of plates may be turned one to another on 10-50° corner. The "swalow tail" twins have been met also.

Some flattened intergrowings have appearense as flat octahedral triangular contoured cristals. Their side faces are not crystallorgaphycally expressed and have coarse-layered relief. Some other grains have either hexagonal or polygonal contours.

The grains surface microrelief is complicated by plastic deformation structures and corrosion ones. The deformation structures are shown like steps, seams or combs on the diamond surfaces. The orientation of this structures make two or three directions systems. Almost all grains carry the solution traces.

The surface relief features are due to formation of numerous corrosional pits, complex channels system and various positive forms.

The internal heterogeneousness of diamonds is displayed both in dispropotional dissolution of their surfaces and producing of directly oriented polyhedral solution "hills".

The coarse sculpture on the grains surfaces is explained as the result of the gas-corrosion processes effect during the postcristallisational period. The fine sculpture of internal solution channels walls is unusual. They have the fineglobular constitution with the globuls united in thin fibres, which are regularly oriented on the flat surfaces.

The such microrelief elements are supposed to be the newforms, that substitute the crystals corrosion defects.

EXSOLUTION CHARACTERS OF ILMENITE PLACERS AROUND THE BAY OF BENGAL AND THEIR GENETIC RELEVANCE.

S.Mitra and S.Ahmed, Department of Geological Sciences, Jadavpur University, Calcutta-700032, India.

Exsolution features in the Fe-Ti Oxide phases were studied from the beach samples collected from four sectors around the Bay of Bengal (Fig.1) : Cox's Bazar (CB),Bangladesh, in the eastern sector; Digha(D) and Puri(P) in the northern sector; Pondichery(PD) in the western sector and Kanyakumari(K) in the southern tip. The exsolutions are classed as : (A) ilmenite - hematite,(B) magnetite - ilmenite, (C) hematite - ilmenite - rutile, (D) hematite - rutile, (E) ilmenite - rutile, (F) magnetite - ilmenite-spinel and (G) ilmenite-spinel. The unexsolved ilmenite content in CB

(45%) are significantly less compared to other areas (P=90%, PD= 80%, K = 85%).

The eastern sector (CB) is remarkably enriched in exsolutions (>50%) of which type (A) is dominant (70-80%), followed by (B), (C),(D) and (E) ; but others are non-existant. In (A) type, the microscopic modal analysis shows ilmenite : hematite ratio to be about 70 : 30. The common exsolution products are lamellae of ilmenite (or hematite)in hematite (or ilmenite) host with bimodal distribution. The early generation lamellae were formed at 700°C fast diffusion process and the finer o s formed at later stage of crystallisation by slow diffusion at 500-600°C. As no pseudobrookite is found in CB it may be presumed that the temperature of the ilmenite crystallising environment was less than1000°C. Enriched ilmenite (> 85% $ilmenite_{ss}$) exsolves continuously while ilmenite with greater Fe_2O_3 content exsolves discontinuously[1]. The latter type may produce bimodality in a type environment as is reflected in the samples of CB. Type (A)was formed in a more oxygeneted part of the basaltic fraction in the upper mantle, which was tapped during 110 $\pm$ 5 m.y. at the early phase of volcanism as Sylhet-Rajmahal trap in the eastern India as a prologue to the Gondwana break up leading to the massive Deccan volcanism in central India.

Type(A) shows various textural patterns viz., seriate (most common), emulsion, granular, triangular and graphic textures.

57Fe Mössbauer spectra of ilmenite concentrate from CB show ilmenite Fe^{2+} doublet (at RT, I.S. = 0.97 mm/sec.,Q.S. = 0.68 mm/sec ; at 100 K,I.S. = 1.09 mm/sec., Q.S. = 1.01 mm./sec, superimposed on hematite Fe^{3+} sextet (at RT, I.S.= 0.34 mm./sec., Q.S. = 0.39 mm./sec., hf = 487 KOe; at 100 K,I.S. = 0.41 mm./sec.,Q.S.= 0.39 mm./sec., hf = 512 KOe) with a ratio of 28 : 72 corresponding to the optical modal data (70:30). XRD and wet chemical study also support this. The Mössbauer spectra substantiates the predominance of type (A) but almost obscures the presence of other varieties.All Indian ilmenites show considerable leaching effects and alterations (70-80%) and have higher content of titanium than CB ilmenites (36-40% TiO_2).

In contrast to CB samples,ilmenites from other areas show significantly lesser (10-20%) content of exsolutions. In these areas (B), (C), (D), (E), (F) and (G) types of exsolutions dominate as much as the (A) type (dominant in CB).

Beach sands of CB are derived from the rocks of the eastern Bangladesh highlands[2].The ilmenite and other opaques,however, were contributed by the material carried from the northern part of the Bengal Basin covered by Sylhet - Rajmahal basltic trap rocks. During the Himalayan orogeny these traps sagged to form a part of the Bengal Foredeep, sediments of which may be carried far down into the tertiary basin of the Bay of Bengal serving as the repository of sediments carrying heavies from the Sylhet Trap basalts.

The ilmenite of other placers were mostly derived from rocks

of the Eastern Ghat and the granulites/charnockites/anorthosites in the South Indian Precambrian shield.

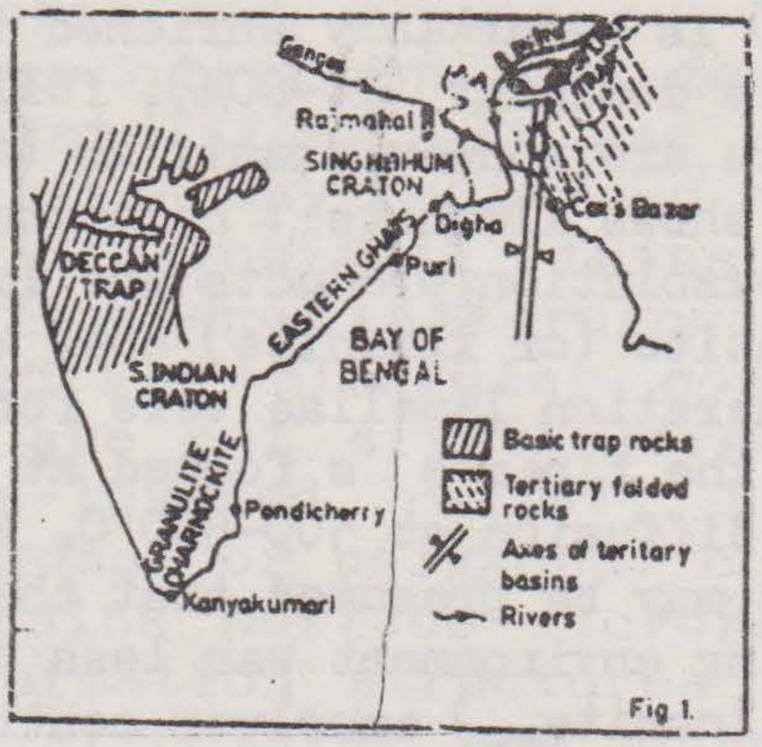

Fig 1.

1. Kretchsmar, U.H. and R.H. McNutt (1971). Can.J. Earth Sci., 8,947.

2. Mitra,S. and S.S.Ahmed (1990). J.Geol.Soc. India, (in press).

1.42P

PROBLEMS IN HIGH-REDUCED AND HIGH-OXIDATED MINERAL FORMS.

M.I. Novgorodova, IGEM, Academy of sciences of the USSR, Moscow, Staromonetny, 35, 109017, USSR

In the space of ten years mineralogical investigations showed that it is possible for most of elements to be in native state in nature. Native metals were founded among of lytophilic elements (Si, Al, Mg, Ti), more wide become list of chalcophilic and syderophilic elements observed in native form in native (Cd, Co, Mn, Cr, Re, In).

As estimated, high-reducred mineral phases are present in a small quantity in magmatic, sedimentary, metamorphic rocks and in ores of different type, mostly in gold deposits. Formation of high-reduced mineral forms is connected with reducing fluids rich in hydrogen and hydrocarbons.

There are carbides, silicides, rare phosphides and carbon in form of grafite and carbon matter that is considered as fine-grained disordered mixture of polymorphic compounds of carbon, natural elementoorganic compounds and hard polymeric hydrocarbons, in paragenic association with native metals. The associations are formed by decomposition of volatile elementoorganic compounds that are considered as migrating forms of oreforming elements in endogenetic processes. As by-products there are sulfur, halogen, hydroxyl and water groups so native metalls and carbon are accompanied by micas, chlorites, hydroxides, oxides, sulfides etc.

Just as immediate crystallization is impossible for a number of well-and low crystallised phases so idea of its formation in result of activity of reducing fluids of system C-H-O-N was suggested an.

As supposed, such fluids may be producted at different depths within of upper mantle and earth crust. Transformation of H_2O-CO_2 fluids in reducing ones is possible in result of action of flows of H_2 and CH_4 connected with deep degasation of earth along main breaks within of reftogenic zones.
There are produced proofs, that in local parts of earth crust fluid systems with crystallisation of some minerals by VLS-way are possible.
In addition to deep-formed flows of recucing gases there are also migration of enriched of oxigen gases along penetrable zones of breaks and draining system of vadose waters into endogenic mineralforming system.
Increase of oxigation potential due to mixing of hydroterms and vadose waters lead to formation of unusual mineral associations with high-oxidated elements in composition of minerals. As exsample of it may be consider associations of native gold with carbonates and tellurates of bismutile, widespread in endogenic gold ores out of the zone of hypergene oxidation.
Interaction of reducing fluids with atmospheric gases which penetrate from surfase by fracture zones sometimes lead to local explosions, that are accompanied by formation of minerals in high temperature- and pressure gradient conditions. Exsamples of this phenomena ar showed.

HYDROTHERMAL-FLOTATION MECHANISM OF GOLD-ORE SHOOTS AND BONANZAS FORMATION

P114

Nikolai S. Ostapenko

Amur Integrated Research Institute Far East Branch of the USSR Academy of Sciences, Relochniy 1,Blagoveshchensk, 675000, USSR

Veins of filling in gold deposits are characterized by variation in thickness and extremely irregular distribution of native gold,as well as by gold ore shoots and bonanzas. In different deposits gold mainly concentrated during one of the intermediate stages of ore-forming processes, besides gold concentration extended over considerable time interval. It is confirmed by the fact,that gold particles show different composition,and the varia-

tions in fineness range up to 100-200°/$_{oo}$. The parts of veins adjacent to selvages,as well as their upper layers are enriched in gold compared to other parts.Usually,the gold enriched portions are steep shoot-like bodies.They are confined to swells,particularly their upper portions, also to the wall rocks framing the middle-seized veins laterally and from the top.

For the Amur Region deposits the absence of substantial vertical temperature gradients in veins in the gold-formation processes has been established.Unlike those in quartz,the inclusions in gold,though posessing similar composition are either saturated with gases or purely gaseous. It's worth mentioning,that native gold belongs to the group of hydrophobic minerals and posesses natural flotation properties. The proposed data bring to a conclusion,that the main factor in gold-ore formation is rather pressure than temperature. Intermittent opening of ore-hosting fractures is supplemented by pressure fluctuations, resulting in repeated phase differentiation and oversaturation of fluids with such components as gold and gas.Consequently,there formed conditions for newly originated gold particles flotation owing to rising of gas bubbles which resulted in concentration of gold in the above mentioned portions of veins.

The author holds that hydrothermal-flotation mechanism accounts for the origin of higher gold concentrations in veins of filling and stockwerk zones within deposits with different depths,but particularly it is true in cases of shallow vein deposits.The arguments in favour of this mechanism and some evidence to illustrate its work are given in the paper.

1.13P Typomorphic Properties of Sphalerite as Indicator of Ore-forming Processes

Z.V. Otkhmezuri, R.A. Akhvlediani, R.T.Rodonaia,Djanelidze
Geological Institute of Academy of Science of Georgian SSR Zoia Rukhadze Str. 1, b. 9, 380093 Tbilisi USSR

1. typomorphic properties of sphalerites are investigated at lead-zine deposits and ore manifestations of the Kvaisa ore filed (Georgia USSR). They are situated on the Southern slope of the Greater Caucasus, confined to the system of parallel E-W trending faults and are localized in Middle Jurassic basaltoid volcanics and Upper Jurassic reef limestones.Ore bodis represented by veins, veinlet-impregnated ores of stockwork type and metasomatic lodes. The ores are built of sphalerite, galena, calcite, quartz, barite and some rate sulphide minerals. Sphalerite is predominantly of cleiophane type lightbrown and lightyellow. Kvaisa sphalerites are characterized by colloform structure.

2. Statistical distribution of izomorphic admixtures of Fe (from 0.08 up to 5.2 weight %),Mn (from 0.02-0.29 w %) and Cd (from 0.05 to 0.304 w %) in Kvaisa sphalerites exposing rather complicated relations,unsubmitted to the rule of normal distribution, it proves the heterogeneity of mineralforming system, determined by heterogeneous composition of country rocks influencing the mineralforming regime.

3. Sphalerites, studied structurally, apart from purely cubic polytypes constituting 35.3% of total sum of excerption are represented by mixture with rhombic polytype R_{15} (60.8%)and also rather seldom by R_9 (3.9%) polytype. It is stated, that small admixture of main izomorphic elements up to 6% has insignificant effects on sphalerite lattice parameter (from 5.4050 to 5.4056 Å), and increase in admixture sum causes the increase of the parameter up to 5.4090 Å. It may be expressed by the following regression formula a =5.4039 +0.005655 Mn +0.0051 Cd +0.000276 Fe.

4. Calculation of thermodynamic conditions of ore formation, based on distribution of isomorphic admixtures and structural pecularities in comparizon with the date on fluid inclusions enabled us to state, that the mineral formation of Kvaisa deposites had taken place under moderate and low temperature condition in 320-200° C interval,at pressure of 0.8-1.2 K bars from the calcium-hydrocarbonate-sulphate solutions at pH very close to neutral with the value from 6.3 to 8.8 and sulphur fugacity-$lgfs_2$ -6-9 .

EPIDOTE: AN INDICATOR OF PALEOCONDITIONS OCCURRING IN

THE FOSSIL HYDROTHERMAL SYSTEM OF SAINT-MARTIN.

Patricia PATRIER, and Daniel BEAUFORT.
Laboratoire de Pétrologie des Altérations Hydrothermales, URA 721 CNRS, Université de Poitiers, 40 avenue du Recteur Pineau, 86022 Poitiers cédex, France.

The geothermal field of Saint Martin (Lesser Antilles) emplaced during the thermal evolution subsequent to the intrusion of a 30 MY old quartz diorite. Epidote is a common mineral in the roots of this geothermal system. It crystallized as far as 2,5 km from the intrusion, for temperatures ranging from 220 to 350°C. This mineral shows a progressive enrichment in iron and/or manganese (X_{PM+PS} increases from 0.21 to 0.30) coupled with an increase of chemical dispersion with increasing distance from the pluton. The most iron rich epidotes appear in hematite bearing paragenesis. The iron enrichment is correlated with the oxygen fugacity which may locally depend on the bulk rock chemistry. It may reflect an increasing influence of meteoric fluids.

For a better understanding of epidotes chemical dispersions, Mössbauer spectroscopy has been performed on five samples. If Fe^{3+} ions accommodated in M(3) sites represent the great majority of the total iron present (≥90%), few amounts assigned to M(1) sites have been evidenced. An ordering parameter has been deduced from the Fe^{3+} occupancy. An increase of epidotes disorder with the distance from the intrusion has been demonstrated. A good correlation is observed between the ordering state of epidotes and the paleotemperature distribution (estimated from fluid inclusion study). A rapid crystallization cannot explain the disequilibrium state displayed by some samples. Kinetics of ordering are slow, the more ordered minerals coincide with those affected by longer cooling event. However, variations of external physicochemical conditions (meteoric contamination...) in the external part of the hydrothermal system probably accentuated the disequilibrium state of the outer epidotes. Epidotes, which display a greater chemical dispersion and disequilibrium state, are also characterized by smaller grain sizes.

The quantitative analysis of crystals size has been performed on eight samples representative of the thermal diffusion gradient developed around the intrusion, or located in thermal anomalous zones. In order to obtain accurate results, this statistical comparative study has been realized in environments providing only temperature dependent crystals size

variations. This condition is verified in epidote + quartz bearing veinlets, where epidotes, developed during one crystallization event, occur as euhedral crystals enclosed in later anhedral quartz. Lengths and widths vary exponentially with increasing temperature, while their ratio is nearly constant. The crystal growth (controlled by interface reactions) displays an exponential dependence of rate upon temperature. These results reveal a close relation between epidote crystals size and estimated temperature which is proposed as a possible geothermometer. It should be now interesting to verify these observations in other geothermal environments.

HYPOGENE SULPHATE–SULPHIDE ZONING IN THE ČELOPEČ COPPER-PYRITE DEPOSIT, BULGARIA

Rumen Petrunov,
Geological Institute, Bulgarian Academy of Sciences, 1113 Sofia, Bulgaria

The Čelopeč ore mineralizations (massive and stockwork) occupy the central parts of hydrothermally altered zones in Upper-Cretaceous volcanic-sedimentary rocks of andesitic and andesite-dacitic composition. In the upper levels, paragenetic ore sequences have been divided into three types of mineralizations including iron-sulphide, copper-arsenic-sulphide and polymetallic assemblages.

Drilling operations have struck an abundant pyrite-anhydrite mineralization in the form of a network of veinlets and veins up to 5-6 *m* thick at depths exceeding 1000 *m*. At higher hypsometric levels, there are pyrite and quartz forming zones of abundant veinlets and veins blending into dense, almost bimineral masses of pyrite and chalcedonic quartz in the uppermost part of the deposit. It is shown that: the pyrite-anhydrite mineralization in depth is spatially divided from the incumbent quartz-pyrite mineralization; the two have identical age relationships with the later *Cu–As*-sulphide and polymetallic mineralizations; pyrite, the common mineral of the two mineralizations, has identical *Co* and *Ni* contents in both of them; this pyrite differs in microcomposition from pyrite of the later mineralizations; in the zone of its formation, anhydrite is partly recrystallized and redeposited along with quartz and base-metal sulphides, the two anhydrites (the primary and the redeposited) having different infrared spectra. All this is interpreted here as evidence of a single calcium-iron sulphate-sulphide stage in the evolution of the hydrothermal process during which the continuous influx of an ascending fluid produced two parageneses: 1) a deeper anhydrite, and 2) an upper pyrite one. Thus, we regard the conditions, which existed at a depth of about 1000 *m* in the Čelopeč deposit, as a specific geochemical threshold at which the nature of mineral formation abruptly

changed from a prevailing sulphate (anhydrite) deposition in depth to a sulphide one (pyrite) in the upper levels producing the well-defined sulphate-sulphide vertical zoning in the hydrothermal system of *Ca*, *Si*, *Fe* and *S* components (Fig.). This zoning reflects the evolution of sulphate- and sulphide- sulphur activities controlled by the temperature-pressure variations, by the exchange of components with the host rocks, and by transitions into the solid phase in the mineral-forming system.

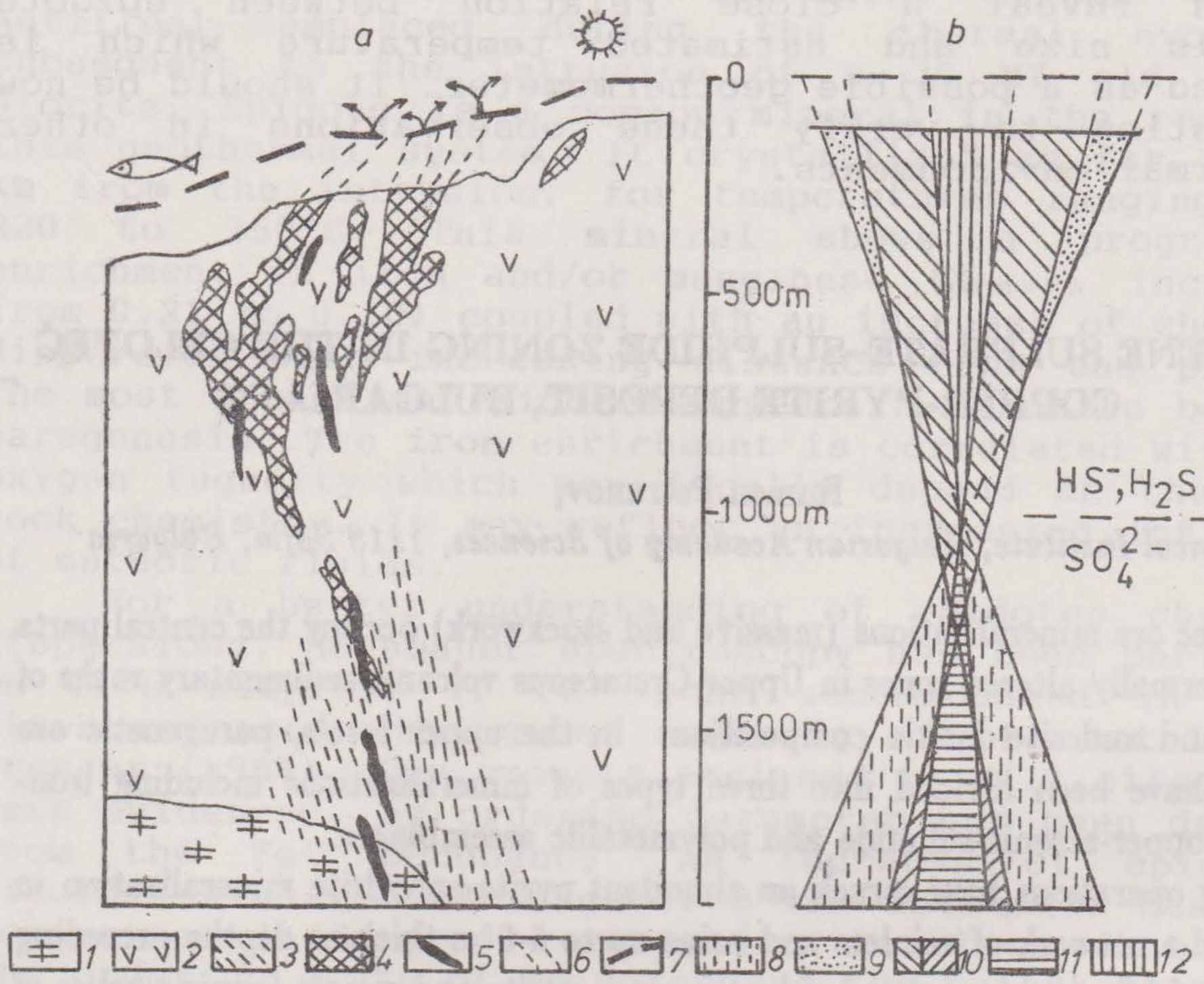

Fig. A model of the calcium-iron sulphate-sulphide stage with the superimposed later processes. a - generalized geological cross-section; b - scheme of vertical development of mineralizations: 1 - basement; 2 - volcanics; 3 - anhydrite; 4 - copper-pyrite ore bodies; 5 - polymetallic mineralizations; 6 - denuded section; 7 - paleodenudation surface; 8 - anhydrite paragenesis; 9 - pyrite paragenesis; 10 to 12 - superimposed mineralizations: 10 - *Cu-As*-sulphide; 11 - quartz-sphalerite-chalcopyrite (with redeposited anhydrite); 12 - barite- galena-sphalerite.

1.32H

OCCURRENCE AND GENSIS OF ZEOLITES FROM BASALTIC ROCKS OF MALWA PLATEAL, INDIA

Dr. Vilas L. Punwatkar, Assistant Professor of Geology, Department of Geology, Holkar Science College, Indore–452001, Madhya Pradesh, India

The Malwa plateau area belongs to middle traps of India. It is predominantely constituted of basaltic flows of massive, fine grained, porphyritic, vericular and amygelaloidal

charactres having considerable variations in thire thicknesses. Zeolites occur particularly wide spread in volcanicclastic strata and developed either as fillings in the amygdular carities or as products of alterations due to late hydrohhermal carities. Zeolites are recorded from trops of variable altitude, some time shows zoning nature. The identified varieties are heulandite, stilbite, mesilite, Laumantite, Chabazite, thomsonite and clinopti lite. The local variations in the composition of each variety are over a short distance. A genetically the order of crystallization of specific zeolites are important as they lead to their frequent zonal distribution. The species and amount of zeolite as function of texture and composition of the host rock, composition of interstitial water, age and temperature. The enlargement of zeolite bearing amygdoles by corrossion of the adjacent basalt, but is likely that the bulk of the zealites in the carities crystallized from materials migrating from the surrounding rock. The trend of zeolite formation within one fracture of amygdale as well as within a set of them may be normally from high temperature to low temperature ones and from those high in alymina to high in silica or Viceversa. The inter–related zeolite sequences paragenesis and their normal reverse trend is of importance both for tracing the tectomic history of an area and the conditions of formation of zeolite assemblages.

Zeolite are formed by the precipitation of the fluids which permeated the basalt in the earlier formed vericles, pipes and fractures. It seems that a fluid reacted with wall rocks to dissolve various components within are necessary for the formation of zeolites. The abundants glass in the host rock appears to have played an important role in zeolitisation and chloitisation by the effects of hydrothermal activity. The temperature of formation of minerals (Quartz and heulandite) attains a maximum of even 240 ℃, presented that the cirolating meteoric water must have been heated due to some exothermic processes causing hydration of the ferromagnesium minerals and formation of the zeolites.

Zeolites possess a typical micro porous structure which filled with water molecules and exchangable cations. It has adsorption properties which is useful for calalyst purifies of gases and liquid and orgenic fertilizer. Thermal analysis, XRD, IR and microstructural analysis are made useful in the indentification and characterization studies of zeolites in order to find more applications. The study will help in assessing the potential of zeolites, when country is facing an actute shortage of the indigineoys resources of molecular sieves and adsortants.

1.274
P01.26

STUDY OF PROSPECTING MINERALOGY OF SPINEL GROUP IN KIMBERLITES IN CHINA

Qin Shuying Deng Chujun Guo Yuemin
(Institute of Mineral Deposits, Beijing, PRC)

Prospecting Mineralogy is one of main direction of the contemporary mineralogy. As we all know, spinels, which can be easily

selected from heavy sand of river system and kimberlites, are the main associated minerals of diamond. In the late sixties, because widespread using of electron microprobe analysis, spinels play an important role in the process of diamond-finding.

It is our intention to reveal the regional characteristics of mineral chemistry of spinels, based on the studies of spinels in some kimbertites provinces and comparing with those in other regions in China and USSR. The authors use the method of diagram of minal components of spinel group, that simplies the classification of G.A. Sokotov and N.V. Pavlov, making it convenient for the ore searching use.

1. The diagraming and classification of spinel group

The main end members of spinels are chromite, spinel, magnetite, magnezioferrite and ulvospinel. The triangular diagram was made by using the contents of tribasic cations and was divided into eight parts with no mineral projective points falling in the eighth part (Fig.1). In Fig.1, 1-chromite, 2-spinel-chromite, 3-chromite-spinel, 4-spinel, 5-magnetite-chromite, 6-chromite-magnetite, 7-magnetite. The first part was subdivided into two subparts (1a and 1b). The content of Mg and Fe was subdivided into the range of 1.00-0.75 and 0.00-0.25, 0.75-0.50 and 0.25-0.50, 0.50-0.25 and 0.50-0.75, 0.25-0.00 and 0.75-1.00 and were prefixed with magnezio-, ferromagnezio-, magnezioferro- and ferro- respectively.

2. The distribution characteristics of spinel group in kimberlites and their ralative rocks

From the diagrams, we find out that there are obvious regional differences among the spinel group in the different regions of kim-berlites in China.

(1) The points of spinels in kimbertites in Shandong and Liaoning provices fall in 1. Most points of chromites in kimbertite rocks rich in diamond fall in 1a. Most points of spinels in the rich diamond zone of Shandong, with more Ti than Southern Liaoning's, fall in the right(Fig.2), while the points of Liaoning fall in the left (Fig.3). Those of Northern Liaoning are placed in the 1b and 2, 3, (Fig.3), showing poor content of diamond.

(2) The points of spinels in kimberlites in Yangtze platform fall in 1b, indicating the content of Al and Fe increasing, but the content of diamond decreasing (Fig.4-1).

(3) The points of spinels in kimberlites in Henan provice and in picrite-porphyrite in Hubei provice are placed in the low left of 1b and 2, 3, without diamond (Fig.4-2, 4-3).

(4) The points of spinels in basic-ultrabasic rocks in Northern Jiangsu provice and Hebei province are placed in the low part of 1b and 5, 6 (Fig.5-2, 5-1).

(5)The points of spinels in ultrabasic rocks in Inner Mongolia geosynclinal area fall in 2, 3 with high content of Al (Fig.5-3).

(6)There are some similarity of spinels in kimbertites between Yakut, USSR and China. The points of intergrowth spinels with diamond or conclusion in diamonds in USSR, fall in the near top of 1a.

3. Conclusion

The diagrams of the spinel minal components show,(1)The method is exact and easy, and the classification is reasonable; (2)In the

process of diamond-search, studying and comparing the spinel regional characteristics of known and unknown areas is an important way for prospecting.

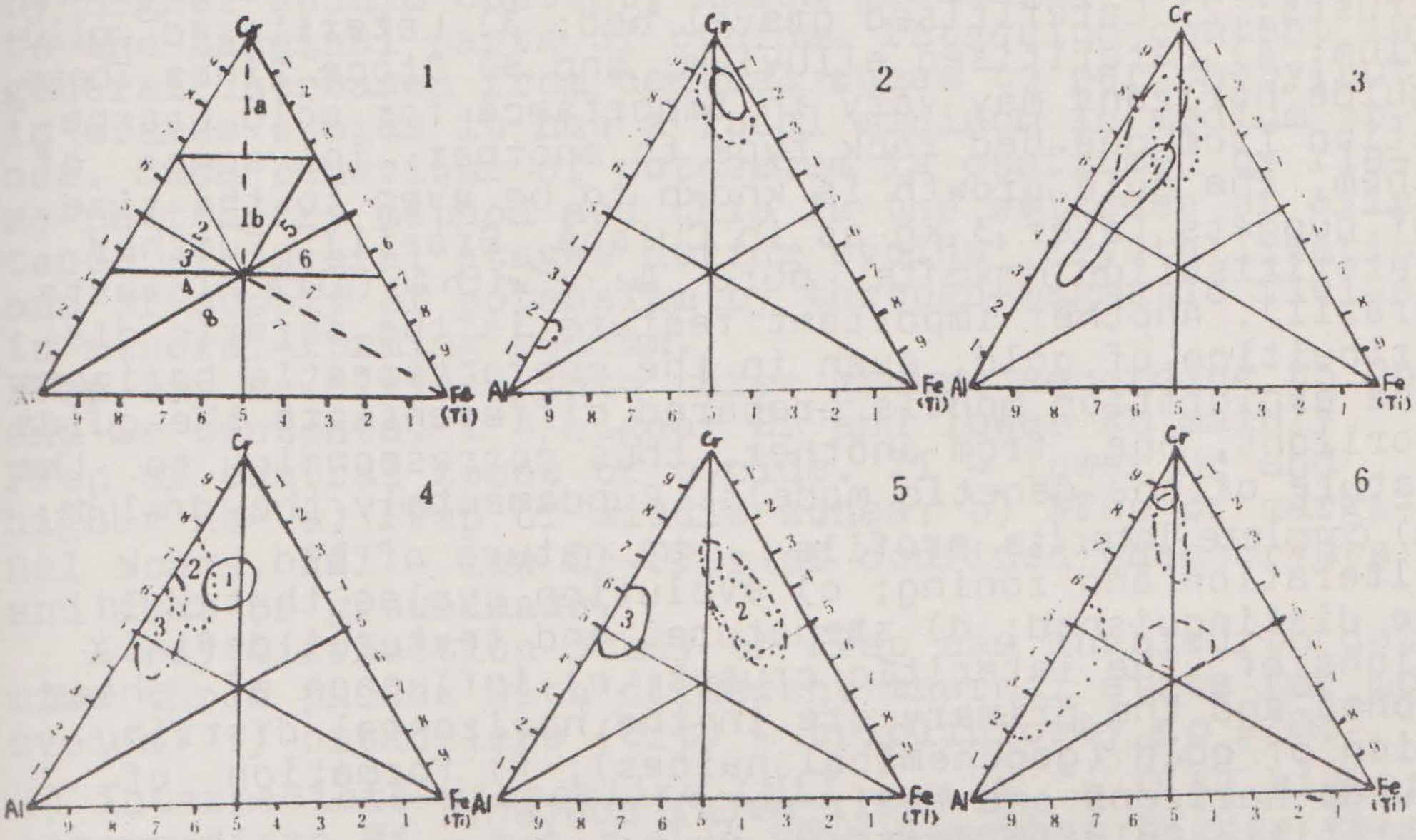

LATERITIC GOLD: SOME MODELS FOR EXPLORATION

A. Bhaskara Rao & Jessica B. Carvalho, Dept. of Geochemistry & Mineral Resources, University of Brasilia, 70910 - Brasilia, Brazil.

Laterites are known extensively in the Third World (lat. 30°N to 30°S) and have called the attention of scientists only recently as hosts of important mineral deposits, of which both Au and Pt are included. Compact laterite coverings over any type of bed-rock could be developed in tropical, subtropical and subarid conditions. Under equatorial climate, laterites form soils and could favour the formation of "stonelines". The supergene enrichment favours the concentration of elements in these surficial deposits, derived from a protore of low tenor. Thus, in Australia, India and Brazil deposits of lateritic nature are being constantly discovered.

For the preparation of a genetic model of auriferous lateritic deposits, the basic parameters are: a) bed rock type; b) topographic nature during the laterite evolution; c) climates dominating at that time; d) alteration processes resulted in degree of decomposition, solution, migration and deposition; e) chemical activitions and formation of metal complexes; f) dessication resulting in precipitation of diferent minerals, giving rise to vertical and horizontal zoning and control.

It is important to mention here typical guide horizons with Au, based on a structural classification of the laterite crusts, as follows: 1) Pisolithic and nodular crusts; 2) Lateritised gravel bed; 3) Lateritised colluvium; 4) Lateritised elluvium; and 5) Stone lines. These guide horizons may vary in importance for gold prospection from one bed rock type to another. In some of them, the gold growth is known to be even to the size of nuggets (over 3 Kg as in Cuiabá, Brazil). Further, lateritisation deposits pure Au or with Ag (Alta Floresta, Brazil). Another important feature is the erratic distribuition of gold, even in the characterestic horizons. The exploration models prepared differentiate the guide horizons, one from another, thus corresponding to the nature of the genetic models. Fundamentaly they include: a) complete laterite profile; b) nature of bed rock alteration and zoning; c) evolution cycles that could be distinguished; d) structural and textural definitions of the lateritic crusts; e) influence of shear zones and the primary ore in the horizontal distribution of gold (geochemical haloes); f) formation of guide horizons and their metal content.
Lateritic Gold is destined to contribute very effectively in the development of small mines in great number of countries in the Third World, enhancing the production at low cost and guiding detailed prospection for primary ores by geochemical patterns.

1.21V

ONTOGENESIS OF POTASH FELDSPAR OVOIDS FROM RAPAKIVI GRANITES

Rundquist, N.D. Geology Department, University of Leningrad. University embankment, 7/9, Leningrad, 199034, USSR.

Developing the ideas of minerals' ontogenesis theory, the ovoids of potash feldspar (PFsp) from rapakivi granites of the Wiborg massif were researched with the aim to distinguish the conditions and succession of their formation. According to classification (which is accepted in the Soviet Union) two phases of rapakivi granites contain ovoids: wiborgite (II phase) and trachytoid rapakivi (III phase).
The morphostructural investigation of ovoids has enabled to determine the gradual transitions in their shape, size and extent of development of plagioclase mantles. The extremely and the most characteristic vovoids type were revealed, as well as zones in their internal structure. The chemical composition of PFsp, perthites and inclusions of other minerals in diffe-

rent zones of various ovoids' types was studied on microanalyzer. PFsp of central zones of ovoids differ by higher soduim content, which gradually decreased to the marginal parts of ovoids. Potassium content in general increased from central zones to periphery, but in coarse ovoids it has a local minimum in medium zones. Such behaviour of potassium is confirmed by flame-photometry method and this is the evidence of existence of several stages during ovoids' crystallization and of supply of potassium by through-magmatic fluids in mineral-forming medium.

PFsp may be divided into three groups according to Rb and Sr contents. I - higher Sr and lower Rb mainly PFsp of central zones of ovoids. II - lower Sr and higher Rb- a) PFsp of middle zones; b) PFsp of marginal zones. III - low Sr-PFsp of confined phenocrysts and that of groundmass.

X-ray diffraction study of PFsp has enabled to determine three phases with different thermal state for most ovoids: 1) orthoclase (Ort) - triclinicity $\Delta\rho = 0$; 2) intermediate microcline (Mi) - $\Delta\rho = 0,4$; higher intermediate Mi - $\Delta\rho = 0,7$. The somewhat higher thermal state is characteristic for ovoids' central zones (subordinate PFsp with $\Delta\rho = 0; 0,4$) and slightly lower thermal state for marginal zones (subordinate Mi with $\Delta\rho = 0,7$). Some ovoids have higher thermal state and Ort phase in these ovoids is predominant. There are two kinds of confined phenocrysts: 1) with higher thermal state-subordinate Ort and Mi with $\Delta\rho = 0,4$; 2) with lower thermal state - subordinate intermediate Mi with $\Delta\rho = 0,82$. PFsp of groundmass has the thermal state which is close to that of ovoids' periphery zones, and slightly lower than PFsp of ovoids as a whole.

Summarizing the data it can be supposed, that there were some stages of ovoids' crystallization. The crystallization of central parts in comparison with middle - periphery zones of ovoids was under higher temperature conditions, and the composition and structure of PFsp confirm this, The entire "history" of ovoids formation is reflected in coarse ovoids. Crystallization of middle - small size ovoids corresponds to individual stages, often final, of coarse ovoids vformation. Crystallization of confined phenocrysts, as that of groundmass PFsp began during final stage of ovoids formation.

FACTORS CONTROLLING THE RADIOACTIVE ANOMALIES IN GRANITES S.E. ASWAN TOWN, EGYPT

G.M. SALLOUM

AL-Azhar University, Cairo

As a result of radiometric investigation, field measurements and regarding the distribution of the radioactivity in each rock type, it can be concluded that, each of the different rock-units has its distrinctive range of gamma radioactivity. The coarse grained granite and the related dykes, the fine grained granite and pegmatites are of particular interest from the radioactivity point of view. It is possibly to conclude that, the high radioactivity in the area underconsideration is attributed to the Uranium present in the accessory minerals, such as, Zircon, Apatite and Sphene as well as the presence of K_{40} present in the potash feldspars and iron oxides. In addition the presence of Uranium and Thorium mineralization .

The radioactive anomalies are lithologically and structurally controlled. Concerning the origin of the radioactive mineralizations, three concepts namely : leaching, syngenitic and hydrothermal have been proposed and discussed in detailed .

Spacial and Genetic Relationship of Travertines with Endogenic Metallization of Various Genesis.

VLADIMIR SEDLETSKI, GRIGORI SEMENOV, DMITRI KHOLODNY
Rostov State University, Institute of Physical and Organic Chemistry
USSR

Travertines widly spred in the regions of tectono-magmatic activity have been treated by now (Baikov, Sedletski, Se-

menov, 1982, 1983, Semenov, 1984, etc.) without relating them to the endogenous and exogenous processes bringing to their origination which led to the formation of ore mineral deposits of various origin. In sprite of the fact that travertine bodies themselves are the concentrators of the commercial amounts of manganese and tungsten - deposits Unsia (Bolivia), Salin Valley (California), Mayer (Arizona), Golconda (Nevada), of arsenic - Nalachevskoye (Kamchatka peninsula) earlier only ore commercial type of travertine deposits was emphasized (Babkin and others, 1976). The mercury mineralization as metacinnabarite and cinnabar concentrated in travertine formations as of siliceous (geyserite,opal,chalcedony and silicon) and carbonate (aragonite, calcite) compounds. By their form and sedimentation they are either subaerial formation type of flows and hats (Pui-Pui, New Zealand; Apapel, Kamchatka; Sulphur Bank and Noksvill, California) or cross-cutting bodies filling gaping cracks and also karst cavities (Terlingua,USA).

At the same time travertine formation processes being the final phase of polycyclic chemical reactions of the major reagents-hydrothermal solution (water fluid)-enclosing substance is an evidence of ore concentrations in the depth which is supported by travertine spreading over the deposits and by the manifestation of varios genesis in Bolivia, USA, USSR and other countries. This fact allowed us to reccommend travertines as a new searching evidence of endogenous mineralization in the regions of tectono-magmatic activity for example the Caucasus.

The spacial and genetic relationship is established between travertines and mineralization in the bounds of the Caucasus. Mercury mineralization and travertines of Tsess deposit in Naro-Mamison ore area (Tsertsvadze, 1972) are related genetically. Here cinnabar is established in travertines of aragonite composition which cement the Quaternary deposits. Travertines exhibit the spacial relationship with the Cimmerian and Alpine rare-metal ores of Tyrnyaus (The Centre Caucasus) and also with realgar-orpiment ores of Darrydag (The Transcaucasus) Travertines are spacially related with polymetallic metallization of Sadon ore area (The Centre Caucasus), copper-pyrrhotite metallization of Kizil-Dere deposit (The Eastern Caucasus) and mercury metallization of Kyshkit (The Western Caucasus).

In the last case we deel with for the first time asolated in the Caucasus siliceous-carbonate paleotravertine deposit before latepermian age (Bykov, Semenov, 1983). Ferruginous-carbonate lens-like body is known in the north-east part of quartz albitophyre massif of river Kysh-Kit which is a right tributary of river Aksaut. The extent of lens is about 180m and thickness is under 20m. The centre part of body is consists of light-grey calcite with admixture of fine-disperceably increeses nearer to the periphery.Also the presence of quartz, chalcedony,opal and pyrite is noted.The formation

of ferruginous-carbonate rocks is connected by us with postvolcanic carbonate and siliceous-carbonate paleotravertines depositing in the area of thermal spring issues with the following lithification of travertines.

Lens-like bodies of Devonian travertines is known (Ohapkin, 1961) among eruptive-sedimentary deposits of Kopievo series in Minusinsk intermontane trough (Eastern Siberia). Maximum thickness of lenses is 90m and length is under 2000m.

In those cases when we don't observe carbonate neogenesises in general genetic series: ore body-travertine deposit this may be connected on the one hand with the loss of hydrothermal solution of the gaseous components at the approach to the day surface which is seen in a powerful calcitization of enclosing rocks, on the other hand travertine deposits may be destroyed in the result of erosion by water or diagnosticated as limestone of normal sedimentological series. It isn't excluded that processes of travertine formation on the day surface in a number of cases coincided with postcarbonate stage of most ore deposits on the depth.

Therefore in the regions of tectono-magmatic activity travertine formation is a final phase of ore-forming processes which occured in the considerable depth and formed ore deposits of various genesis.

RESEARCH ON TYPOMORPHISM OF GOETHITE FROM GOSSAN--TYPE GOLD DEPOSITS IN MIDDLE AND LOWER REACHES OF YANGTZE RIVER , CHINA

SHAO Jielian;LI Lipimg, Department of Geology, China University of Geosciences, Wuhan, Hubei 430074, People's Republic of China

In the middle and lower reaches of Yangtze River, China , goethite is the chiefest component as well as the chiefest gold carrier mineral of gossan-type gold deposits. The authors classified the shapes of goethite in Daijiachong and Wujia gold ores into three types, i.e. ,compacting, powdery and needle-like. Because of the difference of these three types goethite in water content, crystallinity, grain size and crystal structure compacting degree, their reflection, colour indices, X-ray diffraction spectrum, cell parameter,differential thermal effect, infrared spectrum, Mössbauer spectrum and even gold-bearing ability are different. The typomorphism of goethite is provided in this paper.

In conclusion, the powdery goethite with the the richest gold capacity has such typomorphs for rich ore deposits as follow:weak peaks, ocurence of platforms on most peak tops, or existence of not sharp tops of X-ray diffraction spectrogram ; cell volume larger than 139$Å^3$; heat absorption valley teperature of differential thermal curve between 325 to 363°C; hydroxyl vibration δ-OH of infrared spectrum higher than 895 cm^{-1} (the highest being 902 cm^{-1}); quadrupole splitting of Mössbauer spectrum between 0.4 to 0.45 ; and chemical composition with more than 0.3% Cu, 0.1% p_b, 0.15% Zn, 0.2% As, 0.01% Ni, and 0.06% Mn.

ORE MINERALOGY AND GENETIC MINERALOGY OF "QIYUGOU TYPE" GOLD DEPOSITS, CHINA

1.294

Shao Kezhong, Li Shengrong, Luan Wenlou, Hebei College of Geology, Shijiazhuang, Hebei 050031, China

The "Qiyugou type" of gold deposits in Qiyugou area, Henan province, China, is a poly–type gold deposit system dominated by explosive breccia. In this type of gold deposits, there is variety of species of Bi–sulfosalt and Bi–telluride minerals though they are not large in quantity. The Bi–sulfosalts include cosalite, galenobismutite, lillianite, wittichenite and tetradymite, and the Bi–tellurides are represented by tsumoite, tellurobismuthite and two other unnamed ones. The appearance of these minerals has provided geochemical evidence for establishing Bi–Au or Te–Bi–Au type of ore deposits. Tsumoite was first discovered in our country. In view of the fact that these Bi–bearing minerals occurred in the middle to late (especially late) stage of metallization and in the gold–rich blocks, so they can be taken as an important hint for prospecting gold ore bodies.

Gold minerals are dominated by native gold. These {111} simple crystal and {111}+{110} combination crystal form high bismuth content and {110} euhedral crystals of late stage of mineralization all indicate a gold–rich block. Therefore, they are important signs for prospecting and evaluation of gold deposits. Pyrite, being large in quantity, is a major gold carrier. The occurrence of {100}+{111} combination forms of pyrite is a mark of gold mineralization. Compared with standard ones, this particular pyrite possesses lower hardness, reflectivity and a_0 value, and higher specfic gravity, and can be regared as single electronic type conductor. These are all typomorphic characters of gold mineralization. Quartz is a dominant gangue mineral. Its thermoluminescent curves show prominent differences, providing solid basis for setting up three "vanward–","major–" and "late–" phases of mineralization; its double–peak type of thermoluminescent curves are effective prospecting indication. The CO_2 optical density(D_{CO_2}), Ag, Bi and As+Sb+Bi contents of quartz are positively related with its Au content, and they, hence, are considered as composition typomorphic marks for this type of gold deposits. The greyish white fine–grained xenomorphic quartz closely associated with biotite, and the colorless coarse–grained hexagonal prismatic quartz closely associated with calcite, respectively signify the end of "vanward mineralization period" and whole mineralization of deposits, and represent weak gold mineralization stages. On other hand, the subhedral quartz closely associated with poly–metallic sulfides and orthoclase has a intimate relation with gold mineralization, being and thus can be looked at as guiding mark for prospecting and exploration of "Qiyugou Type" of gold ore deposits.

126H

THERMOELECTRIC TYPOMORPHISM OF PYRITE IN GOLD DEPOSITS OF EASTERN SHANDONG PROVINCE

Shao Wei, Chen Guangyuan, Division of Genetic Mineralogy, Chinese University of Geosciences, Beijing, 100083, PRC

Research in semiconductor minerals and thermoelectricity of pyrite had been carried of during 1950′s–1980′s in U.S.A. and USSR, but the study of thermoelectric typomorphism of pyrite from gold deposits is rare. A summary of systematical investigation in thermoelectricity of pyrite from seven gold deposits in eastern Shandong province is given below.

1. Their variation of thermoelectric coefficients is summarized as following in Tab. 1.

Tab.1. Thermoelectric coefficients ($\pm\alpha$ μV / ℃) of pyrite in gold deposits from eastern Shandong province

Genetic type		Quartz vein				Wall alteration		
Gold deposit		Liukou	Qixia	Western Linglong	Eastern Linglong	Xiadian	Luofeng	Sanshandao
Measured samples		640	88	87	3486	127	5000	220
N–pyrite	$-\alpha$	−45～ −297	−11.3～ −198.9	−195.3～ −369.1	−12～ −433	−35.1～ −377.0	−20～ −458	—
P–pyrite	$+\alpha$	+12～ +502	+52.6～ +441.1	+275.5～ +342.4	+11～ +585	+24.5～ +567.4	+19～ +545	+37.2～ +430.1

2. Distribution of their thermoelectric coefficients varies with mineralization stage their disperse range is large, while in the middle strong mineralization stage it is narrow, as is shown in Tab.2.

Tab.2 Dispersion of thermoelectric coefficients of pyrite from gold deposits in eastern Shandong province

Genetic type	Gold deposit	Early stage	Middle stage	Later stage
Quartz vein	Liukou	−269～+502	−297～−46	
	Qixia	−296～+441	−199～−11	−191～−97
	Western Linglong	−370～+444	+102～+459	+14～+569
Wall alteration	Xiadian	−377 ～+526	−281～+567	−284～+219
	Luofeng	−297～+410	+286～+360	+234～+383

3. Distribution of their conduction types is different in different mineralization stages in different deposits. From early stage to late stage conduction type of pyrite is transformed from mixed type (N+P) to or nearly to single type (N or P). Evolution tendency to P type is typomorphic of large deposit independent of their genetic types, is shown in Tab.3.

Tab.3 Frequency of conduction types of pyrite (%) in different mineralization stages

Genetic type	Gold deposit	stage			Evolution tendency
		Early	Middle	Late	
Quartz vein	Liukou	P(53) > N(47)	n(100)	—	P+N→N
	Qixia	P(50.3) > N(49.7)	N(100)	—	P+N→N
	Eastern Linglong	P(60) > N(40)	P(96.7) ≫ N(3.3)	P(100)	P+N→P
Wall alteration	Xiadian	P(42.3) < N(57.7)	P(34.3) < N(65.7)	P(29) ≪ N(71)	N+P→N
	Luofeng	P(98.6) ≫ N(1.4)	P(100)	P(100)	P+N→P
	Sanshandao	P(100)	P(100)	P(100)	P→P

4. As–rich pyrites belong to P–type while replacement of Fe by Co and Ni converts them to N–type. High frequency of P–type is typomorphic of large deposits (Tab.4).

Tab.4 Relation between conduction type average contents of As, Co+Ni of pyrite and reserve of gold deposits in eastern Shandong province

Genetic type		Quartz vein						Walll alteration
Gold deposit		Liukou	Qixia	Western Linglong	Eastern Linglong	Xiadian	Luofeng	Sanshandao
Reserve of deposit		Small	Medium	Large	Large	Medium	Large	Large
Pyrite (ppm)	As	307.69	425.90	689.00	914.74	509.15	1187.68	7530.70
	Co+Ni	1557.76	231.80	135.80	263.33	407.00	72.32	100.57
	P(%)	18.8	35.3	78.2	87.1	37.9	97.1	100

5. Mineralogical mapping of pyrite thermoelectricity reveals:

(1) Distribution of gold mineralization;

(2) Downward extention of gold orebodies;

(3) Location of blind ores:

(4) Relative displacement on both sides of postmineral fractures;

For example mineralogical mapping of pyrite thermoelectric coefficients demonstrated that the orebodies in Luofeng gold mine is distributed mainly over $\alpha = 300–350$ $\mu V / ℃$ part.

6. In upper part of orebodies P–type pyrite dominate, while in lower part of orebodies N–type pyrite dominate. Such vertical zonation distinct in Eastern and Western Linglong, Xiadian and Liukou gold deposits can be used as criteria for judgement of degree of denudation of the deposits.

Note: The financial support is from the NSFC–4860100

PROSPECTING AND TECHNOLOGICAL PROPERTIES OF MINERALS

G.A.Sidorenko, B.S.Gorobetz, Ministery of Geology, All–Union Scientific–Research Institute of raw materials / vims / , Moskow, Staromonetny per., 31, 109017, USSR

Physical methods of minerals investigation in rocks and ores, based on the emission signals analysis within X–ray, optical, infrared and radio frequency ranges, help to determine some diagnostic and typomorphic features of minerals. There features depend on the composition and the structure of minerals, which, in their turn, reflect the peculiaraties of minerals formation and bedding. Being extremely weak, these features demand high sensitivity methods for their study, for example, to control the impurities content up to $10^{-5}–10^{-6}$%. The most suitable are the resonanse and diffraction spectroscopic methodes providing for wide scale of investigations from electron to radio wave–length frequencies. Among number of mineral features only few can be successfully used for prospecting and tecnological purposes, due to their economical and ecological advantages compared with the abilities of traditional methods of analysis and enrichment of ores. The follosing are the most illustrative examples of some recently studied properties of minerals.

1. Prospecting properties. Radiospectroscopic methods. ESR can observe E_1, –centers, $Al^{3+}$and Ge^{4+}ions in the structure of quartz, which indicate radioactive anomalies

and rare metals pegmatite ores. Mossbauer spectroscopic method helps to analyse cassiterite content in tin ores from 0,01 up to 1,5% of SnO_2. Field spectroscopic apparatus are availafle for realising the both methods. Infrared spectroscopic method helps to reveal pyrophosphate bonds in the structure of apatite corresponding to increased redox potential existed when forming the rocks genetically related to the mantle. Such apatite discovered in sands serves for local prospecting of abyssal ore–bearing deposits such as kimberlites or carbonatites. Optical spectroscopy helps to discover diamond–containing kimberlites and eclogites by means of color centers in pyrops: Cr^{3+} / Fe^{2+}–and ($Fe^{2+}Ti^{4+}$) correspondingy. Luminescence helps to identify cassiterite in complex tin ores; helps also to discover silver halides / kerargirite, embolite / in oxidized zones of silver deposits. In the both cases luminescence is excited either by mercury lamp after cooling the samples in liquid nitrogen, or by UV laser at common temperatures. Weak violet glow of apatite containing the impurity centers $Ce^{3+}$and Eu^{2+}may indicate its genetical relaion to the mantle rocks and together with pyrophosphate groupes, identified by infrared spectra the whole complex of these indicators helps for local prospecting of kimberlites and carbonatites. X–ray phase and structure analysis reveals subtle peculiarities in rockforming minerals–feldspars, layer silicates. It helph to carry out mineralogic mapping of an area to be prospected, to discover metasomatic alteration zones probably ore–bearing, to evaluate technological properties of ores and to control the process of extraction of different components.

2. Technological properties related to phase composition of ores can be used for radiometric enrichment of ores. The main methods are photometric and luminescent separation of ores. In photometric method are used different optical reflection and absorption properties of dark and light–coloured minerals / in ores of quartz, microcline, calcite, magnesite, pollucite, lasurite, boxites, barite / . Even much more selective and sensitive are the luminescent properties based on different spectral and kinetic caracteristics of minerals excited by X–rays or ultraviolet lasers. Hitherto are elaborated the methodes of luminescence separation of ores of diamonds, scheelite, spodumene and eucryptite, fluorite, apatite, calcite and dolomite / as by–products of enrichment of phosphorite ores / , datolite, danburite, barite, celestite, microcline and plagyolase, silvinite.

VARIATIONS OF MINERALOGY OF KIMBERLITES DEPENDING ON THEIR STRUCTURAL ENVIRONMENT

Andrei Sinitsyn, Research Institute "Horizon", Leningrad State University, 198904, U.S.S.R.

Diamonds being minor, though very important constituent of kimberlites, are present in kimberlites but rarely - they are mat in economical quantaties in 1% of pipes and in mineralogical quantaties not more than in 10% of pipes.

T. Clifford (1966) was first to note that all African economically diamondiferous kimberlites are regulary found in the areas of ancient cratons. D.Dawson (1970) advanced this concept, showing world wide validity of T. Clifford`s rule.
This offered certain opportunities, since starting prospecting in any new region, it seems worth to start by exploring its Precambrian tectonics to outline the ancient cratons, so far as only those rather small terrains are in any way promising for economically productive pipes.
Beyond any doubt, diamondiferous kimberlites are specific by their accessory mineralogy, though, as it has shown N.Sobolev (1974), this pecularities are rather subtle, revealing only under close investigation of garnets, ilmenites and chromespinelides chemical compositions. Such mineralogical study is often of the same labour consuming scale, as large volume ampling aiming direct diamond assaying.
Meanwhile diamondiferous pipes due to the local features of the underlying ancient cratons petrology reveal one important pecularity - they usually do not contain feldspar granulite xenoliths, abundant in barren pipes, intruding mobile belts terrain. The only exclusions among the intercratonic kimberlites with reported granulite xenoliths are South African Orapa, Newlands and Klipfontein pipes (Dawson, 1980). But all of them intrude the outer edges of the Kaapvaal Archeaen craton, characterized by the so called "along the edges" granulites, differing sufficiently from typical inner mobile belts granulites. The prospecting corollary is that kimberlites containing abundant granulites xenoliths are usually nondiamondiferous.

1.31H

57.4.21. V

ABUNDANCE OF THE $2M_1$ BIOTITE POLYTYPE IN NATURE

S.V.Soboleva, V.V.Nasedkin, Institute of Ore Deposits, Mineralogy, Petrography and Geochemistry, Acad. of Sciences, Moscow 109017, Staromonetny 35
I.U.Schwelidze, Geological Institute, Georgia Acad. of Sciences, USSR, Tbilisy, 380093, Ruckadze str., 1

Rare $2M_1$ polytype of biotite occurs mainly in volcanic and metamorphic rocks and some times in high pressure zones. The electron diffraction oblique texture method proves to be very successful for the determination of the nature and structural perfection of sheet sicicates. We applied this method for the analysis of a great number of biotite samples from Georgia metamorphic rocks and from volcanic rocks from Kamchatka and

Armenia. It was established that $2M_1$ polytypes usually crystallized in the conditions of the dry metamorphism when the partial oxygen pressure is much more higher then the vapour H_2O pressure. As a consequence the anion sublattice is enriched by O^{2-} and has a composition $O_{10+x}(OH)_{2-x}$ $(0 < x < 0.5)$

The proton deficiency in the octahedral apexes decreases the repulsion between the interlayer cations and protons and stabilizes the rare $2M_1$ polytype.

The investigation of metamorphic biotites from Georgia reveals the increasing of $2M_1$ polytype occurence with the metamorphic degree from metapelites to metabasites. Analysis of igneous biotites shows that the $2M_1$ polytypes mainly occur in near surface volcanic focus during the non-equilibrium crystallization. The proton deficiency is compensated by isomorphous replacement of octahedral cations Mg^{2+} for Al^{3+} and Fe^{3+}.

Po 1.16 GENETIC-MINERALOGICAL RESEARCH ON THE SERIES OF MINERALS OF SCHEELITE-POWELLITE

Su Changzhi, Center of Roch and Mineral Analysis, Bureau of Geology and Mineral Resources of Henan Province, Zhengzhou, People's Republic of China

Molybdenum and tungsten have similar crystalochemical properties and geochemical behaviours, so they can replace each other to make up the continous series of minerals of CaWO3 - CaMoO3. It is feasibe in the theoretical analysis and also has been verified by the compound experiment. This essay illustrates that there is a mineral series of scheelite-powellite in the nature which existed in the skarn-porphyry molybdenum(tungsten) orefield of Luanchuan, Henan Province. Various experimental data and classification of chemical composition and fluorescent colour are listed in table 1.

Genetic-mineralical characters of the series are as follow: Their formation is related with the syntectic granitoid of Yanshan Period; They have high molybdenum; Molyboscheelite and W-bearing powellite formed in magnasian skarn stage, which assoicated with magnetite, salite,

cliondrodite and magnesium-peridotite. At the later stage , molybdenite mineralization piled on which formed at high temperature. However, scheelite-molyboscheelite's containing low Mo formed at calciskarn stage or hydrothermal period, which associated with grossnlarite, ratite, ferrosalite, hedenbergite, vevianite, wollastomite, othoclase ; Mo-bearing scheelite-molybdenum-scheelite formed at quartz-sulphide stage; powellite is found in oxidation zone.

Table 1: Table of classification and features of the series of minerals of scheelite--powellite

items \ names / content %		1 scheelite	2 Mo-bearing scheelite	3 molyboscheelite	4 yellow scheelite	5 tungsten powellite	6 W-bearing powellite	7 powellite
classification	$CaMoO_4$ molecular	0·0—1·0	1·0—5·0	5—30	30—50	50—70	70—95	95—100
	MoO_3	0·0—0·72	0·72—3·6	3·6—21·6	21·6—36·0	36·0—50·4	50·4—68·4	68·4—72·0
	WO_3	80·5—79·7	79·7—76·5	76·5—56·4	56·4—40·3	40·3—24·2	24·2—4·0	4·0—0·0
	CaO	19·5—19·6	19·6—19·9	19·9—22·1	22·1—23·7	23·7—25·4	25·4—27·5	27·6—28·0
practical experiments	$Mo\ O_3$	$\equiv_1$ 0·24—0·52	$\equiv_2$ 0·75—1·53	$\equiv_3$ 5·54—6·74	$\vdash_{B17}$ 22·17	$\vdash_{W3}$ 41·61	$\vdash_{B6}$ 52·07	$\equiv_{17}$ 69·63
		$\vdash_{20}$ 0·04—0·24	$\vdash_{14-1}$ 0·11—2·27	$\vdash_{W1}$ 7·0	$\vdash_{W2}$ 30·18	$\vdash_{W4}$ 43·10		72·67
	WO_3	$\equiv_{\pi}$ 79·13	$\equiv_2$ 78·83	$\equiv_3$ 74·26	$\vdash_{B17}$ 53·30	$\vdash_{W3}$ 32·21	21·08	
		$\vdash_{20}$ 79·78	$\vdash$ 80·4—78·83	$\vdash_W$ 75·25	$\vdash_{W2}$ 50·94	$\vdash_{W4}$ 31·23		
	CaO	$\equiv_1$ 20·14	$\equiv_2$ 19·43	$\equiv_3$ 19·24	$\vdash_{B17}$ 23·31	$\vdash_{W3}$ 23·54	27·09	30·37
		$\vdash_{20}$ 18·64	$\vdash$ 18·83—18·9	$\vdash_{W1}$ 17·75	$\vdash_{W2}$ 18·88	$\vdash_{W4}$ 25·66		27·77
proportion (G)		5·96—6·01		5·78		5·09		3·73—3·91
parameter of unit cell Å	a.p	5·238		5·235		5·224	5·18	5·224
	Co	11·36		11·368		11·386	11·394	11·40
dioptre	No	$\equiv_1$ 1·9063	$\equiv_2$ 1·913	$\vdash_{W1}$ 1·9310	$\vdash_{W2}$ 1·9333	$\vdash_{W3}$ 1·9345	$\vdash_{W5}$ 1·9523	1·9345
	Ne	$\equiv_1$ 1·9245	$\equiv_2$ 1·923	$\vdash_{W1}$ 1·9440	$\vdash_{W2}$ 1·9505	$\vdash_{W3}$ 1·9650	$\vdash_{W5}$ 1·9760	
hardness (Hm)		4·4—4·55		4·6				3·8
colour of light		blue	light-blue--light-yellow	bright-yellow	bright-yellow	bright-yellow	bright-yellow	yellow

Notes: (π)1, ⊢20, etc. are symbols for orefield and samples. Except (π), all others are eleton micrascope spectum analysis.

NEW ADVANCES IN MORPHOGENESIS OF PYRITE

Sun Daisheng, Chen Guangyuan, Division of Genetic Mineralogy, Chinese University of Geosciences, Beijing, 100083, PRC.

The present investigated pyrite crystals are collected from 6 gold deposits in eastern Shandong province, namely, Linglong, Qixia, Xiadian, Yuantan, Sanshandao and Luofeng, out of which 8000 are taken into account in statistics, 400 to goniometric measurement and 100 to observation of surface microtopography under SEM. New advances made are given below:

1. 45 forms of pyrite are found: {100}; {210}, {310}, {410}, {510}, {520}, {610}, {710}, {720}, {750}, {760}, {810}, {830}, {850}, {910}, {920}, {940}, {11,1, 0}; {111}; {135}, {251}, {321}, {328}, {421}, {521}, {531}, {641}, {721}, {832}, {841}, {1,3,11}, {10, 6, 25}; {11, 1,3}, {13, 2,7}, {13, 2,9}, {18, 24, 25}, {34, 14, 25}; {211}, {311}, {322}; {113}, {221}, {332}, {441}; {110}.

2. Frequency of forms of pyrite is as follows:

Tab.1 Frequency of appearance of single form among 7000 pyrite crystals from 6 gold deposits in eastern Shandong province

Form of pyrite	Frequency	Frequency ratio (%)	Times of frequency
{100}	5529	78.98	1106
{hk0}	5086	72.65	1017
{111}	597	8.52	119
{hk1}	43	0.61	9
{hkk}	13	0.19	3
{hh1}	6	0.09	1.2
{110}	5	0.07	1

They belong to seven types of crystal forms for pyrite separately. According to the frequency of appearance of single forms in all the crystals is as the following : cube {100} — pentagonal dodecahedron {hk0]— octahedron {111}— didodecahedron {hk1}— icositetrahedron {hkk}–trisoctahedron {hh1}—rhombic dodecahedron {110}.

3. Pyrite with negative striation appears in later stage, being typomorphic of rich ores.

F–cube pyrite is transformed to S–cube pyrite with dense straight striation by de–velopment of step–edged on {210} faces, being typomorphic of rich ores.

4. There is a change in forms of pyrite according to mineralization stages. In earlier stage it is a{100}, a{100}+e{210}—e{210} in intermediate stage and a{100}>o{111}—a{100} in the latest stage.

5. Pyrite crystals are divided according to combination of forms into four types, namely monoform, biform, triform and polyform crystals. In general monoform crystals appear in wall–rocks, while biform to polyform pyrite occur in orebodies. If biform and triform pyrites occur in wall–rocks, it is the indicator for large or high–grade ore.

6. Frequency of composite pyrite forms is different in different mineralization stage. In earlier stage predominates monoform pyrites (75–100%). In intermediary stage predominates biform pyrites (70–90%) with subordinate polyform pyrites (1–30%). In latest stage displays decrease of biform pyrites (4–82%) and increase of monoform pyrite (5–100%).

7. Distribution of pyrite forms displays distinct vertical zonation. As is shown in Linglong gold deposit, monoform pyrites dominate its lower part and biform pyrites dominate its middle part with triform and polyform dominate its upper part of the ore

body.

8. Distribution of pyrite form is different in different types of gold deposits as is shown in the following.

Tab.2 Distribution of forms with in 7000 pyrite crystals from gold deposits in eastern Shandong province

Genetic type	Gold deposit	Monoform %	Combinate form		
			Biform %	Triform %	Polyform %
Quartz vein	E. Linglong	61.90	18.90	12.00	7.20
	W. Linglong	45.90	29.50	13.10	11.50
	Qixia	41.53	27.90	29.40	1.17
Wall alteration	Xiadian	44.33	45.40	9.97	0.30
	Sanshandao	42.90	52.00	4.80	0.30
	Luofeng	46.79	52.43	0.72	0.06

Obviously biform pyrites are less developed while triform and polyform pyrites are more developed in quartz vein type than in wall alteration type of gold deposits.

The above–mentioned investigation is a supplement to the research of Dana (1903), Goldschmidt (1920), Sunagawa (1957), Endo & Sunagawa (1973), Endo (1978) and Murowchich et al. (1987).

Note: The financial support is from the NSFC–4860100

STRUCTURAL KIMBERLITE–CONTROLING CARCASS OF THE SIBERIEN AND CHINA–KOREA PLATFORM

A.E.Tiulenev, department of Metallogeny, All Union Geological Institute, Leningrad, 199026, USSR

Structural Kimberlite–Controlling of the Siberian and China–Korea Platform.

On the basis ofsome cosmoimages of various scales in both regions and information about the distribution of known kimberlite fields in their limits (Mokshantsev, Babsyan et al., 1976; Fumio Kishimoto, 1980) there were determined regional regulatities of distribution of chambers of kimberlite and alkali–ulttrabasic mogmatism. In particular was established rhythm both in orientation and in step of distribution of linear deep kimberlite–controlling faults.

In both regions these faults form structural carcass represented by combination of two types of regmatic lineament lattices; polygonal on the north representing the combination of intersecting north–eastern and sublatitudinal faults (the size of cell – 190 x190 km in Siberia and 150 x 270 km in China) and orthogonal on the south fixed by the intersection of sublatitutinal and submeridional faults (the size of cells in Siberia – 100 x 70 km and in China – 120 x 100 km).

Namely in nodes of intersection of faults there are known and unknown chambers of kimberlite magmatism. The further detaling of the perspective parts in these nodes is done both by way of analysis of large scale cosmoimages and by the use of traditional prospecting methods of investingation: sehlich–mineralogical, geochemical, geobotanical, morphostructural, etc.

1.16P

TRANSFORMATION OF SCHOEPITE INTO DIFFERENT HYDRATED URANATES.

Renaud VOCHTEN, Laboratory of chemical and physical mineralogy, State University Antwerpen, Middelheimlaan 1, 2020 Antwerpen, Belgium.

On principle at first the synthese experiments were started with schoepite [UO2(OH)2.2H2O] obtained from the reaction of CO2, O2 and H2O on U3O8.
The different uranates with general formula (MO)n(UO3)p(H2O)q with M the bivalent ions : Ca2+, Ba2+, Pb2+, Mg2+, Mn2+, Ni2+ were easily obtained by the reaction of solid schoepite at 60°C with aqueous solutions of CaCl2, BaCl2, Pb(NO3)2, MgCl2, MnCl2 and NiCl2 respectively.
From chemical analyses combined with thermogravimetric analyses the crystal-chemical formula was calculated : CaO.6UO3.11H2O (Bequerelite); BaO.6UO3.11H2O (Billiétite); PbO.2UO3.2H2O (Wölsendorfite) MgO.6UO3.13H2O (Mg-uranate); MnO.3UO3.6H2O (Mn-uranate); NiO.3UO3.6H2O (Ni-uranate).Till now only the first three members of this series were found in nature.
From Guinier X-Ray powder diffraction data the cell parameters of the six uranates were calculated by means of the computer program of Cox (1967).
The lattice parameters computed for an orthorhombic cell are of the same greatness for the six uranates which implies the existence of a common sublattice.
From solubility experiments as function of the pH the solubility product is calculated for five of the six uranates. Since wölsendorfite leads to several complex lead-hydroxyl complexes in solution it was impossible to determine the K_{SP} value on an adequate manner.
The dissolution of an uranate can be written as :

$$(MO)_n(UO_3)_p(H_2O)_q + (n+p-q)\ H_2O \rightarrow nM^{2+} + pUO_2^{2+} + 2(n+p)OH^- \qquad (1)$$

Consequently the solubility product is to be written as:

$$K_{SP} = [M^{2+}]^n\ [UO_2^{2+}]^p [OH]^{2(n+p)} \qquad (2)$$

Since several hydroxyl complexes of UO_2^{2+} are known, the computation of the solubility products is relatively complex.
The formation of the different hydroxyl complexes can

be described by the general equation :

$$p\ UO_2^{2+} + q\ H_2O \rightarrow (UO)_p(OH)_q^{(2p-q)+} + qH^+ \qquad (3)$$

for which the formation constant can be expressed as :

$$\beta_{pq} = \frac{[(UO_2)_p(OH)_q^{(2p-q)+}]\ [H^+]^q}{[UO_2^{2+}]^p} \qquad (4)$$

Using these values (Sillen and Martell 1964) the total uranyl-ion concentration can be expressed as a functin of the free uranyl-ion concentration by means of a polynomial.
For becquerelite, billiétite, Mg-uranate, Mn-uranate and Ni-uranate the pK_{SP} is calculated as : 152; 158; 156; 86 and 87 respectively.
In relation to the solubility and the transformation of schoepite into different uranates, the genesis of the natural uranates will be discussed.

THE MINERAL CHARACTERISTIC OF CUPREOUS SANDSTONE DEPOSITS AT YUNNAN PROVINCE AND PROSPECTING SIGNIFICANCE

Wang Gen, Chen Ling, Zhang Daohong, Zhang Fusheng, Geological Institute of Southwest Nonferrous Metals Geological Exploration Corp, CNNC.
Kunming, Yunnan Province, China

The reserves of Cupreous Sandstone deposits in Yunnan is the largest of the same type deposits in China.The genesis of this type deposit is considered from brine. The chloride and sulfate brine, consists of strata primitive water mixed with deep petroleum water. This brine carried with coppery fluid moved cyclically alone the path of fracture, bedded, porous of clastic, replaced and precipitated at the porous and space of fracture, formed the ore deposits.Studing of several cupreous sandstone deposits and occurences in west and central Yunnan, we divided the mineralization system into three stages. Each stage has its copper mineral assemblage and relationship of replacement.

1). The chalcocite stage : The main copper mineral is chalcocite associated with bornite. chalcopyrite, pyrite. The poikilitic calcite cements of clastic, is solubilized and replaced by crystal dolomite. Usually the minerals have obviously horizontal and vertical zoning . The ore bodies with disseminated ore are controlled by fold. The geological age of country rocks is the lower and middle Cretaceous at central Yunnan and the Tertiary at west Yunnan.The ore is

associated with 5-18 g/T of silver and 0.01-0.02 g/T of gold.

2). The silver-rich Chalcocite stage. The silver-rich chalcocite is aggregated by djurlaite (Cu 1.8-1.968 S), blaub leibender covellite (Cu 1.1-1.4 S), digenite and bornite, (and the silver contents is 5000 g/T - 8000 g/T) , with vein enargite. The cements of clasitc are dolomite, mica, quartz. The ore with scatter and veinlet dissmination structure replaced the cements.The ore bodies as vein and ore pocket are controlled by fold and fault. The geological age of country rock are the lower and middle Cretaceous. The silver content is 10-20 g/T and gold content is 0.05-0.1g/T in the ore.

3). Tennantite-Tetrhedrite stage. It is associated with enargite , barite, siderite and quartz, with massive and veinlet disseminate structure. The ore body is vein. The geological age of country rock is the Triassic and the upper Permain. The silver content is >50 g/T and gold is 1-8 g/T in the ore.

Studing of characteristic and sorts of the copper mineral could find good creteria for Cupreous sandstone deposits prospecting, For example in the chalcocite stage,most midium and large copper deposits are occured at central Yunnan, and the small one at west Yunnan. In the second stage and third stage only small copper deposit with high grade are found. If the three stage are superimposed, the deposits will be larger and richer.

TWIN IN NEW TYPE AND ZONAL STRUCTURE OF EPIDOTE FROM DONGSHANDING, FUSAN IRON MINE, CHINA

Wang Gongqing, Wang Anping, EM Lab., Changchun University of Earth Sciences, People's Republic of China

Epidote from this locality usually occurs as perfect short prismatic crystals elongating along b–axis. Generally, they are untwinned crystals, but simple or polysythetic twins with {100} as their twinning plane have been met occasionally. However, there is also a new twinning type with composition plane {101}. Zonal structure with widely variable chemical composition is very common in crystals of this mineral. The average composition analyzed by bulk chemical analysis is: SiO_2 37.20%, Al_2O_3 20.80%, Fe_2O_3 14.95%, FeO 0.23%, TiO_2 0.32%, MnO 0.08%, CaO 23.91%, MgO 0.00%, K_2O 0.06%, Na_2O 0.17%, H_2O 1.80%, and F 1.268 ppm, Total 99.52%. It is near the Fe–rich end member.

Under polarizing microscope, at least 6 zones can be distinguished. The different zones are analyzed with electron microprobe, EDS and WDS respectively. More detailed (WDS) observation can divide it into 8 zones, and more meticulous fine–probe can even find more tiny zones. On the whole, the core of zoned Epidote is deeply colored, then it varies from deep to light tone alternately in direction rim–wards, and become more light in the rim. The analysis shows that the zone of deep color is charactered by enrichmew in iron (TFe O 13.55–19.8%), slightly high content of Ti, but some drop of Al. On the contrary, the zone of light tone has lower iron content (TFeO 11.60–13.50%). The deep color zone of epidote has higher refractive indices (Nm = 1.7651) than the light color zone (Nm = 1.7640).

The decoloration of epidote near calcite veinlet of later stage is due to replacement of calcic hydrothermal solution. Analysis made by use of WDS and

EDS shows that some Ca and Al were introduced (CaO 25.60%, Al_2O_3 25.10%) and Fe were removed (TFeO 11.66%) during replacement. Isomorphic replacement under solid state has caused the color of mineral becoming light and destroyed a part of original zonal structure.

Epidote of this kind occurs as result of contact metamorphism between limestone and diorite at Dongshanding, Fushan Iron Mine, Hebei Province. In another locality, not more than 2–3 km away from Dongshanding, the epidote occurring at the same geological condition from Iron body No.7 is commonly twinned on {100} and the untwinned crystal is scarcely seen . The twin on {101} mentioned above has also not been found yet here, due probably to some different conditions of their formation.

THE INITIAL ANALYSIS OF SILVER ORES MECHAINISM OF ORIGIN IN CHINA

Po 1.18

WANG JINGCHUN, BEIJING INSTITUTE OF MINERAL RESOURCES AND GEOLOGY, BEIJING 100012, P.R.CHINA

Nearly one hundred kinds of silver minerals have been discovered in our country. The most common silver–minerals are: tetrahedrite, argentite, acanthite, pyrargyrite, miargrite, nature silver, Au–Ag compound (Electrum) and silver–halicles.

Studies indicated there's notable difference of existing state and enriching abundance in different origining silver deposits.

As known, silver ore deposits, which related to the hypomagma solution, has larger silver reserve and higher tenor. On the other hand, those, which related to hypermagma solution, is poor (meagre) in both reserve and tenor. The silver ore deposits by cooperration of sedimentation and metasomatism has higher tenors and larger reserves than those by pure sedimentation.

Silver commonly enriched during the middle–later periods of hydrothermal solution activity. In some deposits silver enriched weathering period after hydrothermal solution activity. For example, in volcanic ore deposits, the silver average tenors is higher than 100 g / T, some reach 500 g / T, and the reserves of this kind of deposits, more than a half over 200 tons and quite a few near thousand tons. In this kind of deposits, the mineralizing solution came from deep source, and silver mineralization occured in the hydrothermal stage after the volcame eruption – sedimentation. Then silver minerals crystalized with sulfide simultaneously or a little later. The silver mineralization intensity was decided mainly by diagenesis. If there were different periods of volcanic hydrothermals cooperate, silver usually enriched during the middle and latter periods. Silver has a quite closed relation with the mineralization of lead, zine and copper. The silver contents in ores, during pyritization, which the mineralization temperature was somwhat high, is less than 10 g / T, with the others, which formed during copper, lead andzine mineralization period, are over 100 g / T. the silver content of the lead–zine–poor steeped–stype ores are from 30 to 50 g / T.

The geochemical characteristic of silver decided its chemical affinity for some elements other. During certain mineralizing envirnments, silver could enter into some sulfosalts and sulfides selectedly. In general the selected sequence by silver is from Pb, Bi, Sb, Cu, Au, Zn, Fe, As to Sn. For example, the silver content of galena is about from 770 to 3100 g / T. So we can say that silver has a very closed rela-

tion with lead. Bismuth is also very relative tosilver. In fact, silver ores are often associated with nature bismuth. Another quite relative element to silver is autimony, For instance, the silver content of bournonite is so high up to 1200 g/T. For copper–bearing minerals, the silver content in Cu–Sb sulfosalt is higher than that in Cu–sulfate. For instance, in Yinshan deposit, the silver content in tetrahedrite could be 5700 g/T and in chalcopyrite is only about 95 – 1300 g/T. It is obvious that silver prefers entering Sb–Pb sulfate phase to Cu sulfide phase. Gold is the next object which silver likes to enrich in,the limiteless miscibility between silver and gold may help Au–Ag mixed–compound become one of important silver–bearing minerals. But in huge silver deposits, the silver contents of hyperythrin and Au–Ag ore (Eleelrum) are usually less than 5 percent of general reserves. For example in Yindongshan silver deposit this kind of ore is only 1.24 percent of general reserves there, with 74.11 percent of silver reserves was enriched in Jalpaite. Both gold and silver come from hypo–source, but the difference of their selection to geologic envirnment of deposition is remarkable.

The amount of silver entering sphalerite and pyrite changes regularily as mineralegenelic series doing. In Pb–Zn–Ag or Pb–Zn–Cu–Ag associations, if the mineralizing solution contained more zine, then silver prefered enriching in Zn–sulfide to Fe–sulfide. In fact, in this kind of silver deposits, the silver content in sphalerite is twice to thrice as that of pyrite. On the contrary, in single silver deposit, zine, lead and copper was poor, so silver was enriched in pyrite, by the way the silver content in pyrite would be 700 – 1000 g/T. During supergene mineralizing stage, silver did still firstly associat with lead, the anglesite could contain so much silver, up to 500 g/T. In this kind of carriers, silver came out as micro–enclusure mainly, or some as amorphons phase and lattice–held silver. Silver is miscible with them at high temperaturen and exsolute from them when temperature decreasing. The main reason of that silver could associate with lead, zine and copper closely is that the structural difference between silver sulfide, sulfosalt and Pb–Zn–Cu silfide is small.

The characteristics of silver ore association in volcanic rocks is that they come out as silver–rich mineral phases, for example, argentite–acanthite, nature silver, Au–Ag electrum, jalpaite, stromeyerite, nakaseite, pyrargyrite, polyhasite and hessite. The order of crystalization is: during early period of hydrothermal activity, a little argentite was crystallized and tetrahedrite, pyrargyrite begin to appear until middle period of hydrothermal activity. Electrum began to crystalize at the end of early period of hydrothermal activity when the silver in mineralizing–solution would get more as the time elapsed. Native silver began to crystalize at the later period, and be enrichecl furthur under the supergenesis. During the middle–latter stages of hydrothermal activity, a large number of silver sulfate minerals crystalized. Till later period of hydrothermal activity, silver sulfides and metalmixed–compound (hessite, iodargyyite, chlorargyrite) began to enrich.

GENETIC MINERALOGY STUDY OF YAOGANGXIAN VEIN TUNGSTEN ORE DEPOSIT

Wang Shun–jin, Department of Geology, China University of Geosciences, Wuhan, Hubei, 430074, People's Republic of China.

Yaogangxian tungsten deposit is a vein and skarn ore deposit. In this paper discusses the vein wolframite deposit. The typomorphic characteristics

of minerals, the paragenetic association, fluid inclusion, isotopic chracteristics and polytype are researched.

The mineralization of YGX ore deposit is divided into two periods and five stages. The main of ore–forming minerals occured at higher temperature stage of hydrothermal solution.

The contrast of wolframites which occured in the different direction of wolframite–quartz vein (NNW, NW, NWW) is made known that development of tungsten–bearing hydrothermal solution is regular. Wloframite occuring at early stage of mineralization has lower value of Mn / Fe and higher content of Nb, Ta, Sc, Mg and Ga.In same wolframite–quartz vein, chemical composition of wolframite has the above–mentioned regularity . Study fluid inclusion of quartz, chemical and electron microprobe analyses of wolframite proved wolframite occuring at higher temperature has lower value of Mn / Fe and higher content of Nb, Ta, Sc, Mg. Belt structure of monocrystall of wolframite shows that wolframite has more iron than the later stage.

Hardness of wolframite is in inverse proportion to the content of MnWO4.X–Ray powder diffraction analysis shows that the value of MnO / FeO has positive correlation to d(400) of wolframite and d(111) is related to Ca.

Most of arsenopyrites are positioned in the lower part of the wolframite–quartz vein. Paragenous arsenopyrite with wolframite only occured in a few place of the vein. The value of As / S of arsenopyrite is in direct portion to the temperature of crystallization.

The chemical composition of arsenpyrites of various metallogenic stages and monocrystall showing in Table 1 and Table 2.

Table 1. Chemical composition of arsenopyrites of various metallogenic stages.

Sample	Metallogenic Stage	As	S	Fe	As / S
49–5–2	1	31.33	32.16	36.50	0.974
501–16–2	2	27.84	29.01	43.15	0.960
501–16–2	3	23.72	36.13	40.15	0.657

Table 2. Chemical composition of monocrystall of arsenopyrite

Place of Crystall	As	S	Fe	As / S
core	31.34	36.22	32.44	0.865
margin	27.87	36.23	35.89	0.769

Gold content of arsenopyrite from No.58 vein is 0.5 g / t, 49–501vein is 0.223 g / t (average value).

The mineralization stage of molybdenite belongs to the medium temperature of hydrothermal activity. It is short of Se(0.00014) and Re(0.0007)

(wt%); polytype of molybdenite are 2H and 2H:3R = 1:1.

Feldspar, occurred in tungsten vein of YGX, is orthoclase(Or 62–74%) and microcline(Or 76–96%). The higher content of Rb(Rb_2O 0.205–0.344%) make clear feldspar originates from granitic magma.

According to content of micro–elements and physical properties of muscovite, all of the muscovite occurring in the tungsten–bearing vein are hydrothermal genesis. The polytype of muscovite is $2M_1$.

Cassiterite and bournonite are researched.

The homogenization temperature of inclusion of quartz and isotop of oxygen of quartz and wolframite showed the formation temperature YGX vein tungsten ore deposit is 175–338℃.

Fluid inclusion study of quartz make sure the composition of mineralization fluid is short of F and rich in Ca, Na, Cl and HCO3–, pH = 6.42–7.20.

The mineralization temperature gradient and the variation of chemical composition of minerals showed, YGX ore deposit has rhythmic ventical zonation.

A STUDY OF MINERALOGICAL PROPERTIES AND MINERALIZATION OF WOXI Au-Sb-W DEPOSITS

Weng Lingbao, Fan Jiang, Wang Pu, Department of mineralogy-Petrology-Geochemistry, China University of Geosciences, Beijing 100083, People's Republic of China

Woxi Au-Sb-W deposits occur in the interformational faults developed in purple slates of the Proterozoic Madiyi group.

According to the data obtained from mineralogical studies, we divided the deposit into five stages of mineralization: I. early quartz carbonate, II. quartz scheelite(wolframite), III. quartz pyrite native gold, IV. quartz stibnite native gold, V. later quartz carbonate.

Based on the study of composition, cell parameter, crystallinity and the systematic comparison of data obtained by using electron magnetic resonance, thermoluminescence, infrared spectum and etc., the differ-

ences between mineralized and non-mineralized quartzs are very distinct.

Mineralized quartz has higher content of impure elements, higher intensity of thermoluminescence(1.39×10^{-9}-4.02×10^{-9} mic) and lower temperation of peak(232°c) higher concentration of O^-(Al), E centers, lower crystallinisty grade(CI=0.41-0.51),H_2O and CO_2 absorption band in inclusions infrared spectum are obvious, and has lower D_{H_2O}/D_{CO_2} ratio.

Contrasted with mineralized quartz, the non-mineralized quartz has oppositive characteristies: lower impure elements, lower intensity of thermoluminescence (4.35×10^{-10} mic) and higher temperation(270°c), lower concentration of O^-(Al), E centers, higher crystallinisty grade (CI=0.9), absent CO_2 absorption band.

There are some differences among mineralized quartz of tungsten, antimony and gold.Gold mineralized quartz has the highest content of impure elements, intensity of thermoluminescence and concentration of O^-(Al) centers, but the temperature of thermoluminescence peak and crystallinisty grade lower.

As,Cu,Zn,Cd,Co+Ni have positive correlation with Au in pyrite. Therefore, all of these elements are favourable indicators for gold prospecting. Gold contents in fine-allomorphic-granular pyrite is higher than coarse-idiomorphic-granular pyrite. About 90% pyrite crystal presents P thermoelectricity type, It indicates that the mineralization of the deposits is better at depth.

The content of Al,K,Na in quartz is relative lower and the cell parameter Vo of quartz is less than 113.000Å^3 and Co/Ni<1, S/Se>30000 in pyrite, and the lower content of total rare earth elements in scheelite indicate that the ore-forming process is related to metamorphic and hydrothermal processes.

TYPOMORPHIC PECULIARITIES OF THE GARNET FROM DONGSHENGMIAO POLYMETALLIC SULPHIDE DEPOSIT IN THE NORTHERN MARGIN OF NORTH CHINA PLATFORM: THIER SIGNIFICANCE IN ORE-PROSPECTING

Xia Xuehui, Geological Institute, Ministry of Chemical Industry, Zhuozhou, Hebei

Dongshengmiao polymetallic sulfide deposit is one of the superscale sulfide deposits developed within the polymetallic mineralization belt along the northern margin of north china platform. Stratigraphically, the mining area is characteristic of the middle-late proterozoic Langshan group, a sequence consisting essentially of carbonaceous phyllite, dolomite-marble, and dimicaceous quartz schist, all of low metamorphism as greenschist facies. In addition, volcanic rocks are found in the sequence, and also believe to be an ore-bearing sedimentary formation. The minerals of garnet group, regularly distribuling, commonly in belt over the mining area, have a clase relation to mineralization, so

Table.1 Chemical composition and typomorphic peculiarities of Garnets

Sample number	BG-19-1	BG-19-2	CK160-419	BG-16	CK160-32
Rock(ore) name	Stripped Zn-S ore	Stripped Zn-S ore	Stripped Zn-S ore	Garnet-phyllite	Garnet-phyllite
SiO_2	35.44	36.00	36.28	36.64	36.59
TiO_2	0.27	0.65	-----	0.00	0.05
Al_2O_3	19.17	19.02	20.68	19.16	20.73
FeO	8.62	8.32	9.05	18.18	20.84
MnO	33.44	33.67	29.81	23.63	18.70
MgO	0.56	0.23	0.73	0.00	0.08
CaO	2.38	2.25	2.47	2.44	2.59
Na_2O	0.00	0.00	0.00	0.00	0.00
K_2O	0.00	0.08	0.01	0.00	0.08
Cr_2O_3	0.00	0.24	0.00	0.00	0.29
Total	99.88	100.46	99.03	100.05	100.13
Mn/Fe	3.88	4.05	3.29	1.30	0.90
Cell parameter Ao	11.598	11.594	11.593	11.635	11.610
Crystal form	(110)	(110)	(110)	(211)	(211)
Grain size (mm)	0.2-0.5	0.2-0.5	0.2-0.5	2.5-5.0	2.5-5.0
Refractive index	1.8031	1.8052	1.7976	1.8159	1.8228

the present paper deals with them and gives their typomorphic characters with respect to chemical compositions and physical properties. (Table.1) The garnet minerals reveal an unique radial, similar to the light of the sun, crystal texture, tending to be high in Mn and low in Mg and Ca. The Mn content and Mn to Fe ratio vary as a function of mineralization, as indicated by the progressive increase in the Mn/Fe from 0.9 in the country rocks to 4.05 clase to the ore bodies with these changes, the crystal forms also transit from (211) to (110), the unit cell parameter Ao from long to short, and the crystal colours from brown red to gray white. The meaningful comparison of the pattern (particularly the vibrational band L) of infrared spectrometry with the compositions of the greenlandite points out that the band becomes heighened with the deorease in the molecules of the mineral that is, the two are negatively related.

Based on the above studies, a conclusion is easily drawn that the Mn rich garnets can be attributed to the autometasomation of the hydrothermal fluids derived from submarine exhalations. This means much emphasis on the researches on the garnet minerals, not only on the ground of their mineralogical implications but also of being helpful to ore-prospecting.

THE GENETIC MINERALOGY RESEARCH FOR PYRITE OF POLYMETALLIC SULFIDE DEPOSIT IN DONGSHENGMIAO, INNER MONGOLIA

P. 1.19.

Xia Xuehui, Geological Institute, Ministry of Chemical Industry, Zhuozhou, Hebei Province

Dongshengmiao super-large sulfide, polymetallic deposit is located in the northern margin of North china platform. The deposit was not only controlled by proterozoic characters but also had close relation with the strata and lithological characters of Langshan Group, which belongs to a timecontrol-stratabound deposit. As a major mineral, pyrite is widely distributed over the polymetallic deposit of metamorphic rock system in Langshan Group. This paper refers to the further study on the typomorph and origin of pyrite in order to provide some information for such deposit's genesis and exploration. In Dongshengmiao deposit, the pyrites were formed from the initial sedimentation to regional metamorphism The pyrites can be classified into following five different types according to their occurences, intergrowths and relations between texture and structure: 1. Microgranular pyrite, which appears like stars in the carbonaceous belts of dolomite. The grain size 0.002 mm, and mainly occur as allotriomorphic granulars; 2. Nodular pyrite, the nodules are composed of pyrite, sometimes the micro framboids can be found in it. Nadules are usually enclosed by clnopyrrhotite and sphalerite. They are in different sizes but in high roundness; 3. Concentric ring pyrite, the concentric rings, like ooides and grain size 0.1-0.25mm, can reach 7-9 rings; 4.

Recrystalline-large grain pyrite, they obviously display the mineral annealing recryslalline with foam structure. The triaxial included angles of pyrite are 120° , the grain size 0.25-0.5 mm, and crystal forms are mainly (210), (100); 5. Vein pyrite, this kind of pyrite oecurred as vein and crack fillings. The crystal forms are (100) and grain size 0.1-0.2mm.

The chemical analysis resaults indicate that the atomic ratios of Fe:S are different in above five kinds of pyrites because they were formed in different physical and chemical conditions. In 1. 2. 3. pyrites, the values of S/Fe are high, so some extra S even appeared in them , showing FeS_{2+x}. Calculation indicates that the mineralization often occurred in a high sulfur fugacity environment. Since the sulfur transpiration came into bloom system in 5 pyrite, so it lacked of sulfur. The regular changes of sulfur in pyrites display the sulfur fugacities were getting lower and lower from the pyrites formed in a cut-off systematic sedimentary basin to that in a sulfide active environment. According to calculations, the main reason for lacking of sulfur in pyrites is the sulfur's differential pressures depressed in the open system so that the ideal proportional relation of anion-cation was distroied.

The trace elements show that $Co/Ni < 1$ in 1. 2. pyrites, but $Co/Ni > 1$ in 3. 4. 5. pyrites, especially the pyrite in brecaiated Zn-S ores, $Co/Ni > 5$. The resaults of trace elements analysis from thirty-two pyrite samples on Co-Ni illustration , comparing with the typical deposits abroad and home, reflect that they are not only sedimentation but also hydrothermal process characters.

According to the measurement of cell parameter in pyrites, the higher Co content is, the larger cell parameter Ao is. In vein pyrite, the vacancy of crystal lattice made Fe-S coralent bond stronger and the bond distance got shorter so that cell parameter became small. The cell parameter, reflective power, specific gravity as well as hardness etc, display the typomorphic peculiarities of different genesis for these five kinds of pyrites in this region. Tempretures of forming pyrites were 90-150°C; 230-250°C; 380-400°C. The metallogenetic tempretures were consistent with the mineralize periods.

The mineralogy research of pyrite shows there had been four mineralization periods: initial sedimentation-hot brine metallogenesis-metamorphic recrystallization and local mobilization affected by deute-magmatism. The metallogenesis indicates that the deposit types were from initial sedimentation transitting to hot brine sedimentation. Regional metamorphism and local mobilization could only transform this deposit in different degrees, which made the pyrite body richer.

RESEARCH ON MINERALOGY OF DONGBEIZAI GOLD DEPOSIT FROM SONGPAN, SICHUAN, CHINA

Xu Guofeng, Zhou Xuewu, Department of Prospecting, China University of eosciences, Wuhan, Hubei, 430074, People's Republic of China

Dongbeizai gold deposit is located in Songpan county, Sichuan province, China. It is a fine–disseminated deposit contained in carbonate–clastic formation, and controlled by the Kuashiyia Fault (F1) and associated structures.

This paper has dealed with major mine rals found in Dongbeizai deposit, analyzed native gold, pyrite, realgar and quartz for their morphology, composition, texture, phycical property and spectrum characteristics, deteormined in part properties for stibnite, arsenopyrite, arsenic and calcite, and finally discussed the mineral genesis and typomorphic characteristics for prospecting.

The authors have suggested that the Dongbeizai deposit is an epithermal deposit associated with hot–brine, and is comparable with the Ertaizi gold deposit, Shanxi, and the Carlin deposit in United States. The following minarals can be used as prospecting criteria for "Dongbeizai deposit".

(1) Pyrite: finely disseminated as small pyritohedron, with dull luster, green–yellow colur, rich in As (3100–51600PPm) and containing some Tl (0.8–11PPm), Au(>1PPm), its Co / Ni<1, S / Se = 53600 (in average), the cell parameter a>5.4170Å, the visual reflectaince Rvis<54%, the purity of excitement Pe>13.2%, the thermoelectricity coefficient a=100–300 uv / ℃ (hole conductivity), the microhardness (vhn)<900 kg / mm^2, and with three infrared adsorption spectrum peaks (about 412 / cm^{-1} for the strongest one).

(2) Realgar: occurring in an eyed or striped shape, rich in Sb (4410–5450 PPm) and containing some Tl (0.3–1.2 PPm), with low visual reflectance, low purity of excitement, strong infrared absoption, with two peaks (about 340 / cm^{-1} for the strong and 370 / ϛm^{-1} for the weak).

(3) Quartz: occurring as poly–vein, with gray and white colour, rich in As(5.58–34.56PPm), containing structural aluminium (Al_2O_3: 0.17%–0.26%) and corresponding alkaline elements, its cell parameter V_0>112.985Å^3, with three–peak thermoluminesence curve.

After assessing the gold mineralization at depth of the district, the authors come to a conclusion that the Dongbeizai gold deposit has a vertical zoning with gold occurring beneath realgar, and its potentiality might be considerably large because of its good presoroation.

ELECTRONIC CENTER-HOLE IN PYRITE,THE APPLICATION TO PROSPECTION OF GOLD AND A DISCUSSION ON THE MECHANISM

Xu Hong, Department of Geochmistry, Changchun University Of Earth Sciences,Changchun, Jilin,130026,P.R.China

The nature of electronic center-hole in pyrite might be

reflected by its thermo-valt. The pyrite tested are sampled from Tuling-Shihu Gold Mine, Lingshou, Hebei,which is magmatic hydrothermal quartz veins in genesis. MGT-1 thermo-electronic spectrometer is used to analyse more than 200 pyrite samples (20 grains per sample, 40-60meshesin size). The meassurement shows that some samples yield negative thermo-valt value (electronic center type conductor),some yield positive value (hole type conductor),but the majorities show both negative and positive value.Therefor, compensation valt Vnp (Vnp=DpVp-DnPn, D is the weighting factors of number of grains) is used in discussion.The result is that the Vnp values grade from positive in the centers of the ore bodies outwards into negative in the host rocks.The distribution is symmetric and the positive value is concordant with the ore bodies.The Vnp within the veins decrease downward and the absolute value of Vnp in the host rocks increase outwards.The Vnp of pyrite shows corelation with the burial depth: H=-207.9451+8.5Vnp, r=0.9071>r (critical)=0.811. This is applicable to prospecting ore bodies in the depth, which has been proved by drilling in the mine. The Vnp, however, show no relation with the grade of ores. Steped regression of Vnp with the component of pyrite shows: Vnp=4.3569+2.2696Sb-0.0104Co-0.1370Ni, indicating that the three elements are the principle impurities affecting Vnp value.Observation under microscopes and electron probe reveals that Sb,Co and Ni occur in the form of isomorph .The positive correlation between Vnp and Sb indicats that Sb causes hole in pyrite,while the negative relation between Vnp and Co, Ni in pyrite might be explained by the electronic center resulted from these impurities. Sb substitutes S,which results in the extra negative charge in certain areas of the crystals and subsequently the capture of positive charge--generation of hole. It is generally accepted that the substitution of Fe by Co^{2+} and Ni^{2+} can not result in electronic center unless their valence is higher than Fe^{2+}. It is possible, however, that the introduce of Co and Ni might cause the deficience of S,resulting in electronic center. Synthesis of pyrite was conducted (10 grains per sample),which shows that: the As-bearing pyrite's Vnp is -10.26; the Vnp of Co-bearing pyrite

is -12.82mv and the pure pyrite yield +4.26 Vnp value.The statistics and the expriment indicate that Sb and As result in hole while Co and Ni might cause electronic center. Why the Co, Ni result in electronic center requires further research.

THE INFRARED SPECTRA OF QUARTZ THIN-SECTION AND ITS APPLICATION TO THE STUDY OF MINERALIZAION IN GOLD AND TIN DEPOSITS, EASTERN JUNGGER, XING JIANG, CHINA

Po 1.20

Xu Qingsheng and Shen Xiangyuan, Institute of Mineral Deposits, Chinese Academy of Geological Sciences, Beijing, 100037, People's Republic of China

The infrared spectra of quartz thin-section may be used to study fluid inclusion in quartz and to determine its genesis. In gold deposits, this method can be used to discern auriferous quartz vein from non-auriferous one, and, thus, to assess gold deposits effectively and cheaplyl; in tin deposits, it provides us a new approach to study the physical condition of ore-forming process.

On the infrared spectra of quartz thin-section from six gold deposits in east-

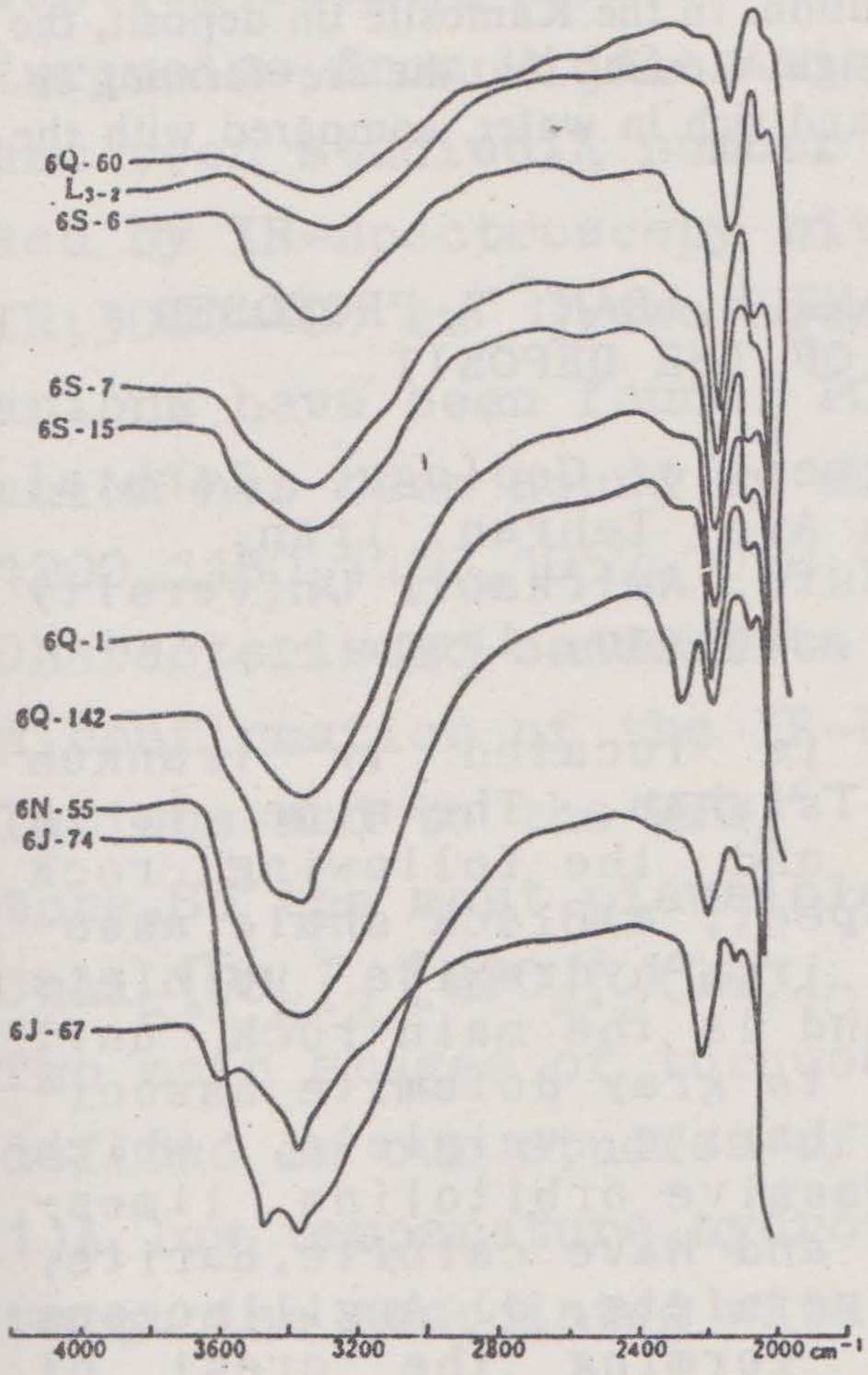

Fig 1. The infrared spectra of quartz thin-section from the gold deposits in eastern Jungger. 6HY--Sabei. 6KA--Kamosite. 6K,6B--Beilekuduke. 6N--Nanminshui. 6S--Jinshan 6Q-1--Qingshui. L_{3-2}--Xiaojingou. 6Q-142--Hongshan. 6J--Jinshangou

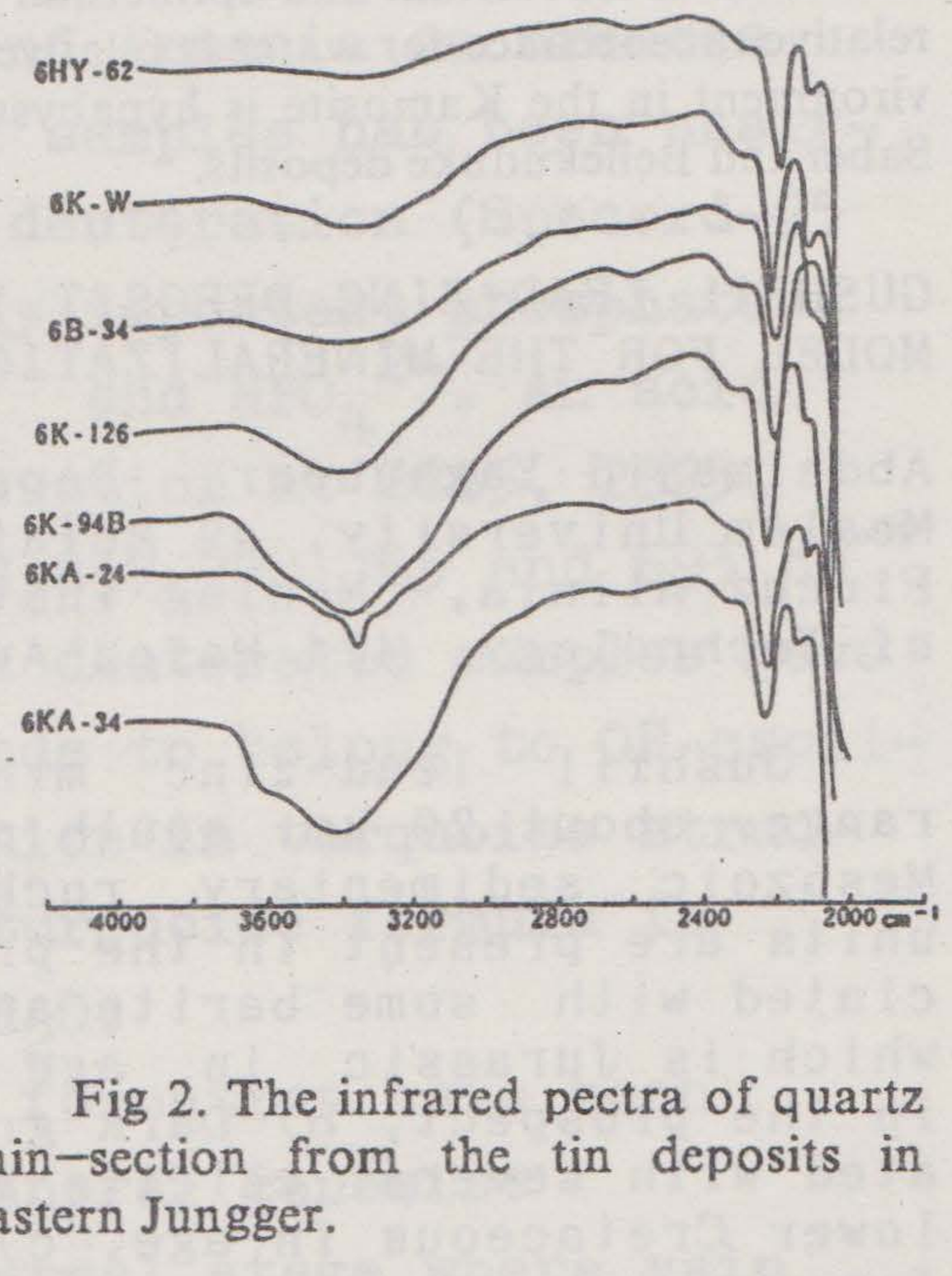

Fig 2. The infrared pectra of quartz thin-section from the tin deposits in eastern Jungger.

ern Jungger (see fig.1), the absorption bands of water are all relatively clear, but show different relative–absorbance for water; the relative–absorbance for water will be higher with the increase of fluid inclusion in quartz. According to the research, if the relative–absorbance for water is higher than one, the quartz probably is auriferous, if the relative–absorbance of water is lower than one, the quartz may be non–auriferous or the gold content of quartz is very low. In the Nanminshui, Jinshangou, Qingshui and Hongshan gold deposits, the relative–absorbance for water is higher than one; in the Jinshan and Xiaojingou gold deposits, the relative–absorbance for water is lower than one, so the gold content of quartz in the Nanminshui, Jinshangou, Qingshui and Hongshan is higher than that of the Jinshan and Xiaojingou (we can draw the same conclusions from the study of fluid inclusion in quartz).

The infrared spectra of quartz thin section from three tin deposits in eastern Jungger(see Fig.2) show that the infrared spectra can not be used to distinguish live quartz vein from non–live quartz vein; the relative–absorbance for water has a definite relation with the homgenization temperature of fluid inclusion in quartz, the higher the homgenization temperature, the lower the relative–absorbance for water. In the Sabei tin deposit, on the infrared spectra of quartz thin–section, the absorption band for water is very weak, it explains that the Sabeitin deposit is mainly formed in a hypogene and poor in water environment, it belongs a kind of hypothermal and in part pneumatolytic deposit. In the Beilekuduke tin deposit, the relative–absorbance for water couldeither be both high or low, so the ore–forming fluid was varied, there should be hypothermal and pneumatolytic in part solution, as well as mesothermal and epithermal solution. In the Kamosite tin deposit, the relative–absorbance for water is relatively high, showing that the ore–forming environment in the Kamosite is hypabyssal and rich in water, compared with the Sabei and Beilekuduke deposits.

GUSHFIL LEAD-ZINC DEPOSIT, IRANKUH, IRAN; A PROPOSED MODEL FOR THE MINERALIZATION OF THE DEPOSIT.

Abdelmajid Yaghubpur, Department of Geology, Tarbiat Mealem University, 49 Mefateh Ave. Tehran, Iran.
Fireuz Alinia, Mining Institute, Amirkabir University of Technology, 424 Hafez Ave., Tehran, Iran.

Gushfil lead-zinc mine is located in Irankuh range, about 20 km. south of Isfahan. The mine is in Mesozoic sedimentary rocks and the following rock units are present in the prospect; a)Black shale associated with some barite and iron-hydroxide veinlets which is Jurassic in age and is the main rock unit in the prospect, b) Dark gray to gray dolomite associated with several calcite and barite veinlets, which lower Cretaceous in age, c) Massive orbitolina limestones,which are gray in color and have calcite,barite, and in part iron hydroxide veinlets, d) Argillaceous marl,grayish-white in color forming the crest of the mountain ranges.

35 borehole samples were logged and the mineralized parts have been drawn in several profiles. Appparently the main ore body is located in the lower

part of the dolomite and the percentage of the lead zinc minerals varies from less than one percent to over 17 percent for lead minerals and from less than one percent to over 30 percent for zinc minerals. The major ore minerals are essentially galena and sphalerite. The main gangue minerals are pyrite, barite, calcite and quartz. The variation of the enriched part of the ore body is also observable in different drill holes to be at different depth. Putting the depth differences together in the profiles parallel to the strike of the beds and prependicular to the strike of the beds it showed that in the Gushfil mine we have a part of an inclined anticline with mineralization occurring as saddle reef type vein on the crest of the fold and in the Gushfil mine the top part of the vein has been eroded and the bottom part showed an aparently reverse sets of the beds which are actually the overturned limb of the fold.

NEW CRYSTALLOCHEMICAL AND GENETIC DATA FOR TURQUOISE

Yakhontova L.K., Plyusnina I.I., Soboleva T.V.
Dept.of Geology,Moscow University,Moscow 119899,USSR

Turquoise from Middle Asia and Armenia occurences has been studied.A number of samples has been analysed by IR-spectroscopy with deuteration (Specord-75 IR;3000-400 cm^{-1});two equally important phosphate anions have been found: PO_4^{3-} and HPO_4^{2-}. An acid anion has been sound by absorption at 2885, 2825, 1200,1180,1160,1057,1012,908,837,770,765 and 693 cm^{-1}. Characteristic bandshifts in deuterated samples gave a confirmation of the IR-bands to belong to OH-oscillations and to the HPO_4^{2-} anion in turquoise structure.So the most plausible turquoise formula is $CuAl_6[PO_4]_2[HPO_4]_2(OH)_{10}\ 4H_2O$.

Two main stages of turquose formation have been defined in our studies of mineral genesis:

1)A low temperature,hydrothermal stage where vein turquoise associated with quartz and pyrite was formed(quartzified turquoise).

2)A hypergenous stage related to the actual weathering processes.It implies an intense kaolinization

of the embedding quartzfeldspathic rocks and evolution of turquoise i.e.impregnation of the mineral with allophane,opal and kaolinite followed by intense amorphisation and stabilisation of the specific relations between Cu, Al and Fe^{3+}.

1.17V

GENETIC CLASSIFICATION AND CHEMICAL COMPOSITION OF CHLORITE MINERALS AND THEIR CHARACTERISTICS OF CHEMICAL EVOLUTION.

YANG MINZHI Tianjin Geological Academy, 42 Youyi Road ,Tianjin, People's Republic of China.

Based on study of geological occurrence, physical features and chemical composition of the chlorite minerals, which occur in sedimentary–metamorphic iron deposits, and in Au.Cu.Mo deposits related with granite, as well as the chlorites related with ultrabasic–basic, acidic, volcanic rocks in districts of North and North East China,

a systematical study has been done on 251 chlorite mineral samples with 11 different occurrence, collected on 24 sites.

Through We have conducted the Polygroup discrimination analysis on the chemical composition and genetic–occurrence of 852 chlorite mineral samples, We tablished. the composition–genetic discrimination formule of chlorite minerls including 3 groups e.g. Magnesio – chlorite, Ferri–magnesio–chlorite, Ferric–chorite, and the average values of chemical composition and the order number of chlorite, and ibentified five geochemical–genetic areas and discribeted. the evolution characteristics and indications on their genesis.

(Ⅰ). The chemical composition–genetic classification of chlorite minerls and their average values of composition are as follow:

1 Magnesco–chlorite minerals: pennine, sheridanite, chinochare; 2 Ferri–Magnesco–chlorite minerals: corundophilite, delessite, prochlorite, and repidalite; 3 Ferric–chlorite minerals: chamosite, thuringite, and daphite, The everage value of composition and their number order about each group of chlorite minerals are: $Mag_{100}Fer_{0}$, $Mag_{80}Fer_{20}$, $Mag_{60}Fer_{40}$, $Mag_{50}Fer_{50}$, $Mag_{20}Fer_{80}$, $Mag_{0}Fer_{100}$.

(Ⅱ). The classification and discremination formula of chlorite Minerals:

Plotting by discremination function F_1–F_2, F_2–F_3, of 3 group chlorite minerals they are concentrated in 3 areas with two lines A.B.as boundaries.

Composition average value mineral	SiO_2	Al_2O_3	Fe_2O_3	FeO	MgO	H_2O^+	Number of Sample	Number of order
Magnesio –chlorite	31.55	16.79	2.01	4.52	30.06	12.39	285	Mag_{100} Fer_0
Ferri–Magnesio– chlorite	28.29	20.50	4.54	17.72	16.47	11.88	175	Mag_{50} Fer_{50}
Ferri– chlorite	26.47	26.40	8.16	24.41	3.49	8.65	392	Mag_0 Fer_{100}

$F_1 = 7.13SiO_2+4.68TiO_2+5.14Al_2O_3+5.98Fe_2O_3+5.87FeO+4.50MnO+6.49MgO+5.13CaO+1.37H_2O^+ +3.62H_2O^- -283.16$

$F_2 = 7.29SiO_2+4.59TiO_2+5.31Al_2O_3+6.26Fe_2O_3+6.25FeO+4.79MnO+6.13MgO+5.28CaO+1.41H_2O^+ +2.49H_2O^- -288.13$

$F_3 = 7.36SiO_2+4.52TiO_2+5.44Al_2O_3+6.47Fe_2O_3+6.45FeO+5.15MnO+5.72MgO+5.29CaO+1.31H_2O^+ +2.68H_2O^- -293.69$

Magnesio–chlorite $F_1 > F_2 > F_3$. Ferri–Magnesio–chlorite $F_1 \approx F_2 \approx F_3$. Ferri–chlorite $F_1 < F_2 \approx F_3$.

(Ⅲ). The geochemical characteristics of evolution on chlorite minerals genetics classification areas According to the analysis and study on their geological occurrence, mineral association and F_1–F_2, F_2–F_3, discremination diagram, Five geochemical genetic area have been determinated as:

Ⅰ.ultrabasic rock genetic area, predominated by Magnesio–chorite

Ⅱ.Basic rock genetic area. predominated by Ferri–Magnesio chlorite, Magnesio–chlorite;

Ⅲ.Intermidiate rock genetic area, predominated by Ferri–Magnesic chlorite.

Ⅳ .Acidic–rockgeneticarea, predominated by Ferri–Magnesio chlorite, Ferri–chlorite;

Ⅴ .Sedimentary–Metamorphic and Sedimentary genetic area, predominated by Ferri–chlorite.

1.The volcanic eruption cycle is shown from basic ➤intermediate ➤acidic rocks and chlorite mineral species form Magnesio ➤ Ferri–Magnesio ➤ Ferri–chlorite sequentially.

2.the evolution of hydrothermal–replacement process of basic rock from Ferri–Magnesio chlorite to Ferri–chlorite.

3.The evolution of hydrothermal process of acidic rock from Ferri–biotite to Ferri–chlorite.

4.The metallogenesis evolution of sedimentary iron deposits form basic volcanic rocks to volcano–sedimentary iron deposits correspondents to

Magnesio–chlorite to ferri–chlorite.

(Ⅳ). The indication significance of the genetic classification and the genetic area. We suggeste thet the genetic diagram and classification of chlorite minerals could be used as the guide to divid the metamorphic phase and zones, the determine their original rock types of metamorphic rock, to correlate the stratigraphy of metamorphic rocks. they also could provide important information on hydrothermal, hydrothermal–replacement process and volcanic eruption cycle and be regarded as the ore–finding marks on Au, Cu, Mo,Fe deposits.

THE DEFECT RESEARCH ON INTERFACE MINERAL CRYSTALS OF GEOLOGICAL SOLID

YU Xinzhen, Li Peilan, Department of Geology, Central–South University of Technology, Changsha, Hunan 410083, People's Republic of China

The interface mineral of geological solid is the basic composing unit of geological solid edge. The history of crustal movements,their nature and intensity, which the geological solid had experienced during the process of crustal evolution, were first recorded by interface minerals,and related information was stored. Based on this concept, multiphase granite bodies in Xihuashan, Jiangxi,are taken as an example and a preliminary research has been made on the defect (micro–structure) character of the interface minerals (orthoclase and molybdenite) of the II–type in the rock bodies.In terms of the rock–forming process of Xihuashan granite bodies, the study suggested that the magma of each phase underwent subsequent differentiation after its intrusion due to liquid immiscibility, resulting finally in formation of the Xihuashan rock bodies.

We studied the defect character of the orthoclase and molyhdenite has been studied by using SEM CL and TEM. It has revealed that all kinds of the orthoclase belonging to γ_5^{2a}, γ_5^{2b} and pegmatoid have the feature of cathode luminescence. but they have different luminescence intensity. After having gone through the simulated experiments of static physical matallurgy, the luminescence phenomena of orthoclase which have different modes of occurance are absolutely different from those which have not undergone relative treatment. The cathode luminescene microstructure of orthoclase shows that not only is the orthoclase luminescene related to its trace ingredients (Fe^{2+},Ti^{4+}),but also to temperature environment and its change. The TEM analysis has revealed only a little free dislocation in the orthoclase having different modes of occurrence and no typical structure of deformed defect has been found, except for exsolution microstructure. It indicates that orthoclase having different modes of occurrence has experienced the same process that changed from the single solid phase to the two phases. The molybdenite having different modes of occurance don't have luminescene phenomena, but there exist common luminescene phenomena of the type of inclusion volume defect. Through physical metallargy experiments and TEM analyses,

we know that a lot of dislocation structures exist in molybdenite crystals having different modes of occurrence, but no typical structures of deformed dislocation has been found.

Study of the aforementioned crystal defect(,microstructure) of the interface minerals (orthoclase and molybdenite) from the Xihuashan granite indicates that the initial state of the γ_5^{2a} and γ_5^{2b}, or γ_5^{2a} or γ_5^{2b}, and pegmatoid is under condition of high temperature liquid phase–high temperature liquid phase interfaces. This implies that the γ_5^{2a} and γ_5^{2b} were products of liquid immiscible phases of magmas after their intrusion. Except for macroscopic geological evidece, this new viewpoint has been supported by the simulated experiments of liqiud separation of biotite granite.

THE NEW RESEARCH ON THE RELATION OF MINERAL FLUID INCLUSION AND ORE-FORMING FLUID

YU Xinzhen, Li peilan, Department of Geology, Central-South University of Technology,Changsha,Hunan, 410083, People's Republic of China

Now they,the national demonstrations on the nature of ore-forming solution,even the theory of deposit-forming cause,are depending a great extent on the researching results of mineral fluid inclutions which are the "samples" of ore-forming (rock-forming) fluid. After researching we think: the mineral fluid inclusion is a type of scattered fluid phase distributed in mineral crystals.It is neither the "sample" of ore-forming (rock-forming) nor the remained substance, however, it is only a part of substance in ore-forming solutions.

Besides some common researching ways,we still used TEW, SEW and SEMF cathode luminescence way in the research. then we found some phenomena which could not be explained by the existing theories, and found that the growing process of nature mineral crystals not only accord with the basic rules of crystal growth.but also had its own character-which was that some nature minerals could be divided into two processes of location growth and non-location growth. According to above-mentioned phenomena,the growing rules of mineral crystals and theories of scattered systems in fluid,we think: mineral fluid inclusions belong to a type of scattered fluid appeared before the growth of mineral crystals,the others were filled with other fluid and formed after the growth of mineral, So the authors

divided above-mentioned scattered fluid system into some kinds as follows: deflegmating fluid (including: interface-layer fluid sub-type, cell-structure fluid subtype), deflocculating fluid,fluid of mineral location-growing enviroment and epienetic fluid. The fluid ingredients and characters of the first three kinds are not completely the same but they are all from the same solution or the same de-simple solution. Although they are not the "sample" of ore-forming, they present the characters of ore-forming fluid from ore side. The ingredients and characters of the forth kind of scattered fluid don't have direct relation with the fluid of mineral-forming.

DIASPORE-BEARING ACID-SULFATE ALTERATION AT AKAIWA IN OTARU, WESTERN HOKKAIDO, JAPAN

1.9.P

Shunzo Yui, Department of Geology & Mineralogy, Hokkaido University, Sapporo 060, Japan

The Akaiwa alteration zone occurs on a steep cliff of the northern coast of the Otaru city, Hokkaido, Japan. The Sea of Japan side of the northern part of Japanese Islands forms a geologic province composed of thick volcanic and sedimentary piles of the Neogene in age. The province is called the Green Tuff region because of characteristic greenish color of the volcanics due to alteration and there occur many ore mineralization including gold-silver veins, kuroko deposits, and base metal veins. Akaiwa is located at the northern end of the Green Tuff region, and is known for beautiful crystals of barite, and there are small abandoned explorations.

Recently an active gold mineralization accompanying hydrothermal-solfataric activity was discovered at Osorezan at the northern end of Main Island of Japan. A north-south alignment of hydrothermal activities through Osorezan is recognized and its northern extension seems to reach Akaiwa.

Mt. Akaiwa(371 m above the sea) and Mt. Shimo-akaiwa(279 m) consist of intensely silicified volcanic rock (andesite?) of the Green Tuff region. The ridge of east-west trend connecting them is very steep and the incline of its northern slope to the Sea of Japan exceeds 45° at places. There are many

pillars of harder rock (irregular pipe-like or more tabular bodies of several to more than ten meters in diameter and several tens meters in height) contrasting to the surrounding softer ground on the slope.

The silicified rock is composed mainly of quartz and partly massive and partly rich in voids. In places, the voids are filled with alunite. The pillars consist of quartz-dickite rock with or without pyrophyllite. In the softer ground, several zones are recognized, which are dickite-, sericite-, and smectite-zones from the silicified rock to andesite(?). The Akaiwa alteration zone, therefore, seems to be deeply dissected analogue of the alteration of Summitville, Colorado described by Stoffregen(1987) although the kaolin mineral in the silicified rock of Akaiwa is mostly dickite, on the other hand, kaolinite at Summitvill.

Diaspore occurs as crystals up to 1 mm in diameter in voids from microscopic to 10 cm in size in quarts-dickite(-pyrophyllite) rock. Fine crystals of quartz project from the wall of voids and crystals of the diaspore occur inside. Some diaspore contains two phases (liquid-vapor) fluid inclusions. The homogenizing temperature is 192°-240°C (19 measurements). Some voids contain zunyite with or without diaspore implying the migration of aluminum and volatile materials in the later stage.

Alunite shows a broad x-ray diffraction profile for 006 reflection with FWHM of 0.5° or more at 31.3-31.5 degree 2θ for CuKα radiation indicating variable content of natroalunite component.

Kaolin minerals in quartz-rich rock is mostly dickite which show sharp x-ray diffraction profiles and that at least, in some softer clayey ground seems to be poorly crystalline kaolinite. Sericite-smectite mixed layer mineral is also detected by x-ray diffraction.

EVOLUTIONAL REGULARITIES OF THE MINERAL WORLD

1.2.P

N.P.Yushkin, Institute of Geology of the Komi Science Centre, Ural Division of the USSR Academy of Sciences Syktyvkar, I67007, USSR

The most essential achievement of contemporary minera-

logy is that it gave rise to the learning on the mineral world evolution which comprises two important trends: the ontogeny and phylogeny of minerals (I,2,3). Evolutional ideas arose and shaped at the dawn of mineralogical investigations favoured by the parallel development of mineralogy and paleontology within the general system of geognosy. The regularities observed by the study of ancient organisms stimulated the search for similar regularities in the mineral world. By the beginning of modern period in the mineralogical science development, a number of basic evolutional regularities were outlined. They found their manifestation in the principle of directed development of the mineral world (Tschermak's principle) as well as in Stenon's principle stating that minerals bear information reflecting conditions of their formation; in the evolutional schemes of crystal form development (Werner's schemes); in the principle of successive mineral formation in mineral bodies etc.

Now evolutional regularities are recognized on various levels of the mineral world organization: beginning with crystal lattices, mineral individuals, mineral parageneses, associations and complexes and ending in the mineral world as a whole (3,4). Main stages of mineral species formation in course of the Earth's development are established.

The most general evolutional regularities are:

I. General growth of the number of minerals, structural complication of the mineral world, enrichment of its diversity in course of geologic time. The diversity manifests itself in the acceleration of all mineral-genetic processes and phenomena, as well as in complication of more recent mineral associations as compared to the earlier ones; in the general growth of the number of minerals formed by recent processes; decrease in the relative energy and crystallochemical density of developing mineral systems; an increasing role of mixing phenomena; increase in the entropy and accumulation of deformations in the structure and shape of minerals, etc.

2. Evolution of the "cubic" or "cubic-orthorhombic" mineral world into the "monoclinic" one that began on the early stages of the Earth's history and is going on up till the modern stage; decrease in the symmetry of substance in contrast to high (and probably increasing) symmetry of the Earth itself.

3. Accumulation of complications of mineral systems in the upper horizons of the Earth's crust, particularly by the geoid surface.

The organic world, life itself, most probably, is a consequence of the mineral world evolution; subsequ-

ently the two worlds (although functionally different) developed in close interaction.
The motive power of the mineral world evolution has energetic origin: it is the propensity of developing mineral systems to equilibrium under the conditions of constant heat loss.

I. Grigoriev D.P. Ontogeniya Mineralov (Ontogeny of Minerals). L'vov, I964, 284 pp.
2. Grigoriev D.P., Zhabin A.G. Ontogeniya Mineralov. Individy. (Ontogeny of Minerals: Mineral Individuals). Moscow, I975, 399 pp.
3. Yushkin N.P. Teoriya i Metody Mineralogii (Theory and Methods of Mineralogy). Leningrad, I977, 29Ipp.
4. Yushkin N.P. Evolutsionnye Predstavleniya v Sovremennoi Mineralogii (Evolutional Concepts in Contemporary Mineralogy) Zap. Vses. Miner. Obshch. I982, part III, vol.4, p.432-442

VARIATION OF THE PRIMARY FIELD OF LEUCITE UNDER WATER DEFICIENT CONDITIONS IN THE SYSTEM Ne-Ks-Q-H_2O AT $PH_2O = 5$ kb

1.10P

Zeng Rongshu, Institute of Geology, Academia Sinica, Beijing 100011, China, MacKenzie, W.S., Department of Geology, The University of Manchester, Manchester M13 9PL, U.K.

Phase relationship of the system Ne-Ks-Q-H_2O at $PH_2O = 5$kb under water-saturated condition have been investigated. Compared with the phase diagrams at 1 atmosphere, 1 kbar and 2 kbar, the primary field of leucite shrinks with increasing pressure. The leucite field of the system Ne-Ks-Q-H_2O at $PH_2O = 5$ kb under water deficient conditions has also been determined.

It was found that nearly 15% H_2O was required to saturate the melt in the leucite-water system at 5 kb. The degree of water saturation changes the liquidus temperatures and the position of the field boundary of leucite in the Ne-Ks-Q-H_2O system. Compared with the size of the leucite field under water-saturated conditions, the leucite primary field expands when the system is unsaturated with water. Thus, for example, bulk compositions $Ne_5Ks_{60}Q_{35}$, $Ne_{10}Ks_{60}Q_{30}$ and $Ne_{20}Ks_{55}Q_{25}$ are located in the feldspar primary field under water-excess condition, but if the water content dropped to 5%, these compositions would crystallize leuxite first

but at higher tempera-tures The position of the field boundary between feldspar and leucite changes to a greater extent than the boundary between leucite and kalsilite with variation in water content at 5 kb pressure.

In discussing the crystallization of k-rich rocks these two factors have to be considered since both affect the order of crystallization of the primary phases.

Po 1.21

THE RELATION BETWEEN UNIT–CELL DIMENSIONS OF TINSTONES AND THEIR MINERALIZING ENVIRONMENTS IN SOUTH CHINA

ZHANG Gendi, FANG Zhong and WANG Xinguang, Department of Earth Sciences, Nanjing University, Nanjing 210008, P.R. China;
ZHOU Yandong, Center of Computation, Hehai University, Nanjing 210024, P.R. China

S. China is one of the famous metallogenetic zones rich in tungsten and tin in the world and, there are a lot of various type of larger tin deposits. Authors have measured unit–cell dimensions for 38 pieces of cassiterites and related trace elements, which were collected from 18 well–known or important tin ore deposits. In combination with the geochemical environments, some knowledge and conclusion have been obtained:

1. The cell dimensions of SnO_2 are $a=4.7308–4.7392$ Å, $c=3.1807–3.1874$ Å, $v=71.211–71.580$ Å^3, and $c/a=0.6720–0.6726$. For the crystals in forms of tetragonal dipyramid and short tetragonal prism, the values of a, c, v are smaller, but for the longer tetragonal prism or needle–like SnO_2, these values are bigger. The equations between dimensions are: $c=0.63581+0.5382\times a$, $(R=0.96)$; $v=-127.8895+42.0865\times a$, $(R=0.98)$; $v=-175.3205+77.4799\times c$, $(R=0.97)$.

2. It is stressed in this paper that as $c/a=0.6720–0.6725$, the a, c, v vs. c/a are in positive relations; but as $c/a=0.6725–0.6727$, their relations are negative. The $c/a=0.6725$ is a turning point of unsymmetrical curve (Fig.1). On the axis of the curve, there are many samples of SnO_2, which are provided with bigger cell dimensions, but the contents of the trace elements are smaller or the smallest. The equation of the curve is: $v=26.8060+43.9707\times (c/a)-803344.500\times (0.6725-(c/a))^2$.

3. As $c/a=0.6725$, the contents of Nb, Ta, Fe, Zr, Ti, W, Cu, Zn, Se and their total in cassiterites are lower or the lowest. All of these values vs. c/a patterns could produce a series of sag curves, though the pattern of In value vs. c/a is shown as a convex curve (fig.2). The Fig.1 and Fig.2 are exactly the opposites. The granitic, pegmatitic and greisen types of tin deposits are hypothermal in origin. For example, the Limu and Huashan ore deposits in Guangxi Province, in which SnO_2 are dispersed on the left side of c/a 0.6725 axis. There are higher values of Nb, Ta, Ti, and Zr, but the cell dimensions and elongation index are

smaller,and the colour of cassiterite is dark. The deposits of SnO_2–sulfide type are hypothermal–mesothermal or mesothermal, as examplified by the Gejiu deposit in Yunnan Prov. and Dachang deposit in Guangxi Prov., where many SnO_2 are dispersed on the axis of 0.6725 or its right side. The values of Nb, Ta, Ti and Zr, and their total are obviously lower ; whereas the a, c, v, c / a and elongation index are larger than other types. The crystals mostly are in light colour.

4. Both contents of trace elements and the related variation of cell dimensions and the c / a ratios of cassiterites are generally controlled by the ore forming temperature and as well as local geochemical background where the tin granites were formed. This can be regarded as a rule responsible for formation of ore deposits in all large or small tin–ore provinces in S. China.

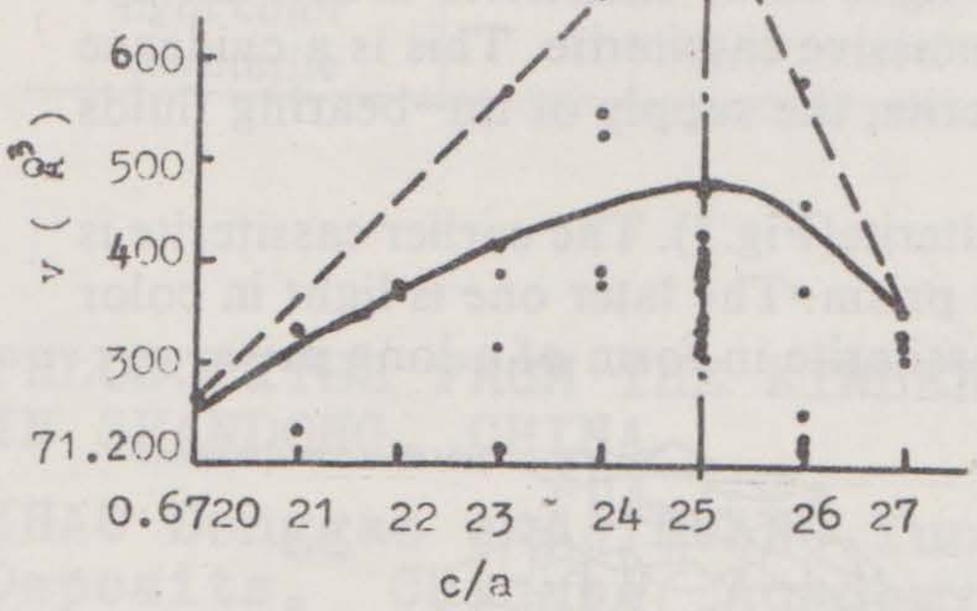

Fig. 1. Unit-cell dimensions vs. c/a volume of tinstones in S. China.

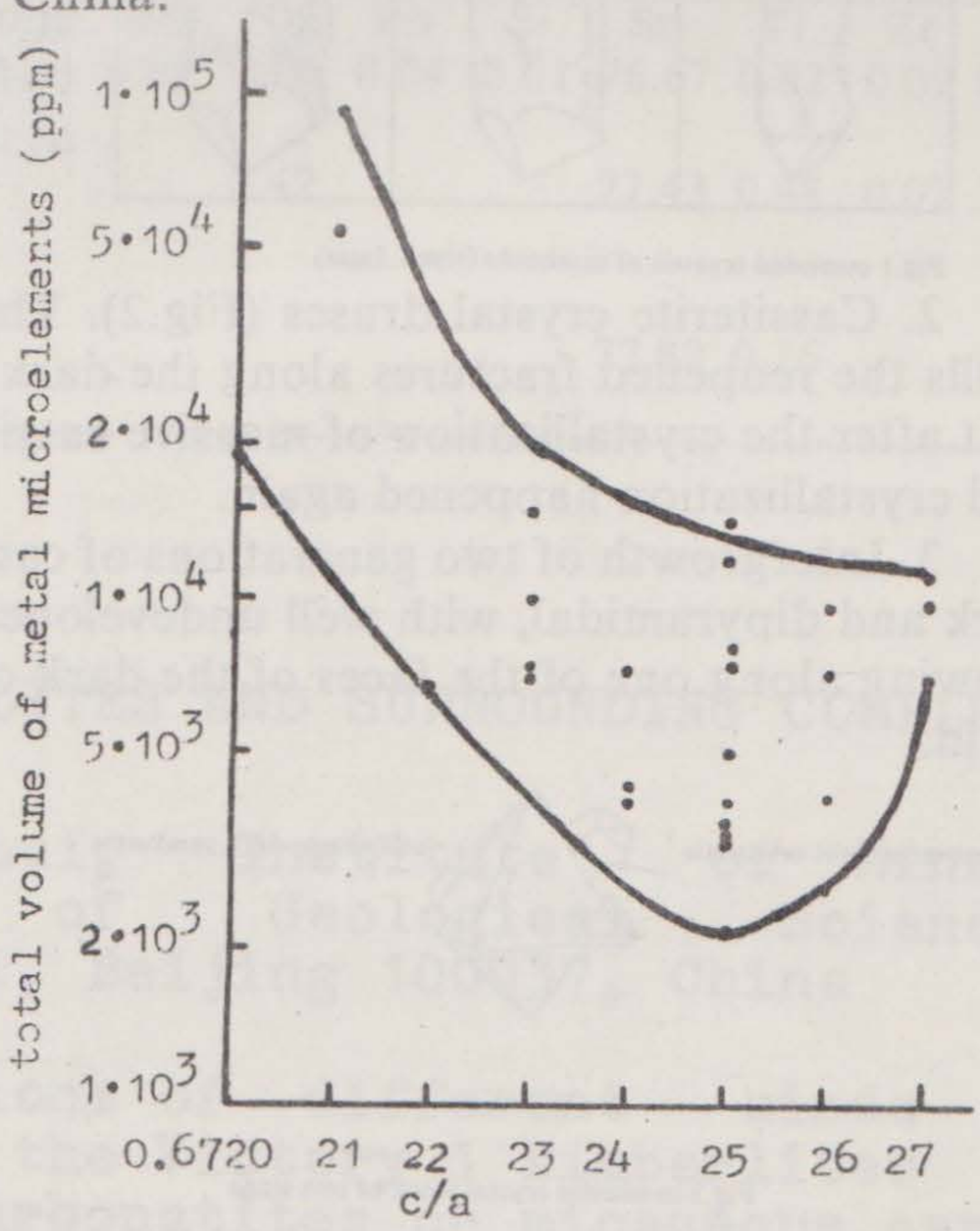

Fig. 2. Unit-cell dimensions vs. the total volume of metal micro-elements (Nb, Ta, Ti, Zr, W, Fe, Cu, Zn, Sc, and In) in tinstones in S. China.

THE CHARACTERISTICS OF MORPHOLOGY OF CASSITERITES IN A VEIN TIN DEPOSIT

Zhang Zengyou, Geological Institute of Southwest Nonferrous Metals Geological Exploration Corp. CNNC. Kunming, Yunnan Province, China

Study of morphology of cassiterites of a hydatothermal vein tin deposit in Western Yunnan has found that the rich ore body has undergone several stages of tin superimposed mineralzation. The characteristics of morphology of cassiterites are as follow:

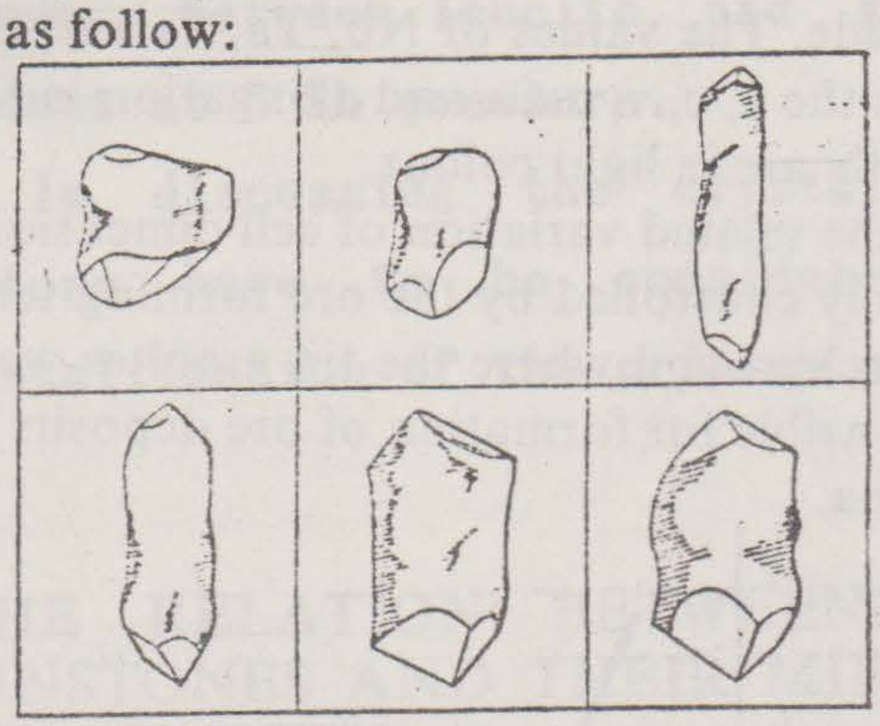

Fig.1 corroded crystals of cassiterite (siye 1.5mm)

1. Resorption of cassiterite crystals (Fig.1). Along with the re–rise of temperature or variation of medium during the later stage, the resorption of cassiterite ocurred. The prism face is easier to be resorbed than pyramid, so the resorbed crystals are ferfectly rounded. It shows that the high solubility fluid activity favourable to pick up the tin appeared at the late stage.

2. Cassiterite crystal druses (Fig.2). The light color cassiterite druses always infills the reopened fractures along the dark massive cassiterite. This is a evidence that after the crystallization of massive cassiterite, the supply of tin–bearing fluids and crystallization happened again.

3. Intergrowth of two generations of cassiterite(Fig.3). The earlier cassiterite is dark and dipyramidal, with well undeveloped prism. The later one is light in color growing along one of the faces of the dark cassiterite in form of a long prism pyramid.

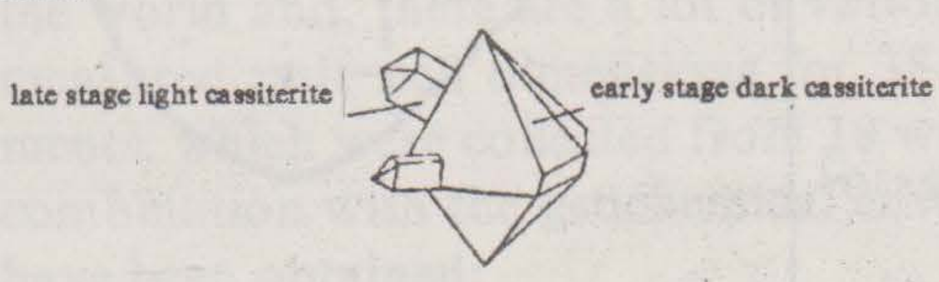

Fig.3 cassiterite crystal stock of two stage

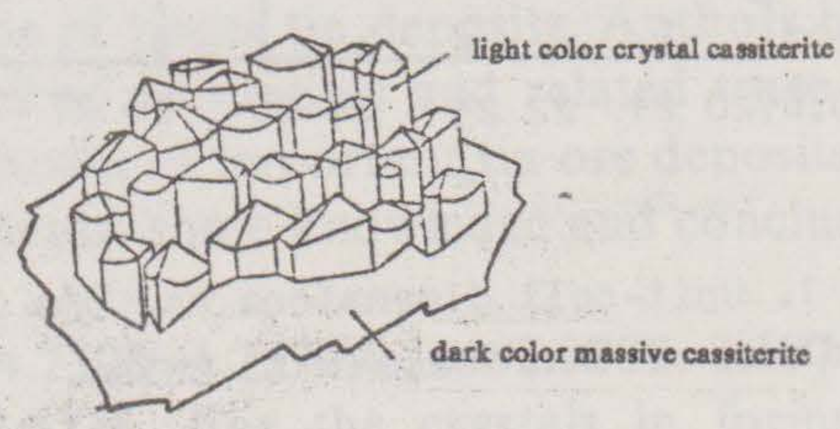

Fig.2 cassiterite crystal drùse (size 5X6mm^2)

4. Poikilitic texture of cassiterite (Fig.4). Fragments of the dark banded cassiterits are enclosed in the light cassiterite crystals, which serves as evidence on the late crystallization of the light cassiterites.

5. Crystallization–resorption–cavity filling of cassiterite(Fig.5).

It seems that three times of crystallization and concerned resorption have happened. The chemical composition of cassiterites shows high contents of Ti, Na, Nb, Zr for the dark ring of cassiterites (Table 1) and the tin mineralization shows pulsatary and continuous properties.

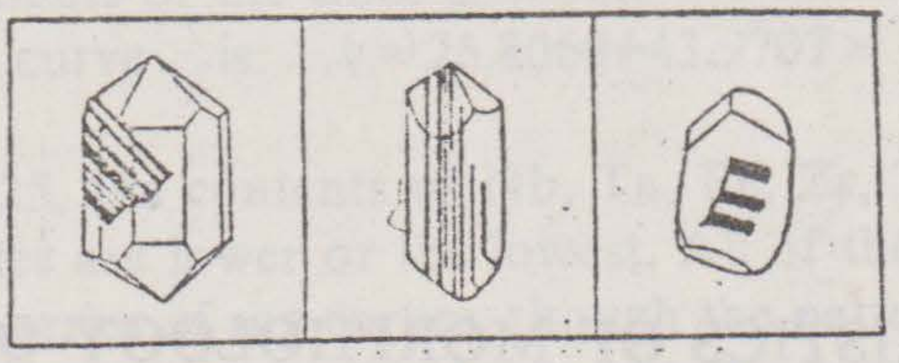

Fig.4 poikillitic texture in cassiterite (1.5mm)

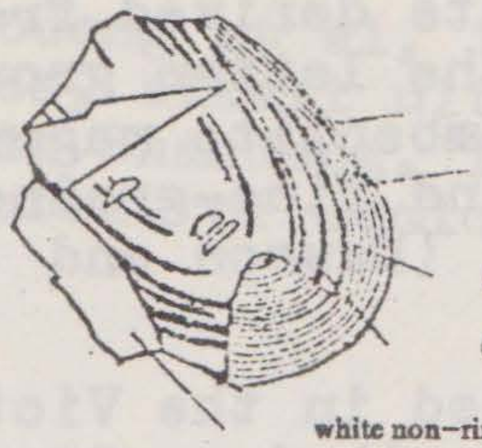

Fig.5 the crystallization, resorption and cavity filling of cassiterite (size 6 × 4cm²)

Table 1. The chemical compositions of cassiterites (laser spectromctry analysis)

	Al	Ca	Cu	Fe	Mg	Na	Nb	Pb	Si	Sn	Ti	Zr	Sc
dark ring cassiterite	0.009	0.01	0.009	0.01	0.01	0.68	0.06	0.04	0.01	76.67	0.82	0.09	0.002
light ring cassiterite							0.42			77.43	0.48	0.02	
light color cassiterite										77.82	0.16		

PHLOGOPITES FROM THE KIMBERLITES AND SURROUNDING COMPLEXES IN SHANDONG, CHINA

ZHAO Donggao and HUANG Yunhui, Institute of Mineral Deposits, Chinese Academy of Geological Sciences, Baiwanzhuang Road 26, Fu Wai, Beijing 100037, China

The compositional variations of different kinds of phlogopites, collected from the Victory 1 kimberlites in Mengyin, Dongshima bedded carbonatites or micaceous carbonatites in Boshan, and Qingyunshan lamprophyre dikes or sills in Linyi, have been studied. Through these studies, the evolutionary trend and the mutual relationship between the kimberlites, located at the center of the western Shandong anticlise, and the surrounding complexes such as carbonatites and lamprophyres, about 80km apart from the Victory 1 kimberlites, have been discussed.

Like the other kimberlites in the world, the Victory 1 kimberlites contain two broad groups of phlogopites: one is strongly resorbed, rounded, distorted, deep brown megacrysts or macrocrysts ranging from several millimeters up to several centimeters in diameter; the other is tiny euhedral-subhedral plate and lath microcrysts whose length are usually smaller than 5mm. These two groups of phlogopites are significantly different in chemical composition, especially in Cr_2O_3 content, the first group being relatively rich in Cr_2O_3 (0.2%) and poor in TFeO, the second being poor in Cr_2O_3 (0.2%) and rich in TFeO. Considering the textural characteristics, the authers think

the former group is possibly xenocrysts derived from primary phlogopites in lherzolites and the latter group is microphenocrysts crystallized from kimberlite magma. This conclusion is based on both coarse- and fine-grained phlogopites instead of on only megacrysts (Dawson and Smith, 1975).

A kind of nodule has been recognized in the Victory 1 kimberlites; this nodule, usually described as "dark mineral aggregate", is dominated by phlogopite (60%) and amphibole (30%), but apatite and some opaque minerals also occur. The phlogopite and amphibole crystals are perfect and coarse, and can include and penetrate each other; the alignment of them is observed. Compared with the other kimberlite phlogopites, the nodule phlogopite has slightly high TFeO content, but is more similar to the microphenocrystal phlogopites in Cr_2O_3 content. The Mg/Mg+Fe values of the micas in the kimberlites, the nodule, and the gneiss xenoliths and wall-rock gneisses are respectively about 0.897, 0.816 and 0.607. Apparently the nodule micas are most similar chemically to the kimberlite phlogopites, so the authers postulate that the nodule is a mantle-derived xenolith similar to the MARID rocks described by Dawson and Smith (1977) in some respects, although a metasomatic origin for such nodule is favored by some Chinese scholars. The further study of the nodule is in progress.

The Qingyunshan intrusions were considered possibly to be lamproite or kimberlite. But the micas in this kind of rocks are significantly different from those in representative kimberlites and lamproites in chemical compositions.

From the Victory 1 kimberlite pipes to the surrounding Dongshima and Qingyunshan, that is to say, from kimberlite ---carbonatite---lamprophyre, the TiO_2 and TFeO contents and the Mg/Mg+Fe values of the phlogopites decrease successively, showing a regular evolutionary trend. Considering the kimberlites and surrounding complexes as a whole, and remembering that the successive decrease of the Mg/Mg+Fe values is a normal evolutionary trend of magma, then we can draw the conclusions that the kimberlites and surrounding complexes in western Shandong anticlise are the products of evolution of cognate magma, and the surrounding complexes are more evolutionary than the kimberlites.

REFERENCES

Dawson, J.B., Smith, J.V. 1975. Chemistry and origin of phlogopite megacrysts in kimberlite, Nature 253, 336-338.

Dawson, J.B., Smith, J.V. 1977. The MARID(mica-amphibole-rutile-ilmenite-diopside) suite of xenoliths in kimberlite Geochim. Cosmochim. Acta 41, 309-323.

Wan Guodong et al, 1983. The relationship between the kimberlites, alkali ultramafic rocks, carbonatites and dark rocks in Shandong. The No. 7 Geological Team of the Shandong Bureau of Geology and Mineral Resources.

CLINOPYROXENES IN BASALT AND ITS PERIDOTITE AND PYROXENITE XENOLITHS

Zhao Hailing and Deng Jinfu, Department of Mineralogy, Petrology and Geochemistry, China University of Geosciences, Beijing, 100083, People's Republic of China

Clinopyroxene is ubiquitous in the basic volcanic rocks and in pyroxenite xenoliths of the basic volcanic rocks. The mineralogical characteristics reflect the physical chemistry conditions of their formation. The study of clinopyroxenes in rocks may provide the characteristics and genetical relationship of the upper mantle and host basalt and approach the rules of evolution of magma formation and differentiation. This paper gives an example of clinopyroxenes in Cenozoic volcanic rocks and the upper mantle rocks in Southeast Coast of China.

Clinopyroxenes in the peridotite xenoliths are Cr-rich diopside and Cr-rich endiopside. Clinopyroxenes in the pyroxenite xenoliths are diopside, endiopside and augite. Clinopyroxenes occur in the basalt as megacryst, phenocryst and microcryst in groundmass. Nearly all of clinopyroxene megacrysts are augite except a few of salite. Most of clinopyroxene phenocrysts and microcryst are Ca-rich. Clinopyroxene phenocrysts and groundmass clinopyroxene in the alkali basalt series are diopside, salite, augite and fassaite. Clinopyroxenes in a few of nephelinites are aegirine-augites. There are augite, pigeonite and bronzite in the tholeiite.

Chemical variation of the clinopyroxenes in the peridotite and the pyroxenite xenoliths and the basalt from the Southeast Coast of China shows that Fe content in the clinopyroxenes increases gradually from the peridotite xenolith to the pyroxenite xenolith to the basalt. The clinopyroxene megacrysts are Ca-poor and Mg-rich compared with the clinopyroxene phenocrysts and microcryst. Composition of Cr_2O_3 in the clinopyroxenes becomes gradually poorer from the peridotite to the pyroxenite to the basalt. These characteristics of the pyroxenes show the genetical difference among them. The trend of evolution of clinopyroxenes is Mg-poor and Ca-rich from the megacrysts to the phenocrysts and microcryst in the groundmass. This trend of evolution is consistent with that from the phenocryst to the microcryst in the alkali basalt series. This shows that the clinopyroxene megacryst crystallizes early from the basalt and indicates that the fractional crystallization of olivine and clinopyroxene is essential during evolution of alkali basalt series in this area.

Chemical composition and optical characteristics of the

clinopyroxenes in the peridotite and the pyroxenite xenoliths and those of the clinopyroxene megacrysts are homogeneous. This shows that they formed at high pressure. Content of Calcium Tschermak's molecule in the clinopyroxene megacrysts is similar to or more than that in the clinopyroxenes in the peridotite and the pyroxenite xenoliths. This shows that the pressure of its formation is similar to or more than that of the upper mantle xenoliths. This is consistent with the results of calculation using thermodynomical method and has been explained using fluid dynamics of magma. The clinopyroxenes of the phenocrysts and the groundmass in the basalt are zoned. Except a few of them are reversely zoned, most of them are decreased in Mg content, and increased in Ca, Fe and Ti from the cores to margin in alkali basalt series.

The trend of evolution of the clinopyroxenes is Ca-poor, Mg-rich and Fe-rich from the phenocrysts to the microcryst in the groundmass in tholeiite, which is different from one of the alkali basalt series. We suggest that the variation trend of major elements of the clinopyroxenes from the phenocryst to the microcryst in the groundmass in the basalt should be significant to distinguish the alkali basalt series from the tholeiite series.

1.22V

PYROXENES OF SKARN DEPOSITS IN CHINA

Zhao Yiming and Lin Wenwei , Institute of Mineral Deposits, Chinese Academy of Geological Sciences , Beijing 100037 , People's Republic of China

Based on the mineral associations of the skarns of 35 major skarn deposits in China studied by the authors, the four types of skarns are divided, i.e. magnesian skarn, calcic skarn , manganoan skarn and alkaline skarn .In different types of skarn deposits exist different types of pyroxenes.

Magnesian skarn may be divided into magmatic magnesian skarn and postmagmatic magnesian skarn . The pyroxenes in magmatic magnesian skarns are generally aluminodiopsides, and are usually associated with spinel, monticellite, forsterite ,and periclase. Aluminodiopsides contain appreciable quantities of alumina (3.64–13.14wt.%), which result in changes of their optical properties, and have strong dispersion of the optical axes angles ($2V_C - 2V_F = 4–14$). The pyroxenes in postmagmatic magnesian skarns are always diopside ($Di_{95–99}Hed_{1–5}$) , associated with forsterite, and overlaid by tremolite ,phlogopite and serpentine . The accompanied mineralizations may have Fe,Cu,Mo,Sn,Au,B. etc.

The pyroxenes in the calcic skarns are of the diopside–hedenbergite series, associated with garnet, wollastonite, and vesuvianite .The systematic investigations show that the compositions of coexisting pyroxenes and garnets in different calcic skarn ore deposits have variety obvious rule , as follows:

The pyroxenes in Fe and Cu skarn doposits are mainly diopside with lower contents of johannsenite molecules. Their associated garnets are generally andradites (And_{63-95}). The pyroxenes in Mo–bearing skarns are chiefly diopside ($Di_{56-93}Hed_{6-41}$). Their coexisting garnets are of transitional types of the grossular–andradite series (And_{17-68}).The pyroxenes in scheelite–bearing skarns are mainly diopside and hedenbergite with certain content of johannsenite molecules ($Hed_{34-59}Joh_{8-10}$). The coexisting garnets belong to transitional types of the grossular–andradite series with comparatively higher content of spessartine molecules ($And_{52-88}Sp_{4-22}$). The pyroxenes in Sn–bearing calcic skarns are predominantly hedenbergite, and subordinately diopside.

To sum up , the metasomatic minerogenetic speciality of the calcic skarns is very obvious . Along with increase of the acidity of skarnizing solutions and decrease of the oxygen fugacity , the valence states of iron are gradually changed from Fe^{3+}in garnets to Fe^{2+}in clinopyroxenes replacing Mg^{2+}. Their accompanied mineralizations are also varied regularly : Fe, Cu→ Mo→W→Sn .

Pb–Zn skarn deposits have some special characters . They occur in relatively shallow environment and usually have a suit of manganoan skarns . The manganoan skarns mainly consist of manganese clinopyroxenes (Mn–hedenbergite , johannsenite , Mn–diopside) and manganese pyroxenoids (rhodonite , bustamite , pyroxmangite , Mn–wollastonite) , which may be accompanied by andradite , Mn–ilvaite , Mn–actinolite . In individual deposit , there appear appreciable quantities of spessartine .

Alkaline skarns occur in the contact zones between syenites and dolomitic carbonate rocks . In the alkaline skarns , the type of pyroxenes is aegirine , associated with many alkaline metasomatic minerals , such as nepheline , arfvedsonite , eckermannite , sodium–tremolite , orthoclase , albite , and phlogopite ,Alkaline skarns are accompanied by U, Th, Tr, Nb, mineralizations .

MINERALOGICAL CHARACTER AND SIGNIFICANCE OF HUANGSHAN COMPLEX IN XINJIANG

Zhong Yingxian, Department of Geology, Chengdu College of Geology, Chengdu 610059, People's Republic of China

Huangshan complex is a mafic-ultramafic complex rich in Cu, Ni sulfide deposits. It thermally intruded into the blastosandstones, philites of the lower Carboniferous of Tianshan fold system. It could be divided into harzburgite, olivine-websterite, websterite, hypersthene-gabbro, and gabbro phases from bottom to top and west to east.

The rock-forming minerals of the complex are olivines (Ol), orthorhombic pyroxenes(Opx), monoclinic pyroxenes

(Cpx), plagioclases (Pl), amphiboles (Amp) , and a few biotites (Bi) , phlogopites (Phl).

Optic and chemical characters of Ol indicate that there are two kinds of Ol, one crystallized after magma intrusion, the other crystallized before magma intrusion. The change of Ni content in Ol shows that the parent magma underwent sulfide immiscible separation.

There are general pleochroism in Opx. The reason is not rich in Fe in Opx, considered by people. It accounts for the higher Ti in Opx.

There are widespread reaction between Cpx and Amp. It does not limit the edges of Cpx. It may appear in the center and any spot in patch on Cpx. It constructs a kind of newly discovered texture of magmatic rocks--Amphibole Reaction Patch Texture. The chemical character of Cpx and relationship between some elements in Cpx indicate that the parent magma undergone immiscible separation belongs to tholeiitic series.

The regular change of An in Pl and En in Opx from bottom to top shows that the complex underwent clear gravitative differentiation.

There are distinct negative normal of Ce in ultramafic rocks in Huangshan complex, it is similar to other ultramafic rocks in the world. The reason is mainly that Opx and Ol possess negative normal of Ce in the ultramafic rocks, it does not show the direct relation with f_{O_2}.

The chemical character in Bi and Phl, show that K,Ba, Th, Hf etc. elements display abnormal geochemical behavior in harzburgite. The reason is not the revolition of magma. It is Bi and Phl possess larger tolerance to K, Ba, Th, Hf etc. elements.

The calculation, according to chemical composition of Ol, Opx, Cpx, Pl, Amp etc., show the physical and chemical condition of complex when formed are: temperature=1500--860 C, pressure=0.26--0.25GPa, fo =10 --10 which is advantageous to form Cu, Ni sulfide deposits.

There is a result through researching the minerals above:

The parent magma of the complex belonged to olivine-tholeiitic series which had undergone immiscible separation, then crystallized under gravitative differentiation and formed Huangshan complex. The physical and chemical condition of complex when formed is just that of Cu, Ni sulfide deposits required.

Po 1.22

A STUDY ON FORMING CONDITIONS OF Ag,Au-TELLURIDES IN SOME HYDROTHERMAL GOLD DEPOSITS

ZHOU Jianping, CHEN Wu, Department of Earth Sciences,Nanjing University, Nanjing, jiangsu, 210008, P. R. of China

In hydrothermal deposits, gold can be concentrated both in mineralization zones of Pyrite, arsenopyrite and Cu-sulfides association and of tellurides, quartz, barite and hematite association. Many volcanic and metamorphic hydrothermal gold deposits in southeastern China contain a number of Ag, Au-tellurides, such as Lishui Au-telluride deposit, Jiangsu, and Huangshan gold deposit,Zhuji,Zhejiang.

Investigation of textural relationships and mineral assemblages among vein-filling minerals which reflect the order of precipitation indicate: (1) deposition of Ag, Au-tellurides succeeds initial deposition of sulfides; (2) in some cases, deposition of tellurides with hight Te/Au+Ag ratios, such as calaverite, sylvanite and tellurium, was followed by those with lower Te/Au+Au ratios, such as petzite, hessite and electrum, however, opposite order of deposition occurred in some other deposits ; (3) hessite and native gold with low fineness (about 820-830) are most common minerals in depths of ore body where calaverite , sylvanite and native tellurium do not occur, indicating a low Te/Au+Ag and high Ag/Au ratio in depths; (4) electrum or native gold were deposited simultaneously with or following tellurides but not before the telluride-bearing stage. The other telluride minerials coexisted with Ag, Au-tellurides are Hg, Pb, Cu, Ni and Fe tellurides etc.

Quartz, hematite and magnetite are main oxides intergrown with Ag, Au-tellurides. Most oxides, except those of Sn and Fe, are unstable with respect to tellurides over the normal range in fo_2 encountered in hydrothermal deposits. Quartz vein containing Ag, Au-tellurides, is generally late, clear, undeformed and contains less inclusions, and often crosscuts or encloses early preexisting milky, inclusion-rich, strained quartz that occupies most of the volume in the veins, Gangue minerals typically include adularia, chlorite, sericite, barite, and carbonates.

The results of experiment of Au-Ag-Te system can be used to explain the occurrence, paragenesis and forming sequence of Ag, Au-tellurides which are of typomorphic significance. It is worth to note the decomposition of γ phase [$(Ag,Au)_{2-x}$ Te, x=0.09-.12] and χ phase (Ag_{11-x} $Au_{1+x}Te$). The assemblage of hessite, stuetzite and petzite (low Te/Au+Ag) and sylvanite (high Te/Au+Ag) is considered as a result of decomposition of γ and/or χ phase below 120°C. Occurrence of paragenetic minerals such as pyrrhotite and studies on fluid inclusions suggest that most tellurides are formed from low salinity ore-forming fluid under the conditions of low temperature (120°-280°C) and low pressure (P<500b).

The intergrowth of high fineness (about 960) and calaverite filling in pyrite fissures in Huangshan and Lishui gold deposits suggests a high $a_{Au}+/a_{Ag}+$ ratio of hydrothermal fluid and $-\log a_{Te}$ value of being 9-10 during the cause of deposition. The range of f_{S_2} can also be defined based on reactions of most common minerals, such as pyrrhotite-pyrite-hematite and chalcopyrite-bornite-pyrite, and a_{Te_2} of formation of Ag, Au-tellurides can be determined according to reactions such as native silver, electrum→ calaverite.

The important variable controlling whether gold is concentrated in sulfides or in Au-tellurides from ore-forming fluid for a given metallic composition is f_{S_2} , a_{Te_2} , and temperature. Fugacity of tellurium

determines if tellurides are deposited from hydrothermal fluid and what kinds of tellurides may occur. There are two ways from telluride undersaturated source to telluride saturated, one is decreasing of temperature, which largely occurs in area where fissure is well developed, and the other is increasing of a Te_2 in hydrothermal fluid. Since the average concentration of Te in igneous rocks is only about 1 ppb, and those rock-forming minerals are obviously uncompatible for Te, three ways of Te concentration are suggested in this study: (1) immiscible sulfide melt rich in Te seprates from silicate melt; (2) Te-rich hydrothermal fluid is derived from late differentiated magma; (3) the reactions between hydrothermal fluid, especially those rich in Ag, Au, Hg and pb, and wall rocks may extract a lot of Te from pyritization zone or copper-sulfide zone. Formation of tellurides from some hydrothermal gold deposits in southeastern China is principally related to the second and the third ways. In this area, the most common occurrence of native gold and Ag,Au-telluride minerals is in epithermal quartz veins associated with volcanic or subvolcanic rocks. The fact that $\delta^{34}s$ values of pyrite from Yinkengshan Ag-Au deposit, Zhejiang, ranges from 3 to 6‰(average about 5‰), is consistent with the sulfur isotope composition of adjacent volcanics. $\delta^{18}O$ values of quartz from the deposit are about -1.75—+3.91‰, which indicates that a majority of the ore-forming fluid was derived from magma. While in some other Au-telluride deposits, such as Lishui, Jiangsu, $\delta^{18}O$ values of quartz from the veins with somewhat metamorphic features containing Ag, Au-tellurides are much higher, about 12-13‰. This implies that replacement and extraction of ore-forming fluid (including metamorphic hydrothermal fluid) on early-formed sulfides might increse a_{Te_2} in some areas, leading to a formation of Ag, Au-tellurides. Local increasing of a_{Te_2} may cause the coexistence of tellurides, such as calaverite, altaite and coloradoite, and native gold with high fineness in fissures or surroundings of sulfide minerals (mainly pyrite and chalcopyrite), and also the crosscutting of some telluride-bearing stockwork veinlets through massive sulfide ores or hydrothermal sulfide veins.

THE ZONING MINERALOGICAL CHARACTERISTICS AND THEIR APPLICATION IN GAOCUN DEPOSIT ,HETAI GOLD ORE ,GUANGDONG PROVINCE ,CHINA

ZHOU Ping, Hubei Institute of Geological Experiment,Wuham,Hubei 430022,People's Republic of China

Hetai gold ore,formed in the mylonite belt , whose wall rocks are Sinian migmatized schists and migmatites, is divided into six deposits,i.e.Gaocun,Yunxi and Houjing deposits,etc.

The No.11 orebody of Gaocun deposit is characterized by its distinctive space zonality in mineralogy. Take the example of the form zonation of pyrite: the cubic form dominates amd only a few other types appear in the upper oreboy;in the middle the dominance of cubic form is substituted by that of various types of combinate forms composed of cub,octahdron,pyritohedron trapezohedron and diploid; the cubic form increases again in the lower orebody. Besides,the face(111) and (hko) on a cube

vary from small to large and back to small sizes with their different places in the orebody.The upper orebody of the thermo-electricity field of the pyrite is characterized by cavity type,while the middle and the lower orebody by the electron type. The major metal mineralogic assemblages are pyrite + chalcopyrite(less) im the upper, pyrite + chalcopyrite + sphalerite(less) + pyrrhotite(less) in the middle,and pyrrho-tite + chalcopyrite + sphalerite(less) + pyrite(less) in the lower orebody.

The analysis of drill samples of Yunxi and Houjing deposits,which are being explored, demonstrates that the mineralogical characteristics of both the deposits are similar to those of the upper-middle and upper parts of the No.11 orebody respectively. It is suggested that the above two deposits extend downwards on a large scale,which is confirmed by the recent deep drill in Yunxi deposit.

STUDIES ON THE TYPE AND THE TYPOMORPHIC CHARACTERISTICS OF THE GARNETS FROM KIMBERLITES AND THE RELATIONSHIP BETWEEN THE GARNETS AND DIAMOND

P 1.25

Zhou Xiuzhong , Huang Yunhui , Qin Shuying , Deng Chujun , Gao Yan and Yang Jianmin , Institute of Mineral Deposits , Chinese Academy of Geological Sciences , Beijing 100037 , People's Republic of China

The 85 samples of the studied garnets are collected primarily from the kimberlite of Shandon and Liaoning Provinces , and secondarily from the eclogite xenoliths of Liaoning and Hebei Provinces , China .

The chemical composition of garnets were analysed by electron probe , their end members were calculated by the partition method of molecular number , and the colors described quantitatively with their dominant λ which were measured by MPV−1 . The classification , and formation conditions of the garnets are discussed based on above results . Meanwhile , the discriminant diagram of the proportion of the Ca , Cr , and Mg component of the garnets is made . It is possible to find out the typomorphic characteristics of the garnets which are closely related to diamond .

The diagram is divided into 5 fields (A−E) with one oblique line (Ca = 15%) and three horizontal lines (Cr = 15% , 10% and 5% respectively) , (see Figure) . Field A , poor in Ca and rich in Cr (Ca < 15% , Cr > 15%) is closely related to diamond .

If put the chemical composition of all garnets into the Dawson and Stephens' (1975)[1] chemical groups , it will be shown that a large amount of garnets belong to the chemical group DG9 and a few garnets belong to the DG1−5 , the rest belong to DG10 , DG11 and DG12 .

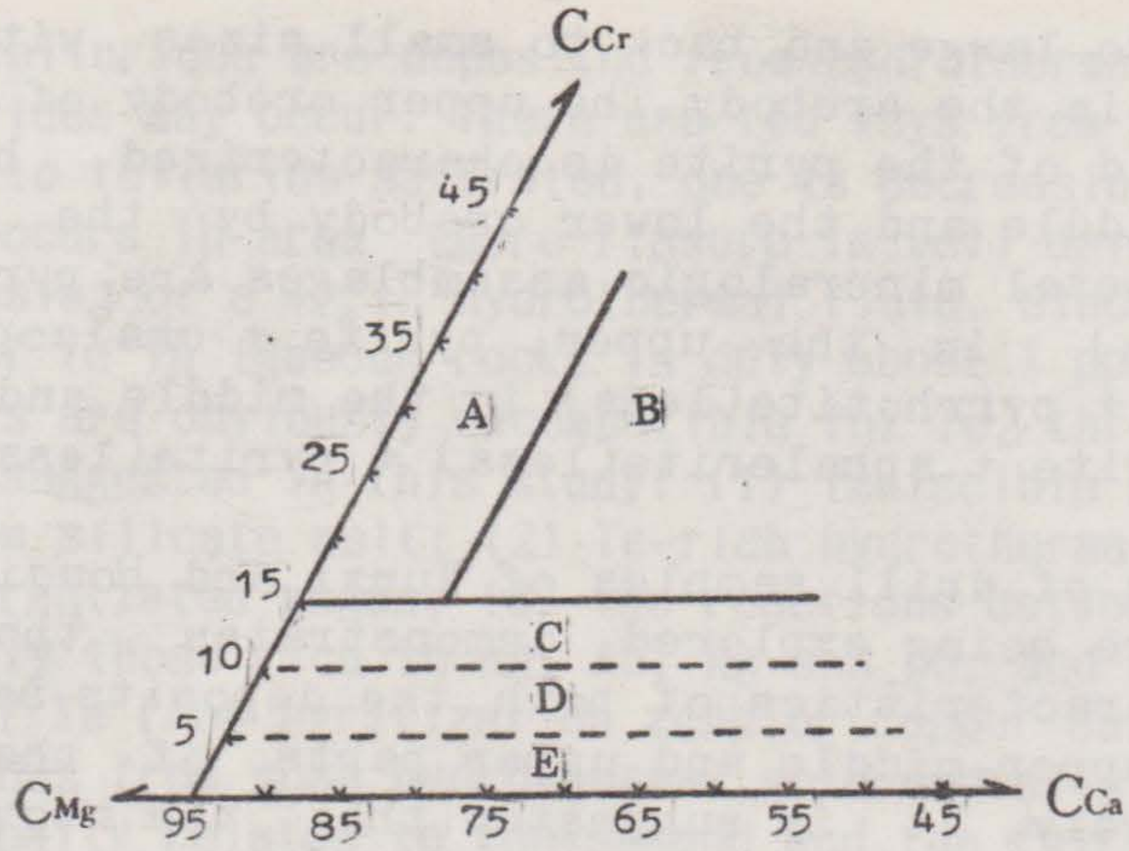

When put the components Ca , Cr , and Mg of these garnets into above diagram , it may be found that both the garnets , belonging to the chemical group DG10 , DG11 and a part of garnets belonging to the DG9 , are fallen in Field A . The garnets of chemical group DG12 which contain highest Cr and medium to high Ca components are fallen in Field B . So it is possible that the garnets , containning high Cr and low Ca components , are closely related to the concentration of diamond .

The garnets which fallen in Field A are collected from Shenli pipe No.1 , Hongqi dike No.1 and No.27 of Shandon Province ; and the pipes No.50 , 51 , 68 , 42 , and 30 of Liaoning Province . They are all the main ore–kimberlite . The garnets of ore–free kimberlite from Hubei and Henan Provinces are fallen in Field B , C , D and E .

The color of the garnets , belonging to Field A , is mainly red , reddish purple , and purple , the individual is bluish green .

Some geologists❷ infer that the formation conditions of the garnets of kimberlite are : temperature 1100–1300 ° C , pressure 4.5–6.5 Gpa and the depth of 240Km . According to the previous investigated results , the authours suggest that the further increase all of the Cr / Cr+Al , a temperature and pressure will be favourable to the formation of diamond .

References :

❶ Dawson , J.B. and Stephens , W.E. , 1975 . Statistical analysis of garnets from Kimberlites and associated xenoliths . J. Geol. 83 : 589–607 .

❷ Irifune ,T.,1985 . Experimental study of the system $Mg_3Al_2Si_3O_{12}$–$Mg_3Cr_2Si_3O_{12}$ at high pressure and high temperature . Journal of the Faculty of Science Hokkaido University , Vol. 21 , No. 3: 449.

MINERAL CHARACTERISTICS IN DIAGENESIS OF THE OSTRACOD SHELLS AND ITS INDICATORS IN OIL EXPLORATION

Zhu Xiaoling and Li Yougui, Institute of Mineral Deposits, Chinese Acade-

my of Geological Sciences, Baiwanzhuang Road 26, 100037 Beijing, P.R.C.

The authors intend to have a comprehensive study to make it possible for ostracod shells to play a role not only in the fields of stratigraphic division and correlation, and geological time determination, but also as important indicatores in oil exploration, on the basis of the phase indentification of the nonmarine Cretaceous ostracod shells and closed carapaces with sediment infills by X–Ray diffraction, in conbination with the analysis of trace–element of the ostracod shells, the colour of carapaces and the ratio between closed carapaces and isolated valves. It is important research subject in the present paper.

This paper on the basis of the analystical outcome of 2000 samples has arrived at the following conclusions:

1. The sample contain 85% of shells ranging from dark brown to black in colour with 92% closed carapaces; the ratio of trace–elements of the ostracod shells:
   Fe / Ca: 0.0172–0.2955, Mg / Ca: 0.0059–0.0909, Sr / Ca: 0.0009–0.0059, Sr / Ba: 2.00–10.00, Organic C: 0.29%–2.25%, S: 1.37%–7.24%; phase identification by X–Ray diffraction of the powder of the ostracods shows:
   It consists mainly of Calcite ($CaCO_3$) and a few Quartz (SiO_2), some Pyrite (FeS_2) and Aukerite ($Ca(Fe,Mg)(CO_3)_2$) are present in it. The sedimentary rocks producing these samples must have been in a reducing environment; high sedimentation rate; in general, the source–rocks or display a strong oil showing.
2. The samples contain 100% of shells ranging from white to light brown, moreover, the isolated valves are more than 50% as opposed to carapaces. The ratio of trace–elements of the ostracod shells: Fe / Ca: 0.0018–0.0571, Mg / Ca: 0.0009–0.0204, Sr / Ca: 0.0008–0.0052, Sr / Ba: 2.00–10.00, Organic C: 0.21%–0.84%, S: 0.06%–1.37%; phase identification by X–ray diffraction of powder of the ostracods shows: It consists of Calcite ($CaCO_3$) and a few Quartz (SiO_2). The sedimentary layers yielding these samples must have been deposited in a weak reducing environment with a lower sedimentation rate, are non–oil bearing layer and display no oil showing.

THE EFFECT OF PIEZOOPTIC CRYSTAL MEMORY AS A NEW

THERMOBAROMETER OF POSTCRYSTALIZATION PROCESSES

Zil'bershtein A.Kh.,VSEGEI,Leningrad,199026,USSR

Sometimes optical anomalies in sinthetic and natural crystals are observed. These anomalies may be induced by internal stresses (X). This stress may be exist due to postcrystalization external pressure (or stress). It's discovered that the value of these anomalies is proportional to the value of external stresses (for different minerals). This is the effect of crystal memory about external stress and pressure in postcrystalization process. The influence of the temperature (T) and exposition (t) of process was investigated. The effective internal stress may be determined from the value of optical anomalies. The effective stress as a function of parameters of process was discovered in view:

$$X = a\ P\ \ln(t)\ \exp(-bT), \text{ for } t < t_o,$$

or $$X = a'P\ \exp(-bT), \text{ for } t \geq t_o,$$

where a, a', b, t_o are the material (mineral) constants. This expression may be used for estimations of Thermodynamic conditions of crystal growth in nature. It is the thermobarometer of new tipe - the optical thermobarometer.

(Ba-K)-FELDSPARS AND BARIAN MUSCOVITE FROM THE KIPUSHI Zn-Pb-Cu DEPOSIT(SHABA, ZAIRE).

Mumba CHABU,Université de Lubumbashi,Laboratoire de Métallogénie B.P. 1825,Lubumbashi,Zaïre.

Barian muscovites and barian feldspars have been observed in association with baryte within the sulfide mineralization of the Kipushi Zn-Pb-Cu deposit hosted by Lower Kundelungu dolomites and dolomitic shales of Late Proterozoic age and by their breccias.

Muscovite changes in composition from normal phengitic muscovite to a highly barium-enriched white mica. The more barium-rich muscovites occur in two mineral assemblages:(i) Ba-muscovite-adularia-hyalophane-baryte-albite-dolomite and(ii) Ba-muscovite-

hyalophane-celsian-baryte-albite-dolomite.

The highest BaO content measured in muscovite is 7.66 weight percent but values around 6 weight percent BaO are more common in barium-muscovite from both assemblages. These micas and the associated minerals occur randomly throughout the sphalerite and dolomite matrix of mineralized breccias.

There is a broad positive correlation between Ba and Al in tetrahedral positions(Fig.1) suggesting that the excess interlayer charge resulting from the replacement of a monovalent element(K) by a bivalent one(Ba), is partly balanced by substitution of Al for Si according to reaction $BaAl=(K,Na)Si$ (1).

Ba is negatively correlated with octahedral occupancy as illustrated in figure 2; this indicates that the excess interlayer charge is also partly balanced by an increase of negative charge resulting from vacancies in octahedral sites.

Mg does not correlate with Ba,but it displays, along with Fe, a relatively well-defined negative correlation with Al. This substitution is the common phengitic substitution of normal muscovite $(Mg,Fe)^{2+}=Al^{VI}\ Al^{IV}$ (2), in which octahedral charge deficiency produced by substitution of Mg for Al in octahedral sites is compensated by increasing Si in tetrahedral positions. The lack of correlation between Ba and Mg indicates that the two substitutions operate independantly.

Feldspars are widespraed in the Kipushi deposit. They are divisible into two groups:(i) albite and(ii) (Ba-K)-feldspars. Albite is the predominant feldspar mineral both in the country rocks and in ores.Its anorthite content ranges from 0 mole percent to 5 mole percent.

Neoformed(Ba-K)-feldspars extend from adularia to celsian. They appear in the same mineral assemblages as barian muscovite although although a Ba-orthoclase has been found to occur outside these associations. Relict grains of baryte were observed embodied in adularia.

The celsian content of (Ba-K)-feldspars ranges from 1.01 to 84.04 percent, but no data were obtained between 5.43 percent and 30.53 percent celsian. Gay and Roy(1968) postulated a composition gap between hyalophane(15-65% celsian)and celsian(85-100% celsian),however the present data indicate that the series adularia-celsian may be continous at relatively low temperature(low grade greenschist facies) suggesting that the reported compositional gap,may fortuitous.

Structural and textural fabrics indicate that Katangan regional metamorphism post-dated the emplacement of the mineralization. It is characterized by low grade metamorphic mineral assemblages of the greenschist facies and it is believed that barium silicates are metamorphic in origin and that their barium content was inherited from baryte present in the mineralization.

References

Fortey,N. J. and Beddoe-Stephens,B.(1982).Mineralogical Mag.46, 63-72.

Gay,P. and Roy,N.N.(1968).Mineralogical Mag.36,914-932.

Seignit,E.R. and Gelb,T.(1970).Australian Jour. Ceramics Soc.6, 12-18

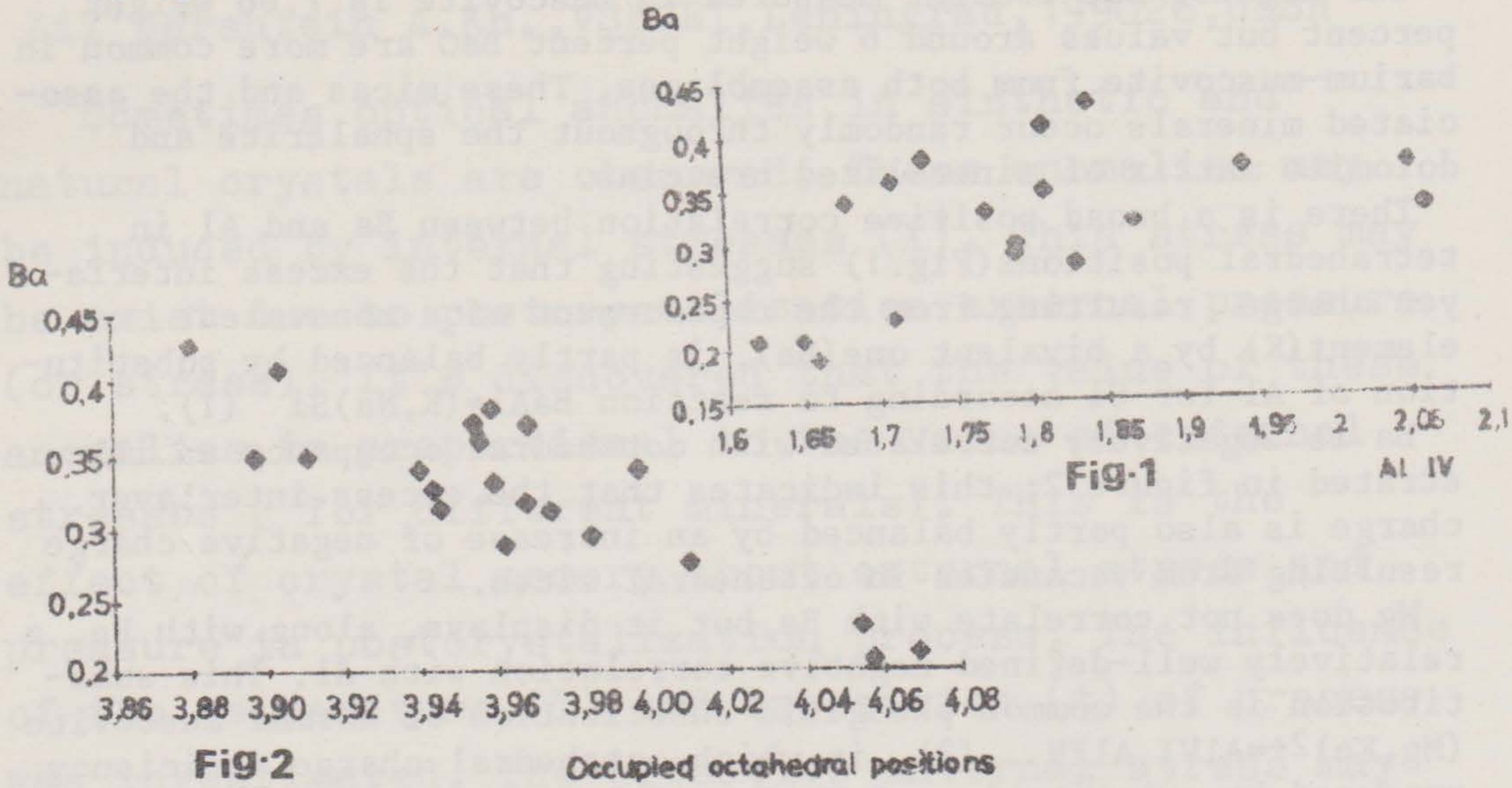

Fig·2

Fig·1

THE GEOCHEMISTRY OF BIOTITE FROM THE KIPUSHI CARBONATE HOSTED Zn-Pb-Cu DEPOSIT(SHABA,ZAIRE).

Mumba CHABU, Université de Lubumbashi, Laboratoire de Métallogénie B.P. 1825, Lubumbashi,Zaïre.

Biotite has been observed in the Kipushi deposit,one of Africa's largest producers of zinc,germanium and cadmium, hosted by Lower Kundelungu group dolomites and dolomitic shales of Late Proterozoic age and by solution collapse breccias. The orebody is located on theeastern edge of a complex breccia field composed on its central part, of huge blocks of different lithologies mainly dolomites derived from Upper Roan Group,stratigraphically below the Kundelungu Supergroup which is host to the mineralization.Some of these blocks have been intruded by doleritic sills prior to their dislocation.

Micrprobe analyses indicate that the biotites are actually phlogopites and that the highest fluorine contents ranging from 4.41 wt.% to 6.39 wt.% and the lowest fluorine intercept values, ranging from 1.04 to 1.90, are found in ore-related Phlogopites associated with phengitic muscovite, dolomite,sphalerite,pyrite and galena or with Mg-chlorite, dolomite,quartz,chalcopyrite and bornite. Its mole fraction phlogopite is also very high(0.68 to 0.95) within the mineralization. A reaction rim is observed around certain phlogopite grains embodied in sphalerite. The mica shows indented edges resulting from silicate-sulfide reactions. Small relict flackes of phlogopite oriented parallel to the phlogopite grain are seen within the reaction rim.

Other phlogopite-bearing mineral assemblages,from barren rocks,

are:phlogopite, Mg-chlorite, dolomite and quartz; and phlogopite, talc, albite, magnesite, dolomite, gypsum, anhydrite and quartz occurring respectively in shales and dolomites above the orebody. Phlogopite, albite and amphibole are major components of doleritic blocks. They are associated with chlorite, epidote and calcite.

In general, mole fraction phlogopite, F and Si vary sympathetically. Phlogopites involved in associations containing gypsum and anhydrite behave differently. They have high mole fraction phlogopite, in the same range as that of F-rich ones, but significantly low F contents(1.09 to 1.78 wt.%).

The best positive correlation between mole fraction phlogopite and F content is shown in micas from barren rocks(Fig1), whereas fluorine enriched ones display an unusual crude inverse relationship in violation of the Fe-F avoindance principle. Mole fraction phlogopite shows a well-defined negative correlation with Al VI (Fig.2). Though very rough a similar relation with Ti is observed.

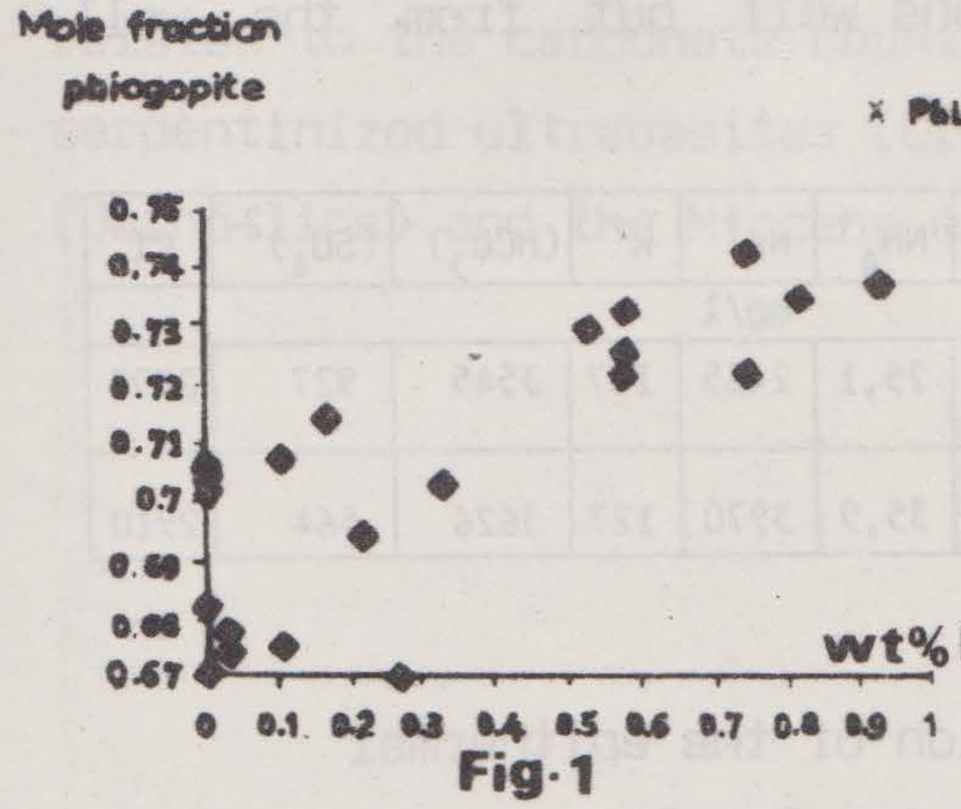

Fig·1

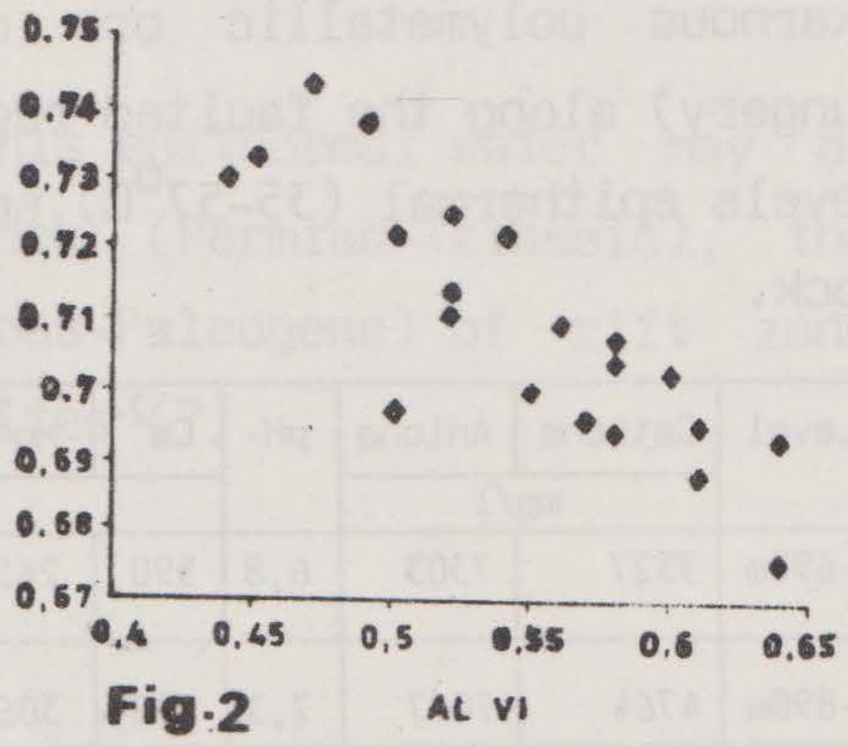

Fig·2

Calculations of $\log(f(H_2O)/f(HF))$ based on calibrated F-OH exchange relations between a fluid and a mica(Munoz and Ludington, 1974; Valley et al.,1982; Munoz,1984) indicate higher relative activity of fluorine in mineralized areas than in barren zones. The observed difference represents at least a one-hundred-fifty-fold increase in relative HF activity towards mineralized zones.

The development of biotite is attributed to metamorphic processes and its F content is interpreted in term of bulk composition influence on metamorphic hydrous minerals geochemistry. This is supported by the presence of similar metamorphic mineral assemblages on a regional scale and by the observed reaction rims around some phlogopite grains, a characteristic feature of silicate-sulfide reactions found in metamorphosed ores(Mallio and Gheith,1972).

References

Mallio, W.J.,and Gheith, M.A. 1972. Mineralium Deposita7,13-17

Munoz, J.L.,1984. Mineral. Soc. Am., Reviews in Mineralogy,13, Baileys, S.W.,ed.,469-493.

Munoz,J.L., and Ludington, S.D.,1974;Am. Jour. Sci.,274,396-413.

Valley,J.W.,Petersen, E.U., Essene, E.J., Bowman, J.R.,1982. Am. Mineralogist 67,545-557

THE FORMATION OF MINERALS BY RECENT HYDROTHERMS AT THE RECSK ORE MINE, HUNGARY

János Kiss[+] and Melinda Jánosi[++], Department of Mineralogy[+] and Department of Petrology and Geochemistry[++], Eötvös University, Budapest, Múzeum krt. 4/a, Hungary, H-1088

During the mining operation of the porphyry copper and skarnous polymetallic ore deposits at Recsk (Mátra Mts., Hungary) along the faulted region in the -690 m and -890 m levels epithermal (35-57°C) solutions well out from the wall rock.

Level	Cations	Anions	pH	Ca^{2+}	Mg^{2+}	Fe^{2+}	NH_4^+	Na^+	K^+	$(HCO_3)^-$	$(SO_4)^{2-}$	Cl^-
	mg/l			mg/l								
-690m	3527	7303	6,8	590	265	0,08	75,1	2465	107	3545	927	2792
-890m	4764	7097	7,3	290	306	0,03	35,9	3970	127	3626	564	2910

Table 1.

Average chemical composition of the epithermal solutions at the two levels

The precipitated minerals are predominantly calcite and aragonite. They form stalactitic masses, oncoides or incrustations. On the surface of these precipitations (or independently of them) as efflorescences, incrustations or as thin coatings the following peculiar mineral paragenesis was observed:
NESQUEHONITE $MgCO_3.3H_2O$, DYPINGITE $Mg_5(CO_3)_4(OH)_2.5H_2O$, NORTHUPITE $Na_3Mg(CO_3)_2Cl$, BLOEDITE $Na_2Mg(SO_4)_2.4H_2O$, THENARDITE Na_2SO_4, HALITE NaCl.
These minerals are accompanied by gypsum and sulphur. In the examined 140 samples more than ten other minerals can be traced in minor quantity.

The water chemistry (see Table 1.) and the precipitated mineral paragenesis are different at the two depths. At the lower level magnesian carbonate and chloride minerals occur in greater amount in comparison with the higher level and we found bloedite exclusively in the samples from the lower level.

There is a considerable similarity between the mineral paragenesis observed at Recsk and the minerals of weathered serpentinite, of evaporites, of the inland salt lakes, of speleothems. A significant difference is, however, that all of the minerals at Recsk discussed here are precipitated from epithermal solutions, and the joint occurrence of these minerals was not recorded so far.

The origin of dissolved ions in this epithermal water may be related to the carbonate country rock (Permian-Triassic), the serpentinized ultrabasites (Cretaceous-Paleogene) of rift zone (Darnó-line) and the Miocene evaporites (?).

ROUTINE IN CL-PETROGRAPHY OF CARBONATE CEMENTS: PROPOSAL OF STANDARD FOR COLOR DESCRIPTIONS

Pascal Amieux, 108 rue Vendôme, 69006 Lyon, France

Problem in communication of results of cathodoluminescence (CL) arise from the difficulties of consulting relevant standards and then the difficulties of using appropriate vocabulary. For description authors refer to "bright" or "dull" luminescence but such terms are relative to their sample suites. Terminology qualifying the low intensities is highly variable because there is no petrographic reference. What is the reality, under the microscope, of a "dark-", "background-" or "non-" luminescent area ? To help overcome these potentially serious problems, description of CL characteristic should be chosen to be as unambiguous as possible wrote John Miller in 1988.

The aim of this communication is to propose a unequivocal standard so that comparisons between the data of different workers may be valid.

As a result of ten years of CL-petrographic investigations, as far I know pyrite shows always a color very similar to black in sedimentary, hydrothermal or plutonic environments. This observation is obtained either with Technosyn or Nuclide Corporation apparatus and also with different kinds of microscope (Leitz, Zeiss, Olympus and Nikon).

Pyrite is a conductive mineral. Considering the energy band model (Garlick, 1964), it exists only a conduction band in the electronic scheme of conductive minerals. This property implies that there is no electronic transition in pyrite which makes emission of photon forbidden. Therefore black color observed in pyrite under electron beam bombardment is a truly non-luminescent response to the electronic excitation. For these reasons I consider that pyrite is an unequivocal standard of black color and of 0 intensity grade level. As pyrite is a widespread mineral in sedimentary rocks large applications to this standard are expected.

For instance comparison of the pyrite standard with very dull colors in carbonates or the so-called "non-luminescent" carbonates is the mean to distinguish black color from very dull blue and very dull brown

colors (Amieux *et al.*, 1989). The pyrite standard allows to use this kind of descriptive terms rather than interpretative locution such as "non-luminescent cement" from which we have no descriptive information.
The geological implication of the improvement of the descriptive methodology offers a better understanding of the carbonate cements precipitating conditions in phreatic environments.
An other application of the pyrite standard is to test CL-apparatus and microscope efficiency. The results should be incorporated in the operating parameters table proposed by D.J. Marshall in 1978. Because pyrite standard represents also an absolute 0 grade of intensity it will be possible to calibrate spectrophotometer and then to create useful scale for CL-intensity.
To confirm these applications I am comparing (work in progress) pyrite standard with carbonate samples coming from other petrographers so interested enough to help in the efficiency of this study (M. Coniglio, University of Waterloo, Canada; S. Dorobek, Texas A & M University, USA; P. Frykman, Geological Survey of Danemark; J.J. Mancuso, Bowling Green State University and J.F. Read, Virginia Polytechnic Institute, USA).

References

Amieux, P., Bernier, P., Dalongeville, R. & Medwecki (de) V., 1989. Cathodoluminescence of carbonate-cemented Holocene beachrock from the Togo coastline (West Africa): an approach to early diagenesis. Sediment. Geol., 65: 261-272.
Garlick, G.F.J., 1964. Luminescence in solids. Science Progress, 52: 3-25.
Marshall, D.J., 1978. Suggested standards for the reporting of cathodoluminescence results. J. Sediment. Petrol., 48: 651-653.
Miller, J., 1988. Cathodoluminescence microscopy. In M. Tucker (editor), Techniques in Sedimentology, Blachwell, p. 174-190.

«CRYSTALLOGRAPHIC» MODELS OF EXCHANGE IN THE HUMAN DENTAL BONE-MINERAL TISSUE.

59.2.1.H

D.K.Arkhipenko, T.N.Grigoryeva, A.M.Gonchar, L.F.Vlasova. Inst.Geology - Geophysics and Cytology-Genetics Sib.Depart.Acad.Sci; Universitats.pr.3, Novosibirsk-630090.

The exposure of dentine and enamel structure to temperature (T), pressure (P) and their combination (T+B) (in autoclave water medium) was studied by difpaction, IR-spectroscopy and micro-chemical methods.

Dentine structure was shown to exhibit the following difference with heating to 800°C: in isothermal

regime the structure transforms in hydroxil-apatite, in dynamic regime carbonat-hydroxil-apatite. Enamel appeared to be more stable: with heating to 600,800°C carbonate ions are still preserved in the structure. At these T-levels IR-spectra showed unusual effect of carbonate ions migration from «B» to «A» positions.

The X-ray reflexes of [hкo], [hoo]-type were shown to increase and those of [ool]-type - to decrease in the enamel and dentine structure after static pressure, it is this very texture which corresponds to the plane of tooth enamel. The texturation effect is also proved by similar reflection spectra from a pressed tablet and lattice side ($10\bar{1}0$) of natural Kovdor F-apatite monocrystal.

The simultaneous (T+P) exposure on the dentine structure (treatment in autoclave filled with H_2O up to 75% of volume at $T \sim 150^{\circ} \pm 2,5^{\circ}C$ which corresponds to $\Delta P \sim 5$ atm) causes partial elimination of CO_3^{--}, H_2O molecules, organic matter and improvement of the crystallinity degree.

The pressure and temperature are the factors, which have constant effect on the bone-mineral tissue. The conformities discovered correspond to that part of exchange which can be conditionally ascribed to the crystallographic model exchange. The total exchange in natural and pathologic conditions depends not only on the temperature and pressure but exhibit more complex pattern.

31.2.17.√

THERMAL ANALYSIS OF CHALCOPYRITE ROASTING REACTIONS

G.Bayer, Institute of Crystallography and Petrography, ETH-Zürich, 8092 Zürich, Switzerland
H.G.Wiedemann, Mettler Instrumente AG, 8606 Greifensee, Switzerland

Roasting of chalcopyrite and of the component copper- and iron sulfides(covelline, chalcocite, pyrrhotine and pyrite) has been the subject of many investigations.The addition of salts in such reactions is of practical interest because it lowers the decomposition temperature and leads to water-leachable sulfates and chlorides.Depending on the kind of salt and on the roasting temperature the separation of copper from iron is easily possible.
The salt roasting of copper bearing sulfides is a very complex process involving numerous reaction steps. Some of the intermediate reaction products are still not

adequately characterized.Therefore it is difficult to describe the salt roasting reactions with simple and specific chemical equations because a number of such reactions takes place simultaneously and/or sequentially, e.g. liberation of sulfur, oxidation sulfide→sulfate, in situ formation of chlorine and direct chlorination.
The aim of the present investigations is to look into the reaction mechanism of sulfide roasting in more detail and hopefully clarify some of the intermediate reaction steps.The combination of thermoanalytical methods(Mettler Thermosystems 3000 and 4000) and X-ray diffraction proved to be very useful for such studies. Mixtures with different ratios of $CuFeS_2$(and also CuS, FeS_{1-x}, FeS_2) and NaCl, KCl or NH_4Cl were heated in oxidizing atmosphere either continuously(heating rates from 0,2 °C/min to 10 °C/min) or stepwise isothermally. Some of the preliminary results are summarized in the following : Pure chalcopyrite starts to oxdize at about 400 °C,which can be seen from the strong weight increase in the TG-curve(Fig.1).The shoulder at about 420 °C points to the formation of an intermediate compound,

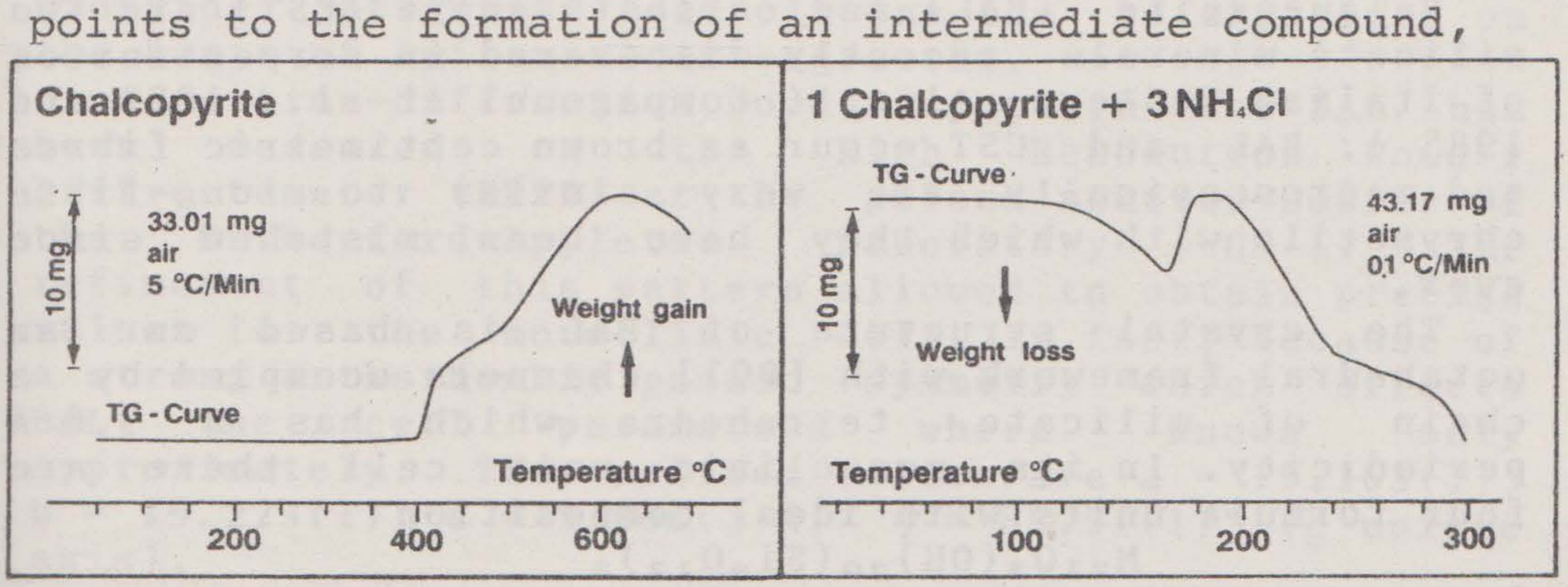

Fig.1.TG-curves of the decomposition of $CuFeS_2$ and $CuFeS_2/3NH_4Cl$

probably $CuO.CuSO_4$. The reaction is complete at 640 °C the reaction products are $CuSO_4$ and Fe_2O_3. Above this temperature $CuSO_4$ decomposes to CuO which reacts at still higher temperatures with Fe_2O_3 to copper ferrite. Addition of alkali chlorides to chalcopyrite lowers the decomposition and oxidation quite drastically, especial-ly in the case of NH_4Cl and KCl. The strong exothermic reaction with corresponding weight increase took place already at about 200 °C and lower in the case of mixtures $CuFeS_2$and NH_4Cl.Important for the completeness of the reaction- especially in mixtures with NH_4Cl - are

slow heating rates through the decomposition region(not faster than 0.2°C/min), covered crucibles and excess of salt addition (preferably 4-5 mole salt/l chalcopyrite). The identification of the mineral phases in the salt-roasted calcines by means of X-ray proved to be most difficult and is still not completed. Some of the intermediate reaction products probably have the stoichiometry of chloro-thionites $(Me)_2CuSO_4Cl_2$.The TG-curve of the mixture $1CuFeS_2/3NH_4Cl$ is an example for incomplete reaction with loss of NH_4Cl followed by only partial oxidation(Fig.1).

25.2.10.P
59.2.4.H

NEW DATA ON THE ASBESTIFORM MINERALS BALANGEROITE AND CARLOSTURANITE

Elena BELLUSO and Giovanni FERRARIS
Dip. Scienze della Terra - Univ. Torino
Via Valperga Caluso 37, 10125 Torino (Italy)

Balangeroite (BAL) and carlosturanite (CST) are two silicate minerals recently discovered in serpentinites of Italian Western Alps (Compagnoni et al., 1983 and 1985). BAL and CST occur as brown centimetric fibres and macroscopically are very similar to long-fibre chrysotile with which they have been mistaken since ever.

The crystal structure of BAL is based on an octahedral framework with [001] channels occupied by a chain of silicate tetrahedra which has a 9.6 Å periodicity. In its monoclinic unit cell there are four formula units with ideal composition

$$M_{21}O_3(OH)_{20}(Si_4O_{12})_2$$

[M = Mg, Fe (major cations), Mn, Al, Ca, Cr, Ti] (Ferraris et al.,1987).

The crystal structure of CST can be obtained from the serpentine layer by preserving the octahedral sheet and by substituting $[\ Si_2O_7\ ]^{-6}$ groups with tetrahedrally arranged $[\ (OH)_6H_2O\ ]^{-6}$ groups (Mellini et al., 1985). In the monoclinic cell (which has the same b and c values of serpentine and a sevenfold a value) there are two formula units with ideal composition

$$M_{21}[T_{12}O_{28}(OH)_4](OH)_{30}.H_2O$$

[M = Mg (major cation), Fe, Ti, Mn, Cr; T = Si (mainly), Al].

A systematic sampling of the serpentinites of the Italian Western Alps brought to the discovery of two and twenty-one new localities for BAL and CST, respectively. While the occurrence of BAL is confined

to the Lanzo Massif, CST is present in all fracturated serpentinites of the explored area; instead, it is absent in the foliated serpentinites. An almost Mg-pure CST has been reported from Taberg (Sweden) (Mellini & Zussman, 1986). CST seems, therefore, to be a major constituent of serpentinites. Possibly, several serpentines which have been found to be Si-poor and H_2O-rich could be CST.

Single fibres of BAL and CST have cross-section of the order of 10^2Å and can be intergrown with various impurities. These impurities could pollute the microprobe analyses because the cross-section of the electron beam can be larger than that of single fibres. Correlations between the analyzed elements have shown that the minor elements really represent substitutions in structural sites of the two minerals. Besides, some analyses of identified single fibres with a TEM/EDS system confirmed the reported compositions, at least qualitatively. The compositions of BAL and CST from Western Alps show little variations, but these are correlated with the localities of occurrence.

Oriented associations of CST with chrysotile, diopside, antigorite, and olivine can be explained on the basis of epitaxial intergrowths.

A neutron-diffraction powder pattern for BAL has been measured on the High Resolution Powder Diffractometer (HRPD) at the pulsed neutron source of the Rutherford-Appleton Laboratory (UK). The refinement of this pattern allowed to obtain precise values for the monoclinic cell. In fact, because of a strong orthorhombic pseudo symmetry which affects BAL, the cell parameters where known only approximately. The refined values are a = 19.163(1), b = 19.223(1), c = 9.606(1)Å, γ = 89.51(1)° (c unique axis).

References

Compagnoni R., Ferraris G. & Fiora L. (1983) - Am. Miner. 68, 214-219.

Compagnoni R., Ferraris G. & Mellini M. (1985) - Am. Miner. 70, 767-772.

Ferraris G., Mellini M. & Merlino S. (1987) - Am. Miner. 72, 382-391.

Mellini M., Ferraris G. & Compagnoni R. (1985) - Am. Miner. 70, 773-781.

Mellini M. & Zussman J. (1986) - Min. Mag. 50, 675-679.

MINERALOGICAL AND CHEMICAL CHARACTERIZATION OF THE ALTERATION PRODUCTS AND ORIGINAL ALLOYS OF VERROCCHIO'S BRONZES.

59.22

CNR - C. S. per la Mineralogia e la Geochimica dei Sedimenti - Florence, Italy
Opificio delle Pietre Dure e Laboratorio di restauro - Florence, Italy
CNR - C. S. sulle cause di deperimento e metodi di conservazione delle Opere d'Arte - Florence, Italy

As a preliminary investigation of the restoration of two outdoor bronze statues by Verrocchio, "L'incredulità di S. Tommaso" (Orsanmichele, Florence, Italy), a program of chemical and mineralogical analyses as been undertaken in order to characterize the alteration products as well as the original bronze alloys. The principal techniques employed were: X-ray diffraction, IR spectrometry, reflected light and scanning electron mycroscopy, ion- and gas-cromatography.

The patinas samples show a structural differentiation in three main layers. The first layer close to the alloy, with a typical reddish color, is composed mainly by cuprite and nantokite. A second intermediate layer, of greenish color, is chiefly made of cupric basic cloride (atacamite). The greenish-gray upper layer, much ticker than the previous ones, shows a very complicated composition, with both corrosion and atmospheric deposition products. The principal corrosion compounds identified are: the sulfates antlerite, brochantite, anglesite as well as a

Fig.1

- 3rd layer
- 2nd layer
- 1st layer
- Original alloy

zinc sulfate, and the oxalate moolooite. Intermixed with these compounds other phases, caused most likely by atmospheric

pollution, were identified. Gypsum is the prevalent mineral among them, quartz is fairly aboundant, feldspars are also present. In more localized areas weddellite, ammonium sulfate, and some nitrates were found. The grayish hue is due to the presence of diffused carbonaceous particulates. A natural crystalline paraffine wax, evenkite, of uncertain origin, was also identified.

The presence of some of the easily water soluble products can be reasonably explained on the basis of the partial protection of the statues, situated in a niche of the church.

The caracterization of the bronze alloys, now under investigation by LMI Italian Company, has a great interest from historical and technological point of view. Preliminary results, carried out parallel with the patinas analyses, seem to indicate a mean copper:tin ratio of about 15:1. Clear evidence of lead micro-isles can be noted on the SEM pictures (fig.1) with an apparently higher frequency near of the surface.

Gian Piero Bernardini, CNR - C. S. per la Mineralogia e la Geochimica dei Sedimenti, via Pira 4, 50121 Florence, Italy

THE DISCOVERY OF THE LACUSTRINE MAGNESITE DEPOSIT IN THE EARLY PLEISTOCENE NIHEWAN FORMATION,YANGYUAN,HEBEI AND ITS SIGNIFICANCE

59-2-3H

Cao Guanqin, Wang Qizheng, Luan Wenlou & Yang Zhusen, Department of Geology,Hebei College of Geology,Shijiazhuang, Hebei, 050031, The People's Republic of China

The magnesite deposit newly discovered by the authors in the Early Pleistocene Nihewan Formation,Yangyuan, Hebei is a lacustrine type of magnesite deposit. It is exposed on the both banks of the Sangganhe River in the Yangyuan Basin, occurring in the uppermost part of the Nihewan Formation. The magnesite-bearing sequence is about 3.5m thick, deposited continuously on "the Marlite Member" of the Nihewan Formation,and situated with angular unconformity under the Late Pleistocene Malan Loess.The buried depth of the sequence is usually only one to several meters below the surface. Preliminary investigations indicate that the horizon of the sequence is quite stable, but that the composition and lithofacies are variable. At Kaiyang village,

located approximately 14 kilometers southeast of the county town of Yangyuan, for example, the sequence is composed mainly of greyish-white feldspar-quartz silt beds with cross bedding and wave ripple and white earthy porous magnesite beds with pseudo-oolitic texture, representing a shore sediment. The silt beds generally contain 20-30% cryptocrystalline magnesite. The main seam of the deposit is 40 centimeters thick,containing up to 80% cryptocrystalline magnesite. At Helangan,located nearly 56 kilometers east of the town, however, the sequence chiefly comprises greyish-white calcite-aragonite lime mud with horizontal bedding, bearing 20-25% cryptocrystalline magnesite and representing a sediment of lake bottom.

China is very rich in magnesite resource, but this type of magnesite deposit has not been reported previously. The scale and genetic model of the deposit are still under investigation.Now available geological information has shown that the deposit seems to have nothing to do with any ultrabasic igneous bodies. In the western part of North China the Nihewan Formation has a widespread distribution in a series of Cenozoic fault basins,covering an area of 10,000 square kilometers.These basins have similar geological environment. For instance,there is a larger area of Precambrian dolomites developed around each basin.Thus,the discovery of the Yangyuan magnesite deposit gives some clues for looking for the same type of magnesite deposits in the basins and for probably existing parental magnesite deposits in the dolomites around them. The industrial use of the Yangyuan magnesite is still under study.

18.2.5P THE LMPROVEMENT OF SLAG PROPERTY

Cao Zhenyuan; Mao Yuwen; Yao Dimin·Univ. of Sci. and Tech. of Beijing
Beijing 100083. P.R. China

The titanium slag in Panzhihua Iron and steel Company contains 16-25% of TiO_2. It is an important resource. Titanium distributes almost in every phase of minerals in the slag. Applying the conventional dressing of original slag collects some concentrated titanium, the tailings still have high tenor of titanium. Changing the state of slag crystallization so as to get TiO_2 relatively concentrated will be favourable to separation and utilization as well. Research indicades that both perovskite and anolite ($TiO_2 \cdot Ti_2O_3$) are minerals with high tenor of titanium. However, the former exists in the slag while the latter rarely does. The purpose of this paper is to seek a process to improve the property of slag.

A series of experiment have been carried out to investigate the crystallization property of slag. Adding different agents into the slag and melting the mixture with different temperaturetime schedules, we·then analyze the results:

Experiments show the regularity of perovskite formation:

1. When the component of the system contains: MgO 16%, Al_2O_3 14%, CaO 25%, TiO_2 25% and SiO_2 24-35%, perovskite is the first crystal phase while cooling the melt slag.

2. The crystal of perovskite will increase with the increase of CaO. If SiO_2 increase, rich titanium augite will crystallize, but very few amount of perovskite is found. Too high (>10%) or too low (<1%) of FeO is unfavourable to the formation of perovskite.

3. With the increase of crystallization time, the crystal of perovskite developes from branched structure into granular, from small to large crystals.

4. If $CaO/SiO_2 > 1$, perovskite will be crystallized, whether it is under oxidizing atmosphere or reducing one.

Table Crystal Phase Found in the Different Conditions

CaO/SiO_2	Natural cooling	Crystallization time	
		2 hours	4 hours
0.78	noly Fassaite crystallita	anolite perovskite	anolite, perovskite more and coarse
0.56	all glass phase	a few anolite	more anolite

The regularity of anolite formation:

1. When the slag contains MgO 4.7%, Al_2O_3 11.6%, CaO 20.7% TiO_2 20.7% and SiO_2 42.2%, anolite firstly crystallizes under oxidizing atmosphere. It can also be formd under reducing condition, if SiO_2 <36%.

2. Anolite only exists in the condition of CaO/SiO_2 <1, otherwise, perovskite may be found. Some experiment results are show in the table as follows:

What mentioned above is the characteristics of crystallization of perovskite and anolite. Addition of some CaO increases the activity. Reasonable selection of CaO/SiO_2 and temperature schedule play an important part in the crystal formation. It is possible to make such a suitable condition in blast furnace so as to improve slag property.

37.2.25 V

MINERALOGICAL CONTRIBUTION FOR THE CLASSIFICATION OF SLAG

CHAUDHURI, J.N.B., Suprova Research Laboratories, 27A, Raja Basanta Ray Road, Calcutta 700 026, India

Considering the possibility of the manifold re-utilization of slag, it is necessary to classify the slag, which in turn is dependent on factors like mineral constitutions, structures and textures, density and/or viscosity, the temperature reached by the slag, etc. The mineralogical studies on the polymetallic dump slag around the Harz mountains, i.e. from Langelsheim (S-La), Lautenthal (LSS) and Sieber (S-Si), revealed the complexity of the smelted products (CHAUDHURI, 1986), where besides the subordinate sulphidic phases, the oxidic phases of calcium, iron, aluminium and silicium represent the main slag constituents. Based on this fact the chemistry of the slag was determined by the modal analysis of the minerals, which were controlled by the XRF, XRD and electronprobe microanalysis methods.

One of the important parameters for the classification of the slag is determination of viscosity-composition-temperature relastionship during the building of the slag, which substantially influences the relationship of components such as CaO (BaO)-(Mg,Fe,Zn,Mn)-$(Al,Fe)_2O_3$-SiO_2 (MANSON and SEGNIT, 1956) and the corresponding mineral formation. By applying the formula suggested by MANSON & SEGNIT (1956) and modified by WINTERHAGER & KAMMEL (1961) to the above mentioned components of samples from the Harz Mountains, and by projecting the values of the quarternary system CaO-ZnO-SiO_2 at a plane of 10% Al_2O_3 content, it can be inferred that:

- the compositions of the slags of Lautenthal and Sieber substantially differ from the admissible computed value for the Pb-slag by showing a higher SiO_2 content; this is

represented by higher content of fayalite, melilite etc. (cf. CHAUDHURI, 1986). The enriched presence of barium in the silicate phases (i.e. hyalophane, Ba-melilite) indicates the application of Ba-rich flux material for the earlier Pb-Zn metallurgy. In contrast, however, the composition of Langelsheim-slag (S-La) is characterized by a higher Zn-content and shows an approximate coincidence with the admissible composition (Gahnite Zone) of the Pb-Zn slag
- in contrast with the slag from Lautenthal (LSS) and Sieber (S-Si), the Langelsheim-slag (S-La) is characterized by an extremely low viscosity (η = 2), which may be attributed not only to its higher content of sulphidic minerals such as sphalerite, pyrrhotite, etc., but also partly to their metallic equivalents.

The temperature reached by the slag is calculated by projecting the main slag-constituents in the basic ternary system CaO+"FeO"+SiO_2 = 100%. It can be established that the temperature reached by the Pb-Zn slag from Langelsheim lays around 1150° C, whereas the temperatures reached by the slag from Lautenthal (LSS) and Sieber (S-Si) were 1400° C and 1250° C respectively.

CHAUDHURI, J.N.B. (1986): Science & Culture, 52 (1), 19
CHAUDHURI, J.N.B (1986): IMA XIV. General Meeting Stanford, Calif. July 13-18. ext. abstr., 73
MANSON,A. & SEGNIT, R. (1956): Proc. Am. Inst. Min. Met., 180, 119
WINTERHAGER, H. & KAMMEL, R. (1961): Erzmetall XIV (h7), 319

MINERALOGY OF THE INTERMEDIATE ALTERATION PRODUCTS OCCURRING DURING THE PYROMETALLURGICAL TREATMENT OF SULPHIDIC COPPER ORE (REVERTS) FROM INDIA

31.2.19

Chaudhuri, J.N.B., Suprova Research Laboratories, 27A, Raja Basanta Ray Road, Calcutta 700 026, India

In connection with an optimal utilization and maximum recorvery of copper out of sulphidic copper ores, the author has carried out mineralogical investigations on their alteration products, which occurred after their pyrometallurgical treatment by the Particle Jet Smelting (PJS) method (KANG et al., 1982). The reverts of Hindusthan Copper Ltd. (HCL, Government of India), consisting of mixed sulphide ores of various copper-bearing minerals viz. covellite, chalcocite, bornite, chalcopyrite, enargite, pyrite, etc. constituted the feed material. The sulphidic ores were ground to the grain size of 50-100 µm, as the finer grain size promotes a higher reactivity (CHAUDHURI, 1985). Apart from a higher metal output (60-80%), the PJS method differs from the existing methods of Outakumpu, Brittingham,

etc.), in having a flash smelting system, where the solid-gas (oxygen) mixtures are subjected to a turbulent axisymmetric burner gas. The downstream fall-off rate of the solids through this (axisymmetric) reaction zone was ca. 33 m/s. The reaction products were finally collected in porcelain beakers.

Ore microscopy, XRD, XRF and electronprobe micro-analyses have revealed that:

- covellite and chalcocite are almost exclusively transformed into metallic copper, the droplets of which are surrounded by a thin rim of digenite
- bornite splits into two different phases of alteration. One is in the matte, which consists of cenopheres containing metallic copper at the core surrounded by a layer, the composition of which corresponds to solid solution of digenite (II) and copper sulphide. The other is in the slag, where finer-grained copper droplets are frequently interlocked between the skeletal magnetites and spinels showing disseminated structures (Cf. AMSTUTZ, 1957-Locking chart). Similar to those of Pb-Zn slag (CHAUDHURI, 1986), some spinels are characterized by a zoning indicating a superoxidation. The later stage of reduction within the slag phase is characterized by the presence of delafossite
- chalcopyrite frequently shows a sequence of alteration from talnakhite (cf. RAMDOHR, 1980) at the outer layer to bornite, and finally to digenite and/or copper sulphide at the core (alteration during oxidation). Sometimes, however, chalcopyrite may also be completely transformed into metallic copper, digenite (I) and digenite (II) (alteration during melting phase)
- Pyrite changes into magnetite with a intermediate alteration phase of pyrrhotite (and/or troilite).

According to the mineral products resulting from the flash smelting of the copper bearing sulphide ores (at a temperature of around 1800 K) three alteration phases can be differentiated, namely (a) alteration occurring during oxidation (b) alteration in the smelting phase and (c) alteration during the slag reduction and cooling phase.

AMSTUTZ, G.C. (1959): Proc. Geol. Assoc. Canada, 11, 104
CHAUDHURI, J.N.B. (1985): Journ. Mines, Metals & Fuels, Febr., 41
CHAUDHURI, J.N.B. (1986): IMA XIV. General Meeting, Stanford, Calif., July 13-18, 73
KANG, J.S., STEINHÄUSER, J. & WUTH, W. (1982): Int. Conf. on Copper Metallurgy, Oct. 19-21, Regnica, Poland
RAMDOHR, P. (1980): The ore minerals and their intergrowths, Pt. II, Akademie Verlag, Berlin

INFLUENCE OF THE DEGRADATION OF IRON SULFIDES CONTAINED IN AGGREGATES ON CONCRETE DURABILITY

Chinchón J.S, Fernández-Turiel J.L., López-Soler A., Querol X. Instituto de Geología "Jaume Almera", CSIC, C/ Martí i Franqués s/n, 08028 Barcelona, Spain.

In the early 1970s, in the Maresme area (province of Barcelona, Spain), serious problems were detected in buildings made of concrete containing aggregates from the Mont Palau quarry (Pineda de Mar).

We studied the mineralogy of the aggregates and that of the weathering products arising from a process in which the most important role is played by the degradation of pyrrhotite and pyrite contained in the aggregates. A pe-pH diagram of the equilibrium reactions of the chemical species involved was constructed, in order to interpret the two different processes of weathering associated with each of the lithofacies that make up the aggregates of the quarry: limestone and shale. The limestones (microesparite) form the "Serie Carbonatada"; the shales have a high organic matter content and occur interlayered with limestones in the "Serie Negra". These lithofacies, both with iron sulfide mineralizations, belong to the Ordovician-Silurian transit series of the northeast of the Iberian Peninsula.

Next, mortars were made using a cement P-450 and aggregates from Mont Palau quarry. X ray diffraction and scanning electron microscopy equipped with an energy dispersive X ray microanalysis system (SEM-EDS) were used to analyse the evolution of the mineral phases of the aggregates and the expansive phases produced by the curing process. Considerable amounts of ettringite produced by the degradation process of iron sulfides contained in the aggregates were detected.

The results show that the ettringite is the main mineral phase that influence the durability of the concrete made up with the aggregates from the Mont Palau quarry (Pineda de Mar).

THE USE OF ANTIOXIDANT CONTAINING MgO-C BRICK ON BOF

CUI Shuxian, Central Iron & Steel Research Institute, Su Liang-ho, China University of Geosciences, Beijing 100083, People's Republic of China.

Previous research has shown that the addition of

powdered SiC to MgO-C brick may give improved suppresion of the oxidation of carbon at high temperature, but no detail in study has been reported. In the present paper, three kinds of used MgO-C bricks have been studied, namely the 12% graphite containing, the 18% graphite containing, and the 12% graphite containing with the addition of 4% SiC MgO-C bricks.The authors find that during smelting,in all the three kinds of bricks,there existed a layer of dense periclase.When SiC is introduced chemical reactions take place,

$$SiC\ (s) + CO\ (g) = SiO\ (g) + 2C\ (s) \qquad 1$$

$$SiO\ (g) + CO\ (g) = SiO_2(s) + C\ (s) \qquad 2$$

The newly formed SiO_2 is precipitated surrounding the periclase grains. Reaction between SiO_2 and MgO, 2MgO, SiO_2 is formed. Since forsterite is easily disolved by the early slag, the anti-slag property is lowered. As a result of detailed petrographic study, and study of the CaO-MgO-SiO_2 ternary phase diagram, the authors will prefer the 18% graphite containing MgO-C brick rather than the two other kinds of bricks

BIOMINERAL AND THEIR CHARACTERISTICS

DAI Yongding, Institute of Geology, Academia Sinica, Beijing 100011, people 's Republic of China.

Based on the present data, more than fifty kinds of biominerals have been found by now, not including their amorphous variant and fossilized mineral. Biominerals are mainly Ca Mg carbonates, Ca Mg phosphates, Si dioxide, Fe and Mn oxides and hydroxides, sulfides and sulfates, halides and organic acid salts. Ca Mg carbonates are mainly Mg calcite, calcite and aragonate. The former two mostly occur in invertebrates and algae; aragonite , mostly occurs in molluscs and green algae. Ca Mg phosphates are mainly dahllite, occur in vertebrates, arthropods and inarticulates, Si dioxide is opal, occurred in diatoms, silicoflagellates, chrysomonales, radiolaria and spongia. Fe and Mn oxides and hydroxides are mainly magnetite, hematite and vernadite, of which, the former one is in magnetobacteria and chiton teeth, the latter two in Fe bacteria. Sulfides are mainly pyrite, occurred in anaerobic sulfur bacteria. Sulfates are mainly celestite, occurred in Acantharid of Radiolaria. Organic acid salts are mainly weddellite, mostly occurring in plants and calculi.

The major characteristics of biomineral are as follows:

A. Weak alkali and weak acid salts They are hard to dissolve and apt to retain. Even if soluble, they can't largely hydrolyze into strong acid or strong alkali to damage organism body.That is the real reason why alkali metal elements K and Na, halogen elements F and Cl, complex anions, nitrate and sulfate, can't composite common biominerals basically.

B. Calcium compound (25 kinds) In fact, common biominerals mostly contain Ca, so it accounts for the overwhelming majority of total biominerals. Ca is a composite element in algal Ca proteinate, Ca pectic acid and enzyme. Its function is extensively to consist cell wall, fix protein, catalysis, electrochemical control, muscle motion and transmit messages. Ca has become the most important metal element in biomineral due to its larger cationic radius than Mg, Fe and Na, weaker alkalinity than K and Na, and more abundant than Sr and Ba.

C. Oxides (12), hydroxides (5) and oxysalts (29 kinds) O is a major element in organism and is necessary for biochemical and metabolic process. Only when the oxygen gas in the atmosphere and hydrosphere increased to a certain level, could Fe and Mn oxides and hydroxides, and microaerobic bacteria occur. Only further increased the oxygen gas in the atmosphere and hydrosphere, could organism be imposed on to increase oxygen reserve in body, promote the metabolism and motion,advance the requirement of calcium, ultimately arise Ca oxysalts deposited.

D. Carbonates (10) and phosphates (10 kinds) Carbon is also a major element in organism and necessary for biochemical and metabolic function. Its redox reaction is the source of energy for organism. P is a necessary element in organism. It composes ATP, DNT, nuclei acid and organic phosphate, also possesses biochemical and metabolic function, and is indispensable for rememberance, thought and inheritance. The development of these two oxysalts are relevant not only to their high contents in the original hydrosphere, but also to their weak acidity.

E. Hydrates (24 kinds) or hydroxy oxysalts (2) Biominerals precipitate out of body fluid slowly. Almost half of them contain crystal water, besides their amorphous variant contains a number of absorping water.During the ontogenetic or fossilized process, they lose crystal water, then eliminate hydroxyl forming more stable minerals.

F. Uniaxial negative or approximate to that. Calcite, dahllite, dolomite, hematite all are uniaxial negative, aragonite is false one. Biogenetic opal also indicates X-ray spectra of christobalite which is uniaxial negative too.That is probably due to one or two directs or planar-epitaxial growth of biomineral. Precursor and pathological minerals are mostly monoclinic or triclinic system and biaxial crystal with large 2V angle. The symmetry in biominerals is avanced along with the loss of crystal water,the elimination of hydroxyl and the extraction of isomorphic ions.

THE GENETIC STAGES AND EVOLUTIONARY TENDENCY OF BIOMINERALS

DAI Yongding, Institute of Geology, Academia Sinica, Beijing 100011, people 's Republic of China

According to their genesis, biominerals can be divided into four stages or facies

A. precursor stage Bofore ossificating, some crystallite, seed crystal or hydrated amorphous mineral are formed. They contain more crystal water. For example, the seed crystal of aragonite is vaterite; the precursor mineral of calcite is monohydrocalcite or ikait; that of dahllite is

brushite and octocalcium phosphate; that of hematite is ferrihydrite; that of pyrite is hydrotroilite. These precursor minerals are well-developed in embryonic and juvenile period, and extremely scarse in adult period. Their contents gradually decrease with ontogenesis.

B. Ossificatia stage Because a great number of biomineral crystals gather together, the molecules of crystal water in biomineral are gradually extracted and the biomineral crystals with no or few crystal waters are formed, constructing a dense biomineral body.Ossificatia minerals are major biominerals, such as magnesium calcite, aragonite, dahllite, opal (christobalite) and hematite.

C. Fossilized stage Biominerals totally lose their crystal water, for example, opal through christobalite translates into chalcedony; then begin losing hydroxyl ions,for example,dahllite translates into franconite; at last, isomorphous mixtures are eliminated, for example,magnesium calcite translates into calcite. So, biominerals change into more stable minerals.

D. Pathological stage When organisms catch a disease, they often secrete some particular minerals, such as whitlockite, calcium pyrophosphate and monetite, besides normal biominerals, such as calcite and dahllite, and precursor minerals, such as octocalcium phosphate and brushite. Whewellite and weddellite are also well-developed at pathological stage.

What mineral the organism adoptes depend on that, during initial biomineralization of this organism, its component elements not only largely exist in the hydrosphere with water soluble compound or complex, but also can be uptaken by this organism as indispensable component, participating in physiologic process, and can precipitate into insoluble biomineral body under certain conditions. For example, the majority of biomineral bodies in living organism are made up of calcite or dahllite and only the minor are aragonite or calcite. It is just contrary to recent marine chemical sediments. This fact reflects that, when the biomineral bodies were generated, the hydrosphere had far more concentrations of Mg cation and monohydrogen phosphate anion and less concentration of Ca cation, so organism adopted these two biominerals, carried on by means of inheritance and lasted up to the present. Owing to the formation of unitive continent, the desalination of sea water and the landing of plant and animal, the biomineral bodies of aragonite and calcite are increased step by step.

The evolution of chemical composition in the hydrosphere also results in a series of biomineral variation. This variation does not mainly display a replacement of one by another in same organism; but an alternation, i.e. one kind of biomineral body (made up of one kind of biomineral) in this taxum of organism may boom along with this taxum and other kind of biomineral body (made up of other kind of biomineral) in that taxum of organism may decline along with that taxum. The essential evolutionary tendency of biomineral is Fe sulfides→Fe and Mn oxides and hydroxides→opal→dolomite →dahllite→Mg calcite→aragonite→calcite, that is sulfides→oxides→oxysalts. It reflects the environmental translation, form reduce to oxidate, in earth surface, and the result from interaction and coevolution between the biosphere and hydrosphere.

ORE-DRESSING MINERALOGY OF KOLA PENINSULA KELSILITE BEARING ROCKS

Dolivo–Dobrovolskaya G.I., Kozyreva L.v. Vladimirov P.S., Korobeynikov A.N., Leningrad institute of mining engineering, Leningrad Geological Institute of Kola Science Centre, USSR Academy of Sciences, Apatyty.

Ín the upper contact zone of apatite–nepheline deposites of Khibiny alkaline massif at Kola Peninsula wide spreading kalsilite among nepheline syenites (rischorrite) was established. This mineral ossurs in a close intergrowths with nepheline and potassium feldspar forming thin (up to 30 m in a cross–section) obling worm–shaped or rarely close to round crystals. The availability of kalsilite in rocks was confirmed by electron microprobe, x–ray diffrectometry and infra–red spectroscopy.

Earlier it had been demonstrated that size dependent properties of pulverised substances play sigtnificant role in process of ore processing. In connection with that it had been proposed to distinguish special variety of substance's state–ultimate clastic particles (UCP). The structure–size dependend properties of clastic particles are given way to prodiction and control, wich make possible to operate with reactions of row materials processing.

In laboratory studies of coagulation of kalsilite ore with limestone the following substances were used: pure calcium carbonate and rischorrite. Ricshorrite is characterized by changeable contents of potassium feldspar and nepheline. Femic minerals are minor constituents of the rock, they include aegirine, alkali amphibole, astrophyllite, eudialite, biotite, titanite and more rarely apatite and aenigmatite.

High potassium content in rocks (up to 15 %) is provided not only by potassium feldspar, but bu potassium feldspathoik – kalsilite also. Kelsilite content in rischorrite rises up to 20 %, at common amount of acid soluble minerals about 50–55 %. Rischorrite was ground to powder with laboratory mill to obtain amount of ultimate clastic particles. Gramilometric analysis was held with Fritsch laser analyzer.

As a result of studies carried cut, it was demonstrated that coagulation process goes on with high velocity on condition that minerals are saturated with structural defects and with content of UCP active phase up to 5%.

PROPERTIES OF DISPERSED MINERALS

G.J.Dolivo–Dobrovolskay, P.S.Vladimirov, V.S.Gsidukova, T.N.Kolibaba, V.M.Sizjakov

Physikal–chemikal properties of substance particles change greatly when their diameter becomes comparable with correlated scale of a physical phenomenon.

Sizes of fractured small particles (–10) are comparable with distorition fields of mechanically deformed crystalls. Stability and dedegree of order of small–size–particles depend upon their aggregated properties which differ substanticles depend upon their aggregated properties which differ substantially from separate particle and solid mineral properties.

Every mineral has peculiar range of particle sizes within which these phenomenon are mostly revealed. Particle and aggregate sizes are variable for different structural types of minerals. Properties of dispersed minerals are variavble in time.

Study of technological fehaviour of minerals of different grindings showed that solid phases interrelation process passes through the aggragation stades vital role in this case belongs to crystallophysical properties of minerals (deffect–capacitance, clearage, piezoeffects) which condition ordering of particles in aggragates promoting their stability. In some cases ordering and stability of aggragates lead to passivation of minerals blend and becomes an obstacle to chemical reactions.

Experimental data obtained during study of size grading of monomineral (model) and polymineral (technological) samples helped to single out some of main aggragate types distinguishing in composition texture and sizes. The most stable are the geterophaseanand monophase aggragates where the central large grain plays the role of orienting base. Fragmental small particles which form the surface of aggragate are by an order of size less then central grain. Zonality and hterogeneity are determined with the presence of more than one mineral phases in the aggragate.

Crystal–optical data were analised with the Madgiscan image analiser which helped to make guantitative cvaluation and classification of different types of aggragate ordering and texture.

25.2.8P

APPLICATIONS OF MINERALOGY TO BENEFICIATION OF THE PYHÄSALMI ORE, FINLAND

Markus Ekberg, A/S Bidjovagge Gruber, Box 160, N-9520 Kautokeino, Norway
Heikki Papunen, Department of Geology and Mineralogy, University of Turku, SF-20500 Turku, Finland

The textures and intergrowths of ore minerals are of prime importance in the beneficiation of an ore. Quantitative determinations of textural indices were made with microscopic sequence analysis of 65 polished sections of the Outokumpu Oy Pyhäsalmi volcanogenic massive pyrite-Cu-Zn ore. The indices calculated were frequency distribution of grain size, specific surface (S_v), index of intergrowth (R_{AB}) and volume of the mineral (V).

The Precambrian sulphide deposit of Pyhäsalmi is metamorphosed and the ore minerals are recrystallized. Hence, the textures are in general homogeneous, only a few weak trends of variation being observed in some parts of the ore deposit. A special ore type shown by the indices is the cataclastic pyrite ore on the +660 level in which chalcopyrite cements the cracks of pyrite. The indices measured also indicate that the content of pyrrhotite in the whole deposit increases downwards and

on the +660 level towards the southern edge of the orebody.The forms of the chalcopyrite and sphalerite grains in the lowermost part of the deposit are disadvantage in the beneficiation of the deposit. The indices calculated are presented in tables and figures.

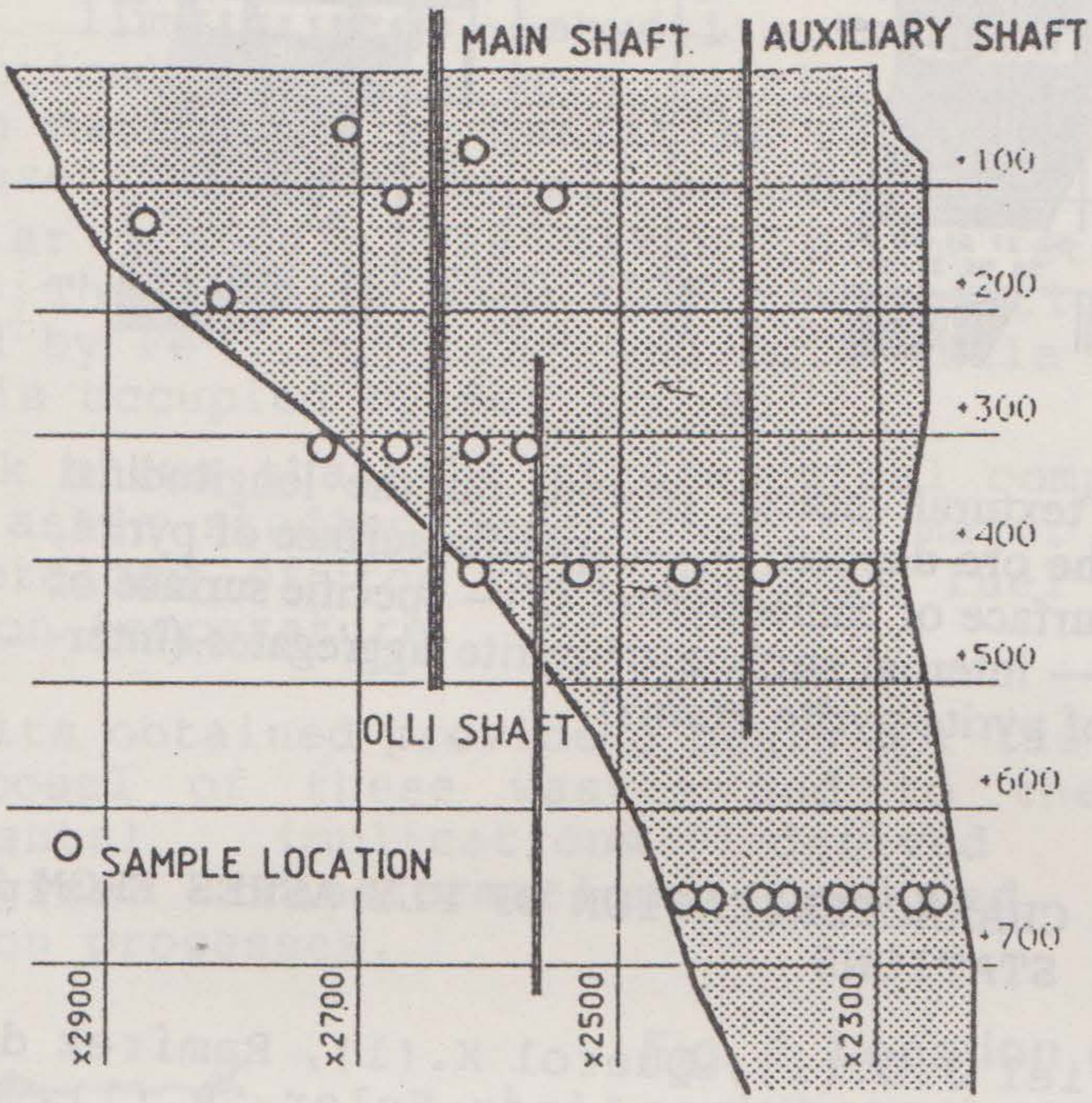

Fig. 1. North-south trending longitudinal projection of the Pyhäsalmi ore deposit with sampling areas. Several samples were commonly taken in each area.

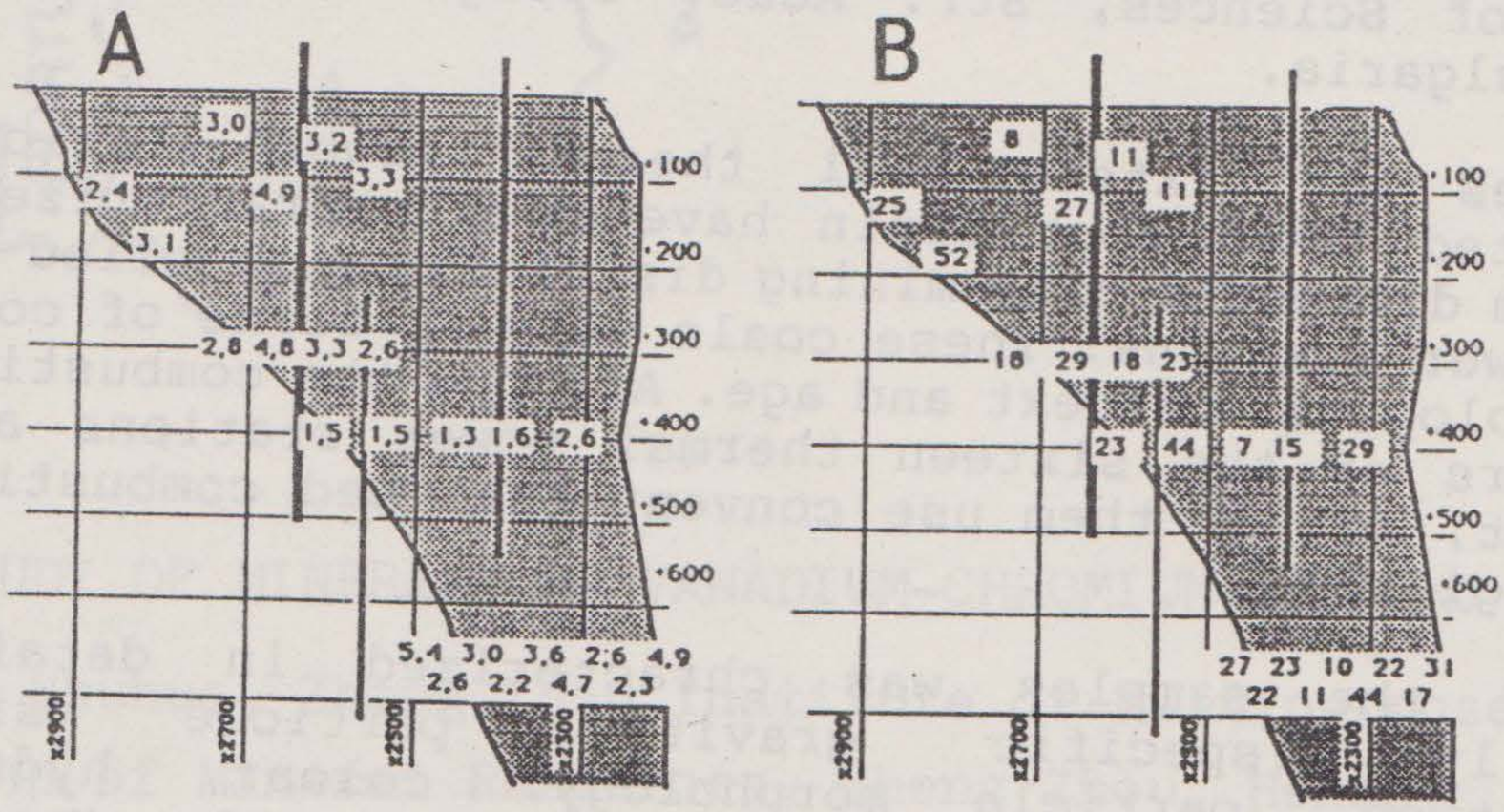

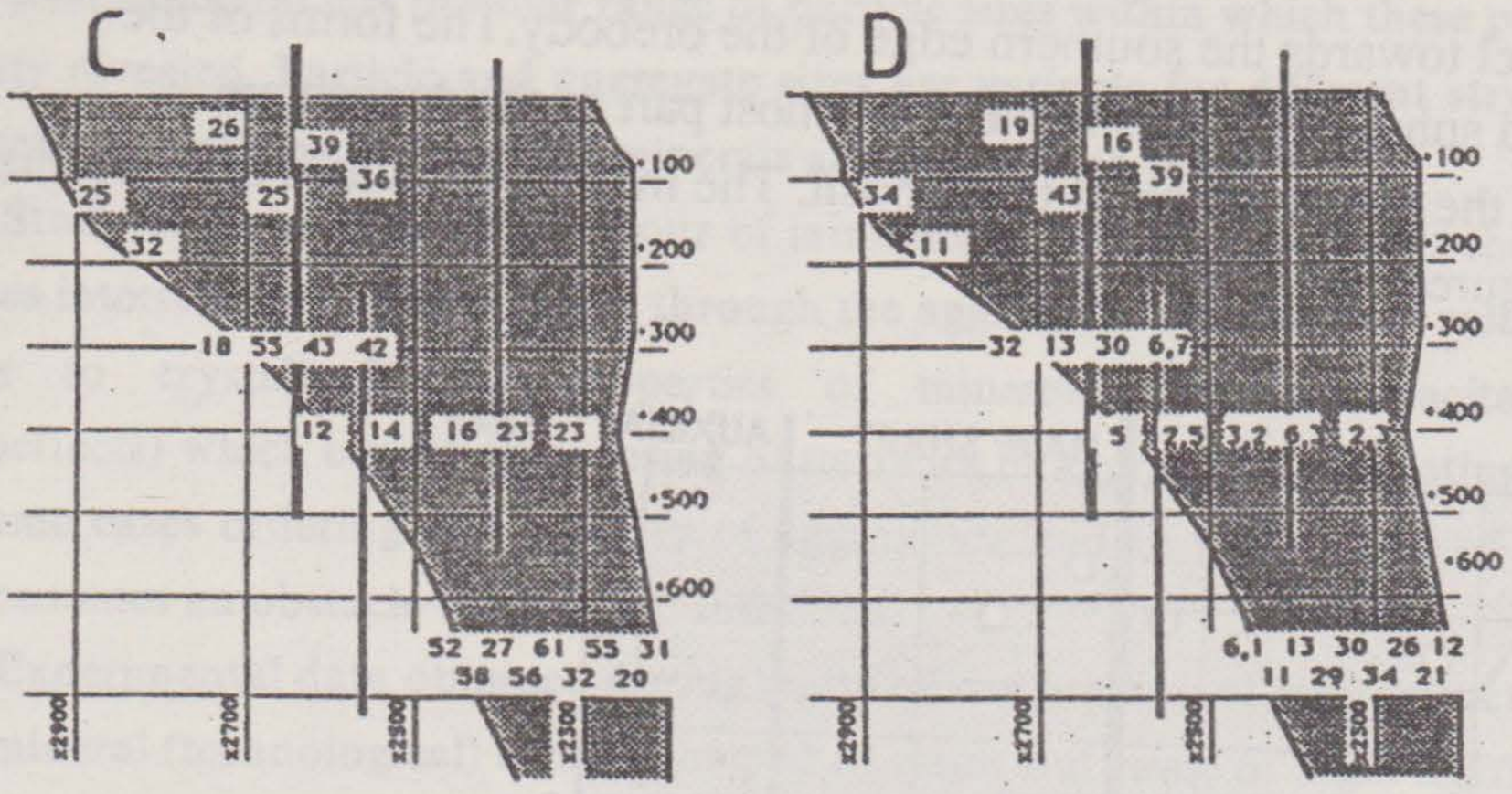

Fig. 2. Some textural indices plotted on the longitudinal projection of the ore deposit: A — specific surface of pyrite, B — specific surface of chalcopyrite, C — specific surface of sphalerite, D — internal surface of pyrite aggregates (intergrowht index of pyrite-pyrite grains)

16.2.7.P

MINERALOGICAL CHARACTERIZATION OF FLY ASHES FROM SPANISH THERMAL POWER STATIONS

Fernández-Turiel J.L.(1), Querol X.(1), Ramírez del Pozo C.(2), Chinchón J.S.(1), López-Soler A.(1), Felipó M.T.(2) and Neikov C.(3). (1) Instituto de Geología "Jaume Almera", CSIC, C/ Martí i Franqués s/n, 08028 Barcelona, Spain. (2) Fac. Farmacia, Univ. de Barcelona, 08028 Barcelona, Spain. (3) Geological Institute of Academy of Sciences, Str. Acad. Giorgi Boncev, 1113 Sofia, Bulgaria.

Fly ashes of sixteen coal thermal power stations distributed throuhgout Spain have been characterized. Coal from different coal-mining districts is supplied to these power stations. These coals vary in terms of coal rank, geological context and age. Althoug the combustion parameters of the sixteen thermal power stations are different, all of them use conventional bed combustion technologies.

Each of the samples was chracterized in detail: physically (specific gravity, particle size distribution, particle morphology, colour, hydric retention and lost on ignition), chemically (major oxides and trace elements: Au, Ag, As, Ba, Br, Cs, Cu, Co, Cr, Hf, Hg, Ir, Mn, Mo, Ni, Pb, Rb, REE, Sb, Sc, Se, Sr, Ta, Th, U, W, Zn and Zr) and mineralogically.

The mineralogical study was carry out by means of X ray diffraction quantitaive analysis, scanning microscopy equipped with an X ray microanalysis system (SEM-EDX) and microprobe.

The fly ashes are made up of alumosilicatic glass, calcium-alumosilicatic glass, quartz, mullite, hematite, spinel, lime, and anhydrite. The quantitative mineralogical analyses were carried out employing the addition method, using quartz as reference phase since this phase is present in all samples.

Particular emphasis was taken in the study of iron spinels. The results show that the position of Me^{2+} is occupied by Fe^{2+}, Mg^{2+}, Ca^{2+} and Mn^{2+}, while the position of Me^{3+} is occupied by Fe^{3+} and Al^{3+}.

This work shows that the mineralogical compositions of the fly ashes studied depends on to major factors: a) the mineralogy of the coal used as fuel and b) the combustion temperature.

The results obtained provide a basis for the utilization and disposal of these wastes and to the study the environmental implications derived from the mineralogical transformations produced during the combustion processes.

Fig. 1. Location of the studied coal thermal power stations.

STUDY OF MINERALS IN VANADIUM-CHROMIUM-BEARING SLAG

37.2.26-V

Ge Shuhua, Zheng Zhou Institute of Multipurpose Utilization of Mineral Resources, Zheng Zhou, Henan, People's Republic of China

Titano-magnetite often contains a little vanadium

and chromium, yet they have economic value, the titanomagnetite of Pan Zhi Hua ore erea contains 0.54% V_2O_3, while that in Hong Ge' 0.53% V_2O_3 and 1.13% Cr_2O_3. After dressing vanadium and chromium were concentrated, then they were concentrated into liquid iron again, in iron making in blast furnace. The liquid iron obtained contains 0.38% V, Hon Ge contains 0.37% and 1.02% Cr . The valuable vanadium and chromium may be retrieved. After blowing, oxidizing, slags are formed and vanadium , chromium retrieved from iron liquid, concentrating into slag. Then the slag becomes beneficial. Vanadium may be concentrated to 17% V_2O_3, when the slag contains a little chromium, the vanadium may be also reduced to 8% V_2O_3 in case slag is rich in chromium. In addition, the V-enriched slag still contains gallium 0.05%.

Minerals composition in slag is simple. The main minerals are rich-V magnetite, V-chromite, silicate fayalite and a little inclusion of metallic Fe. The characterestics of rich-V magnetite and chromite are as follows:

Rich-vanadium magnetite	Rich-vanadium chromite
Chemical formula	Chemical formula
$Fe_{6.31}Mn_{.81}Mg_{.05}Ca_{.09}$	$Fe_{6.79}Mn_{.68}Ca_{.08}Mg_{.04}$
$V_{8.31}Fe_{4.38}Ti_{1.78}O_{32}$	$Cr_{9.92}V_{4.12}Fe_{1.17}Ti_{.06}O_{32}$
Isometric system	Isometric system
Unit cell Z=8	Unit cell Z=8
Cell parameter a=8.476Å	Cell parameter a=8.39Å
Specific gravity 4.85	Specific gravity 4.87
Hardness 764.3 Kg/mm^2	Reflection percentage
Reflection percentage	R=18%(green), 15.3%(red)
R=15.47(481), 16.34%(645)	General crystal form in
General crstal form in	polished section octohedral
polished section octohedral (111), cubic(100)	
(111), cubic(100)	

Phase diagram for the joint Fe-O system at low pressure show that magnetite is stable at high temperature. Isomorphous substituttion of Fe^{3+}, V^{3+}, Cr^{3+} exists extensively in spinel, magnetite and chromite are all the end menber components of spinel solid solution. Crystallizing sequence of oxides mineral (V-bearing magnetite and V-bearing chromite) in iron liquid at about 1400°C don't depend on the decrease of temperature, but depend on sequence of metal oxidizing at temperature condition.

Free energy is the criterion of sequence of formation of metallic oxides. Free energy of element reacted on oxygen in slag is in the following sections.

$4/3\ Cr+O_2=2/3\ Cr_2O_3$	1800K	G^o=-105.24 K Cal
$4/3\ V+O_2=2/3\ V_2O_3$	1800K	G^o=-125.10 K Cal
$3/2\ Fe_{(L)}+O_2=1/2\ Fe_2O_3$	1809K	G^o=-140.80 K cal

L---liquid

The less the free energy G^o, the more prior the oxidizing will take place, After oxidizing of vanadium and chromium and iron produce priorly vanadian magnetite or chromite. Vanadium and chromium content in oxides minerals have close relation to blowing in which time, temperature and oxygen density in air pla an important role.1300-1440°C is the best temperature range of blowing technique adopted. The blowing time, oxygen density are related to oxidizing degree of vanadium andchromium in iron liquid. When over oxidation occurs, according to isomorphous substitution V^{3+} or Cr^{3+} can be replaced by Fe^{3+}, or magnetite lonely be formed. When oxidizing is lacking, vanadium and chromium would remain in iron liquid, Incase blowing proceeds in the best way vanadium content in slag is the most with the decrease of iron loss, otherwise increases, vanadium and chromium grade in slag were low content. V-bearing and Cr-bearing oxide minerals are all solid solution and they floating on iron liquid. Silicon remained in iron liquid oxidized

speedily to be SiO_2(G^oSi+O_2=-135K Cal, 1773°K), while it reacts with FeO melting liquid phase, as they are gluing oxides, then named V-Cr-bearing slag product.

31.2.16 V

THE SLOW COOLING OF CU-NI-S MATTE AND SELECTIVE GRAIN-SIZE FOR MINERAL PROCESSING

Ge Shuhua, Zhu Huijuan, Huang Yaqin, Zheng Zhou Institute of Multipurpose Utilization of Mineral Resources

Pyromettalurgy is mostly used to separate nickel and copper from ore and concentrate them into copper-nickel matte. Then through slow cooling and crushing-grinding-magnetic separation-flotation, the nickel and copper sulfides are separated. The main minerals in the matte are heazlewoodite(Ni_3S_2), chalcocite(Cu_2S) and alloy($CuFeNi_{8-10}$). The purpose of slow cooling is to make the Cu_2S crystals grow larger, because the size of chalcocite grain is the key of separation efficiency. In order to investigate the mechanism of mineral separation, we simulated the industrial cooling speed and got mattes samples at different temperature intervals. Then the samples were quenched by water and tested by determinations and consequently microscopic examination were carried out. It was discovered that the specimens which were sampled above 580°C, all contained 8% of eutectic chalcocite microcrystal remained in the Ni_3S_2 substrate. The eutectic point of the matte is about 580°C, so the slow cooling under the eutectic point(580-400°C) is very important. Recrystallization of the Cu_2S micrystal in this stage is very active, the Cu_2S microcrystal grows larger.

After slow cooling of remelting matte for 50 hours temperature dropped to 390°C, the Cu_2S microcrystal disappeared and all Cu_2S crystals were of the size of more than 100 um being favorable for processing. The re-

melting experments were carried out in a resistance furnace filled with argon in order to avoid oxidization and the specimen was covered with some original fine-grained slags. When temperature reached 1200°S, the specimen completely remelted. After slow cooling, sampling was carried out and specimens were studied.

The copper in heazlewoodite occurs as inclusions of Cu_2S microcrystals in Ni_3S_2 basis, but not as solution. The result of microprobe analysis proved that there was no isomophous substitution between Cu and Ni in Ni_3S_2 and Cu_2S, and they were actually inclusions without mutual solid-solution. Recrystallization and growing of Cu_2S microcrystals depend on the diffusion process. It is mainly vacancy diffusion and lattice diffusion. The higher the temperature, the higher the disordering degree of the crystal therefore the bond force in lattice reduces,the activity of molecules increased recrystallization is more active, so the slow cooling from eutectic point to 400°C is very important.Entropy value of recrystallizaation of Cu_2S is 43.56 Cal°C/mol,

Except about 8% microcrystal of Cu_2S remained in substrate, most of the Cu_2S crystal gains sampled at above the eutectic point(580°C) grew larger, while the cooling time was prolonged. 90% of Cu_2S crystal at 1000°C was greater than 20um, that at 790°C greater than 40um,at 580°C greater than 100um, and under 400°C almost all were greater than 100um.

THE APPLICATION OF PROCESS MINERALOGY TO PYROMETALLURGY

31.2.15.V

Richard D. Hagni, Department of Geology and Geophysics, University of Missouri-Rolla, Rolla, Missouri, USA 65401

Pyrometallurgical products are readily studied by process mineralogical techniques. The techniques involve especially reflected light microscopy, but also include scanning electron microscopy, electron microprobe, and automatic image analysis. The wide variety of pyrometallurgical products that can be studied and include sinters, mattes, slags, drosses, flash

furnace products, ceramic build-ups in electric induction furnaces, and others. Mineralogical studies of those products can contribute valuable information regarding the mineralogy, precise phase chemical compositions, phase abundances, grain sizes, grain shapes, microtextures, phase distributions, partitioning of chemical constituents between phases, and presence of deleterious constituents. The value of such studies can be illustrated by a number of industrial case histories.

The different types of reactions that occur within the flash furnace are especially amenable to study by reflected light microscopy. The solid-gas reaction of pyrite in the furnace feed to form radial fibrous pyrrhotite can be directly observed in all stages of completion. Further oxidation forms radial fibrous magnetite and hematite pseudomorphous after pyrrhotite. The newly formed oxidation products appear at the margins of the falling pyrite particles and gradually progress inward. Pyrite particles that melt prior to reaction and therefore react by liquid-gas reaction form granular pyrrhotite, magnetite, and hematite. Falling chalcopyrite particles that react by solid-gas reactions exhibit angular shapes and a succession of phases that include bornite, digenite, chalcocite, and metallic copper, together with the formation of the oxides, magnetite, hematite, cuprospinel, delafossite, and tenorite. The reaction of chalcopyrite by liquid-gas reaction forms particles that are spheres and cenospheres with intermediate solid solution, bornite solid solution, digenite, chalcocite intergrown in exsolution textures and rimmed by the iron and copper-iron oxides. The extent of agglomeration and fragmentation of the particles during flight through the furnace can be evaluated by reflected light microscopy. The extent of copper entry into the iron oxide phases can be determined by electron microprobe microanalysis.

Cobalt and nickel are very difficult to extract by flotation from the Viburnum Trend ores in the Southeast Missouri Lead District, which contains the second largest cobalt reserve in the United States. Recent pyrometallurgical efforts on cobalt recovery have centered upon submerged bath smelting. Reflected light study of those products shows that cobalt can be crystallized in coarse-grained cobaltpentlandite and as a solid solution substitution in iron-rich sphalerite. Nickel has formed shandite incorporating deleterious lead. The presence of large amounts of air during smelting favor cobalt and nickel segregation.

The mineralogy and character of phases in lead dross that cause lead entrainment during drossing of lead bullion can be determined by process mineralogy techniques. In addition to metallic lead, common phases include metallic copper, galena, chalcocite, albandite, and copper-lead sulfides. Pre-quench crystals are larger and usually exhibit skeletal forms, whereas quench-generated phases are very small and distributed throughout the lead matrix. Skeletal crystals of metallic copper and chalcocite were observed to form three dimensional networks that

entrain large amounts of metallic lead.

Mineralogical differences between "slick" dross and normal lead dross from the Herculaneum, Missouri smelter may explain the causes of the development of drosses that are difficult to handle. Copper occurs as copper-lead sulfide in slick drosses and as chalcocite and covellite in normal drosses.

Reflected light microscopic study of the slag from the Herculaneum lead smelter shows that zinc losses are in the form of olivine, spinel, and glass. Lead losses occur as metallic lead.

Sticky and difficult to handle slags from a secondary copper refinery were found by reflected light microscopy to contain significant amounts of corundum. Corundum forms ring structures that are relic after aluminum wire choppings present in the copper smelter feed.

Process mineralogical study of lead sinter from three Missouri sinter plants has shown that it contains a surprising variety of phases, including lead sulfide, metallic lead, lead oxide, lead-copper sulfide, lead silicate, and wollastonite.

40.2.29.H

CATHODOLUMINESCENCE MICROSCOPY OF REFRACTORIES

Richard D. Hagni and Musa Karakus, Department of Geology and Geophysics, University of Missouri-Rolla, Rolla, Missouri 65401

Refractories are especially well adapted to an examination by cathodoluminescence microscopy because many of the constituent phases show strong cathodoluminescence. The recognition of the various contituent phases, their distributions, grain sizes, grain shapes, variations in chemical compositions, and extent of corrosion by metals are readily studied by cathodoluminescence microscopy. Examples of refractory phases that cathodoluminesce and the character of their cathodoluminescence illustrate the important value of the technique.

The distribution of the bonding phase in refractories, an important aspect in the refractory industry, can be quickly assessed by cathodoluminescence microscopy. The silicate bonding phases in periclase and periclase-chromite refractories, for example, commonly exhibit bright yellowish, locally bright red, and rarely bluish grey cathodoluminescence. In contrast, under ordinary transmitted light microscopy the silicate bond can be obscured by light diffraction at the periclase grain boundaries.

Certain refractory phases that may be easily overlooked under ordinary light microscopy are readily detected with cathodoluminescence microscopy. The presence of ferrite spinel in a magnesite refractory, for example, can be detected by its red cathodoluminescence. Silicate inclusions are revealed by

their yellowish green cathodoluminescence.

In chrome-magnesite bricks, periclase grains typically exhibit a deep orange cathodoluminescence. Where magnesium has diffused into the margins of chromite grains, they are characterized by bluish grey cathodoluminescence in contrast to their non-cathodoluminescent character elsewhere.

Zircon refractories exhibit intense cathodoluminescence in various shades of blue. Zircon sand grains typically exhibit dark blue cathodoluminescence and are readily distinguishable from the fine milled zircon, which shows light bluish grey cathodoluminescence, that sinter the sand grains together in the refractory.
Mullite tends to show a dull violet cathodoluminescence in mullite refractories, and have dull blue cathodoluminescence in fireclay refractories. Corundum in high alumina refractories exhibits dull bluish green cathodoluminescence. Some crystals of silicon carbide in silicon carbide refractories show reddish brown cathodoluminescence although most are non-cathodoluminescent.

Cathodoluminescence microscopy is especially useful in the study of ceramic build-ups that are formed in electric induction furnaces. Ceramic build-ups are undesirable hard and dense deposits that form in or near the throats of channel induction furnaces used in iron foundries as melting and holding furnaces. Under ordinary transmitted light most of the phases have similar properties. Cathodoluminescence microscopy has been found to be ideally suited to the rapid recognition of most phases present in the build-ups. Spinel usually cathodoluminesces bright green, but may show blue-green or red depending upon the presence of various minor activator elements, such as chromium, ferric iron, etc. Compositional zoning may be revealed in spinel crystals by cathodoluminescent red cores and green rims. Corundum usually shows dark red cathodoluminescence, but may also exhibit purple, blue, orange, and yellow-white cathodoluminescence. Periclase usually shows dull brown cathodoluminescence, but it may also exhibit violet blue, reddish, orange, and yellow cathodoluminescence. Forsterite typically exhibits red, and anorthite may show blue to yellow green cathodoluminescence. Hibonite or Ca-hexaluminate has strong medium to dark green cathodoluminescence . Silica usually shows dull blue to dull brown cathodoluminescence, but it also may be pink and red. Mullite cathodoluminesces dull orange. Monticellite commonly occurs as reaction rims around forsterite and shows light blue and pale yellow-orange cathodoluminescence. The gehlenite end member of the melilite series exhibits deep blue cathodoluminescence. Rare earth silicate phases, which are present in small amounts in some build-ups, exhibit pink cathodoluminescence. The calcium sulfide, oldhamite, emits strong yelllow orange cathodoluminescence. Most glasses in the build-ups exhibit

orange cathodoluminescence, but those that are intergrown with melilite crystals are blue. A better understanding of the mineralogy of these deleterious deposits may lead to devising steps that prevent or diminish the formation of the build-ups.

MAKE AN APPROACH OF TECHNOLOGY ON MALACHITE OF Fe-Cu DEPOSIT IN TONG LU HILL

31.2.21 V

Hu Chengcheng, Daya Design and Research Institute of Nonferrous Metal Company, Hubei, China

Tong Lu Hill is located Southwest 3 Km of Daya county, Hubei province. There are tens copper mines from small scale to large scale in Southeast area of Hubei province. Only are there a large number of technological malachite to be found in Tong Lu Hill. The reasons may be: the reserves of copper deposit in Tong Lu Hill belong to large scale. The copper-bearing grade is 1.7% (average). It is the most richest one in copper-bearing in large scale and rich copper deposits in Southeast of Hubei. Therefore, it was provided with material basis for forming malachite. The deposit also is located on the shore of Daya Lake in middle-lower reaches of Yangtze River. The climate belongs to subtropical zone of inland. Air temperature is moderate and full of rainfull. It is a very favourable condition for reaction of oxidize and reduction. The geologica tectonics activity was very frequently in this area since Yan Mountain period. The Cu-Fe skarns deposit was formed by quartz-diorite brought into contact with limstone of Triassic system. The tectonics activity was continued and formed environment of downward enrichment of minerogenetic solution deposit. Moreover, the country rock of this deposit is marble and there are many iron-bering minerals associated with sulfide copper in the ore. As mentioned above, they supplier with material to formed malachite.

The varieties of malachite in this mine have chalcostaktite, dihydrite, etc.. This kind of malachite which can be solved by acid is main variety. The colours have emerald green, blackish green, pink green, sky-blue, etc. . bright and lustrous, pattern quite defferent. The loose texture malachite looks like peacock showing its beautiful feather, velvet and silk-sand satins, jade coming out from miarotitic cavity, shedding its rays in all directions. The compact texture malachite looks like stalacite upside down, ripplep on the blue sea, the Eight Diagrams on the tortoise-shell, pod with grape, mung bean with green leaves, wooden grain of pine tree and cypress. After making into handicarft articl, it became more beautiful which shows beautiful decorative pattern and peculiar prospect. some of them appear discolour, mung bean with green leaves, cat's eye flash of light. These are more valuable variaty of malachite.

Malachite can be classified into two technological types base on quality, texture and technological characteristic.

1. loose texture malachite. This kind of malachite shows loose texture and was mixed up with limonite, light green to dark green. Texture and structure have: plumose, acicular, fibriform, silkiness, radiating, honeycomb, outer covering, network, etc.. They can be made potted landscape or decorative article base on its nature outward appearance.

2. Compact texture malachite. It can be classified into two sub-types according to colour of dark green or pink green. A) . Dark green and fibriform texture malachite. It has green to dark green colour, higher density and hardness, concentric zonal or striped structure, good polishing property. It is an excellent material for making ring-face, heart-shaped, eardrop, necklace. B). Emeral green with striped structure malachite. It has lighter colour, lower-hardness, compact texture and zonal structure, many change decorative pattern. Some look like the moon shed light on green champaign or like running water coming from high mountain or like wave ring sheding its rays in all directions or like cloud layer densely covered, etc.. It is a good material for making seal, necklace, heart-shaped, bow tie.
In short, the malachite of Fe-Cu deposit in Tong Lu Hill is a kind of valuable material of industrial art.

ON OCCURRENCE OF NIOBIUM IN SLAG FROM OPEN HEARTH FURNACE IN BAO STEEL

Huang Fengyin,Department of Geology, University of science and Technology , BeiJing, 100083 PRC

The average Nb content in slag from open hearth furnace of Baotou iron and Steel conp. is 0.3--0.4% . Nb occurreuce in this slag was investigated in 1982 . Nb characteristics and patterns of concentration in different phases of slag were found out .they are :

1. In slag of open hearth furnace Nb can be found in certain minerals,in wh-ich Nb concentrated;

2. Basicity of slag affects the pattern of Nb concentration. When slag havi-ng lower basicity ,Nb content will be higher ,since maneegan-niobite (or niob-ium-bearing firrojacobsite) is formed; the higher the basicity, the lower the content of Nb O ; because Nb gets in isomorphism and is dispersed in niobium-bearing calcium ferroaluminate and other minerals;

3. behavior of Niobium is affected by metallurgical conditions; at the begi-nning of metallurgical process there is reducing atmosphere in furnace ,Nb is in combination with Fe^{2+} .Mn^{2+} forming mangano-niobite (or niobium-bearing ferro-jacobsite);as time goes on, atmosphere inside furnace is getting oxidizing , basicity raises,thus Nb gets in combination with Ca ,Ti forming niobium-bearing uhligite; at the end Nb will be in combination with Fe^{3+} , AL^{3+} forming niobium-bearing calcium ferroaluminate;

4. In author's opinion ; apart from metallurgical conditions and basicity the change of Nb valence alsoplays an important role in Nb concentration and di-spersion.

THE PROPERTIES AND UTILIZATION OF NEPHELINE

59.25 H

Huang Qiang , He Shaoneng and Hang Jialing , Geological Institute of State Administration of Building Materials Industry , Beijing 100010 , P.R.China

As one of feldspathoid-group minerals , nepheline occures in alkaline rocks. The chemical composition ranges of nepheline minerals in plutonic rocks of China are, SiO_2 41-47 %, Al_2O_3 29-34%, CaO 0-1%, FeO 0-0.9%, K_2O 4.9-7.5%, Na_2O 13.9-16.7 %. Compared with the theoretical nepheline, the actual nepheline is always SiO_2-oversaturated but Al_2O_3-undersaturated . The CaO in actual nepheline is due to secondary alteration - cancrinition. Nepheline can intergrow with SiO_2-saturated feldspar minerals but not with SiO_2-oversaturated minerals.

The chemical composition and physical chemistry properties of nepheline give it many advantageous qualities, (1). Intensive fluxing property. Feldspar minerals is used as a fluxing agency in glass and ceramic industries . Because nepheline minerals, compared with feldspar, has high alkalic content and react with quartz at high temperature , it can make quartz to be activated and melt at low temperature . Experiments have proved that the melting point of the glass material prepared with nepheline is 632℃ , while that of the material of the same chemical composition prepared with feldspar is 780℃ .

(2). High effective composition. Both feldspar and nepheline materials are used to supply Al_2O_3 in glass industry. The Al_2O_3 in nepheline is almost actually and theoretically twice as much as in feldspar. The tryout shows that 1 tone nepheline material can replace 1.8 tone feldspar material .(3). High alakli-replacing power. As the main cost of glass industry is from soda, saving alkalis is significant. It can reduces the use of soda in industry to utilize nepheline, which has high alkali content and intensive fluxing property. (4). Reducing the influence of harmful elements. The harmful element content in feldspar material is higher than in silico-material. Therefore, lowering the use of feldspar materials in industry is lowering the influence of harmful elements.

The Glass Experiments . The composition of the experimented material is the same as that of plate glass(SiO_2 72.30, Al_2O_3 2.40, CaO 6.40, MgO 4.00, Na_2O + K_2O 14. 60). In the material, 5.91% of nepheline concentrate (sample No.1) or 8.09% of nepheline syenite (sample No.2) is used. The regulations are, feed the material at 1300℃, raise the temperature to 1450℃ and melt it for 2 hours, then raise the temperature to 1520℃, and reduce the temperature after 2 hour' s purification and fixing up. As a result, the measured top limit temperature of crystallization of No.1 is 953℃, and that of No.2 is 947℃. In the table 1 is the viscosity of the two samples . The experiments

Table 1. The relation between viscosity(P) and temperature(T)

P \ T	1350℃	1300℃	1250℃	1200℃
No.1	416.87	575.44	831.76	1288.25
No.2	407.38	562.34	812.83	1258.93

results have proved that nepheline not only can be utilized as the material of plate glass, but also has energy- and alkali-saving properties.

The Daily Ceramic Experiment. The glaze-preparing experiment, after repeated experiments, we conclude that if 65% of nepheline syenite i.e. 20% of nepheline is used, the best result is achieved, the fluidity of the melt glaze is fine; the melting temperature is lower; the glaze surface is pure white and bright; and there are only a few gas holes in it. In daily ceramic body, after a little amount of nepheline syenite (usually $\leqslant$ 10%) is used, the porcelianization of the body is fine, and its deformation and contraction is little. The white degree is high and melting temperature is lower.

One nepheline deposit with high quality has been found in Sichuan Province, P. R. China and explored now. The content of nepheline is up to 90%. The product has been used in glass and ceramic industries. Its chemical composition is, Al_2O_3 30.31%, Na_2O 15.00%, K_2O 5.31%, CaO 5.50%, Fe_2O_3 0.24%.

4a230 H

CATHODOLUMINESCENCE OF DIAMONDS

J. Just, Jiri Just & Associates, 30 Kay Street, Scarborough, Western Australia 6019

Australia has been known for a long time as a prominent source of many minerals and ores, such as coal, iron, copper, lead, zinc, uranium and, of course, gold. The latest addition to this list are diamonds, when almost two decades of intensive exploration culminated in the discovery of the rich Argyle deposit which put this country very high on the list of diamond producers.

There are many problems in diamond exploration and one of them is, however peculiar it might sound, the actual identification of diamonds. Years of experience suggest that the fastest, and most reliable non-destructive technique is scanning electron microscopy using a SEM equipped with EDS analytical system and operated in the 'differential vacuum' mode (environmental cell). The author has been using a JEOL JSM-2 with ORTEC EDS and a Robinson backscattered-electron detector. As the uncoated scintillator of this detector is sensitive not only to electrons but also to visible light, the device is suitable, in the absence of atomic number contrast, for the detection of cathodoluminescence (CL) and the image observed on the screen is a composite of

topography and cathodoluminescence.
Examination of a large number of diamonds of different provenance indicated that about 85% of natural diamonds exhibit CL to some degree. CL is usually restricted to more-or-less sharply defined areas which apparently reflect the distribution of impurities or growth defects in the crystal. The observations also suggest that the octahedron is the major, if not the only, growth crystal form on natural diamonds and that the other commonly observed forms, to partial resorption of the octahedral crystal (Fig. 1).The cube was found as a growth form only on synthetic diamonds.

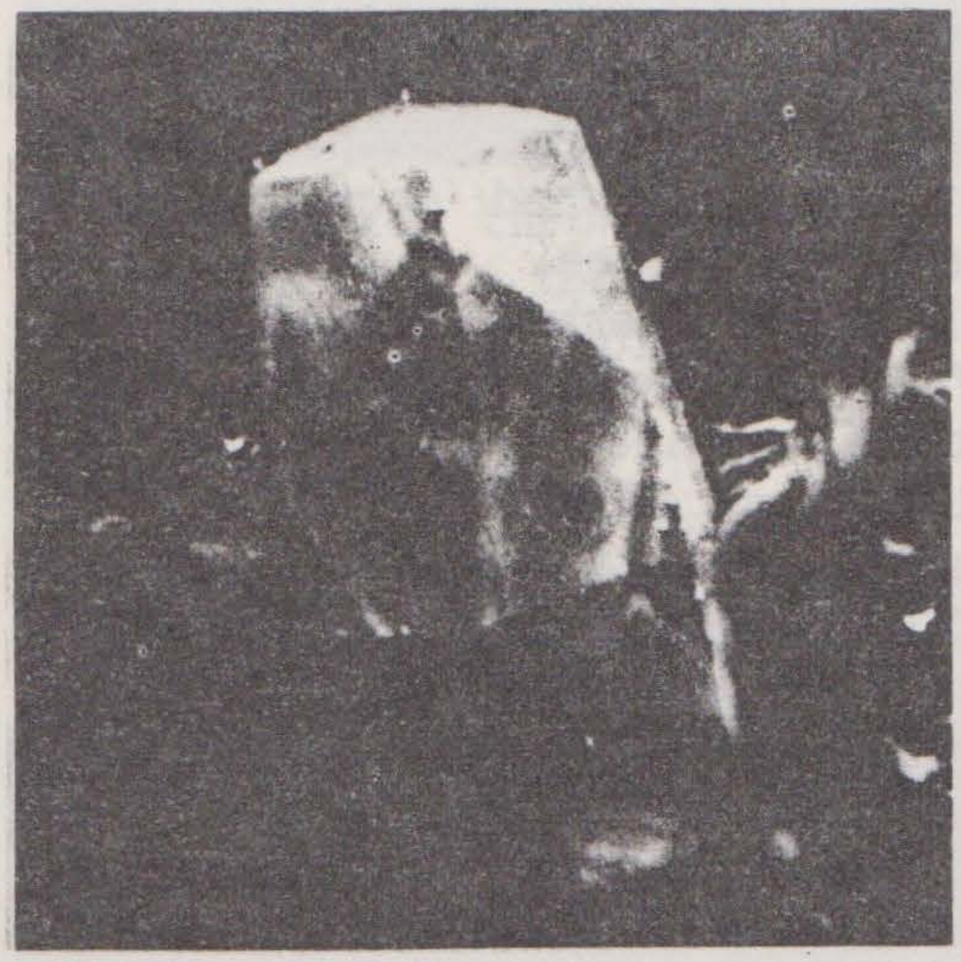

Fig.1. Elongated octahedron reduced to elongated tetrahexahedron by partial dissolution. Octahedral CL pattern clearly visible. Length approx. 1.5 mm. SEM, BE+CL image.

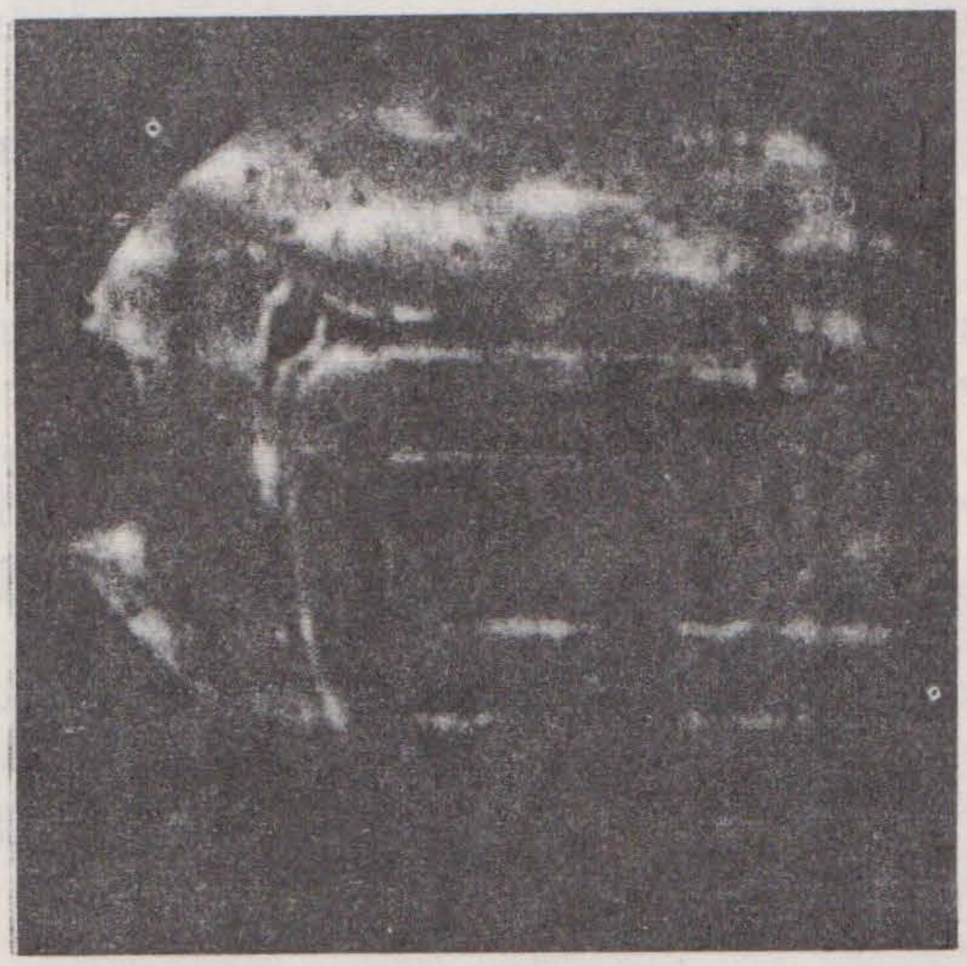

Fig.2. Brilliant cut diamond in a ring. Octahedral Cl pattern clearly visible, table cut almost parallel to (100). Diameter approx. 2 mm. SEM, BE+CL image.

Under suitable conditions single crystals, twins or polycrystalline aggregates can be readily distinguished even on small fragments. As there is no additional instrumentation required, the technique may be used to advantage for the determination of crystallinity, crystallographic orientation or growth defects which might be of importance in diamond exploration e.g. for the interpretation of conditions of formation and subsequent history of the individual diamond grains from a particular locality and in industry for assessing physical properties, e.g. hardness, toughness, etc. of a particular stone and its suitability for a particular industri-al application. The CL patterns may also be easily observed on cut stones and, because they appear to be unique, may serve for 'fingerprinting' of the stones or jewelry pieces (Fig. 2).

37.2.23V

MINERALOGY AND TEXTURES OF ROASTED PYRITE

J. Just, Jiri Just & Associates, 30 Kay Street, Scarborough, W. Australia 6019; J. Graham, CSIRO, Private Bag P.O. Wembley, W. Australia 6014; J. Dunn, Curtin University of Technology, G.P.O. Box U 1987, Perth, W. Australia 6001, J. Avraamides, G. Nguyen, Chemistry Centre, 125 Hay Street, Perth, W. Australia 6000.

Investigation of the behaviour of pyrite during roasting of pyritic gold concentrates was undertaken as part of study of gold recovery from refractory sulphidic gold ores.

Pyrite concentrates representing feed for the North Kalgurli Mines Croesus roaster were roasted at temperatures from 400 to 750°C, various durations and in different controlled atmospheres in a laboratory-scale roaster simulating an industrial fluid bed roaster. The resulting calcines were examined by means of an optical microscope and by a scanning electron microscope JEOL JSM-2 equipped with an ORTEC EDS analytical system and specially modified for work with geological materials. The samples were prepared for examination as conventional polished sections and also as mounts for observation of whole particles.

Essentially two processes are involved in thermal treatment of pyrite: 1. direct oxidation of FeS_2 to Fe_2O_3 and SO_2 and 2. thermal dissociation of FeS_2 to elemental sulphur and a pyrrhotite-like phase with composition close to FeS.

Direct oxidation of pyrite takes place in an oxidizing atmosphere at any temperatures below approx. 550°C (weathering of pyrite in nature may be viewed as "roasting at room temperature"). The reaction is exothermic and therefore selfpropagating. The reaction rate increases with temperature but is limited by the rate of mass transfer of O_2 in and SO_2 out of the grain by diffusion through the relatively impermeable Fe_2O_3 and proceeds in pulses. The resulting Fe_2O_3 has a characteristic concentric texture (Fig. 1).

Thermal decomposition takes place at temperatures above approx. 550°C. The reaction is endothermic, requires an external source of heat and in anoxic atmosphere proceeds only to formation of the FeS phase and sulphur. As the mass transfer is only unidirectional the reaction is continuous and the resulting FeS has a typical spongy texture (Fig. 2). At higher temperatures violent evolution of gaseous sulphur often ruptures the grain (Fig. 3). In oxidizing atmosphere the sulphur gas is continuously burnt off on the surface of the grain (the atmosphere inside the grain remains anoxic while the decomposition is in progress) and after completion or cessation of the thermal decomposition process the FeS is oxidized to Fe_2O_3 and SO_2. The resulting Fe_2O_3 preserves the spongy texture of FeS (Fig. 4) which is much more open and therefore more penetrable than the concentric texture produced by the low temperature direct oxidation of pyrite.

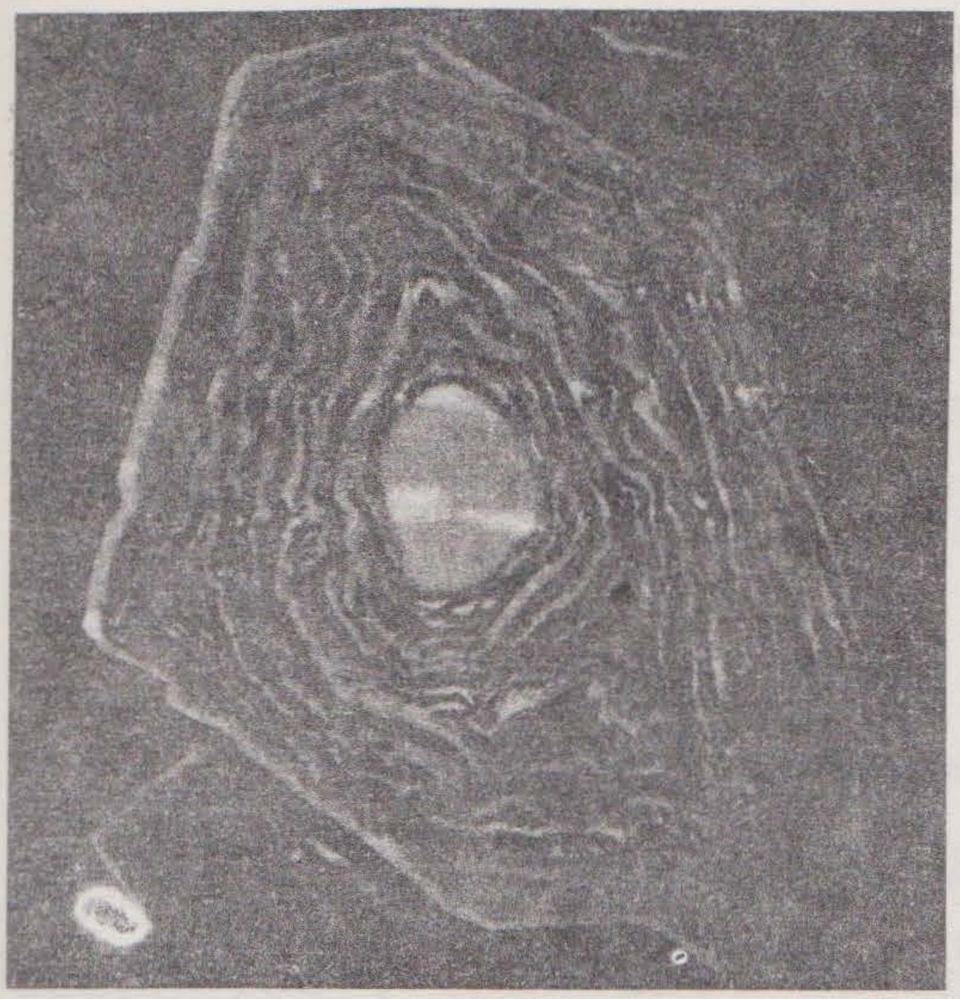

Fig.1. Section through Fe_2O_3 formed by direct oxidation of pyrite at 500°C. Typical concentric texture, pyrite relict in the centre.
SEM, magn. 525x, BE image.

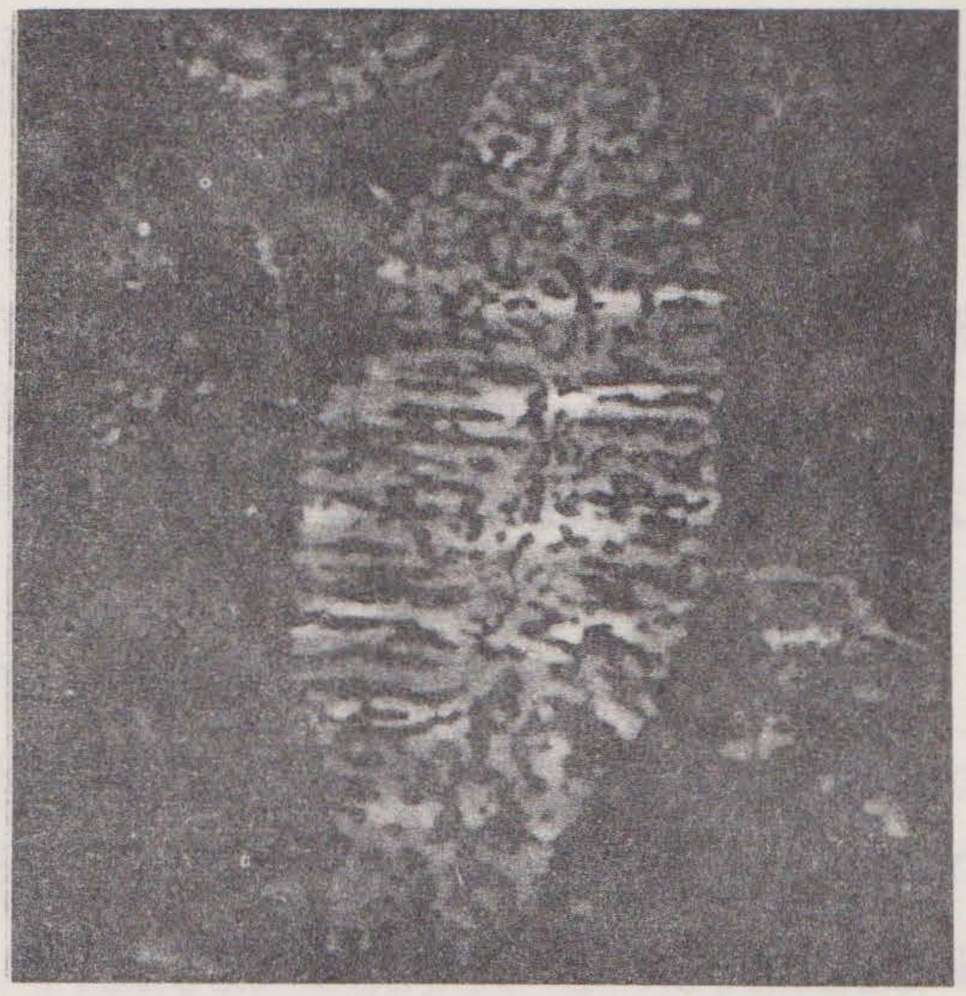

Fig.2. Section through a grain of FeS formed by thermal decomposition of pyrite at 700°C. Typical spongy texture.
SEM, magn. 560x, BE image.

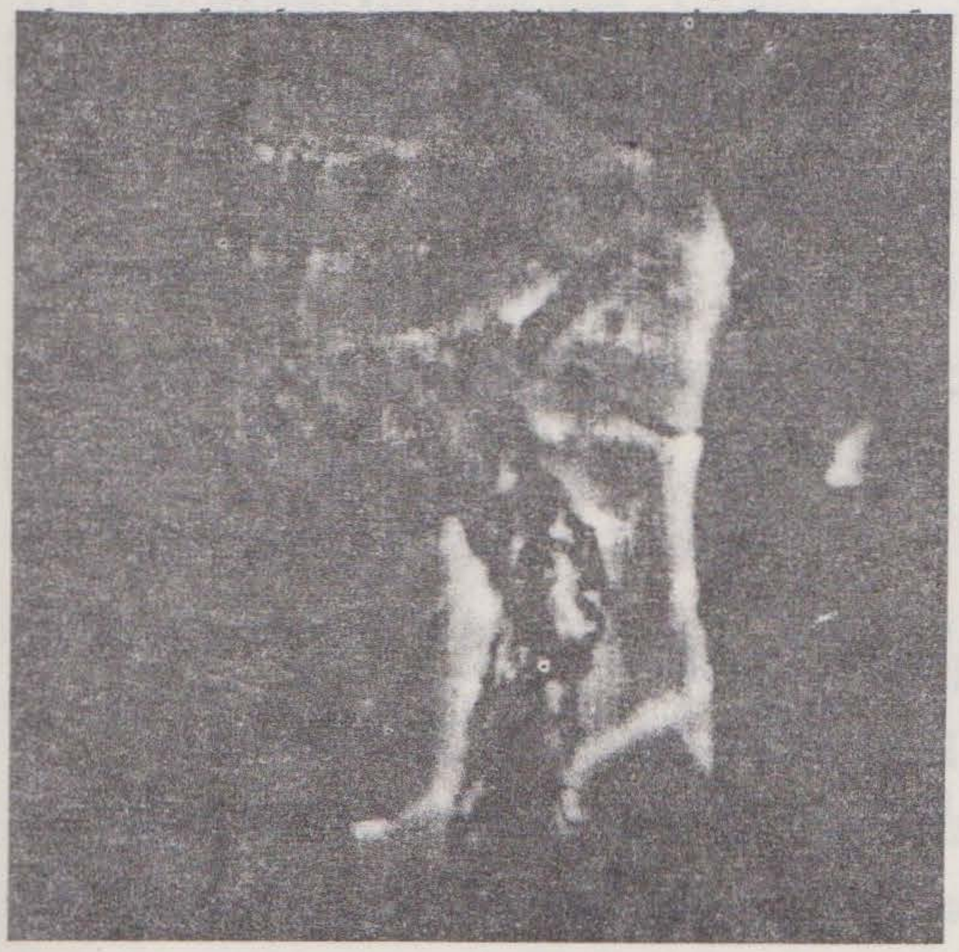

Fig.3. Fe_2O_3 'skin' on spongy FeS formed by roasting of pyrite at 550°C. Grain ruptured by pressure of the evolving gaseous sulphur.
SEM, magn. 730x, BE image.

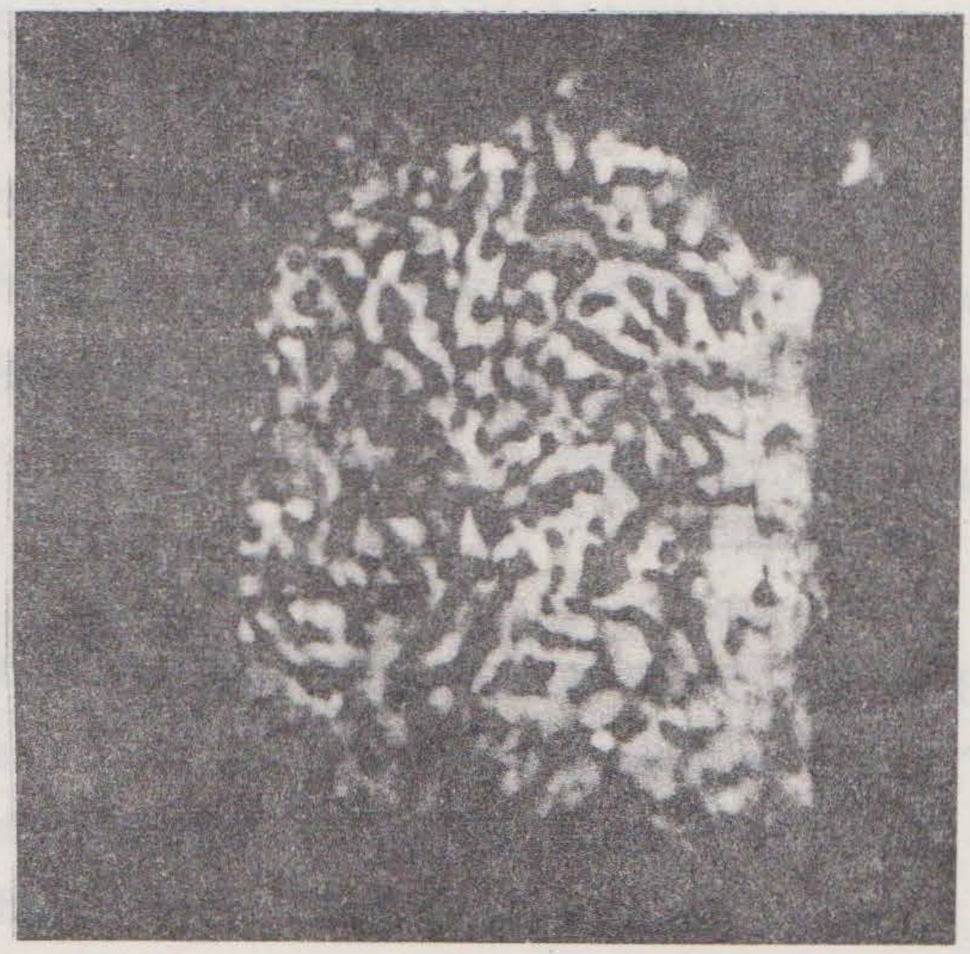

Fig.4. Fe_2O_3 pseudomorph after pyrite formed by thermal decomposition followed by oxidation at 700°C.
SEM, magn. 500x, BE image.

Examination of textures of iron oxide grains in products of laboratory or industrial roasting makes it possible to deduce the thermal history of each grain and assess the efficiency of the roasting process.

18.23P

SELECTIVE ORE TREATMENT — A PREREQUISITE FOR APPLICATION OF PRODUCTION MINERALOGY

Heikki Kauppinen, Kemira Co., Siilinjärvi mine, SF-71800 Siilinjärvi, Finland
Heikki Papunen, Institute of Geology and Mineralogy, University of Turku, SF-20500 Turku, Finland

Most of the mines intermix different ore types to keep the mill feed as homogeneous as possible. However, the homogenization seldom succeeds completely. If the ore types differ in concentratability, the random variation in the proportions of the different ore types results in a continuous need for process adjustment. The delay in adjustment then reduces the recovery of the concentrate.

The best result is achieved by analysing the ore types for their concentration properties and by treating each ore type individually. That way we know how each ore type must be treated in the concentration process. Controlled classification of the ore types and their treatment as individual units requires not only information about the properties of the ore types but also real-time data flow from the stopes to the concentrator. The gain due to optimal milling times and the concentration processes best suited to each ore type is seen in reduced consumption of energy and chemicals and in increased recovery. Classification methods of ore types will be described in detail.

CAPABILITY OF USING BASALT ROCK IN VIETNAM

La The Chich, Hoang Trong Mai, Polytechnical Institute, Hochiminh City, Vietnam

Basalt is largely distributed in Vietnam, particularly on the Southern territory. Due to the authors's studying about Basalt in Vietnam were formed in three stages: Late Miocene, Pliocene–Pleistocene and Pleistocene–Holocene.

The Basalt petrographic compound consists of Basalto–andezit, Basalt toleit, dolerit, alkaline Basalt olivine with their volcanic bombs and tuf.

Basalt is used in Vietnam in constructional materials field. A lot of roads, bridges, hydroelectrical dam, houses sites all use Basalt with different forms.

Dense Basalt is black, after sawing and cutting, grinding smoothly with high aesthetic degree, it can produce paving rock used in the special Architects sites.

At some places have used grinding powder fabricated from melted Basalt at 1400℃ and then it brings about crystallisation slowly and slowly.

With the melted Basalt can produces cotton–glass, stones tubes and stones shelves in

special technologic.

In condition of the humid and tropical climate, on Vietnam Basalt has a weathering crust contained a lot of minerals as bauxite, precious stone, color–powder for constructional branch.

ON MINERAL INCLUSIONS BY MEANS OF CATHODE LUMINESCENE WITH SEM

Li Peilan, Yu Xinzhen, Mai Zhenghong, Dai Daoyang,
Department of Geology, Central-South University of Technology, Changsha, Hunan 410083, People's Republic of China

By means of cathode luminescene with SEM, we have studied more tham 10 kinds of minerals, such as: diamond, quartz, feldspar, calcite, molybdenite, pyrite, wolframite, blende, galena and fluorite. It was found that not only observed there were any cathode luminescene phenomena of inclusions in these minerals, but also did there extensively exist luminescene phenomena of inclusions within transparent and opaque minerals, But with cathode luminescene microscope we could not find this kind of luminescene phenomena. Authors divided luminescene observed into two kinds-direct and indirect.

In the former we can distinguish luminescene of solid phases corpuscles and fluid inclusions, meanwhile directly observe the characters of syngenetic and epigenetic fluid inclusions. For the single inclusion, we can not only directly observe its size, but also observe whether there are inclusions of one-phase or multi-phase and their characters. The ingredients of inclusions are also boverved. In addition

search test and study on sepctroscopy is carried out during direct observation taking advantage of SEM we have contrasted original-position cavity of inclusion characters of fluid inclusions with their luminescene form. Therefore from the above mentioned we can draw conclusion luminescene, caused by cathode ray by means of SEM, has opened up a new potential for the research of mineral fluid inclusions.

In the indirect observing research of luminescene, besides comparison with the former, we directly connected luminescene form with SEM atlas and contrasted them. In combination with energy chart analysis, we have done observation and research on the corpuscles and super-corpuscle mineral phase in the minerals. Hence morphology of cathode luminescene by SEM opens up a new path for the observation and research of corpuscles and super-corpuscles mineral phase.

592.6/1

THE OCCURRING CHARACTERISTICS OF PHOSPHORUS AND ITS EFFECT ON MINERAL DRESSING IN CARBONATE MANGANESE ORE OF HUAYUAN MANGANESE MINE (SOUTHERN SECTION) OF HUNAN PROVINCE

Li Qianmao, Liu Chengxian, Jiang Lixia, Department of Geology Beijing University of Science and Technology. Beijing 100083, China

Ore of Huayuan manganese mine of Hunan province belongs to a kind of high-phosphorus low-iron and poor-manganese carbonate manganese ore. The main chemical composition of this kind of ore is Mn 18.6%, Fe 2.68%, P 0.2%, CaO 6.5%, MgO 3.36%, SiO_2 24.06% and P/Mn 0.011. The main minerals are carbonate minerals, clay minerals, quartz, pyrite and carbonaceous materials. Texture of the ore mainly is of pelitic microcrystal type. Structure of the ore is massive, is banded.

Low content of phosphorus and the fine gains of phosphorus-bearing minerals make research work more difficult. The authors have basically found out that fluorine in the ore occurs in the form of fluor-apatite by using a lot of assay methods (microscope, electron

probing analysis and the process of chemical method). Fluor-apatite in the ore also exists in three forms:(1) of terrigenous fragments(grain size 1-6μm); (2)of well-developed crystals into quartz veins which pass through ore bodies (grain size 6-25μm);(3)trapped in the grains of carbonate manganese minerals as micrograined inclusions(grain size <1μm),this kind of fluor-apatite only takes its up 12% of the total amounts of fluor-apatite. Distribution is nonhomogeneous: 62% distributer in the positions rich in gangue minerals and 17% of fluor-apatite rich in carbonate manganese minerals. Contents of phosphorus and manganese have a negative correlation.

The occurring characteristics of fluor-apatite in the ore have an effect on mineral dressing.First of all there is a great difference of physical and chemical properties between fluor-apatite and carbonate manganese minerals, so intensive magnetic dressing method or "hausmantite" method can be used. As the grain size of fluor-apatite is fine, mechanical selecting method only takes off grains greater than 10μm,but even hausmantite method can not remove the grains of fluor-apatite less than 1μm,resulting in diffculty in concentrating manganese and reducing phosphorus. On the other hand, the nonhomogeneous distribution of fluor-apatite in the ore and the content negative correlation as mentioned can benefit the mineral dressing work of concentrating manganese and reducing phosphorus. By using mechamic dressing method to this kind of ore. Part product of qualified second class or third class can be obtained. This achievement breaks down the past conclusion it is impossible to use mechanical dressing method to reduce phosphorus for this kind of ore.

PROPERTIES AND APPLICATION OF KYANITE GROUP MINERALS

31.2.20 V

Lin Binyin, and Huang He, department of Material Engineering, Wuhan Iron and steel University, Wuhan 430081, China.

Abstract

China has rich resources of kyanite group minerals.They spread over more than 24 povinces,municipalities and autonmous regions.They have significant properties, such as when heating up to a certain temperature, kyanite group minerals can change into mullite irreversibly with volume expansion.The temperature at which kyanite group minerals transform into mullite is influenced by grain size and impurities. So is the total amount of mullite phase formed(Table),

Table The deforming temperatures of kyanite group minerals

Temperature ℃	sillimanite concentrate		Andalusite concentrate			Kyanite Concentrate
	-180 mesh	+180 mesh	-100~+150 mesh	-150~+200 mesh	-200 mesh	-100~+200 mesh
Starting to deform ℃	1400	1500	1350	1300	1300	1100
Completely deforming℃	1650~1700	>1700	1600	1500	1450	1450

kyanite group minerals have less content of impurities. The total content of TiO_2, Fe_2O_3, RO and R_2O(2.5~3.0%) in concentrates are about one half of that in bauxite. Corrosion resistance and creep, thermal shock resistance, etc. The exploitation and application of kyanite group minerals mainly depends on their properties. It is shown practically that kyanite group minerals play an important part in improving the qualities of alumino-silicate refractory. Besides, they are energy saving raw materials.

The author and his researching group have successfully used them in nozzle of large blast furnace(3200M³), hot-blast stove, synthesizing mullite grog, Mullite refractory mortar as well as saggers, etc. The exploitation and application of resources of kyanite group minerals is still in developing in China. The kyanite group minerals are extensive application in the near future.

59.2.7.11

TECHNOLOGICAL CHARACTERISTICS OF FINE MANGANESE CARBONATE MINERAL AND HIGH INTENSITY MAGNETIC SEPARATION

Liu Chengxian, Li Qianmao, Chen Shaolin, Mining Engineering Department, Beijing University of Science and Technology, Beijing 100083, People's Republic of China

It is shown that magnetic property of manganese carbonate ore increases with the manganese grade, the relation found to be a linear equation. From a large amount of measured data of specific susceptibility of Huayuan manganese ore, a regression equation is got as follows, $x = 0.927 + 2.665\ \alpha Mn$, where X is specific susceptibility of ore, αMn is grade of ore, correlation coefficient is 0.999.

After big pieces of ore were crushed to 15~0 mm, 10~0mm, or 6~0mm, in the medium size ore, it was found that there were three kinds of aggregates-rich, low and poor, the grade of manganese is about >25%, 10-25%, <10%, respectively. The difference of magnetic property between these three aggregates and gangue-quartz is obviously, so the medium size ore can be separated a rough manganese concentrate or final concentrate obtained directly. As the grinding cost decreased, middle size high intensity magnetic separator is widely used in the manganese mineral processing plant in China.

For upgrading the rough concentrate or reducing the detrimental impu-

rities, the concentrate should be regrinded and treated by fine size high intensity magnetic separator, such as Model SHP Type high intensity magnetic separator.

CARBON FIBERS IN CAMERA PEGMATITES OF VOLYN'(USSR)

R.V.Lobzova, V.T.Luk'yanova, N.V.Trubkin, Institute of Ore Deposits, Mineralogy, Petrography and Geochemistry USSR Acad. of Sciences, Moscow 109017, Staromonetny 35.

Carbon fibers are very rarely found in nature. They are known in brown coal of Geizentahl, bitumen of Derbishire, graphite bodies of Botogol alkaline pluton. Recently they are found in camera topaz- and morion-bearing pegmatites of Korosten pluton (Ginzburg A.I. et al. 1987). Here carbon fibers are located to brecciated rock cavities of the central part of pegmatite. Cavity sizes are from 5 to 23 cm. Aggregates of fibers are up to 3 kg in bulk.

Fibrous aggregates are composed opaque separations of black colour with round section about $0,002.10^{-3}mm^2$ and 0,005-0,5 mm in long. The fiber ends are subconical and spherical, and there are a lot of dimples that sometimes surrounded with ring growths, and microledges. There are thin intergrowths of fibers with mica and feldspar crystals, globules of sulphides. The chemical composition of fuel matter: C-76,51, H- 5,02, S-0,42, (O+N)- 18,05 mass %; H/C - 0,87, C/(O+N+S) - 4,14.

Study of morphology, chemical composition, trace-elements, the character of thermal destruction, molecoular structure, carbon isotope composition and analysis of fluid inclusions in topaz and morion from the pegmatites, indicates formation of fibers from fluid phase. As it was before established (Ye.K.Lasarenko, 1979) mineralization in Volyn'camera pegmatites proceded at gratual fall of fluid temperature from 600 to 100°C and pressure from 1100 to 200 atm. Possibly, temperatures of carbon fibers origin are 300-250°C and pressure 500-300 atm. rom carbonaceous matters (probably, acetyline). Possibly catalists of processes, as it was taken place in experimentes on pyrolitic carbon fibers synthesis from metan and other hydrocarbons,were iron-, cobalt-, nickel-, potassium-bearing substances and oxygen-bearing gases, and also carbon fibers as themself.

A STUDY OF PROCESS MINERALOGY IN TEST OF BENEFICIATING GOLD MINERAL FROM LI GUO IRON ORE

Chen, Luo, Beijing General Research Institute of MINING AND METALLURGY

Abstract

Li Guo Iron Mine is located in Shandong province, it's iron ore contains 0.88 g/T gold.

The main metal mineral in iron ore are Magnetite, Pyrite, and Chalcopyrite. Gangue minerals are Quartz, carbonate, etc.

Gold exists as independent minerals in iron ore. Most of them are natural gold whose purity is 100%. Others are silver-gold containing 15-44% silver. Gold minerals are very small. The grain sizes of gold mineral range from 0.005-0.020 mm. The maximum one is 0.044 mm.

Pyrite is a main carrier of gold mineral. By analyzing, it is found that the gold content in Pyrite is 79.55% of the total gold content. Others are in Chalcopyrite, few scatter in Magnetite and gangue. Gold minerals exist with other minerals in three ways as following. The first way is that gold mineral is surrounded by one grain of the other mineral. The second is existing in crevice of one mineral grain. That gold is situated between two or in several other mineral grains is the third one. Most of gold minerals exist in the first way in my specimen. What existing in the second and third ways are the few. According to statistics, gold content in Pyrite existing in the first and second ways is 88.67% of the total gold content.

It is not very easy for gold minerals to be separated, since their size are tiny, and most of them are wrapping by other minerals, so a second time grinding is needed before floatating those minerals other than gold. The grinding precision is raised. So single gold mineral, and, part of grain exposing but part to be with others are increased to 92.07%. They are almost full separated. The final rate of reclamation of gold is improved from 40% to 88-90%. The desired result is achieved.

PROCESS MINERALOGY STUDY OF THE PRODUCTS IN THE EXTRACTION OF COBALT FROM CONVERTER SLAG IN JIN CHUAN, CHINA.

Chen, Luo, Beijing General Research Institute of Mining and Metallurgy
Liang-ho Su, China University of Geosciences

During the extraction of nickel, minerals in the converter slag are fayalite, magnetite, and a few sulphides. The fayalite is a cobalt-containing one. Cobalt is extracted by re-melting the converter slag in an electric furnace.

The products of electric furnace are intermediate and slag. The intermidiate consists of alloy and two kinds of sulphides. The alloy phase is about 55-75% of the total, and the grain sizes are about 0.05-0.50 mm. The chemical composition of the alloy phase is about 53-63% of nickel, 25-34% of iron, 4-5% of cobalt and a small amount of copper. The composition of slag of the electric furnace remains the same in all phases.

It is found that the melting temperature of alloy is beneath 1200 c, and the temperature rises with the increase of iron content. This method is available in the extraction of cobalt from converter slag.

DEVELOPMENTS IN COLD CATHODE DISCHARGE BEAM CONTROL AND IN INSTRUMENTATION FOR CATHODOLUMINESCENCE MICROSCOPY

40.2.32/1

by Dr. Donald J. Marshall, MAAS, Inc., Lowell, MA, USA

Important developments have been made in methods for controlling the electron beam in the cold cathode discharge electron gun, typically used in cathodoluminescence microscope (CL) attachments such as the Luminoscope. There are also important new developments in several areas of accessory instrumentation for cathodoluminescence microscopy. This paper will survey a number of these fields as well as indicate some possible directions for future development.

Cold cathode beam regulation: Until recently, cold cathode discharge electron guns and control units did not provide for regulation of either the electron energy or the beam current and this placed demands on the operator to maintain the correct operating conditions. Now technological advances make it possible to regulate both of these quantities through feedback control systems, thereby reducing the amount of operator interaction required and simplifying the acquisition of data using spectrophotometers and EDS accessories. Electron energy can be regulated to +/- 1% or better. Beam current variations can be restricted to short term fluctuations of only a few percent and long term drifts of less than one percent.

Spectrophotometer attachment: Spectrophotometers for CL application need a wide dynamic range, easily variable resolving power, high transmission, and the ability to scan rapidly enough to record transient phenomena. Such a spectrophotometer and its interfacing with the Luminoscope is described. The system is totally computer-controlled.

Cooled stage: Even though it has been well known that some CL emission is enhanced at low temperatures, it is only recently that serious work has been done. This is performed at temperatures near that of liquid nitrogen. At this temperature, for some minerals, there is a dramatic increase in intensity and the spectral peak widths are much narrower. Examples of some of the important information obtained at liquid nitrogen temperatures for diamonds are presented.

Energy dispersive spectroscopy: The observations of CL can now be supplemented with immediate elemental analysis, using the techniques of EDS. Higher energy electron beams (25 kV or higher) and regulated beam energy are important advances which make this technique even more useful than it has been in the past.

Taken together these advances make a CL microscopy laboratory a comprehensive instrumentation center in which not only can a variety of important, interesting research be carried out but also one which can interface with teaching and introduce the student to a wide range of instrumental techniques on a relatively simple, inexpensive instrument.

59.2.9 11

LIQUATION METHOD OF ALUMINIUM EXTRACTION FROM DISTHEN SCHISTS AND KAOLINS

Aleksey A.Marakushev, Valentin G.Moiseyenko, Vyacheslav S.Rimkevich, Yury N.Malovitsky
Amur Integrated Research Institute Far East Branch, the USSR Academy of Sciences, Blagoveshchensk, Relochniy 1, 675000, Amur Region, USSR,
Institute of Experimental Mineralogy, the USSR Academy of Sciences, Chernogolovka, 142432, Moscow Region, USSR

The limited bauxite reserves make it urgent to extract aluminium from silicates and alumosilicates in some countries, possessing powerful aluminium industry, such as the USSR, the USA, Canada and others. In the Far East of the USSR anorthosites, andalusite--disthen-sillimanite schists and kaolin clays are suggested to be promising raw material for aluminium

extraction. The melting of these rocks with special components added results in immiscible melt and effective separation of silica and alumina.

Stable layered melts are formed in the system Al_2O_3-SiO_2-K_2SiF_6 as a result of the Chimchan deposit disthen schists lamination in the temperature interval 750-1100°C and under the pressure up to 50 bar. The immiscible aluminate melts of this system contain 67,48-78,83 wt% of alumina. Two layers structure of the immiscible liquids allows to remove easily the melts, required for further research during or after the experiments. After the removal of hieratite (K_2SiF_6) with high crystallizing ability and good solubility in water aluminate melts have high quality ironless bauxite composition. It is possible to extract alumina from this bauxite with the help of Bayer's method (Pevzner and Raizman, 1983). Only ball liquation isolations take place in the kaolin compositions of this system.

Stable stratum lamination is observed in the system Al_2O_3-SiO_2-K_2SiF_6-NaCl. It comprises silica- and fluoride-rich (I) melts and chloride (II) melts with 2,62-7,84 wt% of aluminium, containing less than 0,5 wt% of silicon with NaCl:KCl ratio, ranging from 1÷1 to 3÷1. Melts II are suitable for electrolytical aluminium extraction by chloride technology (Vetyukov and Borisoglebsky, 1984).

A continuous scheme of the aluminium extraction has been reproduced in our laboratory. This scheme begins with aluminium extraction from starting Chalgany deposit kaolin concentrates, enriched in additional components, and aluminium separation in graphite electrolytic cell from experimental chloride melts ends it. Melts I are exposed to the second lamination by the addition of NaCl. As a result new immiscible fluoride-silicate and chloride melts are formed. Hieratite and mallardite (Na_2SiF_6) extraction from the former melts is possible. Hieratite can be used repeatedly in closed technological process.

The mixture of hieratite and sodium chloride possesses universal ability to extract aluminium from silicate and alumosilicate rocks and minerals: anorthosites, nepheline-syenities, disthen schists, kaolin clays, albite, orthoclase and leucite. It was proved experimentally.

References:

1. Pevzner I.Z., Raizman V.L.(1983): Autoclave processes in alumina production. Moscow: Metallurgy. P.1-128 (in Russian).
2. Vetyukov M.M., Borisoglebsky Yu.V.(1984): Some questions of electrolytic theory of aluminium extraction with the help of chloride technology.

Ion melts and their usage in science and engineering. Kiev: Naukova Dumka. P.13-27 (in Russian).

90.2.31H

FORMATION PROCESSES OF SHOCKED QUARTZ GRAINS FROM MINERALOGICAL DATA

Yasunori MIURA; Department of Mineralogical Sciences and Geology, Yamaguchi University, Yamaguchi, 753 Japan.

Quartz minerals show wide pressure-dependent region (~30kbar) in the low-temperature field, though they have many high-temperature phases with each low-temperature phase [1]. The detailed mineralogical data of quartz silica indicate formation processes of the host rocks.

The Cretaceous-Tertiary (K-T) boundary samples have been discussed from mineralogical, archaelogical and geochemical data by many scientists [cf.2-6]. Anomalous density-variation data and probable formation processes of shocked quartz from four K-T boundary sites (Japan, Italy, Denmark and Tunisia) have been found in the progressive sampling data obtained by powdered X-ray diffractometer [7].

Main purpose of the present study is investigation of large quartz grains with shocked lamellae from K-T boundary sample of Clear Creek North (CCN), Colorado, U.S.A. [8,9] by using the Rigaku four-circle single-crystal X-ray diffractometer, compared with those of the Barringer meteorite crater and terrestrial metamorphic, volcanic and plutonic rocks and tectonic complex to estimate the probable formation process.

Physical properties of shocked quartz: Cell-parameters (as hexagonal cell) of quartz grains with and without shocked lamellae have been obtained from least square method of 25 peaks with higher degree of accuracy, which are summarized as follows. (1) The calculated density (ρ_{cal}) of standard quartz crystals used from Gifu rock-crystal and Yamaguchi granite is 2.645. (2) Three quartz grains (B1M, B3W, B10W) from center of the Barringer meteorite crater show higher value of ρ_{cal}; that is, 2.669. (3) Nine quartz grains from the CCN K-T boundary sample reveal three types of (a) normal rock-crystal (samples Q1, Q2 and SQ4), (b) distorted lower density quartz (SQ1, SQ2 and SQ3) [10], and (c) shocked quartz with higher density (SQ12, SQ20 and SQ21).

Anomalous cell-parameters of CCN shocked quartz: The CCN shocked quartz grains with lamellae indicate the following various cell-parameters and calculated densities: (1) lower a-axis (-1.2% in sample SQ20) and lower c-axis (-0.2% in the SQ20) with the higher density (+2.1%) which is several

times the density than the Barringer-type quartz grains. (2) higher a-axis (+1.5% in SQ3) and lower c-axis (-0.7% in SQ3) with the lower density (-0.6% in SQ3).

The anomalous cell-parameters and densities are due to (a) higher impact process resulted in atomic distortion of the SiO_4 tetrahedra and the compression of stacking direction (i.e. lower c-axis) which is the similar features of the quartz grains in the Barringer impact crater, (b) shocked process with partly glassy multiple lamellae [11].

Probable formation processes: The CCN K-T boundary samples are mixed with those formed by (1) pressure-dependent impact process to show the multiple shocked lamellae with higher density which are probably formed at center of the impact site, (2) temperature-dependent process to make the various distorted quartz grains with lower density and shocked lamellae which are probably formed at deeper place or rim of the impact site.

The present research is partly supported by the Grant-in-Aid for Scientific Research on Priority Areas (Origin of the Solar System) of the Japanese Ministry of Ed., Sci. and Culture (01611005) of the author. The author thanks Prof. W. Alvarez and Dr. G. Izett for sample preparation of the CCN K-T boundary samples.

References: [1]Mason B. and Moore C.(1982): Principles of Geochemistry, 4th Ed., 97. [2]Alvarez L. W. et al. (1980): Science, 208, 1095-1107. [3]Bohor B. F. et al. (1986): Science, 224, 867-869. [4]Miura Y.(1986): LPSC XVII, 555-556. [5]Miura Y. et al.(1988): Global Catastrophes in Earth History, 124-125. [6]Johnson K.R. and Hickey L.J. (1988): Ibid, LPI Contrib. No.673, 87. [7]Miura Y.(1989): Meteoritics, 24(4), 305. [8]Izett G. (1985): EOS, 66, 1149-1150. [9]Izett G. (1989): GSA Special Paper, 249 pp. [10] Miura Y. (1990): LPSC XXI (in press). [11]Xie X. and Chao, E.C.T.(1985): Geochemistry, 4,97-113.

BACTERIAL GOLD MINERALIZATION

Valentin G. Moiseyenko, Sergey A. Marakushev, Amur Integrated Research Institute Academy of Sciences, Blagoveschensk USSR

The genetic properties of ores and placers gold mineralization depend on processes in oxidation and weathering zones. Recent creation and description of accumulation gold microorganizms from Far East ores and placers [1, 2] call for necessity of further investigation of their interaction with precious metals.

Microorganizms were obtained from ore deposits and the system of bacteria - solution of ionic and colloidal gold was the experimental model of biogeochemical areals in nature. An aerobic gramm- positive bacterium Micrococcus luteus proved to be common to all the samples with high gold content and under condition of saturation 1 g of dry biomass sorbs 100 mg of gold, i.e. one cell fixes in average 5 thousands colloidal particles. Was shown that decreasing of gold absorption takes place in anaerobical conditions. The study of this phenomenon showed that cell respiration noticeably increased in the presence of colloidal gold. It suggests the energeticval dependens of absorption process. Inhibitors of the oxdative phosphorilation and the respiration chain diminish dioxygen consumption and gold absorption simultaneously.

Experiments studying the reduction of hydrophobic nitroxile spin probes in the cells by EPR method were carried out in order to evalute the gold influence on the redox situation in membrane chains of electron transfer. The reduction rate in the presence of gold noticeably decreases independently of signal group location inside the lipid membrane bilayer. Therefore, the colloidal gold particles influense on the redox potential practically along the whole membrane profile. This process results in gold recrystallization. At first, gold oxidative complexation by amino acids residues on the surface layer of bacteria take place. Gold ions, related with protein ligands are formed. Later the reduction of gold complexes by exogenous reduction equivalents of redox chain occurs. It was prove by electron microscopic finding out of gold crystalls in this system. After gold colloidal contact with bacteria needle- shaped gold crystalls are found in culture medium by scanning electron microscopy method. In some cases we observed cubic and polyhedral crystals.

Endogenic gold is unstable under exogenous conditions. The average particle size and fineness increases in the row from the initial ores of native deposits through their oxidation zone. The observed crystallization process of ' new' gold on the endogenic gold particle surface can explane the detection of natural gold with high probe cover and edge on the particle surface in placers. This study can affirm that bacteria take part in gold concentration and mineralization.

REFERENCES

1. Marakushev S. A., Balezina T. L., Kovalevskaya A. N., Redox processes in interaction of the heterotrophic microorganisms in the gold deposits with colloidal gold. In; Dokl. AN SSSR, 1988, v. 300, N 5, pp. 1211- 1214 [AN SSSR; Moskow]

2. Marakushev S. A., Kovalevskaya A. N., Moiseyenko V. G. Bacterial recrystallization of gold. In; Dokl. AN SSSR, 1989, v. 308, N 2, pp, 482- 485 [AN SSSR; Moskow, in Russian] .

13.8 P

Biological Implications for Quartz Crystallinity

Y. Nathan[1], Y. Ginott[1,2] and S. Shoval[3,1]

1. Geological Survey of Israel.
2. Hebrew University of Jerusalem.
3. The Open University of Israel.

Crystallinity of quartz in cherts and porcelanites is generally poor. The crystallinity of quartz may be measured by X-ray methods, using the degree of resolution of the d(212) X-ray reflection at 1.382Å (Murata and Norman, 1976), by thermal methods, using the height of the exothermic peak due to the high-low quartz inversion at about 573°C (Deutsch et al., 1989) or by infra-red methods, measuring the degree of resolution of the shoulder at about 1144 cm^{-1} , using the first derivative IR spectra (Shoval et al., 1990). There is good agreement between the crystallinity indices obtained by the three methods. Thermal methods are more accurate for well crystallised samples, whereas IR spectra are more accurate for poorly crystallised ones. X-rays give the best results for intermediate samples. The crystallinity may also be directly observed with a Scanning Electron Microscope (SEM). The poor crystallinity of quartz in cherts and porcelanites appears to be due to the biological origin of the silica via opal (opal A and/or opal C-T).

During a study of diagenesis of silica in the Late Cretaceous of Israel (Ginott, 1990) it appeared that the microfauna, even when originally calcitic, are the first part of the rock to transform into quartz. This is clearly seen in porcelanitic, opal C-T rocks where the fauna is generally quartz, while the rest of the rock is opal C-T. The above implies that microfossils generate a favourable microenvironment for quartz replacement.

18.26 P

STAUROLITE - NEW INDUSTRIAL MINERAL

B.S.Panov, R.M.Polunovsky, V.P.Krivonos,
USSR,
Donetsk Polytechnical Institute,
340000, Donetsk, Artyom Street, 58.

Mineral staurolite that had no practical utilization earlier may be used as alternative source for traditionally used in ferrous metallurgy fluxes-liquescences - fluorite and bauxite. New technology of making steel with staurolite concentrate has been worked out in Donetsk and success-

fully tested at one of metallurgical plants. Addition of staurolite increases velocity and degree of desulphurization of metal in 1.2 - 1.5 times. There is essential reduction of metal costs and steel production increases by 0.28 - 0.65%. Staurolite concentrate is ecologically pure and has a regular granulometric composition. Its utilization instead of Ca fluoride essentially improves ecological surrounding of making steel production that is also of great importance because of problem of ozone strata of Earth.

Staurolite shales often met on Pre-Cambrian shields-platforms may be main sources of production of staurolite. They are rather widely spread in Pre-Cambrian of By Azov part of Ukrainian Shield. There are usually a lot of staurolite's varieties having sometimes disthen and sillimanite. There are from 5 to 35% of staurolite, from 0 to 20% of granate, from 8 to 15% of mical in shales Staurolite forms porphyroblasts in shale with length from 0.1 till 4 cm and also crystal growths. As a rule crystals of staurolite have many ingrowths of quartz, mica, tourmaline and sometimes feldspar.

In cuttings there are lenticular packets with thickness from 5 - 10 till 150 - 300 m along the strike for 2 - 4 km. Productive shales' thickness are metamorphised in conditions of epidote-amphibolite facies and as a rule are not migmatized at all.

Shales containing staurolite are well enriched and give concentrate with 90 - 92% of staurolite. There are 42 - 48% of Al_2O_3 and 32 - 36% of SiO_2 in it. Granite and mica concentrates are also obtained under enrichment. Possibility of getting quartz and feldspar concentrate is being studied. It will allow to carry out conversion of staurolite ores without wastage.

59.28/H

BIOAPATITE CRYSTAL ORIENTATION IN SKELETAL TISSUES

Pavlov D., Turner Orthopaedic Institute, Leningrad, USSR; Ivanov A., Institute of Earth Crust, Leningrad University, Leningrad, USSR

The definition of position of apatite crystals helps to search the process of bone formation. Never the less, there's no common opinion of the crystal orientation, size and formes. Conditions and speed of growth have an influence on the apatite crystal form. In this research the bioapatite crystals were studied by transmission electron microscopy (crystal form and sizes) and X–ray diffraction (crystal sizes and orientation). Results of study show that biocrystals have tabula form, often with hexagonal angles. The sizes of

that crystals are folowing: breadth of tabular – under 1000 Å, thickness about 100 Å. This crystals have normal longitudinal axis of collagen fibril. If fibril is parallel to long axis of bone, tabular crystals are normal to this axis. For example, similar orientation (pynacoidal texture) was found in cross section of compact tissue of tabular bone by X–ray diffraction. Such texture and collagen position was discovered in teeth dental tissue. Prismatic texture is present at basal layer of fossil agnathan aspidin plates, collagen fibrils is formed compact structure parallel to plate surface. Thus, tabular apatite crystals are normally disposed one after the other inside collagen fibril.

A STUDY ON SINTERING MINERAL COMPOSITIONS OF VANADIO-TITANO-MAGNETITE CONCENTRATE AND ITS EFFECT ON SINTER QUALITY

Yunfu Ren, Zhaoxi Chen, Lieying Jiang, Department of Geology, University of Science and Technology Beijing, Beijing 100083, people's Republic of China

This paper deals with the mineral composition and microstructrue of Panzhihua vanadio-titano-magnetite ore concentrate and its sinter and the effect of titanium element on their properties by means of optical microscope, SEM(scan electron microscope), X-ray diffraction, DTA (differential thermal analysis) and TG (thermal gravimetry) etc..

Minerals that separated from the solid solution of vanadio-titano-magnetite in iron ore concentrate are ilmenite and spinel. There are many kind of solid solution elements in the vanadio-titano-magnetite, in which TiO_2 content is 92.39% of total content, V_2O_5 content is 96.93 %. the rest are in titano-hematite, ilmenite etc. These elements make serious crystal lattice defect of mineral, thereby resulting in quickly oxidizing and releasing a large amount of heat in the sintering process.

In the sinter, TiO_2 is mainly present in perovskite which amounts to 37.71% of TiO_2 . the rest is present in vanadio-titano-magnetite and other minerals.

As basicity (CaO/SiO_2) of the sinter is at 1.75 and TiO_2 content in sinter is $>$ 15% , the sinter tumbler strength

decreases obviously, disintegration index increases and reducibility becomes lower.

In process mineralogy it is shown that perovskite increases evidently with the increase of TiO_2 content, consequently, the increase of preovskite is a reason in the mineral composition aspect to make the sinter quality poor. With increasing TiO_2 content the flowability of liquid phase in sinter decreases, thus microstructure of sinter become nonuniform. It is a reason in the microstructure aspect to make the sinter strength lower.

Perovskite crystallizes mostly in the melt when the temperature is over 1200 ℃. There is an inverse relation between perovskite and calcium ferrite in content. The compressive strength of perovskite and calcium ferrite are 8.5kg/mm² and 37kg/mm² respectively.

The best way to improve the quality of sinter of vanadio-titano-magnetite ore concentrate are as follows:

(1) To keep the content of TiO_2 less than 15%;

(2) To sinter at low temperature so as to prevent perovskite formation and increase the content of calcium ferrite.

THE CALCULATION OF MINERAL THEORETICAL STRENGTH

Shen Wenhua, Fang Tingting, Xu Jiami, Department of Nonmetallic Ore Engineering, Wuhan University of Technology, People's Republic of China

PREFACE

For in which minerals are used as raw material, the theoretical strength of a certain kind of mineral is an important parameter, for gem minerals theoretical strength is a major index to its polishing and quality assessing. This article will deals with two parts-calculation of mineral cleavage stress and calculation of tensile strength of mineral fiber.

THE CALCULATION OF MINERAL CLEAVAGE STRESS

The mineral cleavage stress is the maximum stress per unit area. When an ideal crystal plane of a mineral is split. Now let us take diamond for example and give a brief account of the calculation as fallows:

1. Determine the gross bond number of diamond per unit area

$\Sigma N_{[111]}$, when the crystal plane [111] of diamond$_\circ$ is split:
The unit cell parameter of diamond $a_\circ$ is 3.56A.

$$\Sigma N_{[111]} = \frac{n}{s_\circ}$$

Where $s_\circ$ is per unit area perpendicular to external force, it can also be converted by unit cell parameter; n is the gross bond number on an area which is subject to external force. When the crystal plane [111] of diamond is split, the gross bond number is:

$$\Sigma N_{[111]} = \frac{2}{2a_\circ^2 \times \frac{\sqrt{3}}{4} \times (10^{-8})^2} = 1.82\times10^{15}\text{bond/cm}^2$$

2. Firstly we calculate the simple bond energy (also called the dissociation energy) along C-C axis from bond strength of a chemical compound or a simple substance inside crystal and then we can get simple bond force (the dissociation$_\circ$energy along C-C bond is 90000cal/more; the bond destance is 1.54A).

$$Wc\text{-}c(\text{simple bond energy}) = \frac{90000\text{cal}\times4.186\times10^{7}\text{ergs}}{6\times10^{23}}$$

$$= 6.279\times10^{-12}\text{ergs/bond.}$$

$$Pc\text{-}c(\text{simple bond force}) = \frac{Wc\text{-}c}{r}$$

Where r is the bond distance (or covalence radius or ion radius)

$$Pc\text{-}c = \frac{6.279\times10^{-12}}{1.54\ 10^{-8}} = 4.10\times10^{-4}\text{dyhe/bond.}$$

3. Calculate the cleavage stress of the plane [111] of diamond:

$$\sigma_{max} = Pc\text{-}c\times\Sigma N_{[111]} = 4.10\times10^{-4}\times1.82\times10^{15} = 7614.3\text{kg/mm}^2$$

By the same method, We can get the strength of the plane [100] or the plane [110]: σ_{max} [100] = 6610kg/mm^2; σ_{max} [110]=9330kg/mm^2

Therefore for any crystal mineral materal, we can obtain its valence bond value and the simple bond force on its certain split plane, i.e. the corresponding theoretical cleavage stress.

THE CALCULATION OF MINERAL THEORETICAL TENSILE STRENGTH

The theoreticol tensile strength of a certain kind of mineral fiber is the maximum stress (breaking stress) per unit area, when the mineral fiber is subjected to pulling force along its axis and finally breaks. The calculation method is similar to that of mineral cleavage stress. The difference is that when we analyze the applied force bond along the external force, only "principal force bond" stress P (the direction of bond is parallel to force applied calculated because when non-principal force bone stress has not attained its maximum, it need broken.

Here, chrysotile is a example:

Along chrysotile fiber there are two principal force bond Mg-O bond inside octahedron and Si-O bond inside tetrahedron. The gross bond number per unit area is:

$\Sigma N_{Mg\text{-}O}=4.52\times10^{14}\text{bond/cm}^2$; $\Sigma N_{Si\text{-}O}=3.01\times10^{14}\text{bond/cm}^2$.

The simple bond force of Mg-O bond is: $P_{Mg-O}=1.27\times10^{-4}$dyhe/bond.
The simple bond force of Si-O bond is: $P_{Si-O}=4.63\ 10^{-4}$dyhe/bond.
The break stress of each principal force bond is:
σ_{max} Mg-O=5.74×10^{8}dyhe/mm^2; σ_{max} Si-O=13.94×10^{8}dyhe/mm^2
While the sum of the break stress is:
$\sigma_{max} = \sigma_{max}$Mg-O+$\sigma_{max}$ Si-O=2000kg/mm^2
We have calculated several ten kinds of mineral theoretical strength by the valence-bond force formula.

25.2.9P

THE INDUSTRIAL USE OF THE PURPLISH-RED LIPARITE-TUFFITE FROM THE MIDDLE JURASSIC JIULONGSHAN FORMATION OF YANGYUAN,HEBEI —— A NATURAL HIGH-QUALITY MATERIAL FOR GLAZED FLOOR AND WALL TILES

Shao Kezhong, Cao Guanqin, Wang Qizheng,Tian Yuxiang & Song Zichang, Department of Geology, Hebei College of Geology,Shijiazhuang,Hebei,050031,People's Republic of China

The Jiulongshan Formation of Yangyuan County,Hebei Province has a widespread distribution in the area of Mazhubu in the south of the county, consisting mainly of tuffaceous clastic rocks,and being about 280 meters thick.In this paper the authors have demonstrated that the purplish-red liparite-tuffites occurring in the formation are a natural high-quality material for glazed floor and wall tiles.

The purplish-red tuffite of this kind usually contain 60% volcanic debris and 40% normal sediments,generally being of tuffaceous texture, partly developing cross or horizontal bedding, and representing a river bed sediment in a dry climate region. The volcanic debris chiefly comprises volcanic glass,crystalloclastic quartz and feldspar, and s small amount of siliceous detritus.The volcanic glass has become an aggregate of microfilsitic feldspar and quartz or a comb or accordion aggregate of kaolinite due to devitrification.The normal sediments are composed principally of micro-

scaly illite, sericite and other clay minerals as well as quartz and feldspar silt grains. Clay minerals make up about 40% of the rocks by volume (including 27% kaolinite,10% illite and 4% other clay minerals); feldspar 16% and quartz 33% approximately. Moreover, there are a small amount of iron oxide,dolomite and calcite. Chemical analyses have shown that the tuffites contain respectively 61.56-61.64% SiO_2, 17.80-18.33% Al_2O_3, 4.65-5.72% Fe_2O_3, 0.41% TiO, 0.01-1.90% CaO,1.22-2.05% MgO, 2.70% K_2O, 0.31% Na_2O and 7.84-8.71% LOI.

The chemical composition and mineral constituent of the tuffites are quite similar to those of raw material used by some Chinese plants as base of floor and wall tiles. Repeated experiments have indicated that the tiles produced by using the rock of this kind have the following advantages:simple formulation,lower sintering temperature (1100°-1160° C),shorter sintering period (one hour),single firing,lower cost,high quality,etc.

The RISE Of THE INDUSTRIAL PETROLOGY AND OF THE APPLIED MINERALOGY IN CHINA.

37.2.22V

Su Liang-ho, China University of Geosciences, Beijing 100083, People's Republic of China.

In old China,the studies of mineralogy and petrology were restricted mainly as parts of field geologic and economic geologic reports. In new China, many silicate industries were established. The facts that the study of the corrosion of refractories is quite similar to contact metamorphism and the study of metallurgical slags is in genesis similar to igneous rocks, etc, made the petrologist and mineralogists realized the importance of the researches on the industrial petrology and the applied mineralogy. They started to use the theory and method of classical petrology and mineralogy for the benefit of industrial interests.

Many works had been done, such as the study of the metallurgical refractories and slags, and the studies of various ceramic materials,by means of applied mineralogical and industrial petrological techniques.

The iron ore from the Baotou district, Inner Mongolia, is very different from ordinary iron ores. It contains quite an amount of fluorite which is very harmful to the aluminous refractories in the blastfurnace. In 1950's before the establishment of the Baotou Iron and Steel Factory, petrologists suggested the use of carbon brick instead of aluminous ones, which obtained successful results. Latter the mineralogists and petrologists recognized the presence of rare–earth minerals in ths slags, and still latter they found niobium containing minerals existed in the convertor slags, they made all these valuable elements recovered. Now the Factory has become a factory producing polymetallic elements, instead of iron and steel only.

The iron ore from Panzhihua district, Sichuan Province is a vandium–titanium containing magnitite. It is known that such an ore is very hard to handle in the blastfurnace practice. Through the researches of the mineralogy of slags, this problem was solved with very good results.

In 1970's, the Capital Iron and Steel Company started to use oxygen blown convertor in steelmaking. At the beginning, the life of the convertor was very short .It was said that only a few more than 100 times of steel making that the refractories inside the convertor had to be replaced by new refractory bricks. This was uneconomical.The researches, by industrial petrologists with combined studies of the convertor slags and the corrosion of the refractories made the life of the convertor be increased to more than 1000 times at that time.

Other researches in relation to iron and steel works for example, the studies of the petrology of the corroded steel ladels etc. were all earnestly needed by the steel industries.

Our mineralogists and petrologists did researches on ceramics also. In the traditional way of making porcelines, kaoline has been the main source of raw material. Now–a–day, wollastonite, diopside and tremolite,etc. have been used which have the advantages of shortening of the fireing time and lowering of the fireing temperature in the kiln. Energy saving has been a very important topic in the ceramic industry. With this kept in mind, a number of minerals have been studied in making various useful articals.

Under the Committee of The Chinese Silicate Society, the Sub–committee of Technical Petrology had been organized since 1980. Since then, workers on the studies of applied mineralogy and industrial petrology have been increased up to several hundreds throughout the Country.No less than three sessions of The Hole Country Assembly of Technical Petrology had been held up to 1988.

59.2.10.H

THE MINERALOGICAL CHARISTICS AND UTILIZATIONS OF THE ZEOLITIC ROCKS OF UPPERJURASSIC AT DUSHIKOU, CHICHENG, HEBEI, P. R. CHINA

SUN Shanping, WANG Xianqong, LI Jiazhen, WEI Haiquan, WANG Xiqu, China

University of Geosciences, Beijing, 100083, People's Republic of China

There are 8 layers of zeolitic rocks formed by the alteration of rhyolitic tuff and perlite in the third member of Zhang Jia Kou Formation of upperjurassic of Dushikou, Chicheng, Hebei. These autogenic mineral aggregates consist primarily of clinoptilolite, secondly α–cristobalite, montmorillonite and a small amount of mordenite. The content of clinoptilolite is more than 70%. It is one of the best zeolite deposits in China both in quality and prospective reserves.

The Si / Al ratio of clinoptilolites ranges from 4.49 to 4.95. The contents of K are more than Na and (K+Na) more than (Ca+Mg). The contents of (K+Na) are inversely proportional to these of (Ca+Mg). The Ca(+Mg)–Na–K ternary diagram the compositional plots fall entirely in the field of clinoptilolite.

SEM analysis shows that clinoptilolite is microcrystalline in texture in glass fragments and fine–grain volcanic dusts, or regular to irregular tabular forms precipitated in cavities resulting from the decomposition of glass shards and perlite. Mordenite is rare and only found in f_1 layer. It occurs as filbers in the center of shards or adhering to the clinoptilolite. α–Cristobalite occurs as fibers or crypto–crystaline aggregates between montmorillonite and clinoptilolite. Some of the α–cristobalite is found in spherulites on clinoptiollite or filling in the pore space of glass shards. Montmorillonite forms flaky aggregates coating the edges of glass shards and forming the mantle of clinoptilolite. The sequece of formation of those autogenic minerals from volcanic glass is as follows: volcanic glass → montmorillonite→ clinoptilolite, α–cristobalite→ mordenite. These autogenic minerals are primarily formed from the acid volcanic glass through aqueous solution in the alkaline to subalkaline fresh water lake under low temperature and pressure.

We have measured the cation–exchange capacities (CEC) and contents of exchangeable cations of the clinoptilolitic rocks by means of NH3–exchange and found that the former is in a high value. Exchangeable cations are primarily Ca and then K, Na and Mg. The selective cation exchange decreases in the order of NH4 > K > Na > Ca > Mg.

Clinoptilolite could be transformed into K–, Na–and Ca–type by cation exchanges. It is found that the heat–stabilities and absorptions of clinoptilolitic rocks of various cation types are different. During heating treatment, the crystal structure of K–type and Na–type of clinoptilolite are stable up to 700℃, but Ca–type and natural clinoptilolite are destroyed at 500℃. The thermostable sequence is K–type > Na–type > natural sample > Ca–type. The order of absorption is Ca–type > Na–type > natural sample > K–type. Although Si / Al radio is a dominant factor on the thermostability and absorption of clinoptilollite, yet the cation type plays on important role.

The utilization of zeolite depends mainly on its chemical properties. Clinoptilolitic rocks at Dushikou are primarily used in cement production at present, however consider-

ing their high exchange capacities and selective properties to NH4, K, and Cs, Sr et. al., they can be used much more widely and with higher industrial value. The best utilization fields of clinoptilolitic rocks at Dushikou are forage additive of livestock, soil reclamation of farm crops and water pollution treatmant.

MAKE AN APPROACH TO SPECULAR GLOSS AND MEASUREMENT OF DECORATIVE STONES

Tang Suren, Dept. of Non-metallic Mineral Engineering,
Wuhan University of Technology, P. R. China

Specular gloss of a decorative stone is defined as the relativity reflectivity of the polished surface of the stone in the specular direction when incident beam is inclined on to the specimen surface. It is a very important index for evaluating industial value of decorative stones. Why do we use specular gloss to express the reflectivity of decorative stones while we do not use luster? It is because, based on theory of energy-band and electron orbital, these minerals consisting decorative stones also are transparent minerals with binding electrons mainly. They only absorb a few light wave while transmission capacity is very strong. Their reflectivity is weak and the reflective index is only about 5%. Their luster belongs to the category of glassy luster in outward appeance. It is very difficult to distiguish that which is strong or which is weak between two of their luster by peruse. However, it would be much better to express the property of luster of luster of decorative stones using relative value of reflectivity of polished surface of stone (during mono-incident beam) to distiguish strong or weak luster than using directly reflective index. According to the calculative principle of reflective index of mineral, the specular gloss of decorative stones can be calculated approximately as follow:

average specuiar gloss of mineral

$\bar{G}=1/2\ (G_o+G_e)$ (suit for monoaxial crystal mineral)

$\bar{G}=1/4\ (G_g+2G_m+G_p)$ (suit for diaxial crystal mineral)

where G_o, G_e; G_g, G_m, G_p (the principal specular gloss of monoaxial and dixial mineral respectively)

sum specular gloss of decorative stones

$$G=\frac{\bar{G}_1 S_1 + \bar{G}_2 S_2 + \cdots + \bar{G}_n S_n}{S_1 + S_2 + \cdots + S_n}$$

where $\bar{G}_1$, $\bar{G}_2 \cdots \bar{G}_n$ average specular gloss of various kind of mineral

S_1, $S_2 \cdots S_n$ content or occupied area of various kind of mineral on polished surface

The major minerals consisted marble such as calcite, dolomite are high double refractive index (former N=1.486, 1.658 latter N=1.500, 1.679) and they always present orientation arangement in the marble, through a large number of measurement and study. It has been approved that there are orientation for specular gloss of decorative stones (major refer to marble). Therefore author make a suggestion: the method measuring specular gloss of decorative stones using SS-75 photoelectric glossmeter, as follow: We measure alternatirely five points in perpendicular directions where they are in the center and four of corners of two diagonal line on the polishing surface of decorative stones (see fig.) and take arithmetic mean as specular gloss. The conspicuous advantage of this method is to pay attention to both orientation of mineral arrangement and to consider representative and rationlity of measuring position.

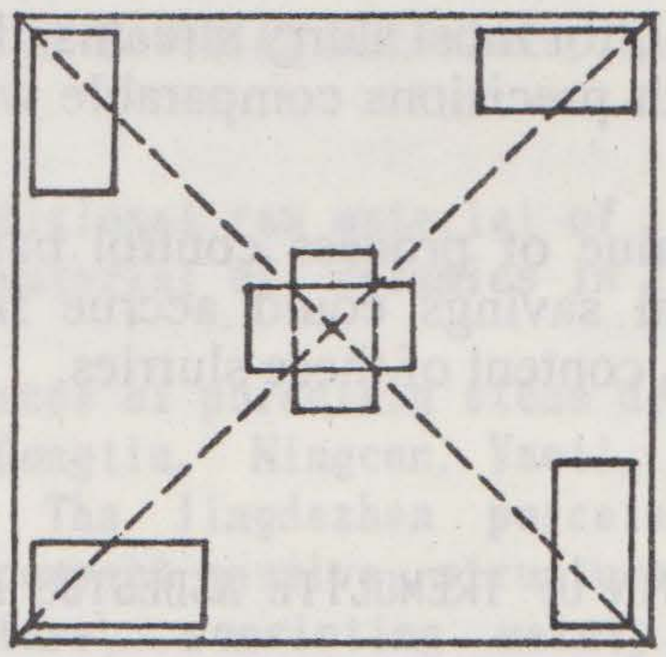

25.2.12.f

QUANTITATIVE ANALYSIS OF FLUORSPAR-CONTAINING SLURRIES: A COMPARISON OF TWO X-RAY DIFFRACTION GEOMETRIES

J.P.R. de VILLIERS, W. CLARK, and P.C. van den HEEVER
MINTEK, Private Bag X3015 RANDBURG, 2125 SOUTH AFRICA

The quantitative on-stream analysis of fluorspar-containing slurries of concentrate, feed, and tailings samples was evaluated using two different diffraction geometries.

The first instrument consisted of a scanning goniometer equipped with a diffracted-beam monochromator and a scintillation detector for sequential measurements. The second instrument was based on the Guinier geometry, and consisted of an incident-beam monochromator and two fixed scintillation detectors. Both instruments operated with a transmission geometry, irradiating a flat slurry sample.

A recirculating slurry-mixing and presentation system was used for both instruments. This consisted of two peristaltic pumps and a mixing vessel for

representative sampling of the slurry, and a windowless sample presenter which presented a flat curtain of slurry to the X-ray beam.

It was found that both instruments could measure CaF_2 concentrations in slurries of concentrate, feed, and tailings with sufficient precision for process control. The precision of the diffracted-beam and incident-beam monochromator instruments are compared with the analytical variations in the chemical analyses by two laboratories.

Instrument	Precision (% CaF_2)		
	Feed	Tailings	Concentrate
Scanning instrument	0.8	0.4	2.5
Guinier-geometry instrument	1.3	0.3	3.5
Chemical analysis	1.0	1.3	2.3

It is therefore evident that, for most slurry streams, the on-stream instrumental methods give results with precisions comparable with those of conventional wet-chemical methods

An evaluation of the value of process control based on these instruments indicated that substantial savings could accrue from the rapid on-stream measurement of the CaF_2 content of these slurries.

CHARACTEISTICS AND ORIGIN OF TREMOLITE ASBESTOS PARAGENETIC WITH NEPHRITE

Chunyun Wang(a), Rongqi Xu(a) and Guohao Ren(b) a, Guangzhou Branch, Institute of Geochemistry, Academia Sinica, Wushan, Guangzhou, GD 510640, P.R.C.; b, Department of Silicate Engineering, Wuhan University of Technology, Wuhan, HB 430070, P.R.C.

Tremolite asbestos from Wenchuan, Sichuan, paragenetic with Longxi nephrites, occurs within clastic belt of tremolite schists and dolomitic marbles. Certain amount of dolomites and trace talcs, chlorites and illites are usually mixed into it. Observations by polarising microscopy revealed that fibres are closely aligned to form bundles which insert intensely cataclastic dolomites and exhibit apparent straight extinction and weak undulous extinction. SEM studies also showed rounded vicinal faces, flattened (100) faces and stepped fracture faces of tremolite fibres.

Electron diffractions and micrographs of dispersions revealed that widespread existence of (010) multiple-chain faults and (100) twinnings in tremolites favours splitting of fibrils, sheet silicates take the form of tremolite fibre and possible talc-inserted layer exists among tremolite structure. In low-resolution electron images of ion-thinned cross-section, tremolite asbestos consisted of irregular and curved small crystallites that have their c-axis fairly well aligned but are rotated about this direction as indicated by (010) faults, thus displayed a cellular structure. Low-angle grain boundaries are structurally coherent, whereas high-angle grain boundaries between individual crystallites, also favouring fibre formation in tremolite asbestos, are typically incoherent and the structural mismatch is compensated partially by unfilled holes or possibly by sheet silicates fillings.

The cellular structure is likely to be achieved by multiple independent nucleation from a supersaturated hydrothermal system of CaO-MgO-SiO2-H2O-CO2 in an opening fracture of cataclastic dolomitic marbles, and subsequent ultrafast growth of nuclei oriented with the fastest growth direction(c) nearly normal to the fracture, the latter of which may favour part of the planar defects in tremolites. It can also provide excellent conduits through asbestos for hydrothermal fluids to result in additional abundant chain-width errors in tremolites and even cause them to alter partially to sheet silicates through retrograde hydration reactions.

CHINA'S JINGDEZHEN PORCELAIN STONE AND ITS DIOCTAHEDRAL SERICITE

Wang Ling, Sichuan Institute of Building Materials, Mianyan, Sichuan 621002, People's Republic of China

Porcelain stone is a traditional raw material of ceramics in China and also the most important raw material of ceramics in the famous porcelain capital, Jingdezhen.

There are abundant resources of porcelain stone deposits in Jingdezhen area, such as Liujiawan, Dongliu, Ningcun, Yaoli, Sanbaopeng, Nangang, Yikeng and Zhuangling, etc.. The Jingdezhen porcelain stone appears in white or greyish colour, compact massive structure, and lepidoblastic texture and quincunx texture*, consisting mainly of fine-grained qtz. (about 57%) and ser. (about 34%), with a smaller amount of fs., Cc., chl., pyrite, etc.. The contents of relict feldspar are in proportion to the strength of mineralizing alteration. The chemical component, K_2O+Na_2O is 4.241% in average and $K_2O>Na_2O$; while that of Fe_2O_3 is less than 1%, averagely 0.695%. White degree of the stone is higher. The mean contents of silica and alumina are 75.464% and 15.239% respectively. So Jingdezhen porcelain stone has technological property of porcelaining by itself.

Sericite is an important content in porcelain stone, and has technological properties of porcelaining both feldspar and clay. The sericite of Jingdezhen porcelain stone exhibits microlepido or lepidoblastic, and is isodimension or petaloid with pointness under SEM. The characteristic peaks of sericites are quite evident, sharp-pointed and symmetry in X-ray patterns, which suggests that sericites are characterized by high crystallinity and low hydration. The polytypes of sericite are mainly $2M_1$, fewer being 1M; 1M is more than $2M_1$ in exceptional deposit(Table 1). On the basis of study on the peak widths W_1-W_2 data of basal reflection 10A and 5A, Jingdezhen porcelain stone almost don't contain montmorillonite (interlayer) minerals. According to the result of chemical analysis of pure sericite specimen, there are a small amount of interlayer cations NH_4^+ in the sericite of Zhuangling and Ningcun porcelain stone. According to characters of values of d(060) and 530cm^{-1}

---

* Quincunx texture, It is a characteristic texture of Chinese procelain stone. In thin section, quartz grains show perforating or harbor-like

which appears as plum blossoms, less homogeneously distributed in microlite or lepidoblastic sericites.
band frequency, there are almost no Fe+Mg in the octahedron of sericite.

Table 1 X-ray and ID characteristic data for dioctahedral sericite of some Jingdezhen porcelain stone

No.	Specimen	Polytype	Peak Position(A)			Peak Widths(°)			d(060)	530
			d_1	d_2	d_3	W_1	W_2	W_3	A	cm^{-1}
1	QX02	$2M_1$	9.968	4.991	3.329	0.380	0.340	0.340	1.495	535
2	QD02	$2M_1+1M$	9.976	5.002	3.336	0.320	0.300	0.300	1.494	536
3	QD03	$2M_1+1M$	10.015	5.006	3.339	0.320	0.300	0.320	1.495	536
4	QD011	$2M_1+1M$	9.913	4.983	3.328	0.300	0.300	0.300	1.496	534
5	QD063	$2M_1+1M$	9.999	4.998	3.338	0.360	0.320	0.300	1.496	535
6	GF06	$2M_1+1M$	9.960	4.993	3.335	0.340	0.340	0.320	1.494	536
7	GF011	$2M_1+1M$	9.992	5.000	3.334	0.320	0.320	0.320	1.494	536
8	GL08	$1M+2M_1$	10.015	4.991	3.339	0.320	0.360	0.300	1.494	533
9	GL010	$1M+2M_1$	9.960	4.985	3.324	0.380	0.340	0.340	1.492	538
10	GN02	$1M+2M_1$	10.039	5.010	3.339	0.400	0.340	0.320	1.493	537

1. Yikeng porcelain stone. 2-5. Zhuangling porcelain stone.
6-7 Dongliu porcelain stone. 8-9. Liujiawan porcelain stone.
10. Ningcun porcelain stone.

From the above-mentioned, it is indicated that the quality of Jingedzhen porcelain stones are excellent, and naturally serves as a kind of the best raw materials of porcelain industry production.

REFERENCES

[1] Shirozu and Shoji Higashi, Clay Science, 4(1972), 137-142.
[2] Shoji Higashi, Memoirs of the Faculty of Science, Kochi University, series E, Geology, 1(1980), 1-39.
[3] Wang Ling, Ceramics Research, (2)(1986), 25-29.
[4] Wang Ling, Li Chaoyi and Song Gongbao, Effective Development and Utilization of Non-Metallic Minerals. Proceedings of the Second World Congress on Non-metallic Minerals, International Academic Publishers, I(1989), 219-222.

CHANGES OF MINERAL PHASES OF SINTER IN THE BLAST FURNACE.

Wang Shutong, Jiang Lieying, Department of Metallurgy, Beijing University of Science and Technology, Beijing 100083, China

The dissection investigation of an experimental blast furnace ($23m^3$) in Shoudu Iron and Steel Co. China, with self-fluxing sinter in furnace burden, was carried out in 1979-1981. This paper deals with the phase change of sinter minerals and the formation process of slag by

petrographic analysis.

Mineral constituents of the sinter before being charged into the furnace are shown as follows:

Mineral	Fe_2O_3	Fe_3O_4	FexO	$CaFe_2O_4$	glass	$CaFeSiO_4$
% (V)	13	54	2	13	8	5
Mineral	Ca_2SiO_4	$Ca_2FeSiAlO_7$				
% (V)	3	1-2				

Reduction of iron bearing minerals: Process of phase change from αFe_2O_3 through γFe_2O_3 to Fe_3O_4 was observed. In the crystals of newly formed Fe_3O_4 appear with many micropores. $CaFe_2O_4$ transforms to FexO and MFe earlier than Fe_3O_4. MFe can be directly formed from Fe_3O_4, but the great majority of MFe are formed step by step through FexO reduction.

Formation of blast furnace slag: In the stack and belly, a great deal of $CaFe_2O_4$ are reduced, CaO enters into the slag, then $CaFeSiO_4$ and Ca_2SiO_4 increase and the glass phase disappears gradually. The alkalis are enriched, at the surface of holes in the slag phase $KSiAlO_4$ appears. In the upper part of bosh, slag and iron are separated from each other. In the slag $Ca_3Mg(SiO_4)_2$, $CaSiO_3$, $MgAl_2O_4$, $CaMgSiO_4$, CaS appear, and Ca_2SiO_4 increases obviously. After deferrization $CaFeSiO_4$ gradually disappears. In the lower part of bosh, the amount of $MgAl_2O_4$ decreases, $CaSiO_3$, $Ca_3Mg(SiO_4)_2$ and Ca_2SiO_4 continuously transform to $Ca_2MgSi_2O_7$ - $Ca_2AlSiAlO_7$, a network structure of $Ca_2MgSi_2O_7$ - $Ca_2AlSiAlO_7$ with Ca_2SiO_4 is formed. In the hearth of the blast furnace, the coke ash enters into slag, which is mainly of $Ca_2AlsiAlO_7$ - $Ca_2MgSi_2O_7$, and the "final slag" is formed.

THE MODIFICATION AND BENEFICIATION OF TITANIUM-BEARING BLAST FURNACE SLAG

WANG Xiuwen, ZHANG Qiang, LI Zhenglong, Institute of Mining and Mineral's Engineering, Beijing University of Science and Technology, Beijing 100083, People's Republic of China

The blast furnace slag studied contains about 23—25% TiO_2 and 12% Fe. On account of higher titanium content it can not be used as raw materials for the production of building materials, e.g., as that of slag

cement production. The comprehensive utilization of the slag would be therefore of significance.

According to the mineral composition analysis titanium in the slag exists prodominately in the form of perovskite ($(Ca,Fe)O(Al,Si,Ti)O_2$) and titanaugite ($(Ca,Na)(Mn,Fe,Ti)(Si,Al)_2O_6$). Obviously it is very difficult to recover titanium and thereby to decrease titanium content of the slag to required level by conventional physical separating methods, although iron in the slag can be recovered by magnetic separation as desired. In our study the original slag was retreated in blast furnace to form two simple slag phases, the one is titanium-riched anosovite (Ti_3O_5), and the other is low-titanium non-crystal phase (known as glass). After crushing and grinding the two phases of materials were separated by conventional physical separating methods. This paper concerns mainly the measurement of the beneficiation properties and the separating study of the two materials—anosovite and glass. The test results were also discussed.

The measurement of specific gravity was made by pycnometer method. The values obtained are 3.118 for anosovite and 3.063 for glass. It is evident that to separate anosovite from glass is difficult by gravity separation. The measurement results of susceptibility show that both anosovite and glass are weakly magnetic materials. Yet the difference is so small that they can not be separated by magnetic separation.The dielectric constants measured are 9.26 for glass and >81 for anosovite. The difference between them is so large, in theory, that to separate them each other by dielectric separation is effective. The separating tests show that both flotation and electrostatic separation are the effective methods to separate the crystal phase anosovite from the non-crystal phase glass. By artificially mixing coarse anosovite with glass, the grade of which is 25% TiO_2, the concentrate grade by electrostatic separation can reach 71.20% TiO_2 with recovery of 60.74% TiO_2 and 94.11% of anosovite. By using hydroximic acid as collector and sodium silicate and sodium hexametaphosphate as depressant anosovite can be separated from glass in fine fraction by flotation. The flotation mechanism is due to selective adsorption of hydroximic acid on the surface of anosovite. The effect of depressants on separation of the two materials may also play an important role. Measurement and test results as mentioned above show that synthetic anosovite and glass differ largely from natural minerals with same or similar chemical composition in beneficiation properties, particularly in magnetic properties and flotation properties.

CHARACTERIZATION AND LEACHING BEHAVIOUR OF FERROCHROMIUM - A MINERALOGICAL STUDY

18.2.1

A. WEDEPOHL and P. ELLIS
MINTEK, Private Bag X3015 RANDBURG, 2125 SOUTH AFRICA

Differential leaching of the phases in ferrochromium, is relevant to a variety of industrial processes. A mineralogical study was therefore made of a range of high-carbon ferrochromium samples produced by the South African ferrochromium industry. According to specification, high-carbon ferrochromium must have a chromium content of more than 50%. The samples chosen for this investigation had carbon values of 6 to 7% and silicon values ranging from 1.13 to 8.26% by mass.

In general, it was found that the major phase present is the carbide $(Cr, Fe)_7C_3$. The second most abundant phase depends on the silicon content of the sample. In low- to medium-silicon samples (1.5 to 4% by mass), this phase is ferrite, i.e. a solid solution of α-iron and chromium, which can dissolve large amounts of silicon, up to approximately 14% by mass. In high-silicon samples (4.5 to 8% by mass), ferrite is replaced by the silicide $(Fe,Cr)Si_3$ containing stoichiometric silicon, i.e. 14.4%. In these samples, there is a further high-silicon phase containing approximately equal amounts of chromium and iron, together with 12% silicon. This phase is denoted as the σ-phase, the presence of which is the main cause of brittle fracture in specific steels, particularly those with high chromium contents. It is known in the steel industry that particular alloying elements, including silicon, enhance the formation of the σ-phase.

The most useful information was gained by the study of several specific particles in polished sections, both before leaching and after leaching for selected times, by means of scanning electron microscopy and analysis of the phases by energy-dispersive spectrometry (EDS). After the initial selection and analysis of particles, the polished sections were subjected to attack by sulphuric acid (20 g/*l*) at 90°C, for the required time. It should be noted that extra ferrochromium fines were always present in the leaching vessel to ensure reducing conditions.

It was found that leaching for 4 hours dissolved a large percentage of the carbide in all the samples. Where the major secondary phase was ferrite i.e. in the low- and average-silicon samples, the ferrite initially dissolved faster than the carbide and had a pockmarked appearance. However, after the first half hour the ferrite particles appeared to have become passivated and the rate of carbide dissolution overtook that of the ferrite. Where the major secondary phase was silicide, i.e. in the high-silicon samples, the silicide phase showed no sign of dissolution, and appeared to have a high resistance to acid attack. In these samples it was observed that the σ-phase was totally dissolved within half an hour in sulphuric acid. X-ray diffraction patterns of all bulk leaching residues, whether the starting material had been high- or low-silicon ferrochromium, showed the residue to consist of primarily $(Fe,Cr)_3Si$ with minor amounts of the carbide $(Cr,Fe)_7C_3$.

This, together with the observation of the leaching behaviour of individual phases in polished sections, led to the hypothesis that the leaching of ferrite is analogous to the dezincification (or de-alloying) process in brass. In this process, pitting corrosion of yellow brass (Cu 65%, Zn 35%) is caused by dissolution of the brass with subsequent recrystallization of pure copper on the corroded surface. Pure copper is relatively resistant to acid attack.

It is suggested here that, in the case of ferrochromium, the surface of a particle of ferrite containing large amounts of silicon in solid solution is rapidly dissolved by the sulphuric acid. All the elements except for a small percentage of the chromium, which stays in solution, are then redeposited on the surface of the source particle as silicide, which is resistant to acid attack. The removal of a small percentage of chromium would increase the silicon content of ferrite in these samples by about 0.5%, giving it a composition equivalent to $(Fe,Cr)_3Si$. EDS analyses of the surfaces of ferrite particles at different stages of leaching were consistent with this theory. This dissolution of the ferrite beneath the passive silicide layer can still take place, since the silicide has a porous nature.

Finally, it is concluded that the silicon content of charge chrome plays a major role in its leaching and corrosion behaviour.

31.2.18 √

STUDY OF MULLITE IN REFRACTORIES

WENG Runsheng, China University of Geosciences, Beijing 100083, People's Republic of China

This paper deals with mullite in refractories.

1. The fused Al_2O_3–ZrO_2–SiO_2 refractories usually contain approxmately 0–3% mullite. It is mainly distributed in the glass phase of AZS refractories. Mullite is colourless, but some refractories contain mullite with light colour. Probably a little Fe_2O_3+$TiO_{\frac{1}{2}}$ is dissolved in it. It is acicular in shape. The reasons are due to as follow:
   (1) The fused cast refractories have approximately 1.2–1.5% sodium oxide. It would promote mullite dissolution prohibition its formation in the silicate melt.
   (2) The products of fused-cast refractories are produced under high temperture and reduction. However this is not favourable for mullite formation.
   (3) According to phase diagram of Al_2O_3–ZrO_2–SiO_2 system after baddeleyite and corundum with included ZrO_2 have been crystallized. Mullite begins to crystallize at that time. The silicate melt has a high viscosity, which make mullite uncrystallized.
2. Andalusite hornfels, sillimanite concentrate powder and kyanite concentrate powder are respectively pressed into column which are sintered at 1300℃, 1600℃ for six hours. It is proved that mineraliser AlF_3 lowers the transformation temperature of sillimanite which grain of mullite is of special netted texture The sintered products show that both andalusite hornfels and kyanite concentrate powder can make mullite and cristobalite formation. However sillimanite concentrate powder form a little amount while heat-

ing at 1600℃.

Adding 10% AlF_3 in the concentrate powder heating at 1500℃ for 6 hours. The complete transformation is attained. It is proved that the mineralizer of AlF_3 decrease the transformation temperature of sillimanite and mullite form a special netted fexture.

ON THE PHYSICO-CHEMICAL CONDITIONS FOR THE FORMATION OF MINERAL ASSEMBLAGE IN THE SHELL FOSSILS

Wu Mingqing, Song Yunhua, and Ouyang Ziyuan, Institute of Geochemistry, Chinese Academy of Sciences, Guiyang, Guizhou, 550002, People's Republic of China

Based on the mineral compositions of shell fossils, it has been found that all the known biogenic minerals were calcium-minerals and two third of them were composed of calcium phosphate just prior to Cambrian period. With the evolution of biota the compositions of marine skeletons apparently had changed when the Phanerozoic sea was dominated by calcite-secreting inverbrates, Cenozoic and modern seas were characterised by organisms which secreted aragonate and Mg-calcite skeletons, and Mesozoic sea contained roughly equal number of each. The question is why the mineral compositions of shell fossils are so special and what factors controll the biominerazation of shells. This paper will discuss thermodynamically the problems.

1. Thermodynamic criteria of formation sequence of carbonate and phosphate minerals

Under the condition of modern seawater, i.e. assumed pH is 8, the total concentration of carbon is 1.2×10^{-3} M, and that of phosphorus is 2×10^{-6} M, the calculation indicates that, in this case, $a_{CO_3^{2-}} = 8.44 \times 10^{-6}$ M, and $a_{PO_4^{3-}} = 3.51 \times 10^{-9}$ M, respectively. According to the mass-action rule and the Ernst's equation $\Delta G^{\circ}_r = -RT \ln K$, the calculated results of $a_{Ca^{2+}}$ which make the $CaCO_3$ and $Ca_3(PO_4)_2$ precipitated are:

For carbonates $a_{Ca^{2+}} = 10^{-3.28}$ M (calcite),

$a_{Ca^{2+}} = 10^{-3.06}$ M (aragonite);

For phosphate $a_{Ca^{2+}} = 10^{-3.93}$ M.

The calculations above show that the precipitation of phosphate took place first followed by the calcite, the last was the aragonite mineral in seawater condition.

2. Activity—pH diagram of carbonate and phosphate minerals

Based on the fact that there were two types of mineral assemblage, i.e. carbonate (calcite or/and aragonite) and phosphate in shell fossils, these elements, that is C, P, and Ca, are taken into account. As H_2CO_3 and H_3PO_4 are polyprotonic acids, the imcomplete polyorder dissociations will take place in solutions. Thus, the $a_{CO_3^{2-}}$ and $a_{PO_4^{3-}}$ will be controlled by the pH of solutions. The lowest activities of Ca^{2+} under which $CaCO_3$ and $Ca_3(PO_4)_2$ precipitations take place can be calculated by means of the $a_{CO_3^{2-}}$ and $a_{PO_4^{3-}}$ present in solution at various pH. Using these calculated results, the $\log a_{Ca^{2+}}$—pH diagram can be constructed.

3. Paleoenviroment analysis for the formation of shell fossils

The $\log a_{Ca^{2+}}$–pH diagram shows that the precipitation of the phosphate minerals take place at pH ≥ 2.2, but it does not mean that the phosphate shells can form at the early stage of paleo-ocean evolution under which the pH values were very low in paleo-seawater. It has been revealed from some geological information that before Proterozoic the phosphate deposition took place in local area on small scale. At Sinian the whole earth deposition of phosphates began on large acale followed by the formation of the phosphate shells. It was not before long that the carbonate shells formed widely, we can inferred that the pH of seawater could be close to 6 at the end of Proterozoic. With the increase of pH in sea water reached 6.45 at Cambrian, carbonate shell, particularly calcite shell with lower solubility, were widely devoloped. In Mesozoic the formation of aragonite and calcite shells was the result of pH values increase of seawater. From Cenozoic to present the pH values of sea water increased gradually up to about 8.1 today. During this period the aragonite shells were dominate.

37.2.27 P

STUDIES ON QUENCHING CRACK OF QUARTZ CRYSTAL

Yang Jun, Research Institute of Quartz Glass, China Building Materials Academy, East Suburb, Guanzhuang, Beijing 100024, China

The size reduction flowchart of the raw materials of quartz crystals for making quartz glass is as follows: quenching — crushing — grinding. Because of the volume effect and anisotropic expansion of quartz during its phase transition water quenching results in cracks. The crack pattern controls the shape of quartz particles. While quartz powders mainly being of rod- or needle- like particles have more influence on mobi-

lity and melting, those predominantly being of equi-granular particles benefit mobility and melting. This paper deals with quenching cracks of quartz crystal at different temperature. It is found that the higher the quenching temperature, the greater the length/width ratio of crack unit and the more the rod- or needle- like particles. The crack direction is mainly parallel to $(1\bar{1}01)$ or $(11\bar{2}1)$. Moreover, the higher the temperature, the greater the crack density. The change in crack density at the phase transitional temperature is the greatest. The experiment results are listed in table 1.

Table 1. The results of quartz crystal quenching experiments

quenching temperature (°C)	heating time (h)	appearance	size of crack (mm·mm)	equi-mesh of crack unit	density of crack (cells/cm^2)	length/wid. ratio of crack unit
200	0.5	transparent	8 x 8	2	1.56	1.00
300	0.5	less transparent	3 x 4	4	8.33	1.33
400	0.5	light opal color	2 x 3	6	16.67	1.50
500	0.5	opal color	1 x 2	10	50.00	2.00
600	0.5	opal color	0.3 x 0.5	35	666.67	5.00
700	0.5	opal color	0.26 x 0.31	52	1240.69	10.53
800	0.5	opal color	0.25 x 0.30	54	1333.33	11.64
900	0.5	opal color	0.15 x 0.18	90	3703.70	21.21

ON THE FIBROUS SUDOITE IN DEBAO, GUANGXI

59.2.11. H

Yang Yaxiu,Di Sumei,and Zhang Wei,Geological Institute,State Bureau of Building Materials Industry,Beijing,100010, People's republic of China

Sudoite, a very rare fibrous di-trioctahedral Al-Mg chlorite, has been found recently in coal-series strata of the Heshen group of Upper Permian Period (P_2h) in Debao County, Guangxi, China. This is a white, fibrous mineral, generally in the form of long and thin bars when observed under SEM. Its optical properties have been determined as follows: Ng'=1.572; Np'=1.569; mostly parallel extinction; (+) elongation; (-) 2v<10°. Electron probe analyses show its structure formula to be $(Mg_{1.73}Al_{3.13}Fe_{0.02}Cr_{0.01})_{4.89}[(Si_{3.10}Al_{0.90})_4O_{10}](OH)_8$. It is indicated that the total number of its octahedral cations, mainly containing Al and

secondly Mg, is slightly under 5. The XRD data of the sudoite (table 1) indicate that d(001)=14.17±0.01Å; d(060)=1.5098±0.0009Å; with the 003 reflection being the strongeat but with the 001 the strongest after heating at 500°C for two hours. The corrected cell parameters are: a= 5.226±0.002, b=9.061±0.003, c=14.285±0.005Å; β=97°11'±2'; V=671.±0.4Å^3; monocline system. The DTA curve of sudoite appears between that of Mg-chlorite and of Al-chlorite, showing two endothermic peaks, one(the larger) at 660°C and the other (the smaller) at 840°C, with a sharp exothermic peak at 940°C. The IR absorption band shows respectively 3650(W) 3615(S) 3520(S) 3350(M) 1070(W) 1000(S,B) 940(W) 832(W) 700(S) 557(W) 532(S) 470-459(S) 408(S) 410(W)cm^{-1}.

Closely associated with sudoite is a small amount of paragonite, which usually appears in a flaky interspersed form amidst the sudoite fibres. The country rock of sudoite is a black carbonaceous clay with flaky texture, composed mainly of rare rectorite containing a layer of water and paragonite, as well as a small amounts of sericite, kaolinite, pyrite, etc. Sudoite fibres are usually to be found along cracks, situated inside or between rock beds, or around pyrite cumular spharolith. It can be therefore, concluded that sudoite was formed by alteration and filling-up of solutions (or hydrothermal solutions) during swelling-up this area after diagensis.

Table 1 The XRD data of sudoite from Debao

hkl	d(Å)	I	hkl	d(Å)	I	hkl	d(Å)	I
001	14.16	50	201	2.497	35	205	1.8032	6
002	7.08	75	20$\bar{3}$	2.404	14	008	1.7731	1
003	4.720	100	006,202	2.364	6B	31$\bar{1}$,20$\bar{7}$	1.7115	2B
110,020	4.488	28	040	2.264	1	20$\bar{8}$	1.5559	10B
004	3.539	72	20$\bar{4}$,133	2.226	4	060	1.5099	15
005	2.833	25	007	2.026	11	062	1.4771	4
200,20$\bar{1}$	2.607	2	204	1.9778	17			
20$\bar{2}$	2.541	11	126,20$\bar{6}$	1.8704	5			

CHARACTERISTICS OF MINERALOGY OF LEIZHUANG QUARTZ STANDSTONE AND ITS EFFECT ON CRUSHING AND Fe_2O_3 ELIMINATION

37.2.28.V

Yao Shudian, Su Fenwei, Beijing Graduate School of Wuhan University of Technology, Guanzhuang, Beijing 100024, China

Leizhuang Quartz Sandstone mine, in eastern of Hebei province is one of the largest Mines to produces Silicious Material required in plate glass industry in China at present. It is the major problem in processing for many years that Fe_2O_3 content of Quartz sandstone is so difficult to be removed that it can not meet the requirments of float process glass manufacture. This article studied in detail the characteristics of ore mineralogy. It has been proved by test that Leizhuang Quartz Sandstone belongs to regrowth type granular texture. The rock consists of framents and cement, the ratio of the two parts is 14:1. The major component of the fragment is quartz, and its content is more than 99%, the rest are feldspar and heavy mineral. Most of the quartz particles are 0.15-0.25 mm in size, Part of them are 0.25-0.45 mm. The size of the feldspar particles is similar to that of the quartz particles. Most of the feldspar particles are slimed, and are mainly

Particles Size Distrubtion & Fe_2O_3 Content of the Products by Different Crushing Methods (Table 1)

Size range mm	Rod mill, Yeild %	Fe_2O_3 %	Crushing rolls Yield %	Fe_2O_3 %
+0.5	1.71	0.110	8.66	0.03
-0.5+0.315	19.70	0.087	14.20	0.05
-0.315+0.2	28.14	0.094	20.34	0.06
-0.2+0.1	36.28	0.110	31.32	0.05
-0.1+0.076	3.72	0.195	4.33	0.12
-0.076	10.45	0.510	21.25	0.24
Total	100.00	0.146	100.00	0.094

Chemical Composition of the Quartz Ore and Test Results (Table 2)

Component	SiO_2	Al_2O_3	Fe_2O_3	CaO	MgO	K_2O	Na_2O	TiO_2	Igloss
Raw Ore %	98.54	0.47	0.087	0.039	0.090	0.20	0.025	0.032	0.23
Laboratory Test %	98.98	0.24	0.054	0.060	0.042	0.22	0.027		0.24
Pilot Test (2.7 T/h) %	99.01	0.45	0.040	0.160	0.020	0.16	0.020	0.02	0.31

distributed among the quartz particles. The heavy mineral are mainly tourmaline, the grainy zircon is also rarely seen.

The cement are mainly silicious, most of it has secondary-grown onto the quartz fragments. Its optical properties remain the same as that of quartz particles, but it is clearly visible at the adges of the quartz particles. Some of it is in the voids between fragments.

It has been found by further study that most of the Fe_2O_3 content in raw ore exists in fine particle size fraction of less than 0.1 mm in size, and most of it consists of the iron generated in the comminution process and membranous iron (iron oxide). There are different effects on distribution of Fe_2O_3 content in each particle size fraction when using different crushing methods (Table 1).

According to above and the laboratory research results, the following results have been obtained from the pilot test that productive capacity is 2.7 T/h:Fe_2O_3 content reduces from 0.24% to 0.040%, the yield of quartz concentrate is 77.3% (Table 2).

40.2.34.11

RELATION OF CATHODOLUMINESCENCE PROPERTIES OF CARBONATE MINERALS TO THEIR ELEMENTAL COMPOSITIONS

Ying Fengxiang and Wang Yanqi, Central Laboratory, Research Institute of Petroleum Exploration and Development, Beijing, 100083, PRC.
Xu Long, Department of Geology, Jianghan Petroleum Institute, Shashi, Hubei, 434102, PRC.

In recent years cathodoluminescence properties of the minerals have become one of the important contents in the study of diagenesis. They are beneficial to examining the minerals and inferring the impure elements within them. Moreover, they may be also used for determining the cementation order of different generation cements, restoring primary structures and textures of the rocks, judging how the minerals originate and where they come from, observing the features and distinguishing secondary porosity, etc.

It is very important to study cathodoluminescence (CL) of various kinds of carbonate minerals which exist in the cements of clastic rocks. In recent years by observation of CL it is found that CL characteristics of carbonate minerals is fairly complicated.

Sometimes CL of the same minerals, such as calcite whose CL may be different, yellow or orange, yet CL of different minerals may be alike. For example, CL of both calcite and ferroan dolomite are yellow. Therefore, in order to distinguish exactly the carbonate minerals and understand why it is different in CL, it is necessary to know their elemental composition by CL in combination with other techniques.

Some representative carbonate minerals have been selected. A total of 46 points are analyzed by electron probe to measure respectively Ca, Mg, Mn and Fe in the minerals. 184 data are obtained, and Ca/Mg, Fe/Mn or Mn/Fe and Fe/Fe+Mg ratio are calculated respectively.

While electron probe performed, X-ray diffraction, atomic absorption spectrophotometer, EDS and CL microscopy analyses are also analyzed. The results indicate that the content of the elements mentioned above is different in various kinds of carbonate minerals. On the basis of the difference it is indicated that calcite, ferroan Calcitte, dolomite, ferroan dolomite and ankerite may be distinguished and that the control factors of CL intensities of various kinds of carbonate minerals may be found.

STUDY ON THE APPLIED MINERALOGY OF QUARTZ SANDSTONE AND ITS APPLICATION

25-2-13p

Zhang Jingwu, Institute of Multipurpose Utilization of Mineral Resources, Ministry of Geology and Mineral Resources, Emei, Sichuan, 614200, People's Republic of China

Quartz sandstone is the main source of siliceous raw materials, but in most cases it needs treatment before being used. Longchang quartz sandstone mine is a huge deposit of siliceous raw material with chemical composition: SiO_2 97.28%, Al_2O_3 1.06%, Fe_2O_3 0.3% and TiO_2 0.24%. Only after treatment for reducing the contents of impurities of Fe and Ti ($Fe_2O_3<0.1\%$, $TiO_2<0.1\%$) can it be used as raw material for making high-quality plate glass. The main mineral phases in the quartz sandstone include quartz, kaolinite, ferrohydrite, hematite, magnetite, rutile, tourmaline and zircon, etc. Here quartz is a valuable mineral, while iron and titanium minerals are harmful and must be eliminated. Therefore further investigation should be required.

The grain size of minerals mentioned above is in the range of 0.7-0.001 mm,and it is further divided into seven grades.The grain size distribution and content of each mineral species in every grade have been studied in detail. The properties of mineral and ore, such as specific gravity, specific susceptibility, volume specific gravity,bulk specific gravity, coefficient of volumetric expansion, compression strength in different directions and refractoriness have also been determined.As the psephicity of the quartz particle is not perfect,it's not suitable to use as the foundry sand of precision castings.There are subtle gas or liquid and mineral inclusions in quartz, and aluminium is enriched obviously on the edge of the quartz particle. By agitating and scrubbing, the ore can be powdered easily, because the weathering of hematite and ferrohydrite has loosened the ore texture. The sand is in fine and medium grained arenaceous texture, basement and contact type cementation, compact block structure, brittle and low strenth. Because the cementation between mineral particls is not strong, it's easy to be crushed. Furthermore, the mineral grains can be liberated quite easily even under action of a weak external force. Hence the sand is easy to be treated.

Occurrence manner and distribution of Fe and Ti in the original mineral

Occurrence manner of Fe and Ti		Fe_2O_3 distribution (%)	TiO_2 distribution (%)
1. Fe and Ti within the quartz grains		20.5	31.0
2. Fe and Ti minerals	iron mineral	23.5	
	rutile		31.4
3. Fe and Ti in clay		26.0	37.2
4. Fe and Ti contaminated on the quartz surface		30.0	0.4

The equilibrium coefficients of metal amounts of Fe and Ti in four kinds of occurrence manner in the original mineral are 97.3% and 94.2% respectively.

According to descriptions as mentioned above and industrial requirements, the treatment procedure for the sand should be: impact crushing (-3 mm) → strong agitation and scrubbing → classification (o.1 mm).Adopting this procedure,the production cost can be quite low, and good results are obtained. At the same time, it prevents the original granularity of quartz particles from being over crushed,it is beneficial to industrial production and getting high recovery. On the other hand, it cuts down the contents of iron and titanium to the maximum extent, and Fe and Ti in 2nd , 3rd and 4th occurrence manners as mentioned above can be eliminated easily.

On the applied mineralogy and the occurrence manners of iron and titanium, the theoretical contents of iron and titanium in quartz sand concentrate are calculated as Fe_2O_3 0.051%, TiO_2 0.085%. They are very close to the chemical analysis results of the ore dressing products: Fe_2O_3 0.055%, TiO_2 0.09%. It is proved in practice that the ore dressing flowsheet and the production indexes are quite satisfactory, thus making the once large inactive mine (because of high Fe and Ti contents) into a exploitable mine.

It is indicated that research results about applied mineralogy

and occurrence manner of elements can be used as the important basis for deposit evaluation and ore treatment process as well.

TECHNOLOGICAL MINERALOGY OF SYNTHETIC BLUE-BLACK FUSED ALUMINS

Zhang Naixian, Guo Jingxiong, Liang Chunlin, Institute of Geology Academia Sinica, People's Republic of China.

Blue-Black Fused Alumina is electrically fused, using bauxite as a main raw material, and crystallized at high temperature. This is a polyphase abrasive material made up of α-corundum, as a predominant crystal phase, and hercynite, secondary crystal phase, and is a new product of great hardness, high toughness, affinity to water and high refractoriness.

Based on the appearance, structure and mineral constitute, the welded block of BBFA devided obviously into four zones: centrical zone, top zone transitional zone and marginal zone. The petrological features of these zones are influenced by composition of the raw materials and technological condition. The main petrological feature as follows: (1), holocrystalline granular texture, porous and compact-structure; (2), the main mineral compositions consist of predominant α-corundum and hercynite, and secondary ilmenite, iosiderite, mullite and hyalite; (3), the α-corundum is mainly euhedral crystal, its shape is rhombohedron, tabular and granular. The corundum crystal of the centrical zone is the biggest and the most complete. From center to margin, the crystals become gradually smaller and smaller. (4), hercynite is a sort of important accessory mineral. 1t grows vertically on the face of α-corundum. They appear as euhedral, skeleton crystals, and being a cement phase; (5), Ilmenite and iosiderite appear as cement phase to fill in the pores of α-corundum aggregates.

The colour of α-corundum in BBFA is blue-black. It indicates that colouring anions hsve entered into crystal lattice of α-corundum. According to ESR spectroscope measurements, Fe^{3+} and Ti^{3+} entered into ctystal lattice, and Ti^{3+} in lattce is nonhomogeneous.

Ctystsl structure of α-corundum in centrical zone is complete by electro microscope, but the α-corundum ctystsl in transitional zone and marginal zone have shown defect including the row of dislocation and layer dislocation and so on, which resulted in colour of α-corundum crystal. crystal cell a , value is positive relation with TiO_2% contents. This indicated that Ti and Fe anion entered into corundum lattice. They replaced Al by part or filled in octahedral space or formed oxides and appeared as solid solution to fill in lattice. It resulted the crystal lattice occurs micro-twisting. The hardness of corundum is in negative

relation with TiO_2 contents. The hercynite crystal devided into two stages in grows. First, it is automorphic crystal of excellent octahedral shape, second, it appears as crossed or branched crystals to fill in porous of corundum aggregates. The unit cell $a_0 = 8.172$ Å, The chemical structural formula is: $Fe^{2+}_{1.00}(Ca_{0.04}Mg_{0.58}Fe^{2+}_{0.15}Ti_{0.01}S_{0.03}Al_{1.19})_2O_4$.

Based on Mossbauer measurements, Fe locates at tetrahedral site. and the value of Q and S are different. The hercynite possesses structute of positive spinel type. Meantime, due to secondaty nearer action, it appears as four-polar double peak. It indicated, there are two sorts of Fe-O tetrahedron (A_1-, A_2-) which is tiny different in crystal structure. (111) plane net of hercynite and (001) plane net of corundum are close conjunct, because the spacing of (001) plane net between two oxygen atoms for corundum equal to 5,14Å and the spacing of (111) plane net between two oxygen atoms for hercynite equal to 5,77 Å. Both values are very similar. Thetefire, they are easily connected.

The success of the research of the BBFA have started a new way of synthesis of polyphase abrasive material and a new way of comprehensive using bauxite resources. A great deal of secondary degree bauxite can be used in China.

25.2.11.P

THE APPLIED MINERALOGICAL STUDY OF FIBROUS SEPIOLITE IN EAST QINLING, CHINA

Zhang Shaohua, Zhang Wei, Wang Lutian
Geological Institute, National Bureau of Building Material Industry, Beijing, 100010, China

The fibrous sepiolite deposits in the East Qingling district are now the only fibrous sepiolite ones that can be mined economically in China. For the industrial uses, we have, for the first time, systematically studied the applied mineralogical features.

1. Chemical composition and crystal chemical formula. The purity of fibrous sepiolite mineral for chemical analysis should be more than 99%, and be checked by infrared spectral technique. The preparation of sepiolite sample is chiefly made by manual method. The purified fibrous sepiolite mineral is composed of silica, magnesia and water, for example, The chemical composition of the purified fibrous sepiolite mineral(Bw-6) in Sangping, Xixia is SiO_2 (55.61%), MgO(24.68), H_2O(17.72%), Al_2O_3(0.061%), Fe_2O_3(0.59%), FeO(0.22), K_2O(0.20%), Na_2O(0.05%), CaO(0.55%), SO_3(0.06%), MnO(0.013%). Its crystal chemical formula is, $(Si_{11.88}Al_{0.02}Fe''_{0.1})_{12.00}(Mg_{7.38}Fe''_{0.07}Fe^{3+}_{0.06}Mn_{0.03})_{7.53}O_{22}Ca_{0.11}K_{0.03}Na_{0.02}$
The result shows that the fibrous sepiolite in the East Qinling district is of the Mg-rich type.

2. X-ray diffraction analysis has been made. The X-ray diffraction patterns

of fibrous sepiolite show that d(110)=12.227A diffraction line is most characteristic, and this kind of sepiolite mineral is well-crystallized, polyhydrosepiolite. Being heated at 200,300,.....1000℃ for 1 hour, the samples were analysed by X-ray diffraction of unit cell parameter show that the size of unit cell decreases with the increase of temperature.

3. Infrared absorption spectral analysis shows that the stong band in the range of 3700-3000cm^{-1} was due to the OH in octahedron led to the fomation of the absorption peaks at 3694and3679cm^{-1};the vibration of the coordination water produced the absorption peaks at 3625 and 3535cm^{-1}; the existence of zeolitic water/absorbed water caused the absorption peaks at 3569,3380 and 3240cm^{-1}; the absorption band in the field of 1700-1600cm^{-1} reflected the OH bending vibration in the coordination water;the absorption band in the 1300-900cm^{-1}region was due to Si-O stretching-contraction vibration;and the Si-O bending vibration resulted in the absorption band in the field of 600-400cm^{-1}. After being heated,at 200,300,.....1000℃ for 1 hour the specimen showed a series of changes in spectrum such as amalgamation and disappearing,which are the reflection of the existence and activity of water of varions states.

4. Differential thermal analysis(DTA) has been carried out. In the DTA spectrum,the strong endothermic valley in the range of 130-140℃ was caused by the removal of waters(i.e.absorbed water and zeolitic water) from the sepiolite region;and the weak endothermic valley(398-401 C,588℃) was due to the removal of crystal water;the endothermic valley at770-841℃ represented the de-hydroxyl process of sepiolite;and exothermic peak at 795-855 ℃ was produced by the phase change of sepiolite.On the TG curves,the total weight loss is 17.5-20%.The weight loss sharply increased at 25-200℃,representing the removal of zeolitic water/absorbed water(9-9.7%);rapidly increased at 200-400℃,showing the removal of 1/2 crystal water(3%);relatively increased at 400-780℃,representing the loss of another1/2 crystal water(3.3-3.6%);and again sharply increased at 770-841℃,suggesting the removal of hydroxyl water(about 2%).

5. The electron-microscope study shows that the rhombohedral lattice in sepiolite is well developed,crystallized order is very good.There was no impurity and any defect in lattice and crystal stock with palygorskite mineral and trace transformed sepiolite into other mineral structures.

6.Study of changes in sepiolite crystal structure at the different grainding times have been made.

7. After treated with different concentrations of Hcl,NaOH,study of changes in sepiolite crystal structure have been made.

8. Study on practicability of fibrous sepiolite for cigarette filtering medium have been carried out.

9. A series of experiments on the specific resistivity, electrodynamic potential, tensile strength, specific surface area, magnetism, acid resistance, alkali resistance, heat resistance, heat conductivity, filtering,

cation exchangeability, specific gravity and decolouriztion of fibrous sepiolite have been made and obtained a large quantity of firsthand data.

APPROACH TO THE RELATIONSHIP BETWEEN THE CHANGE OF VALENT STATE OF IRON ON THE SURFACE OF MARMATITE AND WETTABILITY

59.2.12 H

Zhang Weishai, Institute of Mining, Beijing University of Science and Technology, Beijing 100083, People's Republic of China

Sphalerite is a kind of zinc mineral which often found in multimetallic deposit containing Pb and Zn, and whose distribution is very extensive in earth. Because Zn^{2+} and Fe^{2+} both belong to four coordination and are very similar, thus Fe^{2} in sphalerite is more easy to replace Zn^{2+} than other elements. So sphalerite usually contains Fe, even over 20%.

It is shown that floatation of marmatite is worse than the common sphalerite. Floatation of sphalerite is deteriorates with the increase of iron content. Therefore it is very important to study the property of floatation of sphalerite and the influence factors. Many factors affect floatation of mineral, but influence the nature of surface is the main.

I. Distribution of element in sphalerite

By analysing distribution of elements in mineral, we can determine whether it is of single or multiple minerals. Aalytical results of element concentration and the scanning map show that distribution of Zn and S is uniform, but that of Fe is not very uniform. This illustrates that marmatite is complete single mineral.

II. The X ray photoelectron spectrum (XPS) study on marmatite

Mixed samples of sphalerite with different iron contents magnetite were studied by XPS at the same condition. Conclusion as follows:

1. Because of the existence of Fe^{2+} and Fe^{3+} in the samples mixing show that magnetite with hematite, the XPS analytical results of element Fe in samples conclusion are, either the bound energy or the chemical shift is the same as in marmatite. Results show the existence of high valent iron on the surface of marmatite.

2. The XPS of marmatite show that the marmatite not only contatins Fe, Zn and S, but also oxygen. From this , we consider the ferric oxide exists on the surface of marmatite.

III. Heating experiment on marmatite

In order to verify, once more, the existence of high valent iron in oxide on the surface of marmatite, we carriedoute two kinds of experiments, one is the method of single floatation which only selects sphalerite and oxide it is shown that the effect of mixing is better than the single.

Obviously the surface of rich Fe-sphalerite presents the property of oxide, the higher the concentration, the more the property exhibits.

Conclusion:

Onaccounts of conversion Fe^{2+} to Fe^{3+} on the surface of marmtite, wettability of surface are clearly differed, thereby resulting is diffeculty of marmtite selection. Applying the method of mixing floatation, it would be much better.

APPROACH TO THE RELATIONSHIP BETWEEN CONDUCTIVITY AND WETTABILITY OF MINERAL

25.2.14 P

Zhang Weishai, Institute of Mining, Beijing University of science and Technology, Beijing 100083, People's Republic of China

Usually crystal of mineral grows more or less in combination with impure elements and exhibits defects in different degree, which effect its various properties, such as specific gravity, magnetism, solubility, hardness, wettability of surface, conductivity and so on. There are organic inter relations between them.

When liquid attaches as on the surface of solid, it might be in various forms, such as ball, flat and semisphere. Whichever form it takes, their surface tensions are in equilibrium, as showsn in the following:

$$\sigma sA = \sigma SL + \sigma ALCOS\,\theta$$

Where S=Solid; L=Liquid; A=Air; θ=contact angle

Contact angle shows the degree of wettability of liquid on the surface of solid. According to the equation $COS\,\theta = (\sigma SA - \sigma SL)\,\sigma LA$, we can measure the contact angle with a special apparatus. If the contact angle is large, the mineral is known as hydrophobic mineral. Most part of the particle exposes outside of liquid, only a small part left inside. When properly slected, the ratio of floatation would be large. If the contact angle is small, it is known as hydrophilic. When properly selected the ratio of floatalion would be small. Thereore we can use floatation method to test the contact angle. Experiments were performed with Hallimond tube.

By the theory of semiconductor, semiconductor conducting by cavity is called P-type, and that by electron is N-type. In fact, there are simultaneously cavities and electrons in a block of semiconductor. If the number of cavity is larger than the number of electron, it is a P-type, otherwise, N-type. Experiments show that there is not only P-type or N-type semiconductor in a mineral, but also N-type and P-type semiconductor coexist in a mineral. For different kinds or the same kind of mineral, conductivity may be different. To study these problems is significant not only in geology and ore deposit but also in the research of wettability and floatation of mineral. In akaline medium, floataion of electron con-

ductive N-type mineral is good, but in acidic medium, that of P-type mineral is good.

On mediun the conception of PH is based on dissociation of water : $H_2O \rightleftharpoons H + OH$

but $(H^+) \cdot (OH^-) = K(H_2O)$

That means the product of (H^+) and (OH^-) is a constant. In the solution with acidic reaction there are more (H^+) than (OH^-), but with alkaline, less (H^+) than (OH^-). In alkaline solution. N-type minerals form two same kind of solid-liquid semiconductor.

Owing to formation of the same kind of charge or the surface of particle which rejects each other, wettability is worse, but floatation is better. In the acidic medium, minerals form opposite type solid-liquid phase semiconductor, in which the opposite charge attracted each other occupies the leading place, so that hydrophilicity is good, but floatation is bad. As the same reason, in acidic medium, floatation of P-type movement is good, but in alkaline medium, floatation is bad.

Usually electrons and cavities move randomly, speed of which even up to 1.2×10^7 cm/sec. Owing to random movement they cancel out each other, and the solution forms a kind of energy field. Hence the electrons and cavities move requlary to the surface of mineral. According to the statistical results of experiment, resistivity and contact angle can be divided into 4 regions: 1). Low resistivity with high contact angle, mainly including the sulfide mineral. 2). High resistivity with high contact angle, mainly the natural sulphur, talc and some minerals whose surface are with special property; 3). high resistivity with small contact angle, including the inorganic mineral with equal ionic bond such as fluorite and calcite; 4). High resistivity with very small contact angle. The mentioned above illustrates that, except minerals with special surface property and with ionic bond in chief, for high resistivity mineral, usually the contact angle is small and wettability is good also, but hydrophobility is bad; for low resistivity mineral, the contact angle is large, wettability is bad and hydrophobilily is good, wettability on the surface of mineral and conductivity depend on the crystalline structure and impure elements and etc. Thus much attention should be paid to research and analysis, surfoce wettability and conductivity of mineral so as to promote the development of floatation art.

18.2.2P

MINERALOGICAL INVESTIGATION IN TECHNOGICAL PROCESSING OF LIGHT ROASTING--MAGNETIC SEPERATION-COMPREHENSIVE UTILIZATION FOR MEISAN'S FINE TAILINGS

Zhang Weishai; Zhao Wanzhi; Wu Guoyu. Institute of Mining, Beingjing University of Science and Technology, Beiingjing 100083, P.R.C

Meisan's tailings divide usually into two sorts: dry and wet, particle size of dry tailings is 0.5-75mm, which used in making building material. The particle size of the wet is 0-0.5mm, which exhausted into the tailing dam by clumper.

By means of the new art of light roasting-magnetic seperation--comprehensive treatment, iron ore in Meisan's fine tailings can be recovered, thereby effectively reducing iron grade in tailings. The tailings then be made into a lot of building materials Hence Meisan's fine tailings can be converted into valuable resource. The reason is that we designed a valid technologecal flowsheet according to the feature of ore processed. In order to sufficiently recover and utilize the tailings, the process mineralogical research should be paid attention.

A. THE FEATURE OF MINERAL COMPOSITION OF MEISAN'S FINE TAILINGS

1. Ferric carbonate is the main mineral.

Concentration of TFe is 23.4%, which indicates lean iron ore. Concentration of carbonate is up to 40%, among them that of siderite is up to 50%, which indicates that high iron is due to the existence of magnetite and siderite.

2. Ignition loss is large, concentration of kaolinite is high

Ignition loss of Meisan's fine tailings is up to 13%. Concentration of clay such as kaolinite is up to 13%.

B. PROPERTY OF THE PROCESSED MINERAL IN THE ROASTING PROCEDURE

Meisan's fine tailings contain a lot of siderite, magnetite and kaolinite. When heating to 600° or so, kaolinite becomes uncrystallized promullite. The reaction is as follows:

$$Al_2O_3 \cdot 2SiO_2 \cdot 2H_2O \xrightarrow{530^{\circ}C} Al_2O_3 \cdot 2SiO_2 + 2H_2O$$

As the uncrystallized promullite has activity, the tailings after ligh--roasting has a good coagulability. But heating at low temperature siderite decomposed and then becomes magnetite as follows:

$$FeCO_3 \xrightarrow{350-400^{\circ}C} FeO + CO_2 \uparrow$$

$$6FeO + O_2 \rightarrow 2Fe_3O_4$$

Therefore quality of tailing improved and the quantity reduced.

1. Roasting temperature and activity

There are a lot of clay such as kaolinite in the tailings, which has good activity, while roasting the from 600℃ to 700℃.

2. Variation of weightless rate with the roasting temperature.

The weightless rate is an important property of tailings, which influences the quantity of tailings. The weightless rate of Meisan's fine tailings increases with the increase of roasting temperature. When the temperature is about 900℃, the weightless rate sharply increases, because a lot of carbonate decomposed after 900℃.

3. Rcasting temperature and conversion ratio of siderite

The conversion ratio of siderite can be determined from the analytical result of magnetism VS roasting temperature. When the roasting temperature is 600℃, it indicates the concentration of Fe_3O_4 is maximum. It is highest that the ratio of siderite changed into Fe_3O_4 .

4. Roasting time and the coversion ratio of siderite

Magnetism and concentration of iron VZ roasting time at 700℃ when the roasting time is 30 minutes, the concentration of iron in tailings is the highest. Magnetism attains the maximum strength, the conversion ratio

of siderite is the highest also.

5. Roasting time and activity

Compression strength of samples at the same formation condition increaces with the increaces of time.

6. Change of tailings with the roasting temperature

In order to explain the change of minerals in different roasting with the roasting temperatures, we did the thermal analysis, X-ray diffraction of tailings in different roasting temperatures and X-ray diffraction of clay (particle size less than 0,05mm.) Results reveal that, 1) the loss of weight of tailings are higher at 400-578℃and 650-800℃, 2) The spectra of magnetite still exhibits at 960℃, which indicates that it remains unchanged. But at 600℃, the main peak 2.798 of siderite disappeared and the main peak 2.77 of calcite became weaker. It also shows that calcite had partially decomposed and siderite almost decomposed at 600℃ during roasting. 3) At 700℃ the peaks of kaolinite disappeared which reveals that kaolinite all have converted to uncrystallized promullite.

Finally we draw the following conclutino:

Meisan's fine tailings belongs to the type of ferric-carbonate-clay. Roasting at 600-700℃ and keeping 30 minutes, siderite have almost converted to magnetite the property of tailings have got a big change, the activety is the best, as known, "light-roasting activation". Results reveal that the light-roasting tailings give a possibilities of comprehensive recovery of iron resources a favorable condition for comprehensive utilization.

THE APPLICATION OF MINERAL IN SOME FIELDS OF ECONOMY AND TECHNOLOGY

Zhang Yen, Tianjin Geological Academy of M.M.I., Tianjin 300061, China.

1.Mineral geochemistry and metallurgical technique

In the treatment of metal ores mineral composition and chemical behavior of elements have direct influence on metallurgical technique and the products (including wastes). On the basis of traditional method employed in the metallurgy of bauxite ore, the technique of adding lime is worldwidely used to increase leaching out aluminium. To make further improvement of the treatment, the method leaching out AL from bauxite ore in alkaline solution under high temperature and high pressure was carried out in China, but it was unsuccessful due to blockage in the preheater's tubing by Ti、Si sinters which resulted from Ti、Si、Ca、Mg、Al、Na in the ore minerals under certain physico-chemical conditions. The aim of this paper is to solve the problem. First, the occurrence of Ti was found as rutile, anatase, ilmenite and sphene, and that of Si as kaolinite, hydrokaolinite、quartz、sericite and chlorite. Further more, three new mineral phases derived from them in the different stages of wet metallurgy were identified as $Na_2O \cdot Al_2O_3 \cdot 1.7SiO_2 \cdot nH_2O$、$Na_2O \cdot 3TiO_2 \cdot 2.5H_2O$ and (Ca、Mg) $O.TiO_2.nH_2O$. Then the physico-Chemical process of dissolution, migration and precipitation of the minerals and

elements during treatment was simulated by high T.P.experiment used in mineral geochemical test. As a result proposal was made to put several high-pressure tanks in different T.P.ranges for preventing preheat tube's block, and a new technological process in which no addition of lime are attained was put forward. This technology can thoroughly overcome the problem generating a large quantity of Ti sinter by the refractory new mineral phase from Ca. Ti in Ore. At the same time leached out AL-O can reach the industrial standard.

2.Mineral physics and remote sensing technology.

The mineral physics, especially, the study of electro-magnetic wave of minerals is beneficial for the further application of remote sensing technique in the earth science, geological prospecting and other fields. Some characters of the visible-infrared reflected spectrum of minerals can be used to enhance the satellite images and raise their detectivity. At certain temperature range, the thermal emission property of petromineral is related to their chemical composition and structure. Under certain condition, dielectric constant of mineral and rock in the microwave frequency is corresponding to the data of brightness temperature measured by microwave radiometer. The thermal parameter of mineris now is used to charting thermal inertia. In general, physical character of mineral and rock and their electro-magnetic spectral data are a valuable part of fundamental parameter for every stage of remote sensing, such as technical method, ground spectral measure in the field, space detecting and treatment of remote sensing information in the laboratory.

3.Synthesis of minerals and technological material.

Utilization of chemical composition of mineral has a long history, but study and application of their physical properties such as infrared, semiconduction, microwave, illumination, piezoelectricity, dieclectric etc.remains inadequate. Use of some natural minerals as new types of heat-proof and microwave dielectrical materials has developed in China for recent years. Acheivements have made in synthesis and artificial growing of some mineral materials with physical property of superhardness, piezoelectricity and infrared. Based on characteristic of types I_a. I_b. II_a. II_b of natural diamond and occurrence of nitrogen in it (" small flake" nitrogen and dispersed paramagnetic nitrogen) an ameliorative technology was put forward (including filtering N into synthetic materials, adding Co powder, improving pressure material, synthetic pressure, temperature, time and proportion of composition) , and the quality , output and graininess of the synthesized diamond were increased. Therefore, study of conditions under which natural minerals are formed, their composition, structures and mineral syntheses is significant to development of some technological materials.

4.Mineral and Chinese medicine.

A remarkable progress in the study and application of minerals in Chinese medicine has made in recent years. Confusion of some mineral medicines is found yet. For example, the Chinese traditional medicine of Hanshuishi some one designate it as gypsum, while the others take it as calcite; and Zishiying is dominated by fluorite in Chinese medicinal shops.

According to the character described in the book of "Chinese Materia Medica" well-known over world, the author agree with that Hanshuishi should be warthite; Zishiying, amethyst. In accordance with the NMR spectrogram, the gypsum in spectral line width ($\triangle H = 11.8G$) and area is smaller than the warthite ($\triangle H = 13.4G$). To increase the value of mineral medicine, biochemical and physical effect of minerals and microelements contained on human body are yet left to be explored and revealed.

60.2.13.H APPLICATION OF MINERALS FOR DENTAL PORCELAIN

Zhao Liangchao, Wen Xianglin and Hu Ya-an, Jilin institute of geological sciences. 30, Kuan Ping road, Changchun, China.
Huang Kegui, Changchun hospital of air force. 1 Nan Hu road, Changchun, China.

The dental porcelain is a repair materials for dental prosthetics. It is essentially a glassy ceramics of the $SiO_2-Al_2O_3-R_2O$ system in which the leucite presents as crystalline phase. In general, It consists of opaquers, body porcelains and incisal porcelains. Three porcelain powders are in turn welded on the casting metal crown of the Ni-Cr-Mo alloy. This low melting porcelain is developed recently at abroad. A native dental porcelains have not been offered now at the market at home. We have accomplished the investigation and production of dental porcelains, and provide 32 opaquers and 32 body porcelains according to the difference of tooth color.

Because the leucites have higher thermal expansion and its suitable optical property, it is selected as a raw material of dental porcelains. Sufficient natural leucites, however, are not found in nature in China. The artifical leucites have been synthesized in the laboratory, based on "FAK method" designed by ourselves. The resultant leucites occur as a sphere crystals about 0.01 mm in diameter under microscope.

A special glass containing a great many of potassium has been made from feldspars and fluxes. The internal stress in the glass has been eliminated due to subject to annealing in water. This glass is one of most important component of dental porcelain, and is ground into fine powder of 5-100μm particles. It is a key that this component assures the dental porcelain to produce superior modelling properties and solid dimensional stability both during and after firing. The technology flow of the smelting glass are completed.

An abundant knowledge in mineralogy is combined with more than thousand stain tests to study successfully the pigments: the artifical pigments are substituted by the natural. It is the first time in the world that the

natural minerals as colorant were used in dental porcelain,and it is of a important contribution for the dental materials.Six group of colors of natural minerals are selected,and they further are divided into 32 colors according to a grade of color.

The glass powders are admixed with the leucite,emulsifier and colorant as their proportion.Thus the resultant admixtures become the dental porcelain product. The determination of a physial function shown that the linear cofficient of thermal expansion,hardness,impact strength and fritting temperature of dental porcelin meet the demand of the design.

The further discussion is as follows:

1. The feldspars as raw materials both artifical leucite and glass are about 80% total composition of dental porcelain.The experiment of clinical treatment shown that low tempurature ordering max.Microclase,and no exsolution phase and small Fe,Ti elements in it, is most suitable as raw materials for their preparation. The selected K-rich feldspars are of very importance for keeping built shape of tooth reform to prevent plastic flow during high temperature.

2. A fritting temperature of dental porcelain is mostly dependent upon the composition of glass and the content of leucite.The experiment shown that the fritting temperature vs the content of leucites have indicated a excellent liner relationahip.The content of leucites in dental porcelain has obviously influence on the transparency of porcelain tooth.

3, It is very difficulty that the color,transparency and strength of porcelain tooth are equal with neighboring tooth,but it is not impossible.Owing to our successfully prepared the leucite,glass and colorant,especially mineral colorant.The difficult task was fulfilled.Many minerals with color may be used as colorant. It is,however, absolute prerequistite that natural minerals possess the structure of spinel type,of sphene type and of garnet type,and do not have discoloration during high temperature.

COMPREHENCIVE UTILIZATION OF TITANIUM SLAG THE RECOVERY OF Fe & Ti AND THE UTILIZATION OF THE REMAINS

37.2.24. V

Zhao Wanzhi; Cao Zhenyuan; Wang Xiuwen Univ. of Sci. & Tech. of Beijing, Beijing 100083, P.R.C

Iron Plant of the Panzhihua Iron and Steel Company, China, Produces about 3 million metric tons of titanium slag each year. There are two

characteristics of the slag. One is the high output, the proportion of slag to iron is 0.8--0.9, 1 to 2 times higher than that of other blast furnaces in China. The other is the high content of TiO_2, 16-25%. How can we handle the slag? This is the main diffculty that troubles the company. This is due to the fact that as steel production is developing increasingly, the output of the slag increases with the yield of iron. Now, the volume of slag dump located near the Jinsha River is supersaturated. To open a new slag field is a formidable and expensive construction since Panzhihua is of unfavorable geographical condition. Hence, development of Fe & Ti recovery, and its comprehensive utilization is a very urgent task in aiming at the prolongation of the existing dump service, this paper is to select the corresponding dressing process for recovery of Fe & Ti and make use of remained slag as raw materials for production of a series of building materials. On the basis of chemical and mineral composition and their characteristics.

1. Iron exists both in the form of element and compound in the slag. The solid solution of titano-iron spinel and small iron balls are worthy to recovery. Iron balls, which are always covered with nitride titanium and carbide titanium on the surface, are ill distributed, and differ in size. Such a process of "Grinding-classification-magnetic separation" can effectively separate iron and other composition (βTFe 80%, εTFe 77%, γ 18%).

2. There is a relationship between the contents of TiO_2 and FeO. The content of titanium increases with iron, when TFe is below 10%. But it drops rapidly as iron surpasses 10%. The basicity of slag has influence on the contents of titanium. The high the basicity increases, the more titanium and perofskite exist in slag and vice versa. Anolite only exists in low basic slag. Raising the basicity, perofskites are formed from the reaction between anolite and CaO.

After the magnetic separation, the tailings are re-grinded to -400 mesh. About 80% of perofskite is cloven with other minerals in this case and can be separated by floatation process. It is simple in construction and suitable for industrial purpose. (β TiO_2 30%, ε TiO_2 78%).

3. The remains of the floatation process, most of which are silicate minerals of titanium, are very fine and inactive in chemical property. Adding some binder and admixture, they can be pressed into colour tiles, floor tiles etc.

This can not only convert waste into utility, but also make use of a lot of tailings, thereby resulting in renovating environmental contamination.

INVESTIGATION ON PHASE CHANGING PROCESS OF DIRECT REDUCTION FOR OXIDIZING PELLECT OF TITANOMAGNETITE

Zhou Yixin and Zhang Keren, the Institute of Multipurpose Utilization of Mineral Resources of Ministry of Geology and Mineral Resources, Emei, Sichuan , 614200, People's Republic of China

The phase of iron-titanium oxides in oxidizing pellets of titanomagnetite (concentrate) from Pan-Xi district, Sichuan, China, is almost single titanohematite, and is only a small amount of pseudobrookite (Fe_2TiO_5). Titnaohematite is a complex solid solution, with main components of Fe_2O_3 and TiO_2, and with chemical formules in ideal form: $x(Fe,Mg)TiO_3 \cdot (1-x)Fe_2O_3$, here $x=0.3\pm$.

The reduction of oxidizing pellets is mainly the reduction of the titanohematite. In reduction processes, again formated two phases of magnesium-bearing ulvospinel [$(Fe, Mg)_2 TiO_4$] and magnesium-bearing ilmenite [$(Fe,Mg)TiO_3$], which are similar to original ore in composition and difficultly farther reduced.

Table phase changing process of direct reduction for oxidizing pellet of titanomagnetite

Sequenles	Chemical Reduction	explaination
1	$5[x(Fe,Mg)TiO_3 \cdot (1-x)Fe_2O_3]+2CO \rightarrow 3[y(Fe,Mg)_2TiO_4 \cdot (1-y)Fe_3O_4] + 2yTiO_2 + 2yCO_2$	hematite molecules in titanohematite(ss) is firsty reduced to magnetite molecules, then convered to titanomagnetite(SS) (600℃± - 800℃±)
2	$[y(Fe,Mg)_2TiO_4 \cdot (1-y)Fe_3O_4]+pCO \rightarrow p(Fe,Mg)_2TiO_4+3pFeO+pCO_2$	magnetite molecules in titanomagnetite(SS) is reduced to wustites(FeO), then convered to magnesium-bearing ulvospinel. (1050℃-1100℃+)
3	$pFeO+qCO \rightarrow qFe+qCO_2$; $(p-q)Fe_2TiO_5 \rightarrow (p-q)Fe_5TiO_8$	most of wustites(FeO) is reduced into α-Fe, and small part combined with pseudobrookite (Fe_2TiO_5), then convered to titanomagnetite(SS)
4	$(mFe,nMg)_2TiO_4+qCO \rightarrow [(m-q)Fe,nMg]_2TiO_4+1/2qTiO_2+qFe+qCO_2$	a part of FeO in magnesium-bearing ulvospinel is reduced into α-Fe, when Mgo content increases, then gradully converted to reic-Mg ulvospinel.
5	$[(m-q)Fe,nMg]_2TiO_4+qTiO_2+q'CO \rightarrow (1+q)[(m-q-q')Fe,nMg]TiO_3+q'Fe+q'CO_2$	FeO in rech-Mg ulvospinel is continously reduced, when $(m-q-q')+n=1+q$ and with excess of TiO_2, then converted to magnesium-bearing ilmenite.
6	$[(m-q-q')Fe,nMg]TiO_3+q''CO \rightarrow 1/2[(m-q-q'-q'')Fe,nMg]Ti_2O_5+q''Fe+q''CO_2$	FeO in magnesium-bearing ilmenite is continously reduced with $(m-q-q'-q'')+n=0.5$, then converted to ferro-bearing karrookite (~ 1200℃±)

Consequently it appears very complex law of step by step reduction as compared with common iron ores.

Using microssopical method to compare the observing results of pellets with different metallic rates which are produced by direct reduction with (solid or gas) reduction agents, the phase changing process are found out (see table). It's characteristics are as follow:

1. Without independent hematite (Fe_2O_3) and magnetite (Fe_3O_4) in pellets, as a result lack of "free" FeO in it, so the difficulties of pellets reduction increase step by step in the whole process, the final residues will be ferro-bearing Karrooite or ferro-bearing magnesoanosovite [$(Fe,Mg)Ti_2O_5$] which can not be directly reduced.

2. The results of chemical analyses and calculations indicate that at the end of chemical reaction (3), metallic rate of pellets possibly reaches to 64%±, in reaction (5) may reach to 83%± and in reaction (6) probably to maximum 92%±.

3. The reaction (1-5) has progressed in background of original grains, metallic iron grains with the size of 1μm±, when the reaction (6) begins grains boundaries gradully dissappear, metallic iron grains will incrense to 1-3μm+, then up to 10μm+, and may appear as irregular crystal stock of various forms.

ORE MINERALOGY

PROPERTIES AND TEXTURES OF ORE MINERALS IN BACCU LOCCI (SE SARDINIA, ITALY) MINERAL DEPOSIT AND THEIR GENETIC RELEVANCE. 3.10P

F.Bakos, G.Carcangiu, A.Mazzella, E.Pani, R.G.Valera - Istituto di Giacimenti Minerari, Piazza d´Armi, 09123 Cagliari, Italy.

The Baccu Locci mineral deposit is the result of a complex genetic evolution, proved by the coexistence of stratabound concentrations and discordant veins.

1) The concordant orebodies contain arsenopyrite, pyrite, pyrrhotite, chalcopyrite, sfalerite, galena, bedded in roughly alternating layers, lenses and nodules, according to the general texture of the metasedimentary host rock. Arsenopyrite occurs either as hydioblasts in the host rock, or as euhedral crystals in groups or masses. Pyrite is also abundant, pyrrhotite less frequent with pentlandite exsolution flames. Chalcopyrite and sfalerite belong to a late stage of the crystallization and show mutual exsolutions: sfalerite starlets in chalcopyrite, chalcopyrite droplets in sfalerite, dispersed // to crystallographic directions. Galena is last, anhedral among other sulfides, often intergrown with fibrous silicates. All the characters, namely: mineral association, exsolutions, intergrowth sulfide - silicates, microbrecciation of the former sulfides, bedded texture, point to the evolution of an original deposit (protore) through the influence of the Hercynian regional metamorphism, responsible of a low grade greenschists facies in the area. The layered sulfide mineralization was deformed, mobilized and recrystallized during different tectonometamorphic events.

2) The discordant veins and lenses, locally associated with lamprophyres of the late Hercynian magmatism, are characterized by a low temperature, last phase Au-Ag and sulphosalts mineralization, concluding a former stage of higher temperature. The mineral association is therefore given by two main groups, whose deposition was separated by intermineralizing movements. The first group includes quartz I, pyrite

I, pyrrhotite with abundant intermediate products, sfalerite I, chalcopyrite I, galena I. The second group is represented by quartz II, chalcopyrite II-III, sfalerite II, galena II, antimonite, electrum, meneghinite, bournonite, freibergite, boulangerite, stylotipite, accompanied by calcite garlands. These minerals fill, as late inclusions, all the open spaces and fractures of the former minerals. Au-Ag are mainly bound to chalcopyrite - freibergite; Sb suddenly appears, playing an important rôle in the formation of large variety of sulphosalts. Typical textures describe the evolution of the last mineralizing process. The early sfalerite shows chalcopyrite unmixing segregations dispersed along the grain boundaries, as "imtergranular films" (Ramdohr, 1980). Tiny and rare sfalerite stars in chalcopyrite II may be referred to as inclusions due to a rapid process of crystallization (Marignac, 1989). High speed of crystallization, together with a sudden drop of temperature and the appearance of Sb, Au and Ag is testified by the sulphosalts, whose random association and spatial relations probably depend on very variable local equilibria. Also the widely observed myrmekitic intergrowths, particularly bournonite-galena, are to be considered as the result of decomposition of early compounds and solid solutions. Electrum (Ag up to 50%) is chiefly associated with chalcopyrite III, but its deposition is continuous until the end of the mineralizing process, occurring also together with the sulfosalts.

This study was performed with grants of the Italian Council of Researches, through the Centro Studi Geominerari e Mineralurgici - Università di Cagliari.

REFERENCES

Marignac, Ch.: Sphalerite stars in chalcopyrite: Are they always the result of an unmixing process? Mineral.Deposita 24,176-182(1989)

Ramdohr, P.: The ore minerals and their intergrowths. Pergamon Press, 2nd ed., 2voll. (1980)

Zucchetti, S.C.: The lead-arsenic-sulfide ore deposit of Bacu Locci (Sardinia, Italy). Econ.Geol. 53, 867-876 (1958)

10.3.1P

MOMI, A COMPUTER-SUPPORTED SYSTEM FOR MICROSCOPIC IDENTIFICATION OF ORE MINERALS BY MEANS OF QUALITATIVE AND QUANTITATIVE PROPERTIES

H.-J. Bernhardt, Institut für Mineralogie
Ruhr-Universität, 4630 Bochum, FRG

MOMI (Microscopic Ore Mineral Identification System), a computer-supported system for ore mineral identification, which combines the use of quantitative data and qualitative properties in determination, is presented for discussion.

In a data base, spectral reflectance curves, color values and Vickers hardness numbers are stored for the various minerals as well as all qualitative properties of interest for identification which can be observed with the reflecting polarizing microscope. In addition some general data (e.g. information on crystal system or chemical composition) are stored. A set of classification terms for all properties (e.g. colors) was developed. Intensities (e.g. for anisotropy, color etc.), relations (mineral A compared to mineral B) or frequencies are classified in a 7 step scale. If a mineral can show a property in various ways, this information can also be stored. All data are converted to a numerical code from which it is possible to generate a complete mineral description in plain text, thus largely avoiding the use of descriptive tables or textbooks.

The user may choose the determination criteria and their order. For example it is possible to work completely without quantitative data or to rely solely upon them.

The identification is made in two steps: starting with all stored minerals, those are excluded which have an incompatible match with the observed properties of the unknown mineral. Incompatible means the measured values do not fall within the allowed data ranges (including errors), or the observations are inconsistend with the stored classes of frequencies (always or never present) or intensities (not present or extremely strong). For the remaining minerals, the similarities between measured and stored reflectance curves can be determined. In addition, the matches of observed qualitative properties with the stored data are judged in a manner, which simulate the line of reasoning of a trained microscopist. For each property, a value is computed that depends on the differences in class numbers and an individual weighting factor. The result is a list of possible minerals, combined with the mean values of the match computations.

While the "quantitative part" of the system has largely been tested, the "qualtitative part" is still beeing developed in order to optimize the judgement

structures and algorisms. The system is programmed in HP-BASIC, it runs on a Hewlett-Packard 9816 computer.

3.B

NATIVE GOLD IN GOLD DEPOSITS OF CHINA

Cai Changjin, Gold Geological Research Institute,Langfang, Hebei, China.

Native gold is the most major economic gold mineral in gold deposits of China. Native goldfields in some gold deposits of China have been studied recently by present author and the research results are discussed briefly as follows.

Chemical composition: Au. Many analytic results show that native gold is rarely pure, generally contains some Ag. The Au–Ag series, as judged by composition,is completely continuous. According to the content of Au and Ag,this series may be divided into four subspecies: native gold (Au 100–>80% , Ag 0–<20%), electrum (Au 80–>50%,Ag 20–<50%). Kustelite (Au 50–20% , Ag 50–80%), native silver (Au<20–0%, Ag>80–100%). The analytic data also shows the presence of the following elements: platinum family elements, Cu, Hg, Bi, Sb, Cr, Fe, etc. These elements generally are less than 0.0n%. But in some gold deposits some elements may have higher contents.

X–ray powder pattern and unit cell parameter: the strongest lines of powder pattern are 2.3547–2.3500(10)(111), 2.0394–2.0359(4–5)(200), 1.4423–1.4407(3–5)(220), 1.2300–1.2289(3–4)(311). The unit cell parameter(a_0) is 4.0789–4.0781Å. With an increase of Ag content in Au–Ag series, $a_0$values decrease(gold–electrum) at first, and then increase (electrum–silver).

Morphology: the crystals with good crystal form are uncommon, but are observed nearly in all gold deposits investigated. According to the observations done with scanning electron microscope, the crystals of simple form such as cube, octahedron, terahedron etc. are rare and mostly are combinations consisting of two or more simple forms. The complete idiomorphic crystals are uncommon, mostly are hypidiomorphic crystals with partly developed and distorted crystal faces. The growth striation, setched holes and overgrowth crystals etc. are observed on the crystal faces. The twin crystals, twilings, trillings etc. are observed, but the most common morphology is various polycrystalline aggregates. There is a great variation in grain size of gold.

Main physical properties : both the colour and streak of pure native gold is deep golden yellow, the measured value of density is 18.9g / cm^3(contains Au99.55 wet.% , Ag 0.45 wet · %). VHN = 39.5–103.3 kg / mm^2, averaging 70.6 kg / mm^2.With an increase of Ag content, the colour and streak change gradually from deep to light yellow, the density decreases linearly with increase of Ag%, the VHN firstly increases (gold–electrum) and then decreases (electrum–silver).

Optical property: in reflected light, isotropic. The reflecting colour of pure native

gold is deep golden yellow and varies to light yellow with an increase of Ag content. The reflectivity and the colour index of the native gold of various compositions in 405–700nm of several wavelengthes have been measured and calculated. The reflectivities(%) and colour index of pure native gold(Au 100%) are respectively: 34.43(405), 35.40(436), 38.0(480), 65.33 (426), 75.00(546), 83.85(589), 86.80(644), 89.20(656), 86.32(700nm); Rvis = 74.26%, x = 0.4038, y = 0.3978, $\lambda\alpha$ = 579nm, Pe = 0.3991.

Inclusion study: native gold often contains various kinds of solid mineral inclusions and gas–phase inclusions as H_2O, CO_2 etc. The commonly observed mineral inclusions are such sulfides as pyrite, such tellurides as altaite and the nonmetallic minerals as quartz etc.. The results of thermometric measurements for native gold from 6 mines by burst method show that there are 2–3 ranges of burst temperature: mainly between 315°–375℃, secondly between 254°–286℃. There is also a range of burst temperature between 123–188℃ in some deposits.

Occurrence and association: native gold may occur almost in all types of gold deposits and is always the main industrial gold mineral in most gold deposits. According to origin, the gold deposits of China are mainly magmatic hydrothermal and metamorphic hydrothermal. Volcanic and subvolcanic hydrothermal and underground hydrothermal(brine) leaching gold deposits have recently been discovered one after another in China, and displayed a good prospecting. Placer gold is also one of the important types.

The associated minerals of native gold are various, the most common and closest are pyrite, electrum and quartz etc.. The property and mineral association of native gold in different types of gold deposits display certain differences.

A STUDY OF METACINNABARITE AND TIEMANNITE FROM ZONE OF MERCURY ORE DEPOSITS IN HUNAN AND GUIZHOU

Po 3.1.

Chen Dianfen and Sun Shuqiong, Institute of mineral Deposits, Chinese Academy of Geological Sciences, Beijing 100037 People's Republic of China

Metacinnabarite and tiemannite are two end members in HgS—HgSe isomorphous series. The metacinnabarite occurs in quartz veins, carbonate veins and dolomite–quartz miarolitic cavities in Dadongla, Zhifang and Chatian mercury ore deposits. The tiemannite occurs in altered quartzite around Xinhuang mercury ore deposit.

Commonly selenium and zinc substitut respectively for a part of sulfur and mercury in metacinnabarite. The metacinnabarite from the Dadongla mer-

cury deposit has the highest selenium content (1—2%). The metacinnabarite from the Chatian mercury deposit generally contains abundant zinc (5.7—6.75%), therefore, guadalcazarite, a variety of metacinnabarite, formed. Tiemannite is different from metacinnabarite in isomorphous replacement. Usually a little sulfur substitutes for selenium in tiemannite and sulfur content in tiemannite varies in a range between 0.74% and 1.25%.

Just like other isomorphous minerals, these two minarals are very similar in physical and optical properties, X—ray powder diffraction pattern and infrared absorption spectra, and the characters between them show some requlars changes, that is, from metacinnabarite to tiemannite, specific gravity, reflectivity and cell dimension increase, the micro—indentation hardness decrease, and the location of infrared absorption spectral band moves from low to high frequency (Table).

Metacinnabarite associates with sulfides such as cinnabar and sphalerite etc. It formed in the physico—chemical environment rich in sulfide sulfur, and the temperature of formation is low, ranging from 190 to 220℃. Tiemannite associates solely with quartz, without any trace sphalerite and cinnabar. It formed in the physico—chemical environment poor in sulfide sulfer, and the formation temperature is higher, ranging from 230℃ to 260.

	metacinnabarite	tiemannite
Specific gravity	7.41—7.59	8.4
Hv(Kg/mm^2)	69	84
Rvis (%)	24—24.2	28.31—28.54
Cell dimensions a(Å)	5.8822—5.8929	6.04668—6.04681
stretching vibration place of Hg—S bond or Hg—Se Bond	600 cm^{-1}	625cm^{-1}

ORE PETROLOGY

Chen Zheng et al., Institute of Mineral Deposits, Chinese Academy of Geological Sciences, 26 Baiwanzhuang Road, Beijing, China

This book comprises two parts. The first part deals with the fundamentals of ore petrology and the second part deals with the descriptive ore petrology. These two parts were bound in two volumes.

Volume one introduces the basic concepts of ore petrology and the general methods of study . It includes five chapters in total .

The first chapter treats of certain basic ideas of ore petrology . The writer explains some technical terms , such as ore and ore formations , mineralization stages and epochs , and generation of a mineral ; talks about the meaning of a mineral assemblage ; and lastly discusses the relationship between ore petrology and other branches of geological sciences .

The second chapter treats of the principle groups of ore minerals and their common characters and occurrences . In this chapter , the basic and important parts of crystal chemistry are introduced .

The third chapter treats of the structures and textures of ore and ore minerals . It may be safely said that nearly all kinds of the fabrics of crystal grains and ores formed by crystallization , replacement , sedimentary and metamorphic processes are described .

The fourth chapter treats of the meaning of mineral assemblages , the principles of phase rule and phase equilibrium . Some common methods of mineral synthesis are described . The common characteristics of unitary , binary and ternary phase equilibrium diagrams are explained . Besides these , the relation between phase euilibrium and chemical thermodynamics are introduced . The writer tends to put stress on the application of different types of phase diagram to explain the practical mineral assemblages and the use of chemical thermodynamic calculation in determining the physical–chemical condition of mineral equilibrium assemblages .

The fifth chapter deals with the types of origin of the formations . The writer rather detailly describes the important characters of the magmatic , skarn , hydrothermal , volcanic–sedimentary , weathering and supergene , sedimentary , metamorphic ore and that of the different kinds of country rock alteration .

Volume two is the part of descriptive ore petrology . In this volume , the principal ore formations of chromite , nickel , gold , silver , antimony , mercury and manganese ore are described . According to the authors viewpoints , ore formation represents a typical kind of ore deposits ,which must have charicteristic mineral assemblages , a definite ore genesis , certain special occurrences and fabrics . Besides these , it should be a rather widespread type and possesses a certain scale of economic value . Once an ore formation is established , the constitution , the texture and structure , the occurrence , the mother rock and country rock alteration , and ore genesis which includes mineralization stages ,epochs and the physical chemical condition related to them should be detailly described .

This volume includes seven chapters :

The first chapter treats of the chromite ore formations . Two ore formations are established and described . (1) The stratiform chromite ore formation ,
2) The podiform chromite ore formation.

The second chapter treats of the nickel ore formation. Three ore formations are established and described . (1) The nickel sulfide ore formation de-

rived from gabbro kindred magma . (2) The nickel sulfide ore formation derived from komatite . (3) The weathering crust nickel oxide–silicate ore formation . The latter two are omitted in this volume because they had beem published in Journal of Chengdu college of Geology , 1987 and 1988 .

The third chapter deals with the gold ore formations . There are four ore formations to be established and described . (1) The volcanic–subvolcanic hydrothermal ore formation .(2) The green stone gold–quartz ore formation .(3) The gold bearing conglomerate ore formation .

(4) The migmatitic granite hydrothermal gold ore formation . The latter two are omitted in this volume .

The fourth chapter deal with the silver ore formations . There are four ore formations to be established and described . (1) The mesothermal–epithermal Ag–Pb–Zn ore formation. (2) The metamorphic polymetallic ore formation . (3) The sedimentary Ag–V ore formation .(4) The porphyry polymetallic Ag ore formation . The last one had been published in Bulletin of the Institute of Mineral Deposits , Chinese Academy of Geological Sciences . No. 21, 1988 , so it is omitted in this volume .

The fifth chapter deals with the antimony ore formations . There are four ore formations to be established and described . (1) The stibnite–quartz ore formation . (2) The Sb–Au–W ore formation . (3) The Sb–polymetals ore formation . (4) The stibnite–clay ore formation .

The sixth chapter deals with the mercury ore formations . There are two ore formations to be established and described . (1) The cinnabar–quartz–carbonates ore formation . (2) The cinnabar–opal–orgillite ore formation .

The seventh chapter deals with the manganese ore formations.There are four ore formations to be established and described . (1) The sedimentary Mn ore formation . (2) The metamorphosed Mn ore formation . (3) The supergene enrichment Mn ore formation . (4) The deep sea ferrimanganese nodules ore formation . The last one had been published in Foregin Mineral Deposits , Institute of Mineral Deposits , Chinese Academy of Geological Sciences , so it is omitted in this volume .

As mentional above , this book establishes and describes 22 ore formations in seven kinds of ores in total .

This book is written by a number of specialists in the Mineral Section , Institute of Mineral Deposits , Chinese Academy of Geological Sciences .

If you want to know more deailly the content , please consult the english contents attached to the end of volume two .

ORE MINERAIS IN CHAROITE ROCKS.

Dobrovolskaya M.G., Malov V.S. Institute of Geology of Ore Deposits, Petrography, Mineralogy & Geochemistry of the Academy of sciences of the USSR, Moscow 109017, USSR.

The charoite rocks of the Murunsky alkaline massif in

East Siberia are largely used as the material for jewelry. The beautiful rocks with lilac colour which is proper to charoite are unique by the high alkaline silicate association (canasite, aegirine, quartz, feldspar, K-arfvedsonite, K-richterite, fedorite, tinaxite etc.), also by the composition of ore minerals.
The main minerals like galena, chalcopyrite, idaite, chalcocite, bornite, more rare sphalerite, pyrrhotite pentlandite, digenite, covellite occur as veinlets, small aggregates, impregnation. There are specific K,Tl-bearing sulfides djerfisherite, murunskite, thalcusite sometimes associated with native copper, silver, iron.
For the first time the minerals of platinum-group metals (sperrylite, frudite, sobolevskite and other mineral phases) are found in charoite rocks. They associate with parkerite containing Pt and Pd (0,05-0,06 wt.% respectively).
The analyses of charoite rocks with impregnations of ore minerals revealed the concentrations of Pt and Pd like 0,05-0,2 and 0,1-1,25 g/t respectively, of Rh (0,0015-0,01 g/t), of Ir. (0,001-0,01 g/t).
Thus the alcaline rocks of Murunsky massif contain unusual association of potassium minerals with those of platinum-group metals. One should look for such minerals in the early magmatic rocks of the same massif as well as in alkaline formations of other regions.

AN ILMENITE-ILLITE-CARBON-QUARTZ-CHAMOSITE ASSEMBLAGE

P. Dragov, G. Čatalov, D. Stefanov, J. Uzunov, H. Neykov
Geological Institute, Bulgarian Academy of Sciences, 1113 Sofia, Bulgaria

A low-metamorphic volcanic-sedimentary series formed in a "geosynclinal" (island-arc?) environment hosts an ore bed of composition which has no analogs. It is an alternation of chlorite schists and quartzites. Chlorite schists consist of chamosite (70 - 90 %), organic matter (1 - 15 %), ilmenite (1 - 15 %), illite (0.1 - 10 %) and quartz (0.1 - 5 %). Quartzites contain up to 10 % illite and/or chamosite and about 1 % ilmenite. The bed is 0.2 - 20 *m* thick, 2.5 *km* long, extension in depth unknown. Host rocks are largely metapelites and some basic metavolcanics. They belong to the so called Stoilovo Formation (Lover Triassic?; Strandja Mt., SE Bulgaria; Čatalov & Stefanov, 1988). In an earlier preliminary communication, this rock, which at the same time is titanium-iron ore, has been called stoilite (Dragov at al., 1986).

Optical microscopy, microprobe analyses, X-ray diffractometry, thermogravimetric and wet chemical analyses have been used to characterize the chlorite schist mineral composition, as follows.

Chamosite occurs as fine flakes and blasts parallel to the foliation; oolites or relics of oolites are completely absent. The polytype is IIb ($\beta = 97°$). End compositions:
$(Fe^{2+}_{2.30}Fe^{3+}_{0.41}Al_{1.49}Mg_{1.22}Ca_{0.06}Mn_{0.04})^{+0.94}(Si_{3.05}Al_{0.95})^{-0.95}$ and
$(Fe^{2+}_{3.44}Fe^{3+}_{0.62}Al_{0.98}Mg_{0.86}Mn_{0.04})^{+1.48}(Si_{2.51}Al_{1.49})^{-1.49}$.

Illite is intergrown with chamosite. Its polytype is $2M_1$with crystallinity indices of IK = 0.21 ($°2\Theta$) and IWb = 146. End compositions:
$(K_{0.94}Na_{0.03}Ca_{0.01})^{+0.99}(Al_{1.75}Fe_{0.16}Mg_{0.07})^{-0.29}(Si_{3.30}Al_{0.70})^{-0.70}$ and
$(K_{0.78}Na_{0.05})^{+0.83}(Al_{1.76}Fe_{0.19}Mg_{0.11})^{-0.12}(Si_{3.29}Al_{0.71})^{-0.71}$.

Ilmenite forms fine flakes of uniform size (0.1 – 0.2 *mm* long, 0.005 *mm* thick) parallel to the foliation or of quasiradial orientation if included in chamosite blasts. It shows no exsolutions or twinned aggregates. Its composition and X-ray powder pattern are almost identical to those of synthetic ilmenite. Quartz occurs as separate fine grains and as small lenses of conformation mosaics. Organic matter is found in two varieties: a structureless finely dispersed one and a graphitized material of combustion temperature 660 $°C$. Accessories are dominated by apatite. Trace elements in the schists show clarke concentrations except for *Cr*, *Co* and *Zn* which are of increased contents.

Illite crystallinity indices and the chlorite + zoisite/clinozoisite assemblage found in the metadiabases imply a degree of metamorphism that belongs to the early greenschist facies.

Protogenesis is an essential problem. Sedimentation near a weathering crust over basic or ultrabasic rocks can be rejected as a possibility. One should account for the fact that ilmenite occurs exclusively in the chamosite masses and is metamorphogenic as indicated by its composition and texture. It is absent from the adjacent chlorite and "sericite"-chlorite schists as well as from those intercalations in quartzites which do not contain chamosite. The original silty material, containing finely dispersed organic matter and titanium oxides or silicates, should has been deposited in a sea-floor depression of stagnant water. Besides chamosite, the deposit may have contained ferrosmectite as well. Titanium and iron came from a common source - submarine hydrothermal fluids associated with the basic volcanism. Part of the iron combined with titanium to form ilmenite during the metamorphic crystallisation.

References

Čatalov, G., D. Stefanov. 1988. Lithology and mineralogy of the metapelites

from Stoilovo formation (Lower Triassic?) in Strandja zone (SE Bulgaria). - Palaeont., Stratigr. and Lithol., 26; 50 - 64 (in Bulgarian).

Dragov, P., G. Čatalov, J. Uzunov, D. Stefanov. 1986. A new type titanium-iron ore: ilmenite - iron chlorite schists. - Compt. rend. Acad. bulg. Sci., 38, 8; 89 - 92.

MINERALOGICAL FEATURES OF ORE FORMATION UNDER HYPABYSSAL CONDITIONS (in light of gold-bismuth mineralization)

Po.3.2

G.N.Gamyanin, Yakutsk Institute of Geosciences, Yakutsk, 677981, U.S.S.R.

Gold-bismuth mineralization of the Yana-Kolyma folded system is localized in exo-, endocontact zones of granitoid massifs in extensive batholith intrusive belts. It is represented by quartz veins, crush zones, sulphidized skarns associated with cobalt-, nickel-bearing arsenides, diarsenides, and by a gold-bearing complex of bismuth minerals: bismuthine, ikunolite, tetradymite, joseite A and B, minerals C, D, F, E, K, tellurobismuthite, hedleyite, maldonite, gold-bismuth sulphide, bismuthite, bismuth. The association of bismuth minerals is very sensitive to the instability of shallow physicochemical conditions of mineral formation, which is reflected in their compositions and structural-textural characteristics.

Non-stoichiometry is a characteristic feature of bismuth sulphotellurides and tellurides. Their compositions are rarely ideal and exhibit significant shifts towards excessive bismuth or varying Te:S ratios. Compositions may vary even within a single grain: from tetradymite to mineral E, joseite B to mineral K, hedleyite to Bi_2Te. Low-purity gold (600°/..) composition in this association varies smoothly by 100-200°/.. in ore segregation.

Isomorphism is widely developed. Main isomorphic elements are lead, antimony, and selenium. Selective isomorphism is observed. Maximum amounts of lead occur in tetradymite (up to 8%), of antimony in bismuthine (up to 18%), of selenium in ikunolite and bismuthine (up to 5%). Different impurity content of adjacent grains and uneven impurity distribution within a grain are typical. Mineralizations of individual metallogenic zones are characterized by a predominance of one isomorphic element found in all bismuth minerals.

Presence of metastable minerals and their breakdown textures. Such minerals include maldonite Au_2Bi, gold-

bismuth sulphide Bi_5AuS_4, and ikunolite Bi_4S_3. The latter breaks down into bismuthine with dots of submicroscopically impregnated bismuth. Maldonite breaks down to form subgraphics of bismuth or bismuthite and pure gold, whereas gold-bismuth sulphide breaks down into bismuthine and pure gold whose ichthioglyphs occur among bismuthine. There are tiny prismatic segregations which consist of a very fine mixture of pyrrhotine and bismuth. They have stable proportions of components, and the mixture composition corresponds to a possible mineral of $Fe_4Bi_6S_{13}$ type.

Exsolution textures are developed rather widely not only among bismuth minerals but also among those crystallized simultaneously with them. Most typical are exsolution textures in the form of fine, lenticular intergrowths of joseite A in joseite B or vica versa, joseite A and B in tetradymite, subgraphic textures of bismuthine and sulphotellurides, emulsion textures of chalkopyrite and pyrrhotine in sulphotellurides. Chaotic distribution of such textures in both large clusters of bismuth minerals and single grains is observed. A typical feature of bismuth mineral associations is simultaneous crystallization and intimate intergrowths of bismuth sulphotellurides and tellurides with hypogenic bismuth oxides.

Thus, nonstoichiometric composition of bismuth minerals, uneven distribution of isomorphic impurities, presence of metastable minerals, their breakdown textures, exsolution textures, simultaneous crystallization of oxide and sulphur compounds are typical features for gold-bismuth mineralization under unstable, shallow physicochemical conditions.

312.

MINERALOGY OF THE COMPLEX SULFIDE ORES FROM NEVES-CORVO

O.Gaspar,Laboratório da DGGM,P-4465 S.Mamede de Infesta

Neves-Corvo lies in the Portuguese sector in the Iberian Pyrite Belt (I.P.B.) and consists of five ore bodies, Neves, Corvo, Graça, Zambujal and Lombador, occurring on the top of the acid volcanics of lower Carboniferous age.

The ore bodies show a strong vertical and lateral zoning making it possible to identify and exploit various types of ore :cupriferous ore, complex ores, tin ore and barren pyrite.

With current mineable Graça and Corvo cupriferous ore reserves of some31Mt grading 8,03% Cu and tin ore reserves currently amount to some 2,8Mt at an average grade of 2,7% Sn, Neves-Corvo is the ri - chest copper and tin deposit in the I.P.B..

Since 1980 a systematic ore microscopic study has been carried out aiming at the beneficiation of the sulfides by differential froth

flotation.
Finegrained mineralization, ore textures and mineralogy of the Cu-Zn-Pb ores are very similar to the other sulfide deposits of the I.P.B..More complex are the mineralogy and paragenesis of Cu-As-Sb sulphosalts and tin ores.
Tetrahedrite and tennantite frequently occurring together have a changeable composition and carry variable amounts of Ag and Hg.
Although cassiterite and stannite related minerals have always been observed in small quantities in the other sulfide deposits of IPB, they occur in huge amounts in Neves-Corvo.
So far two different kinds of cassiterite occurrences could be established: 1) as microscopic stripes of euhedral cassiterite in recrystalized pyrite and being replaced by sphalerite and chalco - pyrite; 2) as main constituent of metric massive lenses intergrown with quartz and replaced by carbonates and sulfides, overlaing the Corvo cupriferous ores and sometime with Sn grading up to 30%.
Stannite, kesterite, stannoidite and mawsonite occur in big quan - tities in the cupriferous of Corvo and Graça ores. Their occurrence in complex ores (5.72% Zn , 1.13% Pb and 0.4% Cu) is scarce.
Microscopical observation indicates that introduction of later and hotter Cu-rich hydrothermal solution on primitive pile results in the replacement and migration of the Zn-Pb ores. Very interesting sphalerite replacements by chalcopyrite and tetrahedrite are always present in the rich cupriferous ores.

GOLD IN ARSENOPYRITE

James Graham, CSIRO Division of Mineral Products,
Private Bag, PO Wembley, Western Australia, 6014.

3.4.

Some recent papers have confirmed the existence of invisible gold in arsenopyrite in some gold deposits, and have described its non-uniform distribution, and its correlation with antimony or with iron deficiency in the arsenopyrite lattice (Cathelineau et al, 1988; Johan et al 1989; Graham et al 1988,89). There seems to be a growing consensus that the gold may be in solid solution in the host lattice, and this has been supported by a careful high resolution electron microscope study (Cabri et al 1989). However, a colloidal distribution has been demonstrated in pyritic Carlin type ores (Bakken et al 1989), and there is every likelihood of a continuous transition from particles to solid solution. The distinction is probably largely academic as far as commercial extraction is concerned.

It is possible to confirm the presence of such gold in several ways, listed in order of increasing cost. a) by pyrolysis followed by optical examination,
b) by electron microprobe analysis, or
c) by ion probe analysis.
The microscopic method a) should be suitable for gold

concentrations down to 1ppm or less; electron probe microanalysis can have a sensitivity of up to 10ppm under optimum conditions, and has the best spatial resolution, while the ion probe with mass spectrometric detection can reach 250ppb or better. In every case, quantitative macroscopic information is difficult because of the non-uniform distribution patterns. Hence a matching of mineralogical and metallurgical gold balances is nearly impossible.

The pyrolysis method is interesting; on heating gold-containing arsenopyrite in a vacuum or inert atmosphere at about 600C, gold is redistributed in the recrystallizing sulphide host as the arsenic volatilises. The result is small visible globules of gold.

While Johan et al demonstrated a nice correlation between gold content and iron deficiency for deposits at Chatelet and Villeranges, a compilation of data on arsenopyrites from many sources shows a more complicated story, including very wide non-stoichiometry between sulphur and arsenic, so that iron deficiencey is not a definitive criterion for gold in solid solution in the crystal. Also, the fact that arsenopyrite is present in a gold deposit does not necessarily mean that it is a host for gold.

Invisible gold is found in other hosts such as pyrite, stibnite, loellingite, gersdorffite, pyrrhotite and chalcopyrite, generally at a lower level (see also Cook and Chryssoulis, 1990). Of these, pyrite, gersdorffite and pyrrhotite are well known to show ranges of non-stoichiometry. There is some evidence to link gold content with arsenic content in pyrite.

REFERENCES:

Bakken, B.M., M.F. Hochella, A.F. Marshall and M. Turner (1989) High-resolution microscopy of gold in unoxidised ore from the Carlin mine, Nevada. Econ. Geol. 84, 171-79.

Cabri, L.J., S.L. Chryssoulis, J.P.R. de Villiers, J.H.G. Laflamme and P.R. Buseck (1989) The nature of "invisible" gold in arsenopyrite. Can. Mineral. 27, 353-62.

Cathelineau, M., M.C. Boiron, Ph. Holliger and Ph. Marion (1988) Gold-rich arsenopyrites: Crystal chemistry, gold location and state, physical and chemical conditions of crystallization. Bicentennial Gold 88, 235-40.

Cook, N.J., and S.L. Chryssoulis (1990) Concentrations of "invisible gold" in the common sulphides. Can. Mineral. 28, In Press.

Johan, Z., E. Marcoux and M. Bonnemaison (1989) Auriferous arsenopyrite: Mode of substitution of Au in the structure of FeAsS. Comptes Rendus Acad. Sci. Paris 308 II, 185-91.

Graham, J., J. Just, G. Nguyen and B.W. Robinson (1988) Electron beam techniques in gold mineralogy. Perth Gold 88 (Randol), 137-40.

Graham, J., B.W. Robinson and R.K. Walker (1989) Gold in arsenopyrite. Min. Pet. Symp., Sydney, Aus. I.M.M., 55-57.

MINERALOGY OF MANGANESE NODULES FROM NORTHERN EQUATORIAL PACIFIC OCEAN

38P

GUO Shiqin, SUN Wenhong, XIAO Xuqi, LIN Yueying, YANG Mingming, CHEN Yongzhi, Institute of Mineral Deposits, Baiwanzhuang Road 26, Beijing 100037, China

Deep sea manganese nodule is a complex polymineralic aggregate. It contains hydrated ferromanganese oxides or oxyhydroxides, clay minerals from various sources, minerals of zeolite and small amounts of detrital minerals. Most of the minerals are authigenic, poorly crystallized or colloid. They intergrow intimately and sometimes grow epitaxially, so it is impossible to obtain pure mineral specimens, and many modern methods such as microscope, TEM, SEM, XRD, EMP, IR, MS and DTA have been used for comprehensive analyses.

According to the composition of the minerals in manganese nodules we divide the minerals into three groups.

1. Manganese minerals

XRD and TEM analyses show that vernadite and todorokite are the principal manganese minerals in the nodules from CP(central Pacific basin) and CC(the area between Clarion and Clipperton fractures). Birnessite is rarely found.

Vernadite is the dominator in hydrogenous nodules with smooth surface which are distributed mainly in CP area and several stations in the north of CC area, occuring in the area of sea mounts and of the steep slopes of mounts. It is cryptocrystalline or amorphous, reflectivity is about 11%, reflection color under ore microscope is bluish grey. The based reflections are present at d = 2.4 and 1.4 Å, sometimes at 2.2Å in XRD and SAD patterns. Vernadite is always rich in Fe, and has a Mn / Fe ratio less than 2.

Todorokite is a principal mineral in early diagenitic nodules. In mixed genetic nodules it is nearly equal to vernadite in quantity It shows microcrystalline aggregates, yellowish white, and the reflectivity is about 16%. Marked anisotropy can be seen under the cross polariscope, so it can be distinguished from vernadite easily in nodules.

With the exception of enrichment in Mn, Cu, Ni, Zn, it has higher MgO,

generally 4——6%. We can differentiate todorokite from vernadite in Mn–Fe–(Cu+Ni)×10 and Mn–Fe–Mg×10 triangular diagrams.

Birnessite is rarely present, except in a few nodules from CC area. Care must be taken in birnessite determination for phillipsite and montmorillonite also have the diffraction at 7Å.

We have made experimental heat treatments with specimens in which todorokite is principal. The specimens were heated to 50, 80, 110 and 140 ℃ respectively for 6hrs, then examined with XRD. We found that the intensity of the diffraction at 7Å becomes stronger and the diffraction at 10Å weaker as the temperature increases. It suggests that todorokite can be changed into birnessite as a result of dehydration with aging.

Manganosite has been found with clear electronic diffraction pattern.

2. Iron minerals

Mossbauer spectrums measurement shows that iron–bearing facies have two double peaks. The parameters are IS=0.360–0.366, QS=0.535–0.578mm / s for inner double peaks and IS=0.363–0.368, QS=0.877–0.953mm / s for outer double ones. According to the Mossbauer spectra of known minerals and environment factors we designate the inner peaks as geothite, and the outer peaks may represent akaganeite and ferrihydrite.

3. Silicate minerals

We found that many cores of the nodules from deep sea plain are composed of consolided argillaceous sediments. It has two mineral combinations. The one is dominated by phillipsite and other is by sodium harmotome. A small amount of illite, montmorillonite and quartz are present. In ferromanganese oxide layers outside the core, the impurities are quartz and phillipsite.

The mineralogy of manganese nodule has a close relationship with their chemical composition, structure and the types ,and these factors in turn are controlled by the sea floor topography and regional environment.

STUDIES ON LEAD–ZINC SULPHIDE MINERALIZATIONS IN THE RED SEA COASTAL ZONE EGYPT

M.M.Hassaan, Al–Azhar University, Faculty of Science, Cairo Egypt

Twelve occurrences of Pb–Zn sulphide mineralizations of established Middle Miocene age have been known to occur in several rock units cropping out along the Red Sea Coastal Zone in Egypt namely; basement rocks, Late Cretaceous Sandstones of Nubian facies and Middle Miocene limestones, sandstones and evaporites. The localization of the mineralizations are chiefly controlled lithologically and structurally. Most of the mineral deposits are localized in the sandy limestones when intersected with NW–SE faults and tectonic zones favoring their gydrothermal origin.

The chief primary minerals are sphalerite, galene, pyrite and marcasite. The secondary minerals are cerussite, smithsonite, hydrozincite, calamine, anglesite, hematite, limonite, wulfenite, pyrolusite, psilomelane and zincite.

The chief associated elements are Mo, Ag, Cd, Tl, Hg, Mn and V which distinguish telethermal occurrences. The hydrothermal origin is also supported by pockets and lenses of smoky dolomites, iron and manganese carbonates and silicification occurring within the alteration zones at Zug El Bohar, Um Gheig, Gebel El Rousas and El–Anz located between Quseir and Mersa Alam on the Red Sea Coast. Gossans rich in Fe_2O_3characterise these occurrences. Small ochre occurrence associated with pronounced Pb and Zn contents occur at Um Griefat.

The epigenetic hypogene Pb–Zn deposits occur in the following modes of occurrence:– Pitch and flat, Gash vein and disseminated deposits.

Deposition of sulphides as a result of decrease of temperature of hydrothermal solutions is due to the paragenetic sequence: phrite, sphalerite, galena and marcasite. Vertical geochemical zoning is observed at Um Gheig where zinc increases with depth and vice versa for lead. Lateral geochemical zoning is also detected where at the periphary of the deposit iron and zinc increase while lead decreases. Regional zoning controls distribution of Fe–Mn, Cu and Pb–Zn hydrothermal mineralizations along the Red Sea Coastal Zone where Pb–Zn occurrences at the center are replaced to the north and to the south by Cu and Fe–Mn hydrothermal mineralizations.

The studied mineralizations could represent the Middle Miocene phase in the northern African hypogene Pb–Zn sulphide mineralizarions where there is a tendency of decrease of age of mineralization from the Paleozoic in Morroco to the Pleistocene and Recent for the hydrothermal hot brines in the Red Sea deeps through the Cretaceous in Aljeria and Tunis.

HEAVY MINERAL INCLUDING ILMENITE ALONG VIETNAM'S COAST

P03.3

Hoang Trong Mai, La Thi Chich, Polytechnical Institute, Hochiminh City, Vietnam.

The heavy mineral that includes Ilmenite is distributed along the coast of Vietnam from Quang Ninh to Vung Tau. Its mineral composition is various but the mineral group accompanying Ilmenite usually includes Rutile, Zircon, Monacite, Tourmaline and Magnetite. As compared with continental heavy mineral number of mineral form is smaller, but its mineral association is not as various.

The chemical composition of heavy mineral meets industrial requiments. Its TiO_2amounts to over 50%, its ($FeO + Fe_2O_3$) is approximately 45%, with $FeO > Fe_2O_3$. Other mixtures are in significant.

The thickness of layers of Ilmenite is various. Those lying between high tide level and low tide level tend to taper off. Towards the shore where granularity is high, the composition of heavy mineral is relatively simple. Where the sea meets krans, the sedimentation is

not easy and the layers of Ilmenite are very thin. The source of heavy mineral is determined by the complexes of continental igneous rock and metamorphic rock. The conditions of sedimentation of heavy mineral depends upon the rivers, the winds and the slope of the marine terrace.

Magnetism fractionation and gravity fractionation can be used in the complex exploration of Ilmenite, Zircon and Monacite ore for different industrial branches.

33.P

THE APPLICATION OF THERMAL ANALYSIS IN QUANTITATIVE ANALYSIS

Huang Kaihan, Institute of Comprehensive Utilization of Mineral Resources, Ministry of Geology and Mineral Resources, Emei, Sichuan, 614200, People's Republic of China

This paper describes the method of quantitative analysis of matters and elements in terms of TG curves coupled with DTA curves.

In the process of heating sample, if the masses of n kinds of matters change, and the changing rates of No.a pure matter and sample in b temperature region are respectively P_{a-b} and P_b, the general equations to calculate contents X of these n kinds of matters are as follows:

$$P_{1-1}X_1+P_{2-1}X_2+\cdots\cdots+P_{n-1}X_n=P_1 \quad (1)$$
$$P_{1-2}X_1+P_{2-2}X_2+\cdots\cdots+P_{n-2}X_n=P_2 \quad (2)$$
$$\cdots\cdots\cdots\cdots\cdots\cdots\cdots\cdots\cdots\cdots$$
$$P_{1-n}X_1+P_{2-n}X_2+\cdots\cdots+P_{n-n}X_n=P_n \quad (n)$$

The author applied these equations to the determination of the contents of thermogravity-active matters with indefinite chemical formulae, such as montmorillonite, hydromica and so on, or the matters with overlapped mass changes, such as kaolinite and calcite, gibbsite and calcite etc, or matters with superimposed mass changes, such as kaolinite and halloysite, montmorillonite and kaolinite etc.

The thermal reaction equations have been used to determine the contents of thermogravity-active matters with definite chemical formulae, such as kaolinite, magnetite, siderite etc and some of their specific assemblages.

The determinatoin of FeO in sample, in which there is only mass increase when ferrous in ilmenite, magnetite, chromite, slag and so on is oxidized, is very typical.

The chemical formulae and thermal reaction equations have been used to determine in samples the contents of elements, which are present in thermogravity-active matters with definite chemical formulae, such as kaolinite, chromite, ammonium ferrous sulfate etc and some of their specific assemblages.

The chemical formulae of thermogravity-active matters with indefinite compositions, such as pyrrhotite, slag containing vanadium and so on, have been determined.

If the chemical formula of one matter with isomorphism is$(A_1, A_2, \cdots, A_n)_c B_d$; its molecular weight is M; the number of molecules taking part in the reaction is e in the thermal reaction equation and the mass change is Δm_1; the mass change on TG curve of pure matter with mass m is Δm; the atomic weights and contents of elements B, $A_1, A_2, \cdots, A_n$ are respectively M_b, M_1, $M_2, \cdots, M_n$ and b, $a_1, a_2, \cdots, a_n$, the general equations to calculate the number of atoms X of these n kinds of isomorphous elements are as follows:

$$eM/m = \Delta m_1/\Delta m \quad (1)$$
$$M_b d/M = b \quad (2)$$
$$M_1(1-X_2-\cdots-M_n)C/M = a_1 \quad (3)$$
$$M_2X_2\,C/M = a_2 \quad (4)$$
$$\cdots\cdots\cdots\cdots\cdots\cdots$$
$$M_{n-3}X_{n-3}C/M = a_{n-3} \quad (n-1)$$

These general equations have been used to determine the number of atoms of isomorphous elements Fe, Mg in ankerite and Fe, Zn, Mn in manganess-zinc siderite.

The mass changing rate method can be used in quantitative analysis only when the standards containing the same constituents as the sample are available. If the mass changes of the components to be analyzed are superimposed, quantification can be made only when their mass changing rates are quite different. With these exceptions, all thermogravity--active matters can be quantified using the thermogravity method.

The method of thermogravity quantification of elements is applicable to all thermogravity-active matters which have definite chemical formulae and of which contents are measurable. Quantification of elements in the thermogravity-active matters with indefinite formulae or isomorphism requires a prior determination of the formulae.

The absolute difference between thermal analysis results and actual values falls within the range of 0.03-0.58% (0.20% on average) for quantification of matters, 0.12-0.91%(0.44% on average)for elements, and 0,003-0.023 atom(0.009 atom on average) for atom numbers.

According to 10 measurements of calcite in one sample, the average is 99.71%, the variance 1.53×10^{-6}, the standard deviation 0.12%, and the maximum error 0.12% (with a confidence level of 0.99 and a confidence coefficient of 3.25).

THE Cu - Te - S PHASE SYSTEM AT 350, 450, 550, 675 AND 800 °C

Po3.7

S. Karup-Møller, The Institute of Mineral Industry, The Technical University of Denmark, Building 204, DK-2800 Lyngby, Denmark.

The condensed system Cu - Te - S has been studied at 350, 450, 550, 675 and 800 °C using dry charges annealed in evacuated silica glass tubes. The products were evaluated by means of microscopy, microprobe analyses and X-ray diffraction.

At 300°C three ternary phases were identified. One of these is

goldfieldite with univariant chemical composition $Cu_{3.17}$ $Te_{1.17}$ $S_{4.00}$ and a_0 = 10.267 ± 0.005 Å. The two other phases A and B have not been found in nature. Phase A is hexagonal (a = 4.450 ± 0.001 Å and c = 5.906 ± 0.002 Å) and has the following univariant chemical composition $Cu_{1.27}$ $Te_{0.98}$ $S_{2.00}$ (Z =1 and $d_{calc.}$ = 4.42 gr/cm^3). Phase B is cubic (a = 10.220Å) with a chemical composition ranging between $Cu_{1.00}$ $Te_{0.32}$ $S_{0.29}$ (Z = 30, d_{calc} = 5.30 gr/cm^3) and $Cu_{1.00}$ $Te_{0.55}$ $S_{0.86}$ (Z = 30, d_{calc} = 6.33 gr/ cm^3).

When associated with phase B, chalcocite contains almost 4 mol% Te, but less than 0.5% when associated with goldfieldite. Covelline contains less than 0.5 mol% Te. The three natural Cu-Te phases weissite, richardite and vulcanite may dissolve up to 1.5 mol% S. A small liquid field of the Cu-Te join at $Cu_{0.69-0.71}$ $Te_{0.31-0.29}$ may contain as much as 2 mol% S. On the Te-S join a liquid field exists between pure S and approximately $S_{0.75}$ $Te_{0.25}$ at 350°C. The Cu-content of the liquid is negligible.

At 450°C phase A and vulcanite have disappeared. Goldfieldite, phase B, chalcocite, covelline and richardite have approximately the same chemical composition as at 350°C. Weissite may dissolve up to 3.5 mol% S. The small liquid field on the Cu-Te join at 350°C has increased in size, stretching along the Te-S join and from Te towards a composition of Cu_{45} Te_{55}. The field lies close to the two boundaries of the phase diagram.

At 550°C goldfieldite has disappeared. Weissit may contain up to 7 mol% S and chalcocite up to 11% Te. The compositional field of phase B has slightly expanded and it ranges between $Cu_{1.00}$ $Te_{0.29}$ $S_{0.32}$ and $Cu_{1.00}$ $Te_{0.58}$ $S_{0.83}$. The compositional field of richardite has not changed significantly. At 550°C the liquid field extends as a long narrow tongue from the Te-corner deep into the phase diagram reaching a position of approximately Cu_{48} Te_{28} S_{44}.

At 680°C the phase richardite has disappeared. Complete solid solution exists between chalcocite and weissite. The compositional field of phase B is nearly the same as at 550°C. The liquid field has expanded considerably from the central portion of the phase diagram towards the Cu-corner of this.

At 800°C phase B has disappeared and the liquid field lies very close to the chalcocite-weissite join. Remarkably, towards the S-corner of the phase diagram the boundary of the liquid field has virtually not changed position with increase in temperature from 500°C to 800°C.

Po3.5

DETERMINATION OF SOME MINERALOGICAL PARAMETERS OF VARYING Ag-CONTENT IN SYNTHETIC Au-Ag ALLOYS

Kim, Won-Sa, Dept. of Geology, Chungnam National University, Daejon 302-764, Korea: Kim, Soo-Jin, Dept. of Geological Sciences, Seoul National University, Seoul 151, Republic of Korea

The correlation of Au-Ag ratio in Au-Ag alloys and its variation with depth of gold mineralization has long been of interest. Chemical composition of the alloys can be determined by electron microprobe analysis, an outstanding non-destructive method, preserving the relationship between gold-silver minerals and their surroundings (wallrock, coexisting minerals, etc.) on the polished specimen. The equipment is costly and therefore not a practical technique for companies working with smaller budgets. Thus, development of simple but reliable methods by which the Ag-content of the Au-Ag minerals can be determined has been of interest among the applied mineralogists.

As a first step to meet this goal, quantitative mineralogical parameters such as cell constant, reflectivity, specific gravity and micro-indentation hardness have been measured for the synthetic Au-Ag series alloys prepared at 5 at.% intervals. The unit cell parameter for each alloy has been refined by a least-squares method, using X-ray powder data taken with 114.6 mm Debye-Scherrer camera. The cell constant gradually becomes larger as Ag-content increases. The reflectivities of the Au-Ag compounds have been measured for 2 wavelengths 480 and 546 nm, using spec. pure platinum as a standard. The range and mean values have been determined after 20 measurements for each specimen. It is suggested that use of 480 nm is preferable for the reasons that the range between R values for silver and gold at this wavelength is more than twice that at 546 nm and that R values are more sensitive to the composition of the alloys. Specific gravity measurements also illustrate gradual changes with Ag-content. However, Vickers hardness numbers determined using loads of 25 and 50 gf are so variable regardless of the composition that no apparent trend is seen.

A POSSIBLE EPITAXY OF LAURITE ON RUTHENIRIDOSMINE FROM OPHIOLITICCHROMITITE: GENETIC IMPLICATIONS

P03.6

Olivier Legendre, GIS B.R.G.M.–C.N.R.S., 1A rue de la Ferollerie, 45071Orleans Cedex 2, France.

A detailed scanning electron microscope investigation of platinum–group minerals included in ophiolitic chromites from the "Massifdu Sud" (New Caledonia) has been made. The association of laurite and rutheniridosmine was found to be very common. This association is unusual in that the laurite crystal is always attached to the tabular face (00.1) of the rutheniridosmine. The laurite crystal is always smaller than the rutheniridosmine crystal.

Such association is explained by epitactic overgrowth of the laurite crystal on the rutheniridosmine. The growing plane of the laurite is postulated to be (111) on the (00.1) face of the rutheniridosmine, since those planes comply with the two conditions required for epitaxy i.e.:

– similar symmetry for $(111)_l$ and $(00.1)_r$, trigonal in this case,
– good coincidence between row parameters for $[111]_l$ and $[00.1]_r$, which is within 3.5%.

Genetic implications which can be drawn from this epitaxy in accordance with a_{S2} curves for Ru / RuS_2, Os / OsS_2 and Ir / IrS_2 are:

– Os, Ir, Ru alloys and laurite do not crystallize at the same time,
– whether the Os, Ir, Ru alloy or the laurite crystallizes depends on a_{S2} (assuming weak temperature variation),
– evidence of an increase in a_{S2} during crystallization of ophiolitic chromitites.

DACHANG ORE FIELD --- A DEPOSIT WITH THE MOST ABUNDANT SULFOSALT MINERALS IN THE WORLD

Li Xilin, Institute of Geochemistry, Academia Sinica, Wushan, Guangzhou 510640, Guangdong province, P. R. C.

The well known Dachang cassiterite-sulfides ore field in Guangxi Autonomous Region is a deposit with exceedingly abundant sulfosalt minerals and sulfide minerals. It is, therefore, an ideal place for investegating the sulfosalt minerals. Up to now, 181 species of minerals have been identified by the author, including 47 species of sulfosalt(may up to 60 species from all the literatures), 40 species of sulfides(with antimonides, arsenides and tellurides) and 94 species of other groups of minerals.

The abundant reservoir and the numerous mineral species of sulfosalt minerals in Dachang ore field does come first on the list of sulfosalt mineral deposits in the world. Thus, the ore field was named "the country of sulfosalts" by the author in 1985. All sulfosalt minerals have been studied carefully and have the datum of electron microprobe analysis, reflective colour index, X-ray power diffraction analysis, differential thermal analysis, infrared ray, Mossbauer analysis, specific gravity and hardnesses.

The name of 47 species of sulfosalt minerals are listed as following.

Pb-Sb sulfosalts		
jamesonite	mangunoan jamesonite	benavidesite
boulangerite	zinkenite	semseyite
madocite		
Pb-Sb-As sulfosalts		
jordanite	geocronite	
Pb-Sb-Cu sulfosalt		
bournonite		
Pb-Sb-Ag sulfosalts		
diaphorite $Pb_5AgSb_6S_{14}$	andorite $ZnPb_3Ag_5Sb_5S_{14}$	owyheeite
Pb-Sb-Sn sulfosalts		
franckeite	cylindrite	
Sb-Ag sulfosalts		
pyrargyrite $Ag_5Sb_3S_7$	miargyrite	stephanite
Sn-Ag sulfosalt		
canfieldite		
Cu-Sb-Ag sulfosalts		

tetrahedrite	freibergite	zincotetrahedrite
argentian tetrahedrite		polybasite
argentian zincotetrahedrite		
Sb-Fe sulfosalt		
berthierite		
Pb-Cu-Sn sulfosalt		
$Pb_2(Cu,Zn)_2SnS_5$		
Bi-Pb sulfosalts		
galenobismutite	cosalite	lillianite
weibullite	wittite	
Bi-Ag sulfosalt		
matildite		
Bi-Pb-Ag sulfosalts		
gustavite	schirmerite	pavonite
benjaminite	$PbAgBiS_3$	$Pb_5(Ag,Cu)(Bi,Sb)_5S_{13}$
Bi-Pb-Sb sulfosalts		
kobellite	tintinaite	
Bi-Pb-Cu sulfosalts		
soucekite	eclarite	
Bi-Sb-Ag sulfosalt		
aramayoite		

EFFECT OF STRUCTURAL STRESS TO THE SUBSTITUTION AS ISOMORPHISM —— TAKING THE LEAD-ZINC ORE DEPOSIT OF LUJIAPUZI AS AN EXAMPLE

LIU Hongbo, Department of Geology, Northeast University of Technology, Shenyang, Liaoning Province 110006, People's Republic of China

Research on external factors, such as temperature and concentration of metallogenic component, which affect the substitution as isomorphism, has been reached conclusive understanding, but has not been so about pressure. To take it as an example that the change trend of minor elements substituting host one as isomorphism in monominerals of magnetite and sphalerite of lead-zinc ore deposit of Lujiapuzi, Liaoning province here, the effect of structural stress to the substitution as isomorphism is discussed.

1. The Amount Trend of Minor Elements in Monomineral

The change trend will be found after figuring the amount of minor elements substituting Fe in eight magnetites from eight different elevations: (1)there is an increasing trend of Fe^{3+}, V, In, Mn^{2+}, Cr, Zn, Ga, Ge, Sn, Ti, Mg, Cd, Al from lower to upper; (2)decreasing of Fe^{2+}, Co, Ni, Pb, Cu from lower to upper; (3) little change of Se.

The change trend will be found after treating six blendes as same as mag-

netite: (1)there is a decreasing trend of Fe, Co, Ni, Mn, Cu from lower to upper; (2)increasing of Ga, Ge, In, Cd, Se, Te from lower to upper.

2. Status of Structural Stress at Different Level

There are two granite masses on the Earth surface, one is in the west and the other in the east of the mining district. They intruded during the metallogenic epoch. Judging from the information of drill log, the two masses are linked together underneath. A triangular field enclosed by faults of NE, NW, NWW, is situated in the middle of them. Ore bodies are located in the NW fault. The agency of uplift yields compression at the depth and stretch at the shallow when magma intrudes, namely, the structural stress at the depth is more than that at the shallow. The metallogenic temperature, of course, reduces gradually from the depth to the shallow.

There is an opposite effect of the replacement as isomorphism between temperature and structural stress under the geological environment mentioned above. Why there is actually regular change of the amount of minor elements replacing host one as isomorphism in two monominerals? It is suggested here that the regular change of amount is resulted by structural stress, an prevailing factor affecting the replacement as isomorphism in this district, acting on the atomic structure of minor elements; and it is the reflection of geochemistry in replacement as isomorphism. No attention was previously paid to that.

3. Interpretation of Tectono-Geochemistry

According to the adjusting and differentiating principle of tectono-geochemical dynamic, element that is of small density, unstability, large atomic volume and radius tends to deposit in the space of less structural stress, and one that is of large density, more stability, small atomic volume and radius does oppositely.

Comparing the parameter of atomic volume, radius and density as well as stability of minor elements substituting Fe or Zn with that of Fe or Zn, difference would be seen. Then, it is easy to understand the change trend of the amount of minor elements in magnetite and blende at different level taking into account of both of the adjusting and differentiating principle of tectono-geochemical dynamic and metallogenic enviroment.

4. Conclusion

The substitution of one element to another as isomorphism is affected sensitively and strongly by structural stress. It realizes in such way that structural dynamic adjusts the deposition space of elements that is of different atomic parameter, and further differentiates the concentration of metallogenic component, lead eventually to influence the amount of substituion of elements as isomorphism in minerals. It might be described as $C=f(P.\ V.\ d.\ R)$, where C is the amount of substitution, P, the value of structural stress, V, the atomic volume, d, the atomic density, R, the atomic radius.

THE FIRST DISCOVERY OF α—$(AuAg)_3Hg$ AND MIHARAITE IN CHINA

Lou Zhenkuan, Wang Manzhi, Guan Kang, Wang Chuantai, Tianjin Geological Academy, Minisrty of Metallurgical Industry, Tianjin, 300061, People's Republic of China

α—$(AuAg)_3Hg$ and miharaite is first found in China from the samples collected in gold-bearing quartz veins in Sanjia gold mine, Qinlong county, Hebei province.The gold-bearing quartz veins, occuring in Archean metamorphic basic volcanic rocks of Qianxi group, are controlled by NE-NNEtrending compresso-shear faults.Mineralization is related to magmas intruded around the mining district including both Dushan granitic batholite and granitic stock. Minerals are dominated by quartz, pyrite and a little calcite, galena, chalcopyrite, bornite, sphalerite and minor tennantite, wittichenite, aiklinite, miharaite, gold, kustelite and α—$(AuAg)_3Hg$.

1.α-$(AuAg)_3Hg$

α-$(AuAg)_3Hg$ is a kind of natural mineral containing Hg, Au, Ag, which generally has a intergrosth with gold, electrum and Bi-bearing sulfosalt minerals and occurs in the fissures of pyrite and quartz in the form of veinules and irregular particles.Its reflection color is rosy yellowish-yellow white.It is characterized by isotrope, low hardness, no bi reflection and pleochoism and high reflectivity with 480nm (62.55-80.56%), 546nm (72.18-85.78%), 591nm (75.7-88.28%), 654nm (77.63-91.41%) measued under MPV-1 microphotometer. Its VHN equals to 91.23kg / mm^2. The formula is (Au, $Ag)_3Hg$ with Au 18.08-27.37%(average 41.73%), Hg32.12-38.02%(average 35.66%), analysed with the JCXA733 microprobe.The strong lines of x-ray powder analysis are , 2.3822(9), 2.0599(6), 1.2449(10), 1.1944(5).It belongs to isometric system with a_0-4.129Å, similar to JCPDS4-0784 α-(Au_5Hg).It is referred as a new minerla varity, which has the same structure but different composition than α-(Au_5Hg).

2.Miharaite ($Cu_4FepbBiS_6$)

Miharaite was entiled as a new mineral at Mihara Copper Mine, Okayama Prefecture, Janpan in 1980.Miharaite identified by the authors first in China occurs in gold-bearing quartz veins at Sanjia gold mine, which generally has a paragenesis intergrowthing with galena, chalcopyrite, wittichenite, aikinite and occurs in the fissures of pyrite and quartz in the form of veinules or irregualar particles.Its reflection color is pinkish gray;

polarization color is darl–blue–gray to brownish.It is characterrized by slight bi reflection and middle–low reflectivity (see table 1 measured under MPV–1 microphotometer), similar to miharaite occured in Mihara Copper Mine, Janpan.Its formula is $Cu_4FePbBiS_6$. The chemical composition analy sed by JCXA–733 microprobe is listed in table 2, also similar to Mihara's miharaite.The results of X–ray powder analysis with Gandolifi camera may be compared to those of miharaite within Mihara Copper Mine (table 3).

Based on above studies, it is proposed that this mineral is miharaite.

Tablel. Reflecivity of Miharaite

wave length(nm) location	480	546	591	654
SanJia	27.4–31.0%	28.8–31.9%	29.3–32.8%	30.4–33.4%
wave logth(nm) location	480	548	589	657
Mihara	29.6–30.3%	30.8–31.5%	31.7–32.6%	32.1–34.2%

Table2. Chemical Composition of Miharaite

element location	Cu	Fe	Pb	Bi	S	Total
SanJia	26.48	6.30	23.40	22.47	20.92	99.57
Mihara	28.24	6.05	22.72	22.75	20.60	100.36

Table3. Data of X–ray powder analysis of miharite

SanJia	d	3.729	3.257	3.142	3.068	3.005	2.648	2.182
	I / I_0	2	5	9	10	2	1	7
Mihara	d	3.75	3.25	3.11	3.03	3.00	2.64	2.18
JCDS33–46	I / I_0	60	70	55	100	90	80	60

P039.

MINERALOGY AND GEOCHEMISTRY OF THE ORE– BEARING WEATHERING CRUSTS IN HANOI REGION

Dr. Mai Trong Nhuan, Department of Geochemistry, Hanoi State University, Vietnam

In Hanoi region there are 3 geochemical types of the Weathering crust – feralitic (laterite FWC), ferosialitic (lithomage, LWC) and sialitic (clay, SWC). They are different in zonality, mineralogical, chemical composition, ore–bearing etc. The FWC composes of 3 zones – saprolite, ferosialite and feralite; the LWC profile has lost the feralite zone. The SWC has two zones–saprolite and sialite. Each of these xones is characterized by the definite value of minerals and chemical element content and geochemical coefficients.

The main minerals of the SWC are kaolinite, hydromicas, quartz and the rare ones – chlorite, feldspars .... In the FWC and LWC there are the main minerals such as goethite, hydrogoethite, kaolinite, quartz. The rare minerals of these two types are hydromicas, chlorite, ilmenite, gibbsite, manganite.... The content of goethite and hydrogoethite (43,3 –

47,8%) in the FWC is more than in the LWC (12–30%). The SWC is characterized by the highest content of SiO_2(59,2 – 65,6%), K_2O (1,81–3,76%), Rb(198–300 ppm) and the lowest content of Fe_2O_3(1–4,50%). The FWC has the highest content of Fe_2O_3(42,7 – 45,2%), the lowest content of SiO_2(23,50 – 29,86%); Al_2O_3(11,4 – 15,84%), K_2O (0,09 – 0,17%), CaO (0,03 – 0.04%), MgO (0.04 – 0,1%), Na_2O (0,006 – 0,12%), Rb (12 – 40 ppm). The three weathering crust types are not much different in contents of TiO_2(0,55 – 0,92% for the FWC; 0,36 –1,87% for the LWC; 0,43 – 0,79% for the SWC), MnO (0,01 – 0,1%; 0,02 – 0,19%; 0,01 – 0,006%); Pb (20 – 86 ppm; 30 – 80 ppm; 24 – 83 ppm) Cu (61 – 100 ppm; 43 – 86 ppm; 15 – 40 ppm) Zn (35 – 76 ppm; 37 – 137 ppm; 30 – 92 ppm).

There are many mineral resources related to the weathering crusts – kaolin and clays in the SWC and LWC; puzzolite, colour pigment, laterite stone, gold, iron and tin ores in the LWC and the FWC.

The mineralogical and chemical composition, geochemical characteristics as well as the ore–bearing of the weathering crusts depend first of all on the petrographycal type of parent rocks, geomorphological properties and hydrodynamic conditions of the region.

CATHODOLUMINESCENCE AND CHEMISTRY OF PRIMARY, ALTERED AND SECONDARY WILLEMITE FROM THE STERLING HILL ORE DEPOSIT, NEW JERSEY, USA

40.233.H

Emil Makovicky, Institute of Mineralogy, University of Copenhagen, Oster Voldgade 10, DK–1350 Copenhagen K, Denmark and Brian J. Skinner, Dept. of Geology Geophysics, Yale University, 210 Whitney Avenue, New Haven, CT 06511, USA

Microscope studies of cathodoluminescence of different willemite, Zn_2SiO_4, varieties from the Mn–Zn ore deposit of Sterling Hill reveal a complex pattern of cation leaching, metasomatism, replacement and overgrowths which record the post–peak, retrograde metamorphic and hydrothermal history of the deposit.

The primary, high–metamorphic "black willemite" contains on average 1.0 wt % MgO, 4.8 wt % MnO and 2.9 wt % FeO. Primary "red willemite" has 7.2–8.6 wt % MnO, 0.4–1.1 wt % FeO and 0.4–1.5 wt MgO. They are practically non–luminescent because of luminescence quenching by admixtures. On fractures or in swarms of dislocations, "black willemite" contains fine particles of black franklinite. These features fluoresce because MnO and FeO in adjacent willemite has been reduced to 2.5–3.7 wt % and about 1.4 wt %, respectively. Hydrothermally altered willemite and the associated willemite overgrowths luminescence brightly due to MgO contents reduced to traces, MnO to 0.9–1.5 wt % and FeO to 0.3–0.6 wt %.

The clear primary "red willemite" is largely altered along a dense network of fractures, with only 3.0–3.4 wt % MnO, 0.1–0.5 wt % FeO and 0.5–1.0 wt % MgO. Fluorescent zones along individual fractures are only about 8 μm broad. Numerous cavities and

secondarytephroite and red fraklinite are formed. Large veins of secondary willemite are brightly luminescent, sometimes with multiple fine zones of nonluminescent willemite with less than 0.3 wt % MnO or FeO alternating with zones of brightly luminescent willemite with 0.89–2.0 wt % MnO. Associated are cd–bearing sphalerite and franklinite. In the zincite ore, tephroite is the primary silicate mineral; willemite occurs only as brightly luminescent, fine–grained replacement aggregates with 3–4 wt % MnO. The described alterations of black willemite grade from retrograde metamorphic to hydrothermal; those of red willemite do not show clear differentiation. All these phenomena suggest substantial reactivity and even mobility of willemite in retrograde metamorphic and hydrothermal processes.

3.7.

EXPERIMENTAL STUDIES ON PHASE SYSTEMS RELATED TO THE MINERALOGY OF PLATINUM–GROUP DEPOSITS

E. Makovicky, S. Karup–Moller, M. Makovicky and J. Rose–Hansen, Inst. of Mineralofgy, University of Copenhagen, Oster Voldgade 10, Dk–1350 Copenhagen K, Denmark and Danish technical University, DK–2800 Lyngby, Denmark

In the present project supported by the European Economic Community, phase systems were studied that describe and explain the mineralogy of platinum–group elements in magmatic and postmagmatic ore–forming environments. Dry condensed sulphide and arsenide systems Fe–Ni–Pd–S and Pt–Fe–As–S were studied by means of charges annealed for extended periods in silica glass tubes and analysed by reflected–light microscopy and microprobe.

The phase system Fe–Ni–Pd–S was investigated at 900, 725, 550 and 400℃. Sulphide melt is extensive at 900℃. It recedes from the partial system Fe–Pd–S at 725℃ and recedes further towards the Ni–Pd–S boundary at 550℃. At 900℃, PdS and $(Fe,Ni)_{1-X}S$ do not coexist; the assemblage $Fe_{1-X}S$–PdS–melt is stable at and below 725℃. Solubility of Ni in PdS increases substantially with decreasing temperature. Besides Fe–Ni–Pd alloys, important collectors of Pd are $(Fe,–Ni)_{1-X}S$, high–temperature $Ni_{3\pm X}S_2$and $(Ni,Fe)_9S_8$. (Ni, Fe)S_2dissolves up to 1.5 at %Pd at 725℃. Pentlandite associated with alloys contains measurable Pd contents only when alloys have more than 50 at % Pd. The highest Pd contents in pentlandite are observed for alloy–free associations at 550 and 400℃.

The phase system Pt–Fe–As–S was studied at 850 and 470℃. At 850℃, it contains the typical assemblages (1) $PtAs_2$(sperrylite) –PtS–PtFe–$Fe_{1-X}S$, (2) $PtAs_2$–PtSPtFe–(Pt,As)melt, (3) $PtAs_2$–PtAs (platarsite)–PtS–$Fe_{1-X}S$ and (4) Pts–PtS_2–$Fe_{1-X}S$–PtAsS. Solubilit of Pt in pyrrhotite increases from 0.1 at % to 0.5 at % Pt on passing from assemblage (1) to (4). Solubility of sulphur in $PtAs_2$(an important indicator!) increases from about 2.5 at % in (1)to over 15 at % in assemblage (3). At 470℃, pyrite and arsenopyrite appear;neither dissolves platinum. The principal associations are (1) $PtAs_2$–PtS–(Pt,Fe), (2) $PtAs_2$–PtS–$Fe_{1-X}S$–Pt_3Fe and (3) $PtAs_2$–FeAs–Pt_3Fe–FeS.

S–rich regions of the system contain pyrite, pyrrhotite, PtS and PtS_2. Sulphur solubility in $PtAs_2$exceeds 8 at %. However, in association with pyrite and pyrrhotite, $PtAs_2$contains only 5 at % S. Only traces of Pt are found in pyrrhotite at 470℃ . Several applications of our experimental results to natural Pt and Pd associations will be described.

GEOLOGY, GEOCHEMISTRY AND ORE MINERALOGY OF GOLD DEPOSITS IN GRANULITES AND AMPHIBOLITES OF THE QIANXI GROUP, HEBEI PROVINCE, NE-CHINA

P.03.7.

G. Morteani and G. Lehrberger, Technical University of Munich, D-8046 Garching, Fed. Republic of Germany, and Li Zhiliang and Bai Hongsheng, Ministry of Metallurgical Industry, Beijing, P.R. China

In the Yanshan mountains of the Kuancheng and Qinglong County of Hebei province several gold deposits and occurrences are known within the Archean Qianxi Group.
The country rocks are mainly amphibolites and granulites with magnetite layers, which are intruded by later dykes and granites of Proterozoic, Paleozoic and Yanshanian (Jurassic) age.
Syn- and post-Yanshanian tectonic movements caused fracturing of regional dimension forming a block mosaic limited by mainly NE-SW and E-W trending faults.
Gold deposition can be observed only along the post-intrusive fractures and shear zones. The mineralization is regarded to form at a late to post-magmatic stage with a probable maximum age of 190 My, as determined for pre-mineralization granites.
The gold mineralization is mainly found in quartz veins together with pyrite, chalcopyrite, galena and sphalerite. Calcite and fluorite occur as gangue minerals.
Microscopically gold is found rarely as minute inclusions in early pyrite but frequently in fractures of pyrite together with chalcopyrite, galena and sphalerite.
Geochemically gold is clearly correlated with the quantity of sulphide minerals. Particularly an association of high gold contents with high Cu and locally Bi contents is evident. Silver contents in the veins range from 25 to 150 ppm.
Microprobe studies of gold grains show silver contents of 10 to 30 %.
Wall rock alteration occurs along the mineralized shear zones in the amphibolites and the intrusive rocks. Compositional changes in the rocks are used to interpret the type and source of the mineralizing fluids. Fluid inclusion studies to determine the character and temperature of the fluids are ongoing; stable isotope studies of carbonate also provide important informations.

NATIVE GOLD AND ANTIMONY IN THE ORES OF ANTIMONIAL DEPOSITS OF KIRGHIZIA.

S.K. Mustafin, Institute of geology, Academy of sciences of Kirghiz SSR, Frunze, Dzerzhinskogo, 30,720481, Kirghiz SSR, USSR.

The native elements: antimony, mercury, arsenic, gold, silver are known in the ores of antimonial and comlex

antimonial-mercuriferous deposits of the Middle Asia province.
Native gold and antimony have been discovered and investigated in the ores of antimonial deposits of jasperoid type localized in anticline structures formed by Pre-Cambrian marbled limestones and crystalline slates. Native gold occurs as irregular dissemination in quarts of quarts-antimonial ores in the subscreen sheet-like metasomatic jasperoid deposits. Morphology of gold particles is interstitial, the size are 0,01--3 mm. The structures of natural growth, autoepitaxis and epigenetic deformations were discovered by means of the electron-microscopic study.
Native gold of some generations is met in the ores from crosscutting and subconcordant intraformational zones of crushing the schists laying over jasperoids. In early arsenopyrite there was established syngenetic dense (sometimes with the plots of thin filmy aggregates) dissemination of submicronic rounded natural gold particles, decorating the zones of growth of crystals of the mineral-concentrator.
In quartz-pyrite association there are interstitial gold particles in quartz. The sizes of dimensions are 0,01-1 mm., probe is 900-920; the main impurity is silver.
Gold with cloddy and more seldom dendrite-like morphology of the secretions (sizes are 0,05-4mm., probe is 890-900) associated with crystal-like quartz.
In the composition of antimonial ore there are intergrowths native antimony and gold with spongy structure and perhaps formed at the expense of aurostibite decay. Gold has secretions with sizes of 0,05-5 mm. and is characterized with high probe (990-999); antimony is as an impurity there.
Native antimony forms continuous aggregates to 10 sm across and makes up 50% of the mass of quartz-antimonial ore of separate bodies. Antimonite is formed at the expense of sulphurizing the native antimony, that is confirmed by the network structure of replacement. Antimony is characterized with the absence of visible impurities. Native antimony of the 2nd generation is found in the granulated quartz-antimonial ore where it forms dissemination or more seldom veins with thickness of 0,01-1 mm. The formation of this mineral generation is connected with dynamic metamorphism of the ores.
The results of native gold and antimony researched in the complex ores of the antimonial occurrences will be useful enough while solving the problem of mineralization genesis and working out the optimum schemes of ore enrichment and change.

CASSITERITE AND TRIPLITE FROM BERYKUPLI, GOVINDPAL AREA, BASTAR DISTRICT, MADHYA PRADESH, INDIA

P03.8

V.K.Nayak, Department of Applied Geology, Indian School of Mines, Dhanbad 826004, India

In 1973, the discovery of mineralized pegmatites in Bastar District, Madhya Pradesh, Central India, by the State Directorate of Geology and Mining (DGM) and the Geological Survey of India (GSI), upsurged a great interest for potential tim deposit. As a result, several researchers and organisations have contributed on various aspects of the Bastar Tin Province which covers an area of more than 400 sq. kms. During the last one decade information on geology and structure of the area, nature and types of pegmatites, varied mineralogy and genesis of tin deposit has appeared in the literature (Mookherjee et al. 1979; Geological Survey of India, 1983; Singh and Mukherjee, 1985; Babu, 1986, 1989; Lamba and Agarkar, 1988). It is now recognized that the Sn–Nb–Ta–bearing pegmatites are unique and appear to be genetically related with the granitic activity in the area.

This contribution presents the results of polished sections and electron microprobe investigation of cassiterite and triplite collected in 1986 and 1988, from zoned pegmatite, at Berykupli, Govindpal area (18 ° 42′ N : 81 ° 54′ E), Bastar District, M.P., India.

Cassiterite: The examination of polished sections revealed that it contains numerous tiny inclusions of diverse nature and these appear to be optically homogeneous or sometimes consist of two minerals. However, under the electron microprobe they are shown to contain numerous different minerals, most of them far too small to provide reliable analyses. One grain is tentatively identified as Microlite and another grain is most probably Manganotantalite. The other grains contain variable amounts of Nb, Ta, Fe and Mn. Analyses of four cassiterite specimens show varying amounts of Nb_2O_5(0.1–1.65 wt. %), Ta_2O_5(0.86–6.48 wt. %), FeO (0.22–1.35 wt. %) and sometimes traces of MnO (0.05 wt. %).

Triplite: The physical, optical and electron microprobe analyses of two specimens confirm the identity of triplite. The mineral is blackish–brown and sometimes pinkish in colour. The surface is covered with brown material that sometimes shows pitchy lustre and concentric layers of Fe–Mn hydroxides which are considered to be alteration product of triplite itself. The Fe–Mn hydroxides fill the cracks and veins in the mineral. The veins also contain small grains of columbite–tantalite like minerals. Triplite also contains Mn–bearing fluorapatite and different (Fe, Mn) (Nb, Ta)–oxides with traces of Sn and W (0.2–0.5 wt. %). Two analyses of triplite gave respectively:

$P_2O_5$32.1, 32.6, FeO 19.9, 19.7, MnO 39.5, 39.6, MgO 0.07, 0.12, ZnO 0.18, 0.36, CaO 2.09, 2.58, F 8.26, 9.08, Less 0 = F 3.48, 3.82, Total 98,62, 100.22 wt %. This leads to the formulae: $(Mn_{2.50}Fe_{1.24}Ca_{0.17}Mg_{0.01}Zn_{0.01})$ $(PO_4)_{2.03}(F_{1.92}OH_{0.08})$ and $(Mn_{2.47}Fe_{1.21}Ca_{0.20}Mg_{0.01}Zn_{0.02})$ $(PO_4)_{2.03}F_{2.11}$ in both cases with double formula–unit.

Based on mineralogical and chemical considerations of the Sn–Nb–Ta and rare metal pegmatites, a genetic model is proposed and discussed.

3.10-

STUDY ON BOURNONITE FROM YAOGANGXIAN,HUNAN, CHINA

NIU Xinxi, WANG Wenkui, BI Xianmei, China University of Geosciences (Wuhan), Wuhan 430074, P. R. China

Bournonite is a common sulfosalt mineral occurring in hydrothermal veins formed at moderate temperatures, associated with sulfide of Pb, Cu, Zn etc. and quartz. In China, as we know, the only place, where well developed and wholly remained crystals have been found, is Yaogangxian in Hunan province. The present paper provides a significant result of study systematically on the physical and chemical properties and crystal morphology of bournonite crystals from Yaogangxian, by means of optical / electron microscopy, electron microprobe analysis and crystallometry.

Yaogangxian tungsten ore deposit shows a typical "five– floor–building" structure. The bournonite occurred mostly in the 49–501 vein of 16th mining level (820m above sea level), some in idiomorphic and others in massive. Crystals of bournonite were found in geodes of that vein, associated with chalcopyrite, sphalerite, galena, stannite, stibnite, tetrahedrite and jamesonite etc.. It is steel grey to lead–greyish in colour, black–greyish in streak, opaque with metallic luster. Its cleavage (010) imperfect, fracture is uneven, brittle. Microhardness is 159.8 kg / mm^2, and the relative hardness observed from polished surface of section is higher than that of galena. Specific gravity is 5.84. Reflectivity is 16.24% in average at a wave length of 530nμ, smaller than common probably because of the imperfection of polished surface. Chemical composition of bournonite crystal from Yaogangxian measured with EPMA is in table 1. Compared with the composition of bournonite calculated from the ideal formula and others from C. Palache (1946), this is a typical bournonite undoubtedly. The formula derived from these data is $(Cu_{0.9464}Zn_{0.0008}Fe_{0.0012}Ag_{0.0009})_{0.9493}Pb_{0.9347}(Sb_{0.9451}Bi_{0.0057}As_{0.0272})_{0.9780}S_3$. Simplified to $CuPbSbS_3$.

Table 1. the EPMA data of bournonite crystals.

No	Ag	Cu	Sb	As	S	Pb	Bi	Zn	Fe	Total
1	0.070	12.933	24.063	0.402	20.363	41.740	0.411	0.000	0.017	99.999
2	0.006	12.787	24.527	0.574	20.336	41.582	0.192	0.013	0.017	100.034
3	0.002	12.789	25.094	0.332	20.887	40.673	0.160	0.019	0.008	99.964
4		13.01	24.91		19.69	42.40				100.00

Note: 1, a long–prismatic crystal; 2, a granular crystal shown in fig.1; 3, a massive compact; 4, calculated from its ideal formula $PbCuSbS_3$.

Bournonite belongs to orthorhombic crystal system. There are three types of

crystals in Yaogangxian: long–prismatic, short–prismaatic and granular crystals.Some of them twined or / and regularly connected quite complicatedly. Generally, its {hk0} faces striated vertically, (100) and {h0l} faces sometimes striated horizontally,{010} face and {001} faces smooth. Crystallometry shows that,the heavy striated irregular prism faces and (001) are well developed whileother terminal faces seldom occur on long–prismatic crystals usually; on short–prismatic crystals, common prism faces a{100}, b{010},m{110} and terminal faces c{001},o{101},y{111}, n{011} and u{112} generally developed equally and regularly, and twins very common, repeated to complicated aggregates; granular bournonite crystals were almost the same as short–prismatic crystals, only its terminal faces seem to more develop with respect to short–prismatic one.

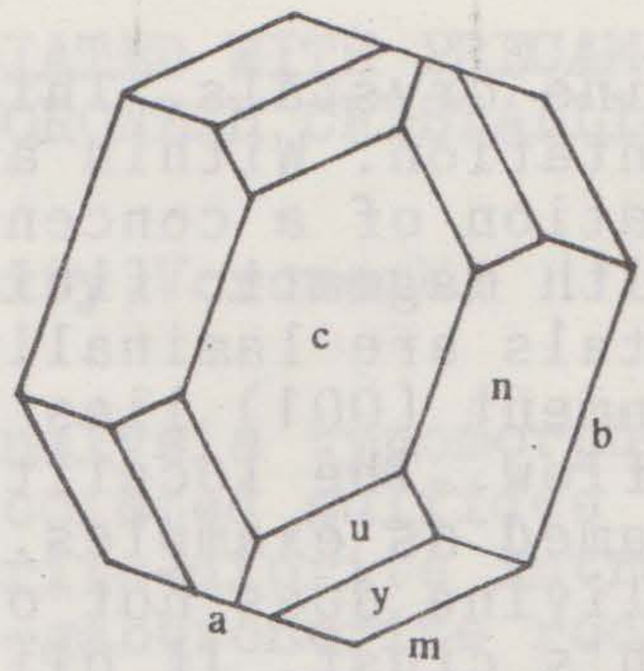

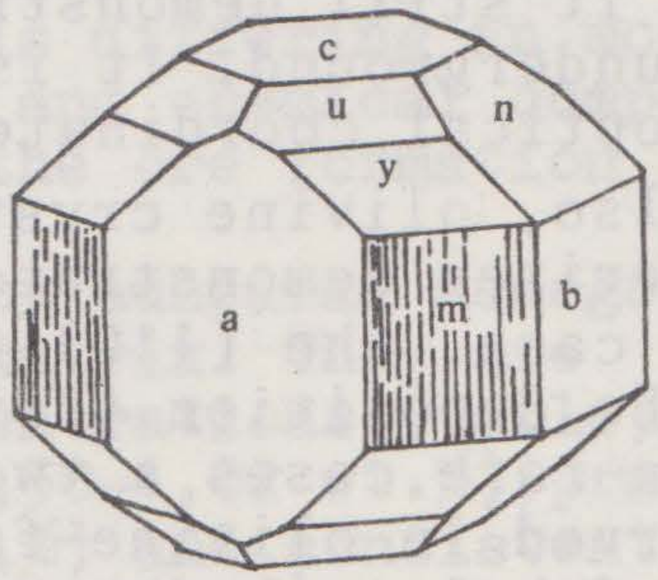

Fig.1 The ideal drawing of a granular bourno–nite crystal.

Fig.1 is an ideal drawing of a granular crystal of bournonite from Yaogangxian showing the development of single forms.

THE FORM OF ORE BODIES IN RESPECT TO THE ORIENTATION OF OLIVINE

3.14.

Paulitsch, P., Institute for Mineralogy TU Darmstadt,

During the last few years, we have analysed the preferred orientation of olivine in various paragenesis by optical methods, using the x-ray texture goniometer, as well as the x-ray universal stage (developed in the Darmstadt Institute) and the electron microscope.Olivine demonstrates great diversity in its orientation in relation to magmatic lamination.

1. The orientation of the crystal face (010) - parallel lamination - is widespread. This orientation is also found in basalt nodules. Because of this widespread distribution in shists as well as in basalt nodules and peridotites, this type can be designated as "Durchläufer"-fabric; PAULITSCH, (1979).
2. The crystal faces (010) of pure metamorphic olivine rocks from the Alps, New Zealand and Japan form an (ac)-girdle with the rotation axis as a folding axis.
3. Occasionally there is a recrystalization of the

olivine crystals. This is depicted in a new type of orientation. Within an (ac)-girdle this results in the formation of a concentration in (HOL)of the peridotite.
4. With magmatic fluid olivine fabrics, the olivine crystals are laminally formed to (010); the crystal alignment (001) lïes in most cases in the direction of the flow. The localities Skaergaard and Stillwater can be named as examples.
5. Olivine does not only appear as a mineral in the earth's crust. If olivine comes from the earth's mantle, it still demonstrates a relict orientation from the underground. It is the preferred orientation of the optical coordinate N-gamma.
6. Also, olivine crystals which have been found in meteorites demonstrate a particular orientation. In this case, the (110)-faces lie parallel to the plane of the deposition (Keil, USA.).
7. In rare cases a two-crystal position has been observed in olivine-fabrics. There then exists a twin-fabric, (Ladurner, 1956, Turner 1942).
8. In peridotites from Norway, there occur both horizontal as well as verticale fold axes. In isolated rocks, both fold axes are present at the same time (Ekremsäter, Norway). In addition, there are also olivine girdels which are at an acute angle to each other (Aalesund).
Therefore, at least 8 types of olivine orientation can be shown whose formation can be associated to the mantle, the crust and meteorites.
The shapes of chromite ore bodies are connected to these observed types of olivine orientation. They can be differentiated accordingly: 1) parallel (ab) layered chromite bodies, 2) (ac)-chromite bodies which are perpendicular to the fold axis (Clar, Hiesleitner, 1948) and 3) chromite layers which cross the magmatic layering at an acute angle (Paulitsch, 1953) Anghida, Greece.
The different geometry of ore bodies is also connected with a different chemical chromium concentration. The amount of chromium content in (ac) layers is higher than in (ab) layers. Analogous connections to further deposits for iron and titanium are also known.

Determination of the Orientation of Olivine Using the Electron-Microscope-Universal-Stage.- Texture, Vol. 1, p. 209, 1974: Doering, E. & Paulitsch, P.

Olivingefüge.- Fortschr. d. Min., Bd. 57, 1979: Paulitsch, P.

CHROME-SPINELS IN SULFIDE ORES ASSOCIATED WITH PRECAMBRIAN NORITE-DIORITE INTRUSIONS OF VORONEZH CRYSTALLINE MASSIF (EUROPEAN PART THE USSR)

A.N.Plaksenko, Voronezh State University, Voronezh, 394693, USSR

By means of electrone microprobe analysis typomorphic features of chrome-spinels and associated sulfides from nickel-cobalt ores-related to norite-diorite intrusions of early Proterozoic peridotite-gabbronorite rocks of Voronezh Crystalline Massif have been ivestigated.

Three generations of chrome-spinels differing in morphological features, internal fabric and chemical composition related to certain stages in the ore formation process have been distinguished.

Chrome-spinels 1 are represented by euhedral homogenious octahedra enclosed in sulfide matrix. They are characterized by unusually high concentrations (table) of Cr_2O_3(59,81-63,42 wt.%), low MgO(0,30-1,82 wt.%), practical absence of Al_2O_3(0,00-0,08 wt.%) and consistent trace amounts of MnO(0,75-2,22 wt.%), ZnO(1,02-1,69 wt.%) and V_2O_3(1,79-2,43 wt.%), which reliably differ them from accessory chrome-spinels inmineralized norites. Specific fea ture of their internal fabric is constant occurence of idiomorphic sulfide inolusions, represented by assamblayes of phyrrotite or phyrrotite-pentlandite, reraly, phyrrotite-chalcopyrite. All these facts lead the authors to the conclusion of chrome-spinels to have crystallized directly hrom an oxide-sulfide melt, what is in full agreement with liquation-magmatic genesis model of sulfide ores associated with norite intrusions.

Chrome-spinels 2 are representel by anhedral grains intergranular to large sulfide aggregates often in association with sulpharsenides and devoid if sulfide inclusions. From spinels 1 they differ by notably lower contents of Cr_2O_3(43,61-56,01 wt.%) and MgO(0,20-0,83 wt.%) and higher contents of Al_2O_3(7,50-11,88 wt.%) and ZnO (2,18-4,48 wt.%).

Chrome-spinels 3 occur exeptionally as rectionary rims around silicate grains enclosed in sulfide matrix. Specific feature of their composition is further depletion in Cr_2O_3(38,80-40,26 wt.%) and considerable enrichment in Al_2O_3(19,75-20,87 wt.%) and ZnO(6,07-6,22 wt.%).

The anthors consider the origin of crome-spinels 2 and 3 to be the result of metamorphic recryslallization of primary sulfide ores and the origin of spinel phase on the sulfide-silicate boundary is determined by the reactionary interaction processes between the latter two which lead to the formation of excessive Al and Zn diffusing from silicate and Cr and Fe - from sulfide.

Thus, the data obtained concerning the variability in morphological types and chemical compositions of spinels

in the sulfide ores suggest that the latter were formed as a result of complex multistage processes including magmatic (major) and metamorphic (secondary) stages in ore genesis.

Table

Electron microprobe analyses of typical chrome-spinels from sulfide ores

Component	Generations 1	2	3
TiO_2	0,02	0,8	0,03
Al_2O_3	0,06	7,50	20,73
Cr_2O_3	60,50	52,09	39,80
Fe_2O_3	5,60	5,56	3,61
FeO	28,82	27,46	28,82
MgO	0,80	0,30	0,32
MnO	0,95	0,72	0,00
ZnO	1,51	3,85	6,12
V_2O_3	1,82	0,93	0,46
NiO	0,03	0,10	0,00
CoO	0,09	0,09	0,00
Total	100,20	99,40	99,89

A.A.Sliouniaev,Laboratory of Mineragraphy,IGEM Academy of Siences,Moscow,109017,USSR

DISTRIBUTION AND CHEMICAL STATE OF GOLD, SILVER AND ADMIXTURES ON THE NATIVE GOLDMSURFACE.

R.A.Amosov, Yu.V.Schegolkov, V.Sh.Ivanov. TCNIGRI, Mingeo, Moscow, Warshavskoye sh.,129 B, 113545 USSR.

The X-ray photoelectron spectroscopy (XPS) has shown that silver accumulates in the near-surface layer of native gold from primary ore deposits and it has been confirmed that silver content commonly decreases on the surface of gold grains from weathering crusts and oxidation zones /1/. The AES and SIMS methods permitted to identify O, C, S, CI, B, F, Mg, Al, Na, Ca, K on the surface of primary and placer gold. The O and C being adsorbed from the atmosphere, as is supposed, while chemical state of the other elements is not discussed /2/. We recorded Auger- and XP-spectra of several dozens gold grains from primery and placer deposits as well as Auger-spectra of 14 reference gold-silver alloys. For analysis of element distribution scanning and ion bombardment have been applied. The principal results are as follows.

1. For the reference alloys having composition between 95%Au+5%Ag and 5%Au+95%Ag a linear relationship

between fineness and value H69eVAu/(H69eVAu+H351eVAg) intensity ratio has been established. This allows to assay native gold within the whole range mentioned above without using element sensibility coefficients.
2. The O, S, Ag, Fe, C, Al, Pb, Hg, Te have been identified on the surface of placer gold. A lateral distribution of these elements is homogenous (for O, S,C) or discrete - in form of circular, elliptical and ring islands. A successive scanning of one portion of the surface in characteristic emission of the elements identified by spectra allows to determine morphology of individual phases and their provisional composition by coincidence of the areas of concentration of different elements, such as silicon and oxygen (SiO_2), aluminium and oxygen (AlOOH?), mercury and sulfur (HgS) and so on. The determination of AuC_xS_y and $AgAl_xO_y$ phases seems to be most interest indicating the Au and Ag separation in hypergene conditions. The growing mineral phases have distinct boundaries and assotiate with mechanical substrate defects such as slip lines originating during transit. In the periods of burying placer gold in intermediate collectors thin layers of iron oxide precipitate on the gold surface thus preventing from nucleation of other mineral phases. In particular, mercury sulphide incrustations are selectively developed on the gold particles free of iron oxide.
3. The primary gold surface contains a relatively small set of admixtures. A permanent presence of sulphur, oxygen and carbon, sometimes, iron is recorded; their lateral distribution is commonly homogenous.
4. To specify chemical state of gold the Auger-spectra of synthesed gold sulphide, oxide and chloride have been analyzed. When comparing metallic and native gold spectra with those of gold compounds, some peculiarities of detailed peak structure were recorded that allowed to suppose chemically bound state of part of gold in primary deposits: there is a difference between primary and metallic gold in ratio of peak altitudes in NVV-doublet and detailed structure of peaks in the 140-170 eV interval.

References

1. Nefedov V.I., Zavoroncov N.M., Matchavariany G.V. a.o. Surface, 1982, N4,p. I44-I49.
2. Petrovskaya N.V., Aleshin V.G., Novgorodova M.I., Nemoshkalenko V.V. Dokl. Acad.Sci.USSR, 1987,N5, p.1241-1244.

THE PETROLOGY AND MINERALOGY IN A TIN–DEPOSIT RELATED WITH ALKALI– GRANITE IN EASTERN JUNGGER, XINJIANG, CHINA

Shen Xiangyuan, Bi Chengsi, Xu Qingsheng, Institute of Mineral Deposits, Chinese Academy of Geological Sciences, Baiwanzhuang Road 26, Beijing 100037, China

The tin–deposit discovered lately located in the west part of Eastern Jungger district, Xinjiang, China. The ore bodies lie in a riebeckite–granite. By means of the research of the petrology and mineralogy for this granite and tin deposit, it is confirmed that the deposit is closely related with alkali–granite. There is an assemblage of cassiterite, quartz, riebeckite. hematite and magnetite which appeared hardly ever in nature, and it could be no report on this type of the association till now.

The chemical composition of this riebeckite–granite is characteristic by high SiO_2, enriched in alkali, $K_2O > Na_2O$, poor in CaO and MgO, lower in $Al_2O_3$and TiO_2, $(K_2O+Na_2O) / Al_2O_3 = 0.997$. The graphic, granophyric and myrmekitic structures made by alkali feldspar and quartz are developed well. A small amount of metapegmatite appeard incompletely in the granite. Major rock–forming minerals determined under microscope are quartz(38%). perthite(18%), albite($Or_{0.5}Ab_{99.5}$, 6%), K–feldspar($Or_{95}Ab_5$, 29%), the microcline with quadrille structure(4%), The triclinicity($\triangle_{131}$) of K–feldspar is 0.879. The order degree (δ) is 0.8, They are maximum microcline. There is no plagioclase in the granite. Mafic minerals(1–1.5%) are mainly riebeckite and aegirine, in general they are tin–bearing. The main accessory minerals are composed of orvillite, sphene, hematite, magnetite, fluorite , cassiterite and rutile etc. According to QAP classification, it is alkali–granite for all plotted points gathering near or on the QA line. Its abundance of the trace elements were determined: Sn(12ppm), Pb, Bi, F, are on the higher side, also the bigger cations Zr, Ga(22ppm) and rare earth elements.

The mineralogical and petrological charactristics involved in all above are simillar of Kuiqi alkali–granite, Fujian, China, the A–type granite in Australia and the anorogenic alkali–granite in Africa.

The mineral composition in the tin–deposit is close to that in the riebeckite–granite, but it is quite differ from other type of tin–deposits. The ore mineral assemblage is simple, the major is cassiterite and hematite, the second specularite and magnetite, and it could be seen that some stokesite and hydro–cassiterite are around the cassiterite. There are less sulfide in the ore, such as chalcopyrite, pyrite, chalcocite, bornite etc. In the gangue minerals, quartz is over 90%, the next is riebeckite, aegirine, a few flourite, sericite, tuhualite and rutile etc. The content of the riebeckite and aegirite in ore is about 1%–5%, both of them are tin–bearing minerals, their Sn–content is about 10–20 times higher than that in these two minerals from granite.

The ore has banded, lumpy and ring–like structure. In the section, it is much obvious that cassiterite is in the center of the band, hematite is mixed with cassiterite or filled in the broken cassiterite, the riebeckite and aegirine are around cassiterite

Table: The average content of SnO_2(%) in riebeckite and aegirine measured with electron microprobe

occurrence	in granite	in ore–vien
riebeckite	0.03 (n = 3)	0.68 (n = 2)
aegirine	0.22 (n = 1)	1.82 (n = 2)

and hematite, the aegirine is replaced by riebeckite, and quartz is in the most outside. Therefore the forming sequence of the minerals is cassiterite–magnetite–hematite–quartz–aegirine–riebeckite–quartz. The hematite is acicular and foliated aggregate. The hematite and magnetite had several forming ways including both replacement and cavity filling: (1) residual magnetite in the hematite, (2) pseudomorphous hematite, (3) lattice replacement hematite in the magnetite, (4) hematite pellets in the hematite vein. It indicates that the fugacity was higher at first , then turned into lower in the mineralization.

There are abundant inclusions with lower gas / liquid ratio in the quartz from the ore–bearing veins. The ore–forming fluid composition is K^+–Na^+–Cl^- (F^-) type. The homogenization temperature of quartz is 334℃ (270–400℃). The decrepitation temperature of the cassiterite is 409℃ (375–475℃) (without pressure correction). The saltness (measured with freezing method) is lower, about 3.4%(0.2–6.4%), the density about 0.6–0.68g / cm^3. Thus the mineralized fluid is a kind of fluid which has higher temperatute, lower saltness and density.

DETERMINATION AND SIGNIFICANCE OF MICROINDENTATION HARDNESS OF PYRITES EXPERIENCED DIFFERENT DIAGENETIC AND METAMORPHIC GRADES IN TWO SULPHIDE DEPOSITS OF INDIA.

3.2.P

K.L. Shrivastava, Department of Geology, Faculty of Engineering, University of Jodhpur, Jodhpur, 342 001, India.

In the present study, microindentation hardness of pyrite samples collected from a wide and graditional range of geological conditions covering early diagenesis to high grade metamorphism at Amjhore pyrite deposit and Rajpura-Dariba polymetallic sulphide deposits of India have been presented to establish a relationship of Vicker Hardness Number (VHN) with the increasing grades of diagenesis and metamorphism.

The most common VHN determination method have been employed using Vickers indenter on polished pyrite surface under reflected light microscope and calculations made on the basis of indentation. To minimise the errors by variations in load and time applied, mineral texture, orientation, composition, bound strength and unit cell relationship; each category of pyrite sample has been

determined as many as 75 ± 5 times with fixed 15 second duration of loading and loads of 100 gf and 200 gf for half and rest of the half samples respectively. The average values so determined have been taken into consideration for each category of samples.

In sedimentary Amjhore deposit, the globular and framboidal pyrites from carbonaceous shale layers, massive pyrite from thick pyrite layer in carbonaceous shale and massive pyrite also cemented with secondary pyrite from pyrite bed stratabounded within carbonaceous shale showing VHN 850, 1153 and 1235 respectively. In Syn-sedimentary metamorphosed polymetallic Rajpura-Dariba sulphide deposit, the pyrite samples collected from mildly metamorphosed calc-silicate rock, garnet-graphite-mica schist, coarse diopside vein in calc-silicate rock and kyanite-graphite-mica schist demonstrated the VHN as 1032, 1265, 1480 and 1530 respectively.

It is concluded that in general, the results show a directly proportional relationship of VHN with the grade of diagenesis and metamorphism of pyrite samples encountered. The sudden decline in the VHN at the initial stage of metamorphism, an exception to the above generalization has probably occurred because of accompanying recrystallization at this stage, which may release the stored energy. However, metamorphism too, in rest of the stages, leads to substantial hardening as advances to the higher grades.

Po3.11.

GEOCHEMISTRY, RB-SR AND OXYGEN ISOTOPIC COMPOSITION OF YANSHANIAN GRANITOIDS IN THE ANJIAYINGZI GOLD DISTRICT, INNER MONGOLIA, P.R. CHINA: CONSTRAINTS ON THE AGE OF MINERALIZATION

R.B. Trumbull, Technical University of Munich, D-8046 Garching, Fed. Republic of Germany
M. Satir, Institute of Geochemistry, University of Tübingen, Fed. Rep. of Germany
Sun Qizhen and Quo Deyou, Ministry of Metallurgical Industry, Beijing, P.R. China.

The Anjiayingzi gold district of southern Inner Mongolia is located in a fault-bounded uplift cored by late Archean metamorphic rocks and Yanshanian (late Mesozoic) granitic plutons. Most of the gold production comes from polymetallic sulfide-quartz veins associated with fracture zones within the Yanshanian Jiguanzi granodiorite. The Jiguanzi pluton intrudes the much larger Kalaqin granite, which is also assigned a Yanshanian age. Although the same structures occur in both granitoids only the Jiguanzi hosts important gold deposits.
Porphyritic rhyolite dikes cut both granitoids along the same fracture system as the mineralized veins. The dikes are pre- or syn-mineralization.
This study of the geochemistry and Rb-Sr, ^{18}O-^{16}O isotopic composition of the

Kalaqin and Jiguanzi plutons and rhyolite dikes seeks to clarify the age of the mineralization and the origin of the host granitoids.
The following results were obtained by the Rb-Sr whole-rock method; for the Jiguanzi granodiorite whole rock and mineral data (K-feldspar and biotite) were combined.
Kalaqin granite: 164 ± 6 Ma; $(^{87}Sr/^{86}Sr)_i$ = 0.7063 ± 9; MSWD = 1.55
Rhyolite dikes: 122 ± 1 Ma; $(^{87}Sr/^{86}Sr)_i$ = 0.7061 ± 4; MSWD = 0.53
Jiguanzi granodiorite: 128 ± 1 Ma; $(^{87}Sr/^{86}Sr)_i$ = 0.7057 ± 3; MSWD = 2.2.
These data confirm the Yanshanian age for the granitoids, and show that there were clearly two phases of magmatism. The initial $^{87}Sr/^{86}Sr$ ratios of all three granitoids are nearly identical at 0.706. The rocks are considered to be juvenile; they cannot have originated by partial melting of the Archean basement, which contains significant granitic components.
The gold mineralization is related to the younger of the two magmatic events. Its age is less than or equal to 122 Ma, which is the age of the penecontemporaneous rhyolite dikes. This age is confirmed by single mineral ages of 123, 120, and 118 Ma for K-feldspar from intensely mineralized and altered zones in the Jiguanzi granodiorite.

Unaltered samples of the Jiguanzi granodiorite have del ^{18}O values of 7.9 - 8.1 per mil. Samples adjacent to mineralized zones and those near the pluton contacts are depleted in ^{18}O by up to 5 per mil.
All rhyolite samples are strongly depleted in ^{18}O, with a range in values from -0.5 to 5.2 per mil. The depletions are attributed to hydrothermal alteration associated with the mineralization.
The unaltered Kalaqin granite has del ^{18}O values of 7-8 per mil. Depletions in ^{18}O of up to 5 per mil at the contact with the Jiguanzi granodiorite are attributed to hydrothermal alteration associated with intrusion of the latter pluton.

TYPES OF SURFACES OF ALLUVIAL GOLD IN THE EASTERN RHODOPES

Po 3.12

Vendulka Tsvetkova-Goleva, Geological Institute of Bulgarian Academy of Sciences, III3 Sofia, Bulgaria

Alluvial nuggets from sediments and bed rocks of Kulidjick river are studied with SEM and electron microprobe analysis.
The area of drainage includes two different fields of supply: Paleogenian dreccia-conglomerates (left tribularies) and old phillites and gneisses (right tribularies).
A high fineness of gold is establisched - 87-90 % of material more than 850 and 27 % more than 972.
The schape, frequency and content of nuggets in the

sediments from the two areas are similar. There is a considerable change in the content of Cu and Hg which predominates in the nuggets from the left tribularies.

The main differences can be distinguisched from the features of the nugget's surfaces. The types can be summarised in the following groups:

I. Phenomena connected with marks of mecanical influences - grooves, trails and imprints (simple and complicated),all of them with (or not) crystal growth.

2. Corrosion surfaces - listen-like, mushroom-like or lump-like surfaces with (or not) crystal growth.

3.Growths with idiomorphic crystals: cubes, octaedres and cubeoctaedres, globules, spirals and fern-leaves.

4. Strongly variated surfaces with pits, holes with different size and debth connected (or not) in chaines, craters, fissures and typical shears of joint.

The types 1 - 3 can be observed on the nuggets surfaces on the two areas. The typ 4 is spreaded in the nuggets from the metamophic rocks.

On the basis of this data an attempt is made to use the peculiarities of the nugget's surfaces to reach a conclusion about genesis, transport's conditions and diagenetic modifications of the alluvial gold.

3.5P

PYRITE - PYRRHOTITE RELATIONSHIPS IN NATURAL AND SYNTHETIC SYSTEMS : SOME NEW OBSERVATIONS.

David J. Vaughan and Alistair Lennie, Department of Geology, The University, Manchester M13 9PL, England; James R. Craig, Department of Geological Sciences, Virginia Polytechnic Institute and State University, Blacksburg, Va 24061, U.S.A.

Pyrite - pyrrhotite relations are very important in defining conditions of formation in sulfide ore deposits, but are only well characterized at higher temperatures. A critical

examination of the existing experimental data has been undertaken and preliminary new data acquired from electrochemical measurements. Both published data on composition and structure of naturally occurring pyrite - pyrrhotite assemblages, and new determinations from a wide variety of deposits, have been collated so as to employ these data as the results of "natural experiments". In particular, coexisting pyrite porphyroblasts that have grown in contact with pyrrhotite during retrograde cooling of metamorphosed massive sulfide deposits preserve evidence of the changing compositions of coexisting phases as a function of temperature. Compositional gradients have been recorded in hexagonal pyrrhotites from deposits such as those at Ducktown, Tennessee, with increasing distance from large (> 10 cm) pyrite porphyroblasts. The compositional variations reach up to 0.3 at % Fe over distances as great as 30 mm and also provide insight into the diffusion processes operative in this system.

A CRYSTAL DRAWING OF JAMESONITE, DACHANG, GUANGXI

WANG Wenkui, NIU Xinxi, China University of Geosciences (Wuhan), Wuhan 430074, P. R. China

19:4P

English mineralogist R. Jameson discovered jamesonite in Cornwall, 1820. As for crystal with remarkable faces is so rare, that no reliable drawing of crystal form recongnized during the past 170 years. In 1914, Slavik worked on this problem and gave one drawing of top view. But V. Goldschmidt wrote in 1918 and 1928 that Slavik's work is questionable.

Great quantity of jamesonite occurred in Dachang tin deposit as prismatic and hair–like aggregates. Three grains of jamesonite crystal with rather good faces are found, and one of them has been studied in detail as the following.

1. Chemical composition:

$Pb_{4.016}(Sb_{5.594}As_{0.275}Sn_{0.115}Bi_{0.002}In_{0.002})_{5.983}(Fe_{0.860}Mn_{0.005}Zn_{0.016})_{0.881}S_{14}$

2. X–ray powder diffraction data:

4.080(34), 3.841(33), 3.709(16), 3.425(100),3.088(27), 2.950(20), 2.722(34).

3. Physical properties:

Steel grey, short prismatic, metallic luster, and opaque. Microhardness (HV) 113kg / mm^2, calculated as Moh's hardness 3.3. Practical specific gravity is 5.53.

4. Data of goniometry:

Monoclinic; prismatic–2 / m.

$a : b : c = 0.81021 : 1 : 0.20908$, $\beta = 91^\circ 52.5'$

$p_0 : q_0 : r_0 = 0.25806 : 0.20897 : 1$

$r_2: p_2: q_2 = 4.78538 : 1.23491 : 1$, $\mu = 88^\circ 7.5'$

$p_0' = 0.25820$, $q_0' = 0.20908$, $e' = 0.03274$

5. The practical and ideal crystal drawing of jamesonite is shown in fig. 1 a and b respectively.

The crystal drawing of jamesonite occurred in Dachang fills the blank of crystal form in the world mineralogy, since the discovery of the mineral 170 years ago.

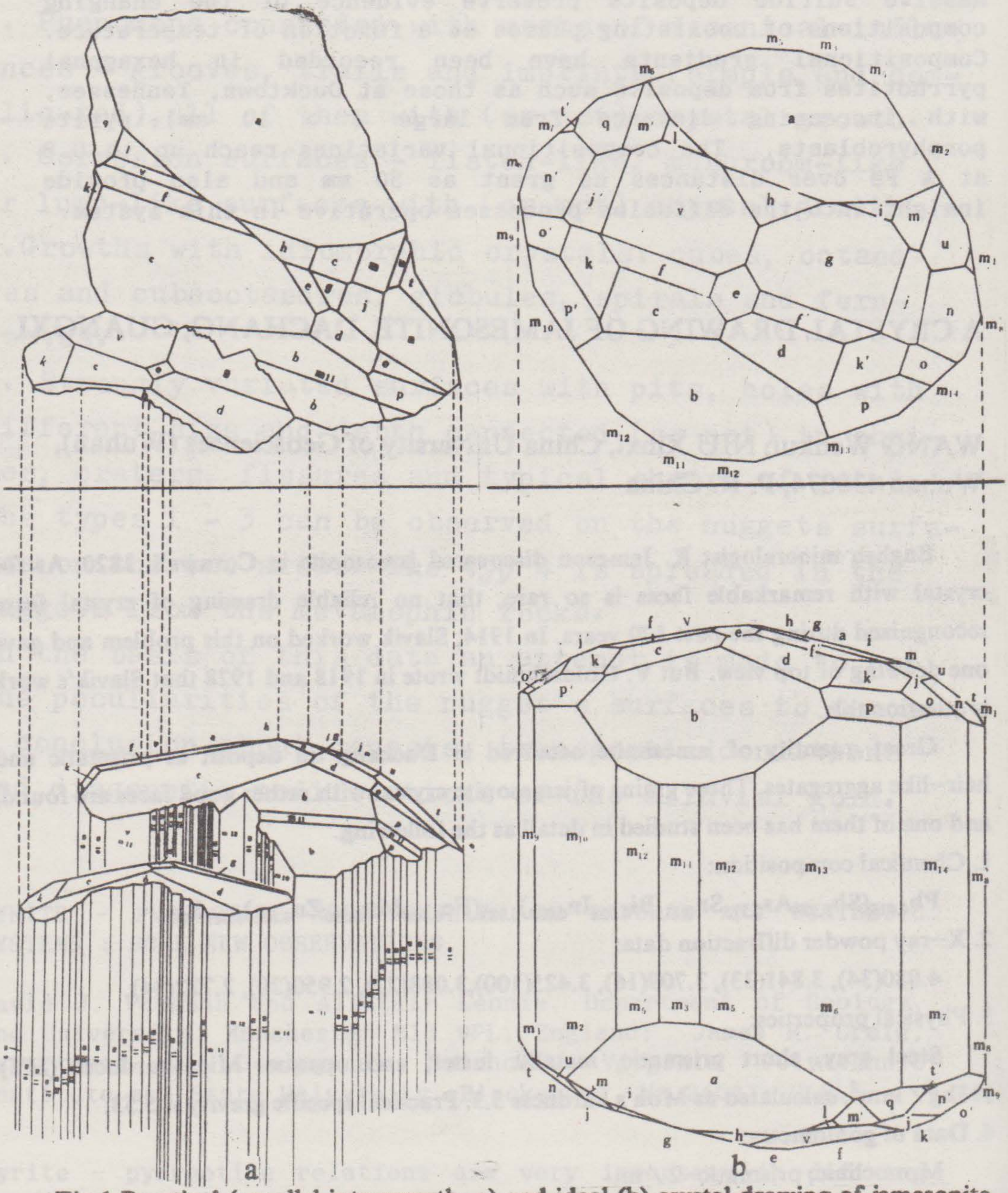

Fig.1 Practical (parallel intergrowth, a) and ideal (b) crystal drawing of jamesonite, Dachang, Guangxi, China.

STUDY ON THE EXPERIMENT OF MIGRATION AND DEPOSITION FOR LEAD–ZINC IN QINGCHENGZI LEAD–ZINC ORE DEPOSIT IN LIAONING PROVINCE

Wang Yu, Tianjin Geological Academy of the Ministry of Metallurgical Industry, Tianjin 300061, People's Republic of China

Some rules of migration and deposition of lead–zinc in Qingchengzi lead–zinc ore deposit have been reserched with the high–pressure and temperature experiment. Onthe basis of the geological environment of the ore deposit. experiment conditions are selected. By means of studying on the physic–chemical conditions of ore formation, the temperature, pressure, PH–value and ore–forming component in ore deposit have been ascertained. The samples of galena and sphalerite were gotten from Qingchengzi deposit. The mono–hole high–pressure caldron made of titanium–steel was used for experiment.

We can get some conclutions from the experiment:

1. When pressure and PH–value are not changeable the solubility of galena and sphalerite increased with the rising of the temperature.

2. As temperature, pressure and PH–value are constant, the solubility of lead and zinc has been raised along with the concentration of the medium.

3. When temperature, pressure and medium concentration are constant the solubility of galena and sphalerite is very low in alkaline solution. the solubility rised as the PH = 5.5 in acid solution, and when PH–value is 3.1 the solubility of lead and zinc grows quickly.

4. The solubility of lead–zinc is lower in certain extent when some $CaCl_2$ and $MgCl_2$ is added into solution.

The experiment in solubility of galena and sphalerite shows that activation is controlled by such factors as temperature, concentration and PH–value of the medium. Higher temperature and medium concentration, lower PH–value are favorable for activation and migration of lead–zinc, conversely, favorable for deposition and concentration of lead and zinc. The inclution composition shows that the major anion in the ore–forming fluid is Cl^-, so that lead and zinc in it are transported in the form of chlorite complexes.

The mechanism of migration and deposition for lead and zinc has the lead and zinc geochemical characters, the complex thermordynamic properties of lead and zinc, and the principle of solubility product, besides, carbonate rocks which contain many calcium and magnesium ions influence deposition of lead and zinc in some extent.

Po3.13

STUDY ON A KIND OF UNDEFINED MINERAL WITH PERFECT CRYSTAL MOR-PHOLOGY(WE TEMPORARILY CALL IT CHENXIANITE FOR CONVENIENCE.)

WEI Tiejun, Committee Policy & Legislation Department of Ministry of Geology & Mineral Resources,Beijing 100812,P.R.C.
WANG Wenkui,China University of Geosciences,Hubei 430074.

1. Geological occurrence

Chenxianite occurs in the oxide zone of Fe,Mn-multimetal deposit of Manaoshan,Chenxian,Hunan,China. The authors first discovered it in 1987.

2. Chemical composition

Chenxianite is studied with SEM,electron probe and chemi-cal analysis.The chemical analysis result is:MnO_2(59.61),MnO (18.44),PbO(7.91),ZnO(0.6),CuO(0.003),Al_2O_3(3.95),Fe_2O_3(0.29) H_2O^+(7.05),SiO_2(1.01),MgO(0.12),CaO(0.24),Na_2O(0.05),K_2O(0.29) TiO_2(0.007),BaO(0.28).The calculated crystallochemical formula is $AlMn_3Mn_8O_{16}(OH)_9$.

3. Crystal morphology

Crystal angle measurement of chenxianite by use of perfect grain(1-2mm in size) gives its convincing crystal morphologi-cal drawing and constant(P_0=1.0662,C=0.9234,ρ_1=61.5°,ρ_{10}=46.6°). Chenxianite is belong to trigonal scalenohedral class D_{3d}-3m($L^3 3L^2 3PC$); its monomorphisms are : r{$10\bar{1}1$},e{$01\bar{1}2$},s'{$06\bar{6}1$}, a{$11\bar{2}0$},m{$10\bar{1}0$}.

4. Cell parameter

The powder diffraction data: 7.532(20),3.975(30),3.427(19) 2.963(61),2.528(100),2.100(50); cell parameter : a=8.73762, c=8.09093(Å),Z=1.

5. Physical character

Chenxianite has brown black colour, brown streak, metal lustre,density of 3.55,hardness of 2.75-3.39,{$10\bar{1}1$} cleavage.

6. Others

The authors also studied it with reflecting microscope, infrared spectra and differential thermal analysis.

7. Initial conclution

Chemical composition of chenxianite is definite and its cell parameter is convincing; its results of our measurements are completely new up to now.We temporarily name this undefin-ed mineral as "CHENXIANITE" according to its place of origin and shall further study it .

REFERENCE : WEI Tiejun,1989,Study on Mineralogy of the Oxid-ized Manganese Deposits in Hunan Prov.& Guangxi Zh.N.A.R.with Expecially Experiments of Mineral Crystal Growth (A thesis for M.S.degree in geology,China University of Geosciences)

THE PHASE RELATIONS IN THE SYSTEM $Ca(Nb,Ti)_2O_6$-$Ce(Nb,Ti)_2O_6$-$Y(Nb,Ti)_2O_6$

Wu Daqing and Diao Guiyi, Guangzhou Branch, Institute

of Geochemistry, Academia Sinica, Wushan, Guangzhou 510640, People's Republic of China

The phase relations in the system $Ca(Nb,Ti)_2O_6$-$Ce(Nb,Ti)_2O_6$-$Y(Nb,Ti)_2O_6$ at 850°C were investigated with the boric acid flux techniques. The powdered CeO_2, Y_2O_3, TiO_2, Nb_2O_5 and $CaCO_3$ with better than 99.9% pure were choosed as starting materials and the chemical reagent H_3BO_3 were used for salt flux. The ratio of atoms Nb/Ti was maitained to 1 in all synthetic samples. Five mineral phases were found in this system: fersmite, aeschynite, euxenite, β-fergusonite, and rutile. Aeschynite and euxenite have a limited ranges of solid solutions. About 15at.% Ce can be replaced by atoms Ca and Y in aeschynite solid solution. Meantime, about 20 at.% Ce and 45 at.% Ca may dissolve in euxenite solid solution by substituting for Y atom. In the B-sites of crystal aeschynite and euxenite, the occupany of the titanium atoms is no more 0.78 and 0.62 atoms, respectively. The deviation of occupany value from the theoric value may implicate that about 13-15 at.% of total cerium was ceric ion Ce^{4+} in synthetic aeschynite, Under microscope synthetic aeschynite is tabular rectangular crystals with brown color, and euxenite and fersmite are transparent crystals.

MINERALOGICAL STUDY OF DICKITE IN FENGDONGYAN, SONGYANG, ZHEJIANG PROVINCE IN CHINA

YANG Xianzhong, Nan jing Institute of Geology and Mineral Resources, 534 East Zhongshan Road, Nan jing, Jiangsu 210016, People's Republic of China

The dickite ore deposit in Fengdongyan. Songyang, occurs in upper Jurassic crystal–vitric tuff of the fouth layer of "a" Member, Moshishan Formation (Jm^{a-4}). The ore body is apparently controlled by fault structure and occurs in stratoid, lenticle and vein shape. The ore with pale–blue, yellowish–pink, grey and yellowish–white displays dense texture and massive structure. The ore consists mainly of dickite, mixed–layer

dickite–kaolinite, quartz, and minor kaolinite and hematite. Based on characteristic features of ore body and mineral assemblages, it is suggested that the dickite ore is formed in hydrothermal alteration. The forming temperature of the ore is about 110–114℃, not exceeding 160℃ (Chen Yunqing, 1984; Janet Hoffman et al., 1979).

Six dickite samples studied in this paper were collected from Fengdongyan dickite ore deposit. Based on study of micromorphology with polarized microscope, scanning electron microscope and transmission electron microscope, and also based on chemical determination and spectral analysis (including X–ray diffraction, differential thermal analysis and infrared spectroscopy) for the dickite samples, some conclusions have been drawn.

1. The ore of the Fengdongyan deposit is composed predominantly of three minerals which form three mineral assemblages: 1)pure dickite; 2)dickite+disorder mixed–layer dickite–kaolinite; 3)dickite+quartz.

2. In polarizing microscope, the dickite commonly presents fine scale shape, perfect (001) cleavage and displays the first grade grey of interference color and inclined extinction. In scanning electron microscope, it usually has pseudohexagonal plate shape with clear outline.

3. Mixed–layer dickite–kaolinite is discovered. It displays fan–like myrmekite shape in polarizing microscope and presents banana–like shape in scanning electron microscope. On the spectral chart, it also shows some characteristics. It is, therefore, considered that the mixed–layer dickite–kaolinite might be intermediate, product formed in transforming process of kaolinite to dickite (Ren Leifu, 1988).

4. The relation between crystallinity (HI) (Hinckley, 1963) and total iron content (X, %) of the dickite has been discussed. HI is negatively correlated with X, and their correlation equation is $HI = 1.811 - 5.787X$, the coefficient of correlation (r) is −0.9731, indicating that the crystallinity of dickite is apparently controlled by content of iron entering the dickite in isomorphous substitution.

5. The relations between the cell parameters (a_0, b_0, c_0) and total iron content (X, %) of dickite are: $a_0 = 5.146 + 2.101 \times 10^{-2}X$, $b_0 = 8.925 + 5.835 \times 10^{-2}X$, $c_0 = 14.426 + 3.976 \times 10^{-2}X$, $\beta = 96.842 + 0.56X$, their coefficients of correlation (r) are 0.2697, 0.9670, 0.9400 and 0.9132 in order. Poor correlation between a_0 and X might be due to migretion of $(-1/6)\,a_0$ along "a" axis in dickite structure, the relatively good correlations between b_0, c_0, β and X indicate that, as the ion radius is bigger than that of aluminium, with increasing isomorphous substitution of iron for aluminium the distance in $\perp$ (001) direction, i.e. c_0, and the distortion of octahedra would increase, meanwhile the increase of distortion of octahedra subsequently results in the increase of b_0 and β.

References

1. Chen Yunqing, 1984, Discovery of Mixed–layer Dickite–kaolinite in Sedimentary Rock and Discussion on Its Origin. Acta Sedimentologica Sinica, Vol.2, No.2, 91–97.
2. Hinckleym D, N. 1963, Variability in "Crystallinity" Valued among the kaolin Deposits of the Coastal Plain of Georgia and South Carolina: in Clays and Clay Minerals, Proc. 11th Natl. Conf., Ottawa, Ontario, 1962, Ada Swineford, ed.,

Pergamon Press, New York, 229–235.
3. Janet Hoffman and John Hower, 1979, Clay Mineral Assemblages as Low Grade Metamorphic Geothermometer– Application to the Thrust Faulted Disturbed Belt of Montana U.S.A.: Soc. Econ. paleontologists and Mineralogists Special Publication Tulsa. Oklahoma, No.26, 55–77.
4. Ren Leifu, 1988, Intermediate Structures of Clay Minerals During Transformation, Acta Sedimentologica Sinica, Vol.6, No.1, 80–87.

PHASES RELATED TO THE $Cu(Pt,Ir,Rh)_2S_4$–$Pb(Pt,Ir,Rh)_2S_3$–$(Ni,Fe)_9S_8$ NEW SYSTEM AND THEIR NEW GENETIC MECHANISM FROM PLATINUM COMPLEX COMPOUND IN YANSHAN, CHINA *

3.6P

Yu Zuxiang, Institute of Geology, Chinese Academy of Geological Sciences, Beijing, 100037, People's Republic of China.

A lot of PGE sulfide phases of iron, nickel, copper and lead were found, which is not a simple compound, but composed of solid solution from two or three phases of $Cu(Pt,Ir,Rh)_2S_4$, $Pb(Pt,Ir,Rh)_2S_3$ and $(Ni,Fe)_9S_8$, in proportion as 1:1 or 3:1, to form a series of superstructure products.

1. $Cu(Pt,Ir,Rh)_2S_4$(Malanite) – $Pb(Pt,Ir,Rh)_2S_3$ binary system [or Ir > Pt > Rh, Rh > Pt > Ir].

a. In proportion as 3:1, to form $Cu_3Pb(Pt,Ir)_8S_{15}$,$Cu_3Pb(Ir,Pt)_8S_{15}$(Inaglyiite, P6 / m etc., a 7.03, c 16.44Å, but formula $Cu_3Pb(Ir,Pt)_8S_{16}$ is error), $Cu_3Pb(Rh,Pt)_8S_{15}$, (Kondorite, a 7.02, c 16.48Å, but formula $Cu_3Pb(Rh,Pt)_8S_{16}$ is error).

b. In proportion as 1:1, to form $CuPb(Pt,Ir,Rh)_4S_7$(Code name Y.H. trig. $P3_112$, $P3_121$ etc., a 7.05, c 34.12Å), $CuPb(Ir,Pt,Rh)_4S_7$(W.H. a 7.02, c 33.94Å), $CuPb(Rh,Pt,Ir)_4S_7$(L.H. a 6.91, c 34.16Å).

The phase of $Cu(Pt,Ir,Rh)_2S_4$ is continuous transform to $Cu_3Pb(Pt,Ir,Rh)_8S_{15}$ and $CuPb(Pt,Ir,Rh)_4S_7$(fig. 1), and atoms S are decrease with Pb / (Cu+Fe) increase. Their relation is corresponded to the equation :

$$(Cu,Pb)_{4+2x/3}(Pt,Ir,Rh)_{8+4x/3}S_{16-2x},\ \text{where } x = Pb / 2\ \text{Atoms}$$

2. In the $Cu(Ir,Rh)_2S_4$–$(Ni,Fe)_9S_8$ binary system [or Rh > Ir; Fe > Ni].

In proportion as 1:1, to form $Ir(Fe,Ni,Cu)_2S_3$(Z.U. trig. R3m, a 14.14, c 34.34Å), $Ir(Ni,Fe,Cu)_2S_3$(Z.A. trig. a 14.10, c 34.29Å), $Rh(Fe,Ni,Cu)_2S_3$(Z.Z. a 14.07, c 34.21Å), $Rh(Ni,Fe,Cu)_2S_3$(Z.H. trig. a 14.04, c 34.14Å). In these formulae the PGE are trivalenct and Fe and Ni are divalenct. A lot of their analyses are put in fig.2.

3. In the $Cu(Ir,Rh)_2S_4$ – $Pb(Ir,Rh,Ir)_2S_3$ – $(Ni,Fe)_9S_8$ ternary or in the $CuPb(Ir,Rh,Pt)_4S_7$ – $(Ni,Fe)_9S_8$ binary system [or Rh > Ir, Fe > Ni].

In proportion as 3:1, to form $IrFeNiCuPbS_{8+x}$(trig. $P3_112$, $P3_121$ etc., a 7.03, c 68.72Å).

I supposed these upper valency PGE^{3+} are come from alkali hydrothermal solution in latest mineralization stage, in the form of complex compound, when reacted with H_2S, it forms a series of PGE phases.

$$2[Pt(NH_3)_6]^{4+}+2[IrCl_6]^{3-}+[Cu(NH_3)_2]^{2+}+[Pb(NH_3)_2]^{2+}+7H_2S+3H_2O+O\rightarrow$$
$$CuPbPt_2Ir_2S_7+12NH_4Cl+4NH_4(OH)$$

* It's an item of Chinese national natural scientific foundation.

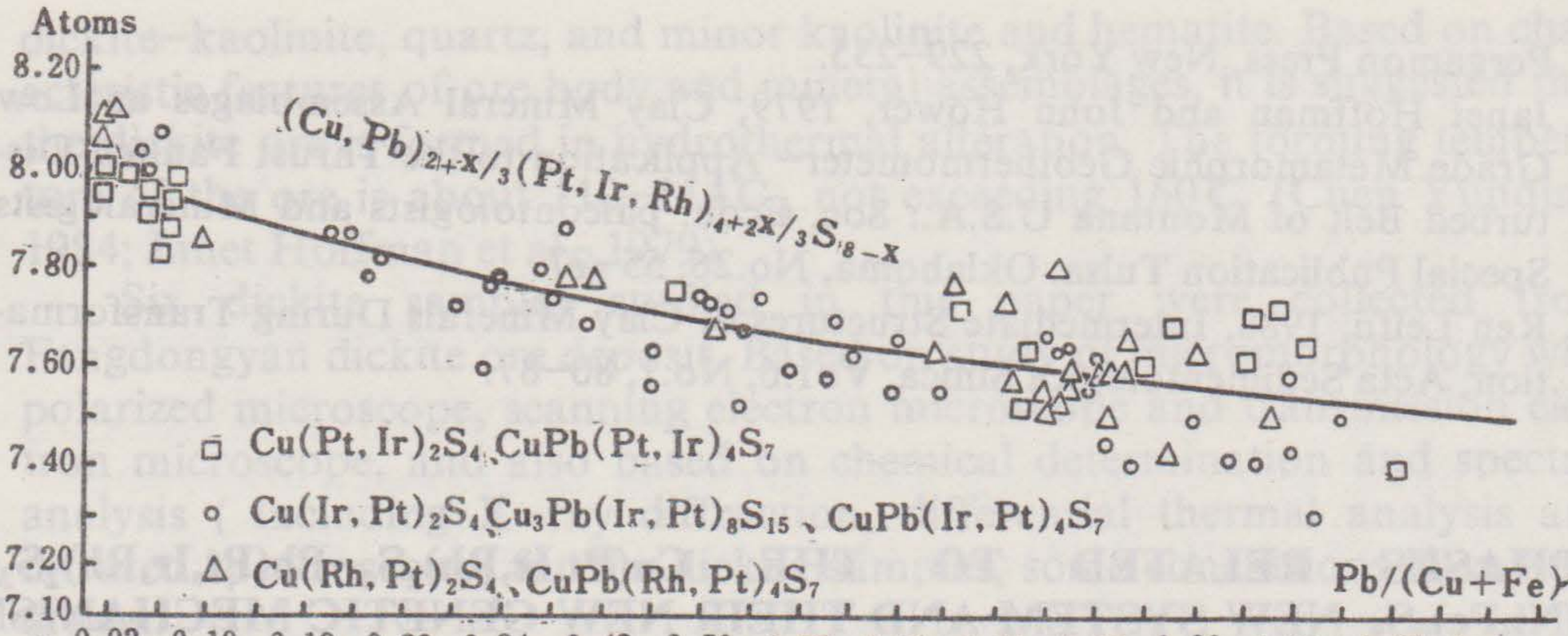

Fig. 1, S Atoms are related to Pb/(Cu+Fe) in $Cu(Pt, Ir)_2S_4$–$Cu_3Pb(Pt, Ir)_8S_{15}$–$CuPb(Pt, Ir)_4S_7$ Mineral Series

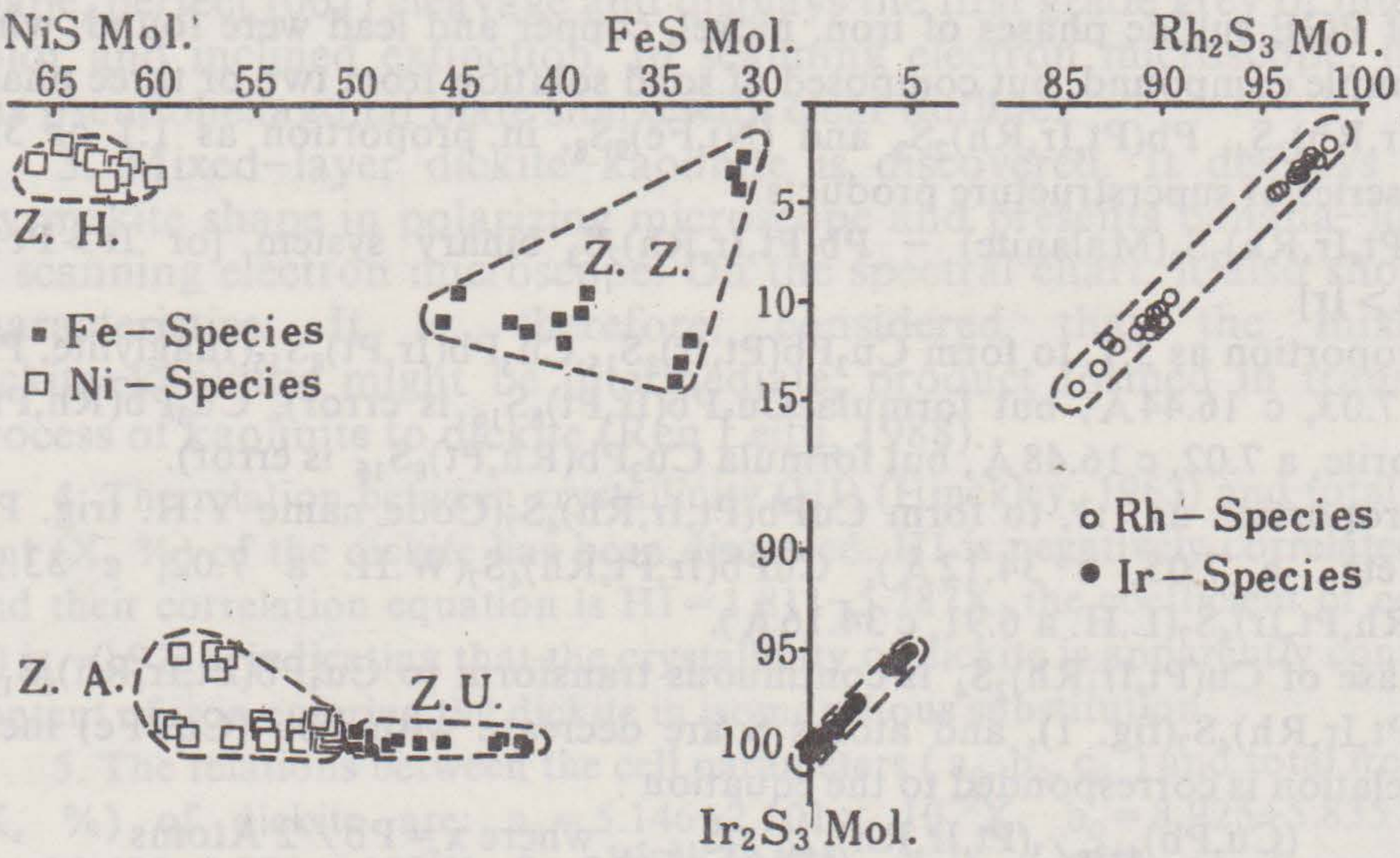

Fig.2 $(Ir, Rh)(Ni, Fe, Cu)_2S_3$ Minerals Group and It's Species

STUDY ON FORMATION OF ACANTHITE

Yue Shuqin , Institute of Mineral Deposits , Chinese Academy of Geological Sciences , Baiwanzhuang Road , 26 , Beijing , 100037 , China

Synthesis experiments of Ag–S system indicate that,in this system there are three polymorphs of Ag_2S between 25 ° C and the liquidus . Ag_2S 111 , acanthite is monoclinic , from 176.3 ° C (Ag–rich) to 177.8 ° C (S–rich) , Ag_2S 111 inverts to Ag_2S 11 , argentite , which is body–centered cubic . Between 586 ° C (Ag–rich) and 622 ° C (S–rich) Ag_2S 11 inverts to Ag_2S 1 , which is thought to be face–centered cubic . Ag_2S 1 is stable at the highest temperature 838 ° C

(Kracck , 1946) .

Acanthite is one of wide spread mineral in Au–Ag–S system in many epithermal deposits of Au–Ag and Ag–Pb–Zn . Acanthite as seen at Yin Keng Shan and Ba Bao Shan of Zhejiang Provinces hes about three kinds of origin .

The first kind is that , the acanthite from these deposits occurs in the quartz veins as regular and irregular grains , intergrows with electrum , talnakhite , chalcopyrite , or in thin rims around chalcopyrite , pyrite and electrum . These acanthites are inverted from argentite due to decreasing temperature during mineralization proccss .

The second kind is that , the acanthite in platy crystals closely intergrows with quartz . This acanthite appears to have been deposited during a late stage of mineralization process under epithermal condition , such one was mainly found in Ba Bao Shan of Zhejiang Province .

The third kind is that , the single crystals of acanthite grow into arrow-shaped and acicular-shaped radial aggregates on the surface of ore specimen . It is obvious that the acanthite was formed in superficial environment .

It is interesting to mention that , when the author washes with alcohol the heavy mineral concentrate of gold–silver–sulfide ore from Yin Keng Shan , there is no acanthite in the concentrate , but after several days , acanthite can be seen newly formed in it , with radial acicular aggregates . So it is clear that acanthite can be formed at ordinary temperature . So the above mentioned third kind acanthite formed in superficial environment belongs really to this type of formation .

The chemical composition of acanthite determined with electron microprobe and scaning electronscope analyses is given in table 1 , it can be seen that the composition of acanthite (no.3) formed at ordinary temperature is more pure than that (no.1, 2) deposited in the epithermal condition and it does not contain impurity , but its Ag-content(no.3) is in excess of stoichiometry of Ag_2S .

Table 1.The Chemical Composition of Acanthite

Sample no.	Ag	Au	Cu	Fe	Bi	Pb	Sb	Te
					(%)			
1	83.48	–	2.71	0.05	0.4	0.27	0.08	–
2	84.98	1.8	–	0.04	–	0.08	–	0.14
3	88.73							

no.	S	Total	Formula
1	12.39	99.38	$Ag_2Cu_{0.04}Pb_{0.003}Bi_{0.005}S$
2	12.59	99.63	$Ag_{2.005}Au_{0.023}Te_{0.003}S$
3	11.27	100.00	$Ag_{2.336}S$

X-Ray diffraction data of various origion acanthite are all analogous to those of A.S.T.M. 14-72 (acanthite).

The origion of acanthite thus formed are all related to the reaction of S with Ag at ordinary temperature and under neutral medium condition.

It is obvious that the discovery of acanthite in this occurrence may provides a valuable data for further studies of geochemical character of Ag.

REFERENCE

Kracek, F.C., 1946, Phase relations in the system sulfur-silver and the transitions in silver sulfide:Am. Geophys. Union Trans., V.27, P. 364-374.

3.9

ANTIMONY - BISMUTH MINERALS IN VOLCANO - SEDIMENTARY ORE DEPOSITS OF BERGSLAGEN, SWEDEN

ZAKRZEWSKI, M.A., Dept. of Geology, Free University, 1081 HV Amsterdam, The Netherlands

Antimony and bismuth minerals are common constituents of polymetallic volcano - sedimentary ore deposits. Their distribution shows typical zoning with Bi confined to proximal and Sb to distal facies in accordance with the preference of Bi for higher and Sb for lower temperature environment. Less common are ores with both Sb and Bi minerals, and exceptional are occurrences with Sb together with Bi build in single mineral phases. In the Bergslagen metallogenic province in central Sweden, the Sb-Bi substitution was observed in 16 minerals from 6 abandoned mines: the Cu-Co mines of Vena, Tunaberg, and Håkansboda; Pb mine of Hornkullen; pyrite mine of Sätra, and Cu deposit of Vindfall.

The Vena mine is type locality for kobellite with the Sb/(Sb+Bi) ratio of (0.37-0.45), jaskòlskiite (0.65), and co-type of izoklakeite (0.40-0.56). Other minerals with both Sb and Bi include an unknown sulfosalt (0.38), bismuthian jamesonite (0.71), stibian bismuthinite (0.15) and stibian cosalite (0.10). In Sätra occurs bismuthian benavidesite (0.95), in Håkansboda bismuthian ullmannite (0.98), in Hornkullen bismuthian meneghinite (0.87). In the Tunaberg mine Dobbe (1988, and pers. comm.) found bismuthian varieties of: meneghinite (0.81), ramdohrite (0.61), andorite (0.75), antimony (0.85), tetrahedrite (0.80-0.59), as well as stibian: bismuthinite (0.37), gustavite (0.30) and bismuth (0.22). In Vindfall Kieft and Eriksson, (1985) found bismuthian tetrahedrite and annivite (0.78-0.34).

The sulphide ore deposits of Bergslagen are related

to Proterozoic complex of felsic metavolcanites and metasediments. Detailed investigations on ore mineralogy in about 300 occurrences have shown contrasting associations of elements. One related to Cu ores in metavolcanites and in clastic sediments, with Cu, Bi, Mo, W, Te and Se, and second association related to Pb ores in carbonate rocks with Pb, Sb, Ag, Hg, Ni, and Sn. The segregation of elements is primarily governed by the contrasts in temperature that produced the proximal Cu ores with Bi minerals, and the distal Pb ores with associated Sb minerals. On the other hand, the relation of ore type with certain lithology suggests a geochemical control of the differentiation.

The six ore deposits of Bergslagen in which the Sb-Bi substitution was observed did not follow the general rules of zonation. They display an overall character of Cu type proximal ore with substantial admixture of elements of the Pb group, but they are located in carbonate rocks. These apparent contradictions suggest that all the involved elements are of common source and that they were released from a feeder zone localized in submarine carbonate facies surrounding. The rapid cooling of the metal bearing solutions resulted in the precipitation of all elements together and the carbonate environment formed a geochemical barrier that prevented a secondary dispersion and differentiation.

Dobbe, R.T.M., 1988, Space and time relations in the Tunaberg area in the metallogenic province of Bergslagen, central Sweden. M.Sc. thesis Free University, Amsterdam, The Netherlands.

Kieft, K., and Eriksson, G., 1985, Regional zoning and metamorphic evolution of the Vindfall Pb-Zn ore east central Sweden. Geologiska Föreningens i Stockholm Förhandlingar, 106, 305-317.

IDENTIFICATION OF ORE MINERALS AND STUDY ON OPTICAL PROPERTIES OF ORE MINERALS USING REFLECTION SPECTRA

Po 3.14

Zheng Chusheng, Institute of Geochemistry, Academia Sinica, Guiyang, Guizhou 550002, People's Republic of China.

Reflection spectrum of minerals is a curve of the reflectance of the minerals as function of the wavelengths of reflected light and it is measured microscopically under linear-polarized light with a photoelectric method in directional polished section (except isotropic minerals).

Reflection spectrum of minerals provides some useful information on many optical properties and each mineral is characterized by its unique spectra, so it can be used as an identification tool. A set of nine identification diagrams are compiled by the author. These diagrams afford a practical means for ore minerals determination on the basis of reflection optical properties of minerals.

Reflection spectra can be used to describe optical properties of ore minerals quantitatively too. The characteristics of optical properties of each mineral are determined by the number of main reflection spectra of the mineral (1, 2 or 3) and their interrelationships. All the optical properties can be calculated quantitatively using the data of the main reflection spectra. Some of them can be shown in the form of quantitative data varying with wavelength(λ). Only reflectance(λ) and reflection color can be calculated, because of one reflection spectrum for a isotropic mineral. Many optical properties can be calculated, such as reflectance(λ)(e,o), reflection color(e,o), absolute bireflectance(λ), relative bireflectance(λ), angle of rotation properties(λ), reflectance under cross-nicols(λ), reflection color under cross-nicols, optical sign(λ) and length fast or slow(λ) for uniaxial crystals, and reflectance(λ)(g,m,p), reflection color (g,m,p), abselute propertied(λ)(g-m, g-p, m-p), relative bireflectance(λ)(g-m, g-p, m-p), angle of rotation properties(λ)(g-m, g-p, m-p), reflectance under cross-nicols(λ)(g-m, g-p, m-p), reflection color under cross-nicols(g-m, g-p, m-p), optical sign(λ), orientation of optical plane(λ) and length fast or slow(λ) (g-m, g-p, m-p) for biaxial crystals.

P.3.15. STUDY ON SILVER-BEARING MINERALS (AG-SULFOANTIMONITES) OF SILVER-SULFIDE DEPOSIT IN THE MIDSOUTH OF DAXINGAN RIDGE AREA

Zhu Zhongxiou,Li Henian,Zhang Peiping,Changchun University of Earth Science, Changchun,Jilin 130026, People's Republic of China

In the midsouth of Daxingan Ridge Hercynian Zone of fold, some silver-sulfide deposits have been discovered. Representatively there are Mengentaoligai and Chaganchulu Ag-Pb-Zn deposit, Dajinzi Ag-Cu-Sn and Eyingtaolegai Ag deposit.In these deposits lots of silver-bearing minerals are discovered .Recently there are 12 species of these minerals are

appraised, but most of those are Ag-sulfoantimonites.Since the silver-bearing minerals are very small,the study of them is very difficult. We appraise the silver-bearing minerals only with electron microprobe and microscope, under which the reflectivity and hardness are identified. Besides natural element-silver,simple sulfides-argentite,polybasite,stromeyerite, canfieldite, most of them are Ag-Sb-S minerals-pyrargyrite, pyrostilpnite,stephanite; Ag-Pb-Sb-S minerals-diaphorite,freieslebenite; Ag-Cu-Sb-S minerals-freibergite, polybasite. The variation of rich As-bearing minerals are not been discovered. The charcter of Ag-sulfoantimonites are:

1.Pyrargyrite:It is more important silver-bearing mineral of the deposit and distributed in leadlike irregular granular it is. Reflecting colour is light blue gray,strong optic anisotropic. Internal reflection is dark red, R= 26.2-27.7, VHN50=125-128kg/mm^2 , chemical composition: Ag 61.84-63.38%, Sb 20.83-22.78%, As 0.55-0.70%, S 15.71-17.94%.

2.Pyrostilpnite: It is Strong optic anisotopic. Internal reflection is light yellow,R=26.0-27.1, VHN50=123-125,chemical composition: Ag 61.28%, Sb 23.94%, As 0.37%, S 17.24%.

3.Stephanite: R=27.4-28.6, VHN50=154,chemical composition: Ag 69.62-71.09%,Sb 13.39-16.32%, As 0.27-0.45%,S 14.94-15.24%.

4.Diaphorite: Optic anisotrope, R=31.8-33%, VHN50=198, chemical composition: Ag 24.33-26.12%,Sb 26.88-27.57%,Pb 27.41-31.72%, As 0.49-0.61%, S 17.80-18.38%.

5.Freieslebenite: reflecting colour is gray-white, weak optic anisotropic, R=36,1-36.6%,VHN50=117.

6.Freibergite: It is the most important silver-bearing mineral of the deposit, optic isotrope, R=28.4-30.6%,VHN50=252-301,chemical composition: Ag 28.5-44.68%, Cu 24-46.9%, Fe 5.7-1.02%, Zn 1-1.88%, Sb 24-28.37%, As 0.36-1.42%, S 17-22.3%.

7.Polybasite: Strong optic anisotrope, R=31.2-28.8%, VHN50=135, chemical composition: Ag 72.02%, Cu 0.59%, Sb 9.96%, As 0.529%, S 16.6%.

In the deposits, all of the silver-bearing minerals are distributed regularly. In space, from shallow to deep it is zoning vertically,which is from silver-sulfoantimonites sulfide. Among the sulfoantimonites, Ag-sulfoantimonites and Ag-Cu-sulfoantimonites are located on shallow,but Ag-Pb-sulfoantimonites are deeper.In the same mineral (for example: freibergite and pyrargyrite), the content of Ag increase gradually from shallow to deep. From early to late during mineralization, Ag-sulfide and Ag-sulfoantimonites are formed earlier, and Ag-Cu-Fe-sulfoantimonites are formed earlier than Ag-Pb-sulfoantimo-

nites,but silver is formed later. This forming order depends on geochemical quality of elements;the composition of hydrothermal system and the physical-chemical conditions during forming. In the deep of deposit, it is reduction enviroment, and the concentration of S^{2-} is bigger,sulfides are formed. Upward, the fugacity of oxigen increase and S can combine with Sb forming composite negativeion easyly, sulfoantimonites are formed.Approach to the surface of earth,S is oxidized further and SO_4^{2-} is formed, but Ag forms natural silver.
(reflectivty R is measured by λ=589nm;VHN50--microcopic hardness)

CRYSTAL STRUCTURE AND CRYSTAL CHEMISTRY OF MINERALS

POWDER DIFFRACTION STRUCTURE ANALYSIS OF NATURAL AND CATION EXCHANGED GONNARDITES

56.4.2 V

G. Artioli and M.R. Torres Salvador, Istituto di Mineralogia e Petrologia, Università di Modena, 41100 Modena, Italy

Natural zeolite gonnardite from Palagonia, Sicily, Italy, has been fully characterized through x-ray powder diffraction and Rietveld profile refinement.

Some differences in the location and occupancy of the water molecules in the zeolite cavities exist with respect to previously reported structure results of gonnardite from Norway (Mazzi et al. 1986).

Samples of gonnardites from the same locality (Palagonia) were used in cation exchange experiments at the University of Naples (Ciambelli et al. 1989). We performed Rietveld structure analysis on their ammonium and potassium- exchanged gonnardites.

The refinements show large rotations of the tetrahedral chains and distortion of the Si,Al tetrahedra in both structures. Also the location and occupancy of the cations and the water molecules in the channels are substantially different from those observed in natural gonnardites.

Space groups and cell parameters for the three samples, as resulting from the refinement are as follows:

sample	Space group	a	b	c	δ
natural	I $\bar{4}$2d	13.246	13.246	6.600	
K-exchanged	I $\bar{4}$2d	13.727	13.727	6.558	
NH_4-exchanged	I 112_1 (non st.)	13.073	12.815	6.620	91.11

Ciambelli P., Franco E., Notaro M. and Vaccaro C. (1989) in Recent Research Reports, Zeolites for the Nineties; Jansen J.C. Moscou L. and Post M.F.M. eds., Amsterdam, 63, 147-148.

Mazzi F., Larsen A.O., Gottardi G. and Galli E. (1986) N. Jb. Min. Mh., 219-228.

56.4.3.V

SYNTHESIS AND CRYSTAL CHEMISTRY OF ANHYDROUS NICKEL ARSENATES.

Jacques BARBIER & Chris FRAMPTON, Department of Chemistry, McMaster University, Hamilton, Ontario L8S 4M1, Canada.

Using hydrothermal growth (P= 1 kbar, T= 600-800°C) and synthetic annabergite, $Ni_3As_2O_8.8H_2O$, as starting material, the following $Ni_3As_2O_8$ polymorphs have been synthesized in single crystal form: a low-temperature green orthorhombic form (Cmca, a=5.94, b=11.26, c=8.16 Å, isostructural with $Mg_3V_2O_8$ (1)), synthetic green xanthiosite (2) ($P2_1/c$, a=5.79, b=9.58, c=10.22 Å, β=93.5°) and a yellow tetragonal form ($I\bar{4}2d$, a=6.79, c=18.78 Å, isostructural with $Mg_3As_2O_8$ (3)). The results of X-ray structure refinements of these phases will be presented and discussed.

Preliminary data relative to other new anhydrous nickel arsenates synthesized during the course of a survey of the NiO-As_2O_5 system will also be presented. These compounds include a monoclinic red phase (C-centred, a=10.630, b=14.486, c=6.668 Å, β106.3°), a monoclinic green phase (C2/m, a=9.30, b=9.03, c= 5.15 Å, β=98.6°) and an hexagonal green phase (a=12.63, c=5.15 Å, possibly another high-temperature form of $Ni_3As_2O_8$).

(1) Krishnamachari N. & Calvo C. (1971) Can. J. Chem. 49, 1629

(2) Davis R.J., Hey M.H. & Kingsbury A.W.G. (1965) Mineral. Mag. 35, 72

(3) Krishnamachari N. & Calvo C. (1973) Acta Cryst. B29, 2611

56.4.4.V

CRYSTAL CHEMISTRY AND SPECTROSCOPY OF $2M_1$ BIOTITES

L.V.Bershov, R.M.Mineeva, S.V.Soboleva, Institute of Ore Deposits, Mineralogy, Petrography and Geochemistry USSR Acad. of Sciences, Mosoow 109017, Staromonetny 35

The occurence of trioctahedral mica in nature and among the synthesis products in 1M polytype is due to the uniform distribution of the octahedral cations. The known structures of the volcanic and metamorphic $2M_1$ biotites demonstrate the ordered distribution of the octahedral cations with the localisation of Al^{3+}, Fe^{3+} and Ti^{4+} in cis-octahedra M2. Therefore OH vector is inclined to (001) plane and directed to the octahedron M1, mainly occupied by divalent cations.

The proton localisation by the method of electrostatic minimum calculation reveals the deviation of OH

vector on 20-25° from the normal to the (001) plane in the structures of $2M_1$ biotites.

The unregular cation distribution and vector OH inclination in natural biotites from the metamorphic (Georgia) and volcanic (Kamchatka, Armenia) rocks were proved by spectroscopic methods (EPR, Mössbauer, IR). The character of the ordered cation distribution has a great influence on the OH vector orientation and hence affects the relative disposition of the adjacent mica layers with the $\pm 120°$ rotation, correspond to the $2M_1$ polytype.

CENTROSYMMETRIC AND NON-CENTROSYMMETRIC ONE-LAYER POLYTYPES OF METASOMATIC SERICITES IN THE UPPER DEVON OF THE TUVA THROUGH

A.M.Bloch, All-Union Institute of Mineral Resources, A.P.Zhukhlistov and B.B.Zvyagin, Institute of Ore Mineralogy (IGEM) USSR Ac. Sc., 109017 Moscow, USSR

Metasomatic argilizites of sericite composition are for the first time described for sedimentary sequences of the upper Devon of the Tuva through, regions of their display correlating with zones of high jointing. They develop along intergrain joints, substitute aggressively the calcite of the cementing mass and fragmental grains of feldspar and effusive rocks, corrode the transsecting carbonate streaks. The sericites are commonly accompanied by pyrite. The country sedimentary sequences contain ore concentrations of polymetals, molybdenite, cobalt-nickel mineralization, etc. According to the oblique-texture electron diffraction data, the sericites under study are represented both by the usual 1M (33033) polytype (space group C2/m) consisting of centrosymmetric layers with the trans-octahedra vacant and by its mixtures with the 1M (15015, C2) polytype consisting of non-centrosymmetric layers with one of the cis-octahedra vacant. The two sericite varieties differ significantly in particle morphology, arrangement and intensities of 021, 111 reflexions and range in the β angle variation (greater and less than $\beta_{ideal}=\arccos(-a/3c)$). This implies the absence of intermediate cation distributions over octahedra and the impossibility of uniform structures consisting of both layer kinds.

As products of low-temperature hydrothermal acid leaching processes such sericites may develop in the country sequences of the ore formations not only in Tuva, but also in the whole Altai-Sayan folded region, and, especially, in the Ore Altai. Under such condi-

tions their genesis should be revised in favour of its endogenic interpretation.

56-4.5.V

ON THE ROLE OF HS^- ION IN SULFIDE STRUCTURES

G.B. Bokij, M.T. Dmitrieva, Yu.P. Dikov, B.A. Boronikhin

Institute of Ore Deposits, Mineralogy, Petrography and Geochemistry, U.S.S.R. Academy of Sciences, Moscow, U.S.S.R.

Many of the natural sulfides are known to deviate from ideal stoichiometry. Bokij et al. [1,2] suggested that in some sulfides defects occur in connection with the presence of HS^- ions in the structure. To confirm this various sulfides were studied by X-ray and X-ray photoelectron spectroscopy. The samples ranged from pyrrotites, a classical example for non-stoichiometric sulfides, to sphalerites, for which a deviation from stoichiometry was never observed or discussed. The sphalerites under investigation were obtained by hydrothermal synthesis in solutions with various HS^- ions concentrations. A clear correlation between the results obtained by X-ray method and by photoelectron spectroscopy was found.

Pyrrotite was investigated in detail by X-ray photoelectron spectroscopy as to the 2p electron band of sulfur. In the spectrum a characteristic sharp line with a maximum of bond energy of 163 kV was observed corresponding to the standard value of bond energy in iron monosulfides. Further, a maximum of low intensity was registered at 161.2 kV. Such a maximum is characteristic of the HS^- type bond, similar to that, observed in the sphalerite spectrum.

The results support the concept of a partial substitution of S^{2-} ions by HS^- ions, causing vacancies in the cationic part of the structure.

1.Bokij G.B., Bondar A.M., Dokl. AN SSSR, 248, 956 (1979).
2.Bokij G.B., Dmitrieva M.T., Dikov Yu.P., Acta Cryst. A40 suppl. C-207 (1984)

THE STRUCTURAL SIMILARITY AND THE STRUCTURAL DISTINCTION FERRIFAYALITE AND LAIHUNITE

G.B.Bokiy, Z.V.Vrublevskaja, I.V.Ginzburg, Institute

of Ore Deposits, Mineralogy, Petrography and Geochemistry USSR Acad. of Sciences, Moscow 109017, Staromonetny 35.
D.Yu.Pushcharovsky, N.A.Yamnova, Moscow State University, Moscow, USSR.
The complete structure investigation of ferrifayalite $\square_{0.5}Fe^{2+}_{0.5}Fe^{3+}_{1.0}SiO_4$ from granit rock (Middle Asia, USSA). was carried out (automatic single-crystal diffractometer P1 "Syntex", R=0.129). Unit cell parameters: a=4.806, b=10.20, c=5.76Å, α =90,89°. The ferrifayalite crystal-chemical data are considered in comperison with laihunite (1), having the similar composition. The ferrifayalite distinguishs from laihunite by higher content of Fe^{3+}, by some other structures features. Cation position M1, occupied by Fe^{2+} and vacancies in laihunite structure splits on two position M1, M3 with partly ordered location Fe^{2+} (M1 -0.66%Fe^{2+} , 0.33% vacancies, M3- 0.33%Fe^{2+} , 0.66% vacancies), whereas in laihunite structure Fe^{2+} and vacancies are completely ordered. In ferrifayalite as in laihunite Fe^{3+} are located in M2 position. The tetrahedral are completely occupied by Si. In accordance with octahedra composition the partly vacant octahedron M1 by ferrifayalite is smaller than vacant octahedron M1 by laihunite. The M2 octahedra volumes in laihunite and ferrifayalite structure are similar. The revealed partly ordered cation arrangement in ferrifayalite indicates the less equilibrium conditions of the crystallisation process of this mineral in comparison process of this mineral in comparison process of this mineral in comparison with laihunite.

1. O.Tamada, B.Shen, N.Morimoto, Min.Journal, 1983, 11, 8, 382.

CRYSTAL CHEMICAL RELATIONSHIPS AMONG FELDSPATHOIDS IN THE DAVYNE-MICROSOMMITE GROUP

46.4.12 K

E. Bonaccorsi, S. Merlino & M. Pasero, Department of Earth Sciences, University of Pisa, Via S. Maria 53, 56126 Pisa, Italy

Three distinct feldspathoids with the same tetrahedral framework, but differing in the chemical composition and ordering of the ions in the cavities of the structure, have been found in the Somma-Vesuvius volcanic area, Italy. The three

minerals, davyne, microsommite and a new phase (n.p.: its complete chemical and structural characterization is in progress), present hexagonal unit cells with $P6_3/m$ (davyne) or $P6_3$ (microsommite, n.p.) space groups, similar c axes and related a axes, with a(micr.)=$\sqrt{3}$·a(dav.) and a(n.p.)=2·a(dav.).

The common features of the three minerals are: a) cancrinite-type tetrahedral framework, with ordered alternation of silicon and aluminum tetrahedra; b) "undecahedral" cages, built up by five six-membered rings and six four-membered rings: within these cages ...Ca-Cl-Ca-Cl... chains develop parallel to the c axis; c) larger channels hosting alkali cations, sulphate and/or chlorine anions.

The chemical and structural analyses indicated the following crystal chemical formulae for the three minerals:

	channels	cages	framework
davyne	$\{Na_4K_2(SO_4)_{0.5}Cl\}$	$\{Ca_2Cl_2\}$	$\{Si_6Al_6O_{24}\}$
microsommite	$\{Na_4K_2(SO_4)\}$	$\{Ca_2Cl_2\}$	$\{Si_6Al_6O_{24}\}$
n.p.	$\{Na_4K_2Cl_2\}$	$\{Ca_2Cl_2\}$	$\{Si_6Al_6O_{24}\}$

when the three distinct structural elements are emphasized. The results of the structural refinements indicated that these phases differ not only in the sulphate/chlorine contents, but also in the distribution of the alkali cations in the large channels, disordered in davyne and ordered in microsommite and n.p.. As the order-disorder relationships among the three phases may be related to both temperature and sulphate/chlorine contents, anion exchange experiments as well as high temperature structural studies have been planned and preliminary results will be presented.

A mineral phase with the same space group as microsommite and similar unit cell dimensions was found in Pitigliano, southern Tuscany, Italy. Chemical and structural investigations point to the crystal chemical formula $\{Na_4K_2(SO_4)\}\{Na_2(H_2O)_2\}\{Si_6Al_6O_{24}\}$, which indicates that ...Na-H_2O-Na-H_2O... chains substitute for ...Ca-Cl-Ca-Cl... chains within the "undecahedral" cages.

Interestingly a compound with microsommite-type structure and composition $\{Na_3K_3(SO_4)_{0.67}(OH)_{0.67}(H_2O)_{0.5}\}$ $\{Na_2(H_2O)_2\}$ $\{Si_6Al_6O_{24}\}$ was prepared and studied by Klaska & Jarchow (Naturwiss., 64, 93, 1977). The crystal chemical relationships among this synthetic phase, microsommite from Vesuvius and "microsommite" from Pitigliano will be presented and discussed.

EFFECT OF OCTAHEDRAL COMPOSITIONAL VARIATION ON THE CRYSTAL STRUCTURE OF 1M BIOTITES

41.4.7.H

Maria Franca Brigatti, Dipartimento di Chimica, Università della Basilicata, Potenza, Italy

This work examines the effect of the octahedral compositional variation on the crystal structure of 1M biotites.

Accordingly, data from previous crystal–structure refinements have been assessed along with those from eight new refinements.

C2/m setting and reflections with $I > 5\sigma(I)$ were employed.

b cell dimension increases fairly smoothly with the substitution of Fe for Mg although Ti substitution causes more marked decreases in the *c*-cell parameter.

Examination of the trends in the structure and geometrical parameters with compositional variation reveals that:

- the tetrahedral ring distortion is not affected by the octahedral composition, whereas it is linked to the geometry of the ditrigonal cavity occupied by the interlayer cations;
- the octahedral sheet distortion shows similar trend for M1 and M2 sites; in Fe–richer biotites the "average" distortion of octahedral layer decreases and M1 is more distorted and larger than M2;
- in Fe–rich terms the number of electrons of M1 site is slightly higher than that of M2 thereby suggesting slight preference of Fe^{2+} for M1;
- M1 site distortion increases with Ti increase and decrease when Mg/Σ_{oct} (where Σ_{oct} is the octahedral occupancy) decreases;
- all biotites exhibit limited ordering of Mg cation over the octahedral

sites with preferential centering of the M2 site when $Mg/\Sigma_{oct} > 0.6$;

– the octahedral thickness decreases with Ti increase.

INVESTIGATION OF THE CRYSTAL STRUCTURE OF VANADINITE*

Chen Guoying, Li Wanmao and Wang Qiguang, Department of Geology and Instruments analysis & Research Center, Lanzhou University, Lanzhou, Gansu,. 730001, People's Republic of China.

Vanadinite is considered as a isostructural mineral of pyromorphite series of apatite group since it has been found and named in 1838. The crystal structure of vanadinite which occured in the oxidated zone of Xiaotieshan mine, Gansu province, China. The study shows that the vanadinite not only has no apatite type structure, it is not a vanadate, too. In reality, the mineral is a Pb and V complex oxide.

Vanadinite is a major secondary mineral in the oxidated zone of Xiaotieshan mine. The mineral usually occurs as prismatic aggregates, crystal druses and granular aggregates. Well-developed single crystals are common. Crystal habit short or long hexagonal prismatic. Brownish red to black brown-red in colour. Biaxial negative (–). Measured density 6.948g.Cm^{-3}.

The chemical analysis of the mineral were carried out by means of electron microprobe. The mean values are, PbO 78.13, V_2O_5 18.70, As_2O_5 0.40, P_2O_5 0.48, SO_2 0.08, Cl 2.65, Total 100.44 wt.%. The sum of oxygen atoms within the unit-cell which was obtained from the chemical analytic values and cell volume of the mineral is 26. The empirical formula (based on O=26) is, $Pb_{4.00}(V_{3.00}P_{0.09}As_{0.03}S_{0.01})_{3.04}O_{12.44}Cl_{2.04}$. The simplified formula is $Pb_4V_3O_{12}Cl_2$.

A crystal 0.2×0.2×0.3 mm was mounted on a CAD-4 Enraf-Nonius diffractometer for X-ray analysis, using MoKα radiation (λ=0.7107Å) with graphite monochrometer. Frist, prelaminary cell parameters were determined from 25 arbitrarily selecting reflections with autoindexing procedure. The accurate cell parameters which were obtained by least-squares method from the 25 well-centered reflections are, a=10.282(3)Å, b=7.291(4)Å, c=10.273(4)Å, β =120.0(3)° , V=666.8Å^3, Z=2.

The intensity data collection were carried out by the ω/2θ scan technique, using a variable scan speed. A total of 1587 reflections were collected to $0 \leqslant h \leqslant 16$, $0 \leqslant k \leqslant 12$, $-16 \leqslant l \leqslant +16$ out to a maxium 2θ of 54°. By averaging equivalent intensities, 1265 independent reflections with $I > 3.0\sigma$ were used to the refinement of the structure. The structure was solved by heavy atoms method. Fristly starting from the isostructural relation between vanadinite and apatite, the position of Pb atom was derived from the Patterson

function according to $P6_3/m$ space group. However, as a whole, the crystal structure of the mineral may be only belong to $P2_1/m$ space group because the systematic absences are only 0k0 with k not times of 2. Changing over from the space group $P6_3/m$ to $P2_1/m$, the positions of four Pb atoms were found by equivalent point transform of $P2_1/m$ space group. Then the positions of three V atoms, nine O atoms and a Cl atom were found from Fourier syntheses. Therefore it can be determined that the vanadinite belongs to monoclinic system, $P2_1/m$ space group.

The bond lengths and bond angles calculated from the coordinating parameters and atomic radii show that the V-O distance vary 1. 161Å to 2.129Å, and the bond angles vary from 34° to 175°. It seems that there is no a coordinating tetrahedra $(VO_4)^{-}$ groups within the structue of vanadinite. For this reason, the vanadinite could be a Pb and V complex oxide but not a vanadate mineral. The complete structural information will be reported after the structure refinement is performed.

STACKING VARIATIONS AND NON-STOICHIOMETRY IN THE BIXBYITE-BRAUNITE POLYSOMATIC MINERAL GROUP

47.7.1.K

Johan P.de Villiers, Peter R. Buseck, Department of Geology and Chemistry, Arizona State University, Tempe, ARIZONA 85287, USA

Bixbyite, braunite, neltnerite, and braunite-II are manganese rich members of a mineral group based on the ca tions of the fluorite structure type, with general formula MgO_2 (M= Mn,Fe,Ca,Si). They consist of layer modules of (Mn,Fe)O octahedra stacked in various arrangements depending on the coordination of interlayered M-cations.

The structures of the 21 possible layer assemblages up to a thickness of eight layer modules have been generated using stacking vectors derived from the known mineral varieties. These structures have been used to simulate the observed images obtained by electron microscopy.

Non-stoichiometry has been observed in braunites from several localities and is manifested by variations in

their M^{2+} and Si contents.High-resoluton transmission electron microscopy(HRTEM) revealed the presence of several polysomes of varied thicknesses.In addition to the 2-module bixbyite,the 4-module braunite,and the 8-module braunite-II,new 3-,5-,and 8-module assemblages have been observed .These assemblages have calculated SiO_2 contents that vary from 0 to 10% by mass.

Very fine intergrowths of bixbyite and braunite- have also been observed by HRTEM.These intergrowths consist of varied amounts and thicknesses of the two components and also account for non-stoichiometric variations in the M^{2+} and Si contents lower than those for braunite-II.

56.4.6. V

Cr-BEARING VARIETIES OF SCHREYERITE AND VUORELAINENITE

M.T.Dmitrieva, S.P.Korikovsky, V.A.Boronichin,
A.A.Koneva Institute of Ore Deposits,Mineralogy, Petrography and Geochemistry,U.S.S.R. Academy of Sciences,Moscow,U.S.S.R.

The two new vanadium-bearing minerals have been recently discovered and described - schreyerite $V_2Ti_3O_9$ [1] and vuorelainenite $(Mn,Fe)V_2O_4$ [2]. We succeeded in thus far identifying unknown Cr-rich varieties of these two minerals in metamorphosed schists in Baikal region. Schreyerite is the first find in the territory of the U.S.S.R. and the third find in the world.In contrast to the two schreyerites described earlier the mineral from the U.S.S.R. contains up to 20-28% of $Cr_2Ti_3O_9$. Cr-bearing schreyerite coexists with rutile as a rule in thin intergrowth and rather seldom occurs as homogeneous mineral grains.Medenbach and Schmetzer noticed that it was difficult to separate schreyerite for X-ray investigation due to the intergrowth with rutile and the grains studied showed predominantly rutile in the powder pattern [1]. Of all reflections only five belonged to schreyerite phase.X-ray investigation with Gandolfi and Debye-Scherrer (114.6 mm) cameras performed in the frame of this study showed

predominantly schreyerite.For the first time,a rather complete X-ray pattern of schreyerite has been obtained.Comparison of interplanar spacings of investigated schreyerite with those of synthetic phases Fe2Ti3O9 and (Cr,Fe)2Ti3O9 revealed good correlation. The d-values have been indexed according to a primitive monoclinic cell and the unit cell parameters have been refined: a =7.055, b =18.828, c =5.004, β=119.76° .The X-ray investigation confirmed the isomorphic relation between chromium and vanadium.As to the crystallochemical peculiarities, schreyerite is the first natural analog of an Anderson phase with general formula M2Mn-2O2n-1.

Electron microprobe analyses of spinels from Baikal region have shown large variation in V2O3 and Cr2O3 content (24.3-39.5% and 23.4-43.8% correspondingly) with constant MnO,FeO,and ZnO.According to the chemical and X-ray data the investigated spinels belong to the vuorelainenite-manganochromite series with 60% of manganochromite-vuorelainenite and 40% of chromite-coulsonite components.The spinels of such composition have been found for the first time.As the result of the considerable replacement of V3+ by Cr3+ a continuous series exists between Cr-bearing vuorelainenite and V-bearing manganochromite.

Reference

1.Medenbach O., Schmetzer K. -Amer.Miner.,1978,V.63, p. 1182-1186.
2.Zakrzewski M.A. et al., - Canad.Miner.,1982,V.20, pt.2,p.281-290.

SYMMETRY OF THE SUBSTANCE OF EARTH'S SHELLS AND THE PHASE TRANSFORMATIONS

56.4.7.V

Dolivo-Dobrovolsky V.V.,Department of Mineralogy, Crystallography and Petrography,Mining Institute, Leningrad, USSR

The prevailing symmetry of crystalline matter making up the Earth's shells is changed with a depth in the following succession: triclinic (granite-metamorphic

shell A_1), monoclinic (granulito-basitic shell A_2), orthorombic (upper mantle B), orthorhombic + cubic (transition sone C_1), middle systems + cubic (transition sone C_2), cubic (deep mantle D). The change of symmetry of the matter in the shells is essentially connected with the phase transformations in mantle. The increase of pressure causes the phase transformations in silicates which are accompanied either with the decrease of symmetry (mainly with the security of Si coordination number) or with the increase of symmetry (mainly with increase of Si coordination number). The change of the matter symmetry of external shells (the Earth's crust) depends on the general direction of the evolution of Earth's substance in the global scale.

46.4.10K

ENVIRONMENT OF CRYSTALLIZATION OF TOPAZ AS INFERRED FROM CRYSTAL CHEMISTRY AND INFRARED SPECTRA

Foord, Eugene E., Jackson, Larry L., Taggart, Joseph E., Crock, James G., and King, Trude V. V., M.S. 905, U.S. Geological Survey, Box 25046 Denver Federal Center, Denver, CO 80225

Topaz, $Al_2SiO_4(F,OH)_2$, is usually found as a vapor-phase or hydrothermal crystallization product in three principal geologic associations: in lithophysal cavities in rhyolites(R), pegmatites and greisens(P), and hydrothermal veins(H). The mineral also occurs as a liquidus phase in ongonites and some rhyolites. Compositions of 65 topaz samples (8R, 40P, 17H) are distinctly grouped in terms of H_2O^+(>105°C), F, and trace element content. The average H_2O^- content for all samples was 0.04(±0.01) wt. %. H_2O^+ contents (in wt. %) for 7R topaz ranged from 0.06 to 0.11, for 40P topaz from 0.20 to 0.91, and for 17H topaz from 1.69 to 2.67; fluorine content is inversely related to water content (Fig. 1). One late-stage sample of topaz from rhyolite from Boiler Peak, NM contained 0.50 wt. % H_2O and was likely deposited from hydrothermal solutions rather than a vapor-phase. One sample of topaz from a high T and P metamorphic environment (rutile-quartz-sillimanite gneiss) contained 1.04 wt. % H_2O. A maximum of about 30% of the F site is occupied by OH in H topazes (Fig. 2). The F-OH ratio correlates with, and possibly is controlled by the temperature of crystallization.

Trace and minor elements which vary by association include Li, Fe, Cr and Ge. The average Li content of R topaz (50 ppm) is ≥ five times

that of P and H topaz. All samples contain trace amounts of Fe (as much as 0.3 wt. %). Chromium, present in some samples of H topaz, and derived from host schist or ultramafic host rocks, is the chromophore in the pink-red and orange-red crystals from Ouro Preto, Brazil and Katlang, Pakistan; pink to burgundy colored crystals from both of these localities contain 400 - 500 ppm Cr. Purplish-red topaz from Sanarka, Orenburg district, USSR contains about 2700 ppm Cr. Germanium contents are elevated in four samples of P topaz (200 ppm Mt. Antero, CO; 500 ppm Little Three mine, Ramona, CA; 550 ppm Maple Lode mine, Aguanga Mtn., CA; and 400 ppm Satao (Viseu), Portugal).

Other physical properties, e.g. density, unit-cell data, and optical data vary linearly with the substitution of OH for F. Measurement of any of these properties may be used to determine the F or OH content and to predict topaz type and environment.

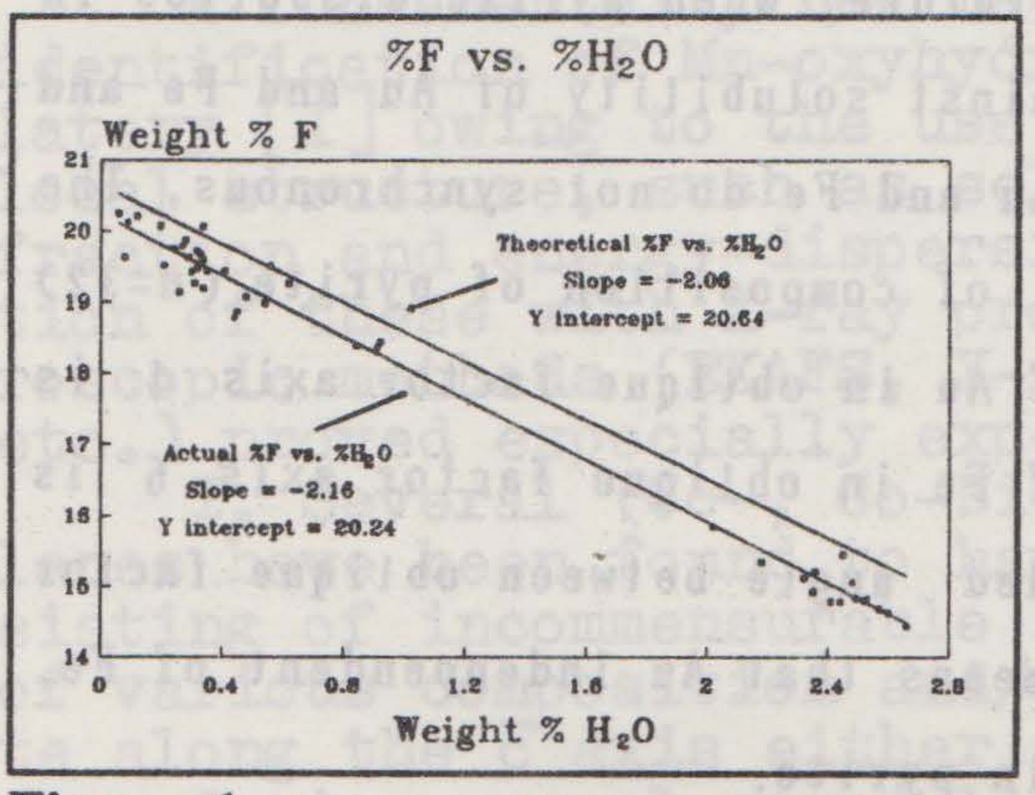

Figure 1

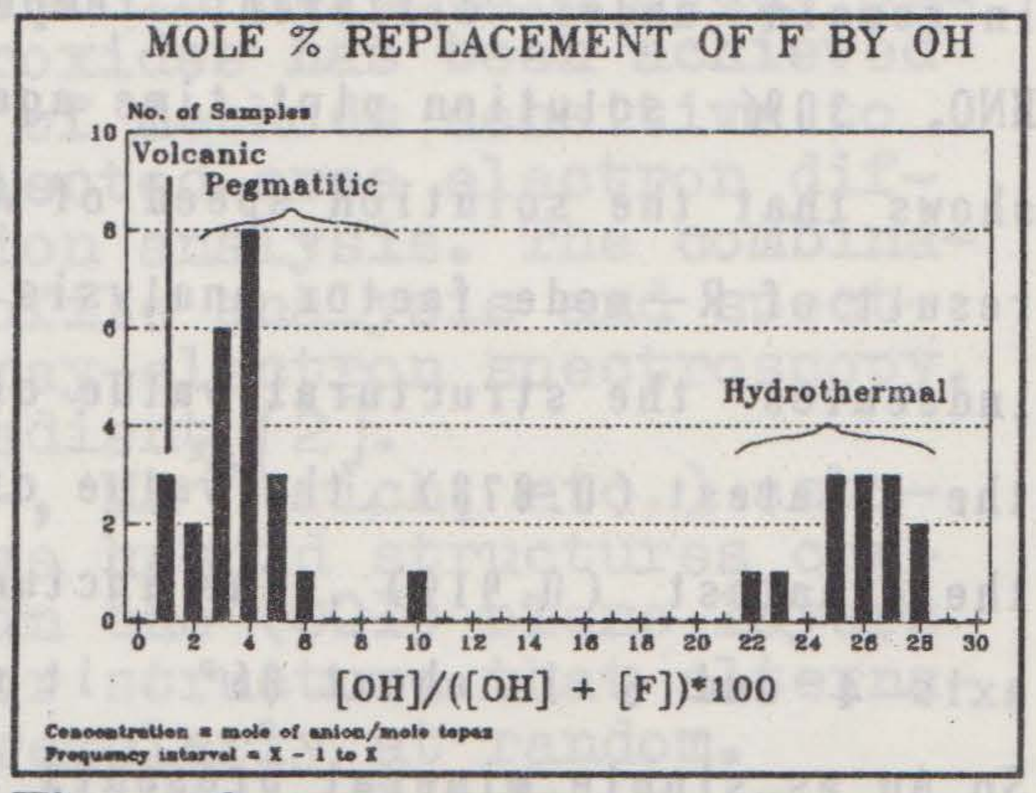

Figure 2

IR reflectance spectra of F-rich (R type topaz) and OH-rich (H type) are distinct. Three narrow, well-defined, OH absorption bands are characteristic of R topaz (3400 to 3800 cm^{-1}). P topaz shows OH absorption features from 3400 to 4200 cm^{-1}. Hydroxyl-rich topaz (H type) displays a more complex series of OH absorption bands between 3400 and 4200 cm^{-1}. Hydroxyl-rich topaz also contains CO_2 as indicated by a sharp peak at 2300 cm^{-1}. Disorder of OH - F is indicated for the OH-rich material which is consistent with its known triclinic symmetry.

THE PRESENT STATE OF Au IN PYRITE IN TULING—SHIHU GOLO DEPOSIT, HEBEI PROVINCE

Gao Xue Jun Chang Chun College of Geolgy, Chang Chun, Ji Lin 130026, People's Republic of China

Tuling—shihu gold deposit is the type of Au—bearing quartz

vein of magmatic hydrothermal. It is evidenced that Au in pyrite presents as either mineral of gold (or electrum) or ion (Au^*). The major methodes of investigation and analyses are EPM, SEM, EPR, mineral phase analysis and R-mode factor statistics of composition. The conclusions as follows:

1. Au in Au—bearing pyrite is mainly single mineral——gold (or electrum). The result of EPM, the picture of face distribution of X—ray and back scattering electron of Au appears cleacly with the simple of pyrite. Mineral phase analysis (n = 8) shows: when pyrite dissolves in HNO_3 10% solution Au of pyrite appears mainly in remain under different temperature; when pyrite dissolves in HNO_3 30% solution plot time against solubility of Au and Fe and shows that the solution speed of Au and Fe do not synchronous. The result of R—mode factor analysis of composition of pyrite (n=32) indecates the structural value of Au in oblique factor axis 4 is the greatest (0.878), the value of Fe in oblique factor axis 6 is the greatest (0.919). The included angle between oblique factor axis 4 and 6 is about 86°, it means that Au indenpendent of Fe. So Au as single mineral presents in pyrite.

2. Besides single mineral——gold (or electrum) there is a few ion Au——Au^* in the crystal lattice of pyrite. The analysis of mineral phase (n = 8) indecates: whether pyrite dissolves in HNO_3 10% under different temperature or in the HNO_3 30% under different time there is the Au of ion state in the solution, the consistency of ion Au is relative lower. The investigation of the spectrum of EPR (n=8) shows, Au—bearing pyrite has the FS spectrum line of Gauss line—type of narrow and isotropy and its $g = 2.001 \pm 0.001$. Considing the spectrum line is due to the pyrite which contains ion Au——Au^*, but the consistency of Au^* is lower. The result of SEM indecates: the diagram of face distribution of the feature X—ray composition of pyrite shows that the distribution of Au element is even and simillar to that of Fe and S, it indecates these all elements occupy crystal lattice in pyrite.

RECENT DEVELOPMENTS IN CRYSTAL CHEMISTRY AND GENESIS OF MANGANEZE OXYHYDROXIDES.

Gorshkov A.I. (IGEM, USSR Acad.Sci.), Drits V.A. (GIN, USSR Acad.Sci.), Dubinina G.A. (Inst. of Microbiology, USSR Acad.Sci.)

Manganeze oxyhydroxides from oceanic (or marine) crusts and nodules, and laterite weathering crusts and other continental formations are normally poorly crystallized and often form complex mixtures with one another and other minerals. Therefore their structural and crystal-chemical investigation by conventional methods (X-ray diffraction and microprobe analysis) is extremely complicated, which hampers estubli-shing their genesis.

A fundamentally new level in structure study and identification of Mn-oxyhydroxides has been achieved latery [I] owing to the use of methods sensitive to local structure, such as selected-area electron diffraction and energy-dispersion analysis. The combination of these with X-ray profile analysis and spectroscopic methods (EXAFS, X-ray-electron spectroscopy, etc.) proved especially expedient [2].

I. Several (Co-, Co-Ni-, Mn^{3+}-rich, etc.) asbolanes have been found to have hybrid structures consisting of incommensurable in the (OOI) plane layers of various composition and/or structure that alternate along the $\vec{c}$ axis either regularly at random.

2. An unusual mixed-layer mineral have been found in oceanic Fe-Mn nodules whose structure contains asbolane-like packets alternating at random with buserite-like ones.

3. Crystal structures have been determined for a number of new Mn-oxyhydroxides. I4 Å-Ca-birnessite, clinobirnessite, buserite-II have layer structures; achtensite and Mn-ferroxyhite have pseudolayer structures.

4. Structural and crystal chemical features were established birnessite, Fe-vernadite and iron-free vernadite.

5. A new chalcophanite variety has been found, namely, Ni-chalcophanite having a rhombohedral unit cell.

6. Three different todorockite structural varieties have been identified.

7. A new crystal-chemical classification of channel-structure manganeze minerals has been proposed including structural characteristics of the known and hypothetical minerals. A number of new minerals have been predicted on this basis.

The crystal-chemical data obtained for Mn-oxy-

hydroxides as well as their diffraction characteristics were used in investigating the localization and genesis of the mineral formations in question. Thus the oceanic crusts and nodules were shown to be associated with definite sets of ore minerals. These are pseudolayer-structure Fe-vernadite and Mn-ferroxyhite in hydrogenic formations, layer-structure buserite-I and interstratified asbolane-buserite in diagenic nodules, and channel-structure todorockite, 7A-birnessite and often I4A-Ca-birnessite and clinobirnessite in hydrothermal sedimentary crusts. Mixed-layer samples were also found.

Biogenic nature of the basic ore components (Fe-vernadite, Mn-ferroxyhite) in oceanic hydrogenic Fe-Mn-crusts and nodules was substantiated. Mn^{2+} and Fe^{2+} cations as well as any Mn-Fe-minerals and colloid particles of oceanic (marine) or terrigenic genesis may serve as the raw material for biogenic formation of vernadite-ferroxyhite associations.

Solid-phase ageing processes were detected in crusts and nodules leading to transformation of buserite-I into 7A-birnessite, replacement of hydrothermal todorockite and buserite-I by buserite-II, and iron-free vernadite biogenic substitution for todorockite and birnessite.

Asbolane in laterite weathering crusts is normally formed through transformation from buserite-I via interstratified asbolane-buserite.

I. Chukhrov F.V. et.al. Hypergenic oxides of manganeneze, Nauka, Moscow, I989, 350 pp. (in Russian).
2. Chukhrov F.V. et.al. Miner.zhurn., I988, IO, N 2, pp. 78-92.

STUDY OF SODIC-AMPHIBOLE FROM BLUE-SCHIST BELT IN NORTH HUBEI PROVINCE

Guan Yaxian, Liu Baoliang, Sun Yanxiao, Huang Junjie, Chang Chun University of Earth Science, Changchun 130026, Jilin, People's Republic of China

A large blue–schist belt extends in central China, between the south of Sino–Korea platform and the north of Yangtze platform. It begins from northern Sichuan province, passing through southern Shanxi province to northern Hubei province, Anhui, Jiangsu and Shangdong proince, and then dives into Yellow sea, extending discontinuously for more than 2000km. Such an ancient blue–schist belt is rarely seen elsewhere in the world, while the Northern Hubei blue–schist belt is in the middle part of the whole belt.

The major rock types of northern Hubei blue–schist belt comprise glaucophane chlorite sericite schist, glaucophane albite chlorite actinolite schist and glaucophane muscovite quartz albite schist. Their protolith belong to basic

volcanics, acidic volcanic sedimentary rocks, argillo–arenaceous rocks and carbonatite, occurring at the tectonic setting of a continental rift. Its major mineral association: Mr+Ser+Chl+Q, Mr+Sti+Epi+Ac+Ab, Cro+Mus+Epi+Ab+Spe+Q. symptomatic metamorphic minerals occurring in this area include amphiboles, stilpnomelane, phengite, garnet, epidote, piedmontite and albite, quartz, calcite, dolomite, etc. However, no typical high–pressure low–temperature minerals such as lawsonite, jadeite and aragonite have been found yet.

Minerals of amphibole group in the area can be divided into three series according to Leake(1978):sodic–amphibole are magnesio–riebeckite and crossite;sodic–calcic amphibole is winchite; and calcic amphibole is actinolite.

The chemical composition of sodic–amphibole shows $Mg/Mg+Fe^{2+}$, 0.48–0.75, $Fe^{3+}/Fe^{3+}+Al^{VI}$, 0.36–0.91. Crossite and magnesio–riebeckite have refractive indices respectively: Ng=1.668,1.698; Nm=1.664,1.666; Np=1.653, 1.656. There is a little variation of parameters in the unit cell of sodic–amphibole: a_0=9.546–9.68A, b_0=17.751–17.976A, c_0=5.295–5.340A, β=103.60–103.72, V=883–893A. It is found that the more Mg and Al are substituted by Fe^{3+} and Fe^{2+}, the higher the values of a_0, b_0, V would be , but it's not the case for c_0.

A linear relationship is found among peak intensities of X–ray diffraction(I_{110}, I_{310}, I_{330}, I_{240}), composition of sodic–amphibole(numbers of atom in unit cell) and Fe,Mg content in site C ($M_{<1>}$,$M_{<2>}$,$M_{<3>}$).

The parameters of Mossbauer spectrum: Fe^{2+} $M_{(1)}$ I.S= 1.118–1.136mm/s, Q.S=2.773–2.867 mm/s, GW=0.277–0.296 mm; Fe^{2+} $M_{(3)}$ I.S= 1.093–1.213 mm/s, Q.S=2.231–2.443 mm/s, GW=0.304–0.40 mm; Fe^{3+} $M_{(2)}$ I.S= 0.352–0.413 mm/s, Q.S=0.415–0.461 mm/s, GW=0.267–0.309 mm. Mossbauer spectroscopy studies show that: In sodic–amphibole, Fe^{2+} is located in sites $M_{(1)}$, $M_{(3)}$, and Fe^{3+} in site $M_{(2)}$. So Fe–ion in sodic–amphibole is distributed orderly.

Amounts of Fe^{2+} in sites $M_{(1)}$ and $M_{(3)}$ are approximate, with their maximum difference being of 3.7%.

In sodic–amphibole,occupancy of Fe–ion has relation to the age of the beds in which the amphibole exists the occupance of Fe^{2+} in sites $M_{(1)}$, $M_{(3)}$ increases, while that of Fe^{3+} in site $M_{(2)}$ decreases, as the age of the beds becomes older. At Suixian–Yinshan district, for example, the numbers of Fe^{2+} in sites $M_{(1)}$, $M_{(3)}$ of sodic–amphibole from the underlying Huangzhiwang formation of Suixian group are 0.9412 and 0.4523 respectively, which higher than that from the overlying Baizhaoshan formation(0.6403 and 0.4005). However, Fe^{3+} at site $M_{(2)}$ of sodic–amphibole from the former is 1.0364 which is, on the contrary, lower than that (1.2982) from the latter.

Occupancy of Fe^{2+} in sites $M_{(1)}$,$M_{(3)}$ is calculated by absorption band at 3600–3700cm^{-1} in IR absporption curve which is the comparable with the result by Mossbauer method. In Junxian–Liangyun district, for instance, the number of Fe^{2+} in $M_{(1)}$, $M_{(3)}$ sites of sodic–amphibole from the underlying Yiaolinghe group are 1.028 and 0.451 respectively which is higher than that, namely, 0.696 and 0.394. the overlying Doushantuo, However, that of Fe^{3+} at $M_{(2)}$ site from the former is 1.276, which is, on the contrary,lower the number of Fe^{3+} in the former and 1.38 from the latter.

Studies show that the formation temperature of sodic–amphibole of the blue–schist belt in this area is about 300–450℃ , pressure about 0.6–0.75Gpa, which are somewhat higher in temperature, lower in pressure than that from typi-

cal blue–schist at abroad. It may correspond to a transitional glaucophane–green schist facies. This blue–schist belt was formed at late proterozoic, having the age 7.44 Ma, as a result of ancient intracontinental plates collapsion–collision movement, when subducted Yangtze platfrom come into collision with north China platfrom.

STRUCTURAL MINERAL CHANGES IN THE PROCESS OF FINE GRINDING

T.S.Jusupov, D.K.Arkhipenko - Institute of Geol. and Geophys. Sib. Br. Acad. Sci. USSR, 630090-Novosibirsk

There were observed some regularities and sequences of transforming a mineral structure with different types of chemical bonds in the process of fine grinding.

Mineral having mainly ionic type of a bond (CaF_2 and others) demonstrates rather slight distortion during grinding; mainly, the size of blocks of coherent scattering decreases.

The grinding of minerals mainly with covalent types of bonds (sylvite: galena, arsenopyrite, chalkopyrite) results in the most intensive microdistortions the physical and chemical properties changing.

The layer silicate having a different set of types of bonds demonstrates a rather great structural distortion. There are indentified some changes depending on the medium: in the air medium - the bonds in octahedral layers are the first to distroy; in the water medium there is the break in the interlayer space, the structure of polyhedral being preserved.

As the content and structure determine mineral properties, but grinding brings to their changes the information concerning the structure is very important for obtaining some nessesary adaptable properties.

46.4.14.K

CRYSTAL CHEMISTRY OF 7Å PHYLLOMANGANATE MINERALS

Kim, Soo Jin, Department of Geological Sciences, Seoul National University, Seoul 151-742, Korea

7Å phyllomanganate minerals refer to hexagonal manganese oxide minerals that are characterized by a layer structure with basal d(001) spacing in the range of 7.1-7.6Å. The minerals include rancieite, birnessite and related phases and show widespread occurrence in marine and terrestrial manganese deposits. Although the name birnessite was originally given to the Na-dominant member of the 7Å phyllomanganate minerals, it has been also applied in many previous studies to other cation-dominant members with d(001)=7.1- 7.4Å regardless of their chemistry. Confusion also arises in the differentiation of birnessite and rancieite, e.g., the phyllomanganate mineral with d(001)=7.4Å was named birnessite by one and rancieite by the other. Further confusion has arisen from takanelite which has been named to the mineral having the same X-ray powder diffraction pattern as rancieite.

7Å phyllomanganate minerals have hexagonal layer structures with variable c-dimensions which depend on the nature of interlayer cations and content of water molecules between edge-shared [MnO_6] octahedral layers. Approximately one out of nine octahedral sites is statistically vacant, leading to the general formula $R_{2x}Mn^{4+}_{9-x}O_{18}\cdot nH_2O$, where R=Ca, Mn^{2+}, Mg, K, Na ; x=0.8-1.3 ; n= 3-8. The minerals of this formula fall under the name of "rancieite group". It includes Ca-dominant (rancieite), Na-dominant (birnessite), Mn^{2+}-dominant and Mg-dominant members. Minerals of the rancieite group occur predominantly in two different hydration states, i.e., n=3-4 and/or 6-8 in the formula. The present author proposes that minerals with higher hydration be called species (i.e., rancieite etc.) and those with lower hydration be called dehydrated varieties (i.e., dehydrated rancieite etc.). The Mn^{2+}-dominant member of rancieite group in this work may be the true Mn^{2+} analogue of rancieite rather than takanelite.

ELECTRON_HOLE CENTERS IN SOME GEM CRYPTOCRYSTALLINE AND AMORPHOUS VARIETIES OF SILICA

46.4.8.K

Ruslan I. Kostov, Geological Institute, Bulgarian Academy of Sciences, Sofia 1113, Bulgaria

Numerous studies have been provided on natural and synthetic quartz by electron paramagnetic resonance (EPR) spectroscopy which display many electron-hole centers (for review see Weil, 1984; Kostov, Bershov, 1987). whis is important both from a theoretical and practical point of view as being

used for crystallochemical, geochemical, morphological, physicochemical and dosimetricinterpretations.

Further,on studieswhichhave been carried out on chalcedonies of different colour and index of crystallinity,two main signals have been descibed in their EPR spectra - a broad signal attributed to iron-bearing microphases correlating in most cases to the intensity of colour and a narrow signal at g=2 assumed to be one or more centers. The intensity correlates with decreasing index of crystallinity (Plyusnina, Kostov, 1988). In certain cases in the EPR spectra of cryptocrystalline silica the g=4.3 center, attributed to Fe^{3+} has also been observed (Kostov, Bershov, 1984).

In the EPR spectra of some opal varieties of different colour,the following main signals have been observed - a broad signal attributed to iron microphases, a signal of Fe^{3+} at g=4.3,a six-component signal of Mn^{2+} and a narrow signal at g=2 attributed to organic matter,both last signals being typical for the black or dark coloured opal varieties (Kostov, Pojarevski, 1988). Similar data have been obtained for bioopal and Australian vein opal (Ikeya, Golson, 1985).

The observed EPR signals in cryptocrystalline quartz, chalcedony and opal have beem also described in the EPR spectra of natural glasses as tektites and impactites (Mineeva et al., 1984),or perlites (Calas et al., 1988).

References

Calas, G., S.Angelov, Y.Yanev, R.I.Kostov. 1988. - Geologica Balc., 18, 5, 53-60.

Ikeya, M., J.Golson. 1985. In: ESR Dating and Dosimetry (Ed.: M.Ikeya, T.Miki), IONICS, Tokyo, 281-285.

Kostov, R.I., L.V.Bershov. 1984. - Izvestiya Akad. Nauk SSSR. Seriya Geolog., 11, 93-105.

Kostov, R.I., L.V.Bershov. 1987. - Izvestiya Akad. Nauk

SSSR. Seriya Geolog., 7, 80-87.
Kostov, R.I., I.M.Pojarevski. 1988. - Compt. Rend. Acad. Bulg. Sci., 41, 7, 63-66.
Mineeva, R.M., L.V.Bershov, A.S.Marfunin, V.I.Feldman, A.V.Speranskii. 1984. - Mineral. Zhurnal, 6, 2, 30-35.
Plyusnina, I.I., R.I.Kostov. 1988. - Geochem., Mineral. and Petrol., 25, 20-27.
Weil, J.A. 1984. - Phys. Chem. Minerals, 10, 4, 149-165.

STRUCTURAL PECULIARITIES OF TOURMALINE FROM QUARTZ VEINS OF THE SUBARCTIC URALS

L.M.Krivoputskaya, R.V.Rodionova, S.M.Solntseva, R.I.Mashkovtsev, I.I.Urosov. Institute of Geology and Geophysics, Novosibirsk-630090, USSR

A complex of methods has been used to study asbestiform specimens which are fibrous-diverse aggregates of greyish blue colour with a silky luster. Some fibers are up to 2-3 cm long and hundredths of a millimeter in diameter. The mineral under study appears in quartz veins on the western slope of the Subarctic Urals. It is associated with quartz body-host rock contacts and does not exceed 5-10 cm in thickness.

The crystallochemical formula of the mineral $^{Na}_{0.446}{}^{K}_{0.120}{}^{Li}_{0.004}{}^{Mg}_{0.969}{}^{Mn}_{0.004}{}^{Fe^{2+}}_{1.092}{}^{Fe^{3+}}_{0.207}$ $^{Al}_{6.159}{}^{Si}_{9.762}{}^{Ti}_{0.020}{}^{O}_{27}{}^{B}_{2.61}{}^{(OH,F)}_{4}$ corresponds to tourmaline. An increased content of Si is due to quartz present in the sample. On the basis of IR-spectroscopic and X-ray data the specimen under study was stated to be related to the schorl-dravite series with isomorphic impurities being distributed statistically among the Y-sites. In EPR spectra, broad lines are observed in the range g~4, which is typical of the Fe^{3+} ions in the distorted octahedron coordination.

The comparison with a number of natural and synthe-

tic tourmalines shows that the structure of the asbestiform specimen is characterized by a more narrow spectrum of isomorphic substitutions. The unit cell parameters and main interplanar distances - 3.99(10), 2.58(70), 1.59(50), 1.64(30) - correspond to the tourmaline structure, a significant re-distribution of reflex intensities, however, being observed. At a relatively high perfection of the crystal structure the defect quantity in the specimen under study is significantly higher than in crystals of verdelite and rubellite varieties: s_{stud}=0.39, s_{verd}=0.11, s_{rubel}=0.14. The crystallite sizes are 910, 1790 and 1400 Å, respectively.

The asbestiform tourmaline under study is also sensitive to mechanical effects. The correlation of a mechanical load with a value of thermal and X-ray characteristics is stated. An increase in mechanical effect duration and load value is followed by a decrease in temperature of endothermic peaks from 985°C in the initial sample to 970 and 965°C in those affected mechanically for 20 min and 40 min, respectively, with the intensive development of microdistortions (0.39, 61 and 82, respectively), by a decrease in crystallite size (910, 460 and 280 Å), by loss of constitutional water and mineral amorphization.

The investigations carried out allow the asbestiform mineral to be identified as tourmaline and the evolution of mineral formation medium to be followed in the region under study.

INVESTIGATION OF TYPOMORPHIC CHARACTERISTICS OF ZONAL CRYSTALS OF FLUORITE

L.M.Krivoputskaya, R.V.Rodionova, S.M.Solntseva, I.I.Urosov, Z.K.Mazurova. Institute of Geology and Geophysics, Novosibirsk-630090, USSR

Fluorites from pegmatites of the Kent deposit of the Central Kazakhstan have been investigated by a complex of techniques. The specimens under study are crystals of a cube-octahedron habit of 6 to 17 cm in size with a distinct zonality. There are 8 structural mineralogical zones revealed from the core of crystals to the periphery, and fluorite in each of these zones is distinguished in colour (light-blue to dark-violet), nature and quantity of isomorphous impurities, values of some structural characteristics. A wide range of elements entering the structure as isomorphs such as: Y, Mn, Gd, Si, Ti, P, Cu, Cr, Mg, K, Na, Al - has been revealed in various generations of fluorite. A distinct regularity, however, of a decrease in their contents from early to later generations has been stated only for Y^{+3}, Gd^{+3}, Mn^{+2}. Variations in concentration of these elements in the fluorite structure result in changing the specimen colour. An increase in quantity of these elements in the structure was shown to change the specimen colour from light-blue to blue, violet and green. In particular, the intensively coloured varieties contain more yttrium than the light ones, the Y contents being higher in the zones of green colour than in the violet ones and the violet varieties have more Y than those of light-blue colour.

The presence of impurity elements in crystals correlates with values of a number of structural characteristics. An increase in concentrations on Mn^{+2}, Gd^{+3} and Y^{+3} leads to a decrease in the "a" parameter of unit cell from 5.4644 to 5.4627 Å, the crystal perfection being changed from early generations of fluorite to later ones. The perfection degree is determined by microcrystal size, defect amount, concentration and character (ion size) of elements that enter the structure as isomorphs. A decrease in crystal structure

perfection degree from $0.1 \cdot 10^{-4}$ to $0.2 \cdot 10^{-2}$, decrease in microcrystal size from 1860 to 1230 Å and increase in value of microdistortions from 0.02 to 0.19 are observed for the distinguished zones from the crystal center towards the periphery.

The investigations carried out on composition and structure of fluorite resulted in revealing the typomorphic characteristics that allow the changes in colour of the specimens to be explained and conditions of mineral formation to be determined more precisely.

IRRADIATION INDUCED DECORATION OF MINERIS AND STUDIES OF NATURAL CRYSTAL STRUCTURES

Komov I.L. Kulish E.A., IGFM, USSR

Internal structure of natural minerals revealed by γ–irradiation is found to contain information on crystal growth and development history. Decoration patterns of natural crystals have shown a number of elements attesting inhomogeneity of their internal structure (zoning, sectoral division, mosasic pictures, traces of solution–regeneration). Contrast of different structures and constitutions which reveals itself in colour of mineral is a characteristic feature to measure the inhomogeneity. Crystals grown in relatively stable environments are more or less homogeneous, their colour being uniform in the whole volume of the material.

Difference in colour intensity and a kind of rhythmic colour zoning are indicative of temporal changes in composition of the mineral–bearing fluids. These pictures allow us to reconstruct the intricate dynamics of changes taking place in the environments in certain time intervals. Decoration of crystals by γ–irradiation makes it possible to study the mechanism of the commonest natural phenomenon–that of solution–regeneration. Transparent quartz which seems to be absolutely homogeneous presents crystals having varying number of solution–regeneration zone. There have been found from 2 to 7 such in some crystals. The regenerated parts of some broken or dissolved crystals have more intense colouring as compared to the contemporaneous material. Dissolving and consecutive formation of cones and "funnels" begin at the top of the crystal and then take over the whole belt of the prism faces. Citrine zones dissolve faster than the smoky ones.

Irradiation allows us to determine limits of displacements and those of the mosaic blocks. Smoky crystals have mosaic structure as a rule, the mosaic block borders being seen on the faces of main rhombohedra showing a sort of streamline distribution pattern for colours. Highly mosaic crystals have usually low density of colours. Smoky–citrine quartz has been found to demonstrate inherited mosaics localized at the base of the crystal

though quickly wedged out. Coarse blocks have been found a characteristic feature of amethysts.

Mosaics of growth as revealed by irradiation may serve a piece of evidence for heterogenous, unstable environments of quartz growth, possibly in solutions supersaturated by silica and rich in impurities.

The density of colours has been found to increase near twin borders because free surface energy related to the twin interfaces adds at that boundary to the free energy of the radiation defects. Impurity and point defects concentrate on twin borders, there being notably a lower number of these defects in any other region. γ–irradiation is found to be a very promising tool to study the internal structure of minerals.

564.8. V

CRYSTAL STRUCTURE OF ZINCOVOLTAITE*

Li Wanmao, Wang Qiguang and Chen Guoying, Department of Geology and Instruments Analysis & Research Centre, Lanzhou University, Lanzhou, Gansu, 730001, People's Republic of China.

Zincovoltaite is a new sulphate mineral discovered at Xitieshan mine in China, 1984. In this paper, the crystal structure of the new mineral has been studied.

A crystal 0.2*0.2*0.2mm was mounted on a CAD-4 Enraf-Nonius diffractometer. Cell dimensions and orientation matrix for data collection were calculated by least-squares refinement from 25 centered reflections using MoKα radiation (λ=0.710Å) with graphite monochromator. The cell parameter gives a=27.169(2)Å, V=20055Å^3, Z=16($K_2Zn_5Fe_3Al(SO_4)_{12}*18H_2O$). Diffraction intensities for reflections were measured by the ω/2θ scan technique, using a variable scan speed. A total of 4713 reflections were measured up to a maximum 2θ of 56°. 1142 with I<3σ was classified as unobserved reflections. The systematic absence hkl,h+k,h+l,k+l≠2n;hk0,h+k≠4n; hhl,h,l≠2n uniquely define the space group as Fd3c. By averaging equivalent intensities, 745 independent reflections with I>3.0σ were obtained. All reflections were corrected for standard intensity, Lorents. and polarization factors.

The structure was solved by model methods and Fourier syntheses. The sites in the space group Fd3c for Fe, Zn and K atoms were fixed based on the space group of the mineral, and culminated in a trial model. The oxygen atoms were found from Fourier syntheses. H atoms could not be found out because of the disordered distribution completely of water molecule. The anisotropic thermal parameters for all atoms by block-diagonal least-squares were refined. The refinement converged to an R of 0.057. The crystal structure of the zincovoltaite may be considered that a 3-dimensions continuous framework consists of $[Fe^{3+}O_6]$. $[ZnO_4(H_2O)_2]$ octahedron and $[KO_{12}]$ polyhedron linked by $[SO_4]$

tetrahedron, and $[Al(H_2O)_6]$ octahedron disordered distribution filled in the great holes from the above arrangement. Fe^{3+} ion is located at the origin of the cell, namely symmetric center, and surrrounded by six oxygen atoms belonging to $[SO_4]$ with a mean Fe-O distance 2.018(5)Å. Zn^{2+} ion is surrounded by four oxygen atoms belonging to $[SO_4]$ and two oxygen atoms belonging to water molecule. The Fe^{3+} ions have two different possible occupancies. One is that a part of Fe^{3+} ions occupy firstly 32 equivalant sites in the unit-cell and the rest of Fe^{3+} ions occupy 96 equvalant sites together with 80 Zn^{2+} ions. Another one is that the Fe^{3+} ions occupy half of all 96 equivalant sites in the unit-cell. The Mössbauer spectrum of the mineral confirmed that the Fe^{3+} ions of zincovoltaite distribute in according to the former pattern.

K^+ ions occupy the holes between the $[FeO_6]$ and $[ZnO_4(H_2O)_2]$ octahedron, and each K^+ ion is surrounded by 12 oxygen atoms. The $[KO_{12}]$ polyhedron and $[ZnO_4(H_2O)_2]$ octahedron linked by sharing bridge oxygen corners. Because the K-O(3) distance (3.223Å) is significant longer than K-O(4) distance (2.876Å) with a difference of 0.347Å the coordination of K and O atoms must be considered to be a 6+6. Al atom was found from 3-dimension Fourier synthesis and surrounded by 6 oxygen atoms belonging to water molecule. The $[Al(H_2O)_6]$ octahedron filled in the great hole giving rise from the arrangement of the $[FeO_6]$, $[ZnO_4(H_2O)_2]$ octahedra, and $[KO_{12}]$ polyhedra. This fact shows that the Al atom is one of the essential constituents of zincovoltaite.

* Project is supported by the National Natural Science Fundation of China

11.4.6.H

EXPERIMENTAL STUDIES IN THE FELDSPAR SYSTEM $CaAl_2Si_2O_8$ - $Na_{0.5}La_{0.5}Al_2Si_2O_8$

F. Liebau and H.-J. Kneip, Mineralogisches Institut der Universität Kiel, D-2300 Kiel, Germany F.R.G.

Feldspars $M[(Al_{2-x}Si_{2+x})O_8]$ show remarkable chemical variation with regard to the non-tetrahedral cations M which can be monovalent ($M^+ = Na^+, K^+, Rb^+, NH_4^+, Tl^+$) or divalent ($M^{2+} = Ca^{2+}, Sr^{2+}, Ba^{2+}, Pb^{2+}$). In contrast, incorporation of trivalent non-tetrahedral cations into the feldspar framework has only been observed for $M^{3+} = La^{3+}$ [1] and, to a minor extent, for the larger rare earth cations Ce^{3+}, Pr^{3+} and Nd^{3+} [2]. To gain insight into the structure of such feldspars, gels of composition $Na_xLa_xCa_{8-2x}[Al_2Si_2O_8]_8$ have been heated to 1300°C and the pro-

ducts studied by X-ray powder diffraction, electron microscopy and diffraction, X-ray fluorescence microanalysis, and ^{29}Si-NMR. The following results have been obtained.

(1) In the whole composition range ($0 \leq x \leq 4$) the unit cell volume increases continuously with x following the linear equation

$$V = 7.609x + 1341.5 \quad (R = 0.996).$$

(2) Deviations from 90° of the triclinic angles decrease with x; above x = 3.05(5) the feldspars are monoclinic.

(3) Decreasing intensity and increasing diffuseness of b reflections on single crystal electron diffraction diagrams indicate that the Al/Si distribution becomes less ordered as the $2Ca^{2+} \longrightarrow Na^{+} + La^{3+}$ replacement increases. In accordance, NMR spectra show that the portion of $Q^4(3Al)$ units increases; for $x \geq 1$ even $Q^4(2Al)$ are observed.

(4) Decreasing intensity and increasing diffuseness of c and d reflections as x increases indicate that the distribution of the M cations is disordered and that the monoclinic feldspars ($x \geq 3.05$) are I-centered with the most probable space group I2/c.

(5) Even with high resolution electron microscopy no exsolution into two feldspar phases has been observed.

(6) Albite-law (010) twinning has frequently been observed in triclinic, Carlsbad-albite law [001](010) twinning in triclinic as well as monoclinic feldspars of the system.

(7) In the Ca poor part of the system under study there seem to be slight deviations of the chemical compositions of the feldspar crystals from the formula $Na_xLa_xCa_{8-2x}[Al_2Si_2O_8]_8$.

[1] Bettermann, P. & Liebau, F., Naturwiss. 63, 480 (1976)

[2] Grammenopoulou, S., Diplomarbeit, Mathem.-Naturwiss. Fakultät, Universität Kiel, 1978

56.4.9H

GENESIS TYPES AND CRYSTALCHEMICAL CLASSIFICATION OF IRREGULAR ILLITE / SMECTITE INTERSTARTIFIED CLAY MINERALS

Lu QI, Lei Xinrong, Liu Huifon, Test Center, China University of Geosciences, Wuhan, Hubei 430074, P.R. China

Irregular illite / smectite interstartified clay minerals (I / S) are of great significance to study diagenesis, classify strata, research quasicrystal structure, etc..

I / S can be grouped into three types according to its geneses: diagenetic, weathered, and volcano hydrothermal.

The characteristic of diagenetic I / S is that, along with the diagenetic degree's increasing, the I layers in I / S get raising, but S layers become less. It indicates the evolutionary process of clay from smectite to illite. The structural feature is that, at the early stage, I / S is wholly random along Z direction, but at the later, partly regular. On the basis of a great many XRD patterns and data of I / S (the samples are from pellites and sandstones of Cainozoic, Mesozoic,and Palaeozoic groups), it is concluded that the process always shows discontinuity, i.e. the I layers in I / S are jumped from below 60% to above 80%, which just corresponds to the first and the second oil–forming zones.

Weathered I / S has the feature that: the struture is wholly random, and I layers in I / S are below 60%, with their formation being controlled by the weathering degrees. This type I / S includes degenerated froms.

The volcano hydrothermal I / S are well–crystalized, and have symmetrical XRD peaks, and are partly regular in structure. The I layers in I / S remain almost fixed in number. This type of I / S often can be found at P–T (Permian–Triassic system) boundary. Both field and experimental studies as well as synthetic experiment showed that the I / S are formed in an acidic medium, above 300. Based on the properties, the authors support the view that at the P–T boundary, there was cosmic dust falling down onto the earth surface, or volcano ejecting occurring on a large scale.

Having studied more than one thousand I / S samples from every geological times and based on the features of chemistries and structures, I / S can be classified into 3 groups: whooly random, partly regular and quasicrystal groups.

In the first group, the I layers in I / S are less than 60%, and they are poorly crystalized, the XRD peaks are very broad, sometimes could hardly even be found at a fixed position.

The second group includes IS, ISI, and ISII regular forms.

Based on the theory of quasicrystal particle fractional dimension model, and after analysing the I / S at the P–T boundary layer, it is found out that the I / S possesses two–dimension crystal and one–dimension quasicrystal structure, i.e. crystal structure is shown along X and Y, and quasicrystal along Z direction. By calculation, the authors proposed four types of quasicrystal I / S structure sequences (the details will be in another article being in press):

1. ISIIIISIISIIIISIIIISIISIIIISIISIIIIS.....
2. IIISIIIIIISIIIISIIIIIISIIIIIISIIIISI.....
3. ISIISISIISIISIISISIISISIISIISISIISIISIS.....
4. ISISIISISIISISIISISISIISISISIISISIISISIS.....

The I layers in the above four sequences are 76.51%, 84.71%, 61.80%, and 58.20% respectively. They are just equal to the compositions of the I / S at the P–T boundary of the four provinces (Hunan, Hubei, Sichuan and Zejiang) in China.

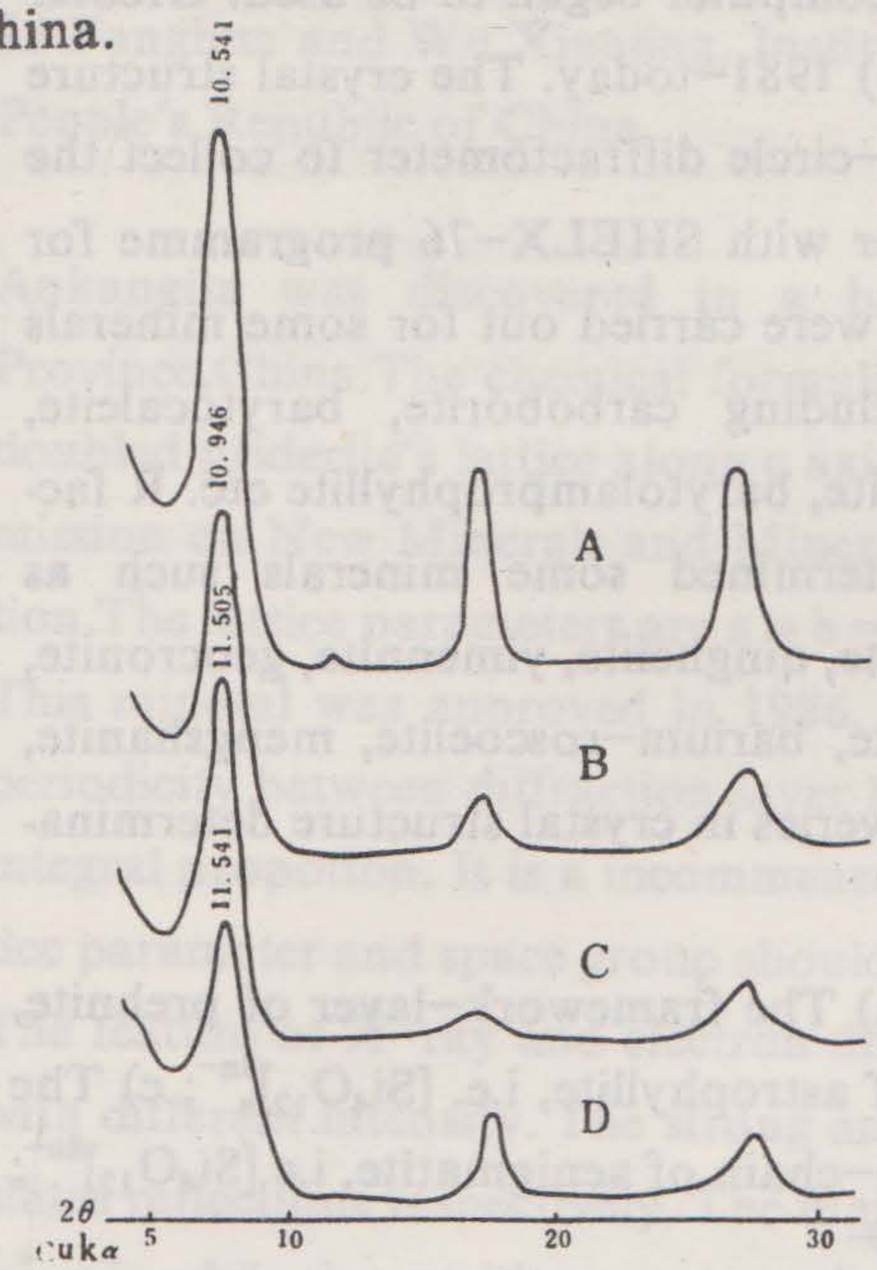

Fig. XRD patterns of I / S at P–T boundary layer.

A:Huangshi, HUBEI
B:Sangzhi, HUNAN
C:Guangyuan, SICHUAN
D:Changxing, ZHEJIANG

A BRIEF INTRODUCTION OF RESEARCH WORK ON CRYSTAL STRUCTURE OF MINERALS IN CHINA UNIVERSITY OF GEOSCIENCES

41.4.3H

Ma Zhesheng and Shi Nicheng, China University of Geosciences, Beijing,100083, People's Republic of China

In 1957, the famous mineralogist and crystallographer—Peng Zhizhong completed the structure analysis of prehnite. This work filled the blank in this research area in China. He set up an X–ray laboratory and guided us in the new period on crystal structure of minerals in China.

The research work can be divided into three periods: 1) 1956–1966. During this time, we determined some structure of minerals such as prehnite, barytocalcite, baotite, bertrandite, bafertisite, monoclinic astrophyllite, taaffeite, nigerite, szaibelyite, chevkinite, suolunite, aenigmatite, baryto–lamprophyllite, triclinic–astrophyllite. We collaborated with the Institute of Atomic Energy and determinated the structures of cassiterite and barite by using the single–crystal neutron diffraction method. At that time only the photographic method was available in our laboratory and the intensities were estimated by eye. Although the values of the conventional R factor were rather high (they were about 0.2 to 0.3), later experiments proved that all these structure were initially correct; 2) 1973–1980. In this period, we determined balipholite,carboborite, paracostibite, omeiite, isomertiete,cebaite. These structure

analyses were being performed while we were coordinating with some other institutions to determine some minerals which were rather difficult to be identified. An X–ray generator with a rotating anode was used for photography. The computer began to be used. Greater accuracy was achieved. R indices about 0.09 to 0.18. 3) 1981–today. The crystal structure determination entered into a new stage, as we used 4–circle diffractometer to collect the three dimensional data and used special minicomputer with SHELX–76 programme for calculating. The refinement of some crystal structures were carried out for some minerals which were determined in the earlier period including carboborite, barytocalcite, balipholite, taaffeite, parahopeite, volborthite, chevkinite, barytolamprophyllite etc. R factors ranged 0.04–0.05. In the meanwhile, we determined some minerals such as Mg–nigerite, tin–ludwigite, carbocernaite, dagingshanite, qingheiite, yimennite, geocronite, d'ansite, cebaite, ganziite, qitianligite, wolframoixiolite, barium–roscoelite, mengshanite, ankangite etc. The following are some important discoveries in crystal structure determination of minerals during the above periods:

1) Discovering several new Si–O radical in silicates: a) The framework–layer of prehnite, i.e. $[Si_3AlO_{10}]_n^{5n-}$; b) The band form of Si–O radical of astrophyllite, i.e. $[Si_4O_{12}]_n^{8n-}$; c) The tetragonal–ring of baotite, i.e.$[Si_4O_{12}]_n^{8-}$; d) The branch–chain of aenigmatite, i.e.$[Si_4O_{12}]^{8n-}$; e) A special double tetrahedra of bertrandite,i.e.$[Si_2O_7]^{6-}$.

2) Discovering the eight–layer closest packing of taaffeite.

3) Discovering the special phenomena of the polymorphism (4 modifications) of the chevkinite group and the polytypism of astrophyllite.

4) Discovering the second order (or higher order) superstructure of F–RE fluo–carbonate.

5) Discovering the order–disorder phenomena of the vacancy of laihunite.

6) Discovering the mode of ordering of various cations and anions and some rare ordering mode of additional anions.

7) Discovering the phenomena of "opposite–crystallographic shearing" in the structure of hechite.

8) Having collaborated with other units, we discovered many new minerals and new species by structure analyses, including: magnesio–astrophyllite, barytolamprophyllite. ortholamprophyllite, balipholite, furongite, xiangjingite, orthobrannerite, ruarsite, anduoite, clinotyrolite,tongbaite, tin–ludwigite, yimenite, daqingshanite, qingheiite, xillingolite, qitianglingite and ankangite etc.

Recently, the research on crystal structure of minerals enters a wider field. We took a lot of time to do the modulation structure of minerals: The sine wave modulation structure was discoverd in franckeite and cylindrite by TEM. A kind of one dimensional incommensurate modulation was determined in ankangite. The research on surface structure of minerals started with STM(Scanning Tunneling Microscopy). Having collaborated with Prof. Tibor Zoltai we investigated the surface structures of graphite and jamesonite.

46.4.13K

THE STUDY OF THE CRYSTAL STRUCTURE OF ANKANGITE

Ma Zhesheng, Shi Nicheng, Zhou Jian, Liu Wei, China University of Geosciences, Beijing; Li Fanghua and Wu Xiaojing, Institute of Physics, Chinese Academy of Sciences, Beijing, People's Republic of China

Ankangite was discovered in a barite mineral deposit of Ankang Shiti in Shanxi Province,China.The chemical formula is $Ba(Ti,V,Cr)_8O_{16}$. The structure was considered as doubled priderite's lattice along c axis, when it was reported as a new mineral to the Commission on New Minerals and Mineral Names of the International Mineralogical Association.The lattice parameters are $a = b = 10.127$, $c = 2.978 * 2 = 5.956$ Å. Space group is P4 / n. This mineral was approved in 1986. During the structure analysis, it was found that the periodicity between diffraction layer lines in oscillation photograph along c axis was not in integral propotion. It is a incommensurate modulated structure. Therefore, the original lattice parameter and space group should be corrected.

The feature of X–ray and electron diffraction patterns is that there are two kinds of spots with different intensity. The strong and weak spots correspond to main reflections and satellites reflections respectively. The main reflections can be indexed by reciprocal vectors a^*, b^*, c^*, while the satellites can be written as

$$H = ha^* + kb^* + lc^* + mq$$

where $q = rc^* = 1 / 2.27c^*$

The characteristic of the reflections are as follows: a) The regulated periodicity of the main reflections is 2.956 Å along c axis. The periodicity of the satellites corresponding to a certain main reflection is $1 / q = 6.72$ Å; b) The distance between satellite and center of two main reflections along the c–axis is $u = 0.81$ Å; c) With the extinction of the main reflections, the corresponding satellites are absent.

The determination of the substructure of ankangite follows. A crystal, 0.2 * 0.25 * 0.40mm in size, was mounted on the NONIUS 4–circle automated diffractometer (The Department of Chemistry, University of Minnesota, USA). The intensity data of the main reflections were collected with MoKα radiation.535 independent diffractions were obtained in the range of $2\theta < 80^\circ$. The Lorentz and polarization corrections and absorption corrections were made.The sub–cell parameters are $a = b = 10.139(4)$ Å, $c = 2.961(2)$ Å. Space group is I4 / m. The substructure is isostructural with priderite. The least squares method was applied to refining the atomic fractional coordinates and anisotropic temperature factors, $R = 0.039$.

The atomic coordinates and thermalparameters are shown in Table 1.

Using high resolution electron diffraction image and X–ray diffraction method, ankangite was finally identified to be a one–dimensional incommensurate modulated structure along the c–axis. The modulation wave vector is $q = c^* / 2.27$. According to classification of

Tabe 1. Atomic Coordinates and Thermalparameters of Ankangite

Atoms	x	y	z	Beq
Ti(V)	0.1652(1)	0.3494(1)	0.0000	0.55(6)
O1	0.2026(2)	0.1556(2)	0.0000	0.43(2)
O2	0.1673(2)	0.5390(2)	0.0000	0.57(3)
Ba	0.0000	0.0000	0.3790(6)	2.60(2)

Bravais class derived by De Wolff, the incommensurate modulated structure is $P^{I4/mmm}_{1\,111}$ (No.21). The four-dimensional super space group of ankangite is $P^{I4/m}_{1\,1}$, since the space group of its substructure is I4 / m. The modulated structure is caused by occupancies and displacements of Ba cations in the tunnel.

* Project supported by the National Nature Science Fund of China

LOCAL STRUCTURES AROUND Ti, Cr AND Fe ATOMS IN GLASSES OF ROCK-FORMING SILICATE SYSTEMS

F.Marumo, Y.Tabira, T.Mabuchi and H.Morikawa, Research Laboratory of Engineering Materials, Tokyo Institute of Technology, Nagatsuta 4259, Midori, Yokohama 227, Japan

It is well known that some transition-metal elements show large effects on crystallization of rock-forming minerals from silicate melts, whereas others have only trivial influence on phase relations. For example, addition of a small amount of $MgCr_2O_4$ into the system Mg_2SiO_4-$CaAl_2Si_2O_8$-$CaMgSi_2O_6$(Di) expands significantly the spinel primary field, but the addition of $CaTiAl_2O_6$(Tp) affects the liquidus phase relation only slightly. The difference is supposed to have some correlation to the local atomic structures around the respective transition-metal elements. With the intention of elucidating the correlation, the coordinations of Ti, Cr and Fe atoms in silicate glasses were investigated with X-ray diffraction and EXAFS spectroscopy, by choosing the systems Di-Tp, Di-$CaCrAlSiO_6$(CaCrTs) and Di-$CaFeAlSiO_6$(CaFeTs).

Glasses with compositions of Tp10, 20, 30, 40 and 50 wt% and Di end member were prepared from reagent grade chemicals by melting their mixtures and then dropping into ice water. The glasses prepared have the compositions with 1.5, 2.5, 4.0 and 5.0 wt% CaCrTs, and 20, 40, 60, and 70 wt% CaFeTs in the systems Di-CaCrTs and Di-CaFeTs, respectively. The diffraction data were collected on a powder X-ray diffractometer with Mo Kα radiation. The Ti K, Cr K and Fe K EXAFS spectra were measured on the glasses with an EXAFS spectrometer at the Photon Factory in the Institute for High Energy Physics, Tsukuba. As for Tp10, Tp30 and Tp40 samples, diffraction data were also collected on the molten state with an X-ray diffractometer specially designed for use of synchrotron radiation.

The analyses of the observed data showed that a significant

part of Ti atoms take fourfold coordinations both in the melts and glasses of the Di-Tp system, whereas Cr atoms in the Di-CaCrTs system take entirely sixfold coordinations even in the composition range with a small amount of CaCrTs. The strong preference of Cr^{3+} to octahedral sites seems to stimulate crystallization of spinel, where Cr^{3+} ions occupy the octahedral sites with a slight distortion. On the other hand, Ti^{4+} ions can occupy either octahedral or tetrahedral sites, and addition of Tp does not extensively change the structure of the melt. The fact seems to be a reason why the diopside primary field covers a wide range of the Di-Tp system.

The Fe K EXAFS spectra indicated that Fe atoms take both octahedral and tetrahedral coordinations in the Di-CaFeTs glasses, giving practically constant mean Fe-O distances. Therefore, drastic structural changes are not expected also in the melts of this system, when the CaFeTs component is increased. The phase diagram of this system has again a wide pyroxene primary field.

The above observations suggest a close relation of the coordinations around transition-metal atoms in amorphous silicate materials to crystal-field stabilization energy. The Cr^{3+} ion has a large crystal-field stabilization energy in an octahedral field, whereas the Ti^{4+} ion has no crystal-field stabilization energy in either of the tetrahedral or octahedral field. The Fe^{3+} ion has five 3d electrons and no crystal-field stabilization energy in the high-spin state. Thus, the crystal-field stabilization energy seems to have a primary importance in the process of crystallization from silicate melts containing the first period transition metal elements.

STRUCTURAL AND CHEMICAL TRANSFORMATIONS OF ZIRCONS AT ELEVATED TEMPERATURES AND PRESSURES

56.4.10.V

A.V.Maslenikov, Institute of Precambrian Geology and Geochronology USSR Academy of Sciences, nab. Makarova 2, Leningrad 199034 and N.V.Kotov, Geological Faculty, State University, Universitetskaja nab.7/9, Leningrad 199034 USSR

The crystal structure of metamict zircon is subjected to recrystallization both by heating in air at temperatures up to 1400°C for 10 days and during hydrothermal treatment at 1kbar, 300-600°C in pure water and 2M NaCl solution for 3 days. The structure regeneration is identified by the X-ray powder pattern being confirmed by unit-cell parameters. Fig.1 shows a conjugated linear change of U and Pb-contents from point 1 (initial sample, near concordia) toward point 6 situated near the origin and corresponding to the following conditions: 1kbar, 600°C. The similar behaviour of Pb and U was also observed in crystalline samples of zircon as a result of their treatment by 15% HNO_3,

200°C. Thus, defect domains of matrix are being affected both by hydrothermal treatment and acid leaching. A combined hydrothermal treatment of zircon and vitreous oceanic basalt in two adjacent ampules at 1kbar, 300-600°C revealed no diffusion transport of typical zircon elements: Zr, Hf, Y, Sc, Yb into basalt whose recrystallization results in the formation of smectite and mixed-layer phases with a high sorbtion ability. The electron microscopic (Camscan, Link) study of the reactor walls showed neither material transport in vapour phase nor subtraction of the matter from the ampule with zircon have been found under thermogradient hydrothermal conditions.
These results are important for the interpretation of geochronological data on naturally occurring discordant zircons.

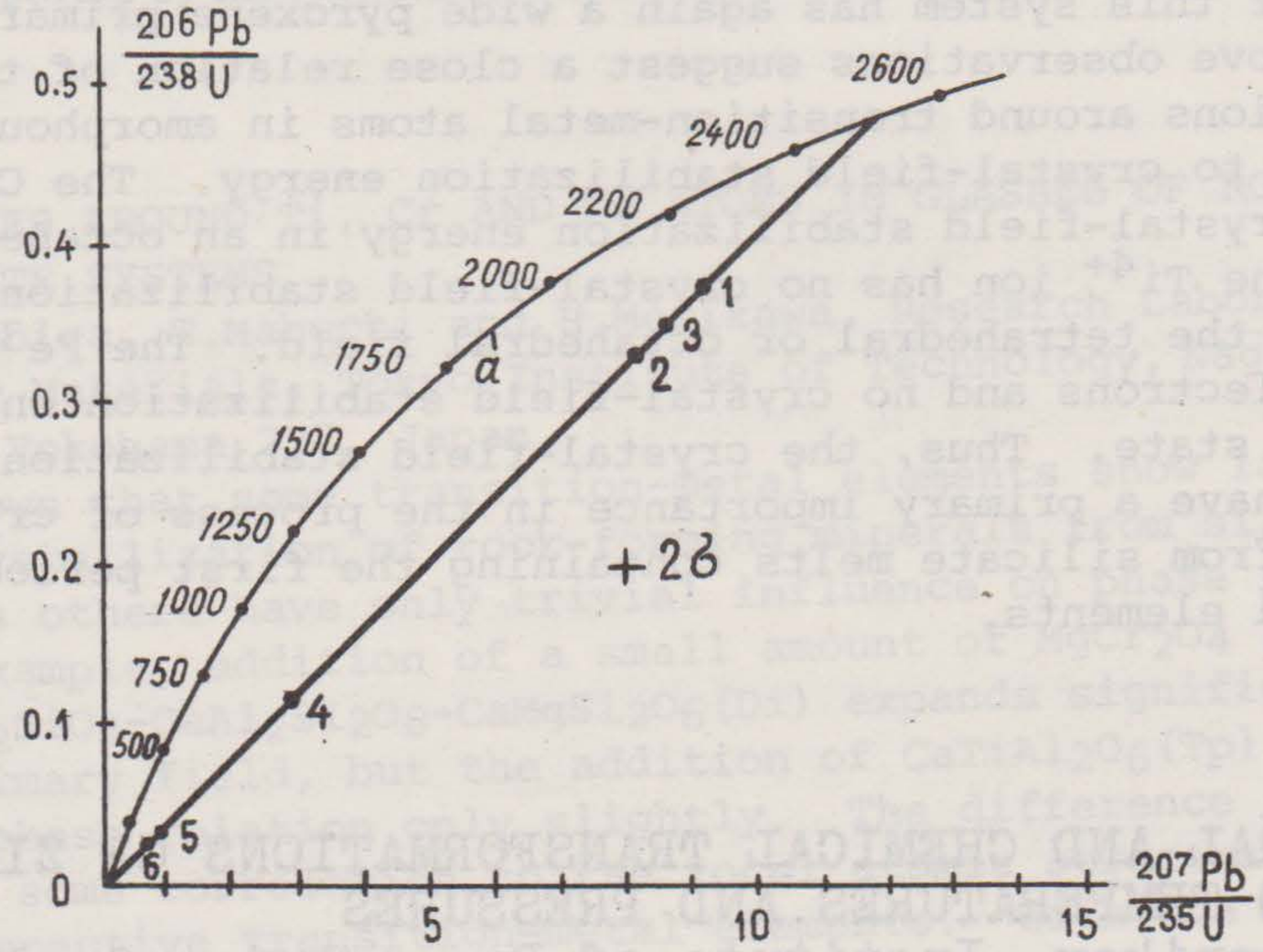

Fig.1. The relative Pb and U mobility at different conditions of zircon treatment: 1-initial sample; 2-300°C, 2M NaCl, unwashed; 3-300°C, 2M NaCl, washed in 15%HNO_3 at 80°C; 4-300°C, 2M NaCl, washed in 15%HNO_3 at 200°C; 5-600°C, 2M NaCl, unwashed; 6-600°C, 2M NaCl, washed in 15%HNO_3 at 200°C. a - concordia

DEVELOPMENT of the IDEA about the ESSENCE of MAIN MINERALOGICAL OBJECT

Powarennych Michael, Institute of Mineralogy, Geochemistry and Crystal Chemistry of Rare Elements,

Moscow, 113127, USSR

Evrystic fruitfulness of the approach to reveal the essence of the main mineralogical object has been shown earlier (Powarennych,Onoprienko,1986;Powarennych,1988,1989,1990). As far as we concern the essence of any natural system as its inner motive - law of self-motion we define that for the "mineral" system consists in the discordance between the condensed and diffused state of substance realising itself in the form of adsorption-desorption in thin layer of space on both sides from the phase boundary. This discordance is settled by formation of "s u r f a c e" - an immanent virtue of any mineral. This virtue does not inherent to the objects of less evolved matter forms such as atoms, molecules and elementary fractions. All history of mineral evolution from generation to its desintegration is imprinted in its surfaces. Any point in mineral volume was the point of its former surface sometimes. It is just on the mineral surfaces that genetic information can be "recorded" as a measure of negentropy in energy-substance distribution in the nearlying sphere of space-temporal continuum. This genetic information is fixed in the structure of arrising mineral body and manifests itself in its properties.

As it is shown in the proposed structural scheme of the object of mineral level of matter evolution (Powarennych,1990) it consists of three following elements (the main triad): m i n e r a l e m b r y o, protomineral (mE), system of i n n e r s u r f a c e s insurted into each other (iS) and o u t e r s u r f a c e (oS), i.e. M(Mineral)= mE + iS + oS . The members of the main triad in their turn consists of triads. For instance, mE consists of:1) e n c l o s e d sphere of space-temporal continuum , which may have Riman topological metrics (eC*),2)clothed by primary surface (s u r f a c i a l) - quasisolid-quasiliquid e a r l y f i l m (eF*),3)stabilised by primary a d s o r p t i o n l a y e r (aL*), i.e. mE = eC* + eF* + aL* . Each element from the iS-system is an enclosed four-dimensional generation and consists of:1)d i s o r d e r e d s u r f a c e with unevenly saturated atomic bonds (dS),2)a d s o r p t i o n l a y e r (aL) and 3)e n v i r o n m e n t i n c l u s i o n s (eI), i.e. $iS=\sum_{n=0}^{n}(dS + aL + eI)_n$. Mineral-medium interaction occurs in the sphere of space on both sides from the phase boundary where substance-energy-information interchange proceeds (s t r u c t u r e d e n v i r o n m e n t , sE). Thus, the o u t e r s u r f a c e (oS) consists of the most disordered outer surface (dS_o), adsorption

layer (aL_o) and structured environment (sE_o), i.e.
$oS = dS_o + aL_o + sE_o$.
As it follows from the proposed scheme one can aproximate the iS-system by the model of spacial crystalline lattice, i.e. the up-to- date adopted crystal chemical paradigma is included in now creating one as a constituent part. It allows oneself for the first time to give an e s s e n t i a l definition of the o b j e c t of mineralogy, compare the definitions of "mineral", "crystal" and "mineraloid" based on the prevaling role of one of three main triad members. One can receive basis of the paradoxical Vernadsky's idea of widening of "mineral" notion. The proposed scheme makes possible to create nonartificial, n a t u r a l classification of mineral level matter evolution objects - Periodic System of Minerals.

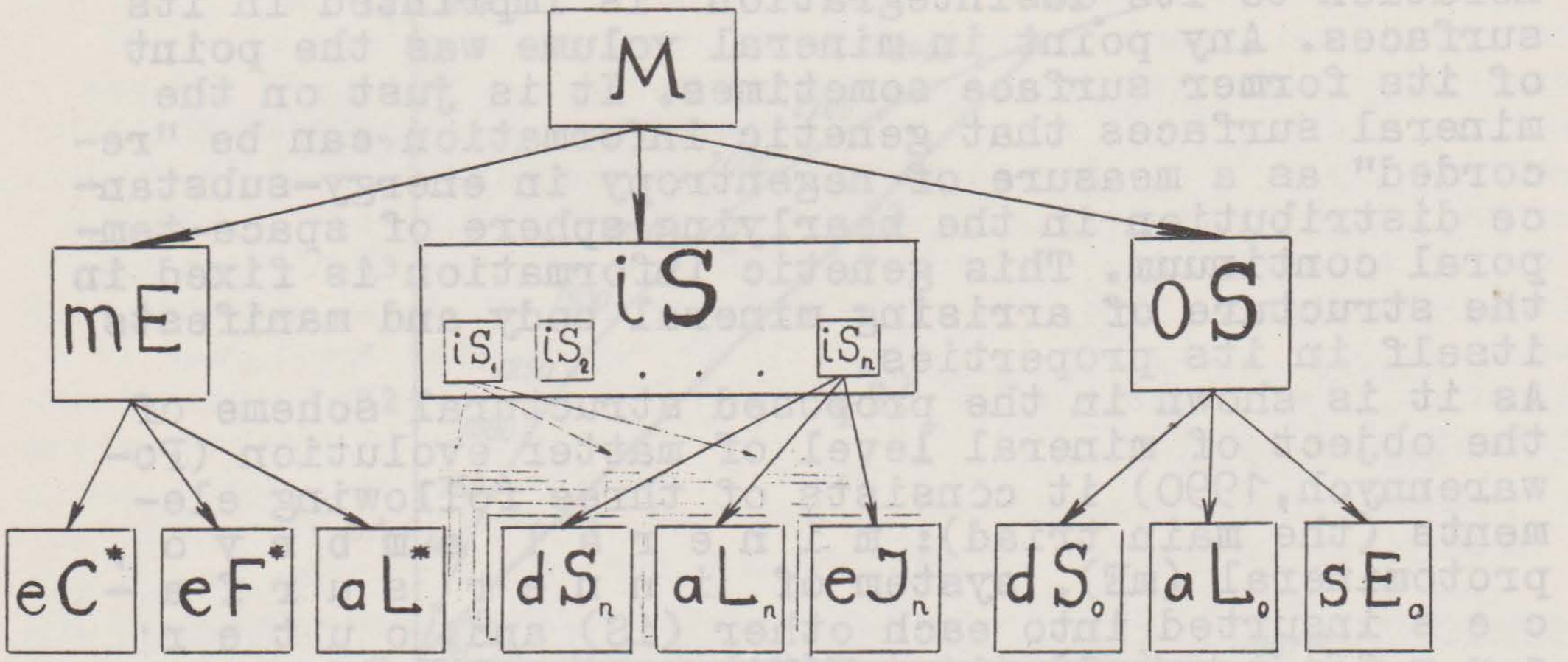

СТРУКТУРНАЯ СХЕМА СТРОЕНИЯ МИНЕРАЛА - ОСНОВНОГО ОБЪЕКТА ФУНДАМЕНТАЛЬНОЙ НАУКИ МИНЕРАЛОГИИ (пояснения - в тексте).

56.4.12V

CRYSTAL STRUCTURES OF RARE-EARTH MINERALS*

Ritsuro Miyawaki, *Ceramic Technology Department, Government Industrial Research Institute, Nagoya, Kita, Nagoya 462, JAPAN*
and **Izumi Nakai**, *Department of Chemistry, University of Tsukuba, Ibaraki 305, JAPAN*

The rare-earth elements (REE)comprise lanthanides (Ln), yttrium (Y) and, in some cases, scandium (Sc). The high oxidation state (3+) together with large ionic radii (about 1 Å) account for the characteristic behavior of rare-earth elements in crystal structures as well as in geological processes.

So far, a total of about 160 kinds of rare-earth minerals have been described. The rare-earth minerals always contain a variety

of rare-earth elements. From a view point of the distribution of rare-earth elements, rare-earth minerals can be classified into the following three groups: a group with the abundance of Y-group rare-earths; a group rich in Ce-group rare-earths; and a group composed of minerals having both Y-group dominant and Ce-group dominant species.

Crystal structures have been reported for about a half of the known rare-earth minerals. The structure analyses revealed that many of them were solid solutions among the rare-earth ions and other heterovalent ions with ionic radii comparable to those of rare-earth ions such as Na^{+}, Ca^{2+} and Th^{4+}, whereas some of the rare-earth minerals had independent crystallographic sites for rare-earth atoms. It is known that the similarity of ionic radii and electronegativities are generally the most important factors for isomorphous substitutions among the physico-chemical properties of elements.

The rare-earth minerals could be classified into the following 6 groups with a few exceptions:

(1) minerals with crystal structures containing isolated triangular anionic groups: e.g., bastnaesite, ancylite,
(2) minerals with crystal structures containing only isolated tetrahedral anionic groups: e.g., monazite, xenotime,
(3) minerals with crystal structures containing anionic groups of tetrahedral ions: e.g., yttrialite, gadolinite,
(4) minerals with crystal structures containing anionic groups of tetrahedral and octahedral ions: e.g., allanite, mosandrite,
(5) minerals with crystal structures containing anionic groups of octahedral ions: e.g., fergusonite, euxenite,
(6) minerals with crystal structures without anionic groups: e.g., fluocerite.

The coordination numbers of Ce-group rare-earths are similar to those of calcium and are generally higher than those of Y-group rare-earths. The coordination numbers of the Y-group rare-earths are from 6 to 9, among which the most frequently observed number is 8. On the other hand, those of the Ce-group rare-earths are from 7 to 12, and the most frequently observed number is 9. Consequently, the isomorphous substitution between Ce-group rare-earths and calcium is more frequently observed than that between Y-group rare-earths and calcium. On the other hand, thorium ions tend to be substituted by Y-group rare-earth ions rather than by Ce-group ions in the octahedral sites as observed in brannerite and davidite. The structure of Y-group rare-earth mineral is different from that of Ce-group rare-earth mineral when these structures belong to the groups (1) and (2) owing to the difference in the ionic radii between the two groups, even if the chemical formulae of the two minerals are similar to each other: e.g., tengerite, $Y_2(CO_3)_3 \cdot nH_2O$ (n=2-3) ——— lanthanite, $La_2(CO_3)_3 \cdot 8H_2O$, and xenotime, YPO_4 ——— monazite, $CePO_4$. These minerals do not have infinite framework structures, and the anionic groups in the structures are isolated each other and connected by rare-earth atoms to form three-dimensional structures. Therefore, the size of RE-polyhedron affects the

whole structure. On the other hand, structures having tight framework as is seen in the structures of gadolinite, allanite and aeschynite, are not affected by the sizes of the RE-polyhedra, because they can accept RE-polyhedra of any sizes without rearrangement of the structure. In addition, the coordination numbers of rare-earth atoms tend to increase in the order of silicate, phosphate, carbonate. This is explained by the decrease in the bond-strength accompanied by the oxygen atoms of SiO_4^{4-}, PO_4^{3-} and CO_3^{2-} ions, which have average negative charges of -1, -3/4 and -2/3 per an oxygen atom, respectively.

The charge compensation mechanisms in the solid-solutions of rare-earth minerals were classified into the following 4 types:
a) substitution accompanying vacancies,
b) coupled substitution within a rare-earth site,
c) coupled substitution at 2 independent crystallographic sites,
d) substitution accompanying valence variations.

---

* Published annually in **Rare Earth**(J. of the Rare Earth Soc. of JAPAN.), #11, 1-133(1987), #13, 1-42(1988), & #15, 1-12(1989).

SOLID-STATE NMR STUDY ON KAOLINITE WITH VARIOUS HINCKLEY INDICES

Ritsuro Miyawaki, Shinji Tomura, Yasuo Shibasaki,
Ceramic Technology Department,
Gov. Indust. Res. Inst., Nagoya, Kita, Nagoya 462, JAPAN
Masaharu Okazaki, Kazumi Toriyama,
Radiation Research Department,
Gov. Indust. Res. Inst., Nagoya, Kita, Nagoya 462, JAPAN
and **Soichiro Samejima,** *Engineering Research Association for Artificial Clays, G.I.R.I.N., Kita, Nagoya 462, JAPAN*

Kaolinite with high plasticity has been widely used as raw material for ceramics. The crystallinity of kaolinite is one of the factors closely related to the plasticity. The crystallinity has been usually estimated by the Hinckley indices which are calculated from the intensities of X-ray powder diffraction patterns. Recently, several attempts have been made to clarify the physical meaning of the Hinckley index(Plançon *et al.*, 1988; Brindley *et al.*, 1986; Komarneni *et al.*, 1985; *etc.*).

In the present study, a total of 10 (5 natural and 5 synthesized) kaolinite samples with various Hinckley indices were examined by high resolution solid state NMR to reinvestigate the relationship between the Hinckley index and the short range ordering. The natural samples examined are Kanpaku kaolinite, API-No.9 standard kaolinite specimen, Georgia kaolinite, Kibushi clay and Gairome clay. The synthesized materials were prepared from amorphous mixture of silica and alumina by hydrothermal treatment (Miyawaki *et al.*, 1989). X-ray powder diffraction patterns of the samples were measured on a RIGAKU RAD-IIB diffractometer using graphite monochromatized Cu$K\alpha$ radiation by the step scanning technique. ^{29}Si and ^{27}Al NMR spectra were

obtained with a BRUKER-MSL-200 spectrometer operated at 39.763 MHz for ^{29}Si and 52.140 MHz for ^{27}Al. Powdered samples were packed in rotors and spun at about 2.5 or 3.5 kHz for Si or Al, respectively, in a magic-angle spinning probe. About 300-1600 scans for ^{29}Si and 120 scans for ^{27}Al were accumulated. The magnetic field strength was 4.7 T. Chemical shifts were measured relative to TMS or α-Al_2O_3 for ^{29}Si or ^{27}Al, respectively.

Although all the ^{29}Si NMR spectra of kaolinite samples showed peaks around -92 ppm, the shapes varied considerably. Doublet peaks were observed in the spectra of kaolinites with higher Hinckley indices, *i.e.*, Kanpaku kaolinite, API-No.9 standard kaolinite specimen and kaolinite synthesized at 300°C. On the other hand, kaolinites with lower Hinckley indices, such as Gairome clay and Kibushi clay, gave broader single peaks. The peak widths at half height of ^{29}Si spectra decreased with an increase of the Hinckley index (Fig. 1). The natural samples and the synthetic ones can be divided into two groups as shown in Fig. 1. The difference between the natural and synthetic kaolinites was also observed in the shapes of ^{27}Al NMR spectra, which show complex powder patterns due to the quadrupole effect.

The dependence of the peak widths of ^{29}Si NMR spectra on the Hinckley index suggests that short range disordering around Si atom in kaolinite decreases the Hinckley index. Hence, the Hinckley index should be related not only to the long range ordering but also to the short range ordering, as opposed to the result of Komarneni *et al.* (1985).

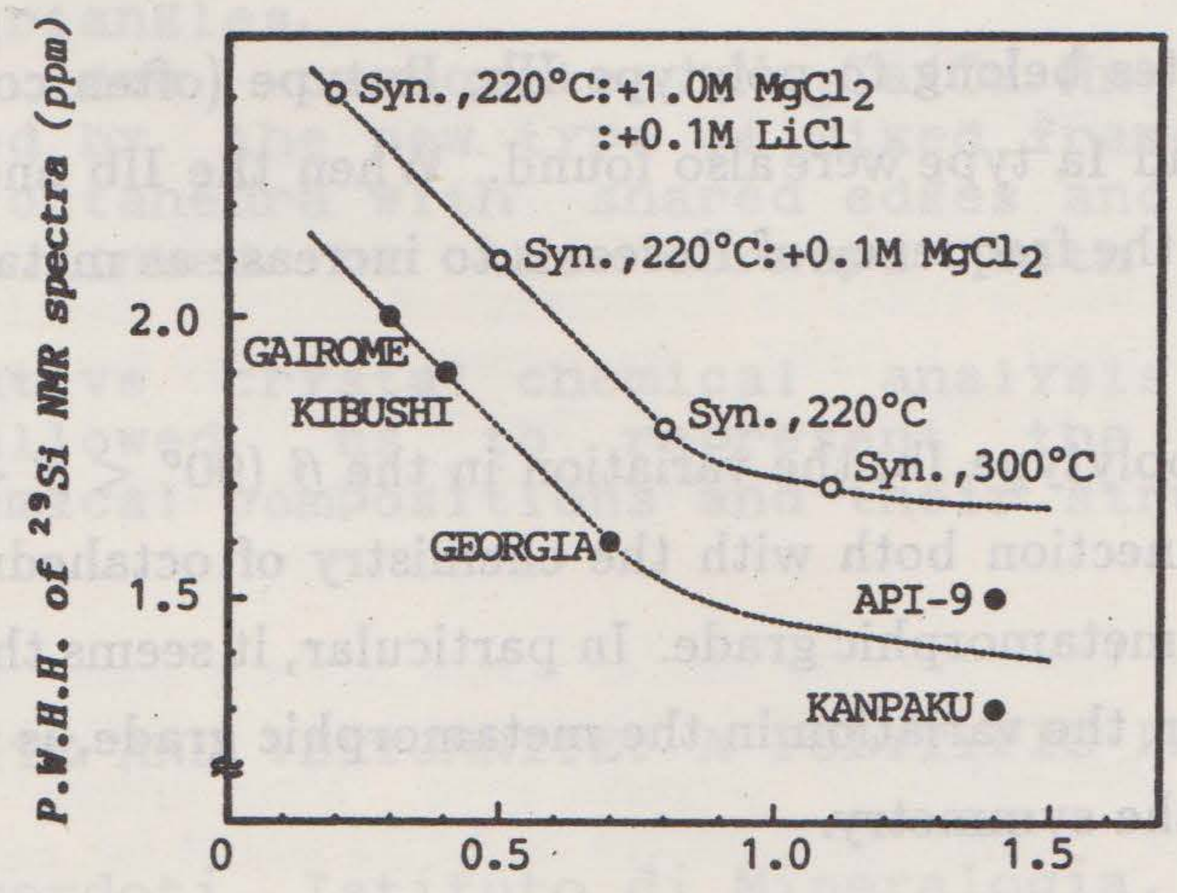

Fig. 1. Relation between the Hinckley index and P.W.H.H. of ^{29}Si NMR spectra.

Brindley *et al.* (1986) *Clays & Clay Minerals*, **34**, 239-249.
Komarneni *et al.* (1985) *Clay Minerals*, **20**, 327-334.
Miyawaki *et al.* (1989) *ABSTRACTS, 9th Int. Clay Conf.*, p.263.
Plançon *et al.* (1988) *Clay Minerals*, **23**, 249-260.

56.4.13.V

CHLORITE POLYTYPES IN PHYLLITES OF CIMA D'ASTA (SOUTH–EASTERN ALPS, ITALY)

Luciano Poppi, Dipartimento di Scienze Mineralogiche, Università di Bologna, Italy

In phyllites *l.s.* of Cima d'Asta (South–Eastern Alps, Italy), there are chlorites with different chemical composition and different polytypism. The aim of this work is to discuss the different polytypes found as far as thermodynamic crystallization features are concerned.

The analyzed samples are from low– to medium–grade metamorphism in a volcanic–sedimentary sequence resulting from interlayering of mafic and felsic metavolcanics with metasediments.

Well–defined correlations between unit cell dimensions and chemistry of the mineral are shown, in particular:

- c decreases as $(Al^{IV} + Al^{VI})$ increases;
- b increases as Fe/Σ^{VI} ratio increases;
- β seems to be linked to the feature of the whole octahedral populations.

Most chlorites belong to polytype IIb; Ib type (often co–existent with polytype IIb) and Ia type were also found. When the IIb and Ib polytypes are co–existent, the frequency of Ib seems to increase as metamorphic grade increases.

Regarding polytype Ib, the variation in the β ($90° < \beta < 97°$) angle is discussed in connection both with the chemistry of octahedral sites of the mineral and the metamorphic grade. In particular, it seems that the Fe/Σ^{VI} ratio, rather than the variation in the metamorphic grade, is responsible for the lowering in the symmetry.

41.4.2H

COMPARATIVE CRYSTAL CHEMISTRY OF NEW MINERALS FROM ALKALINE ROCKS.

D. Yu. Pushcharovsky, N. A. Yamnova, T. N. Nadezhina
Department of Geology, Moscow University, 119899 Moscow, USSR

Five new minerals were recently described in alkaline

rocks of Kola peninsula and North Ural. The review summarizes the results of their structural determinations, realized in the Department of Crystallography (Moscow University) during the last three years.

The structure of grumantite $Na[Si_2O_4(OH)]\cdot H_2O$ (Lovozero alkaline massif) contains a new type of interrupted framework, untypical for the tetrahedral complexes $[T_2O_5]$. It's formation can be connected with the presence of (OH)-groups, which decrease the average negative charge per one tetrahedron.

Clinobehoite $Be(OH)_2$ was found in desilicified pegmatites of North Ural in association with other Be-minerals: bavenite, bityite, ginzburgite. Its structure is composed of 3-layered sheets of Be-tetrahedra linked by H-bonds. The different types of H-bonds are definitively revealed in the IR-spectrum of clinobehoite.

Baniosite $Ba_3(Ti_{1.2}Nb_{4.8})Si_4O_{25.4}$ was identified in carbonatites of Vuorijarvi (Kola peninsula). Its mixed framework contains the octahedral columns with three Nb-octahedra in their sections, linked by pyrogroups $[Si_2O_7]$. The angle Si-O-Si=180° is a peculiar feature of this structure.

Two new carbonates were found in pegmatites of the Kola peninsula. The structure of tuliokite $Na_6BaTh(CO_3)_6\cdot 6H_2O$ contains the isolated mixed complexes,formed by the Th-icosahedron sharing edges with six $[CO_3]$-triangles.

The other new carbonate $Na_3Ca(Ca,Mn)(CO_3)_3F$ is caracterised by the new type of mixed framework, built of the Ca-octahedra with shared edges and of (Ca,Mn)-octahedra, linked by the corners with six $[CO_3]$-triangles.

The comparative crystal chemical analysis of studied minerals allowed us to represent the connections between chemical compositions and their structures.

STRAETLINGITE AND VERTUMNITE: A POLYTYPIC PAIR OF MINERALS

57.4.15 V

Michele Sacerdoti, Istituto di Mineralogia, Università di Ferrara, Romano Rinaldi, Dip.to di Scienze della Terra, Università di Cagliari, Elio Passaglia, Istituto di Mineralogia, Università di Modena, Italy

The crystal structure of straetlingite has been solved (space group $R\bar{3}$, a=5.745(7), c=37.77(1)Å) and compared with that of vertumnite (space group $P6_3/m$, a= 5.755, c=25.12 Å; Galli & Passaglia, 1978). The two mi

nerals differ in the stacking scheme of the two fundamental polyhedral sheets normal to the c direction. In vertumnite the octahedral sheet (O), with ideal composition $[Ca_2Al(OH)_6.H_2O]^+$, and the tetrahedral module (T), with ideal composition $[(Al, Si)_{2.5}O_2(OH)_6.0.12H_2O]^-$, are stacked according to the scheme: O T mT mO, whereby a double tetrahedral layer is obtained by mirror symmetry. In straetlingite such sequence becomes O T -T -O with a centre of inversion as the symmetry operator, hence the lengthening of the c repeat.

New chemical data obtained on vertumnite and their comparison with those of straetlingite are in agreement with the present polytypic structural scheme, thereby further testifying to its correctness.

Reference

Galli & Passaglia, TMPM 1978, 25, 33-44.

57.5.17.V

NEW DATA ON CORDYLITE

Shen Jinchuan Mi Linxiao
China University of Geosciences, Wuhan 430074, China

Cordylite, a rare earth-carbonate mineral, $BaCe_2(CO_3)_3F_2$, was first discovered and described by Flink, G (1901) in Narssarssuk of southern Greenland. Its struture was proposed by Oftedal, I (1931). After then, some new data on cordylite were added by G. Donnay et al. (1955) and T.T. Chen et al (1975). But there has been no reliable chemical and structural data supplied, many points on cordylite still remaining foggy.

We observed that there are many similar points in X-ray powder data and general physical properties among cordylite, baiyuneboite-(Ce)($NaBaCe_2(CO_3)_4F$) and a new mineral $(Ca_{0.5}\square_{0.5})BaCe_2(CO_3)_4F$ proposed by us. After authors' studies of these three minerals in detail, we think the cordylite should be redefined for the following reasons.

(1) The compatibility values (1 - Kp/Kc) of cordylite are very poor (- 0.1896 and -0.2139 respetcively for data given by T.T. Chen (1975) and ideal chemical composition). (2) The structure of cordylite assumed by Oftedal, I (1931) is in contradiction with its optical properties and its space group. (3) The mean occupied volume of the single large cation (unit cell volume / total number of large cations in cell) of cordylite is unusual (86.2 A^3). It is much larger than those in other similar minerals (as cebaite-(Ce), huangheite-(Ce), the new mineral etc. they are about 72 A^3) (4) Cordylite has no coordination polyhedrons similar

to huangheite-(Ce) etc. (5) The structure of cordylite is not comparable with other similar minerals. But the structure and c-axis parameter of new $(Ca_{0.5}\square_{0.5})BaCe_2(CO_3)_4F$ can be deduced from huangheite-(Ce) in such a way : the {F-Ba-F} triple layers (2*0.6259) in huangheite-(Ce) are replaced by the single layer of {Ca+F}. The c-axis value of the new mineral should be (8/12=2/3)*38.40 - 4*0.6259 = 23.0964A, which is very near the c axis value 23.017 A measured by the authors. Comparing the number of large cation (Ba^{2+}, Ce^{3+}) in huangheite (6 Ba and 6 Ce in cell) and cordylite (2 Ba and 4 Ce in cell), we found that the c-axis parameter of cordylite should be less than (1/2)*38.40 = 19.20 A. This value is much smaller than 23.050(5) given by T.T.Chen. Both the chemical composition and structure of cordylite are unreasonable and in contradiction with each other. (6) There are no apparent differences in X-ray powder data, physical properties, DTA, IR etc. except chemical composition and crystal structure supposed by Oftedal among cordylite, baiyuneboite-(Ce), new $(Ca_{0.5}\square_{0.5})BaCe_2(CO_3)_4F$.

Baiyuneboite-(Ce) was discovered by Prof. Fu Pingqiu in 1987. it is a Na-Ba-RE fluor-carbonate mineral. It differs from cordylite described before, by structure and chemical composition. Baiyuneboite-(Ce) is isostructural with $Ca_{0.5}BaCe_2(CO_3)_4F$. Na atoms in baiyuneboite-(Ce) have their own specific sites in the structure. There are no Na atoms existing in cordylite described earlier. According to Dr. J.A. Mandarino, recently Prof. J.Zemann et al. have found that type cordylite from Greenland contains essential Na. Baiyuneboite-(Ce) and type cordylite are identical. But the minerals quoted as cordylite from other locations need not be equivalent to baiyuneboite-(Ce) or type cordylite. For an example, cordylite discovered in Baiyun Obo, China are not a single mineral. They should be baiyuneboite-(Ce) or $Ca_{0.5}BaCe_2(CO_3)_4F$ or a mineral with composition between them.

We affirm that the minerals quoted as cordylite before, discovered in Greenland, Canada, China etc. may actually be baiyuneboite-(Ce) or $Ca_{0.5}BaCe_2(CO_3)_4F$ or other isomorphous minerals. To clarify such confusion, we think it be better to redefine cordylite as a group name; baiyuneboite-(Ce) and $Ca_{0.5}BaCe_2(CO_3)_4F$ as its individual species. The general formula for cordylite can be written $(A_{1-x}, B_{0.5x})BaCe_2(CO_3)_4F$, in which A may be Na^+...; B may be Ca^{2+}.... New mineral species of the cordylite group, containing cations other than Na, Ca, will likely be discovered in the future.

Determination of the Second-order Superstructure of Cebaite

57.4.16. V

Shen Jinchuan(沈今川) and Mi Jinxiao(宓锦校)
China University of Geosciences, Yujiashan, Wuhan 430074, P.R.C.

Cebaite is a Ba-REE fluor-carbonate mineral discovered in the Bayun Obo Nb-Ta-REE iron ore deposit in Inner Mongolia of China in 1964. Its ideal chemical

formula is $Ce_2Ba_3(CO_3)_5F_2$.Since its light(C,F) and heavy(Ba,Ce...) atoms are quite different ,and Ba and Ce are very similar in their X-ray scattering capabilities,the actural structure of the mineral has not been accurately determined experimentally before this work.In this study we have successfully completed the single-crystal structure analysis of cebaite.Samples were obtained from the West Mining District of Bayun Obo.3-D diffraction intensity data were collected with a RASA-5RP Model high-power four-circle single crystal diffractometer.Its precisely determined cell parameters are:$a_0 = 21.338(3)$,

Table 1.simplified atomic coordinates,occupancies of cebaite

Atom	X	Y	Z	K	Atom	X	Y	Z	K	Atom	X	Y	Z	K
Ba1	0.0	0.0	0.0	0.52	Ba2	0.5	0.480	0.0	0.49	Ba3	0.3076	-0.031	0.8916	1.0
Ba4	0.1931	0.497	0.0946	1.0	Ba5	0.5	0.004	0.5	0.53	Ba6	0.0	0.524	0.5	0.49
Ba7	0.3140	0.473	0.4015	1.12	Ba8	0.1875	-0.002	0.5920	0.91	RE1	0.1069	0.491	0.7828	1.01
RE2	0.3968	-0.020	0.2056	1.0	RE3	0.4010	0.514	0.6904	1.0	RE4	0.1005	-0.003	0.3204	1.0
F1	0.130	0.48	0.607	1.0	F2	0.074	-0.01	0.480	1.0	F3	0.428	0.49	0.508	1.0
F4	0.378	1.01	0.382	1.0	O1	0.075	0.28	0.145	1.0	O2	0.079	0.718	0.155	1.0
O3	-0.009	0.50	0.108	1.0	O4	0.382	0.28	0.058	1.0	O5	0.372	0.73	0.065	1.0
O6	0.291	0.50	-0.011	1.0	O7	0.189	0.287	0.411	1.0	O8	0.190	0.724	0.430	1.0
O9	0.102	0.50	0.369	1.0	O10	0.487	0.284	0.313	1.0	O11	0.487	0.717	0.293	1.0
O12	0.406	0.51	0.255	1.0	O13	0.220	0.274	0.773	1.0	O14	0.215	0.723	0.784	1.0
O15	0.304	0.51	0.793	1.0	O16	0.294	0.22	0.220	1.0	O17	0.281	0.78	0.248	1.0
O18	0.191	0.00	0.226	1.0	O19	0.016	0.217	0.678	1.0	O20	0.009	0.772	0.684	1.0
O21	0.107	0.00	0.727	1.0	O22	0.116	0.22	0.938	1.0	O23	0.123	0.773	0.943	1.0
O24	0.202	0.00	0.998	1.0	O25	0.422	0.22	0.842	1.0	O26	0.419	0.78	0.831	1.0
O27	0.510	0.01	0.879	1.0	O28	0.306	0.229	0.590	1.0	O29	0.312	0.78	0.579	1.0
O30	0.397	0.00	0.634	1.0	C1	0.047	0.49	0.142	1.0	C2	0.349	0.51	0.039	1.0
C3	0.461	0.51	0.296	1.0	C4	0.158	0.49	0.404	1.0	C5	0.246	0.50	0.780	1.0
C6	0.151	0.01	0.957	1.0	C7	0.046	0.00	0.693	1.0	C8	0.333	0.00	0.603	1.0
C9	0.451	0.00	0.855	1.0	C10	0.257	0.00	0.228	1.0					

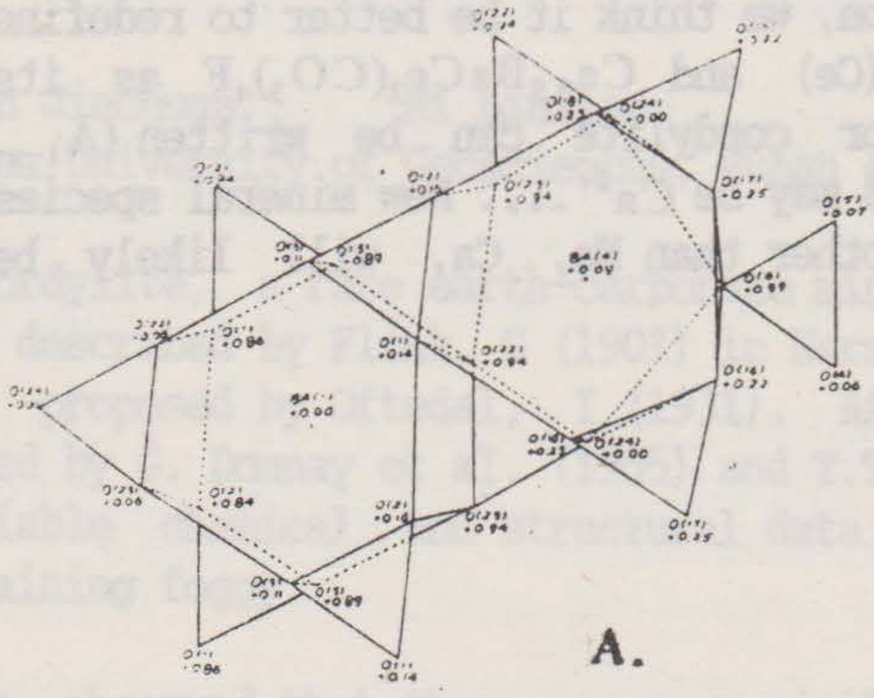

A.

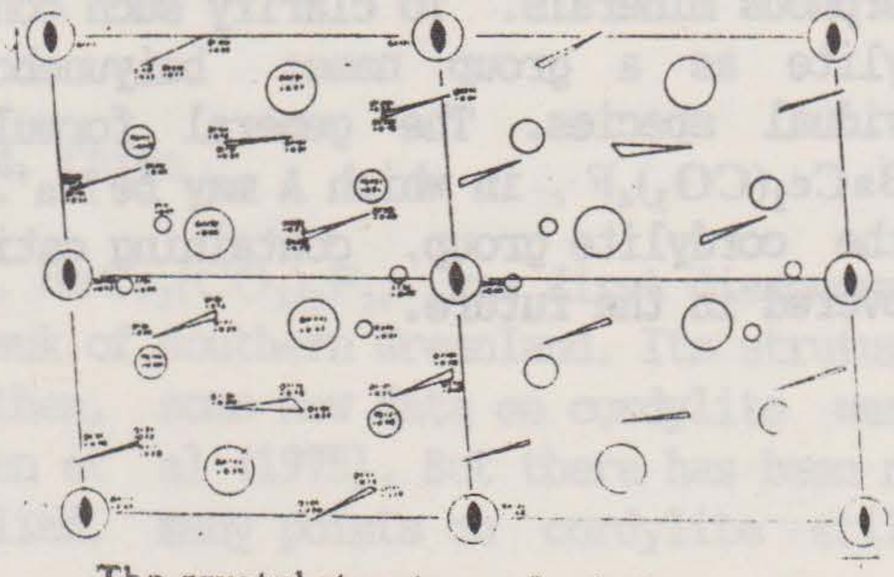

The crystal structure of cebaite

(projection ∥ b axis)

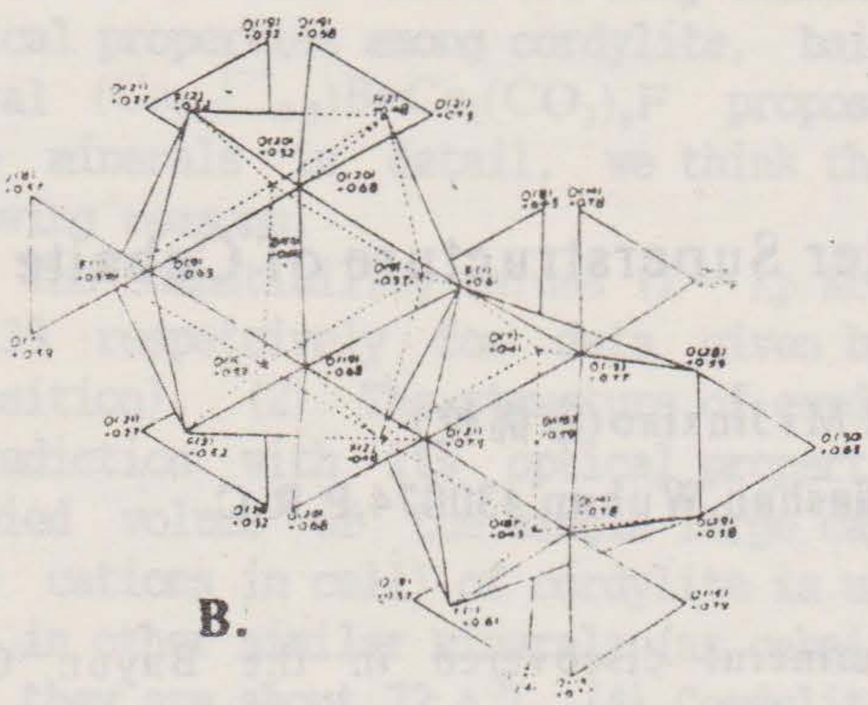

B.

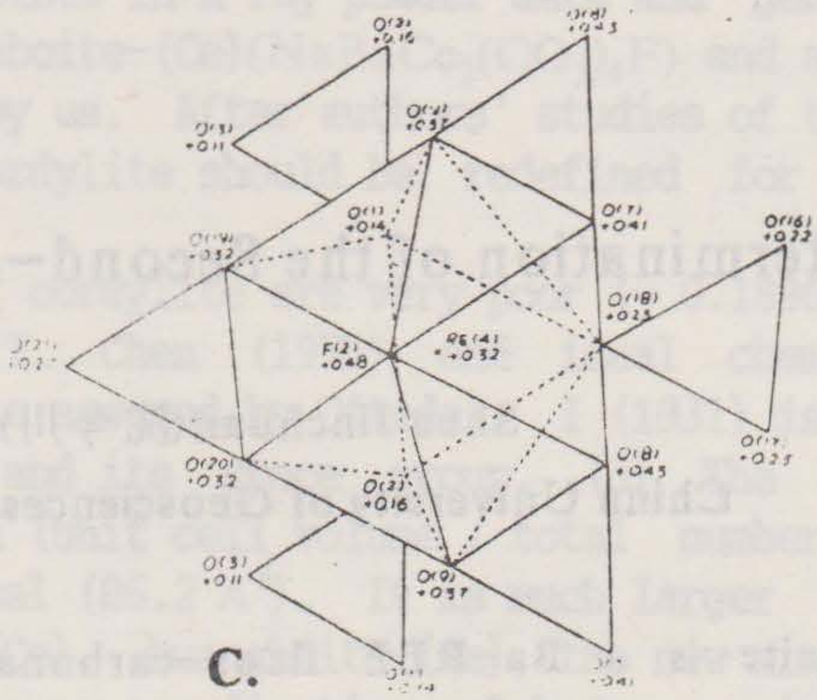

C.

$b_0 = 5.0666(8)$, $c_0 = 13.276(9)$Å, $\beta = 94.76(4)^\circ$, $V = 1430$Å^3, space group P2. 1916 independent data ($F > 5\sigma(F)$) were used to make multi-cycle least squares refinement of 103 variable parameters for the 3-Dcoordinates,site occupancy and isotropic thermal vibration of 56 asymmetric atoms, $R = 0.07$(see Table 1.).

As compared with huanghoite of the same family,cebaite is even more complicated in crystal structure.The heavy atoms Ba and Ce have five different coordination forms with the coordination numbers being 10,11,and 12.(see Figure 1.a,b,c).The coordination polyhedrons of Ba and Ce are linked as a chain in the order of Ba-Ce-Ba-Ba-Ce-Ba-Ce-Ba-Ba-Ce along the [103] direction,and such chains are linked by $[CO_3]^{2-}$ to form a net layer parallel to plane(010).The net layers at $Y = 0$ and $1/2$ are further linked into a three-dimensional framework.The centres of planar triangles of $[CO_3]^{2-}$ and all heavy atoms are approximately located at $Y = 0$ and $Y = 1/2$.The accurate determination of cebaite crystal structure is of great importance in deepening the study of crystallochemistry of Ba-REE fluor-carbonate minerals.

The Crystal Structure of $(Ca_{0.5}\square_{0.5})BaCe_2(CO_3)_4F$

96.4.11. K

Shen Jinchuan Mi Jinxiao

China University of Geosciences, Wuhan 430074, Hubei, CHINA

A new mineral of Ca-Ba-REE (Ce-Series) fluor-carbonate was recently discovered in China by the authors The crystal structure of this new mineral has been solved . It is isostructual with baiyuneboite-(Ce) . The physical properties , cell parameters and space group can be explained properly based on the structure.

EXPERIMENT: Sample was collected from the REE-Fe-Nb ore deposits at Bayan Obo , Inner Mongolia , China . The oscillation photos about the c-axis gives $c = 23.02$Å Weissenberg photos (rotated around c axis , weak spots were ignored) give $a = b = 5.10$ Å, $\gamma = 120^\circ$ .Systematical absense of $l = 2n + 1$ data in hh2hl type reflections indicates that diffraction symbol should be $6/mmm$ $P-/c$. Its possible space groups are $P6_3/mmc$,$P6_3mc$, $P\bar{6}2c$. In the zero-layer of Weissenberg photos (CuKα, 50kv, 120ma, 24hr) some weak spots can be observed with care . If they are taken into account , then a superstructure cell $a' = b' = 2a = 10.20$Å , $c' = c = 23.02$Å , will be obtained .

The data collection was completed on a RASA-5RP Automatic Four-circle Single Crystal Diffractometer in our university. (graphite monochromator , MoKα: 0.70926 Å , 50 kv ,150ma,$2\theta = 2-65^\circ$).The cell parameters refined on this device are as follows: $a = b = 5.093(6)$, $c = 23.017(6)$, $V = 517$Å^3. 821 reflections were collected , of which 344 have $F > 3\sigma(F)$.

SOLUTION AND REFINEMENT OF THE STRUCTURE:The structure was solved by 3D-Patterson P(uvw) and the difference electroh density map . During structure

analysis several space groups were tried ,and only $P\bar{6}2c$ proved to be the best of all .

Isotropic refinement led to R = 0.06 for all 344 independent reflections , anisotropic refinement R = 0.05 . Atomic coordinates, site occupancies and isotropic thermal vibration parameters are given in table 1.

DESCRIPTION OF THE STRUCTURE: The structure has a layer feature($\perp$ c axis) .All heavy atoms(Ba , Ce) and the CO_3group form a hexagonal base-centred net-like framework . At z = 1 / 4 and z= 3 / 4 the hexagonal layer consists of Ca and F atoms , in which each kind of atoms is also arranged in a hexagonal base-centred net-like framework . Those hexagonal layers of atoms are stacked along c axis in the sequence of $Ba-CO_3-Ce-CO_3-Ca(F)-CO_3-Ce-CO_3-Ba-CO_3-Ce-CO_3-Ca(F)-CO_3-Ce-CO_3-Ba$. The plane of CO_3group is normal to c axis, Ca occupy 1 / 2 equivalent sites and are disordered.

Table 1. Atomic coordinates , site occupancies and isotropic thermal vibration parameters

Atom	X / A	Y / B	Z / C	K	U_{11}
Ba	0.0000	0.0000	0.0000	0.1667	0.0098(5)
Ce	0.6667	0.3333	0.1458(1)	0.3333	0.0086(4)
Ca	0.3333	0.6667	0.2500	0.16667	0.035(3)
C(1)	0.3333	0.6667	0.0661(4)	0.3333	0.010(5)
O(1)	0.499(5)	0.540(6)	0.0661(4)	1.0000	0.009(3)
C(2)	0.0000	0.0000	0.1783(4)	0.3333	0.010(5)
O(2)	0.15(1)	0.290(3)	0.1783(4)	1.0000	0.016(2)
F(1)	0.6667	0.3333	0.2500	0.1667	0.036(8)

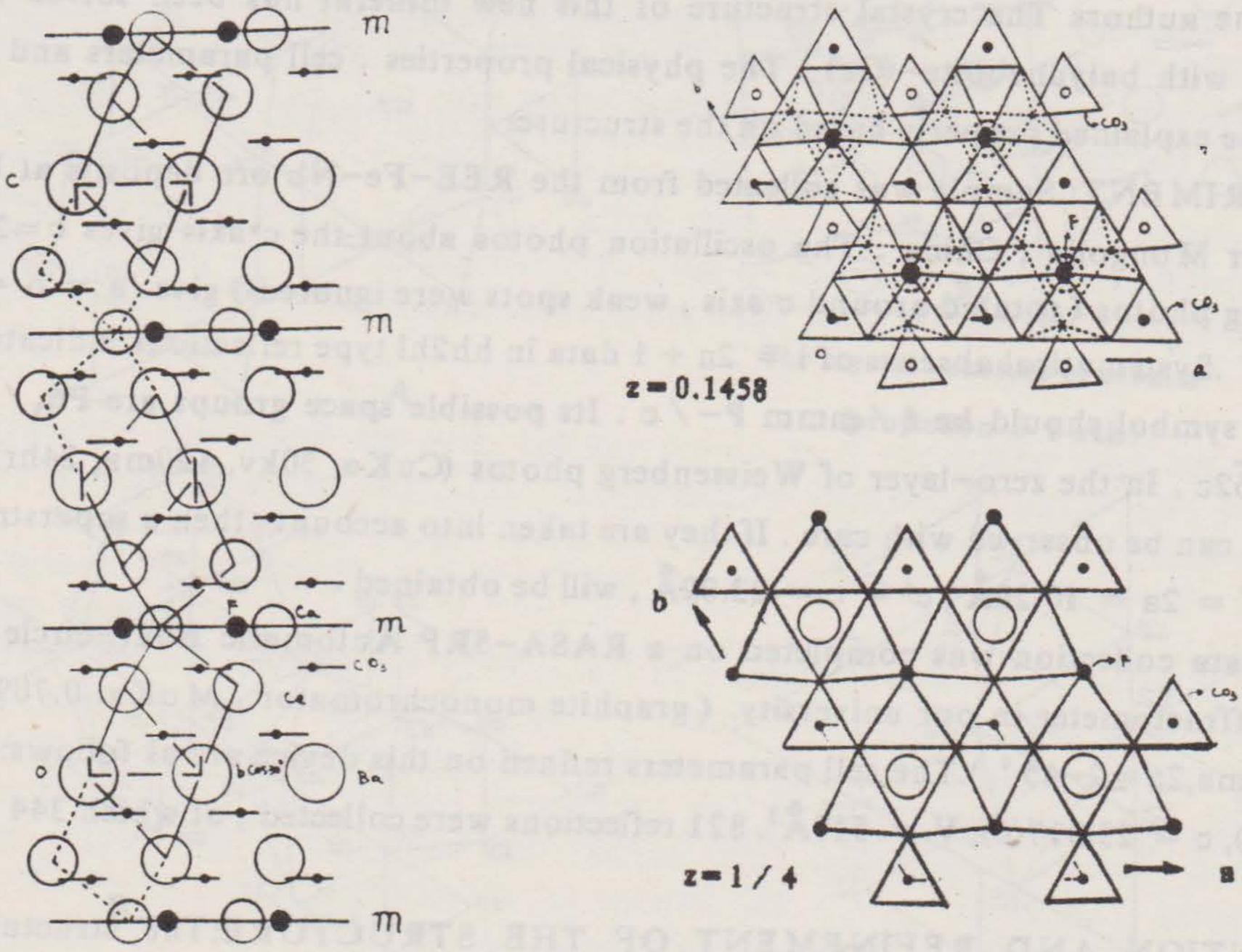

The crystal structure of $(Ca_{0.5}\square_{0.5})BaCe_2(CO_3)_4F$

56.4.11. V

THE RESEARCH ON CRYSTAL STRUCTURE OF DAOMANITE

Shi Nicheng and Ma Zhesheng, China University of Geosciences, Beijing, 100083, People,s Republic of China

The accuracy of determining the crystal structure of daomanite was influenced by very small size of crystal but the basic data and information were obtained. This work is based on the report by Ding et al(KEXUE TONGBAO(1981), No 9. p. 554–557).

The PW–1100 four circle X–ray diffractometer was applied. crystal size 0.28 * 0.19 * 0.04mm, MoK_{α}, graphite monochromator, $3^{\circ} < \theta < 25^{\circ}$, A tolal of 354 independent reflections were collected, of which 183 were applied to intensity calculation. The PL corrections were carried out.The crystal data belongs to orthorhomic system, a = 3.756 Å, b = 15.876Å, c = 5.852Å, V = 348.96Å, space group Cmc2, Dx = 7.598g / cm^3. Z = 4{CuPtAsS}.

The structure was solved by Direct and Patterson method and the coordinate of Pt was obtained, other atomic coordinates were got by Fourier synthesis. The least square method was applied to refining the atomic fraction coordinates and anisotropic temperture factors, R = 0.25, the atomic coordinates and thermoparameters are shown in Table 1. The interatomic distances are shown in Table 2. The PLUTO map of the structure is shown inFig.1.

Table 1 Atomic coordinates and thermoparameter of Daomanit

Atoms	GI	x	y	z	Ueq
Pt	0.5	0.0(0)	0.177(1)	0.312(7)	0.003(4)
As	0.5	0.5(0)	0.267(2)	0.217(8)	0.003(1)
Cu	0.5	0.0(0)	0.449(2)	0.292(9)	0.021(10)
S_1	0.5	0.5(0)	0.085(6)	0.429(18)	0.018(19)
S_2	0.5	0.5(0)	0.383(6)	0.451(17)	0.004(2)

Table 2 Interatomic distances (A) of Daomanite

Pt—(As,S)	octahedron	Cu—S	tetrahedron
Pt—As	2.43(3) * 2	and As–S	bond length
Pt—S_1	2.47(6) * 2	Cu—S_1	2.35(6)
Pt—S_2	2.31(2)	Cu—S_2	2.30(7) * 2
Pt—As	2.53(2)	Cu—S_1	2.19(6)
		As—S_2	2.30(5)

The Pt in Daomanite is coordinated to three As atoms and three S atoms and form an octahedron; the Cu is coordinated to four S atoms and form a distorted tetrahedron. The

octahedrons are linked with each other as shared edges by themself and form octahedral chains along a axis.Octahedral chains are connected by sharing corners and form double octahedral chains. The double octahedral chains are linked with Cu–S tetrahedrons as shared corners. The structure determinetion indicated that Daomanite is a new type complex chain type arsenic sulphide.

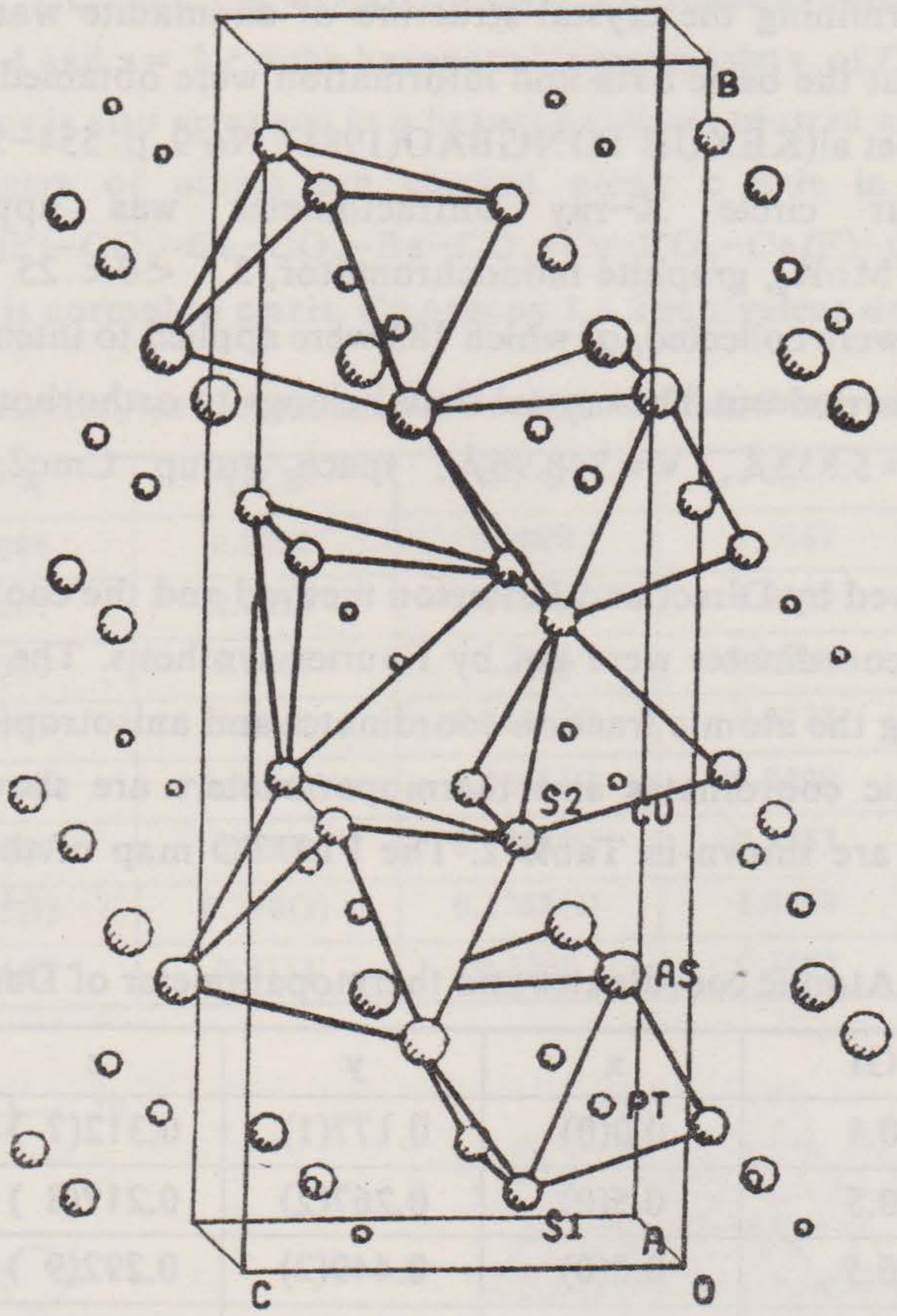

Fig.1 The PLUTO map of crystal structure for Daomanite

57.5.18. V

SEPARATION OF IMPURITY MINERALS IN SUZHOU KAOLINITE

Yasuo Shibasaki, *Ceramic Technology Department,*
Gov. Indust. Res. Inst., Nagoya, Kita, Nagoya 462, JAPAN
Kisato Tone, Akihiro Nishioka, Masanobu Kamori
Engineering Research Association for Artificial Clays,
G.I.R.I.N., Kita, Nagoya 462, JAPAN
and **Yuan-Rong Zheng**, *Xian Yang Res. Inst. of Non-metallic Minerals, Xian Yang, Shaan Xi, CHINA*

INTRODUCTION Suzhou kaolinite, strongly coagulated with impurity minerals, was well-purified by elutriation using a special organic deflocculant assistant and water glass simultaneously. Because of the coagulation with iron impurity, this kaolinite has

been difficult to use as ceramic raw material, being used mainly for non-firing purposes. such as paper filler. Since Suzhou kaolinite deposit is one of the largest deposits in China, and is located near sea shore, expansion of its usage is very important. Therefore, we aimed to use this kaolinite for ceramic white wares using deflocculant of water glass and an organic deflocculant which was produced by one of the authors (YZ).

In the present study, we have compared the separabilities of the two treatments, one of which uses both water glass and the organic deflocculant (treatment 1) and the other uses only water glass (treatment 2).

EXPERIMENTAL Suzhou kaolinite (grade A-0) was provided by Suzhou Kaolin Konsu Co. It was ground and passed 70 mesh sieve (<ϕ212μm), and mixed with water, water glass, and the organic deflocculant No.105. Settling down for 1 hour after stirring well, the suspensions were separated from sediments using siphon tube. Above operation was repeated three times. Mineral compositions of the individual specimens were examined by XRD, DTA, IR, TEM, and their chemical compositions were determined by X-ray fluorescence analysis.

RESULTS AND DISCUSSION XRD and DTA showed that the starting material consists of kaolinite, quartz and FeS_2. Tubular halloysite and platy kaolinite were observed in the material by TEM. In addition, separated two peaks (3620cm^{-1} and 3690cm^{-1}) in IR spectra suggested the presence of halloysite.

Quartz could be removed by the treatment 1, but not by the treatment 2. In case of the treatment 1, the specific surface area of the suspension was higher than that of the tailings. But treatment 2 was less effective.

The result of X-ray fluorescence analysis indicated that the ratio of Al/Si of suspension obtained by the treatment 1 agreed with the theoretical composition of kaolinite, however, that obtained by the treatment 2 was exceed in Si.

Although the contents of iron in the samples decreased, those of titanium did not by the treatment 2. The iron contents as FeS_2 with heavy density should be precipitated during the treatment. On the other hand, the treatment 1 could decrease both of these impurities.

The secondary particles may be aggregated by $Al(OH)_3$ adsorbed on clay particle surface. The functional groups of the organic deflocculant should make complexes with the $Al(OH)_3$ to destroy the secondary particles.

The water film thicknesses on particle surface of samples were measured by DSC. The thickness of the suspension, 13 Å is larger than that of raw materials, 12 Å. Better plasticity clay had tendency to have larger thickness of water film.

The plasticities of the samples were investigated by applying the Pfefferkorn method (Shibasaki *et al.*, 1984). CV(characteristic value of plastic clay) of raw material was 0.71% and that of suspension was 0.78%. This result was agreed with that of DSC. It was indicated that Suzhou kaolinite separated by the present treatment was superior to raw materials

form view point of plasticity.

CONCLUSION It was revealed that the impurity minerals in Suzhou kaolinite was successfully separated by this treatment using the water glass and the deflocculant organic material No.105. The separability estimated by XRD and elemental analysis suggested superiority of the treatment 1. Furthermore, the kaolinite obtained by the treatment 1 showed better Pfefferkorn plasticity and thicker adsorbed water thickness on the kaolinite particle measured by DSC.

REFERENCES

Shibasaki *et al.* (1984) *J. Ceramic Soc. Jpn.*, **92**, 77.

57.5.19. V

COMPOSITION AND TRANSFORMATION OF X-RAY-AMORPHOUS FERRIFERROUS PHOSPHATE-OXIDES FROM PHOSPHORITES

V.I.Silaev,G.S.Nazarova. Institute of geology of Komi Science Centre of Ural Department of Academy of Sciences, Syktyvkar,167610,USSR .

The new phosphorite deposit of the Polarny Ural has been investigated and it determined that their phosphate matter consists of four mineral species: carbonate-fluorapatite,aluminophosphates(besides that calcic, calcic-barium, zincic-copper), ferriferrous phosphates (besides that manganiferous), phosphate-oxide compounds of iron. Particularly the latter are of great importance in some industrial types of secondary phosphorites but until recently they have not been investigated adequately by geologists and mineralogists. Microprobe investigation showed the following combinations of phosphate-oxide occurrences 76-99% Fe_2O_3; 3-6% P_2O_5;0.5-2.5% SiO_2;0-3% Al_2O_3;0.3-0.9% CaO;0-1% MnO_2;0.4-1.5% ZnO;There are also a few impurities as Na,Mg,Ni,Co,Sr,REE,S,As. In IR-spectra of studied samples (IR-investigations were made at (400-1800) cm-1 region on "specord-IR 75" spectrometer) there are the bands which belong to carbonate-apatite (1460,1430,985,1085,1045,585,475 cm-1). X-ray-amorphous phosphates(1085,1045 cm-1);in addition wide bands in 400-500 cm-1 region are caused by amorphous ferriferrous oxides. Wide band 905,800, 400-550 cm-1 are caused by amorphous hydrous ferric oxides. If the samples of phosphate-oxide formations are annealed their IR-spectra change profoundly (see fig. 1).

Already at 220°C annealing the band(400-500) cm-1 decreases very strongly. It can be caused by decreasing the amount of amorphous ferric oxide. If the amorphous hydrous ferric oxides is present in the studied samples the IR-band belonging to the latter disappears.At the same time together with these changes in the IR-spectra the doublet of bands belonging to the new·formed phosphate phase appears

and increases.

Thus,it can be assumed that amorphous phosphate-oxide formations are original hybrid compounds such as studied earlier in natural gels of alumino-ferric-phosphate sulphate composition /1/.At low temperature annealing of phosphate-oxide formations, their transformations take place and the process is expressed by loss of water and appearance of new ferric phosphate. There is no dout that the phosphate-oxides studied are natural examples of compounds transitional between amorphous gels and crystalline minerals.

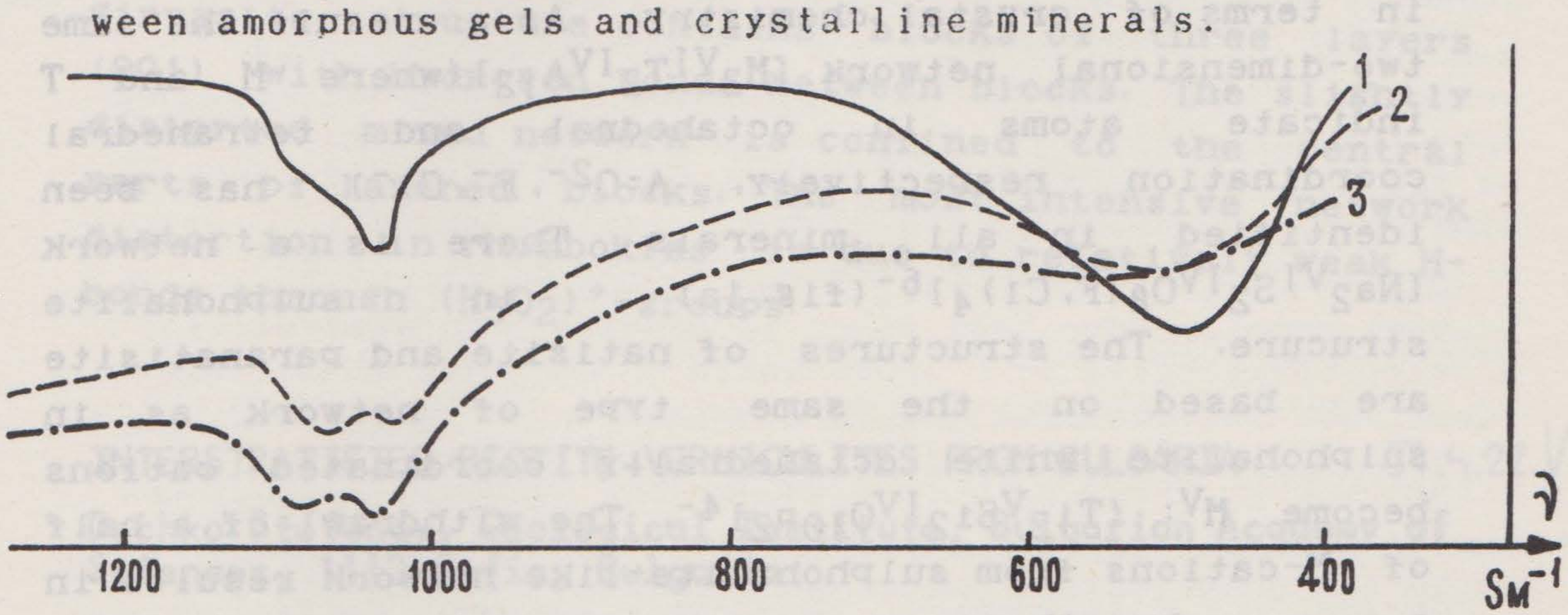

Fig.1. Changes of IR-spectra depended on annealing temperature
1- initial phosphate-oxide;
2- sample was subjected to 40 minutes annealing at 220 C;
3- sample was subjected to 40 minutes annealing at 500 C.

Reference

N.P.Yushkin, G.S.Nazarova. Mineralogy, genesis and phase evolution of colloids of iron-alumino-phosphate-sulphate composition.13 International Mineralogical Association (Physics of Minerals and Ore Microscopy),Sofia,1982,pp 89-97.

MIXED TETRAHEDRAL AND OCTAHEDRAL NETWORK TRANSFORMATION IN STRUCTURES OF SULPHOHALITE-NATISITE, PARANATISITE-GIRVASITE-RHOMBOKLAS

57.4.20.V

Sokolova E.V., Egorov-Tismenko Yu.K., Department of Geology, Moscow State University, Moscow, 119899, USSR

Two new minerals were investigated by single-crystal X-ray method. The first one is paranatisite

$Na_8Ti_{3,5}O_2(OH)_2[SiO_4]_4$ (a=9,827; b=9,167; c=4,799 A, sp. gr. Pmma, Z=1), the second-girvasite $NaCa_2Mg_3(OH)_2(H_2O)_4[PO_4]_2[PO_2(OH)_2](CO_3)$ (a=6,522; b=12,25; c=21,56 A, β=89,48°, sp. gr. P $2_1/c$, Z=4). Both of them were compared with sulphohalite $Na_6[SO_4]_2(F,Cl)_2$, natisite $Na_2(TiO)[SiO_4]$, rhomboklas $(H_5O_2)^+\{Fe[SO_4]_2\cdot 2H_2O\}^-$ and its synthetic Y-analogue in terms of crystal chemistry. As a result the same two-dimensional network $[M_2^{VI}T_2^{IV}A_{12}]$ (where M and T indicate atoms in octahedral and tetrahedral coordination respectively, $A=O^{2-}, F^-, Cl^-$) has been identified in all minerals. There is a network $[Na_2^{VI}S_2^{IV}O_8(F,Cl)_4]^{6-}$ (fig. 1a) in sulphohalite strucure. The structures of natisite and paranatisite are based on the same type of network as in sulphohalite while octahedrally coordinated cations become M^V: $\{Ti_2^VSi_2^{IV}O_{10}\square_2\}^{4-}$. The withdrawl of a half of M-cations from sulphohalite-like network results in a hypothetic structural fragment $[M^{VI}\square^{VI}T_2^{IV}O_{10}\square_2]$ (fig. 1b). An additional partial rotation of tetrahedra leads to the slight distortion

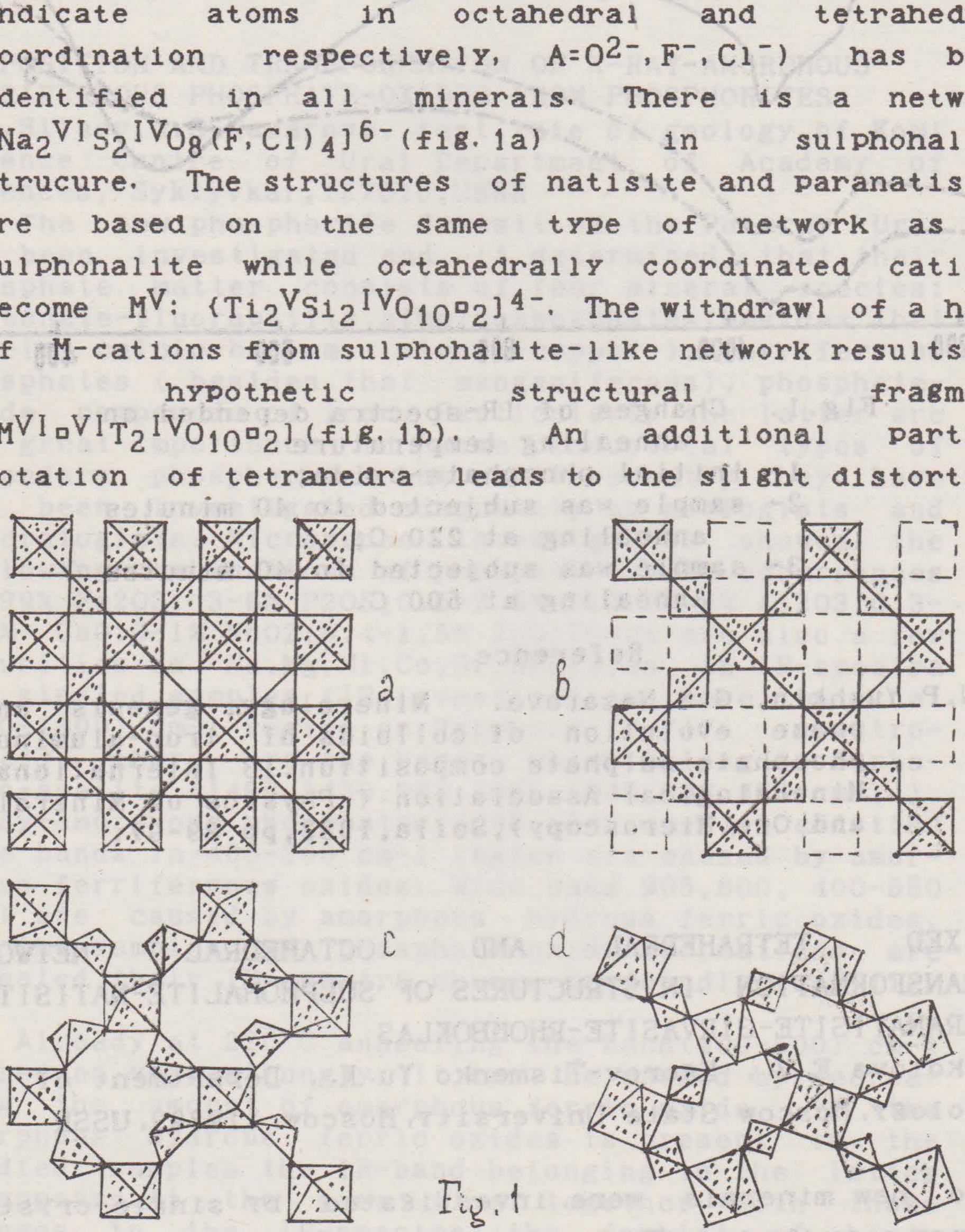

Fig. 1

of the network $[Mg^{VI}\square^{VI}P_2{}^{IV}O_{10}\square_2]^{8-}$ (fig. 1c) in girvasite. The most distorted net is characteristic for rhomboklas: $[Fe^{VI}\square^{VI}S_2{}^{IV}O_8(H_2O)_2\square_2]^{-}$ (fig. 1d) and in its Y-analogue. In compact sulphohalite structure Na-S-nets constitute a framework with additional Na in its voids. The dense net packing in sulphohalite and titanosilicates prevents any net distortion. The girvasite structure contains blocks of three layers (001) with hydrogen bonds between blocks. The slightly distorted mixed network is confined to the central parts of layered blocks. The most intensive network distortion in rhomboklas is due to relatively weak H-bonds through $(H_5O_2)^{+}$-groups.

INTERSTRATIFIED BIOTITE-VERMICULITES FROM BULGARIA

57.4.22.V

Dechko Stefanov, Geological Institute, Bulgarian Academy of Sciences, 1113 Sofia, Bulgaria

The vermiculite deposits in Bulgaria are concentrated in the regions of the Srednogorie and the Rhodope Mts. They are weathering products of ultrabasic rocks and amphibolites transformed by potassic metasomatism into trioctahedral micas. Both the end members biotite and phlogopite, and the intermediate members of the series are found. The later hydration of these minerals has produced vermiculite layers in their structures, thus forming interstratified biotite-vermiculites with varying content of vermiculite layers. This process has finally resulted in monomineralic vermiculite deposits of economic value.

X-ray diffractometry has been used to study the interstratified biotite-vermiculites in order to determine the proportions of vermiculite layers, their stacking sequences, and the types and concentrations of exchange cations.

The study uses the nomenclature of interstratified minerals as recommended by the AIPEA Nomenclature Committee (Bailey, 1982).

The vermiculite deposits of Bulgaria show a great variety of interstratified minerals of the biotite-vermiculite type. In analyzing the diffraction patterns of interstratified biotite-vermiculites, it should be taken into account that the varying proportions of vermiculite layers present (w_v) and the varying amounts of constituent Ca-cations in the vermiculite interlayers have a combined effect on the basal reflection interplanar distances.

The randomly interstratified biotite-vermiculites containing

about 5 % vermiculite interlayers are characterized by broad and asymmetric basal reflections. With the increasing portion of vermiculite layers (to about 15 %), the reflections shift toward the hydrobiotite side. The most common interstratified biotite-vermiculites are those with over 30 % vermiculite layers. Diffractograms record representatives constituting 30-35 % of vermiculite layers with interstratified minerals. With 10-15 % vermiculite layers, however, no periodic stacking is shown thus disobeying the rule CV < 0.75 valid for the regularly interstratified 2 : 1 hydrobiotites, For this reason they are referred to the randomly interstratified biotite-vermiculites. A group of samples has been identified as typical hydrobiotite of $w_v \sim 0.5$, CV < 0.75, and diffraction patterns having series of basal reflections of $d_{(001)} = 24.5$ Å (D'yakonov, 1981; Brindley et al., 1983).

Several samples have been found to contain an interstratified biotite-vermiculite of $w_v \sim 0.6$ which corresponds to an interstratified mineral with the BB combination not described by D'yakonov (1981) or Brindley et al. (1983). Only Weiss (1980) has reported such interstratified biotite-vermiculites in a single-crystal X-ray study.

Using the quantitative method of D'yakonov (1981), the contents of Ca-cations (ξ_{Ca}) in the interstratified biotite-vermiculites have been calculated. Mg-hydrobiotites ($\xi_{Ca} < 10\%$), (Mg,Ca)-hydrobiotites ($\xi_{Ca} > 10\%$), Mg-biotite-vermiculites ($\xi_{Ca} < 10\%$) and (Mg,Ca)-biotite-vermiculites ($\xi_{Ca} > 10\%$) are identified.

The interstratified biotite-vermiculites of varying proportions of vermiculite interlayers ($0.05 < w_v < 0.6$) found in the Bulgarian vermiculite deposits sustain the interpretation of their genesis as the result of hydration of the biotite-phlogopites formed at the expense of the original ultrabasic rocks and amphibolites.

References

Bailey, G. W. 1982. Nomenclature for regular interstratifications. Amer. Miner., 67, 3/4, 394-398

Brindley, G. W., Zalba, P. E., Bethke, G. M. 1983. Hydrobiotite, a regular 1 : 1 interstratification of biotite and vermiculite layers. Amer. Miner., 68, 3/4, 420-425

D'yakonov, Y. S. 1981. New data on the varieties and identification of hydrobiotites. Crystal chemistry of minerals, Leningrad, Nauka Publ. Nouse, 39-46 (in Russian)

Weiss, Z. 1980. Single-crystal X-ray study of mixed structures of vermiculite and biotite (hydrobiotites). Clay Miner., 15, 275-281

INCOMMENSURATE PHASES IN MINERALS AS MANIFESTATION OF QUASI-CRYSTALLINITY

N.G. Stenina, Institute of Geology and Geophysics, Siberian Branch of the USSR Academy of Sciences, Novosibirsk, 630090 USSR

Irrationality is the main characteristic of incommensurate phases (INC), as they result from modulation of a regular atomic chain by a static displacement wave with irrational superperiod λa and amplitude εa Therefore each atom will be displaced from the regular position by an irrational magnitude $\varepsilon a \sin(2\pi\lambda n a)$ where n is the number of the atom considered. The modulated atomic chain thus created is strictly aperiodic, as it cannot be superposed over itself by any finite translation. INC from this viewpoint represents a special one-dimentional case of quasi-crystals, which was discovered in 1984 [1].

Among the known methods , transmission electron microscopy (TEM) gives a most detailed information for the INC identification. It allows us to study the distribution of satellite reflexions in electron diffraction patterns, the fringe contrast, specific for INC, and also to observe directly the atomic displacements waves in high resolution images.

Using these possibilities of TEM, INC was established in some minerals: quartz from pegmatites, plagioclase (labradorite-bitownite) from intrusive rocks and clynopyroxene (omphacite) from eclogites. The studies showed the following. 1. Crystallographic directions of incommensurate modulations as well as the vectors of atomic microdisplacements are determined by rational states of corresponding structures. 2. INC in minerals represent metastable states in the ranges of

structural transitions: $\alpha-\beta$ in quartz, $I\bar{1} \rightarrow C\bar{1}$ in plagioclase; or phase transition: Omph → Pl+Qu. 3.The property of a mineral to transit from one phase into another by INC mechanism; the range of P,T-parameters and the INC stability in minerals depend on the mineral composition, mainly on Al content. 4. There is a dependence of the incommensurate modulations period on such parameters as temperature and kinetics of metamorphism and the decompression gradient.

The mentioned specific features of INC in minerals demonstrate the importance of their investigation for the solution of fundamental problems of genetic mineralogy, petrology and geochemistry.

1. Shechtman D., Blech I., Gratias D., Cahn J.W. Metallic Phase with Long-Range Orientational Order and No Transitional Symmetry. Phys. Rev. Lettr., 1984, Vol.53, P.1951.

QUARTZ - A MODEL PHASE FOR INVESTIGATION OF HYDROTHERMAL ORE-FORMING SYSTEMS

N.G. Stenina. Institute of Geology and Geophysics. Siberian Division of the USSR Academy of Sciences. 630090 Novosibirsk,USSR

Quartz is one of the final products of the development of hydrothermal ore-forming systems. Therefore, the specific features of its real structure provide us with information about ore-formation, especially about its aspects such as the form of transportation of ore elements, the mechanisms of their migration and concentration in vein quartz.

By means of high voltage transmission electron mi-

croscopy combined with an IR-spectroscopy and X-ray microanalysis, the hydrothermal quartz of the following types was studied: i) from the veins with various ore mineralization: copper-molybdenum, gold -silver; ii) from ore veins which underwent postcrystallization transformations (deformation and annealing); iii) from the non-ore veins.

The main difference between microstructural features of ore-bearing and non-ore bearing veins is established. It consists in that the ore-bearing quartz has water in a structurally combined form. The H_2O molecules occupy the positions in a quartz framework between the defective silicon and metal oxide tetrahedra. Non-ore quartz has water in a free form; it enters in the volume of gas-liquid inclusions.

The study of quartz from ore-bearing veins which underwent postcrystallization and a high temperature deformation with a subsequent annealing shows that it stimulates solid state transformations of a "proto-ore" quartz saturated with impurities and structural water. As a result, the metallic atoms diffuse from the structural positions which they occupy according to the heteroisomorphism in quartz: $Me^{3+}Me^{+} \rightarrow Si^{4+}$ to the defective zones like dislocation substructures, microinclusions etc. The molecular water entering the quartz structure is the catalyst of these reactions.

1. Stenina N.G., Sotnikov V.I. et al. Microstructural features of hydrothermal vein quartz as indicator of its ore-bearing capacity. Geokhimia, 1988, N 5, p.641-653.

464.9.K

SUBSTITUTION VECTOR APPROACH TO CHEMICAL COMPOSITIONS OF REAL MICA SERIES

Sun Shihua and Yu Jie, Institute of Geology, Academia Sinica, Beijing, 100011, People's Republic of China

A substitution vector or an exchange vector is the vector representation of an isomorphic substitution. The purpose of this paper is to show how to explain the variations of the naturally occurring mica compositions in terms of substitution vectors.

The substitution vector is a free vector. Its expression can be obtained by rewriting corresponding isomorphic substitution equation directly, or by calculating direction vector of the line linking relevant two ideal minerals. For example, muscovite substitution vector $AM(Fe^{+2}, Al_{VI}, \square_{VI}) = (-3, 2, 1)$ from $3Fe^{+2} \rightarrow 2Al_{VI} + \square_{VI}$, which is just the direction vector of the link from annite to muscovite; Fe–Tschermak substitution $Fe^{+2} + Si \rightarrow Al_{VI} + Al_{IV}$ ($AE(Fe^{+2}, Al_{VI}, Si, Al_{IV}) = (-1, 1, -1, 1)$) is parallel to the link of annite and Fe–analog of estonite. The generalized substitution vector $V = (\alpha_1, \alpha_2, \cdots \alpha_n, v)$, where $\alpha_i (i = 1, 2, \cdots n)$ or v is called substitution component of ion i or vacancy, respectively. Component sum $CS = \sum \alpha_i$. Electrovalent sum $ES = \sum e_i \cdot \alpha_i$, here, e_i represents electrovalence of ion i. CS and ES are the measurements of variations of vacancy and electrovalence in mineral, respectively, due to the substitution.

There are two important groups of substitutions in the 2:1 layer mica: substitutions of octahedral $ES(VI) = 0$ and $ES(VI) \neq 0$. For instance, AM and MT (parallel to muscovite–trilithionite) belong to the former; and AE, AP (annite–polylithionite) and MP (muscovite–polylithionite) to the latter. Coupled two or three independent vectors comprising $ES(VI) = 0$ and $ES(VI) \neq 0$ substitutions make up a basis of simplified–composition space for a mica series, such as Mg–Fe, Fe–Li, Fe–Al or Al–Li micas.

The dominant tendency of compositions of a mica series, or their basic substitution, can be described by a linear combination *on* the basis vectors and determined graphically, or by the principal components analysis. It is found that 99% of the total variation of the simplified two octahedral compositions of Fe–Al micas is localized to the first eigenvector. ES(VI) and CS(VI) calculated from the first eigenvector give an unequivocal explanation that the first eigenvector represents an octahedral (because $ES \approx 0$) vacancy–producing (because $CS \neq 0$) substitution, i. e. muscovite substitution (AM). In fact, the angle between AM and the first eigenvector is only 0.8°. Similar calculation for 13 cation compositions of 141 Mg–Fe micas proves that the first eigenvector accountable for about 80% of the total information in mica data represents substitution 8PA+AM. AM and 8PA+AM are the basic substitutions of Fe–Al micas and Mg–Fe micas, respectively. Therefore, the plane comprising PA and AM (e. g. Foster's (1960) $Mg-(Fe^{+2}+Mn)-(R^{+3}+Ti)_{VI}$ triangle) contains more information about variations of Mg–Fe mica compositions than other planes. The general formula of a mica series could be expressed by a 'starting' mineral plus a linear

combination of basis vectors, or plus only basic substitution. The general Fe–Li mica formula $K_2R^{+2}_x Li_{4-x}R^{+3}_2[Al_xSi_{8-x}O_{20}](OH)_4$(Stone et al., 1988), however, departs far from basic substitution AP of its real micas.

In the two-composition plots, the points of a mica series are trapped by several polygons framed with several lines parallel to or approximately parallel to some substitution vectors. The stagger pattern of the polygons implies compositional discontinuity due to the limit of substitution. A kind of discontinuity occurs between dioctahedral and trioctahedral micas in Fe–Al or Al–Li micas. For instance, Fe–Al micas $K_2Fe_6[Si_6Al_2O_{20}](OH)_4$+mAM+eAE are made up of at least two polygons, which hardly overlap each other: for the most micas, if $m < 3/2$, $0 < e < 1$, otherwise $-1 < e < 0$. In Al–Li micas $K_2Al_4[Si_6Al_2O_{20}](OH, F)_4$+tMT+pMP, when p is fairly samll, the compositions will be limited by $t < 1/3$ ($MT(Al_{VI}, Li, \square_{VI}) = (-1, 3, 2)$). Another kind of discontinuity occurs within trioctahedral micas. The overlapping pattern of the polygons in Mg–Fe or Fe–Li micas suggests that the continuous compositional variation in trioctahedral micas along the direction of their basic substitution is accompanied by changing the extent of substitution of Al (or R^{+3}_{VI}) into octahedral sheet. The change of this extent, locally, is sharp or discontinuous.

In brief, the substitution vector is a strong tool for explaining mica compositions, especially for determining compositional dominant tendency and discontinuity. It has been concluded that there are two kinds of compositional discontinuities, which relate to the limits of substitutions of Al into octa- and tetra-hedral sheets, and are the basis for subdivision of mica series.

ATOMIC CHARGES BY MOLECULAR ORBITAL STUDY AND ELECTROSTATIC ENERGIES OF β-Mg_2SiO_4

57.4.23V

TAMADA, O., Dept. of Earth Science College of Liberal Arts and Sciences, Kyoto Univ., Kyoto 606, Japan.

It is well-known that β-Mg_2SiO_4 has an extraordinary crystal structure which does not obey Pauling's valence balance rule. The molecular orbital study (CNDO/2) has been performed on this mineral to determine the atomic charges. Electrostatic energies of the crystal and the atoms have also been calculated in order to compare them with the atomic charges.

The atomic charges were determined by the following procedure. A fairly large cluster of atoms was constructed around each of eight atoms in an asymmetric unit (Mg1, Mg2, Mg3, Si, O1,, O2, O3 and O4). The cluster was cut out of the areal structure determined by X-ray analysis (Horiuchi and Sawamoto, 1981), setting each of the above atoms near the center of the cluster. Assuming that all the atoms had their formal charges, the charge

neutrality was made to hold in the cluster by introducing H atoms. H atoms were attached to the outer oxygens of the cluster at the standard distance of 0.96Å. Slater-type orbitals (STO) were used as the orbital basis set of atoms. The charges were determined by the standard procedure of charge density analysis for CNDO/2 as listed in Table 1. Unfortunately the calculation in self-consistent iterations does not always converge for such a large cluster as used in this study. In fact, the calculation of Si charge diverged in the cluster. The atomic charges marked by the asterisks in Table 1 were taken as the value when they showed approximate convergence before the calculations diverged.

Electrostatic energies are calculated by the method of Bertaut (1952) using the formal charges as 2e, 4e and -2e for Mg, Si and O, respectively, as listed in Table 2. Electrostatic energies of three Mg atoms are nearly the same and their charge values are also nearly the same.

Electrostatic energy of O1 and O2 are higher and lower, respectively, by about 200 kcal/mol. than those of O3 and O4, which indicate that the Pauling's rule does not hold. The atomic charge of O1 exhibits a smaller value of -0.56e and that of O2 a larger one of -0.66e compared to the charges of -0.59 and -0.61e on O3 and O4, respectively.

The following conclusions are derived from the above results.

(1) The values of the atomic charges of O are different between the atomic sites, while those of Mg are nearly the same. As a rule, the atom with a lower electrostatic energy has a larger atomic charge.

(2) The differences between the charges of four O atoms are not large as expected from the large differences in electrostatic energies.

Table 1 Atomic charges (e) of β-Mg_2SiO_4 and the cluster used.

Mg1	0.68	($Mg_7Si_2O_{30}H_{38}$)
Mg2	0.68*	($Mg_7Si_2O_{28}H_{34}$)
Mg3	0.69*	($Mg_8Si_3O_{34}H_{40}$)
Si		
O1	-0.56*	($Mg_5O_{18}H_{26}$)
O2	-0.66	($MgSiO_{12}H_{14}$)
O3	-0.59	($Mg_7Si_2O_{30}H_{38}$)
O4	-0.61	($Mg_3SiO_{16}H_{22}$)

Table 2 Electrostatic energies (kcal/mol.) of β-Mg_2SiO_4.

Crystal	-5804(3)
Mg1	-1172(6)
Mg2	-1164(3)
Mg3	-1192(3)
Si	-4321(7)
O1	-996(4)
O2	-1427(5)
O3	-1230(6)
O4	-1243(2)

Bertaut. P. F. (1952) Joun. Phys. Radium, 13, 499-505.
Horiuchi, H. and Sawamoto, H. (1981) Amer. Miner., 66, 568-575.

X-RAY STRUCTURE ANALYSIS OF "EASTONITE" AND PREISWERKITE, THE CRYSTAL-CHEMISTRY OF THE Mg+Si = Al^{vi}+Al^{iv} EXCHANGE IN (K,Na)-TRIOCTAHEDRAL MICAS, AND A NEW SITE (X) FOR TETRAHEDRALLY-COORDINATED LOW-VALENT CATIONS (Li, Na, Mg, Fe^{2+}).

57.4.24 V

L. UNGARETTI*, D. C. SMITH**, A. TLILI** & R. OBERTI*.
* CNR, C.S. Cristallografia Strutturale, 27100 Pavia, Italy.
** Muséum National d'Histoire Naturelle, 75005 Paris, France.

The structures of natural specimens of (K,Na)-"eastonite" (EA) and of preiswerkite (PW) have been determined by single-crystal X-ray refinement in the space group *C2/m*, the final R_{obs} factors for ≈ 550 reflections being 2.1 % and 3.8 % respectively.

Sample Q102/2 from the Liset eclogite pod, Norway (Smith, 1988) has a composition rather close to that of ideal EA ($K_2Mg_5Al_1Si_5Al_3O_{20}(OH)_4$) in terms of Al^{vi} and Al^{iv} (Si = 5.1 per 20 O) but some K, Mg, Al^{vi} and (OH) are replaced by Na, Fe, Ti and F respectively. The X-ray diffraction data indicate the presence of only one phase (confirmed by TEM examination of adjacent crystals; K. Livi, pers. comm.), in contrast to the mixed-layer phlogopite + serpentine nature of the "type" EA discredited by Livi & Veblen (1987). The "type" PW (sample KP/4; Keusen & Peters, 1980) has a composition (Si = 4.1) rather close to that of ideal PW ($Na_2Mg_4Al_2Si_4Al_4O_{20}(OH)_4$) with some replacement of Mg by Fe.

The average structure of space group *C2/m* typical of phlogopite (PH = $K_2Mg_6Si_6Al_2O_{20}(OH)_4$) therefore extends along the (K,Na)-trioctahedral mica series to EA and also to PW. This situation of long range disorder (LRD) does not exclude the possibility of some short range order (SRO) (cf. alternating Si and Al in the T sites of margarite) and hence lower symmetry locally. Raman spectra from PW display sharp peaks compared to those of EA, and an intense Si-O-Al vibration but a weak Si-O-Si vibration; both points are suggestive of SRO in PW (Tlili et al., 1988, 1989). Comparison with published and unpublished crystal structure refinements of several micas, in particular of some "phlogopites" and "biotites", permits an evaluation of structural changes along the PH-EA-PW join, which represents the "tschermakitic exchange" Mg+Si = Al^{vi}+Al^{iv} accompanied by the replacement of K by Na and by some variation in minor elements, especially Fe and F.

The T-O mean bond length (mbl) increases from PH to PW, all individual T-O bonds increasing due to the increasing content of the larger Al^{3+} cation (as in K-dioctahedral micas). The T-O(3) (apical) distance strongly increases, since Al^{iv} moves towards the basal oxygens O(1) and O(2) to provide them with more charge, such that T-O(3), which is shorter than T-O(1) and T-O(2) in PH, overtakes in EA and becomes very long in PW (1.708 A) compared to the 1.689 A mbl for T-O(basal).

The M-O mbl's are strongly related to the octahedral cations' charge and size. The M2-O mbl decreases from PH to PW (as in K-dioctahedral micas) suggesting an almost complete ordering of $^{vi}R^{3+}$ cations at this site (2.059 A in EA and 2.009 A in PW)

whereas the M1-O mbl remains similar (2.077 A in EA and 2.060 A in PW, but more iron in EA). As expected, the different values observed for the M1-O and M2-O mbl's become almost equal in PH where both sites have no $^{vi}R^{3+}$.

The W-O mbl (where W denotes the interlayer cation) slightly increases from PH to EA. The W-O (outer) and W-O (inner) mbl's respectively increase and decrease along the PH-EA-PW join (as in K-dioctahedral micas) due to the increasing rotation of the tetrahedra mainly caused by the tschermakitic exchange (di-trigonal array, increasing α, α=12° in EA and 20° in PW). The W-O (inner) mbl drastically shortens from 2.890 in K-rich EA to 2.575 A in almost Na-pure PW (as between phengite and paragonite).

In the refinements of EA, PW and a few "biotites", a new partially-occupied site (here denoted by X) has been discovered. X lies between the normal K and H sites (necessitating the absence of both K and H), almost at the centre of the ditrigonal array of (Si,Al) tetrahedra. It makes a rather short bond with the hydroxyl O(4) and 3 longer bond distances with the basal oxygens O(1),O(1),O(2); the bond angles range between ≈ 102° and 115°, with a mean value of ≈ 109.2°; these feature are suitable for tetrahedrally coordinated low-valent cations such as Li, Na, Mg and Fe^{2+}. In EA the X-O mbl (2.24 A) is appropriate for Na^{iv}, whereas in PW the mbl (2.04) is more appropriate for (Li,Mg,Fe^{2+}) in fourfold coordination (as in the Fe-site of staurolite). The X site might explain the apparent alkali-deficiency observed in many natural micas.

REFS: Keusen & Peters (1980) *Amer. Mineral.* 65, p. 1134; Livi & Veblen (1987) *Amer. Mineral.* 72, p. 113; Smith (1988) chap. 1 in "*Eclogites and Eclogite-Facies Rocks*", Elsevier, 524 pp; Tlili et al. (1988) *Terra Cognita* 8, p.78; (1989) *Mineral. Mag.* 53, p.165.

56.4.1.
57.4.14

GMELINITE: STRUCTURAL REFINEMENT OF A K-RICH NATURAL SAMPLE

G. Vezzalini, S. Quartieri and E. Passaglia

Università di Modena, Istituto di Mineralogia e Petrologia- via S.Eufemia,19-41100 Modena (Italy)

The structure of zeolite gmelinite $[(Na,Ca_{0.5})_8(Al_8Si_{16})O_{48}\cdot 22H_2O$; s.g. $P6_3/mmc]$ is characterized by a framework consisting of a sequence AABB of parallel 6-membered rings. The crystal chemistry study of gmelinites (Passaglia et al., 1978) showed that exchangeable cations are usually Na and Ca, Na> Ca and Mg and K are present in smaller amounts. The

monovalent cation content (Na+K) is correlated positively with c and negatively with a cell parameters. Structure refinements of an Na- and a Ca-rich gmelinite (Galli et al., 1982) confirmed Fischer's results, showing only small differences in the framework angles and in the extraframework site occupancies. The crystal structure of a sample anomalous for K content and cell parameters is reported by Malinovskii (1984), who correlated the high c and low a values with the K content. The author emphasized the presence of disordered intergrowth of chabazite, as already suggested by Fischer (1966) on the basis of weak diffuse streaks in the rotation photographs along c.

The present work reports the X-ray single crystal structure refinement (final Rw=6.6%) of a K-rich gmelinite from Fara Vicentina (VC), Italy $[(K_{2.72}Na_{1.67}Ca_{.39}Sr_{.13}Mg_{.22})(Al_{7.79}Si_{16.32})O_{48} \cdot 23.52\ H_2O]$, with very high c and very low a cell parameters (a=13.621(3), c=10.254(1)). Unlike sample studied by Malinovskii (1984), this sample does not show disordered intergrowths of chabazite and gmelinite frameworks. The structural data show the presence of three extraframework cation sites, one of them (C1) is localized in the offrettite cage, the second (C2) in the large channel near the 8-ring window, both correspond to those already found by Galli et al. (1982) and Malinovskii (1984), but with lower occupancy (about 5%) for C2; the other cation site (C3) is localized inside the double 6-ring with a very low occupancy. The interaction between framework oxygens and cations in C2 sites causes the deformation of offrettite cage with a c shortening and a lengthening. Therefore, the cell parameter values of gmelinite samples, up to now structurally described, may be correlated with the C2 site occupancy; in particular the large c and the small a values of sample here studied are most likely due to the very low occupancy of this site.

A structure refinement based on the combined data from single crystal and synchrotron X-ray powder pattern is in progress on this gmelinite sample.

-Fischer,K.(1966): Untersuchung der Krystallstruktur von Gmelinit. N.Jb.Miner.Mh.,1966, 1-13.

-Galli,E., Passaglia,E. and Zanazzi,P.F.(1982): Gmelinite: structural refinements of sodium-rich and calcium-rich natural crystals. N.Jb.Miner.Mh.,1982, 145-155.
-Malinovskii,Yu.A.(1984): The crystal structure of K-gmelinite. Sov.Phys.Crystallogr.,293 (3), 256-258.
-Passaglia,E., Pongiluppi,D. and Vezzalini,G.(1978): The crystal chemistry of gmelinites. N.Jb.Miner.Mh., 1978, 310-324.

X- Ray POWDER DIFFRACTION CHARACTERIZATION OF PYROPE

WANG Guanxin and GONG Guohong, Institute of Geochemistry, Academia Sinica, Guiyang, Guizhou 550002, People's Republic of China

Pyrope, $Mg_3Al_2(SiO_4)_3$, is an end member of garnet group. The component of natural pyrope is rather complex with wide isomorphous substitution. In it, magnesium may be partially replaced by iron, calcium or manganese, and aluminum by chromium or iron. So, it is difficult to differentiate pyrope from another garnets on the basis of the unit cell parameter, because its parameter, a = 11.53 - 11.65 A, overlaps the dimensions of almandine or spessartine. But, according to the method of structure analysis, the characterization of pyrope can be found from powder diffraction data.

structurally, the garnet belongs to cubic system, space group: O_h^{10} - Ia3d, Z=8. In a unit cell, there are 160 atoms: 24 A(Mg, Fe^{2+}, Ca, Mn); 16 B(AL, Cr, Fe^{3+}); 24 Si and 96 O. Their Wyckoff notation and co-ordinates of equivalent positions were recorded as follows:

A in (c)	0.125,	0,	0.25;
B in (a)	0,	0,	0;
Si in (d)	0.375,	0,	0.25;
O in (h)	x,	y,	z.

Where x, y and z can be obtained in the light of the empirical formula:

$$x = 0.006 + 0.022\langle r\{x\}\rangle + 0.014\langle r[y]\rangle$$
$$y = 0.051 - 0.023\langle r\{x\}\rangle + 0.037\langle r[y]\rangle$$
$$z = 0.643 - 0.009\langle r\{x\}\rangle + 0.034\langle r[y]\rangle$$

Where $\langle r\{x\}\rangle$ and $\langle r[y]\rangle$ are the average of ion radius of A and B, respectively. For example, the ordinates of a natural pyrope, $(Mg_{0.77}Ca_{0.14}Fe^{2+}_{0.09})_3(Al_{0.85}Cr_{0.07}Fe^{3+}_{0.04}Fe^{2+}_{0.04})_2[(Si_{0.99}Al_{0.01})O_4]_3$, can be given:

$x = 0.0340$ $y = 0.0499$ $z = 0.6532$

Then, the structure factors F_{hkl} of the natural pyrope can be calculated based on the structure analysis, two of them as follows:

$$F_{332} = -28.53\ f_O$$
$$F_{422} = 8\ f_A + 16\ f_B + 8\ f_{Si} - 27.16\ f_O$$

Where f_i is the scattering factor of the atom.

Obviously, the F_{332} has only an item concerning with oxygen atom, but the F_{422} with all atoms in pyrope, and it depends on f_A and f_B. Therefore, the relative intensity I_{332} / I_{422}, calculated in direct proportion to structure factors $|F_{hkl}|^2$, can be taken as an identification indicator of pyrope, because the value of F_{422} of pyrope is the smallest in the garnet group, and it is easy to distinquish the pyrope from another garnets. The ratios of I_{332} / I_{422} calculated are listed below:

minerals	I_{332} / I_{422}
synthetic pyrope	1.47
natural pyrope	0.91
almandine	0.61
spessartine	0.56
grossular	0.67
andradite	0.22

MICROSTRUCTURE STUDY OF COMPLEX HIGH-ORDER TWIN OF GRANDIDIERITE

62.7-3. H

Wu Xiuling Yang Guangming Pan Zhaolu Shen Jinchuan
China University of Geosciences. Wuhan 430074

The grandidierite is a rare mineral discovered in Jixi county, Heilongjiang, China (1987). Its ideal chemical formula is (Mg,Fe) Al_2SiBO_9. X-ray diffraction analysis and transmission electron microscopy (TEM) have been used to study the microstructure of grandidierite. The studies show that this mineral belong to orthorhombic with the unit cell parameters a=10.318(2)Å, b=10.981(1)Å, c=5.753(1)Å, and the space group Pbnm.

The microstructure analysis of complex (high-order) twins is very complicated. Formerly, the study to simple high-order twins in metal materials and minerals is more. However, the study to the complex (high-order) twins in the low symmetry minerals is less. When we observed the microstructure of grandidierite studied by TEM in our laboratory, it was the first time that the complex

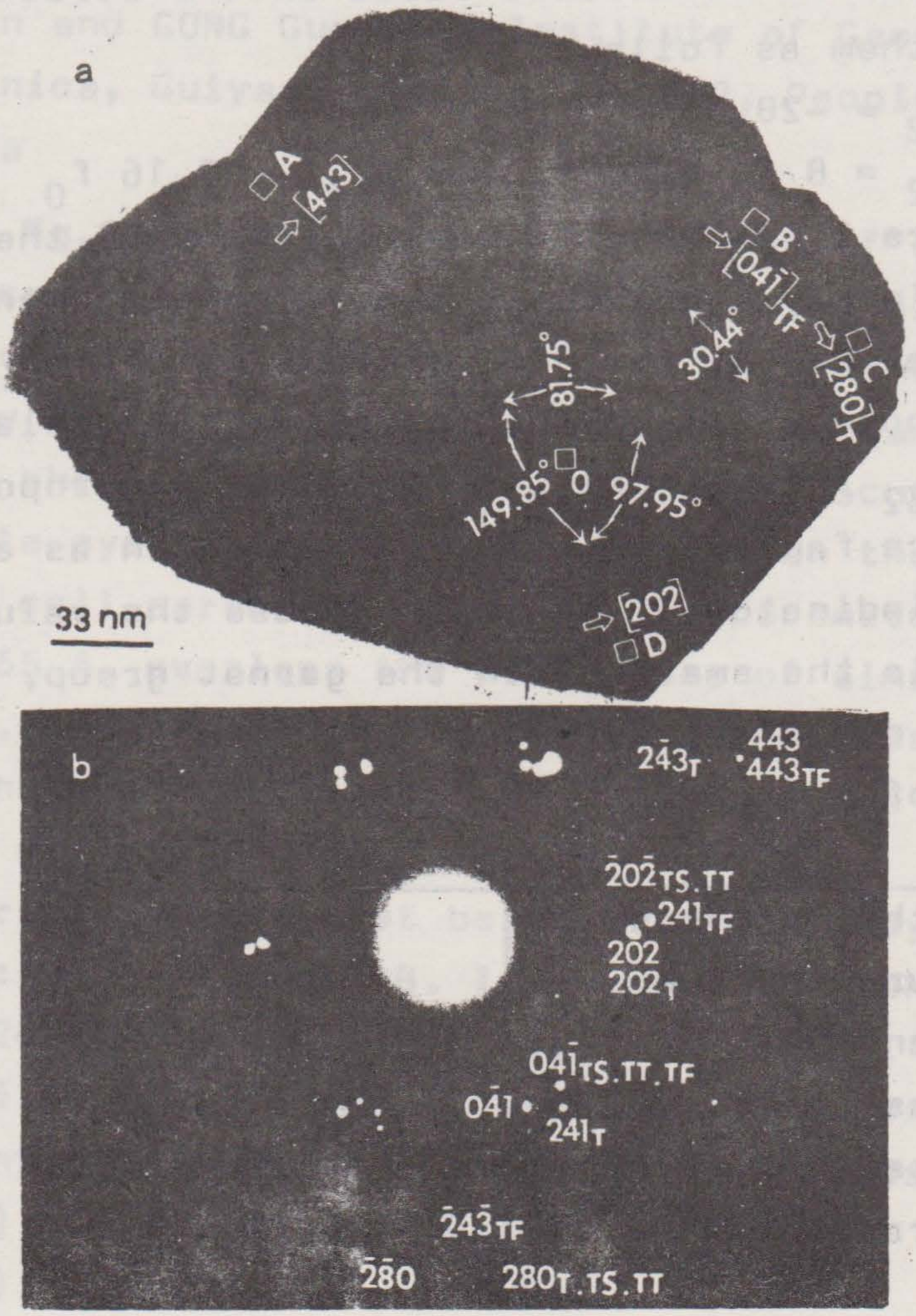

Fig.1a. Electron micrograph of the complex (high-order)twins in grandidierite.

Fig.1b. Composite electron diffraction pattern of the crystal zone axies $[\bar{4}14]$,$[4\bar{1}\bar{4}]_T$,$[\bar{4}14]_{TS}$,$[\bar{4}14]_{TT}$and $[4\bar{1}\bar{4}]_{TF}$of grandidierite and its indexing, projection position of 1 and -1 grade laue spots.

(high–order) twins in the mineral were discovered. The selected area electron diffraction (SAED) and the electron micrograph of the high–order twin were obtained by TEM. Fig.1b showed the SAED pattern corresponding to "o" area in fig.1a.

The combination of SAED and bright field image of TEM has been used in determining the complex (high–order) twins in grandidierite ((202)growth twin , (280)(202) secondary order twin, (04$\bar{1}$)(280)(202) third order twin and (443) fourth order twin). The structure relationship between the complex (high–order) twins in the mineral has been explained and the analysis method of the microstructure for the minerals with low symmetry and complex (high–order) twins has been summarized.

In fig.1b, the arrangement feature of the electron diffraction spots is regular. The experimental result shows that there are splits of electron diffraction spots along [202],$[280]_T$,$[04\bar{1}]_{TF}$,[443], in these four directions (see fig.1b), i.e., there are plane defect on the crystallographical plane (202),$(280)_T$,$(04\bar{1})_{TF}$, (443) in the mineral (In fig.1b, T, TS, TT and TF show first, second, third and fourth order twin spots, respectively).

The discovery and study of the microstructure characteristics of the low symmetry and complex (high–order) twins in borate mineral not only furnished new data for the modern mineralogy, but also gave an example for the study of mineral microstructure.

ELECTRONMICROSCOPIC STUDY ON INCLUSIONS IN SMALL DIAMONDS OCCURRED IN LIAONING

Xiao Xugang, Liu Gang, Department of Geology, Northeast University of Technology, Shenyang Liaoning, 110006, People's Republic of China

Inclusions in small diamonds (max dia.≦0.5mm) occurred in south Liaoning, can be observed with stereomicroscope. Powder samples are prepared by crushing with two plates of W-Ti-Co hard alloy. Three included minerals are discovered with transmission electronmicroscopy.

1, Al-rich Chromite Indexed SAD patterns(fig.1) indicate that this mineral crystal is cubic face-centred and has cell parameter a=0.841nm. Chemical compositions obtained from EDAX are: Mg 20.985%, Al 25.392%, Cr 33.129%, Fe 20.494%.

2, K-feldspar (sanidine, orthoclase) Indexed SAD patterns show as fig.2. After Niggli's reduction, a unique Bravais cell

is determined. This is a momoclinic base-centred cell having parameters a= 0.873mm, b=1.307mm, c=0.737mm, β=118°. Chemical compositions from EDAX are: Al 22.027%, Si 61.013%, K 16.966%. This mineral cam be determined as K- feldspar.

3, Quartz These included minerals are widespred im the small diamonds. Their compositions all are SiO_2 determined with electron probe EIM-810Q. SAD patterms manifest 3- or 6-fold rotation symmetry and contribute cell parameters a=0.497mm, c=0.545nm, so these minerals may be confirmed as d- or β-quartz.

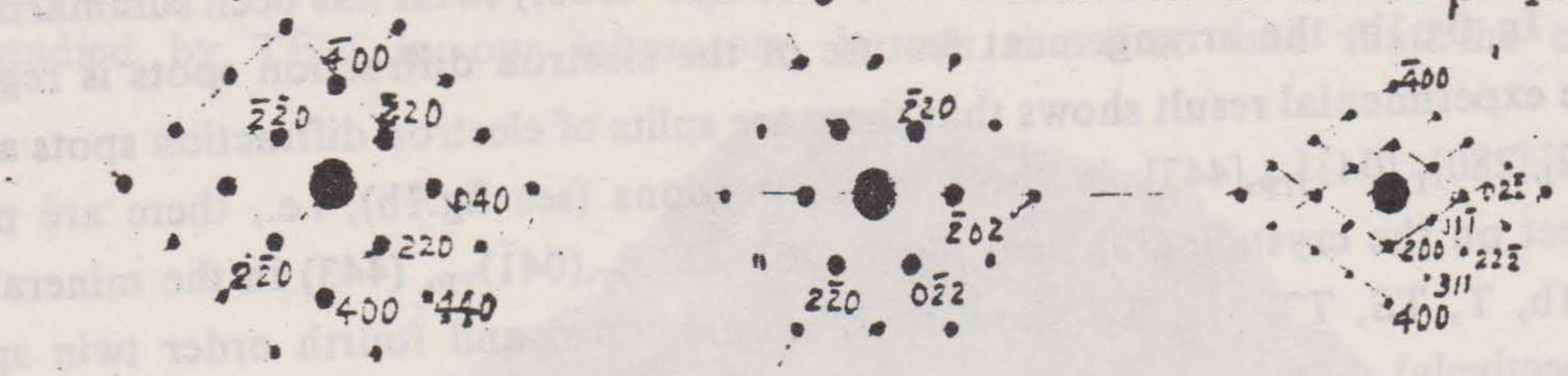

a, (001)*, $\perp C_4$ b, (111)*, $\perp C_3$ c, (011)*, $\perp C_2$

Fig. 1 Indexed SAD patterms of Al-rich Chromite

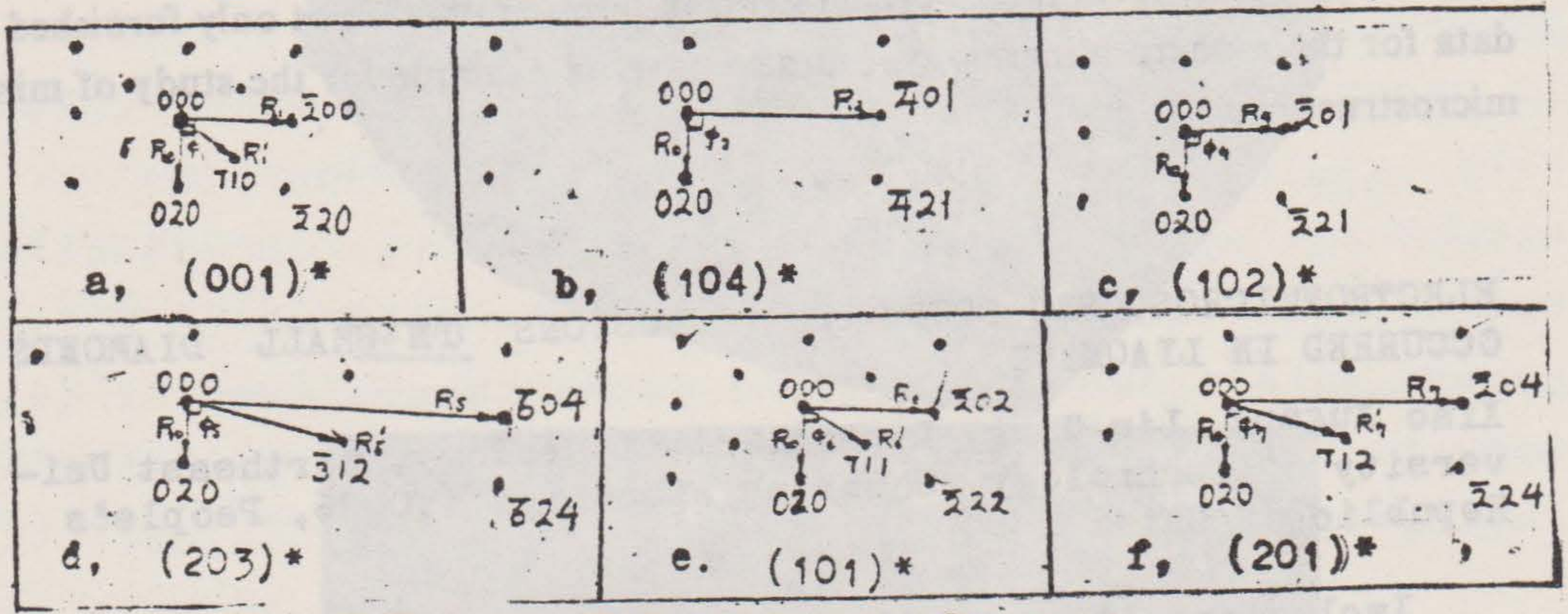

Fig. 2 Indexed SAD patterms of K-feldspar

Fig. 3 SAD patterms of quartz

Conclusiom: Mineralogical composition consisting of above memtioned three minerals included im small Liaoning-diamonds, is mear to that of acidic igmeous rocks, so they are not linked to peridotite suites and eclogite suites.

References

1 , J.D.H. Donnary et al, Crystal Data, 3rd editiom, vol 11

(1973) M-33---M-35

2 , J.E. Field(editer), The Properties of Diamond, (1979), 556-588, Academic Press, London

STUDIES ON THE DEFECT STRUCTURES AND METASOMATISM OF OLIVINE AND PYROXENE IN LHERZOLITE XENOLITHS FROM BASALTS IN FUJIAN AND ZHEJIANG PROVINCES, SOUTH EASTERN CHINA"

Xie Xiande Liu Junsuo Xie Hongsen
Institute of Geochemistry, Academia Sinica, Guiyang, China

Along the east coast of China, Cenozoic basalts and mantle xenoliths therein contained are extensively distributed. Crystals of olivine and pyroxene in lherzolite fragments from Fujian and Zhejiang alkali basalts were examined under a transmission electron microscope, conclusive evidence on metasomatism of an olivine on a submicroscopic scale was found; and a mode for "cryptic" metasomatism in the mantle is proposed.

I. Defect Structures

"Kink band" parallel to (100) with crossing [100] screws and walls parallel to (100) and (001) respectively defining long subgrains dominate the deformation structures of the olivine(with a Pbnm system) from Fujian and Zhejiang. Besides, there are some free screw dislocations of [100] and some fractures, faults and subgrain boundaries. Climb and recovery of dislocations of the olivine from Fujian are remarkable. Defects in the orthopyroxene from both Fujian and Zhejiang are mainly bands of edge dislocations parallel to (100). Lamellae of clinopyroxene parallel to (100) formed both by shear-induced transformation and by exsolution are common. Fractures parallel to {hk0} are often found in the orthopyroxene from Fujian.

The dislocation densities of both the olivine and pyroxene from Zhejiang are larger than those of their Fujian counterparts. This means probably a deeper origin of the xenoliths from Fujian basalts, or a larger geothermal gradient in the area of Fujian.

Bubbles were found existing along the defect structures both in olivine and in orthopyroxene.

II. Metasomatism

Metasomatism on a submicroscopic scale was discovered within an olivine crystal along the subgrain boundaries. There are typical gulf-and-peninsula structures of metasomatism along the metasomatized edges of olivine subgrains; electron diffraction patterns of the metasomatic products are hexagonal, quite different from those of the host olivine. Metasomatized

zones are from about 200 A to 2.5 μm. Another interesting phenomenon probably related to mantle metasomatism is that within an olivine crystal a mica phase was found with dislocation boundaries between mica and its host. The olivine close to the boundary is evidently altered; but the mica near the boundary is not. Electron diffraction patterns show that the mica and olivine have a common lattice plane with the (100) plane of the olivine coinciding with the (001) plane of the mica.

Border rings of a clinopyroxene from Fujian were shown to be an extremely fine mineral mixture in which larger mica crystals were observed. In one case, mica is observed in the ring under the optical microscope.

III. Discussion

Geochemical studies have shown that alkali basalts and their lherzolite xenoliths from Mingxi County, Fujian Province were enriched in LREE (R.Y., Zhang, B.L., Cong, 1987); but no metasomatic structures or phases were found. Similar phenomena were found in many other places in the world. To interpret these phenomena, metasomatism in the mantle was earlier proposed by geochemists. Unfortunately, lacking of structural evidence makes the concept uncertain and restricts its wide reception. To go around this difficulty, the term "cryptic" metasomatism was used to denote the LREE enrichment process(M.F., Roden and V.R., Murthy, 1985). The discovery of metasomatism on a submicroscopic scale within an olivine from Fujian has confirmed the "cryptic" type of mantle metasomatism. In fact, we tentatively suggest in this study that the so-called "cryptic" metasomatism is actually a process in which incompatible element-rich fluids diffuse and alternate the original phases along their defect structures and subgrain boundaries on a submicroscopic scale. The abundant bubbles found existing along the dislocations and subgrain boundaries in both olivine and pyroxene make this suggestion feasible. The metasomatism of an olivine from Fujian along its defect structures in zones less than 2.5 μm in size may be regarded as direct evidence of the proposed mode.

* Supported by the Chinese Committee of Natural Sciences

THE REALIZATION OF POWD12 PACKWGE ON MINI AND MICRO-COMPUTERS

Xie Xilin, Lin Xinyuan & Wang Liben, Institute of Mineral Deposits, Chinese Academy of Geological Sciences, Beijing 100037, China.

POWD12 is a familiar software package which was recommended by the International Committee of Crystallography to the international community for theoretically simulating the patterns of X-ray diffraction. The original copy of POWD12 was created on the IBM370/3030 and CDC6600 computer at Pennsylvania state University of the United States. Based on the magnetic type provided by Prof. Shen Jinchuan of China University of Geosciences-Wuhan, we have transplanted this package on mini-computer PDP11/24 of PW1700 system-PHILIPS, and on micro-computer CASIO of D/MAX 3B system RIKAGU; NEC9801FC of XRD system, CAGS.

In order to read the source program of POWD12 without the help of a magnetic

type unit, the files on that type were first rewritten on 8 inch floppy disk(single side, single density) by using FACOM M-150 computer; then physically read and explained as external files by PDP 11/24. The obtained source program was transmitted to PC computer in the form of unsynchronous communication.

POWD12 package was written in FORTRAN language. The difficulty in executing it on a mini or a micro-computer is lack of internal storage. Fortunately, this long program could be converted into several models which are relatively independent and capable in being executed consecutively. The transmitting of parameters among the models is done by "Real parameter" or "Common Sentence". Therefore, we divided POWD12 into sub-models. The calculating results of the first model will be put into the succissive one through the external equipment(disk). This method in which the Sub-models are executed by stage, the parameters transmitted by disk file, has a general value for realization of a large program package on the micro-computer.

In this way, three copies of POWD12 have been created for the above three mini-and micro-computer systems. Requirement for input data are as that for the original copy. For output, despite printing the diffraction pattern on a printer, we have written the programs for screen display and for plotting. A data file whose structure coincides with that of the data file for a special type of diffraction system is also produced after calculation in order to be directly used by the data processing system of diffractometers.

Some good results were obtained by using this micro-computerized copy of POWD12 packge for studying the structures of superconductors in the low-temperature laboratory of the Peking University, and in the Institute of Chemistry, Academy Sinica.

THE STUDY ON THE ORTHOPYROXENE WITH SPACE GROUP $P2_1ca$

XU Huifang, Department of Earth Sciences, Nanjing University, Nanjing, Jiangsu 210008, People's Republic of China

It has been carried out that all of the k odd diffraction spots violating b-glide are completly present on 0kl electron diffraction patterns of three orthopyroxenes, through detailed TEM study for the orthopyroxene megacrysts [sample 1, hypersthene ($En_{56}Fs_{41}Wo_3$) from Blackhill, Chengde, Hebei Province, NE China; sample 2, enstatite ($En_{94}Fs_6$) from Bamble, Norway; sample 3, ferrohypersthene ($En_{42}Fs_{56}Wo_2$) from Bettola, Italy]. The result shows that k odd diffraction spots are caused neither by C2/c clinopyroxene exsolution lamellea on (100) with fortuitously similar cell parameters or the difuse streaks of orthopyroxene along a* direction, nor by the overlap of certain diffraction from the orthopyroxene itself and/or clinopyroxene neighbouring 0kl diffraction plane of orthopyroxene or multipl diffraction effect (Sasaki et al., 1984).

The result of phase transition is brought out, the whole k odd

spots in 0kl diffraction pattern systermatically disappeared when the sample was heated to about 900℃, according to the SAD pattern in the process under heating stage of TEM for hypersthene (sample 1) (Xu et al., 1989). Thus, author confirmed that the orthopyroxene with space group $P2_1ca$ really exists in nature. Having studied for other orthopyroxenes with different composition and occurrences (sample 4, brozonite ($En_{87}Fs_{13}$) of the lherzolite inclusion in alkali basalt, East China; sample 5, hypersthene ($En_{62}Fs_{35}Wo_3$) of the norite from Blackhill, Chengde, Hebei Province, NE China; sample 6, hypersthene ($En_{65}Fs_{33}Wo_2$) of the gabbro from Jinan, Shangdong Province, North China), author obtained same conclusion. The results from above orthopyroxene samples show that orthopyroxenes with different composition (range from En_{94} to En_{42}), different occurrence (from intrusive rock to volcanic rock) and different geological ages (from Presinian to Cenozoic) display $P2_1ca$ symmetry. It can be inferred that the

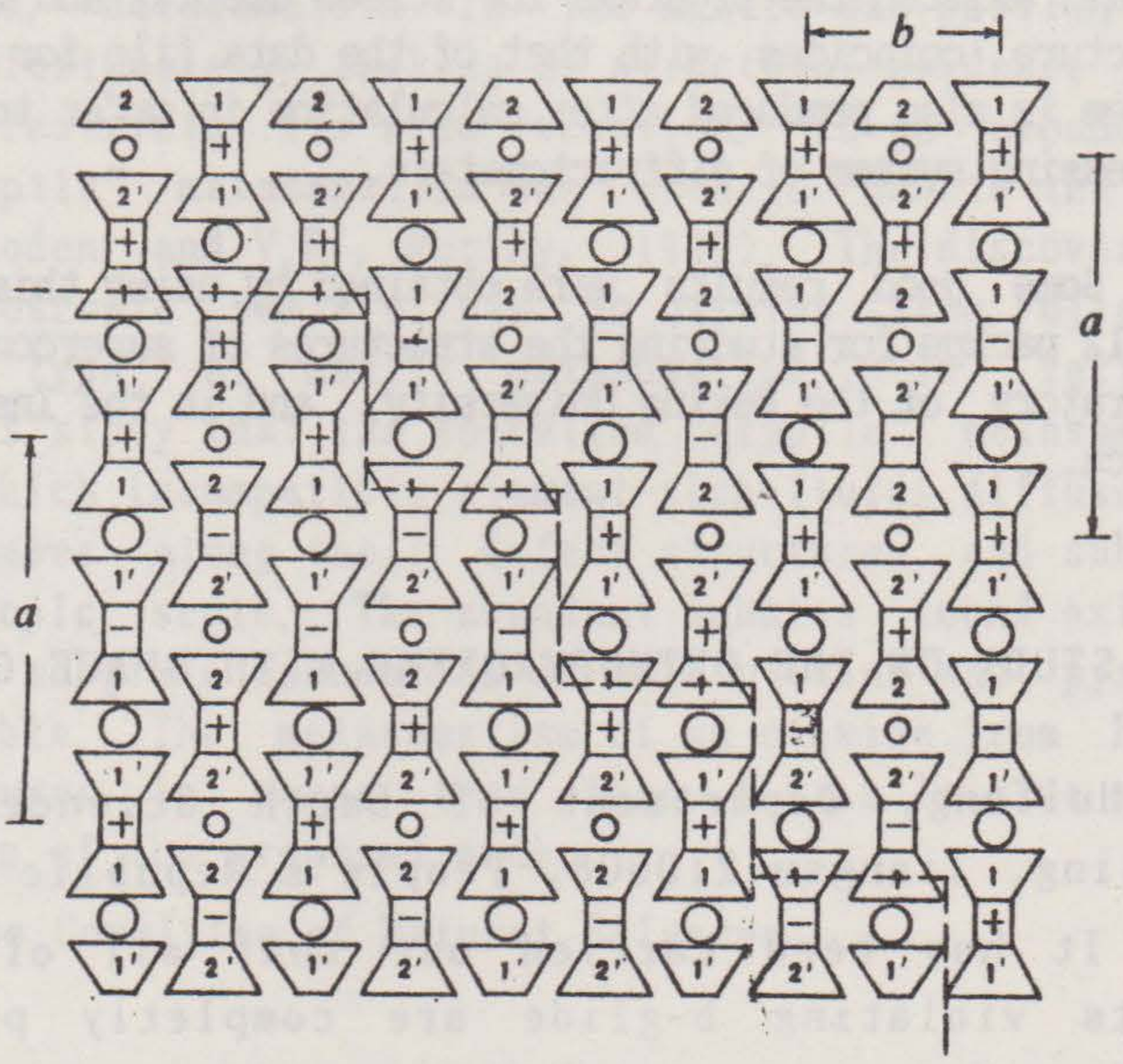

Fig.1 The possible domain boundary in $P2_1ca$ orthopyroxene (broken line represents domain boundary).
1-OA_1; 2-SA_2; 1'-OB_1; 2'-OB_2; o-$M_2A(P\cdot N)$; ○-$M_2B(P\cdot P)$.

space group of all orthopyroxenes should be $P2_1ca$ under normal temperature and pressure condition, rather than Pbca.

Author confirmed that there is a new kind of domain structure in the crystals of $P2_1ca$ hypersthene (sample 1) and $P2_1ca$ enstatite (sample 2) (Xu et al., 1988; Luo et al., 1988). The neighbouring domains are repeated systamatically by the symmetry operation of (100) symmetry plane and the glide of b/2. Two neighbouring domains are in the relationship of anti-orientation for their polar a-axis, and the step-like boundary between two domains costitutes inversion domain boundary (Fig.1). Existence of this kind of domain structure corresponds to the effect of b-glide on (100) plane completly, which conceals the true symmetry and crystal structure, and leads to streak of diffraction spots

(sample 1) and /or satellite spots (sample 2) parallele to a*.
1. Sasaki,S. et al., 1984:Am. Mineral., 69, 1082.
2. Xu,H. et al., 1988:Exploration of Geosciences, 1, 59.
3. Xu,H. et al., 1989:Journal of Petrol. and Mineral., 8, 188.

TYPES OF DOMAIN STRUCTURES IN MINERAL CRYSTALS AND THEIR TRANSMISSION ELECTRON MICROSCOPE STUDY

XU Huifang and XU Ning, Department of Earth Sciences and the Laboratory of Solid State Microstructures, Nanjing University, Nanjing, Jiangsu 210008, People's Republic of China

The domains with cell level (include stacking fault and exsolution caused by spinodal decomposition, in solid solution, in broad sense) extensively exist in mineral crystals, which, affect the crystal structure, chemical composition and physical feature of minerals. It is realy possibole to reveal domain the structures by using of transmission electron microscopy and electron deffraction. The physical chemistry condition and the evolution history of thermal, stress and chemical composition of minerals can be revealled by applying the domain structures from microcosmic angle.

The domain structures can be classified into three main types according to their characteristics and genesis. I: The domain structures constituted by a series of domains with same composition and structure, which include (1). antiphase domain structure [eg. (i) APD in pigeonite formed through the displacive phase transition from C2/c symmetry to P21/c's (Heuer and Nord, 1976; Carpenter, 1979); (ii) APD in omphacite formed throughthe ordering of (Mg,Fe) , Al and Ca, Na in M1 and M2 site in the process of phase transition from C2/c symmetry to P2/n's (Champness,1973; Carpenter, 1978); (iii) extended antiphase domain structure observed in KNbW2O9 crystal (not mineral) below the β to α phase transition temperature with certain width of domain boundaries (Tao, 1988); (2). Domain twin [eg. (i) superlattice orthoclase formed through the ordering of Al in tetrahedra site (Xu et al, 1989) and (ii) super-microtwinning in perovskite and leucite formed through the deforming of crystal lattice]; (3). Inversion domain structure, such as appeared in P21ca orthopyroxene. This kind of domain structure includes the characteristiccs of above two domain structures. The neighbouring domains are repeated symmetrically by symmetry operation of (100) symmetry plane and the glide of b/2 along b-axis (Xu et al, 1988). II: The domain structures constituted by the domains with same composition but differen structure [eg. (i) P21/c and/or C2/c clinopyroxene domains in orthopyroxene crystal, which may be caused by stress, phase transition (Buseck and Iijima, 1975) and/or stacking fault; (ii) long period structure caused by the stacking of different crystallographic layer modules, such

as the chlorite with long period (Xu et al, 1989) and long period polytypes in pyrrhotite. III: The domain structures constituted by the domains with different composition and structure, (in a broad sense) which include (1). exsolution structure caused by spinodal decomposition in solid solution [eg. anorthoclase, sanidine and augite from volcanic rocks], (2). the domain structures caused by polysomatic reaction [eg. chain width disorder and long period modulated structure in inosilicates and mixed layer structure in phyllosilicates], (3). extended domain twin formed through the phase trnsformation by the change of chemical composition [eg. domain twin in laihunite with certain width of olivine domain boudaries (Fu, 1988) which is formed through the phase transformation from fayalite to laihunite by the oxidation, and the domain boundaries are parlleled to (001). If these two types of structure units are arranged periodically, the modulated structure may be formed].

All these types of domain structures show the definitely crystallographyc relationship in mineral crystals, and appear differentely in electron micrograph and electron diffraction pattern. It should be poited out that some kinds of domain structures may display transitio nal features of above types or complex features of above two or more types, such as e-diffraction structure in intermediate plagioclase (Kitamura and Morimoto, 1983).

48.7.5 K

ELECTRON DIFFRACTION STUDY ON MAGNESIOCUMMINGTONITE FROM LONGQUAN, ZHEJIANG PROVINCE

XUE Jiyue, MA Jun, Department of Earth Sciences, Nanjing University;
ZHANG Fusheng, HU Meisheng, Center of Material Sciences, Nanjing University;
WANG Luchun, Laboratory of Solid Microstructure Physics, Nanjing University; Nanjing, Jiangsu 210008, People's Republic of China

The studied magnesiocummingtonite(Mg-Cum) with the form of fribrous or radial aggregate surrounds the peridotite block within Early Paleozoic melange zone of Longquan, Zhejiang Province. The length of its crystals ranges from several mm to about 1cm. Under polarizing microscope it is of inclined extinction, $c\wedge Ng=10^{\circ}-13^{\circ}$, and it coexists with olivine, talc, serpentine, etc.. Its ratio of $Mg/(Mg+FeO^{*})$ is about 0.80. It is poor in calcium and aluminium.

The features of the [001] electron diffraction pattern of Longquan Mg-Cum are: (1) The pattern is composed of a series of diffraction streaks parallel to b^{*} axis, which are overlapped by diffraction spots. It is shown that the Mg-Cum is disordered in long range along b axis; (2) The h00 diffractions of h odd and $h+k/2=2n+1$ ($h=2n+1$) diffractions which violate c-center lattice are very weak and obliterated by the

diffraction streaks. As the 0k0 diffractions, k odd diffractions are systematically extincted; (3) All the k=4n diffraction spots are strongly sharp and circular, whereas the others are somewhat elongated along b* axis and orbicular.

The long range disorder of Longquan Mg-Cum along b axis is verified by its high resolution lattice image. The isolated wide chain lamellae parallel to (010) are commonly seen under TEM. Among these multiple chain lamellae, triple chain is predominant. The interval of multiple chain is irregular.

Based on the existent condition of diffractions for Longquan Mg-Cum, it is known that the space group is $P2_1/m$. After analyzing the [001] electron diffraction pattern, authors believe that it is a sort of Mg-Cum which somewhat deviates from $P2_1/m$ structure. This assumption can be proved as the following: (1) All the k=4n diffractions are sharp and strong imply that there is a subperiod whose length is b/4 and this repeat period is very constant. This length equals the distance between two neighbouring Si^{4+}. When the amphibole-C2/m inverts to the $P2_1/m$ form, it is necessary to transform half of the double chains. The transformation can be completed only by rotating the O^{2-}. Thus, during the course of phase transformation from C2/m to $P2_1/m$ with the decreasing of temperature, the sites of the Si^{4+} basically have no displacement. The arrangement of Si^{4+} in $P2_1/m$-form succeeds to from that in the C2/m-form. It seems that they are strictly arranged at the Bravais lattice positions of $P2_1/m$. In consequence, there is a subperiod of b/4 in the electron diffraction pattern. However, O^{2-} must be rotated. Probably, this rotation will cause the arrangement of O^{2-} to deviate from the Bravais lattice point. As the result, the k≠4n spots are diffuse along b* axis. The more the spots diffuse, the more the O^{2-} sites deviate from $P2_1/m$ lattice. (2) The spots violating the C-centered lattice on the [001] diffraction pattern are barely seen. so that the foil sample has to be tilted slightly. Among these spots, only h+k/2=2n+1 (h=2n+1) spots appear. Again it is another example of incomplete phase transformation. It is common that the diffraction spots appear early in the initial stage of the phase transformation.

According to the previous report, the relative diffraction intensities violating the C-centered lattice change from sample to sample for Mg-Cum. Obviously, they depend on the progress of phase transformation. It is believed that the Longquan Mg-Cum lies in the initial stage of phase transformation from C2/m to $P2_1/m$.

New crystallochemical and genetic data for turquoise

Yakhontova L.K., Plyusnina I.I., Soboleva T.V.

Turquoise from middle Asia and Armenia occurences has been studied. A number of samples has been analysed by IR-spectroscopy with denteration (Specord 75-IR;3000-400 cm^{-1});two equallyimportant phosphate anious have been found: PO_4^{3-} and HPO_4^{2-} .An acid anion has been sound by absorption at 2885, 2825, 1200, 1180,1160,1057, 1012, 908, 837, 770, 765 and 693 cm^{-1}. Characteristic bandshifts in deuterated samples gave a confirmation of the IR-bands to belong to OH-oscillations and to the HPO_4^{2-} anion in turquiose structure. So the most plausible turquoise formula is $CuAl_6[PO_4]_2[HPO_4]_2(OH)_{10}\cdot 4H_2O$.

Two main stages of turquose formation have been defined in our studies of mineral genesis:

1) A low temprature, hydrothermal stage where vein turquoise associated with qurtz and pyrite was formed (quartzified terquoise).

2) A hypergenous stage related to the actual weathering processes. It implies an intense Kaolinization of the embedding quartzfeldspathic rocks and evolution of turquoise i.e. impregnation of the mineral with allophane, opal and Kaolinite followed by intense amorphisation and stabilisation of the specific relations between Cu, Al and Fe^{3+} .

62.7.4.K

THE TRANSMISSION ELECTRON MICROSCOPE STUDIES OF GRANDIDIERITE

Yang Guangming Wu Xiuling Pan Zhaolu
China University of Geosciences,Wuhan 430074

We have studied the cell parameters, micro–twinning structure, crystal defect and lattice image of grandidierite discovered in China recently. The studies gain new data unobtained by optical microscopy and X–ray analysis for grandidierite.

1. A set of the electron diffraction patterns was obtained with the selection area electron diffracting mode. According to the angles relationship between these patterns, reciprocal lattice plane perpendicular to node 0K0 was obtained by geometric building method, the unit cell parameters of grandidierite measured from these patterns are orthorhombic with $a_0 = 10.30$Å, $b_0 = 10.98$Å and $c_0 = 5.74$Å, It is the same with our result by the Four Circle Single Crystal Diffractometer.

2. The diffraction spots obtained by SAED have spliting feafure on the same layer line (Figl–a). Its contrast image corresponding to the Fig 1–a displays distinct boundary with twinning character (Figl–b). In the Fig 1–a, the orientational index of the crystal zone of the matrix and twin is $[\bar{4}14]$ and $[4\bar{1}\bar{4}]_T$respectively. Fig1–c show that the twin spots $(hkl)_T$ and matrix spots $(hkl)_m$ have a symmetric arrangement for the twin plane

(101). $(hkl)_T$ and $(hkl)_m$ overlap each other by rotating 180° around axis [101]. When Hh+Kk+Ll = 5n, the two sets of spot combined upto a set of spot, where,n = 0, ± 1, ± 2,••• ,and HKL is twin axis (simplified divisor index).This arrangement feature showed that the twin belongs to rotation law with[101] (e.g. plane law twin with (101)). Their index hkl is the same , but symbol is opposite.By calculating of the twin index transformation matrix [T], we can determine the positions of the twin spots in diffraction coordinate system of the matrix . The experiment result is the same as our result calculated by index transformation matrix $[T]_{hkl}$ and twin orientation transformation matrix $[\tilde{T}]_{uvw}$.

3. Sometimes, we can observe the longed spots which have periodicity as two layers on an electron diffraction pattern (Figl–d), it is a crystal defect and might be a stacking fault. The grandidierite occured in the region metamorphic rock and associated with high temperature mineral, sillimanite. Its growth defect usually exist. However, the distribution shape of the spots and corresponding lattice fringe image (Fig1–e) from other selected area displays that the crystal is uniformity structure.

The studies show that the mineral structure is imperfect for grandidierite. The micro–twinning structure and stacking fault is main cause that leads to the mineral imperfect. The microstructure detail provided direct criterion for studying genesis of geological body and its evolution process. However, this observation is very difficult for optical microscopy or X–ray diffracting method.

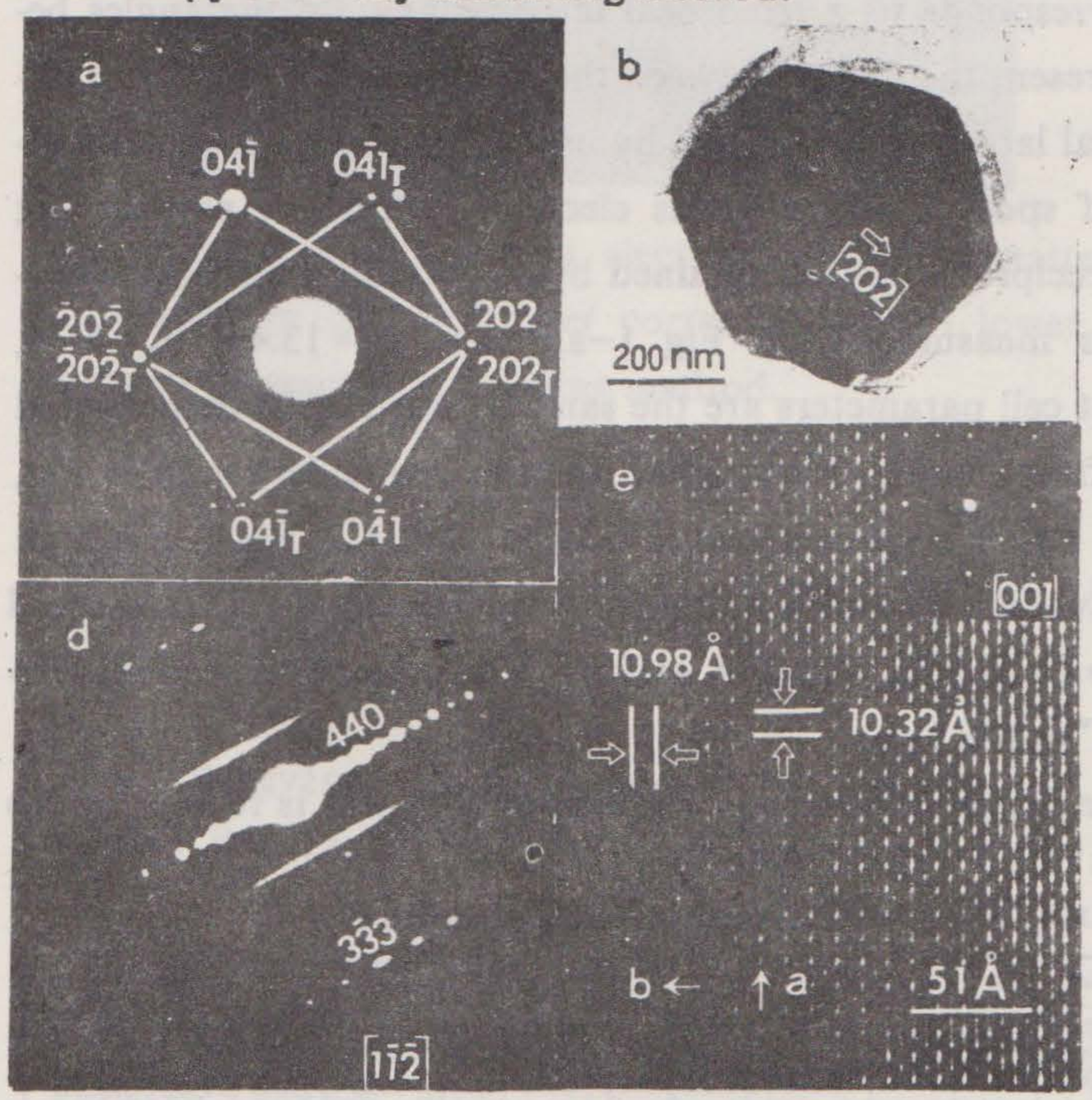

Fig1. a–combined electron diffaction pattern of matrix [$\bar{4}$14] and twin [$4\bar{1}\bar{4}$]$_T$corresponding to b; b–bright–field image of twin for grandidierite; c–indexing pattern extended according to a; d–electron diffaction pattern showing crystal defect; e–lattice fringe image (corresponding to upper right); 120KV, CM12, Philips. China University of Geosciences (Wuhan).

92.7.5.

ELECTRON MICROPROBE ANALYSES AND TRANSMISSION ELECTRON MICROSCOPE STUDIES OF CHEVKINITE

Yang Guangming Wu Xiuling Zhao Wenxia Pan Zhaolu

China University of Geosciences, Wuhan 430074

We studied naturally occurring chevkinite from a rare earth mineral deposit within an aegirine alkali feldspar granite massif in south–western China. The chemical composition of mineral was determined by EMXA with a JCXA–733 superprobe and the results were shown in Table 1. The distribution of the REE weight were obtained by ICPS. The agreements between these two results were quite well. The crystal chemical formula of chevkinite is $(Ce_{1.819}La_{0.951}Nd_{0.408}\cdots Ca_{0.695})_{3.983}Fe^{2+}(Fe^{3+}_{0.716}Fe^{2+}_{0.434}Ti_{0.317}Nb_{0.259}Mn_{0.127}Mg_{0.057}Al_{0.042})_{1.952}T_2O_8[Si_{2.086}O_7]_2$, while ideal formula is $(RE,Ca)_4Fe^{2+}(Fe,Ti,Nb)_2Ti_2O_8[S_2O_7]_2$. Electron diffraction analyses and high resolution lattice fringe observations of the mineral were carried out with a TEM in our laboratory. Fig 1,a–d show the electron diffraction pattern of chevkinite for different orientation. The angles between patterns b and c, c and d with rotation about 0K0 are 44.41° and 23.55° ,respectively. An electron diffraction pattern corresponds to a reciprocal lattice plane. So the angles between the electron patterns represent the angles between the corrsponding reciprocal lattice planes. Fig 1–f is reciprocal lattice plane formed by using geometric building method. Its arrangement feature of spots is the same as electron diffraction pattern Fig 1–a(lower left). It showed the reciprocal lattice obtained by the building method is correct. The unit cell parameters measured from Fig 1–a,b are: $a_0=13.40$, $b_0=5.74$, $c_0=11.07$Å, $\beta=101°$. The unit cell parameters are the same as our results determinted with the Four Circle Single Diffractometer. Electron diffraction law is: h+k=2n in hkl, h=2n in hol, k=2n in oko. Its possible space group is C2 / m, Cm, C2. Fig 1–e is high resolution lattice image of chevkinite (corresponding to lower left,Fig 1–a). It showed that the lattice image with $a_0=13.20$Å, $c_0=11.00$Å and $\beta=101°$ has a reciprocal relationship to the vectors a^* and c^* in Fig 1–a.

Discussion: The chevkinite is rich–Nb in the composition and this is related to Nb

Table 1. Electron Microprobe analyses of Chevkinite.

method		CaO	MgO	FeO	MnO	Al_2O_3	SiO_2	TiO_2	Nb_2O_5	La_2O_3	CeO_2	Pr_2O_3	Nd_2O_3	Sm_2O_3	Eu_2O_3	Y_2O_3	Sum	$\sum TR_2O_3$
EMXA	1	3.45	0.28	12.19	0.70	0.19	19.29	15.25	2.65	11.79	23.85	1.25	5.43	0.30	0.09	0.05	96.74	42.75
	2	3.38	0.18	12.24	0.62	0.22	20.51	14.61	2.98	12.22	24.02	0.11	5.46	0.21	0.28	0.05	97.09	42.36
	3	3.40	0.07	13.01	0.67	0.08	20.58	15.45	2.84	13.02	24.40	0.27	5.48	0.28	0.33	0.12	99.98	43.89
	4	3.37	0.27	12.33	0.62	0.19	20.56	15.08	2.99	12.21	23.86	1.25	5.46	0.30	0.28	0.05	98.81	43.41
	5	2.07	0.17	12.33	1.07	0.16	19.85	13.99	2.38	12.70	23.82	1.54	5.73	0.40	0.20	0.00	96.41	44.39
	∑	3.13	0.19	12.42	0.74	0.17	20.16	14.88	2.77	12.39	23.99	0.88	5.51	0.30	0.24	0.05	97.83	43.36
ICPS		La_2O_3	CeO_2	Pr_2O_3	Nd_2O_3	Sm_2O_3	Eu_2O_3	Gd_2O_3	Tb_2O_3	Dy_2O_3	Ho_2O_3	Er_2O_3	Tm_2O_3	Yb_2O_3	Lu_2O_3	Y_2O_3		$\sum TR_2O_3$
		13.41	22.80	1.14	5.12	0.34	0.06	0.20	0.028	0.04	0.01	0.02	0.004	0.02	0.003	0.088		43.28

Analyzer: EMXA–China University of Geosciences; ICPS–Hubei Geological Research Laboratory.

abundance in the parental pluton; The space group of chevkinite determined by Peng and Pan(1964) is C2/m, while the S.G of chevkinite determined by C.Calvo and R.Faggiani(1974) is $P2_1/a$. In our paper, the study of electron diffraction for chevkinite shows that S.G. is also C2/m. La,Ce in the synthesized chevkinite is replaced by Nd and Fe by Co,Mg. This is a possible cause which leads to space group variation. Up to now, "the chevkinite" containing only Nd has never been discovered in the nature.

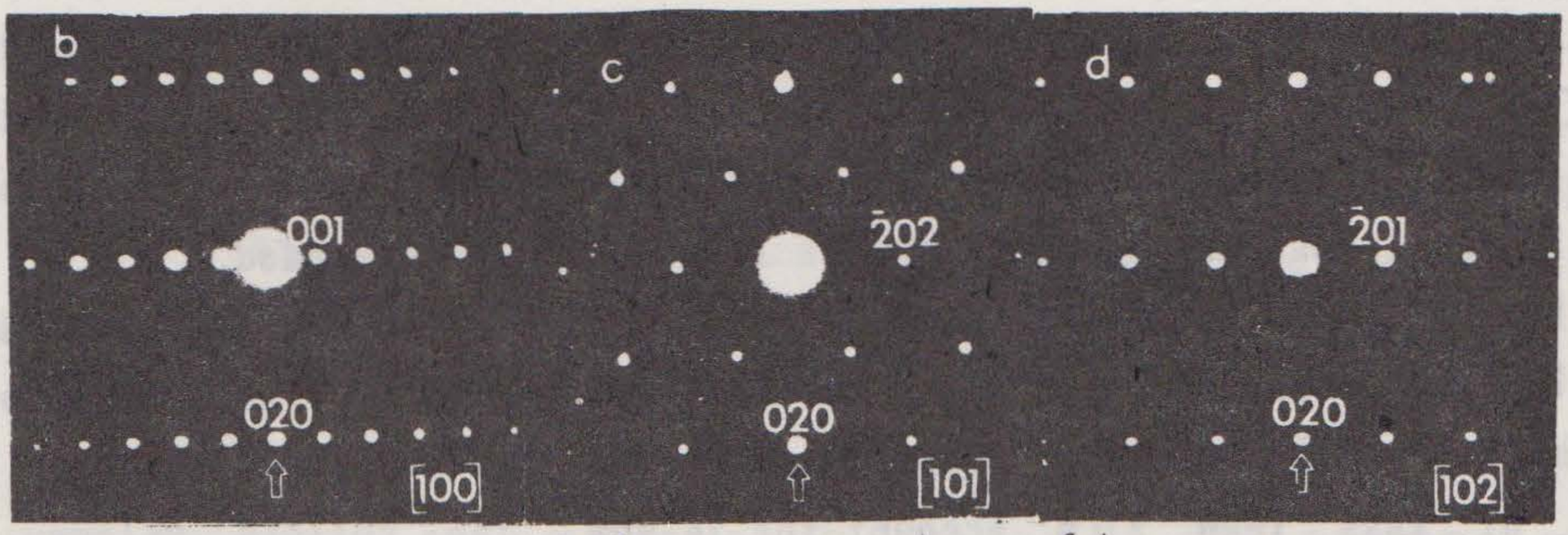

F.1, a,b,c,d—selection area electron diffraction pattern rotated about 0K0; e—lattice fringe image of chevkinite(corresponding to lower left); f—reciprocal lattice plane formed by geometric building method.

RESEARCHES ON THE APPLIED MINERALOGY OF RECTORITE FROM ZHONGXIANG, HUBEI, CHINA

Zhang Rongying, Zhao Lianqiang, Sun Xiaocheng
(Hubei Provincial Institute of Geological Experiment)

ABSTRACT

The Zhongxiang rectorite occurs in Wujiaping Formation of upper series of Permian System. Under polarized light microscope the rectorite is fibrous, parallel extinction and positive elongation. Ng'=1.549-1.553, Np'=1.515-1.522, density=2.76/cm³. Chemical formula is as follows:

mica layer:

$(Na_{0.79}K_{0.39}Ca_{0.26})_{1.44}Al_4[(Si_6Al_2)_8O_{20}](OH)_4$

smectite layer:

$(Ca_{0.55}Na_{0.02}K_{0.01}Mg_{0.03})_{0.61}(Al_{4.1}Fe_{0.09}Mg_{0.07})_{4.26}[(Si_{6.46}Al_{1.54})_8O_{20}](OH)_4 \cdot nH_2O$

It is a Na-rectorite in which the mica layer is paragonite, and smectite layer is possesed of beidellitic composition. The x-ray diffraction data of 00l reflection show a regular integral seriers, σ=0.17, VC=0.688, a_0=5.10Å, b_0=8.89Å, $c_0=\sin\beta$=24.69Å, Infrared absorption spectra are 3640, 3440, 1618, 1110, 1078, 1012, 935, 905, 812, 802, 698, 635, 540, 488 and 468cm^{-1}. The differential thermal curves show four endothermic valleys (110℃, 180℃, 600℃ and 1020℃) and one exothermic peak (1065℃). The loss weigth within 1000℃ is 15.35%. Under electron microscope most of rectorite forms appear irregular schistose, a few of which are fibrous and fold-banded.

Rectorite clay is possessrd of many excellent physicochemical and technological properties, such as colloidal dispersivity, water-absorbing swellability, cation exchange properties, plasticity, stickability, etc. The grains of less then 2μm account for 76-90%. The colloid valency is 60ml/15g, its expanding capacity, 5.8ml/g, the colloidal rate of Na-ionized rectorite, 100%, the colloidal dispersivity, good, the interlayer swell of hydrated rectorite, up to41Å, Its osmosis swell is estimated greater than 100Å. The cation exchange capacities (CEC) are 44.9 mmol/100g, among which ECa^{2+} is 37.8, EMg^{2+}, 1.82, ENa^{+}, 1.44, EK^{+}, 0.68mmol/100g. The d00l of hydroxy-aluminum cross-linked rectorite, the titanium oxide cross-linked rectorite and NH_4^+—dimethyl octadecyl hydroxy ethyl chloride complex rectorite are 28.2Å, 37.9Å, and 29.5Å, respectively. Its plasticity: the plastic index is 49.2, liquid limite, 82.7%, plastic limite, 33.5%. Its stickability is good. Dry and wet compressive strengths are 607.6 K Pa and 58.8 K Pa respectively. Its external specific surface area is 7m^2/g; the internal, 383m^2/g; the total, 390m^2/g. The ammonia absorbing quantity is 6 mg/g. Fire resistance equals 1660℃.

The application study of rectorite is as follows:

1.New-type petroleum catalyst carrier:

Petroleum cracking and catalystic carrier made of inorganic cross-linked rectorite is possessed of good adsorption property, good thermal stability and high tronsformation rate.

2. High temperature-resistant material of drilling mud fluid:

Made of rectorite the drilling mud fluid is possessed of such advantages as the high mud making rate (24.6m^3/t), low dehydration quantity (<13ml/30min), low yield value (<10Pa), thin mud crust (0.5mm) and good heat stability, etc.

3. Freshness-keeping agent for mat straw:

The freshness-keeping agent made of rectorite is homogeneous in mud making, moderate in acidity, thin and uniform coating, quick drying

and sunlight ultra-violet radiation defence and keeping green colour and scent.

4.Suspension agent of coating:

Based on the good suspension of the rectorite in water solution, excellent adaptability to organic substances, etc., it can be utilized for suspension agents of high-temperature resistant steel cast coating and organosilicon resin coating.

5. Cement:

By using the stickability and plasticity of rectorite, it is utilized for the cements of the coating of welding electrode, high-voltage electro-ceramics, cast moulding sand, coal briquette of synthetic ammonia, etc.

A STUDY OF STM IMAGES ON CARBON – GRAPHITES IN CHINA'S GEOLOGY HISTORY

57.5.25 V

ZHENG Zhe, Department of Geology, Peking University, Beijing 100871, People's Republic of China;
YANG Weisheng, YAN Jingjuan, Department of Physics, Peking University, Beijing 100871, People's Republic of China

There are enormous organic matters buried in sediments in various geological periods of China, which can be transformed into carbon materials including kerogen and graphite with different crystalline degree undergoing catagenesis, metagenesis and metamorphism. These carbon materials,which are a kind of carbon skeleton consisting of aromatic molecule, are still an open question. Scanning tunneling microscopy (STM) is one of the newest tecniques to study three–dimensional structural pictures of surfaces of even individual atoms, with which this paper reveals the characters of these carbon materials, and this study is an exploratory one of the series studies.

The samples were taken from the Jiodong group and the Jiling group in Shandong province and Inner Mongolia Autonomous region, degree of graphitization is ranges of 0.72 – 0.78 and 0.85 – 0.91 respectively. The experiments use constant current mode with tunneling current 0.7nA,bias voltage 10mV and scanning speed 150 Hz in X direction, 0.1 Hz in Y direction,Z is the height of tip versus the scan position (X, Y,). The topography of graphite were taken in air at ambient pressure, and resolve carbon atoms in the structure, the six hexagonal ring can be seen clearly,in which six carbon atoms can be divided into two groups,three of them have darker grey scale,the others lighter grey scale. This can be accounted for by the stronger or weaker tunneling effect due to overlaping or no overlaping carbons in the second layer of the graphitic structure. This is in agreement with the result of theorical calculation.The images of graphite demonstrate that most of the hexagonal rings in graphite are nearly regular, though some of them are twisted or zigzag resulting in surface undulations of graphite.

The images of kerogen shows that many aromatic carbon skeleton can be resolved,the details of which are being analysed and studied.

References
Hansma,Paul K, Tersoff, Jerry (1987),Scanning Tunneling Microscopy, J. Appl. Phys., Vol.61, No 2, pp. 1–23
Eling, V, Wild,F., (1988), Tunneing Microscopy on Various Carbon Materials, J. Vac. Sci. Technol. A 6 (2) Mar / Apr, pp. 412–414

EXPERIMENTAL STUDY ON CHEMICAL BONDING OF MILLERITE

Zhu Naijue, Institute of Chemistry, Academia Sinica, Beijing 100080, PRC. Liang Li, Institute of Biophysics, Academia Sinica, Beijing 100080, PRC. Shi Nicheng, China University of Geosciences, Beijing 100083, PRC.

Millerite is a well known metallic sulfide mineral. Its structure parameters are rather simple [1] [2]. only Ni and S two atoms. But its structural reason and the relationship between structure and properties are still not clear after about sixty years from its structure was first determined based on X–ray powder data.

The Ni in millerite is coordinated by five S atoms and two Ni atoms. The S polyhedron is a distorted tetragonal pyramid with three different distances (2.271, 2.283, 2.364 Å). Three Ni atoms are located at the corners of an equilateral triangle with distance of 2.536 Å. The S atom in millerite is also coordinated to five Ni ligands in the form of a distorted tetragonal pyramid. The unusual coodination number and distances in millerite were probably safe to assume there are some unusual bonding interaction. The millerite was reported to be metallic and Pauli paramagnetic which has be due to the short Ni–Ni distance. But it is difficult to explain how the weak metal–metal interaction leads to delocalization of electron throughout all the structure?

The experimental deformation electron density of millerite has been determined from high resolution X–ray intensity data. It is defined as the difference between the total observed density and the density corresponding to a super position of neutral, spherical atom and is sensitive to the redistribution of electron within the molecule as a results of chemical bonding[3].

The distances between nickel and sulphur (2.27–2.36 Å) are too shorter than normal ionic bond length (2.53 Å). These means millerite ~~is~~ not a ionic compound. The deficiencies of electron density in the covalent regions between Ni and S atoms means there are no covalent interaction. So millerite is also not a covalent compound. The distance between nucleus and lone pair electrons of Ni and S in millerite are 0.80–0.97 and 0.85–1.01 A respectively. These distances are longer than 0.50 and 0.588 Å
observed and calculated previously for unbonded lone pair electron of Ni and S. These

means millerite looks like a coordinate complex and the lone pair electrons of Ni and S participate the coordination to S and Ni. So there are double coordinate bond between Ni and S.

The five fold coordination distribution is consistent with the expected dsp3 hybridization at Ni. So the 4S 4Px 4Py 4Pz and 3dx2+y2 orbitals are hybridizated and are filled by lone pairs of sulphur atoms. Remaining 3dxy 3dyz 3dzx and 3dz2 are filled by eight 3d electrons. The general electron distribution of t2g shows four formal orbital which along the four threefold axis of the cube around centre ion as expected by Weiss [4]. According to the distribution of valence electrons in millerite, six 3d electron of dxy dyz and dzx at Ni occupy only three orbitals of above four orbitals. The empty orbital exactly points other Ni atom and be filled by its dz2 electron. So there is normal coordinate bond between Ni and Ni in millerite.

Because the electrons of both Ni and S atom coordinate to each other and these electrons are all move out from their nucleus. It means they are more delocalization than usual case. The some metallic property of millerite may be caused by this delocalization of lone pair electrons of Ni and S. From the consideration of d electron configuration, millerite carries no net spin. The small value of paramagnetic susceptibility is may due to appreciable quantities of Fe and Co in millerite.

We are grateful for research support from Science Fund of the Chinese Academy of Sciences and thank Prof. Philip C Gooddel (Department of Geological Science, The University of Texas) for providing some suitable millerite crystals.

【1】 Grice, J.D. & Ferguson, R.B.: Canadian Mineralogist 12, 248–252 (1974)

【2】 Rajamani, V. & Prewitt, C.T.: Canadian Mineralogist 12, 253–257 (1974)

【3】 Stevens, E.D. & Coppens, P.: Acta Crystallogr., B36, 1864–1876 (1980)

【4】 Weiss, R.J.: X–ray Determination of Electron Distributions. Amsterdam: North–Holland (1966).

PROBLEMS IN STRUCTURAL MINERALOGY SOLVED RECENTLY BY ELECTRON DIFFRACTION STRUCTURE ANALYSIS

A.P.Zhukhlistov, B.B.Zvyagin, Institute of Ore Deposit Geology, Petrography, Mineraligy and Geochemistry, USSR Academy of Sciences, Moscow 109017, USSR

New important data in structural mineralogy have been obtained in the recent years using highly-informative oblique-texture and single-crystal rotation electron diffraction (ED) patterns.

1. The problem of polytypism of palygorskites has been solved and variations in their actual structural features have been revealed. The solution has been promoted by combining the analysis of ED patterns, and the theoretical derivation of structures and predic-

tion of their diffraction properties.

2. Peculiar ingomogeneous mica polytypes have been found having either identical or different parity of layer orientations (symbols: $4M_3$=3135 ([2$\bar{2}\bar{2}$2]), $3M_2$= 561 ([11$\bar{2}$])).

3. Mica having non-centrosymmetric layers (with vacant cis-octahedra) have been found usually in association with centrosymmetric-layer mica (with vacant trans-octahedra).

4. The variations in kaolinite structure and lattice have been analysed depending on formation conditions.

47.4.15 K

ORIENTED GROWTH OF CHRYSOTILE ON LIZARDITE AND ANTIGORITE

Gábor Papp, Eötvös Loránd University, Mineralogical Department, Budapest, Múzeum krt 4/a, Hungary, H-1088

Oriented growth of chrysotile on other serpentine minerals was revealed by transmission electron microscopic investigation of replica and dispersed ground samples of serpentine materials (Papp, 1984).

On the replica samples a triangular network composed of narrow stripes is outlined on a smooth surface. TEM study of the ground samples disclosed that the stripes correspond to hollow fibers of chrysotile, whereas the "base" of the network is lizardite (in other cases antigorite). There is a significant difference between the two assemblages: chrysotile grows on lizardite in all the three directions of a regular triangle, while on antigorite it grows only in two directions.

Selected area electron diffraction patterns showed that $c^*_{CH} \parallel b^*_{1L}$ or $c^*_{CH} \parallel b^*_{2L}$ or $c^*_{CH} \parallel b^*_{3L}$ (CH=chrysotile, L=lizardite, $b^*_{1,2,3}$=pseudohexagonal b^* directions, see Fig. 1a). From these relations and the characteristics

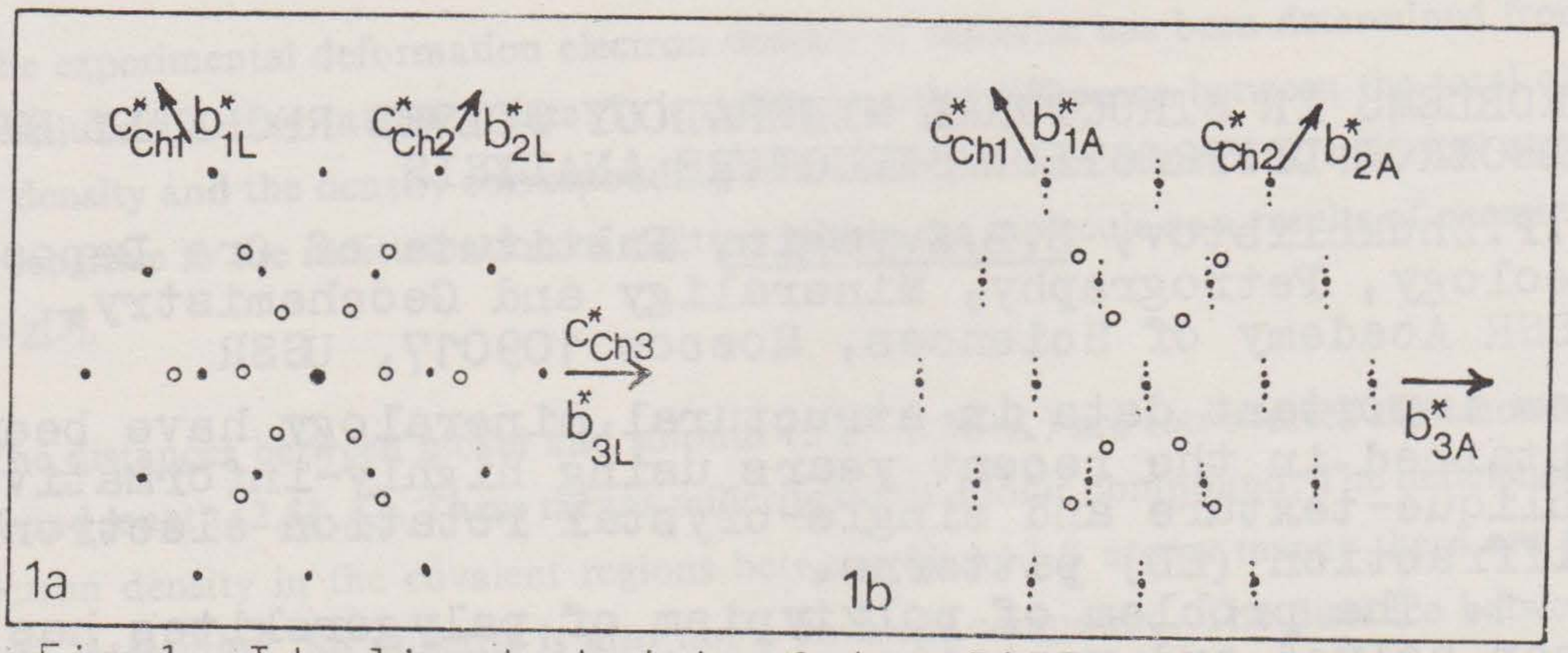

Fig.1. Idealized sketch of the SAED pattern given by (a) chrysotile-lizardite, (b) chrysotile-antigorite assemblage. Abbreviations: see the text; circles: chrysotile reflections

of the cylindrical chrysotile lattice follows that if we theoretically "unroll" a chrysotile tube of the network the structural directions within the layers would correspond to those in the lizardite "basement". In other words, the setting (direction) of the chrysotile network is structurally controlled.

In the case of antigorite [010]* direction seems to be "forbidden" (Fig. 1b, A=antigorite), i.e. chrysotile fibers do not lie in the direction just perpendicular to the structural modulation. This observation correspond to the results of Cressey (pers. comm., 1988) on the "cubic serpentine" from Tilly Foster Mine, described by Aumento, 1967.

TEM investigation of ion-thinned samples revealed a peculiar "sandwitch-texture" of the discussed assemblage. Lizardite (or antigorite) forms thin lamellae, a few tens of nm in thickness and exceeding 1 μm in the direction parallel with the structural layers. Chrysotile tubes are "sandwiched" between the lizardite (antigorite) lamellae. Lizardite (antigorite) lamellae and "layers" of chrysotile tubes may many times alternate one above the other.

Oriented growth of chrysotile on other serpentine minerals was observed in 9 samples so far. Chrysotile-lizardite assemblage was established in 7 samples of the origin as follows: 2 from serpentine veins, 2 from serpentinized carbonate rocks, 3 from serpentinite of pseudomorphic or transition type texture. Chrysotile-antigorite assemblage was found in 2 samples, 1 from a serpentine vein and the other from serpentinized carbonate rock. The number of observations is insufficient for drawing statistical conclusions related to the occurrence of the discussed phenomenon. Nevertheless, "non-pseudomorphous" serpentinization (i.e. serpentine veins or serpentinized carbonate rocks) seems to be preferred environment for development of the oriented growth compared with the "pseudomorphous" serpentinization of ultrabasic rocks.

References:

Aummento, G.F. (1967): Am. Mineral., 52, 1399-1413.

Papp, G. (1984): Diploma work (manuscript). Eötvös L. University, Budapest.

KINETIC (OR CRYSTAL GROWTH) ASPECTS IN EARTH AND PLANETARY SCIENCES

P05.1.

ADULARIA: TEXTURE AND STRUCTURE

Mizuhiko Akizuki and Koichi Murooka, Institute of Mineralogy, Petrology, and Economic Geology, Faculty of Science, Tohoku University, Sendai 980, Japan

Introduction Adularia showing "adularia form" without (010) face represents characteristic internal textures between crossed polars. A transparent K-feldspar with Baveno twin from Alpine fissures shows large (010) faces, and is optically homogeneous. Bambauer and Laves (1960) interpreted the internal textures of adularia in terms of original growth as sanidines and later transformation to microclines with different degree of Al/Si order. Akizuki and Sunagawa (1978), however, attempted to correlate the optical properties, the internal textures, and the growth features observed on the surface of crystal faces from Alpine mineral fissures and valencianite from epithermal veins, and the role of the growth process in Al,Si order-disoder was discussed.

Observations Adularia from Obersubachtal, Austria studied shows a single crystal form with large (010), (001), $(10\bar{1})$, and (110) faces. The surface microtopographs of crystal faces were studied by means of a reflection-type interference contrast microscope and SEM. Special thin sections were prepared in some cases parallel to or perpendicular to the as-grown face so as to correlate growth surface features with internal textures as well as with optical properties. These sections were observed under the polarizing microscope with the universal stage to measure 2V values and extinction angles.

The (110) growth are characterized by the development of many stout prismatic, rhombohedral hillocks and the corrresponding {110} sector is optically triclinic, that is, the unit cell is triclinic. The $(10\bar{1})$ face consists of striations parallel to b axis, and the $(10\bar{1})$ section shows growth bands parallel to b axis under crossed

polarizers. The {10$\bar{1}$} sector is monoclinic. The (001) face shows growth hillocks with growth centers, and the (001) section consists of corresponding internal growth patterns. The sector is triclinic. The (010) face consists of fine growth features, which are observed by SEM. The (001) thin section, which was produced through near the center of crystal, shows large {010} and {110} sectors. The {010} sector consists of two kinds of domains, which are smaller towards the rim of crystal. The orientations of two domains are in a relation of albite twin. The {010} sector is triclinic as well.

The optic axial plane is normal to (010) through the crystal and the 2V values correspond to those of low sanidine structure, not microcline, that is, the crystal is a triclinic disordered K-feldspar.

Discussion The small {010} sectors are found inside valencianite type adularia, which occurs as a gangue mineral in hydrothermal ore deposits, though the (010) face is not observed on the habit face (Akizuki and Sunagawa, 1978). The transparent K-feldspar with Baveno twin from Alpine fissures is optically homogeneous, though the rim shows fine growth bands in some specimens. The present specimens are single in the form, and show large (010) faces. The internal textures and optical properties are similar to those of adularia (valencianite) showing "adularia form". The crystal consists of triclinic disordered structure, and the internal textures were produced during crystal growth, not by a phase transition.

References

Akizuki, M. and Sunagawa, I. (1978) Study of the sector structure in adularia by means of optical microscopy, infra-red absorption, and electron microscopy. Min. Mag., 42, 453-462.

Bambauer, H.U. and Laves, F. (1960) Zum Adularproblem. Schweiz. Mineral. Petrog. Mitt., 40, 177-205

P.o.5.2.

HRTEM AND MICROCHEMICAL STUDY OF PHASES TRANSFORMATION BETWEEN Mn^{3+}- Mn^{4+} OXIDES FROM LATERITIC PROFILES.

M. Amouric*, S. Parc and D. Nahon - CRMCC, CNRS. Campus de Luminy, Case 913, 13288 Marseille, Cedex 9 - France.

Lateritic manganiferous sequences, encountered in tropical and equatorial countries, mainly consist of manganese oxi-hydroxides that can be exploited as ore deposit.

Through the sample of Moanda sequence (Gabon) choiced here, we reported HRTEM, microdiffraction and microchemical examinations of unheated mixtures of manganite and pyrolusite with the main aims to characterize these two phases in greater details and to gain a better understanding of the processes that are responsible for their transformation (Amouric et al.). So two possible ways are directly evidenced in our observations :

a) Pyrolusite ($Mn^{IV}O_2$) is directly obtained after manganite ($Mn^{III}OOH$) oxidation. The crystals of this secondary pyrolusite are clearly shown in structural continuity with the ones of manganite through an irregular and diffuse transformation front, laterally and vertically.

b) Pyrolusite may result from manganite by the way of an intermediate and new transitory phase (γ-$Mn^{III}_2O_3$ or Mn_3O_4). Such a phase is revealed for the first time in this sequence.

These transformations, which preserve the respective lattices strictly in the same orientation, occur through a topotactism mechanism.

As for Mn_5O_8 (Rask and Buseck, 1986), our discovery of unexpected γ-Mn_2O_3 (or Mn_3O_4) transitory phase in unheated microtomed and ion-milled natural samples is of particular interest.

Higher in the sequence, transformations are more complicated. Matrix (illite, kaolinite...) is destabilized and takes part in different reactions.

References :

Amouric M., Parc S. and Nahon D. (1990). HRTEM study of manganese oxihydroxides phase transition in lateritic profile. Am. Miner (submitted).

Rask J.M. and Buseck P.R (1986). Topotacticrelation among pyrolusite, manganite and Mn_5O_8 : a HRTEM investigation. Am. Miner. 71, 805-814.

5.3V

WHISKER GROWTH OF MINERALS

I. K. Bonev, *Geological Institute, Bulgarian Academy of Sciences,*
1113 *Sofia, Bulgaria*

Natural whiskers, ribbon-like and thin platy crystals have considerably larger surface area and surface energy as compared to the equilibrium crystal shapes, which suggests growth under highly non-equilibrium conditions.

The morphological anisometry of whiskers in substances of axial structure is to a certain degree structurally predetermined. However, substances

of isometric or pseudoisometric structures, and of planar structures as well, are also known to form whiskers. In these cases controlling factors are undoubtedly the special conditions and kinetics of crystallization.

There is a diversity of opinions concerning the mechanisms of whisker growth especially in natural whiskers and similar anisometric forms that most commonly grow from solutions. The VLS processes in vapour phase, well known from laboratory practice, have restricted occurrence in nature (e.g. during coal-fires). In turn, the spiral-dislocation mechanism, regarded as more or less universally valid, raises serious objections. The detailed study of a variety of natural whiskers of many minerals with the aid of modern electron microscopic (SEM, TEM, HVEM) and other methods has not confirmed the axiomatic prerequisites of the dislocation hypothesis. Indeed:

1. Whisker side faces are not perfectly smooth as postulated, they show various steps, striations, grooves, hillocks, etc. Having numerous re-entrant angles, these surface irregularities and steps are potential, but not actively operating layer sources.

2. In many cases, thin whiskers do not contain the postulated axial dislocations, either. Yet, remaining highly perfect themselves, some thicker whiskers, ribbons and platelets include volume defects such as axial channels (not connected with dislocations), etc.

3. Whisker terminals often have pyramidal shape, bounded by oblique, rapidly growing faces. Frontal transverse faces with single or double dislocations are not to be observed.

Thus, the real external and internal structure of the highly anisometric crystals is incompatible with the model of dislocation growth at low supersaturation and suggests that whiskers and thin platelets, like the skeletal crystals, grow by $2D$-nucleation in diffusion-limited regime. The base of growing whiskers is any projection on the substrate or it is formed in consequence of the morphological instability of crystal faces. The small cross section of the individual whiskers promotes their rapid growth towards the medium of high supersaturation, while the lateral faces remain in an exhausted environment. The secondary thickenning can be realized only if the supersaturation restores by diffusion at a later moment. Impurities raise the diffusional resistance of the medium.

Different variants of this general model of whisker growth are realized in nature, e.g.: base growth on a porous substrate through supersaturation increasing by evaporation; base growth as the result of surface migration; growth from the tip by solution transport in a surface capillary film, or through an axial channel; growth from stagnant highly supersaturated solutions in a closed space; growth in gels; growth following drastic P, T and C changes (after seismotectonic shoks, mixing of solutions of different compositions and temperatures, etc.); "LLS" growth in solutions through an immiscible melt droplet; metasomatic growth in crystal solid medium by intermediation of solutions, etc.

5.10V

ZONING OF PORPHYROBLAST MINERALS AS AN INDICATOR OF GROWTH-RATE LAWS

William D. Carlson, Department of Geological Sciences, University of Texas at Austin, Austin TX 78731-7909 USA

Rates of porphyroblast growth may be controlled by: (1) the kinetics of dissolution / reprecipitation reactions on mineral surfaces, required to break down unstable precursor minerals and to enlarge crystals of stable minerals; (2) the kinetics of intergranular diffusion, required to transport material from precursors to the growing porphyroblasts; or (3) the kinetics of heat transport, required to supply the energy to drive endothermic prograde metamorphic reactions. Although a metamorphic reaction may progress through stages in which each of these kinetic controls operates in turn (Fisher, 1978, *Geochim Cosmochim Acta* 42:1035), the predominant control on growth kinetics can be identified by examination of the compositional profiles of chemically zoned porphyroblasts. An application of the technique to garnet porphyroblasts in amphibolite-facies pelitic rocks of the Picuris Mountains, New Mexico, USA is presented here. A complete description of the technique may be found in Carlson (1989, *Contrib Mineral Petrol* 103:1).

Kretz (1974, *Lithos* 7:123) described a method for testing the predictions of a specified growth-rate law against observed zoning patterns. Kretz's "normalized radius-rate diagram" is constructed by determining: (1) the *normalized radius* (c^*), that is, the radius at which the midpoint of a chosen narrow compositional interval appears in a crystal, divided by the radius at which the midpoint of the same compositional interval appears in the largest crystal in a specimen; and (2) the *normalized rate of growth* (C^*), approximated by the radial width of the chosen compositional interval in a crystal, divided by the radial width of the same compositional interval in the largest crystal in the specimen. Any growth-rate law specifying the radius of a porphyroblast as a function of time constitutes a function for the normalized radius-rate relationship of the form $c^* = \text{fcn}(C^*)$. If the chosen growth-rate law applies to the specimen being analyzed, then measured pairs of c^* and C^* should plot along the curve $c^* = \text{fcn}(C^*)$ determined for that growth-rate law.

In a surface-controlled process, the radial growth rate is constant and therefore independent of radius; thus c^* is unity, independent of C^* (straight line in figure). In an *isothermal* diffusion-controlled process, the normalized radius-rate relationship has the form $c^* = 1/C^*$ (curved line in figure). In a heat-flow-controlled process in which energy is supplied to the rock at a constant rate, the normalized radius-rate relationship has the form $c^* = 1/(C^* \cdot C^*)$, which would plot as a steep curve to the left and above the curved line in the figure.

In 11 samples from the Picuris Range, in each of which zoning was measured in four to six garnet crystals, none of the above normalized radius-rate relations matched the measured zoning profiles. Instead, the measured radius-rate relations define curves that are roughly parallel to the isothermal diffusion-controlled curve, but that are displaced from it downward and to the right. From this, the hypothesis arose that the measured relations might be explained by a diffusion-controlled growth-rate law that accounts for the acceleration of diffusion produced by increasing temperature during a prograde crystallization event.

When the effects of increasing temperature are considered, it becomes evident that the normalized radius-rate relationship must be different in form (1) for crystals nucleating at different points in the thermal history, and (2) for crystals that experience different amounts of heating during their growth. The first factor is accommodated by including in the expression for the radius-rate relationship a variable τ_i, which represents the fraction of time elapsed during the nucleation interval before the *i*th crystal nucleated. This can be computed from the radius of the *i*th crystal and the rate law for thermally accelerated, diffusion-controlled growth. The second factor is accommodated by including a variable γ, which incorporates the heating rate and the activation energy for intergranular diffusion. This is treated as an unknown parameter to be evaluated by fitting the equation for the radius-rate relationship to the relations measured in the natural sample.

The figure below illustrates the close correspondence between the radius-rate relationship predicted for thermally accelerated, diffusion-controlled growth and the measured radius-rate relations in three garnets from one of the samples from the Picuris Range. The agreement seen in the figure is taken as evidence that the dominant kinetic control on the growth of these garnets was the rate of intergranular diffusion. That inference is confirmed in these rocks by additional evidence from spatial dispositions of porphyroblasts and their crystal size frequency distributions (Carlson, 1989, *ibid.*).

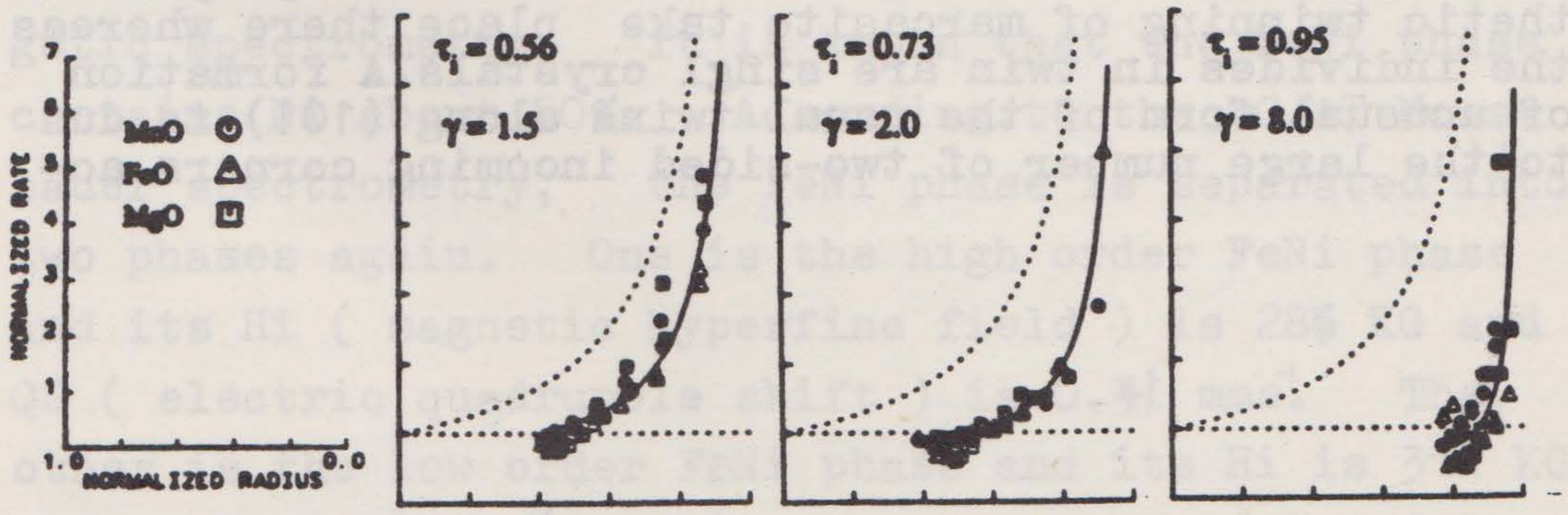

UNUSUAL FORM OF USUAL MARCASITE TWINS.

E.V.Galuskin,N.I.Frishman,IGEM,Academy of sciences of the USSR,Moscow,Staromonetny 35,109017 USSR.

It is well know growth effects connected with a twin crystals such as 1) a crystallization of large twin crystals on a background of small single crystals;2) a formation of twinned plates in cubic and other crystal sistems;3)a capture of alien inclusions alon a twin seam,which depended from existence of two-sided incoming corner and so on.The incoming corners are absent in usual twins of marcasite alon (101)(fig.a).A marcasite from brown coal of Angren(Usbekistan) occur mainly in "speare"-type twins(fig.a), fiveling(fig.c), sceletal form with the beams in twin orientation under 75°("leaf"-type,fig. b).Pyrite epitaxial growth on marcasite twins of "speare" ore "leaf"-type near twinning seam lead to cross-form of profile(Makagonov and Nicandrow,1984)(fig.d).

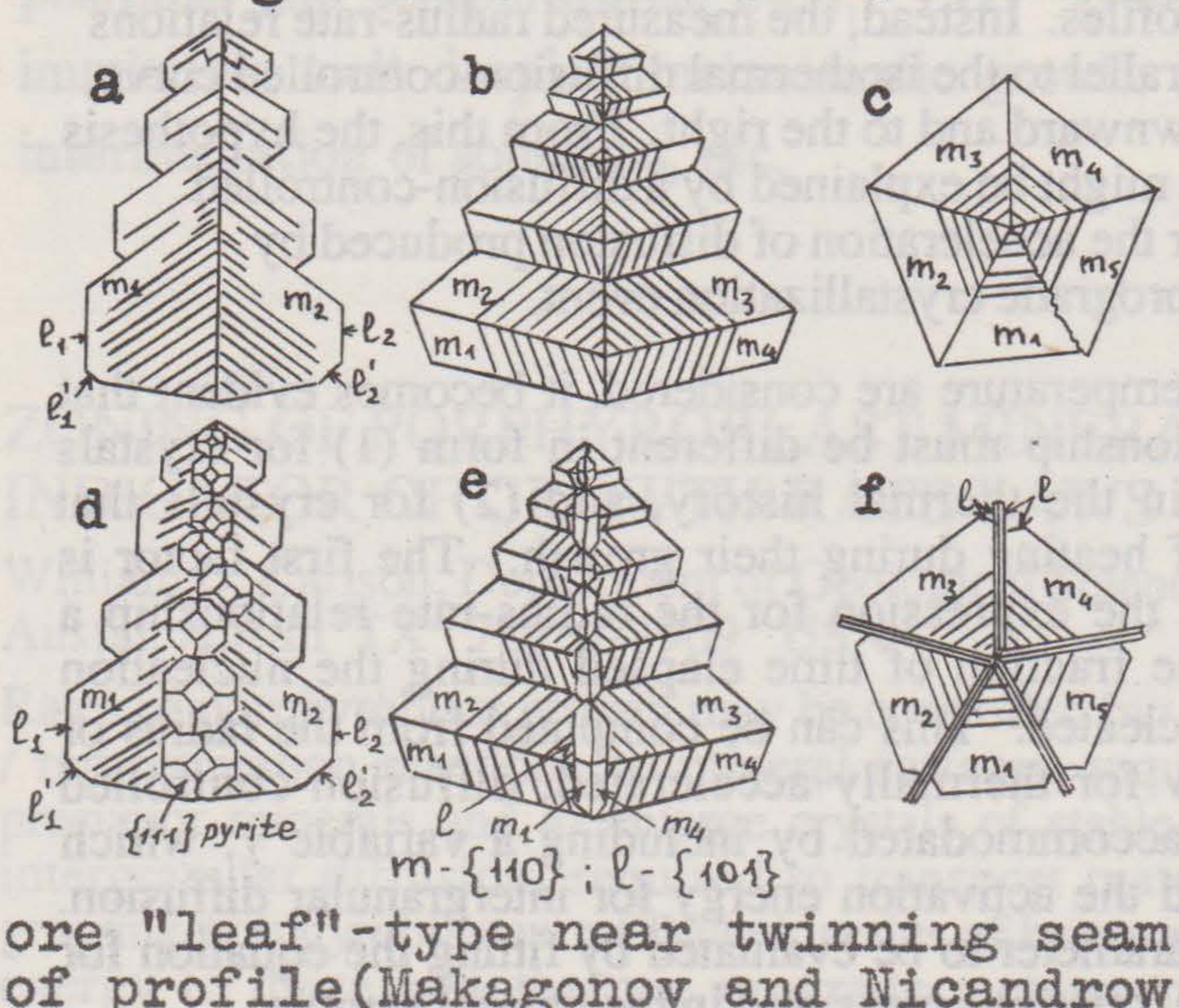

Unusual twins with cross-form section(without pyrite) are found in lower part of coal thickness on the border with with clay.The twins are presented in form of "speare" and "leaf"-type(fig.e).They have fine,notched, plating growth sceletal along twin seam.The plates w wtich are oriented normally to the twin plane are not in the twin position,but sceletal formation oblated on (101),(110),(111) and microfase of the zone of prism. A study of twin seam regionv show that fine polysinthetic twinning of marcasite take place there whereas the individes in twin are singl crystals.A formation of unusual form of the usual twins along (101) is due to the large number of two-sided incoming corners ac-

companing polysinthetic twinning.Appearance of the two-sided incoming corners stimulite the marcasite the sceletal-plates growth along twin plane and lead to forming of the sceletal plates.The same sceletal growth forms on the fiveling lead to the peculiar face (fig.f).Crystal growth in solid state(coal,clay) intensities an anisotropy of the groth speed for the crystal faces.

We show here on the macrolevel the role of twin borders as a special region with certain affinities. A study of the twin seam region allow are not only receive the new characteristics of matter,but also help to explain many natural fenomena and to reach a new level in crystal synthesis.

REFERENCE

E.P.Makagonov,S.N.Nicandrow Polymorphic twin epitaxy of pyrite with marcasite.In: Ontogenegy of minerals in practice geological working.Sverdlovsk,1984(Russian)

ON THE MÖSSBAUER SPECTROMETRY OF ORDER Fe Ni PHASE IN THE CHONDRITE METEORITE OCCURING IN SUIZHOU

GE Yingya, REN Yingxin, Department of Geology, HUA Xin, MA Yihan, Test & Research Centre, China University of Geosciences(Wuhan), Wuhan, Hubei, 430074, People's Republic of China

Using Danon, et al's methed (1), the order FeNi phase has been abstracted from the Fe-Ni alloy in the chondrite meteorite from Suizhou. Through the energetic spectrometry, it is known that the FeNi phase contains Ni about 50%. According to the DC/AT Mossbauer spectrometry, the FeNi phase is separated into two phases again. One is the high order FeNi phase and its Hi (magnetic hyperfine field) is 285 KG and QS (electric quadrupole shift) is 0.41 mms^{-1}. The other is the low order FeNi phase and its Hi is 311 KG and QS is 0.02 mms^{-1}. This phenomenon of high and low order phases in the same meteorite was not reported

before. According to the different order degree, we may infer that the meteorite was heated by lash after it cooled under 593 K.

Reference:

1. J. Danon, R. B. Scorzelli, I. Souza Azevedo, and M. Christophe-Michel-Levy, Iron-nickel superstructure in metal particles of chondrites, Nature, 281, 469-71 (1979).

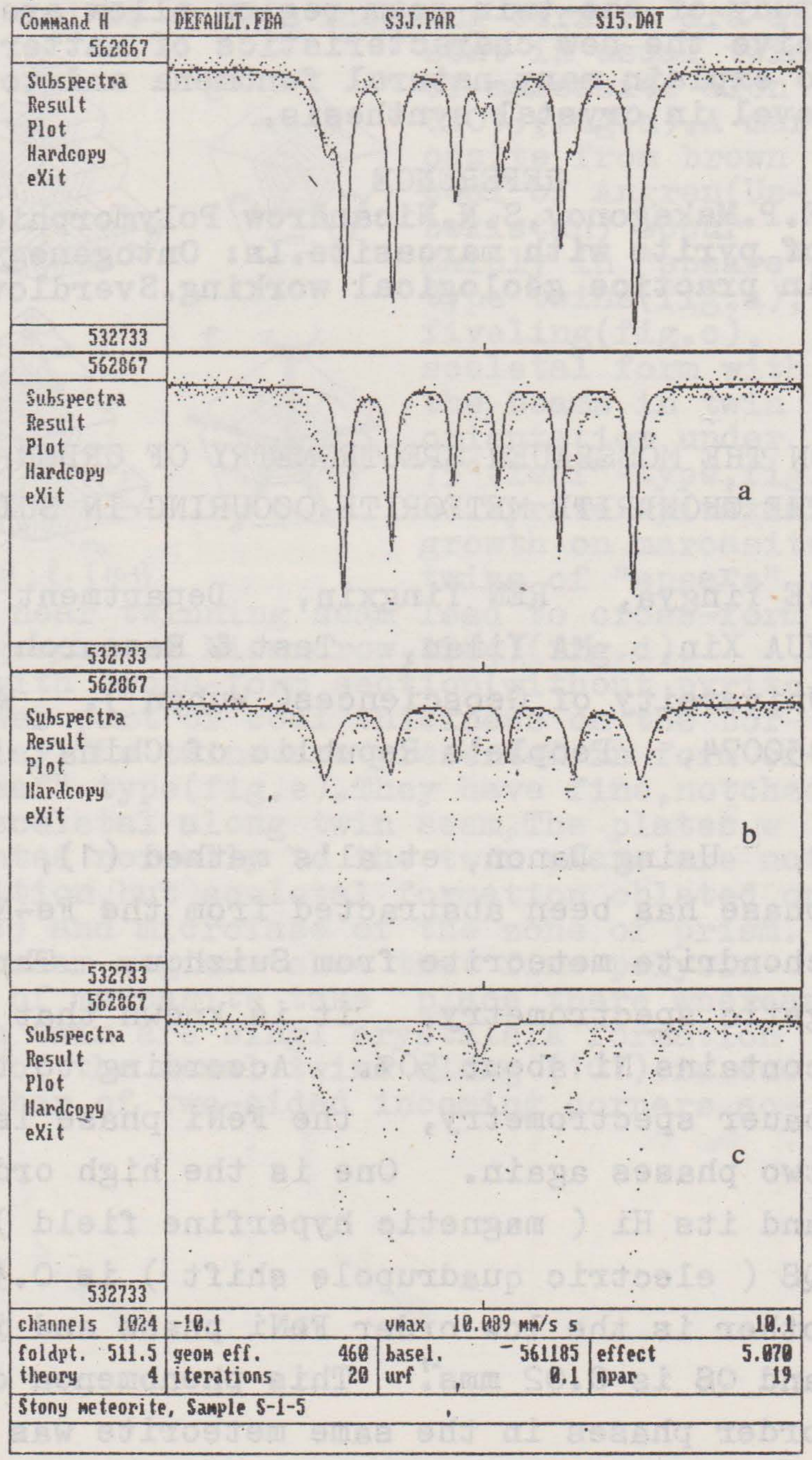

Fig. The Mössbauer spectrum of the order FeNi phase in the chondrite meteorite from Suizhou.

a. High order FeNi phase spectrum,

b. Low order FeNi phase spectrum.

c. Disorder Fe-Ni alloy phase spectrum (Ni 25%).

Measured at room temperature, radioactive source is $^{57}Co/Rh$.

Investigation of nucleation processes in gel.

L.L.Goshka,V.P.Ruzov;Department of physics,
Syktyvkar State University ,
167001,Syktyvkar,USSR

The processes of the nucleation of calcium tartrate crystals are described in this paper. The chosen experimental method for nucleation control is the changing of the acidity of gel-media,by proton implantation.

The experimental results can be summed up as follows:

1) decreasing of the pH value of crystallogenetic media by implantation of protons leads to nucleation suppression and crystals arise in gel only at some depth from the gel-solution boundary (G):

$$G^{1/2} = a \cdot (pH) + b \qquad (1)$$

where a,b - constant parameters;

2) decreasing of the pH value of the media leads to decreasing the nucleus density (N)in the apper layer of crystals ,but the mean mass of one crystal in the test-tube increases:

$$N = k \cdot (pH) + N_0 \qquad (2)$$

where k, N_0 - constant parameters;

3) coordinate of the crystal boundary in gel depends (G) on implantation time (T) and on the molarity of maternal calcium chloride solution: the higher the molarity is, the deeper is the first layer of crystals arising in gel:

$$G^2 = d\,T + p \qquad (3)$$

here d,p - constant parameters;

4) coordinate ofnucleation boundary varies in time:it moves to the gel solutin boundary;

5) the time of the arising of the first crystal (τ)depends on the implantation time (T), but not on the maternal solution molarity:

$$\tau = n\,T + t \qquad (4)$$

where n,t - constant parameters;

The theoretical discription of this fenomena needs the assumption of the 'equivalence condition in the form:

$$\left| \frac{pM - pA}{pM + pA} \right| \leqslant \gamma \qquad (5)$$

where γ - model parameter;
M,A - concentrations of crystal-forming reagent.

The "equivalence condition" (5) in such a form is not so strong as proposed by Henisch, because of logarithmic scale, and it means that the concentration of crystal-forming reagents can't differ very much.

Reference

Henisch H.K.,Garsia-Ruiz J.M.:
J.Crystal Gr.75,203,(1986).

5.13V

HREM OBSERVATIONS OF ULTRASTRUCTURES IN CLINOENSTATITES AND G.P. ZONES IN ORTHOPYROXENES

Huang Wankang, Institute of Geochemistry, Academia Sinica, Box 1131 Wushan, Guangzhou,P.R.C.,Wang Yanguo, Institute of Metal Research Academia Sinica, Kang Zhenchuan, Institute of Metallurgy,Beijing and T. Sameshima, University of Shizuoka,Shizuoka, Japan.

The clinoenstatite occurred in boninite from Népoui, New Caledonia. Two groups of electron diffraction dots in clinoenstatite appear under HREM , they indicate the matrix and the twin respectively. Its high magnification structure image shows that the two variances t_1 and t_2 are related in (100) mirror reflection. Moreover, there are polymorphic transformations of orthopyroxenes and clinoenstatite, which are exhibited by $1\times$ or $2\times a_o$ (18.2Å) of orthoenstatites appearing in CLEN field. On the electron diffractogram of CLEN, the faint strikings along a^* axis imply that the polymorphic transformation is not very frequent.

This low-temperature clinoenstatite (CLEN P21/c) could be formed by inversion of protoenstatite and orthoenstatite as well as high-temperature clinoenstatite(C2/c). Based on the experiments and the fact that the natural Cape Vogel clinoenstatite was inverted into protoenstatite by heating at 1100°C for 3 hours, T. Sameshima suggested that the CLEN phenocrysts in New Caledonia were formed by inversion from protoenstatites.

In nature clinoenstatites only occur in boninite and meteorite. The CLEN in Qinzhen meteorite is believed to be formed by conversion of protoenstatite as well, but it possesses different ultrastructure features. For instance, there are a lot of add number of polymorphic CLEN cell in OREN and 27Å long-period structure appeared by one unit-cell of CLEN and OREN alternating frequently. The different ultrastructures of CLEN in Qingzhen meteorite and boninite may be produced by the transformation of protoenstatite in varying

condition. The boninite, for example, had been suggested to be formed in adiabatic melting condition with high temperature and low pressure and had experienced a high rate of cooling during its extrusion, while the cooling rate of celestial body is very low (n°C/M.Y.). Nevertheless, only a thorough investigation could finally rule out the posibility that the CLEN in boninite may be inversion from the high-temperature clinoenstatite.

The Guinier-Preston zones in two bronzites have been investigated. The sample M-108 is collected from a mela-gabbro instrusion and the another N-14 is separated from a gabbro xenolith in alkali basalt.

Electron micrograph of sample M-108 shows higher number of G.P. zones with one unit-cell thick, while in sample N-14 the G.P. zones are two unit-cell thick. It means that multiple unit-cell thick of G.P. zones could appear in earth and in a Fe-rich orthopyroxene(N-14 : $En_{72.2}Fs_{25.7}Wo_{2.1}$).

For counting the density of G.P. zones semi-quantitively, a statistical method has been proposed. The statistical results of five samples show that they are not influenced by the magnifigation of structure image. Moreover, both the line density and the area density represent the characteristics of G.P. zones. According to the samples from N-14, M-108, Bamble and Webster, there is a positive correlation between the Wo contents of orthopyroxenes and the densities of G.P. zones. It seems that the densities of G.P. zones have some relation with the Ca contents of orthopyroxenes.

This project was supported by National Natural Science Foundation of China.

GENERATION OF BRAZIL TWINS IN HYDROTHERMAL QUARTZ AND AMETHYST AND MICROTEXTURES ORIGINATED THEREFROM

5.5 V

Lu Taijing#1 and I. Sunagawa#2, Faculty of Sciences, Tohoku University, Aramaki, Aoba, Sendai, 980 Japan

Present address: #1 Physics Department, Gakushuin University, Mejiro, Toshima-ku, Tokyo, 171 Japan
#2 Kashiwa-cho 3-54-2, Tachikawa, Tokyo, 190 Japan

Brazil twins are most commonly encountered in amethyst crystals of geode origin, and quartz crystals of epithermal origin, and practically absent in quartz crystals of high temperature origin. Due to the presence of numerous Brazil twin lamelle, various micro-textures, including Brewster fringes, appear in these crystals. Optical microscopic investigations have been made on Brazil twins and micro-textures therefrom, observed in both natural and synthetic amethysts and

natural vein quartz of epithermal origins to understand how and under what conditions Brazil twins are generated and how various micro-textures appear.

Based on the observations on synthetic amethyst, it was concluded that the generation of Brazil twins is triggered by the precipitation of solid inclusions (goethite) and the associated strain fields, which occurs on the growing surface due to fluctuation of growth parameters. Precipitation of polymerized embryonic particles of silica on the surface of solid inclusions precipitated on the growing rhombohedral surface is considered to be respoonsible for the generation of Brazil twins. Brazil twin boundaries are always parallel to the neighbouring crystallographically equivalent rhombohedral faces, but never to the growing surface. This is explained in terms of boundary structure.

When growth conditions are stabilized after the generation of Brazil twin lamellae, Brewster fringes appear. On the contrary, if perturbation took place in growth parameters, alternating band structures with and without Brazil twins, or fibrous textures appear.

5.14.H

DENSITY AND COMPOSITIONS OF PLAGIOCLASES BETWEEN METEORITES AND IMPACT CRATERS

Yasunori Miura; Department of Mineralogical Sciences, Yamaguchi University, Yamaguchi, 753, Japan.

Chemical compositions and calculated densities of various plagioclases are very important to investigate (a) atomic substitution of the crystal structure, and (b) useful indicator of formation process of temperature-dependent (in igneous origin) or pressure-dependent (in impact origin) [cf. 1-5].

Main purpose of the present study are (1) investigations of compositions (esp. An-content and mafic content) and calculated density of plagioclase (-like) phases in chondritic and achondritic meteorites, (2) detailed study of terrestrial impact craters from the center to the rim, and (3) estimation of probable supplied sites of terrestrial and extraterrestrial fragmental rocks from these physical and chemical data.

Calculated density and compositions of plagioclases have been obtained by single crystal X-ray diffractometer

and electron microprobe analyzer, which are summarized as follows.

1) Densities of plagioclases from the Manicouagan impact crater are changed from lower (2.57 in center) to normal (2.70 in rim).

2) Zagami SNC and eucritic achondrites contain higher density plagioclases which are largely different with terrestrial and lunar plagioclases.

3) Mafic content (=MgO+FeO) can be applied as useful indicator of formation process; that is, (a) about 3 times the mafic content of higher temperature-dependent plagioclases of volcanic origin than slow-cooled terrestrial plutonic origin, and (b) 20 times the mafic content in pressure-dependent plagioclase from melt rocks at rim of the Manicouagan impact crater, compared with slower cooled rocks at the central peak.

4) From computer analyses of the compositions, terrestrial and lunar plagioclases show mainly lower density with minor foreign elements (Fe·Mg) and insufficient amounts of Na·Ca·K ions.

5) Eucritic plagioclases reveal higher density with much more foreign elements (Fe·Mg) with complicated variation of ratio Al/Si.

6) Higher density of meteoritic plagioclases suggests different formation process of achondritic meteorites; that is, (a) different source-origins (i.e. different mixing process and chemical evolution on the parent-body, such as asteroids), and/or (b) different crystallization condition after impact events (i.e. relatively rapid-cooling after insufficient mixing with mafic minerals).

7) Density and mafic content of various plagioclases can be applied to as powerful indicator of the formation processes and formed impact sites, and different origins among terrestrial, lunar and meteoritic materials.

The present research is in part supported by the Grant-in-Aid for Scientific Research on Priority Areas (Origin of the Solar System) ofthe Japanese Ministry of Ed., Science and Culture (01611005) of the author. We thanks Drs. B. Mason and R. Grieve for sample preparation and valuable comments.

References:

[1] Stöffler D.S. and Hornemann U.(1972): Meteoritics, 7, 371-394.

[2] Grieve R.A.F. and Floran R.J. (1978): J.G.R., 83,

2761-2771.
[3] Arndt J., Hummel W. and Gonzalez-Cabeza I. (1982): P.C.M., 8, 230-239.
[4] Miura Y. and Kato T. (1989): LPSC XX ,703-704.
[5] Miura Y., Yanai K. and Miura H. (1986): Meteoritics, 460-461.

5.1.V

STRUCTURE AND PROPERTIES OF MODEL MAGMATIC LIQUIDS

Mysen, Bjorn O., Geophysical Laboratory, 2801 Upton St., N.W., Washington, D.C., 20008, USA

The structure of silicate liquids at high temperature and high pressure, and relationships between their structure and properties are necessary to characterize natural magmatic processes. Bulk compositions between depolymerized (nonbridging oxygen per silicon; *NBO/Si* > 0) alkali or alkaline earth silicates and fully polymerized (*NBO/Si* = 0) silica - aluminates represent the structural environment of natural magmatic liquids. Their Al/(Al + Si) typically is between 0.2 and 0.3. Alkali metals are the principal cations for charge-balance of tetrahedrally-coordinated Al^{3+} at 1 atmosphere. The principal network-modifying cations are Ca and Mg (Mysen, 1988). Silicate melts in this composition range consist of coexisting structural units characterized by their average number of nonbridging oxygen per tetrahedrally-coordinated cations (*NBO/T*) equal to 0 (TO_2, or Q^4-species), 1(T_2O_5, or Q^3-species), and 2 (TO_3, or Q^2-species; see, for example, Virgo *et al.*, 1980). The equilibrium in such melts is described with the equation;

$$T_2O_5\ (2Q^3) \Leftrightarrow TO_3\ (Q^2) + TO_2\ (Q^4), \quad (1)$$

where T = Al + Si. The Q^4, Q^3 and Q^2 notations are sometimes used in place of the stoichiometric designations. The superscript in the Q-notation denotes the number of bridging oxygen in the unit.

Physical and chemical properties of natural magmas depend on the properties, detailed structure, and proportions of these individual structural units. In order to provide a structural framework for quantitative characterization of the properties of natural magma, it is necessary to characterize the relationships between pressure, temperature, and the compositional variables. For this purpose, Raman spectroscopy has been used to determine the abundances of individual structural units in the quenched melts. All compositions in this study are on the join $M_2Si_4O_9$ - $M_2(MAl)_4O_9$ (M = K, Na and Li; denoted KS4 - KA4, NS4 - NA4 and LS4 - LA4), with, therefore, *NBO/T* = 0.5. Substitution of charge-balanced Al^{3+} for Si^{4+} results in a systematic lowering of the abundance of T_2O_5 units together with a concomitant increase in the more polymerized unit, TO_2 and the less polymerized one, TO_3 (Fig. 1). The overall degree of polymerization of the melts remains constant (*NBO/T* = 0.5) in this process. Thus, qualitatively, increasing Al/(Al + Si) shifts equation (1) to the right. It is notable, however, that even in the absence of Al^{3+} the larger the ionization potential of the network-modifying cation (Li > Na > K), the mol fractions, $X(TO_2)$ and $X(TO_3)$, are greater, and the $X(T_2O_5)$ is smaller. This observation accords with results from ^{29}Si NMR spectroscopy of analogous melt compositions (Stebbins, 1987).

The distribution of structural units as a function of Al/(Al + Si)

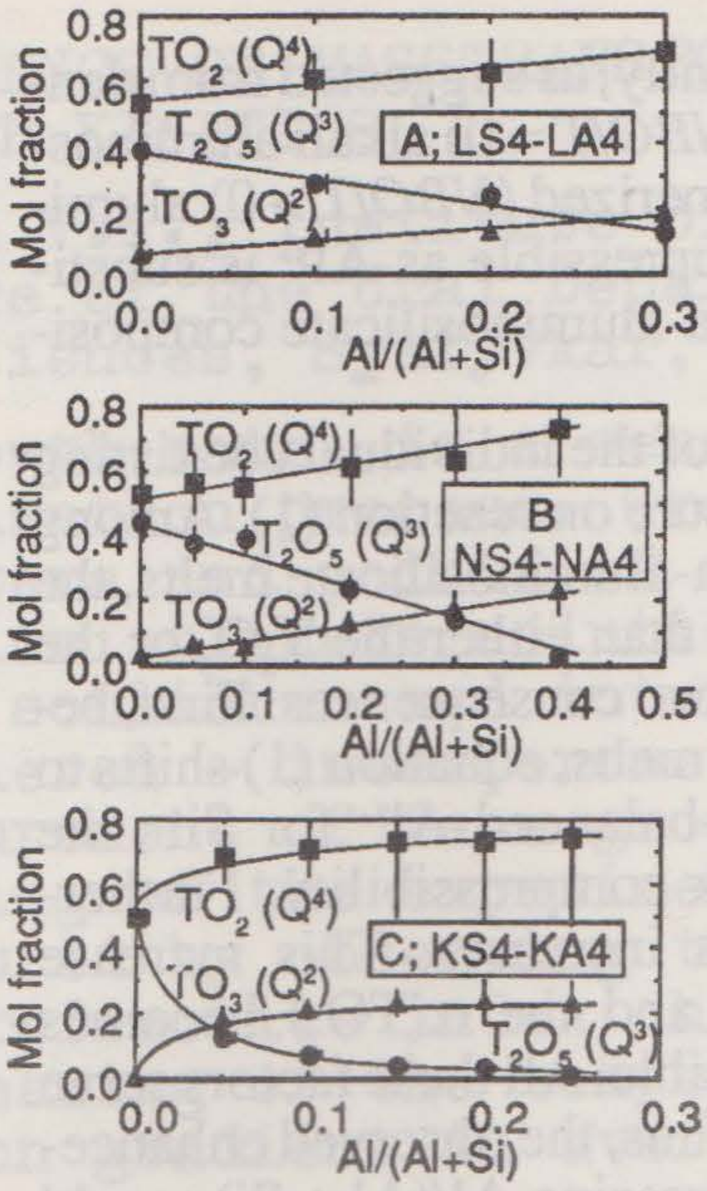

FIG. 1. Mol fraction of structural units in 1-bar, temperature-quenched melts as a function of Al/(Al + Si). A - The join $Li_2Si_4O_9$ - $Li_2(LiAl)_4O_9$ (LS4 - LA4), B - The join $Na_2Si_4O_9$ - $Na_2(NaAl)_4O_9$ (NS4 - NA4), C - The join $K_2Si_4O_9$ - $K_2(KAl)_4O_9$ (KS4 - KA4).

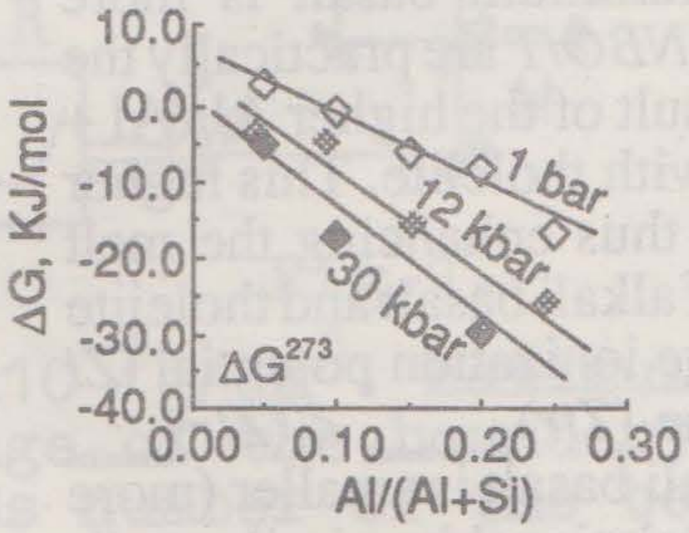

FIG. 3. Free energy for equilibrium (1) at 273K (ΔG^{273}) for melts on the join $K_2Si_4O_9$ - $K_2(KAl)_4O_9$ as a function of pressure as indicated.

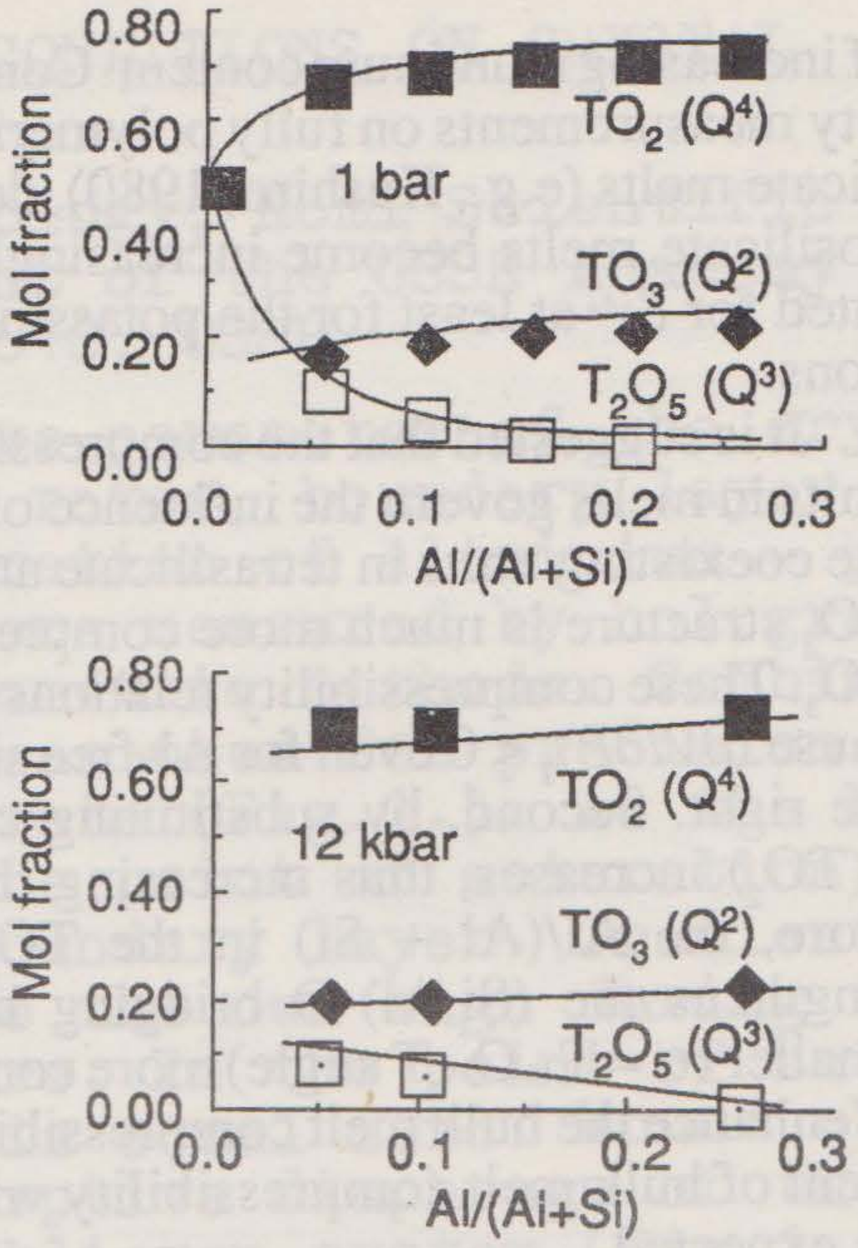

FIG. 2. Mol fraction of structural units in $K_2Si_4O_9$ - $K_2(KAl)_4O_9$ melts as a function of Al/(Al + Si) at the pressures indicated.

follows the same general trends at high pressure (Fig. 2) as at 1 bar (Fig. 1) at least for the potassium tetra-aluminosilicate quenched melts. Qualitatively, from the abundance information in Fig. 2, at a given Al/(Al + Si), the $X(T_2O_5)$ tends to be lower at higher pressure, thus indicating a shift of equation (1) to the right. The equilibrium constant for reaction (1) is positively correlated with temperature yielding ΔH ~ 30 KJ/mol and ΔS ~ 5 J/mol K.

Under the assumption of ideal mixing of the structural units, the free energy of reaction (1) at 273K has been calculated (Fig. 3). The ΔG^{273} decreases with increasing Al/(Al + Si) at constant pressure. Increasing pressure generally results in a further decrease in ΔG. The pressure effect on ΔG for reaction (1) is further enhanced as a function

of increasing aluminum content. Consequently, as suggested from density measurements on fully polymerized ($NBO/T = 0$) alkali aluminosilicate melts (e.g., Kushiro, 1980), depolymerized ($NBO/T > 0$) aluminosilicate melts become increasingly compressible as Al^{3+} is substituted for Si^{4+} at least for the potassium tetra-aluminosilicate compositions.

It is suggested that the compressibility of the individual coexisting units in melts govern the influence of pressure on reaction (1). Among the coexisting units in tetrasilicate and tetra-aluminosilicate melts, the TO_2 structure is much more compressible than either the T_2O_5 or the TO_3. These compressibility relations have two consequences. First, because $(\partial V/\partial P)_T < 0$ even for Al-free silicate melts, equation (1) shifts to the right. Second, by substituting charge-balanced Al^{3+} for Si^{4+}, the $X(TO_2)$ increases, thus increasing the bulk compressibility. Furthermore, the Al/(Al + Si) in the TO_2 units increases. This increase lengthens the (Si,Al)-O bridging bonds, and the $\alpha(TO_2)$ becomes smaller (α = T - O - T angle) more compressible. All these factors serve to enhance the bulk melt compressibility. Thus, the observed enhancement of bulk melt compressibility with increasing Al/(Al + Si) would be expected.

The pressure-composition relationships provides a rationale to understand the behavior of natural magmatic liquids under pressure. (i) Magmatic liquids become more polymerized with increasing silica, or alumina, or both. Thus, the relative abundance of TO_2 units in the melts increases. As a result, the molar volume and the melt compressibility of magmatic liquids increase in the order komatiite < basalt < andesite < rhyolite. (ii) For basaltic melts, high-aluminum basalt is more compressible than tholeiite even though their NBO/T are practically the same (Mysen, 1988). This behavior is the result of the higher Al/(Al + Si) in the high-alumina basalt as compared with tholeiite. This higher Al/(Al + Si) shifts reaction (1) to the right thus enhancing the melt compressibility. (iii) The bulk composition of alkali basalt and tholeiite differs principally in the values of the average ionization potential (Z/r) of the charge-balancing metal cations. The $(Z/r)_{\text{alkali basalt}} < (Z/r)_{\text{tholeiite}}$ with the result that ΔG of reaction (1) for alkali basalt is smaller (more negative) Implying greater compressibility. Relationships similar to (i-iii) would also be expected for all other melt properties that depend on the abundance and character of bridging oxygen bonds in TO_2 units in the magmatic liquids.

References

Kushiro, I., Ch 3 in: *Physics of Magmatic Processes* (ed.: R. B. Hargraves), Princeton Univ. Press, 1980.

Mysen, B. O., *Structure and Properties of Silicate Melts*, Elsevier, Amsterdam, 354 pp., 1988.

Virgo, D., B. O. Mysen, and I. Kushiro, s, *Science, 208*, 1371-1373, 1980.

INFLUENCE OF MASSTRANSPORT CONDITIONS ON CRYSTAL GROWTH KINETICS

P. 5.3

Rakin V.I., Institute of Geology, Komi Scientific Centre of the Ural Department of the USSR Academy of Sciences, Syktyvkar, 167610, USSR

A growth rate is a sensitive parameter of the crystallisation process. Growth rates, boundary layer parameters and points of saturation of aluminium - potassium sulphate solution were measured by holographic, schlieren and interferometric methods. Combined schlieren - interferometer was used for precision measurement of face growth rate (Fig.1.). At the beginning of the experiment the point of saturation was measured by observing the boundary layer. Gradient of the refractive index changes the own sign during the decreasing of the temperature. In the point of saturation gradient in average is equal zero. Round absorptive diaphragm of the schlieren system (Fig.1.) well visualizes this stage. In the course of the process boundary layer width demonstrates weak dependence from supersaturation, while concentration change in the boundary layer has not trivial dependence (Fig.2.). Boundary layers near the faces (OOI),(III),(OII) show similar properties with deviation of concentration about 0.5×10^{-3} g/cm^3. Maximum in the curve indicates the change of the boundary layer structure, However Reynolds number of the boundary flow is smaller then one that corresponds to laminar stream. Transition to the oscillations in the boundary layer comes at the supersaturation about 1.5×10^{-2} g/cm^3 (σ =11%).

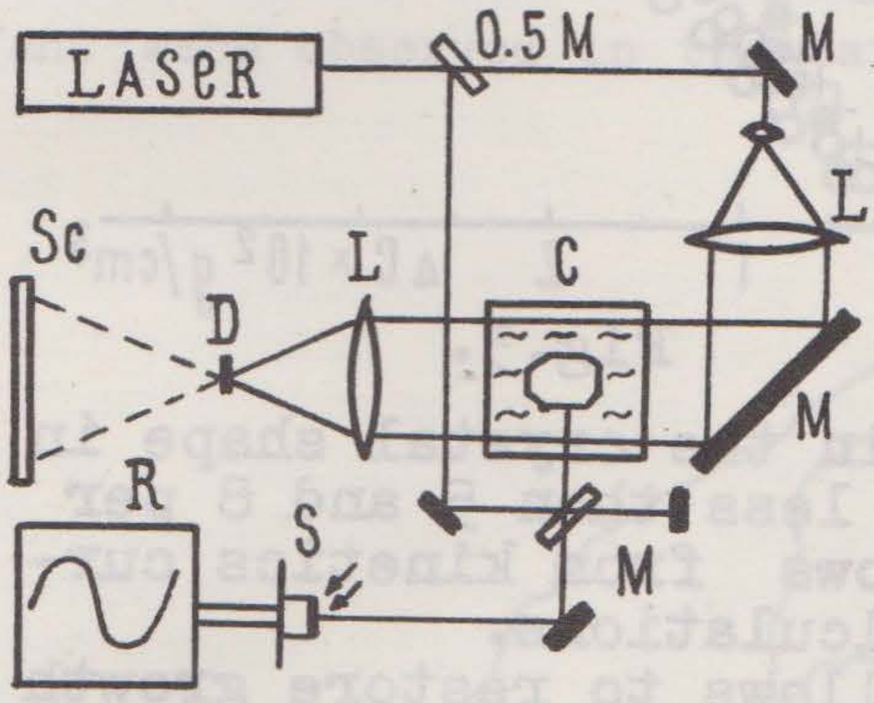

Fig.1.

Growth kinetics data are presented in figure 3. All curves change their behaviour beginning from 0.7×10^{-2} g/cm^3 (σ =5%). Masstransport through boundary layer calculated by means of diffusion coefficient (3.2x

10^{-6}cm^2/s) and concentrational gradient is smaller than 1.5 of measured growth rate at the high supersaturations. Hence it may be proposed that mechanism of "convective diffusion" determines masstransport at supersaturation higher than 5%, that corresponds to kinetics stage of crystal growth.

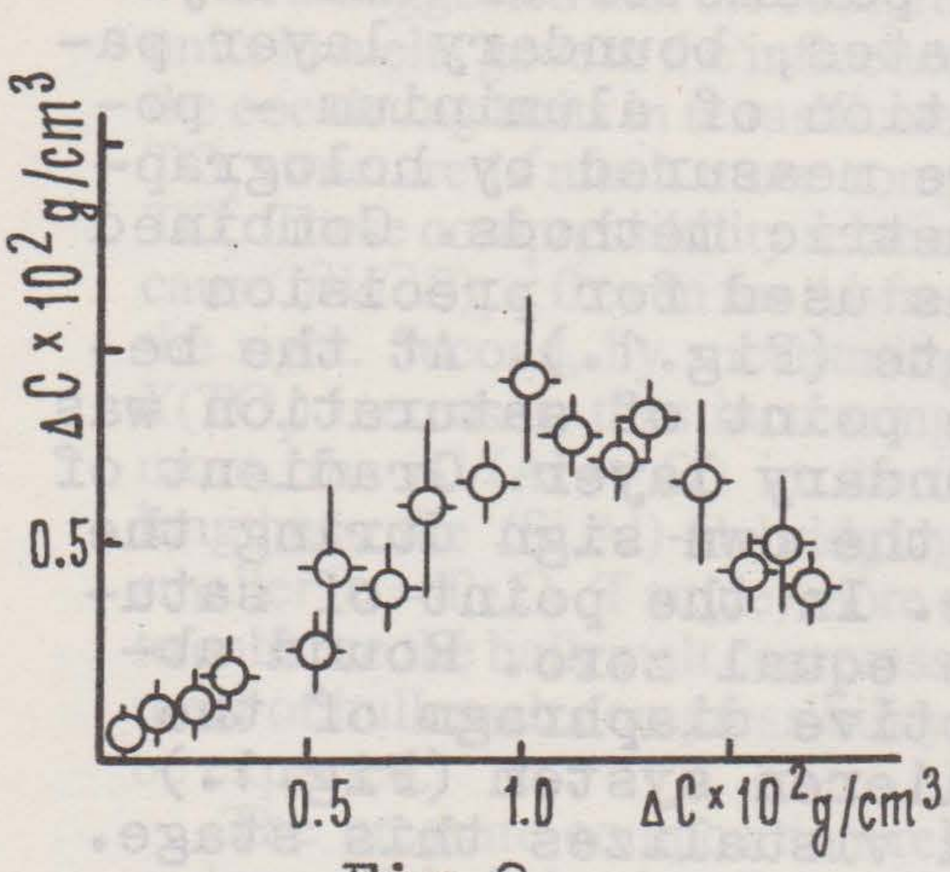

Fig.2.

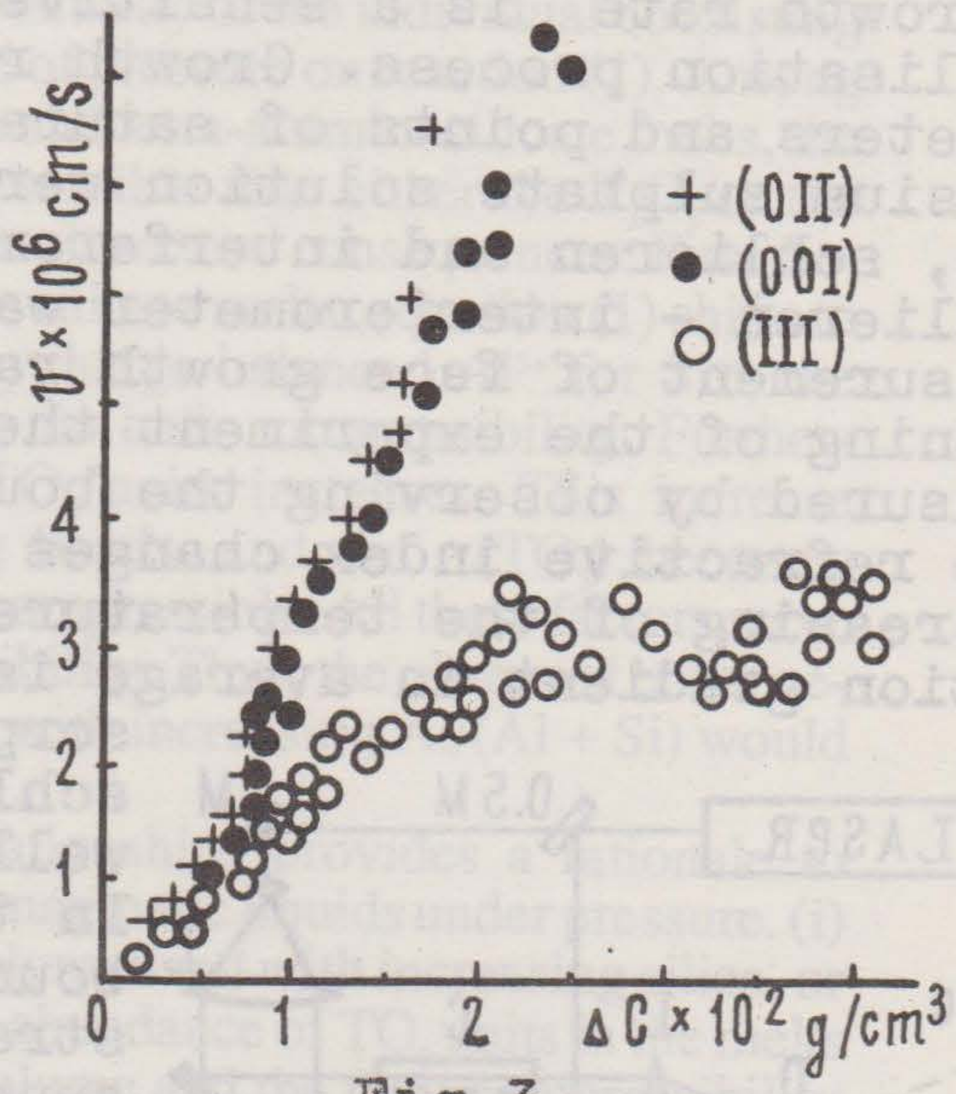

Fig.3.

Faces {0II} and {00I} remain in the crystal shape in the ranges of supersaturation less than 5 and 8 per cent respectively, as it follows from kinetics curves (Fig.3.) and geometric calculations.
Thus morphological analysis allows to restore growth conditions of the crystal, and masstransport conditions in the solutions have been determined exactly by means of behaviour of the boundary layer and growth kinetics data.

5.7.V GROWTH MARKS OF MINERALS BY X-RAY TOPOGRAPHY

Eugenio Scandale, Dipartimento Geomineralogico, Università di Bari-Campus, 70124 Bari, Italy
Giorgio Graziani and Sergio Lucchesi, Dipartimento di Scienze della Terra, Università di Roma, Piazzale A. Moro, 00100 Roma, Italy

The study of growth defects by X-ray topography lead to interesting hypotheses concerning the growth history of minerals. In particular recent results on hydrothermal quartz druses of different proveniences indicated that minerals grown in the same conditions are characterized by the same structural defects (1,2), so defects

can be considered growth marks, characterizing and differentiating the various druses and consequently the various geological growth environments.
The logical development of this type of studies was to verify the possibility of extension of the growth mark concept to other minerals and to other geological growth environments. Therefore beryl crystals from pegmatites have been studied: topographs showed quite perfect crystals characterized by the absence of dislocations and by growth bands (3). Observations, taken as a whole, indicate that structural defects of the examined crystals from pegmatite can be considered growth marks, as for quartz from hydrothermal druses. In particular the absence of basal dislocations, that are common in hydrothermal beryl crystals (4,5), can be considered characteristic feature of the growth environment.
In this paper will be discussed the case of an "horse-shoe" beryl from a brasilian pegmatite (6) in which channels parallel to the c axis resulted the dominating defects and only a few dislocation fans were observed in the latest crystallization stage. The study

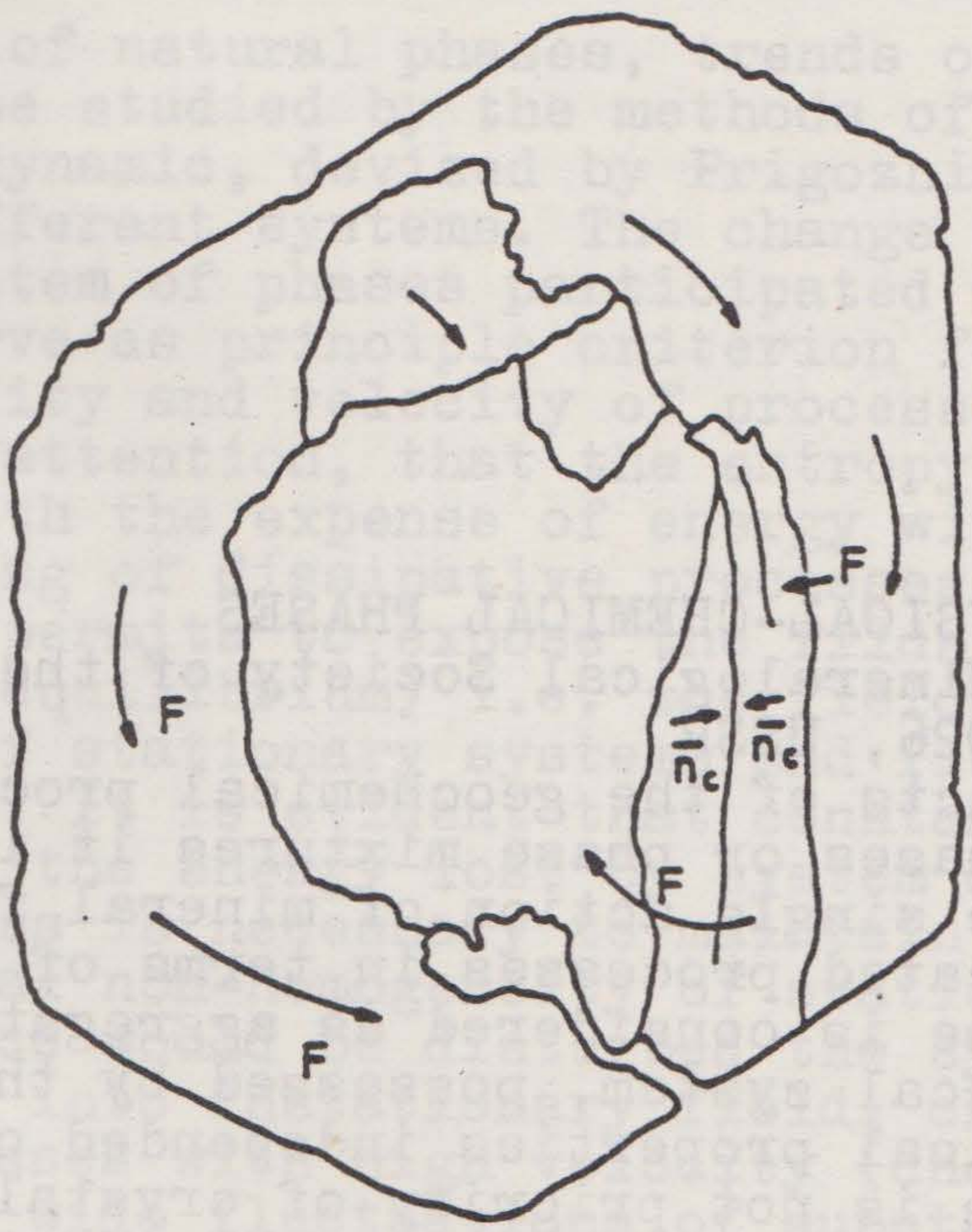

Fig. 1 - Schematic drawing of the crystal growth. The crystal developed from a seed by successive grains progressively recovering the hexagonal polyhedral form, following the F arrows. The $\bar{n}_c$ arrows indicate the growth normals as deduced from the dislocation fan orientations observed in the latest crystallization stage.

of the fluid inclusions contained in the crystal show that the latest crystallization of the "horse-shoe" beryl occurred under hydrothermal conditions. (Fig. 1).
These results could open new perspectives to the role of the growth marks.

References

1 - Scandale E., Stasi F., Zarka A., J. Appl. Cryst. 16, 399, (1983)
2 - Scandale E., Stasi F., J. Appl. Cryst. 18, 275, (1985)
3 - Scandale E., Lucchesi S., Graziani G., Europ. J. Min. (1990) in preparation
4 - Scandale E., Scordari F., Zarka A., J. Appl. Cryst. 12, 70, (1979)
5 - Scandale E., Scordari F., Zarka A., J. Appl. Cryst. 12, 78, (1979)
6 - Graziani G., Scandale E., Zarka A., J. Appl. Cryst. 14, 241, (1981)

5.6.V

THE NATURAL PHYSICAL-CHEMICAL PHASES

T.N.Sokolova, Mineralogical Society of the USSR
Leningrad, 199026, USSR

Since all products of the geochemical processes are represented by phases or phase mixtures it is reasonable to consider the single action of mineral formation as well as complicated processes in terms of notion about phase. The phase is considered as aggregate of parts of thermodynamical system, possessed by the same physical and chemical properties independed on substance quantity. There is not priority of crystalline phases with respect to non crystalline ones. In the terms of organazing levels for matter all physical-chemical phase are the components of the same level of organization, where the ties between elements of level (atoms) possess energy from some unites to hundreds KJ/Mol. Crystalline state is the particular case of organizing matter for the level in a whole. Phases represent the statistical systems, independing on the

grade of structure organization their identification and study are based on the priciples of following physical-chemical analysis: continuity of the characteristic changes within the limits of homogeneity and presence of singular points (lines) on the diagram, which don't change their absciss under conditional changes. The thermodynamic phase characteristics can be described by the Gibbs equation:

$$SdT - Vdp + n_i \mu_i = 0$$

where the entropy value (S) differs from the same substance according to its physical or aggregate state. There are as many Gibbs equations as phases. Comparision of dimentions characteristics for regulated atoms groups (germs of critical sizes, ordered fields within the glass or methamict minerals, micronohomogeneity etc.) shows that the dimensions factor is important for distingwishity of phases as statistical system. It is known that micrononhomogeneities with sizes up to few microns differ from macrophases becous of greate influence of surface properties. Micrononhomogeneities up to 10-100 Å can be considered as components of solution or colloidal system.

The changes of natural phases, trends of their evolution shoul be studied by the methods of non-equilibrium thermodynamic, devised by Prigozhin, Nicols and etc. for different systems. The change of entropy of phase or system of phases participated in the processes may serve as principle criterion for measure of irreversibility and velocity of processes. It should be taken in attention, that the entropy changes are connected with the expense of energy with inviroment and developing of dissipative processes. That kind of analysis permits to expose the filds of linear proceses (near equilibrium) i.e. the fields of existing and change of stationary systems and fields non-linear processes. It is evident that constant energy flow equilibrated the energy lost by system during dissipative process is necessary to maintain equilibrium and structural non-homogeneity of stationary system. If the balance would be disturbed the system could be developed into instationary field, characterized by the processes with high velocity (chemical reactions etc.), wide fluctuations of substance and energy. The system could be developed into the new stationary state through the unstable condition. Hence it follows the reasons for the degradation processes accompanying with the growth of entropy and for evolutional processes developing only in open systems in field of unstability with significant fluctuations, for geological systems.

5.4.V.

IN-SITU OBSERVATION OF CRYSTAL GROWTH AT ORDINARY AND HIGH TEMPERATURES

I. Sunagawa, K. Tsukamoto, T.Abe, K. Maiwa, K.Onuma, H. Nakamura, M. Kawasaki and K. Waizumi, Institute of Mineralogy, Petrology and Economic Geology, Tohoku University, Aramaki, Aoba, Sendai 980 Japan

In any geological phenomenon, the nucleation, growth and dissolution of crystals are involved, irrespective of whether the processes take place near the Earth's surface under ordinary temperature and pressure conditions or in the Earth's interior under high temperature, high pressure conditions. To understand how these kinetic processes take place is immensely important in geological and planetary sciences. Since we can not directly observe the processes of mineral formation, characterizations and deductive analyses of growth histories of mineral crystals have been the main methodology applied to understand kinetic processes of geological samples. Another approach is to verify the mechanism of crystal growth or dissolution, by experimentally measuring the kinetic data and confronting them with the theoretically expected one. Both methodologies are in essence indirect approaches. If in-situ observations of growth or dissolution processes with as high visibility as in the case of characterization could be combined with highly precise rate measurement and well-controlled growth conditions, this would provide the most direct method of investigating the kinetics of crystallization and verifying the mechanism of growth and dissolution of crystals. We have developed such in-situ observation methods for both ordinary temperature aqueous solution system and high temperature silicate solution system. In the presentation, the in-situ observation methods we have recently developed in our laboratory will be reviewed.

(1) Aquous solution growth at ordinary temperature

A wide variety of experimental set ups has been developed by a combination of various optical

microscopies, interferometric methods, light scattering, Raman spectroscopy, flow system, temperature controlling system using personal computers, and recording system with CCD TV camera. The experiments were carried out in a thermostated clean room. Temperature control with fluctuation less than 0.01 C is guranteed, and advancing spiral steps with a height of nm order can be observed in-situ. Using such experimental set ups, the following in-situ investigations are now possible.

a) Clustering phenomenon in supersaturated solution.
b) Visualization and measurement of diffusion boundary layer, buoyancy driven convection, etc. in relation to flow rates of solutions.
c) Measurement of surface super- or under-saturation on a growing solid-liquid interface.
d) Identification of dislocation characters in a growing crystal.
e) Measurement of growth or dissolution rates and slopes of individual growth hillocks or etch pits, and of advancing rates of spiral steps.
f) Growth rates versus driving force relations on individual growth hillocks and surface supersatuations.
g) Morphological variation of bulk crystals and growth spirals in relation to various kinetic parameters.
h) Analysis of impurity effects.
g) Secondary nucleation phenomenon.

(2) High temperature silicate and oxide systems

By preparing thin liquid film of silicate or oxide systems in a small furnace installed on the stage of an optical microscope, in-situ observation of growing or dissolving crystals in high temperature liquid phase by transmitted light has been realized. Personal computers are used to control temperatures up to 1500 C, with less fluctuation than 0.5 C. The following problems have been investigated using this method.

a) In-situ observation of growth or dissolution processes of crystals at elevated temperatures.
b) Direct and precise measurements of melting points of both stable and metastable phases.

c) Morphological variations including roughening transition in relation to driving forces and compositions.
d) Growth or dissolutrion rate versus driving force relations.
e) Measurement of nucleation rates and probability; analysis of nucleation behavior.
f) Metastable nucleation; stability of metastable phases.
g) Visualization of convection and diffusion boundary layer in silicate melt or solution.

References

K. Tsukamoto, T. Abe and I. Sunagawa; J. Cryst. Growth 63 (1983)215
K. Tsukamoto and I. Sunagawa; J. Cryst. Growth 71(1985)183
T.Abe, K. Tsukamoto and I. Sunagawa; Mineral. J. 13 (1987)479
K. Maiwa, K. Tsukamoto and I. Sunagawa; Proc. 1st Topical Meeting on Crystal Growth Mechanism, Tokyo (1988) 71
K. Onuma, K. Tsukamoto and I. Sunagawa; J. Cryst. Growth 98(1989) 377
K. Onuma, K. Tsukamoto and I. Sunagawa, J. Cryst. Growth 98 (1989), 384
K. Maiwa, K. Tsukamoto and I. Sunagawa, J. Cryst. Growth, 98 (1989) 590
I. Sunagawa, in "Dynamic Processes of Material Transport and Transformation in the Earth's Interior, TERRA Pub, Tokyo, 1990"142

5.2.V. **ON THE DIAMOND CRYSTALS GENESIS IN THE EARTH MATLE,**

Andrzej Szymański, Institute of Electronic Materials Technology, 01-919 Warszawa, 133 Wólczyńska Str., Poland.

Genetic analysis of natural and synthetic diamond and especially programmed experiments confirm opinion that most hypotheses on the formation of diamonds as products of magma crystallization in very deep region of mantle are seemingly real only *(Niedbalska, Szymański 1987, Niedbalska et al 1988)*
Graphite/diamond equilibrium plot for eclogites given by Dawson (1980) distingly proved, that industrial processes of HP/HT static synthesis was technically strained by pressure and probably more exceed natural conditions. High pressure technology on his start neglected physicochemical knowledge. Most commercially produced synthetic diamonds grown from graphite in the presence of solvent/catalyst metals up to 1 mm sizes with isometric shape.

Reconstruction technique *(Wentorf, 1971)* used diamond as source of sp^3 orbitals organized carbon for on seed growing stones was developed by *Burns (1988)* to grown large crystals up to 11 cts in weight. The process is determined by the solubility difference of carbon on the precursor/metal and diamond/metal interface.

Localised his synthesis in points deviated 1,2 GPa higher and lower than Dawson's line (Fig.) *Niedbalska and Szymański (1987)* using glassy carbon as precursor received same results as in commercial diamond synthesis based on graphite, but in lower pressure 3,8 GPa. Temperature localization of experimental points (Fig.) were compared with *Sunagawa (1984)* plots of faces growth rates. All good contoured crystals (~0,7 mm in size) are cubooctahedrons with clear (100) and equipondemant or underdeveloped (111) faces. *Niedbalska and Szymański (1987)* suggestion that diamond in the mantle grown from polycondensed and carbonized hydrocarbons was verified by *Sobolev and Shatsky (1986)* who describe diamond microcrystals grown into bubble hydrocarbons inclusions in garnets in pressure below 4 GPa in metamorfic rocks.

On the draft (Fig.) two types of different areas are given: Ts/p (temperature of synthesis) and Tc (temperature of organic precursor carbonization). All discussed experiments *(Niedbalska, Szymański 1987, Onodera et al 1988, Miyamoto et al 1989)* carbonized his glassy carbon to similar temperatures.

Sobolev and Shatsky (1986) diamonds are placed in two points: Ts/p and Tc+Te/p (Te-temperature of epitaxy). Second one is more logical and graphically verify suggestion that future development of HP/HT synthesis to go in the direction of CVD epitaxy and would be low/pressure liquid phase epitaxy - LPLPE (Fig., lined „xx" area).

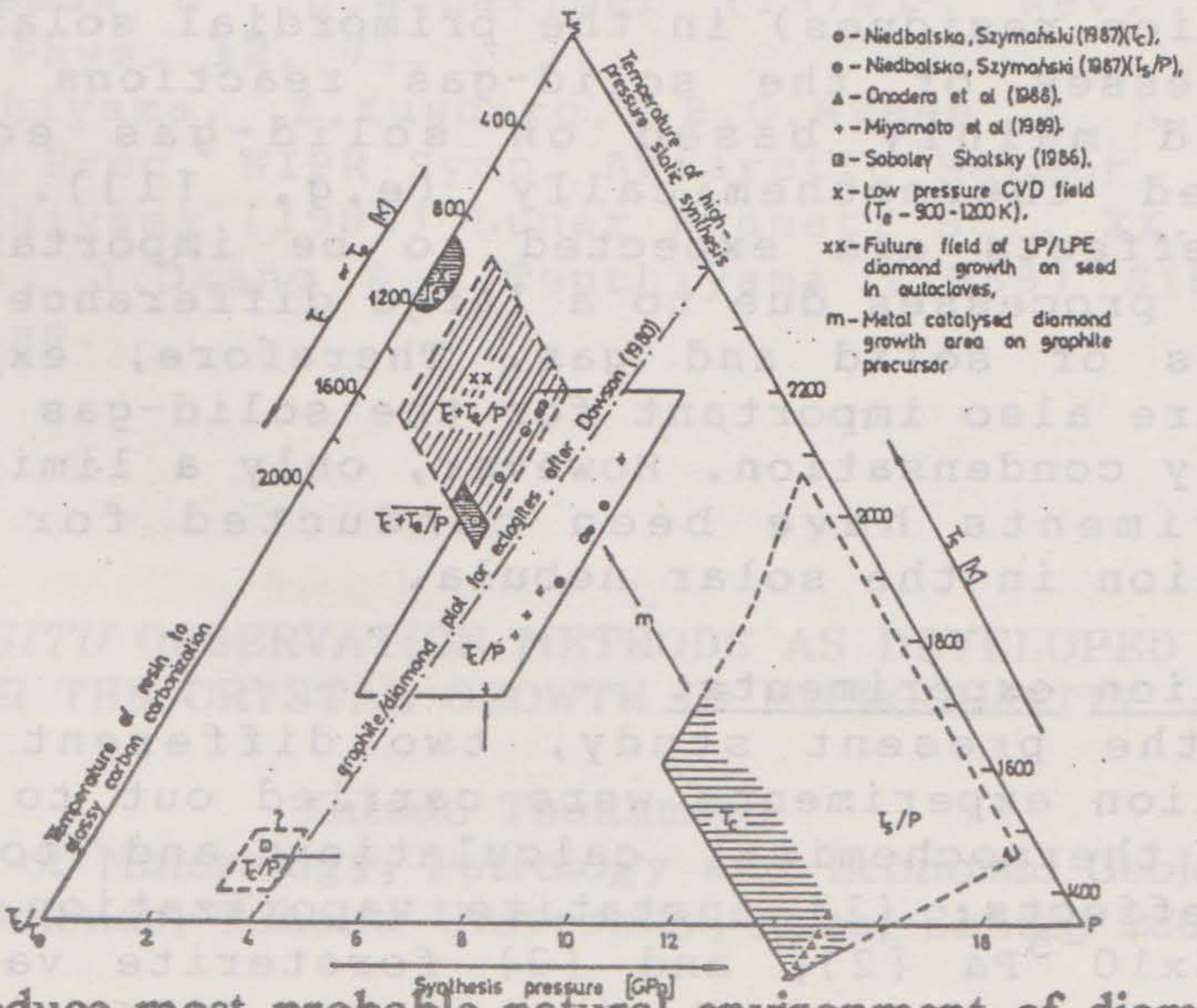

As we may deduce most probable natural environment of diamond crystals grown was liquid hydrocarbons filled deep closed crystal or rock geodes, decomposed to carbon without metal catalyst but with high isostatic partial

pressure under high temperature.

Bibliography:
Niedbalska A., Szymański A. (1987), Proc. XXV EHPRG, Potsdam, pp. 34—37
Niedbalska A., Szymański A., Zalewski S. A. (1989), Abstr. 1st ICNDST, Tokyo, No. 2—19.
Dawson J. B. (1980), Kimberlites and Their Xenolites. Springer Verlag. Berlin.
Wentorf R. H. (1971), J. Phys. Chem., 69, pp. 3063—3069.
Burns R. C. (1988), Abstr. 1st ICNDST, Tokyo, No. 2—12.
Sobolev N. W., Shatsky W. S. (1986), Geol. and Geoph., 7, pp. 77—80 (in Russian)
Onodera A., Higashi K., Irie Y. (1988), J. Mat. Sci., 23, pp. 422—428.
Miyamoto M., Akaiski M., Ohsawa T., Yamaoka S., Fukunaga O. (1989) in press.

5.8 H

CONDENSATION EXPERIMENTS ON EXTRATERRESTRIAL SOLID MATERIALS.

Akira Tsuchiyama, Department of Geology and Mineralogy, Kyoto University, Kyoto 606, Japan.

Solid-gas reactions.

It has been known that solid-liquid reactions (melting and crystallization) are essential processes for evolution of the planets, such as the earth and some meteorite parental bodies, and many experiments have been done on this problem. On the other hand, solid-gas reactions (vaporization and condensation) are essential processes for formation of the planets because they were formed from condensation products (or vaporization residues) in the primordial solar nebula.

Processes of the solid-gas reactions have been discussed mainly based on solid-gas equilibria calculated thermochemically (e.g. [1]). However, kinetic effects are expected to be important in the solid-gas processes due to a large difference of atomic structures of solid and gas. Therefore, experimental studies are also important for the solid-gas reactions, especially condensation. However, only a limited number of experiments have been conducted for studying condensation in the solar nebula.

Condensation experiments.

In the present study, two different types of condensation experiments were carried out to check the previous thermochemical calculation and to evaluate kinetic effects; (1) enstatite vaporization source at $p(H_2)=4.4\times10^{-5}$Pa [2], and (2) forsterite vaporization source at $p(H_2)=1.4$ Pa under different redox conditions [3]. Results of the experiments-(2) show that the condensation sequences are almost the same as

those expected from the calculation although some kinetic effects were seen especially at low condensation temperatures.

Kinetics of condensation.

Several kinetic effects due to a nucleation delay of crystals were found in the experiments although heterogeneous nucleation on substrata (mostly Mo plates) took place. Condensation of metastable crystals including a high pressure mineral (coesite) were recognized at about 1000°C in the experiments-(1). In the experiments-(2), whiskers of forsterite and enstatite grown by a VLS-mechanism, in which metastable melt droplets condensed first, were found at medium temperatures (around 1000°C). Probably, the larger kinetic effect of the experiments-(1) results from the lower pressure in the experiments. Condensation of amorphous silicates at low temperatures (<500°C) were also found in the both experiments.

Isotope fractionation.

Fractionations of Mg and Si isotopes were investigated with products of the experiments-(2) [4]. It was found that large amounts of fractionation (> a few tens of per mil.) took place during the vaporization and condensation. Heavier isotopes were fractionated into solids during condensation at high temperatures (>1000°C) as well as vaporization.

References

[1] L.Grossman & J.W.Larimer (1974) Rev. Geophys. Space Phys. **12**, 71.
[2] A.Tsuchiyama, I.Kushiro, B.O.Mysen & N.Morimoto (1988) Proc. NIPR Symp. Antarctic Meteor. **1**, 172.
[3] A.Tsuchiyama (1989) Lunar Planet. Sci. **XX**, 1136.
[4] C.Uyeda, J.Okano & A.Tsuchiyama (1989) SIMS, **VII**, in press.

IN SITU OBSERVATION METHODS AS DEVELOPED FOR THE CRYSTAL GROWTH IN MICROGRAVITY

5.12 M

Katsuo Tsukamoto
Institute of Mineralogy, Petrology and Economic Geology,
Faculty of Science, Tohoku University, Aoba, Sendai 980, Japan

Although high quality semiconductor crystals can be grown and thus growth of crystals seems to be controlled freely at any

environments, crystal growth in microgravity is almost beyond control, which is realized when we fly only 300km vertically from the earth. It is therefore questionable whether we can analyze the formation of cosmic materials based upon the experiences on earth.

Utilization of microgravity has a lot of possibilities to verify crystal growth theories or to investigate the crystal growth mechanisms from fundamental point of views. This is because in microgravity no buoyancy driven convection such as thermal convection or solutal convection would take place, which leads to no fluctuating environment. So only diffusion, which is largely influenced by fluctuating convection [1], is the transport mechanism of growth units. Although modern crystal growth theories started to include effects of convection in a limited case, crystal growth *via* diffusion process alone would have to be investigated experimentally as a simple case so that critical phenomena, for instance, in morphological stability or in growth zoning could be understood.

A very stable environment in microgravity gives us the other possibility. According to our high temperature *in situ* observation of silicate crystal growth, metastable phases which do not appear in a phase diagram commonly nucleate prior to the nucleation of the stable phase, if the supersaturation is large [2]. It is easily understood from this example that, if there is no gravity and thus no convection, nucleation of crystals in microgravity would become very difficult and needs much larger supersaturation, which would often lead to metastable nucleation that cannot be investigated in gravity.

In order to investigate the difference of the crystal growth between in gravity and in microgravity, varieties of *in situ* observation methods by high resolution optical microscopies or interferometries were developed. A few payloads for the experiments in space were made by installing these optics. The first model is planned to be flown using a NASA space shuttle this year and more payloads were made for rockets. The observation methods [3] are in principle similar each other. Vertically crossing optical axes are used for the observation of a crystal surface at a molecular level and of the concentration gradient around a growing or a dissolving crystal. Newly designed modulation contrast microscopy is employed for the former observation, which enables it to visualize growth steps as thin as 1nm during crystal growth. The concentration around a crystal is visualized and measured by Schlieren method or common-path interferometry.

Although these *in situ* experiments in microgravity have not yet been done, the knowledge through the development of these instruments had great influences upon the progress of *in situ* observation methods, which have been utilized for the experiments in our laboratory. The followings are some of the by-products through the development of these optics and the preparation of these experiments.

(1) Space microscope employing modulation contrast microscopy,

for the observation of a crystal surface at a molecular level and the measurements of crystal growth rate with the help of built-in auto-focus system,
(2) common-path interferometries, which are very stable against vibration, for the measurements of concentration around a crystal in solution or of temperature around a crystal in melt, and
(3) phase shifting two-wavelength interferometry, for the measurements of both temperature and concentration around a crystal. This interferometry achieved 50 times more accurate measurements than ordinary interferometries and much easier analysis with the help of a microcomputer.

Up to now no experiments is planned to use microgravity in the field of mineralogy, however there seems to be many applicabilities especially in the field of meteorite or cosmic materials.

References

[1] (a) K. Onuma, K. Tsukamoto and I. Sunagawa, J. Crystal Growth 89 (1988) 177. (b) K. Onuma, K. Tsukamoto and I. Sunagawa, J. Crystal Growth 98 (1989) 384. (c) K. Onuma, K. Tsukamoto and I. Sunagawa, J. Crystal Growth 98 (1989) 377.
[2] T. Abe, K. Tsukamoto and I. Sunagawa, Mineral. J. 13 (1987) 479.
[3] K. Tsukamoto, J. Crystal Growth 61 (1983) 199.

KINETIC ASPECTS OF SECTOR ZONING IN ARSENOPYRITE

Po 5.4.

I. Vesselinov, T. Kerestedjian, H. Neykov, *Geological Institute, Bulgarian Academy of Sciences, Acad. G. Bonchev Str., Bl.24, 1113 Sofia, Bulgaria.*

Sector zoning, very typical of hydrothermal arsenopyrite, is studied in an assemblage of quartz and needle-like arsenopyrite formed at about 350 ^{o}C in a Bulgarian base-metal vein deposit. Arsenopyrite is bounded by {101}, {210} and {010} (Buerger's setting) and the oriented (001) polished section of a typical crystal (5 x 0.5 x 0.5 mm) shows a zonal pattern involving the (210) and (010) growth pyramids with a well-defined boundary between the two sectors. Sector zoning is especially prominent in electron microscope BSE image. Microprobe point analyses give $Fe(As_{1-x}S_x)S$ compositions which vary in perfect harmony with the changing slopes of the boundary line segments.

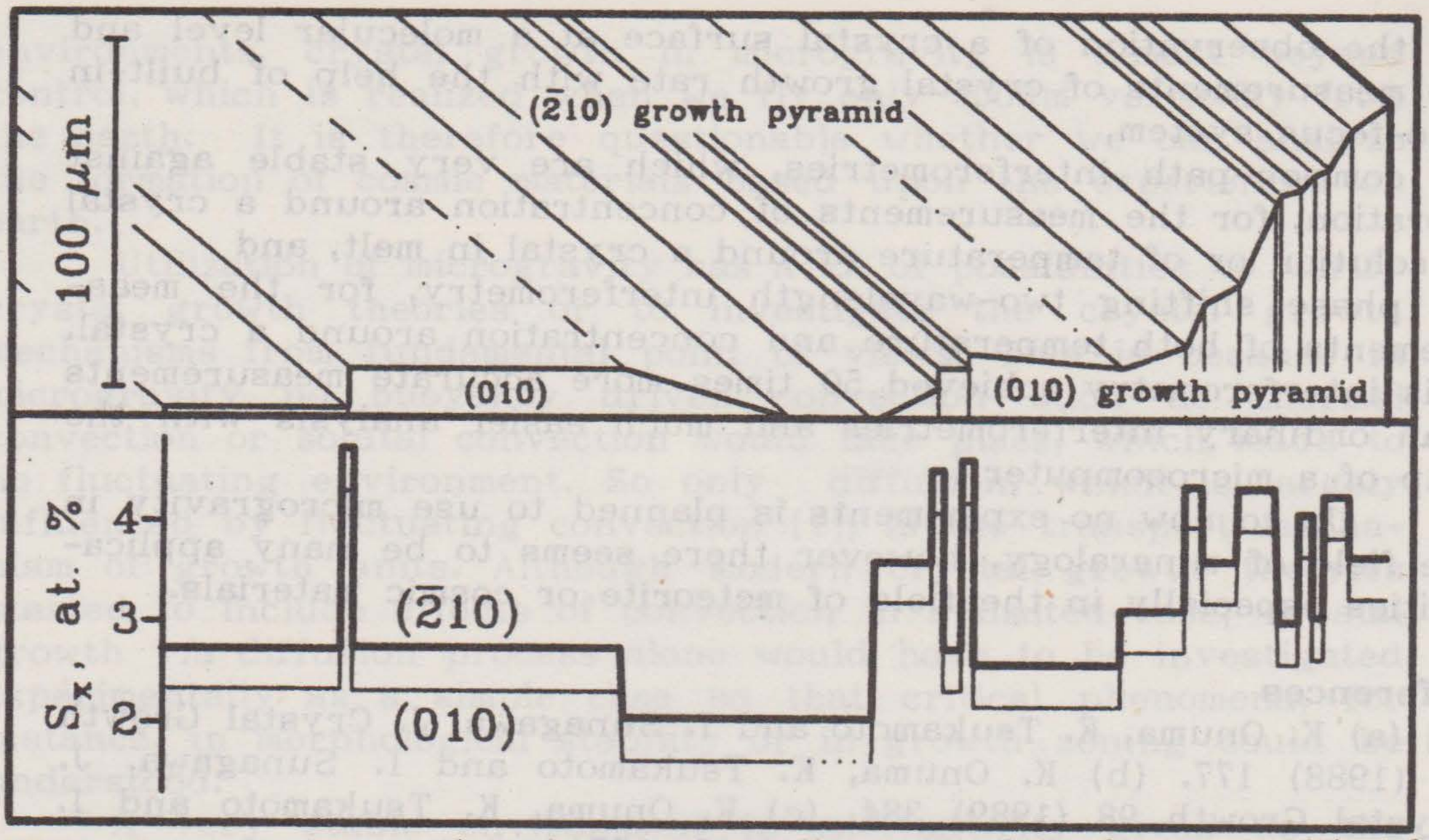

Kretschmar and Scott (1976), not succeeding to explain the compositional zoning of arsenopyrite in terms of equilibrium relations in the $Fe - As - S$ system, have suggested growth kinetics as the likely cause. For hydrothermal arsenopyrite, our specimen conclusively corroborates that suggestion because the boundary geometry, so closely related to the non-stoichiometric S_x content, is dependent solely on the relative growth rates of the two faces, i.e. on V^{010}/V^{210}.

Our study of that effect is based on the theory of sectorial and zonal growth as given by Chernov (1980). We treat S_x as homogeneous impurity trapped at non-equilibrium and use the measured values of its concentration and of V^{010}/V^{210} to derive the S_x solid/fluid distribution coefficients during growth as they influence and are influenced by the growth rates in the (210) and (010) sectors. Variable distribution coefficients, subject to crystallochemical interpretation, and the law of mass action as an agent in controlling supersaturation at the front of the growing faces explain many features of the sector zoning in terms of phenomena taking place close to the growing crystal surface. Such a mechanism releases the constraint of postulating unreasonably varyable hydrothermal environments as responsible for zonal arsenopyrites. It also permits making rough estimates of growth times.

References

Kretschmar U., Scott S. D., *Canadian Mineralogist*, **14**, 364-386, 1976

Chernov A. A. Processes of Crystallisation, in: *Modern Crystallography*, vol. 3, ch. 1, 7-232, Moscow, Nauka Publ. House, 1980 (in Russian)

HOW MINERAL CRYSTALS GROW

Yu.K.Vorobyov
Laboratory of Genetic Minerology, IGEM of Academy of Sciences of the USSR, Staromonetny per., Moscow, 109017, USSR

The natural crystal-forming media are almost always very polluted, that is they include a great number of components besides the main crystallizing substance. The physical models of natural crystallization have been studied in the specially polluted solutions of $NaNO_3$, $NaCl$, $K_2Cr_2O_7$, $Pb(NO_3)_2$, $CuSO_4 \cdot 5H_2O$, alum and others substances. The growth's cinetic curves have been built and the impurity concentrations in the crystallization halo have been measured. It has been found that the growth in polluted natural media is determined by periodic accumulation of the impurities and by rise of impurity barrier stopping the crystallization. Because of that the growth process has a clearly expressed pulsing character (Fig.1). In the crystals' growth in such media the following phenomena have been observed. At first the crystals grow rather homogeneous having the most simple habitus. However not long after because of impurity accumulating before the growth front the faces lose steadiness. The growth becomes slower, and then very quickly the first inclusion zone is formed. Then growing of the pure matter goes on, but very soon it starts to grow slower again and the second inclusion zone is formed. This process is resumed again and again.

In every cycle the following p h e n o p h a s e s of g r o w t h are distinguished.

Phase I - rapid growth of the pure crystallizing substance. As the impurity accumulates in the boundary layer the growth becomes slower and turns into the next phase -

Phase II - the rate of growth reduces to a complete stop:the impurities completely block the crystallization.

Phase III - relaxation of the impurity barrier: during the pause in growing the impurity concentration is decreased slowly by diffusion to a certain threshold level at which the crystallization is again possible.

Because of the supersaturation of the main crystallizing component increases simultaneously, the last phase of the cycle begins -

Phase IV - a stormy growth is accompanied by trapping of a lot of medium inclusions. The growth rate increases about as compared to the growth rate in the end of the phenophase I. Due to this the most polluted part of crystallization halo is trapped by a crystal, forming a medium inclusions zone in the crystal. In accordance with this sequence of growth phenophases the regular alternation of pure and polluted zones occures in crystals of many minerals. Because of the variety of relaxation variants of impurity barrier the polluted zones may be as follows: 1) the zones of inclusions of polluted medium and impurity phases(quartz, caloite, diopside); 2) the periodical sedimentation of impurity phase layers on the growth' front (ilmenite-spinel bycrystals, agates); 3) the periodical trapping of high concentrations of homogeneous impurities (wolframite, granate, cassiterite, fluorite).

Fig. PHENOPHASES OF CRYSTAL GROWTH

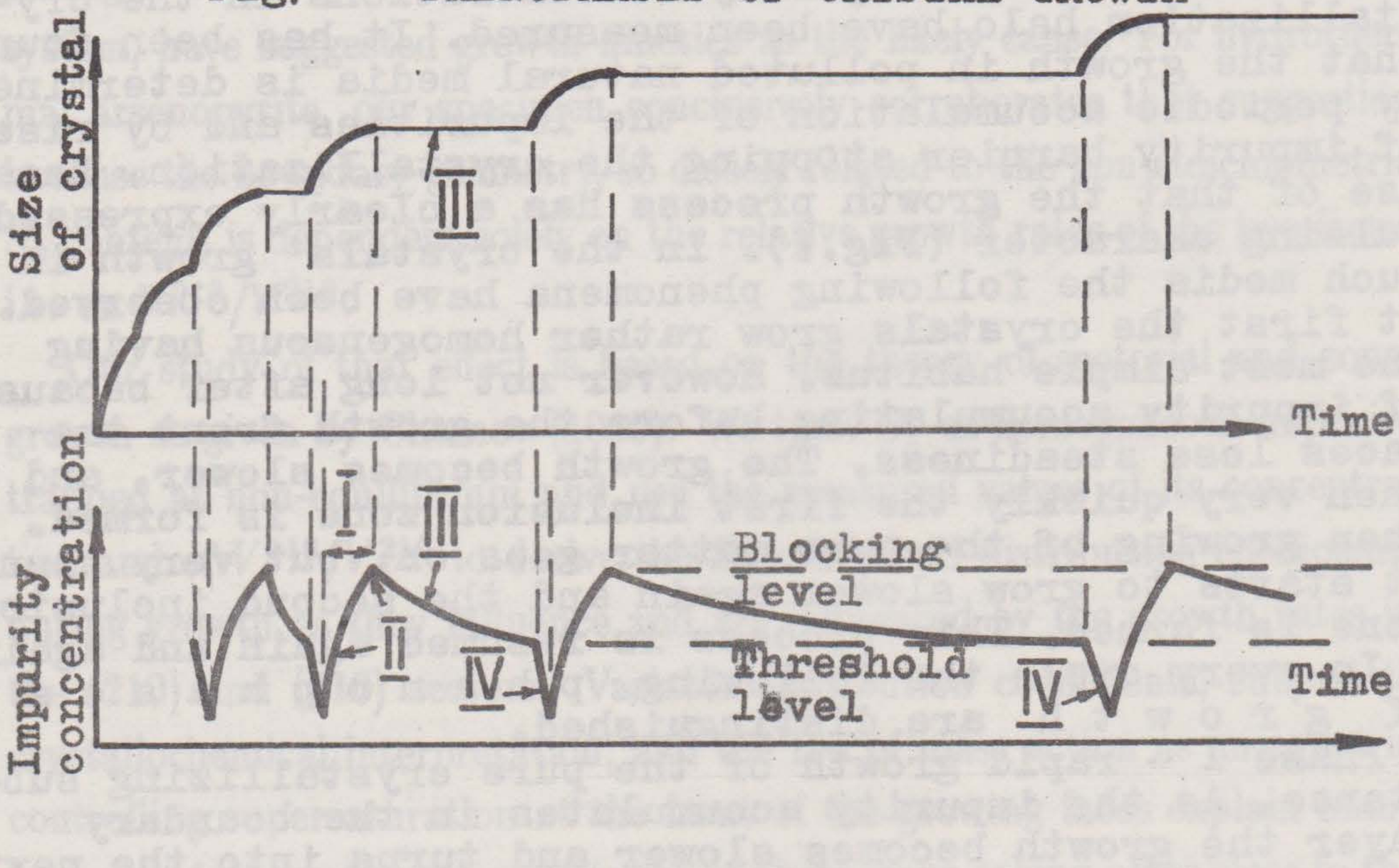

P. 55.

THE PROGRESS OF RESEARCH ON THE CRYSTAL MORPHOLOGY OF CHINA

WANG Wenkui, ZHAO Shanrong & NIU Xinxi, Department of Geology, China University of Geosciences (Wuhan), Wuhan 430074, People's Republic of China

During a long period in history the study of Chinese crystal morphology was in a state of free hand sketch.

In the 40 years after the establishment of New China, the study of crystal morphology got a good beginning and several important contributions. In early 1950's, prof. Zhang Bingxi introduced V. Goldschmidt's crystallometry to the students of Geological Department of Beijing University. Several years later, the Institute of Mineralogy of Beijing College of Geology and prof. Peng Zhizhong first built the laboratory of crystallometry, gave lecture on the course of crystallometry, and published a book of crystallometry (1963). Meanwhile, he complished the research on the crystal morphology of hsianghualite (1964). Xie Xiande took the study of kurnakovite with complete morphological data (1964). This is an important progress in the history of Chinese recent mineralogy. Thereafter for more than 20 years, Zhang Jingyi measured 33 uranium mineral crystals occur in China (1988). In the earlier 1980's, the Institute of Mineralogy of Wuhan College of Geology reestablished the classical course of crystallometry and published An Introduction of Crystal Surface Microtopography (1985), mainly on the work of Sunagawa. The later is a beginning of research of crystal surface microtopography in China. Financed by NSFC, Wang Wenkui et al have completed A Morphological Study of the First Group of 20 Minerals From China, and built the only laboratory for teaching and research of both macro- and micro-morphology of crystals. That has laid a firm fundation for the continuous development of crystal morphology.

Certain Chinese mineral crystals have unique morphs in the world. They are the fundamental material in the study of mineralogy, that is inneglectable for development. For example, the morph of our first new mineral hsianghualite is a combination of 16 single forms. It is the most creditable representative of tetartoidal class (T=23) among minerals discovered in the world. The morph of jamesonite, occurred in Dachang, Guangxi, is the only reliable drawing since 1825 the mineral discovered (Niu Xinxi & Wang Wenkui, 1986). Besides, the morphs of aegirine occurring in alkalinic granite in Kuiqi, Fuzhou, are very beautiful and rich in the world. The development of single forms show that the series of evolution is from complex to simple (Wang Wenkui & Zhao Shanrong, 1987).

Now, there are 80 species of minerals which have been studied on goniometry, including 2 new minerals of China, 33 species of uranium minerals, and more than 40 species of other minerals. They provide about 100 exact crystal drawings and enhanced the basic research and teaching in mineralogy of China.

Recently, the study on genetic morphology of minerals is delightful. Chen Guangyuan (1987) has broadly studied the morphology of pyrite in Jiaodong Au deposits, and showed 5 morphological characteristics of pyrite both in altered rock type and quartz vein type deposits. Zhang Liangju (1987) in the study of Xiao Qinling Au deposits, has mapped the crystal morph of pyrite according to the mineralizing stage to see the evolution. Zhao Shanrong (1988) has studied the natural crystalization of aegirine and arfvedsonite on the light of morphology. She pointed out that the micro bonding on the surface of crystal growth is decided by both internal structure and environmental conditions—degree of supersaturation.

The previous work of mineral crystal morphology is so little that it lag far behind the study of the other branches in mineralogy. Therefore, our task is not only to compensate the lack of the morphological study of mineral species, but also to start along the trend of genetic and prospecting crystal morphology with broad future, so as to discover the unique characteristics of Chinese crystal morphology and enrich the data of world mineral crystal morphology.

5.9.H

THE UNIQUE MORPHOLOGICAL SERIES OF AEGIRINE FROM KUIQI GRANITE, FUJIAN, CHINA

WANG Wenkui, ZHAO Shanrong and NIU Xinxi, China University of Geosciences (Wuhan), Wuhan 430074, P.R. China

Crystals of aegirine occurred in druses of Kuiqi granite are so beautiful and plenty that bear great significance in the traditional mineralogy. The goniometrical study of about 300 crystals with STOE goniometer by V.Goldschmidt's method, and more than 40 exact clinographic crystal drawings[1] show that: (1) the eucentrical pyramidal habit are characteristic for partial aegirne and mainly bounded by d{131} or q{692}, which differs from that of Greenland and Xibin by o{661} or x{461}[2,3]; (2) there exists a remarkable series, not reported before, of morphological evolution from one end of eucentrical pyramidal (fig.1,2,3) through pupa-like (fig.4,5) to simple prismatic (fig.6,7,8), the other end; (3) both the reentrant and closed types of simple contact twinning on (100) (fig.9,10) and parallel intergrowth are typical and plenty.

As a result of internal influence of bond chains and free space for growth, the diminutiom of pyramidal

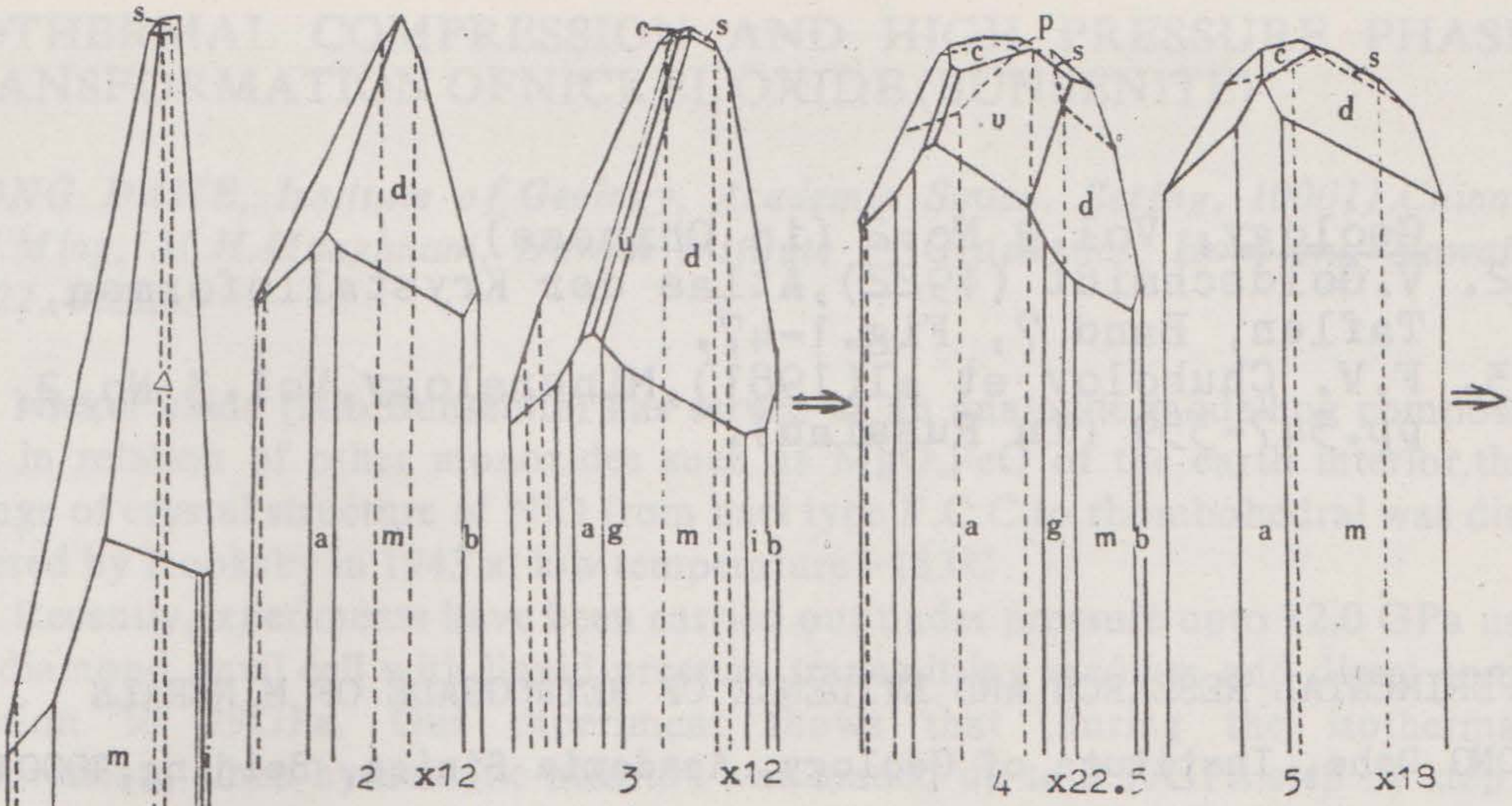

Fig.1 x12 Eucentric needle

Fig.2,3 Eucentric pyramidal

Fig.4,5 Pupu-like pyramidal

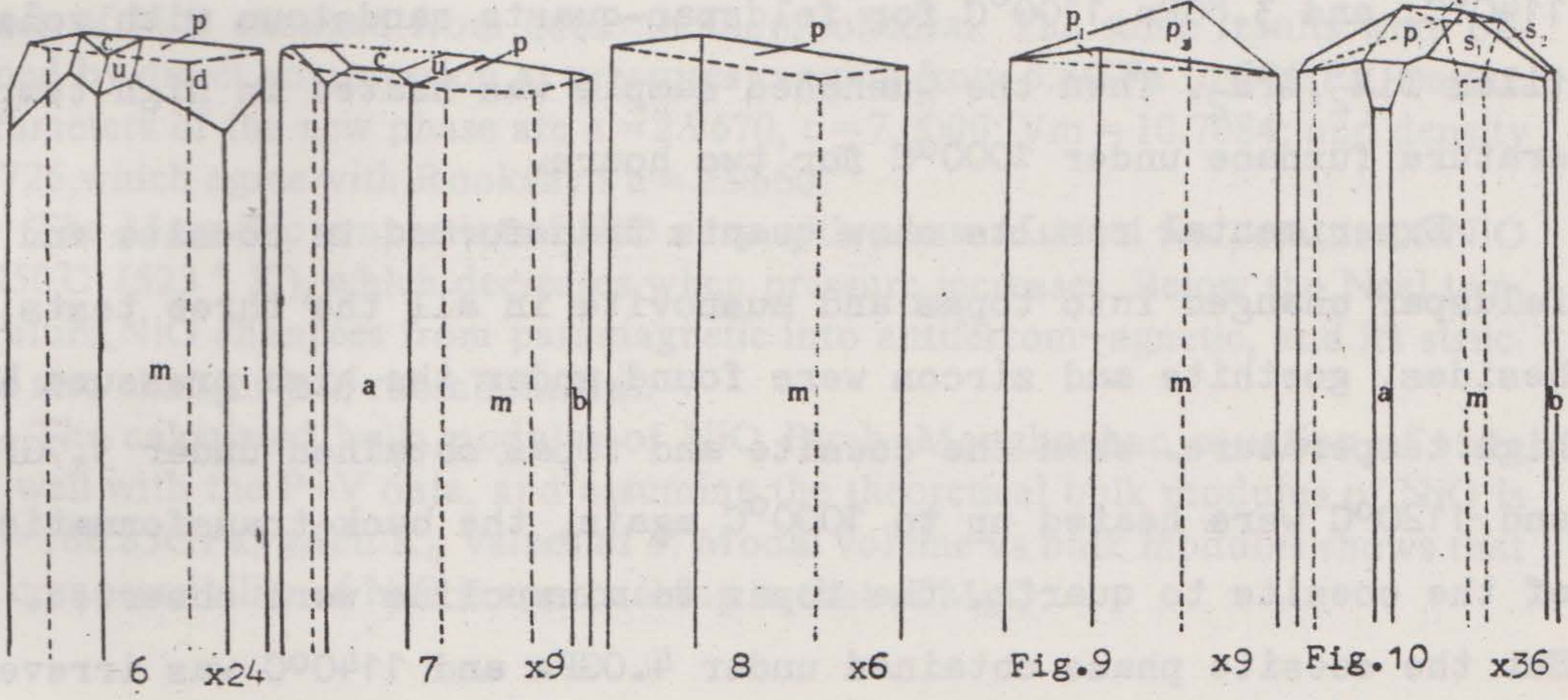

Fig.6,7,8 Simple prismatic

Twin on (100), reentrant

Twin on (100), closed

The morphological evolution series of aegirine, Fuzhou, China (fig.1-8).
c(001), p($\bar{1}$01), d(131), u(111), s($\bar{1}$11), △($\rho\approx90°$), a(100), b(010), m(110).

faces, as well as simultaneously the emergence and development of c{001} or p{$\bar{1}$01} are the main macro indices of the morphological evolution of aegirine.

All of these exhibit an astonishing comprehensive systematic evolution pattern of macro-morphology of aegirine from Kuiqi granite, never disclosed elsewhere before.

References

1. Wang Wenkui, et al (1990), Crystal morphology of aegirine in Kuiqi miraolitic granite, Fuzhou, Fujian

Geology, Vol.9 No.2 (in Chinese).
2. V.Goldschmidt (1922),Atlas der Krystalloformen, Taflen, Band 7, Fig.1-47.
3. F.V. Chuholov et al(1981),Mineralogy,Vol.3 No.2, pp.347-359 (in Russian).

5.11H

EXPERIMENTAL RESEARCH AND EVIDENCE OF RETROGRADE OF MINERALS

XIONG Dahe, Institute of Geology, Academia Sinica, Beijing,100011 China.

Using the cubic-anvil high pressure apparatus, we carried out the phase transformation experiments at 3.7GPa, 1120°C; 4.0GPa, 1140°C; and 3.8GPa,1100°C for feldspar-quartz sandstone with volatiles TiH_2,ZrH_2. Then the Quenched sample was heated in high temperature furnace under 1000°C for two hours.

Experimental results show quartz transformed to coesite and feldspar changed into topaz and muscovite in all the three tests, besides, goethite and zircon were found under the high pressure & high temperature. When the coesite and topaz obtained under 3.7GPa and 1120°C were heated up to 1000°C again, the back-transformation of the coesite to quartz, the topaz to microcline were observed. But the coesite phase obtained under 4.0GPa and 1140°C was irrevers ible, no back-transformation occurred,when heated up to 1000°C again. This probably suggests that 4.0GPa and 1140°C were the criti cal pressure and temperature for coesite stable range.

Employing high temperature diamond anvil cell,synchrotron radiation and energy dispersive X-ray diffraction technique the spinel to olivine back-transformation was observed at 750-950°C for γ-spinel(γ-$(Mg\ Fe)_2SiO_4$).

The experimental results of phase change and back-transformation of olivine and quartz etc. are well with their theoretical phase diagrama. It possibly foretells that reversibility or retrograde of minerals is a important factor of mineral genesis.

ISOTHERMAL COMPRESSION AND HIGH PRESSURE PHASE TRANSFORMATION OFNICKEL OXIDE (BUNSENITE)

P5 5.7.

XIONG DAHE, Institute of Geology, Academia Sinica, Beijing, 100011,China., L.C.Ming, M.H.Manghnani, Hawaii Institute of Geophysics, Honolulu, Hawaii, 96822, U.S.A.

Nickel oxide (Nio,Bunsenite) has served as an analogue modelling composition in relation of other monoxides such as MgO,FeO of the earth interior.the change of crystal structure of NiO from naci type F.C.C.to rhombohedral was discovered by Rooksby in 1943 at low temperature −183℃.

Recently,experiments have been carried out under pressure upto 12.0 GPa using diamond anvil cell with liquid pressure transmitting medium and direct compression to 29GPa. Our experiment shows that ,during the isothermal compression, when hydrastatic pressure was loaded up to 8.87GPa step by step , the lattice parameter and molal volume of NiO changed from ao=4.1824; Vm=11.0099; density 6.7802 at zero pressure to ao=4.1139;Vm=10.4819,and density 7.1254 at 8.87GPa. All data show small deviation from that by Drinkerman and S.K.Agrawal. The diffraction lines (111),(220)of NiO suddenly split when pressure was loaded up to 12GPa at hydrostatic compression, and the phase of NiO changed from cubic to rhombohedral. The same results were obtained by direct compression at pressures ranging from 5.8GPa to 29GPa. Lattice parameters of the new phase are a=2.9670, c=7.0000; Vm=10.7084; and density 6.9726,which agree with Rooksby's a=2.9660.

The Magnetic properties of NiO vary with pressure. Neel temperatureof NiO is 250℃ (523 ° K), which decreases when pressure increases. Below the Neel temperature,NiO changees from paramagnetic into antiferrom−agnetic, and its structure also changes into rhombohedral.

The calculated bulk modulus of NiO Birch−Manghnahan equation of state fits well with the P−V data, and assuming the theoretical bulk modulus of NiO is K_0=166.83GPa, given K_0 values of 4. Modal volume vs bulk modulus shows that the compressibility of NiO is approaching to that of MgO.

THE GROWTH OF CALCIUM CHLORAPATITE CRYSTAL

Yang Xiuming *, W.A.Rachinger **, P.P. Phakey **, J.Palamara**
* Department of geology China University of Geoscience
Wuhan 430074, Hubei, P. R. China
** Department of Physics Monash University
Clayton, Victoria 3168, Australia

Abstract

The calcium apatites are important substances both in the animal and mineral kingdoms. Fluorapatite is the major ore of phosphorous,

hydroxyapatite forms the inorganic component of bone, dentine, enamel and some pathological calcifications. The chlorapatite not only can mixed with fluorapatite constitute the base for the major phosphor compound in fluorescent lamps, but also can convert into a single crystal of hydroxyapatite. Thus the studies of chlorapatite have great significance.

The first part of this paper describes the solution growth methods used for obtaining large crystals of chlorapatite . The solution, from which crystals of chlorapatite were grown, was made up by fusing mixtures of microcrystalline β–$Ca_3(PO_4)_2$ and $CaCl_2$.The temperature of the growth was from 1330°C to 1060°C. The cooling rates were 1-3°C/hr. The largest chloraplatite crystal obtained was 7 mm in length and 2 mm in diameter.

In the latter part of this paper some optical and crystallographic properties of chlorapatite are described. At room temperature, the chlorapatite crystals were monoclinic and optically biaxial negative. Some crystals were highly twinned. It can be concluded from the surface microtopographical features that the twins were not formed during the growth period, but were formed during the cooling period.

P.5.8

THE ZONING STRUCTURE IN THE AEGIRINE CRYSTAL AS INFORMATION OF GROWTH

ZHAO Shanrong, WANG Wenkui, Department of Geology, China University of Geosciences (Wuhan), Wuhan 430074, People's Republic of China

The aegirine crystals occur in the cavities of Kuiqi granite, Fujian. The zoning structure is exhibited in the crystals. In this paper the difference in the composition and the shape between different zones in the same crystal, the growth dynamic characteristic and the growth history of the aegirine are discussed.

Based on the EMP analysis, the relationship between the colour and the composition of the zones is: the dark green zones are rich in K_2O+Na_2O and TiO_2, while the light green zones are rich in ΣFeO; the dark brown zones are rich in CaO and MnO while the light brown zones are rich in ΣFeO and K_2O+Na_2O. According

to the distribution of the zoning in the crystals, two genetic types are divided. One is growth zoning structure which is formed by growing. The zoning is only in the head of the prismatic crystal and composed of dark and light green or/and brown zones alternately. The other is alteration zoning structure which is formed by alteration. The zoning is around the crystal with one or two brown zones.

The growth zoning structure is a kind of dissipative structure. Based on the simplified dynamic equation of crystal growth and the compositional difference between different zones, the dynamic characteristic of the aegirine crystal growth is: the state of the system is supersaturated and is of non-linearity. Some components, such as Na, K, Ca, Fe, Mn, Ti, diffuse slowly in the magma. Then the growing facial state of the aegirine exchanges alternately between different states of concentration under the same environmental condition. therefore, the zoning structure in the aegirine crystals developed. The negative correlation of the ion couples (K+Na-Ca, Fe-Mn and Fe-Ti) shows that the ion prior absorbed on the growing crystal face will result in the other ion at the same crystal-chemical site repelled during the crystal growing. The zoning only appears in the head of crystal because of the faster growing rate along C axis resulting in the relative slowly diffusing rate of the ions in the magma along this direction.

The shape of the zones in same crystal are also different. Outward from centre, the shapes change from simple to complex. It shows that in the early stage of the aegirine growth, the supersaturation is lower and the shapes of zoning are equilibrium form, on the contrary, in the late stage of the growth thesupersaturation is higher and the shapes of zoning become non-equilibrium form. The external zone of the zoning structure is the morphology of the aegirine crystal. It is very various and bounded by many kinds of faces including some high index faces, such as {692}, {661} etc., and some curved faces. That is, in the last stage of growth the supersaturation is very high and the growing rate is very fast, but the cause of the increase of supersaturation in the late stage is not clear so far.

MINERAL PHYSICS

G.11.K.

Si-O BOND LENGTH VARIATIONS IN SILICA PHASES

A. Alberti, Istituto di Mineralogia, Università di Ferrara,
Cso Ercole I° d'Este 32, 44100 Ferrara, Italy

In the last three decades many authors tried to rationalize the bonding forces governing tetrahedral bond length variations in silicates, both by a variety of quantum mechanical calculations, and by the quantitative evaluation of the actual effects of bond angles, bond strength and others, through statistical analysis of experimental data. Bond length variations have been theoretically interpreted by different authors as principally due to either covalent or ionic interaction. Furthermore experimental results might be ambiguously interpreted.

In order to describe the properties of the Si-O bond in silicates and their structural variations, a multiple linear regression analysis of the available data, trying to discern the effect of the different factors which are supposed to influence the tetrahedral Si-O bond length, d(Si-O), was carried out on compositionally simple compounds: SiO_2 silicates.

The factors taken into account are:

1) The Si-O-Si angle and its functions: -sec(Si-O-Si), 1/(1-sec(Si-O-Si))

2) the <O-Si-O> angle and its functions: -sec(<O-Si-O>), 1/(1-sec(<O-Si-O>)), $2/(tg^2(<O\text{-}Si\text{-}O>))$

   where <O-Si-O> is the average of the three O-Si-O angles formed with the bridging Si-O bond

3) the distortion of <O-Si-O> defined as:
   $\sqrt{\sum_{i=1}^{3}(O\text{-}Si\text{-}O - <O\text{-}Si\text{-}O>)^2}$

4) the tetrahedral distortion defined as:
   $\sqrt{\sum_{i=1}^{6}(O\text{-}Si\text{-}O - 109.47)^2/5}$

5) the bonded distance d(O-Si2), and nonbonded distance d(Si1...Si2)

6) the electrostatic energy of ion sites

7) the nonbonded ion repulsion defined as:
$d(Si1...Si2)+ \sum_{i=1}^{3} d(O-O_i)$
where O is the bridging oxygen and O_i are the three other oxygens of the tetrahedron

Seven phases: low quartz, low cristobalite, low trydimite F1, low trydimite Cc, coesite C2/c, coesite $P2_1/a$, synthetic zeolite ZSM-5 with a ratio Al/Si ≈ 0; totalling a number of 448 individual d(Si-O) have been considered.
Almost all the considered variables correlate significantly, at the 99% level or more, with d(Si-O), and multiple regression equations for d(Si-O) were obtained at the 99.99% level of significance. Of interest is the very strong correlation between d(Si...Si) and the Si-O-Si angle over the whole range of Si-O-Si angles. On the contrary, d(Si-O) correlates with Si-O-Si angle more weakly than expected, and the correlation between d(Si1-O) and d(O-Si2) is even weaker. This data suggest that (Si...Si) interaction plays a fundamental role in the bond geometry, thus enhancing the ionic interaction in silicates. It is also worth to point out the significant correlation wich has been found between d(Si-O) and the electrostatic energy of anion site.

REAPPRAISAL OF INFRARED SPECTROSCOPY OF BERYL.

6.10K

Carlo Aurisicchio, Consiglio Nazionale delle Ricerche. Roma, Italia.
Odino Grubessi, Universita'degli Studi di Roma "La Sapienza". Roma, Italia.
Pierre Zecchini, Université de Besançon. Besançon Cedex, France.

In a previous paper [Aurisicchio et al. 1988] the complex crystal chemistry of beryl has been re-evaluated. The results show that the main substitutions concern divalent and trivalent ions for Al in the octahedral site and Li ion for Be in the tetrahedral site. Both substitution need the entry of alkali (Na,K,Cs,Rb,) ions in the channel in the "2a" position between the six-membered Si rings, whereas the "2b" position at the center of each ring is occupied preferentially by water molecules.

The effects of these substitutions on the lattice parameters allows the definition of three beryl series on the basis of the c/a ratio:
"octahedral" beryls -where Al→Me2+; c/a values in the range 0.991-0.996;
"tetrahedral" beryls-where Be→Li ; c/a values in the range 0.999-1.003;
"normal"beryls -where the substitution do not occur or may occur together, though a very limited extent;c/a values in the range 0.997-0.998.

A compositional gap exist between octahedral and tetrahedral beryls.

Although the infrared spectra of beryl have been repeteadly investigated, the assignments of the SiO4 and BeO4 internal vibration is not unanimously accepted (Plyusnina,1964; Gervais,1972; Adams et al.,1974; Hoffmeister, 1987).

To give a contribution to resolve the discrepancies of band assignements and to verify the influence of octahedral and tetrahedral substitutions, alkali and water contents, we analyse the variation of shape and position of IR bands of beryls from different source, on the basis of chemical and structural results.

3800 - 3400 cm-1 range.

As well known, in this range of IR spectra of beryl, observed absorptions bands are due to the Type-I and Type-I water,as defined by Wood and Nassau (1967)

At room temperature three typical spectra, correlated to the octahedral("Type O"), normal ("Type N") and tetrahedral beryls ("type T") were observed:

spectra "Type O": shoulder at 3698 cm-1 strong absorptions at 3663 and at 3600 cm-1;
spectra "Type N": strong absorption at 3698 cm-1 with a very weak absorption at 3663 cm-1 and at 3600 cm-1;
spectra "Type T": an equivalent absorption for both types of water.

Using low temperature measurement (N liquide) infrared spectra,best results were obtained by increasing the absorption band intensities of Type-I and Type-II water .

Low temperature measurements increase also OH absorption (Katz, 1962). That could explain the large increase of the "3663 cm-1" band. This absorption is due to the Type-II water and to OH associated with sodium, both together. OH-(Na) absorption is observable at 3658 cm-1 on spectra from large sodium content samples, this absorption is a shoulder on lower sodium content. 3600 cm-1 absorption could be the combination of OH-(Na) at 3590 cm-1 and OH-(Cs) at 3596 cm-1 with the Type - II water absorption.

A correlation were done with the sodium content and the ratio between the Type-II (3660 cm-1) and the Type-I (3698 cm-1) water absorption heights. The proposed model could explain the decrease of the Type-I water with the increase of sodium content, and the formation of OH in the neighboirhood of alcali in the channels of the beryl.

1200 - 500 cm-1 range.

In our spectra the absorption at 1200 cm-1 become more broaden and shift with the increase of Rf content in the framework channels. In order to clarify this assignement we attempt to compare some our structural data [c/a ratio, Be-O(2)*4, Si-O(1), and Al-O(2) bond distance] versus band positions.

The shift of band at 1200 cm-1 versus c/a ratio, suggests that the band shifting is lied to variation of the Si-O-Si ring bond depending on the octahedral and tetrahedral substitutions. For this band, moreover, not correlation exist between shifting and BeO(2)*4 bond distances, but, on the contrary, a good correlation exist with Si-O bond distances. So, according to Hoffmeister, we suggest to assign this vibration to SiO ring.

The band at 1060 cm-1 appears when the substitution in tetrahedral site T' is › of 0.190 u.a.f. and the band at 1020 cm-1 disappears with the increase of T'site substitution. The band at 1020 cm-1 increase and widens with the increase of the octahedral substitution and the band at 1060 cm-1 disappears.

These two bands may be caused by a variation of the "external bond" Si-O-Be and Si-O-Al rispectively.

The 950 cm-1 band shifting shows a good correlation versus Si-O(1) bond distan cies and versus c/a ratio. Thus, according to all authors we assign this band to SiO vibration.

The 805 cm-1 band shifting shows a good correletion versus BeO(2)*4 bond distances and versus c/a ratio. Therefore, according to Plyusnina we suggest to assign this band to BeO vibration.

At 700 cm-1 and 560 cm-1 , at low temperature, appears two weak shoulders that increase in intensity with the Be-Li substitutions in the T'site and disappears in the "octahedral beryls". These two bands allow to confirm the tetrahedral position of Li in the beryl structure (Tarte, 1964).

The absorption at 525 cm-1 and 500cm-1 show a good correlation versus Al-O(2)*6

bond distances and versus c/a ratio, so we assign this band to AlO6 vibration.

REFERENCE

ADAMS,D.M, GARDNER,I.R.(1974).J.Chem.Soc.,Dalton Trans., 1525-1505.
AURISICCHIO,C., GRUBESSI,O., ZANAZZI,PF. (1988).Am. Mineralogist, 73, 826-837.
GERVAIS,F., PIRIOU,B., CABANNE,F.(1972).Phys.Status Solidi, 51, 701-712.
HOFFMEISTER,A.M., HOERING, T.C., VIRGO, D.(1987).Phis.Chem.Minerals, 14, 205-224;
KATZ, A., (1962). Philips Research Reports, 17(3), 133-279.
PLYUSNINA, I.I.,(1964).Geokhimiya, 1, 31-41;
TARTE,P. (1964) .Spectrochimica Acta, 20, 238-239.
WOOD,D., NASSAU, K.,(1968) Am.Mineralogist,53, 777-800.

SPECTROSCOPIC STUDY OF ISOMORPHISM AND COLORING ROLE OF Fe IN PYROPHYLLITES

Cai Xiucheng, Zhang Huifen, Fu Yude and Tang Rongbin
Institute of Geochemistry, Academica Sinica, Guiyang, Guizhou, 550002, People's Republic of China

Structural characteristics and coloration of pyrophyllites have already been studied[1-3] . The purpose of this paper is to study the isomorphism and coloring role of Fe in pyrophyllites by spectroscopic methods.

18 natural pyrophyllite samples were collected from Zhejian and Fujien provinces. Their EPR spectra at low field consist of two absorption bands: A, g_{eff} =11.4; B, g_{eff} =4.3. The differences in the EPR spectra of 4 pure pyrophyllite samples which were treated at different temperatures were obvious: Below 400°C, both A and B became more intense with increasing temperature; Above 400°C, A decreased with raising of temperature and disappeared at 900°C, but B increased in intensity all the time; B is labeled here as B', because its increasing is related to dehydroxylation; B' at 900°C is more intense than A in initial samples. IR and DTA data showed that the dehydroxylation began at ~500°C and ended at 900°C. Therefore we can get the following interpretations:

1) Reducing-increasing process in intensity between A and B' bands during thermal treatment, and its synchronism with the dehydroxylation demonstrate that A and B(and B') bands are generated by the same paramagnetic ions. Because of the similarity of B' to absorption(g_{eff} =4.3) of Fe^{3+} in octahedral sheets of kaolinite, A ought to be attributed also to Fe^{3+}, which isomorphously replacing the Al^{3+} in octahedral sheets of pyrophyllite.

2) B' at 900°C consists of 4 lines: One(g_{eff} =4.3) is the same with Fe^{3+} line of dehydrated kaolinite and glass, $\lambda = 1/3$. Such Fe^{3+} ions are situated in tetrahedra $Al^{3+}(Fe^{3+})-O_4$; Other three lines(g_{eff} =4.5, 4.2, 4.1) should be attributed to Fe^{3+} ions in trigonal bipyromid $Al^{3+}(Fe^{3+})-O_5$, $\lambda < 1/3$. Thus it may be deduced that in natural

pyrophyllites, isomorphous Fe^{3+} ions have two coordinations: main $Al^{3+}(Fe^{3+})-O_4(OH)_2$; minor $Al^{3+}(Fe^{3+})-O_2(OH)_4$.

3) The facts that both A and B increased with raising of treatment temperature < 400°C, intensity of B' at 900°C exceeds that of A in initial samples propose that isomorphous cation in octahedral coordination are not only Fe^{3+}, but also Fe^{2+} oxidated during heat treatment.

Moreover, relative content of Fe^{3+} (from A) and total iron content(Fe_2O_3) were determined(Tab.1). It is obvious that the concentration of iron(or Fe^{3+}) is closely related to the coloration of pyrophyllite. Optical spectra of initial samples show that absorption band at 5520 Å is attributed to Fe^{3+}; Changes in their intensity and width make the samples to be colored in different tones. Optical spectra of violet-red and pink pyrophyllites treated at 900°C show also that the absorption at 5200Å are generated by Fe^{3+} (charge transfer transition). Therefore, isomorphous Fe^{3+} ions are major origin of violet-red and brick-red colors of pyrophyllites, which is consistent with (3).

Tab. 1 Contents of total iron and Fe^{3+}(A band) in pure pyrophyllites

sample No	Q-6	Q-7	Q-1	Q-3	N-58	N-59
color	violet red	yellow	yellow green	light green	green grey	grey
total iron (Fe_2O_3) %	0.69	0.41	0.37	0.28		
Fe^{3+}(A, rel.cont.) $\times 10^{15}$ sp./mg	0.24	0.22	0.13	0.11	0.04	0.03

References
(1) Литовченко А.С. и др.: 7 conf. Clay Mineral. and Petrol. in Kardlevy Vary, 1976, Geologica Proha, 1977, p.49
(2) Wardle Ronald and Brindley G. W. : Amer. Mineralogist, vol.57, 1972, p.732
(3) 范良明、楊永富：硅酸盐通报，1984年，第5期，第1页

Po6.1.

DIRECT DETERMINATION OF Fe^{2+} AND Fe^{3+} IN IRON-BEARING MINERALS BY ELECTRON PROBE QUANTITATIVE ANALYSIS

CHEN Keqiao, Institute of Mineral Deposits, Chinese Academy of Geological Sciences, 26 Baiwanzhuang Road, Beijing, China

The electron probe quantitative analysis of iron-bearing oxide or silicate at present can only yield the quantitative result of TFe, rather than the separate

quantification of Fe^{2+} and Fe^{3+}. Therefore, for solving the problems of mineralogy, petrology and mineral deposits, the methods such as the residual–oxygen calculation and the velence–balancing of chemical formula of mineral are usually used to calculate the Fe^{2+} and Fe^{3+} contents and the chemical formula.

Studies by domestic and foreign scientists indicate that the Fe^{2+} and Fe^{3+} contents in minerals (the average valence state of iron) are somewhat proportional to the FeLβ / FeLα ratio. We made an electron probe quantitative analysis of each mineral of the ten available standard samples (hematite, goethite, magnetite, titannomagnetite, chromite, ilmenite, epidote, ilvaite, almandine, olivine) using a JXA–733 electron probe microanalyser produced by JEOL (connected with an American TN–5500 energy dispersive spectrometer), and determined the counting rate of FeLβ and FeLα. Then we calculated their respective FeLβ / FeLα ratios and, drew the correlation curves of FeLβ / FeLα ratio versus average valence state of iron.

Four minerals with chemically analytical results and known Fe^{2+} and Fe^{3+} contents are taken as unknown samples; the FeLβ / FeLα ratio for each mineral can be calculated using the results of determinations by electron probe quantitative analysis and FeLβ and FeLα counting rate methods. The average valence state of each mineral can be obtained on the basis of FeLβ / FeLα ratio versus and then the percentage contents of Fe^{2+} and Fe^{3+} are calculated using the following equations:

$$X_{FeO} = \frac{(3-N) \times n_{Fe} \times n_{Fe_2O_3}}{(N-2) \times n_{FeO} \times 2n_{Fe} + (3-N) \times n_{Fe} \times n_{Fe_2O_3}} \times C\%$$

$$X_{Fe_2O_3} = \frac{(N-2) \times n_{Fe} \times n_{Fe_2O_3}}{(N-2) \times n_{FeO} \times 2n_{Fe} + (3-N) \times n_{Fe} \times n_{Fe_2O_3}} \times C\%$$

where X_{FeO} is the true percentage content of FEO in mineral, $X_{Fe_2O_3}$ the true percentage content of Fe_2O_3 in mineral, N the average valence state pf iron in mineral, n the moleculer (or atomic) weight, and C% TFeO percentage content obtained through quantitative analysis by electron probe BA method.

A comparison with the chemically analytical results suggests that the quantitative analyses of Fe^{2+} and Fe^{3+} in several minerals by electron probe are relatively ideal on the whole. Under microscope, the first two minerals exhibit a lot of intergrown quarter crystals that can not separated thoroughly. For such a kind of minerals, therefore, the percentage contents of their Fe^{2+} and Fe^{3+} directly determined by electron probe quantitative analysis are surely better than those detected by wet chemical analysis.

ELECTRON IRRADIATION EFFECTS IN QUARTZ SINGLE CRYSTALS AND POLYCRYSTALLINE MATERIAL

O.W. Flörke*, B. Martin* , K. Röller*, R. Wirth**
*Inst.f. Mineralogie,RUB Bochum, 4630 Bochum, Germany
**Institut für Neue Materialien GmbH, Universität Saarbrücken, 6600 Saarbrücken, Germany

Po62.

Quartz single crystals with different crystallographic orientations (c-cut (0001) and x-cut ($2\bar{1}\bar{1}0$)) have been irradiated by electrons in an electron microscope at 200 kV. The irradiation results in the formation of strain centers followed by a crystalline-amorphous transformation of the crystal. The appearance of the amorphous state is correlated with the generation of streaks and an elliptical elongation of the electron diffraction spots. The deformation of the diffraction spots is a result of the deformation of the single crystal lattice caused by the volume increase of the amorphous state of SiO_2.
Additional irradiation experiments have been carried out at dislocations and grain boundaries. Results:

- Size and number of the strain centers increase with the irradiation time.
- Irradiation damage is enhanced in those samples with the crystallographic orientation ($2\bar{1}\bar{1}0$) compared with samples cut (0001).
- At grain boundaries irradiation generates amorphous regions along the grain boundary. The width of the amorphous region at different boundaries depends on the crystallographic orientation relationship of the two adjacent grains.
- In the vicinity of the grain boundary at both sides of the boundary there is a zone free of strain centers. The width of this zone is different in two adjacent grains and can be correlated with the crystallographic orientation of the grains.
- Similar observations concerning the width of the amorphous regions along the grain boundaries have been made at quartz-mica phase boundaries.

Po 6.3.

PRELIMINARY STUDY OF SILICON-29 AND ALUMINUM-27 MASS NMR SPECTRA OF SOME SILICATE MINERALS

GUO Jiugao,* YE Chaohui, HE Zhihai, CHEN Feng, WANG Zhuming, Laboratory of Magnetic Resonance and Molecular Physics, Wuhan, 430071, People's Republic of China

Since 1980, the solid-state high resolution NMR techniques have been introduced into mineralogy. Among these magic angle sample-spinning (MASS) NMR technique was extensively used. It is shown that this method is a powerful tool for examining the local structural enviroment of a wide variety of atoms in minerals. The most significant application of that will be to those problems that cannot be addressed using XRD or TEM method, these include order/disorder, the structure of amorphous and fine-grained materials etc.. This paper will briefly introduce the results of ^{29}Si and ^{27}Al MASS NMR spectra of

some minerals.

The minerals studied were characterized by XRD.Apart from that some clay minerals mixed with quartz,no discovering any apparent impurity minerals. The spectra were recorded on Bruker MLS-400 NMR spectrometer with magic-angle sample-spinning rotor assemblies. The rotation rates are from about 3 to 5 KHz. Peak chemical shift are reported in ppm from external TMS for silicon-29 and $Al(NO_3)_3$ for aluminum-27. Three sinter mullite examined were fired at 1350℃ ,1500℃ and 1730℃ respectively and one mullite which is a commodity made in England was also measured for comparison. The results show there are three peaks in ^{29}Si MASS NMR spectra, and peak chemical shift is at -97.2, -92.6 and -87.3 ppm which may be due to mullite $Q^2(0Al)$, $Q^2(1Al)$ and $Q^2(2Al)$ separately. The relative intensity of the peaks varies with increasing fire temperature and these ^{29}Si spectra show also systematic variation in full width at half-height which is consistent with the results of XRD. The coordinate state of Al is also varies with fire temperature change.

^{29}Si chemical shift of pyrophyllite, montmorillonite and kaolinite is -95.2, -93.4 and -91.4 ppm, which is identical with published data. The difference in shift among these minerals can be explained according to the difference in structure. ^{27}Al chemical shift of pyrophyllite and montmorillonite is 3.2 and -0.6 ppm separately which is similar with the paper by D.E.Woessner (1989). However, ^{27}Al chemical shift of kaolinite is quite different with the data reported by R.A.Kinsey et al.,(1985). The spectra of four kaolinite and a dickite consist of a narrow peak at -1.1 ~ 2.4 ppm and a shoulder at about 9 ppm, which shows there are two distinct octahedral aluminum sites in these samples.

The ^{29}Si MASS NMR spectra of a natural illite is also consistent with presence of multiple silicon sites,which contain a large peak at -85.8 ppm ($Q^3(1Al)$) and shoulder peaks at -88.5 ppm ($Q^3(0Al)$),and at about -82.0 ppm ($Q^3(2Al)$). Our results are similar with ^{29}Si NMR spectra of a synthetic illite by C.A.Weiss et al., (1987). ^{27}Al MASS NMR spectrum of illite consists of a large peak at 3.0 ppm that is due to octahedral Al site and a small peak at 68.8 ppm that attributes to tetrahedral Al site,which is consistent with the data by Kinsey et al..

G.5 H
Po 14.6.

INFRARED SPECTROSCOPIC STUDY OF PYROPE

GUO Lihe, WANG Wuyi, WANG Alian and ZHANG Andi, Laboratory of Physical Mineralogy, IMD, CAGS, 26 Beiwanzhuang Road, Beijing 100037, China

Infrared spectrum of 124 pyropes from Chinese kimberlites and non-kimberlitic sources were measured. Some typical grains were selected for EMP analysis. As the IR and compositional information are obtained from the same pyrope grain, it is possible to contrast the spectroscopic character with its chemical composition.

Pyrope belongs to garnet group with chemical formula A3B2(SiO4)3, where A=Mg2+,Fe2+,Ca2+...; B=Al3+,Cr3+,Fe3+... . It has a space group Ia3d-Oh10, Z=8(ZB=4). The crystal structure refinement work [Ref.1] indicates that the A,B cations and (SiO4) groups occupy the D2, S6 and S4 sites respectively. The analysis of the normal vibrational mode by group theory gives for pyrope a total of 237 vibrational modes. Besides the 125 non-optical active modes, there are 17 IR active triple-degenerated modes of F1u species and 25 Raman active modes. IR spectrum of pyrope has 10 fundamental viberation bands in the 4000-200cm-1 region (labeled as A,B,...,k Fig.1). Bands(A—D) in 1000-850 cm-1 region and (E—G) in 650-500cm-1 region correlated respectively with V3 anti-symmetric streching viberation and V4 unsymmetic bending viberation of (SiO4) tetrahedra. The bands below 500cm-1, H,I and J,K, mainly correlated with the cations in octahedra and dodecahedra respectively [Ref.2,3,4,5]

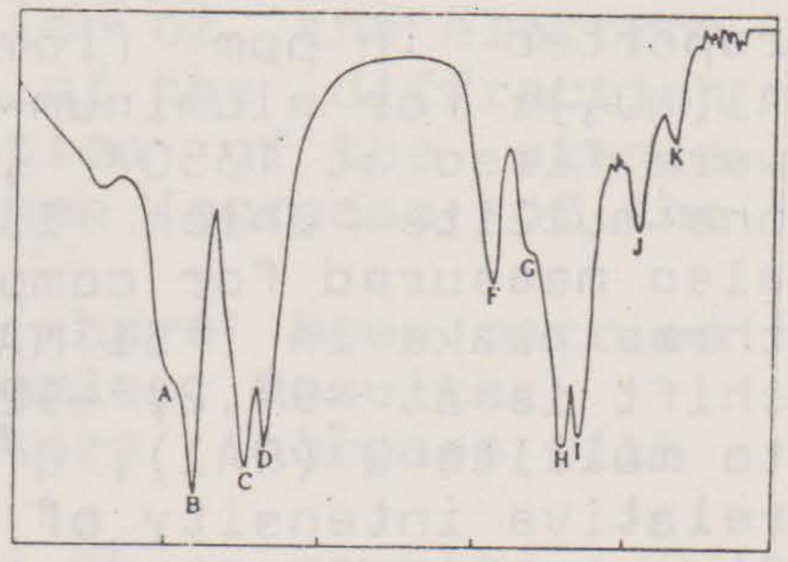

Fig.1 IR spectrum of pyrope

The frequencies of the bands A — G varies with the Si-O bond length of (SiO4)4- tetrahedra. The frequency differences (C-D) and (B-(C+D)/2) of bands B,C,D are assigned to factor group splitting (B——2F1u) and site group splitting (E——A+B) respectively. Both factor group splitting and site group splitting are related to octahedral cations. With the increasing of substitution of Cr3+ for Al3+, the changing extent of the symmetry of force field around tetrahedron will increase, resulting in the increasing distortion of the tetrahedron, which will be reflected in the increasing of site group splitting (B-(C+D)/2); on the other hand, the distance between tetrahedra increases with the substitution, because the radius of Cr3+ (=0.615A) is larger than that of Al3+ (=0.535A). So the interaction between tetrahedra will decrease, resulting in the decreasing of factor group splitting (C-D). this theoritical analysis is verified by our experimental results as follows:

Sample	Cr2O3 wt%	[B-(C+D)/2] cm-1	[C-D] cm-1
B10	0.02	82.3	27.5
B7	1.95	83.3	26.0
B2	6.89	84.8	25.4
B1	11.16	85.6	20
3-1	15.31	85.4	20

Both (C-D) and (B-(C+D)/2) splittings might also be influenced by the substitution of the cations in dodecahedra. In brief, IR spectroscopic characters of pyrope show comprehensive information not only about its chemical composition , but also about its structural features.

IR analysis of pyrope grains from diamondiferous and barren kimberlites,

mantle xenoliths in kimberlite and basalt, and difference types of non-kimberlitic rocks has been done. Relation of (C-D) splitting vs (B-(C+D)/2) splitting is shown in Fig 2. It was found that the pyropes which come from diamondiferous kimberlites and its dunite xenolith have low (C-D) values and high (B-(C+D)/2) values comparatively. It is contrary to that of the pyropes which come from barren kimberlites and non-kimerlitic rocks. Therefore IR spectroscopic characters of pyropes provide the information about the genetic enviroment of the pyropes. Obviously, this technique has the potential as a new method to discriminate the source of indicator minerals in the diamond exploration to come. This work provides the theoretical basis of that method.

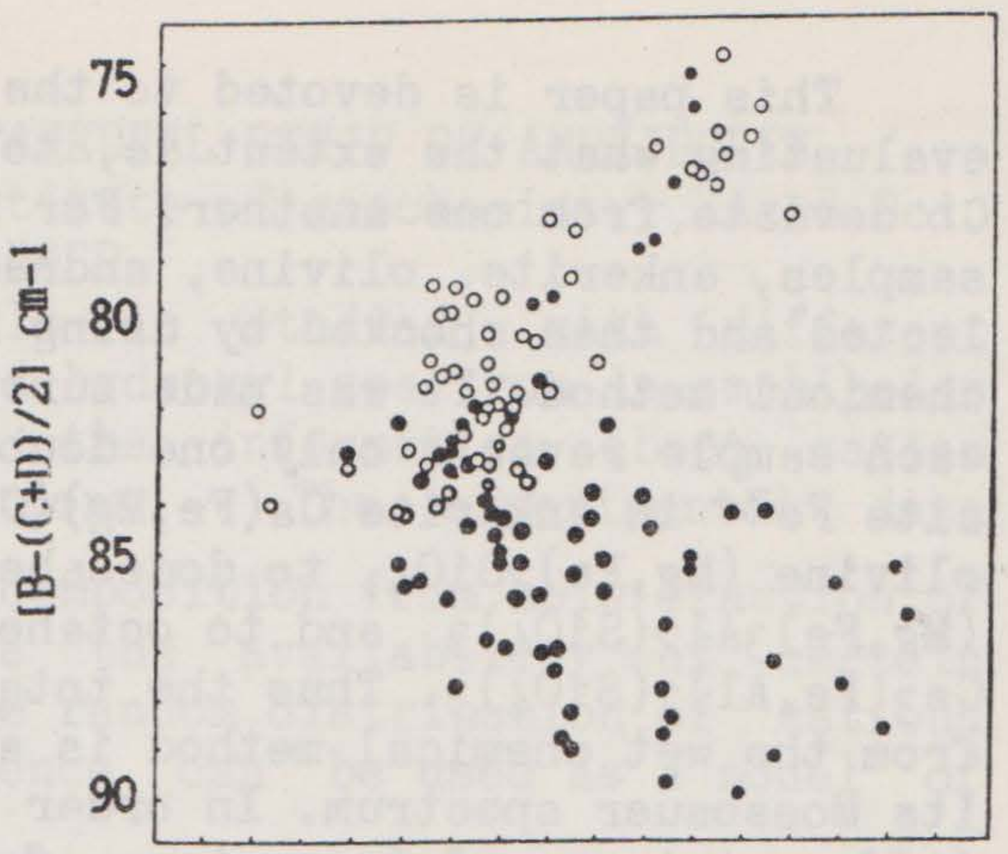

Fig.2 [C-D] vs [B-(C+D)/2] of pyropes
Black point: from diamondiferous kb & its dunite xenoliths; Circle: from barren kb & non-kimberlitic rocks

References

[1] Gibbs, GV and Smith JV (1965), Am. Mineral., 50: 2032-2039
[2] Moore, RK, et al. (1971), Am. Mineral., 56: 54-71
[3] Tarte, P, (1965), Mem. Acad. r. Belg. cl. Sci., 35: 103-119
[4] Wang, A (1987), Ph.D thesis, LASIR. Lille, France
[5] Wang, WY (1988), Master thesis, CAGS, Beijng, China

THE DETERMINATION OF CONSTANT C=Ca/Cb IN MÖSSBAUER SPECTROSCOPY

KAN Xuemin, ZHANG Enlin and LI Yirong; Institute of Geochemistry, Academia, Sinica, Guiyang 550002, P. R. C.

6.9K

The quantitative use of Mossbauer spectroscopy is based on the formula:

$$\frac{Sa}{Sb} = \frac{Ca}{Cb} \cdot \frac{Na}{Nb} \qquad (1)$$

where Sa and Sb are the peak areas, and Na and Nb the concentrations, of different types of iron atoms (a) and (b), respectively, and Ca and Cb are the constants which should be related to the line widths, saturation corrections and recoil-free fractions of the respective types of the iron atoms. As it is difficult to obtain the accurate values of Ca and Cb, in most circumstances people assume $Ca/Cb = 1$. However, it was reported that in some minerals such as garnets Fe^{3+} is held more rigidly in its site, such that the Mossbauer spectrum appears to have more Fe^{3+} than is actually present (Dyar M. D. et al., Amer. Mineral. 72(1987) 792-800).

This paper is devoted to the experimental investigation for evaluating what the extent is, to which the coefficients Ca and Cb deviate from one another. For this purpose four mineral samples, ankerite, olivine, andradite and almandite, were collected and then checked by using Mossbauer spectroscopy and wet chemical method. It was made sure that the Mossbauer spectrum of each sample reveals only one doublet, which belongs to octahedral site Fe^{2+} in ankerite $Ca(Fe,Mg)(CO_3)_2$, to M1 and M2 site Fe^{2+} in olivine $(Mg,Fe)_2SiO_4$, to dodecahedral site Fe^{2+} in almandite $(Mg,Fe)_3Al_2(SiO_4)_3$ and to octahedral site Fe^{3+} in andradite $Ca_3(Fe,Al)_2(SiO_4)_3$. Thus the total iron content of each sample from the wet chemical method is attributed to the only doublet of its Mossbauer spectrum. In order to measure the Ca/Cb ratios for different types of iron atoms, four absorbers, which consist of two different mineral samples each, were prepared: 1. (ankerite + olivine), 2. (olivine + andradite), 3. (andradite + almandite), 4. (almandite + ankerite). For each absorber, Na and Nb are accurately definite with $Na/Nb \simeq 1$. On the other hand, to ensure the measurement of Sa/Sb with satisfactory accuracy, it was carefully checked that the separations of the peaks in the spectra of the absorbers are all larger than 0.4 mm/s. The effective thicknesses of the absorbers are all about 5 $mg(Fe)/cm^2$ and the Mossbauer measurements were accomplished at room temperature. Obviously, only three independent Ca/Cb ratios can be obtained through Mossbauer measurements of the four absorbers. After rewriting Ca (or Cb) into Cakr for ankerite, Colv for olivine, Cadd for andradite and Calm for almandite and choosing olivine for a reference mineral, our results can be shown as follows:

$$\frac{Cadd}{Colv} = 0.964(\pm 0.025)$$

$$\frac{Calm}{Colv} = 0.874(\pm 0.020)$$

$$\frac{Cakr}{Colv} = 0.828(\pm 0.015)$$

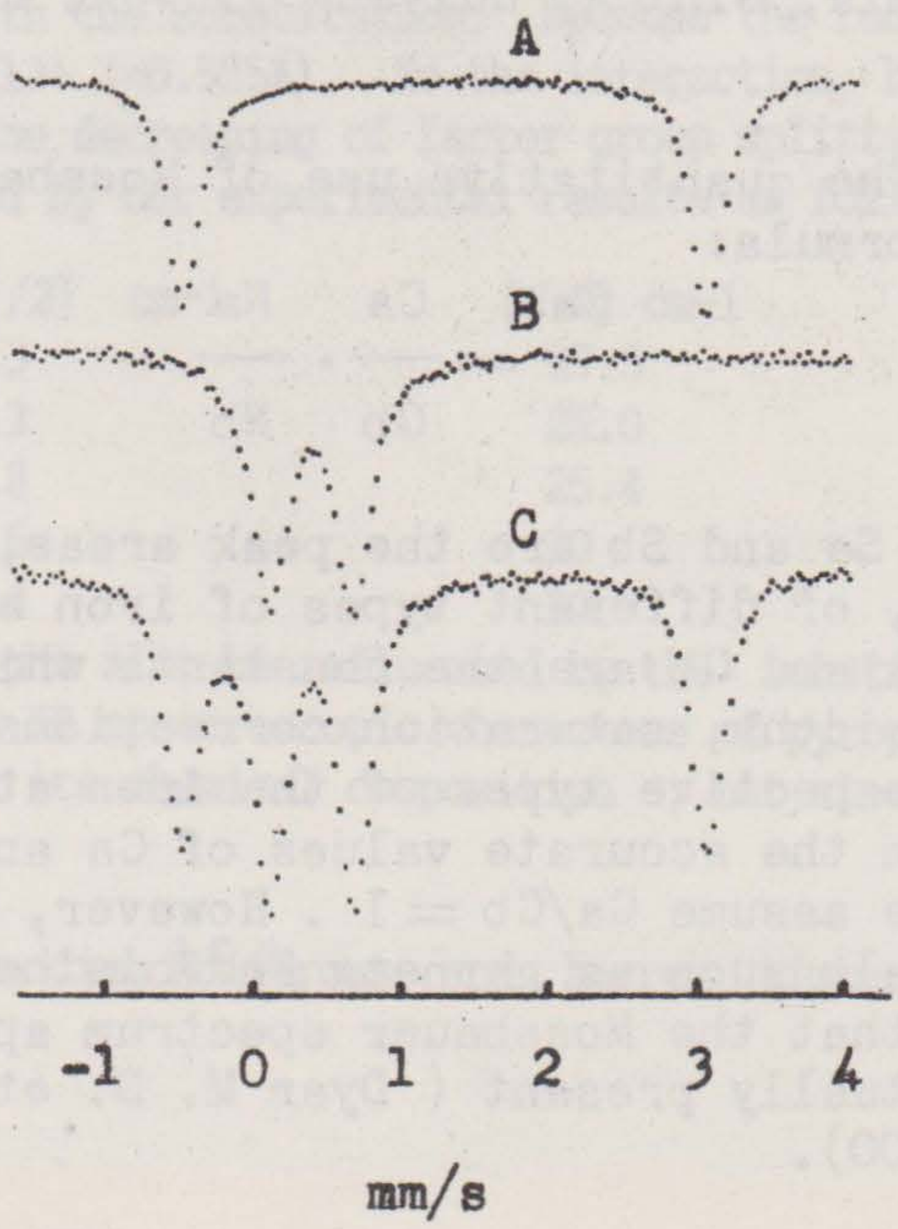

Fig. 1. Mossbauer spectra
A. Almandite
B. Andradite
C. The absorber (almandite + andradite) with Nadd/Nalm = 1.00

MARKOV CHAIN SIMULATION OF THE OCTAHEDRAL STRIP OF AMPHIBOLES.

Lapides I.L., Lustenberg E.E., Institute of geochemistry, Acad.Sci. (Sib.Dept) USSR. Irkutsk, 664033, USSR.

The cations distribution in minerals is studied with different methods. The analysis of infrared hydroxyl spectrum in amphiboles gives the possibility to obtain the information about cation distribution in $2M_1$ and M_3 - positions. The experimental data about dependence of cation triads composition from mole fraction of cations make it possible to suppose the availability of certain objective law which contradict the random distribution of cations on the positions.The symbol sequence can be used as a model of cations sequence.

There are two extreme possibilities in this case: the hard causal dependence between symbols or their full statistical independence. It is interesting to study the correlation between the real cation sequences with these extreme variants.

First and second order Markov's chains (stationary and unstationary) were used for that purpose. The simulation of concrete sequences (binary variant) has been carried out by means of Monte-Carlo method. For the Markov chains of the second order the stochastic simulation has been realized. It is possible, in this case, to append the different restrictions (such as the correlation between near- and long-range order parameters, a chain composition variations etc.) on the transition probabilities. The unstationary Markov chains of the second order provide the best approximation to the experimental data. The number of distributions of chain, the Kolmogorov entropy among them, have been obtained. The facts of derivation from the general dependence, the information significance of received models have been discussed.

THE SPECTROSCOPY OF NORDENSKIOLDINE FROM CHINA

Li Dien and Peng Minsheng, Department of geology, Central South University of Technology, Changsha, Hunan, 410083, China

Nordenskioldine, $CaSn(BO_3)_2$, a rare ortho–borate mineral, was recently found in an andradite–diopside skarn belt between carbonate rock and granite in the Gejiu tin deposit, Yunnan, China. The studies in this paper are focused on the electron paramagnetic resonance(EPR), infrared and Raman spectra of the nordenskioldine.

EPR spectra of the nordenskioldine at 300k and at 77k show a well resolved sextet lines due to $Mn^{2+}$with EPR parameters $g=1.9993$ and $A=89.92\times10^{-4}cm^{-1}$and the signals of $Fe^{3+}$with $g=4.8213$. The EPR signals of $Mn^{2+}$and Fe^{3+}do not change with rotation angles when the applied magnetic field is parallel to c–axis, which means that $Mn^{2+}$and Fe^{3+}, whose electronic configuration is $3d^5$, are in the axial sites. According to the EPR parameters of $Mn^{2+}$and $Fe^{3+}$and the structural data of nondenskioldine, it is reasonable to suggest that $Mn^{2+}$and Fe^{3+}prefer to substitute for Ca^{2+}in the more distorted octahedra

ions is ^2E_g rather than $^2A_{1g}$. Table 1 lists the observed values of the crystal field transition frequencies and g-factors of Cu^{2+} ions in $BaCuSi_4O_{10}$ together with the calculated ones using a point charge model.

2. Similar calculations have been made on dioptase ($Cu_6(Si_6O_{18}).6H_2O$) and $CaCrSi_4O_{10}$. Although Cu^{2+} ions in dioptase are 6-coordinated, as a good approximation, they can be treated as being square planar coordinated because $R_5, R_6 \gg R_1=R_2=R_3=R_4\equiv R$. $CaCrSi_4O_{10}$ is also isostructural with gillespite. The ground term of Cr^{2+} ions in $CaCrSi_4O_{10}$ is expected to split in the same manner as that of Cu^{2+} ions in $BaCuSi_4O_{10}$. The calculated results for dioptase and $CaCrSi_4O_{10}$ are also given in Table 1.

Table 1

Assignment	Transition frequency(cm^{-1})					
	$BaCuSi_4O_{10}$		Dioptase		$CaCrSi_4O_{10}$	
	Obs.[1]	Calc.*	Obs.[3]	Calc.**	Obs.[4]	Calc.+
$^2B_{1g}\rightarrow\ ^2B_{2g}$	12650	12650	10300	10300	14390	14390
$\rightarrow\ ^2A_{1g}$	15100	15040	13050	13348	19570	19705
$\rightarrow\ ^2E_g$	16500 18400	17600	15000 15820	15186	22080	21970
$g_{\parallel}$	2.342	2.342				
$g_{\perp}$	2.063	2.062				

*Using $\eta\langle r^2\rangle/R^3=0.0456$ a.u., $\eta\langle r^4\rangle/R^5=0.0346$ a.u., and $\lambda=-540$ cm^{-1}

** $\eta\langle r^2\rangle/R^3=0.0414$ a.u., $\eta\langle r^4\rangle/R^5=0.0402$ a.u.

+ $\eta\langle r^2\rangle/R^3=0.0602$ a.u., $\eta\langle r^4\rangle/R^5=0.0393$ a.u.

3. The energy level order determined by the AOM is the same as that predicted by LFT.

4. EHMO calculations on a CuO_4^{6-} cluster show that the uppermost state can be either A_{1g} or E_g depending on the parameter values chosen, but in all cases, the energy differences between the a_{1g} and e_g orbitals are too small to account for the observed spectra.

1. Lin Chuanyi et al., Acta Mineralogica Sinica 5(1985) 301(in Chinese)

2.W.G.Clark & R.G.Burns,J.Chem.Soc.,(1967)1034
3.Zhu Hebao et al.,Acta Scientiarum Naturalium Universitatis Guizhou, 3(1988)193 (in Chinese)
4.H.L.Belsky et al., Am. Mineral.,69(1984)771

P065.

Site Occupancy and Local Properties of Fe^{2+} in Orthopyroxenes

Lin Chuanyi[a], Zhang Li, P. Turk, and S. S. Hafner
Institute of Mineralogy, University of Marburg, 3550 Marburg, West Germany

[a] permanent address: Institute of Geochemistry, Guangzhou Branch, Academia Sinica, China

Over the past two decades, many studies have been carried out on the electronic state of Fe^{2+} and its distribution over the M_1 and M_2 sites in pyroxenes. Several questions, however, are still open. For example, the mm2 (C_{2v}) model used by Runciman et al. (1973) or Goldman and Rossman (1977) to interpret the optical absorption spectra of orthopyroxenes (OPX), needs confirmation because the predicted energy interval between the $Fe^{2+}(M_2)$ ground and first excited states has never been observed experimentally. In order to test this model, four samples of OPX were synthesized at 30 kbar and 900°C, x = Fe/(Fe+Mg) being between 0.4 and 0.8.

Lattice constants were determined using 16 unambigously identified reflections for each sample (Table 1).

Table 1 Latice constants of 4 synthetic orthopyroxenes

Sample	x	a (Å)	b (Å)	c (Å)	V (Å^3)
OPX3	0.4	18.309(4)	8.929(1)	5.213(3)	852.30
OPX4	0.5	18.328(3)	8.945(2)	5.218(2)	855.36
OPX5	0.6	18.345(3)	8.972(1)	5.224(2)	859.84
OPX6	0.8	18.372(5)	9.009(3)	5.229(3)	865.41

Mossbauer spectra of ^{57}Fe were taken at temperatures between 4.2 and 78 K and 295 K to study the thermal shifts, TS, and temperature dependence of nuclear quadrupole splittings, QS, at M_1 and M_2. The data were interpreted in terms of crystal field theory, assuming a pseudosymmetry mm2 and an effective axial symmetry for the crystal field at M_2 and M_1, respectively. Predicted signs of V_{zz} for Fe^{2+} at both M_1 and M_2 are positive. For Fe^{2+} at M_2, calculated values of the asymmetry parameter and the predicted orientation of the EFG principal axes system with respect to the crystallographic axes system are also given. These results may be compared with those obtained from single crystal Mossbauer data of a natural enstatite $Mg_{0.86}Fe_{0.14}SiO_3$ (Stanek and Hafner, 1988).

In order to obtain information about the temperature dependence of the Fe^{2+}, Mg distribution over M_1 and M_2, heating experiments were carried out under controlled conditions: (i) 600°C, using a sealed gold tube filled with N_2, P = P_{N_2} = 3 bar, 72 h to 3 weeks; (ii) 600°C, P = P_{H_2O} = 1 kbar, in a Morey autoclave

using a Ag-Pd tube (inner tube, filled with sample and a small amount of water) and a gold tube (outer tube, filled with Fe-Fe_3O_4 buffer and a certain amount of H_2O), 72 h to 3 weeks. Conclusions on the kinetics of the Mg, Fe^{2+} exchange in the lower region of effective temperatures will be presented.

J. Stanek and S.S. Hafner, Hyperfine Interactions, **39** (1988) 235-252.
W.A. Runciman et al., Am. Mineral.,**58** (1973) 444-450.
D.S. Goldman and G.K. Rossman, Am.Mineral., **62** (1977).
151-157.

GENERATION AND DEGRADATION OF PARAMAGNETIC CENTRES IN NATURAL QUARTZ

Lutoev V.P.
Institute of Geology, Komi Scientific Centre, Ural Division, USSR Academy of Sciences, Oplesnina 2, 167610, Syktyvkar, USSR

There are many electron-hole centres in quartz using in mineralogical aims. In order to make them detectable it is necessary to transfer them in paramagnetic state, but this process depends on history and genesis of the sample. The oxygen-hole O_n^{m-}--R^+ [1,2] and modified aluminum centres [3] which structure is still unsufficiently understanded are of great interest. We attempted to find a general tendency of generation and degradation of the set of paramagnetic centres in basic types of quartz crystals alpine veins of Ural deposits.

The investigation was carried on single crystals by EPR at 77 K and 300 K. The generation and degradation of paramagnetic centres were stimulated by gamma-radiation of Cs-source (0-10^6 Gy) and cyclic isochronous annealing on air (75-720 K). Stable centres were studied only. After every step radiation or annealing the set and contents of paramagnetic centres were recorded.

It is possible to select three type of the quartz crystals of the region: smoky, smoky-citrine and citrine, amethists. The colourless radiation-resistant crystals are geneticaly assosiated with amethist and similar to it. E_1'-, E_2'-, E_4'-, [Ge(E_1')]-, [AlO_4]-centres have the same level of contents in all species. The content of [Ge(E_2')H^+], [Ge(A,C)Li^+] and modified aluminum centres B in the second type of crystals is significantly higher and content of O_n^{m-}--R^+-centres is hihger in smoky quartz. [AlO_4LiH]-, [Ti(A)H^+]- centres and modified aluminum centres A are typical only for citrines and smoky-citrines crystals. Iron centres $Fe^{3+}I$, $Fe^{3+}S^1$, $Fe^{3+}S_2$ are present only in amethists and amethist-like crystals.

Two intervals of radiate generation of centres was fixed. The generation and the following radiation-induced degradation of impurity-related electron centres, [AlO_4]- and [AlOLiH]-centres took place before dose of 10^6Gy was accumulated. The general scheme [4] describes this process.

Further radiation caused the radiation-induced degradation of [AlO_4]-, [AlO_4LiH]-centres and the increase of contents of E_2'-, O_n^{m-}-R^+ -, modified aluminum cetrnes.

The annealing stimulated monotonous degradation of electron E_2'-, E_4'-, [Ge(A,C)Li^+]-, [Ge(E_2')H^+]-, [Ti(A)H^+] and hole [AlO_4]-, [AlO_4LiH]-centres. The degradation of these hole centres was accompained by the increase of Si and Ge E_1'-, O_n^{m-}-R^+- and modified aluminum centres content.

Hence the generation of paramagnetic state of O_n^{m-}-R^+ and modified aluminum centres has two stages. The radiation stimulates formation of hole deep traps located on their pre-centres. It is possible that this process proceeds by a loss of protons. At further radiation or annealing these traps re-capture the holes located on the aluminum centres.

Obtained data give a possibility to pick out optimal conditions for the influence on quartz of various genesis. Though the radiation dose or the annealing temperature required for detection of maximal content of paramagnetic centre varied, the variation was a little for samples of the same quartz crystal type.

Reference:

1. Bershov L.V., Marfunin A.S., Speransky A.V. A new stable radiation center in quartz.-Int.Geol.Rev. (1980), v.22, N.10, p.1225-1233.
2. Orlenev P.O., B.M. Moiseev New paleodosemetric centre in natural a-quartz. - Doklady AS USSR (1985), v.283, N.5, p.1274-1277 - in Russian.
3. Mashmeyer D., Nieman K., Hake H., Lehmann G., Rauber A. Two modified smoky quartz centers in natural citrine.-Phys.Chem.Minerals (1980),v.6, N.1, p.145-156.
4. Weil J.A. A review of electron spin spectroscopy and its application to the study of paramagnetic defects in crystalline quartz.- Phys.Chem.Minerals (1984), v.10, N.1, p.149-165.

DETERMINATION OF TRACE ELEMENTS IN ROCKS AND SOILS BY X-RAY FLUORESCENCE SPECTROMETRY

MAO Huixin and ZHANG Mengqun

Center of Materials Analysis, Nanjing University
Nanjing, Jiangsu 210008, People's Republic of China

Based on the matrix correction reported by R. C. Reynolds, the authors have successfully resolved the determination of 26 trace elements (ppm) with the calibration curves obtained from the measurement of standard samples and the regression analysis of their results on the X-ray fluorescence spectrometer "Shimadzu VF-320".

The measured lines of analyzed elements are usually overlapped by some interfering lines of other elements contained in the sample, for example

AsK_α(λ=1.177A) by PbL_α (λ=1.175A),
Y K_α(λ=0.830A) by $RbK_{\beta 1}$(λ =0.829A), and
NbK_α(λ=0.748A) by Y $K_{\beta 1}$(λ=0.741A).

The elaborate and efficient subtraction for these overlapped peaks has been studied and the good calibration curves have been obtained for all 26 trace elements. It has also fulled up the function deficiency of the software in VF-320 computer.

The specimen preparation technique has been improved as well. About 4 grams of each sample ground to 200-mesh powder was pressed into briquette, then the trace elements can be measured successively on the briquette. The expense for this specimen preparation has been reduced to the minimum value. These measured elements are Co, Ni, Cu, Zn, Ga, As, Rb, Sr, Y, Zr, Nb, Mo, Sn, Sb, Ba, Hf, W, Tl, Pb, Bi, Yb, Th, U, Fe and Ti, Mn as well.

SPECTROSCOPIC INVESTIGATIONS OF TOURMALINES

R.I.Mashkovtsev, I.I.Urosov. Institute of Geology and Geophysics, Siberian Branch of the Academy of Sciences of the USSR, 630090, Novosibirsk, USSR

Natural and synthetic tourmalines were investigated by infrared, optical and ESR spectroscopy.

Series of synthetic samples were investigated beginning from alkali-free aluminic tourmalines up to alkali Fe- and Mg-rich tourmalines. With the substitutions of Al ions in Y and Z octahedra by Mg or Fe ions systematic changes in IR spectra of OH groups are

observed. Frequencies of the valence band vibrations of OH_I and OH_{II} draw together and finally make one asymmetric and wide band.

Study of natural elbaites showed that by isomorphic substitutions in octahedra the valence vibrations of OH_{II} groups display the one-mode behaviour type, and two-mode behaviour type is observed in OH_I valence vibrations.

Colourless elbaites frequently turn yellow after gamma irradiation. In this case paramagnetic centers (PC) on defects of the structure are observed. One PC has $g_{//} = 1.994$, $g_{/} = 2.008$ and relates to a vacancy in OH_I position coordinated by three nearest-neighbour Al ions as indicated by hyperfine structure of ESR spectra. The hole type center with $g_{//} = 2.056$, $g_{/} = 1.997$ is localized on oxygen ion. The yellow elbaite shows absorption band at 635 nm, which is tentatively ascribed to hole PC.

Fe^{3+} DISTRIBUTION IN CHROMITES AND THE EVOLUTION OF SUKINDA MANTLE.

Sachinath Mitra, Tapan Pal and Taraknath Pal, Department of Geological Sciences, Jadavpur University, Calcutta - 700 032, India.

Mössbauer spectroscopy and magnetic studies on natural chromites have shown that i) a part of Fe^{3+} ions may also occupy the A-site (tetrahedral) resulting an inverse spinel structure and ii) the B-site (octahedral) may characterised by $Fe^{2+} \rightleftharpoons Fe^{3+}$ electron hopping[1]. Mössbauer investigations on two chromite ores from brown and grey ore horizons of Sukinda complex, Orissa, revealed that the brown ore is characterised by the occupancy of Fe^{2+} in A-site and Fe^{3+} is distributed in B-site as well as in A-site. The grey ore is characterised by total absence of Fe^{3+} in A-site, while Fe^{2+} is exclusively located at B-site along with Fe^{2+} with the consequent accompanying electronic transition $Fe^{2+} \rightleftharpoons Fe^{3+}$, which is

discernable by Mössbauer spectroscopy. The Mössbauer parameters of Fe^{2+} and Fe^{3+} at A- and B-sites in these two chromite types are as below :

	Fe^{3+} (B)		Fe^{2+}(A)		Fe^{3+}(A)		Fe^{2+}/Fe^{3+}	a_o
	C.S.	Q.S.	C.S	Q.S.	C.S.	Q.S.		
Brown ore	0.23	0.46	1.28	0.47	0.16	1.08	0.189	8.284

	Fe^{3+}(B)		Fe^{2+}(A)		$Fe^{2+} \rightleftharpoons Fe^{3+}$(B)			
	C.S.	Q.S.	C.S.	Q.S.	C.S.	Q.S.		
Grey ore	0.19	0.54	1.08	0.34	0.89	1.37	0.890	8.270

Where a_o is a - cell parameter measured from XRD lines and corrected by the Nelson - Riley extrapolation function. Fe^{3+} : Fe^{2+} ratio determined by Lorentzian curve splitting of the Mössbauer spectra and the chemical data led to arrive at the formula of the brown ore and grey ore chromites respectively as :

$(Mg_{3.949}\ Fe^{3+}_{3.872}\ Fe^{2+}_{0.214}\ Ca_{0.014}\ Na_{0.009}\ K_{0.003})$
$[\ Cr_{5.765}\ Fe^{3+}_{8.679}\ Al_{1.400}\ Si_{0.116}\ Ti_{0.032}\ Ni_{0.008}]$
O_{32} and $(Mg_{6.489}\ Fe^{3+}_{0.779}\ Fe^{2+}_{0.682}\ Ca_{0.024}$
$Na_{0.023}\ K_{0.013})\ [\ Cr_{10.982}\ Fe^{3+}_{0.412}\ Fe^{2+}_{0.415}\ Al_{2.992}$
$Si_{0.822}\ Ti_{0.147}\ Ni_{0.230}]\ O_{32}$

Compared to those of grey ores of chromites, the brown ore is coarser in size ($\leq$ 5 mm across) and has higher Cr-content, total Fe as well as Fe^{3+} and lower content of Ni & Al. With decrease in temperaure the decrease in fO_2 is evidenced from the T-fO_2 plot with various buffers. The brown ore formed at high fO_2 condition is presumed to have evolved at the lower part of mantle and with slow rate of cooling at higher temperature compared to the mantle melt crystallising the grey ore.

The authors conclude that there was tectonic inversion during the magmatic emplacement in the folded basin of the Banded Iron-Formations (Archean in age) whereby the mantle rocks hosting brown ores were emplaced earlier than those accompanying the grey ores, although any such spatial relationship is

not observed because of extensive lateritic cover.

[1] Galvao da Silva, E.et al. (1980)Appl.phys. 22,389.

G.3.H

TWO DIMENSIONAL CHEMICAL STATE IMAGING OF MINERALS BY SELECTIVELY INDUCED X-RAY FLUORESCENCE ANALYSIS

Izumi Nakai, Department of Chemistry, University of Tsukuba, Ibaraki, 305 JAPAN, **Akira Tsuchiyama**, College of General Education, Osaka University, Toyonaka-shi, Osaka 560, **Ritusro Miyawaki**, Ceramic Technology Department, Government Industrial Research Institute, Nagoya Kita, Nagoya 462, Japan

Knowledge of chemical states of elements and distribution of trace elements in a mineral is important to study origin of the mineral and its formation condition. Several spectroscopic methods such as Mœsbauer spectroscopy, X-ray and optical absorption spectroscopy have been often used to examine the chemical states of elements. However, these methods do not provide two dimensional data. Recently, a new XRF (X-ray fluorescence analysis) technique based on the selective excitation of specific chemical species by tunable synchrotron radiation (SR) was developed1). This paper reports the first application of this technique to geological problems2). Advantage of the SR-XRF technique in trace element analysis is also examined in this study.

SR-XRF measurement was made at BL-4A at Photon Factory, Tsukuba, utilizing an XRF system with Si(Li) detector. Monochromatic X-ray with desired energy and beam size was obtained with Si(111) double crystal monochromator and a slit system. Two dimensional analysis was carried out by scanning a sample on a computer controlled XZ stage normal to the orbital plane of SR.

Samples used are pseudomorph of goethite after pyrite and two chondrites: Allende and Murchison meteorites. Reference samples as standards for iron in various oxidation states include Fe metal, FeS_2, Fe_3O_4, FeOOH, Fe_2SiO_4, olivine and $YFeO_3$.

XANES spectra were measured by X-ray fluorescence detection. Figure 1 shows Fe K-edge absorption spectra of iron (Fe^0), pyrite (Fe^{2+}) and goethite(Fe^{3+}) indicating chemical shift of the absorption edge depending on their oxidation states. Accordingly, if a sample is excited at 7112.3eV, metallic iron is mainly excited, and at 7117.0 keV, both Fe^0 and Fe^{2+} are excited while at 7598.9eV, total iron should be excited. The pyrite/goethite sample was excited at the latter two energies and the meteorites were at the three energies.

An isolated image of each oxidation state of iron is obtained by a subtraction of two data measured at different energy 1). The results are shown in Fig. 2 a and b, where Fe concentration corresponds to 16 degree of darkness (black is the highest concentration). Fig. 2a indicates distribution of divalent Fe, which corresponds well with pyrite, while Fig. 2b indicates trivalent iron corresponding to goethite. Figure 3 shows an example of the analysis of Allende meteorite indicating distribution of Fe^0 + Fe^{2+}. Two dimensional distribution of trace elements, Cu and Zn was also measured. A separate SEM-EDX analysis using the same sample showed that the chondrule is rich in Mg, Si, the inclusion is fine grained CAI and matrix is rich in Fe and Si. The present analysis indicates that Cu and Cr are concentrated at the region rich in metallic Fe, while Zn is in the fine grained CAI.

This study has demonstrated the capability of chemical state imaging and trace elements analysis of geological samples by the SR-XRF technique. This method is truly nondestructive and has therefore more advantage over electron microprobe because it does not require any pretreatment of sample such as carbon coating and is suitable for analysis of samples containing water.

1) K. Sakurai et al. Jap. J. Appl. Phys., 27, L1768(1988).
2) I. Nakai et al. Photon Factory Activity Report #6, 141 (1988)

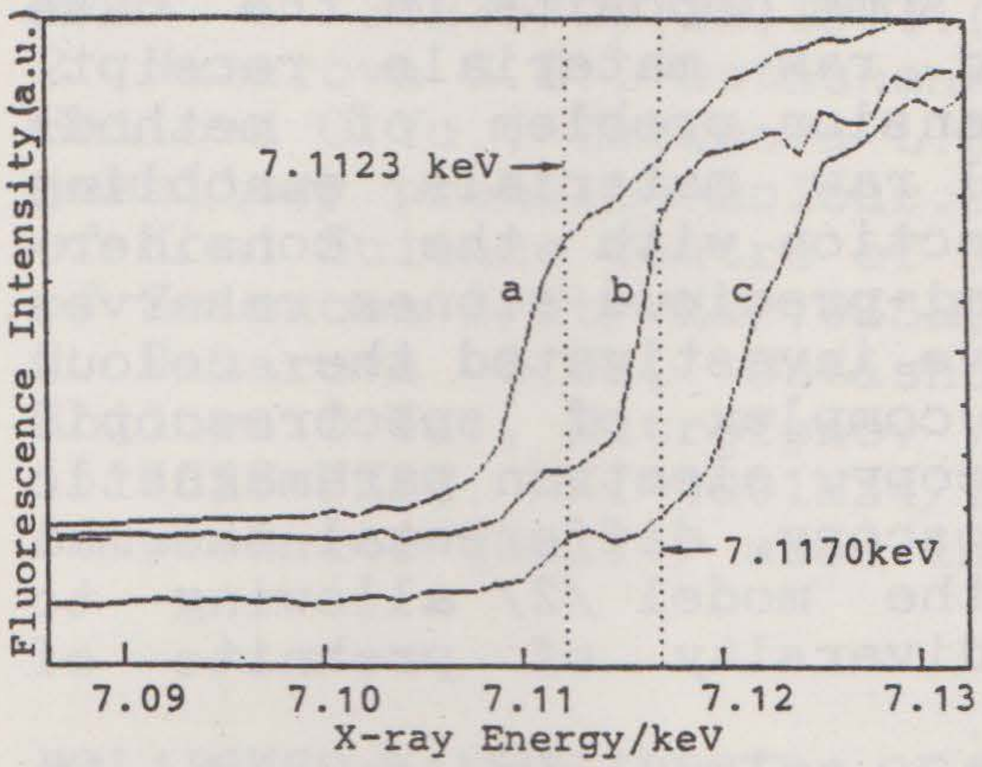

Fig. 1. XANES spectra of (a)iron, (b)pyrite and (c)goethite.

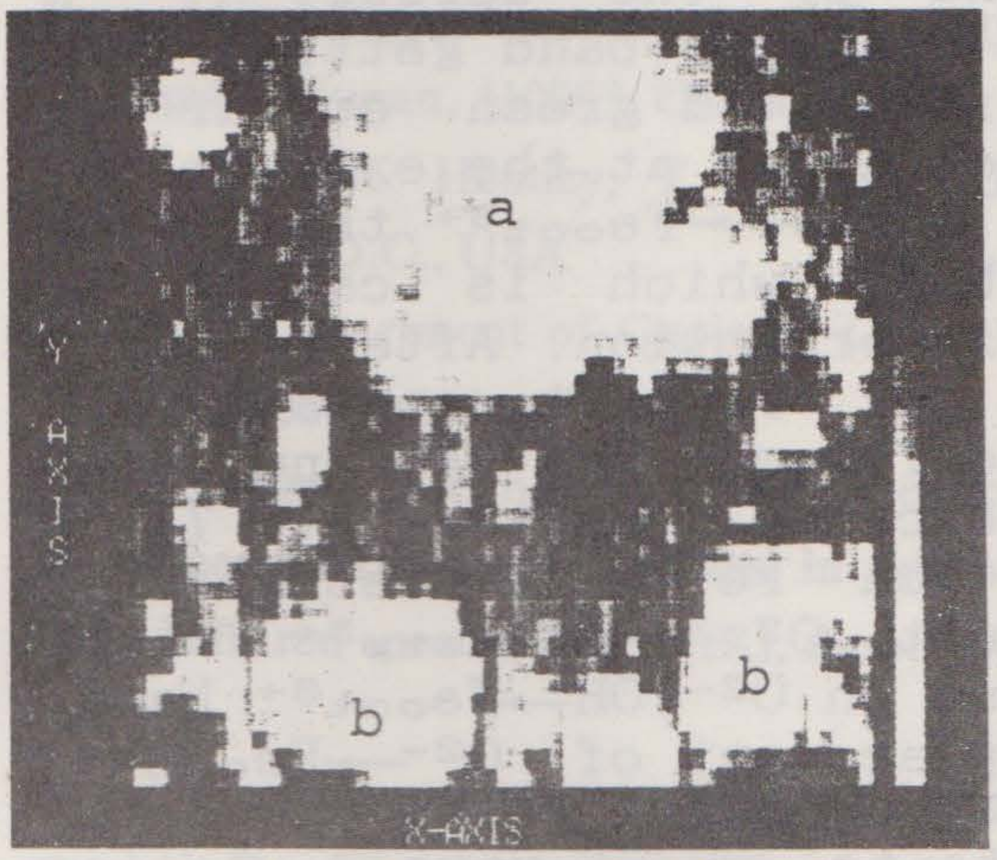

Fig. 3. Distribution of Fe^0+Fe^{2+} in allende meteorite. 57x40 points, 0.13x0.13mm^2 beam, 0.1mm step, 2sec/point.a:CAI,b:chondrule.

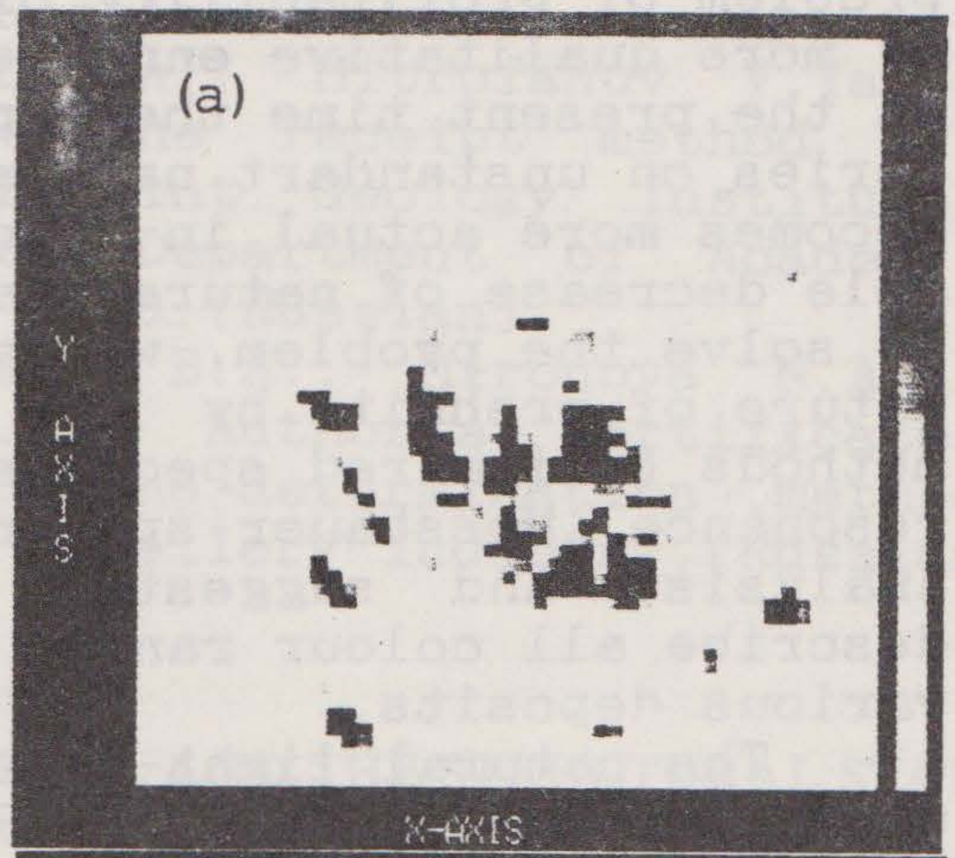

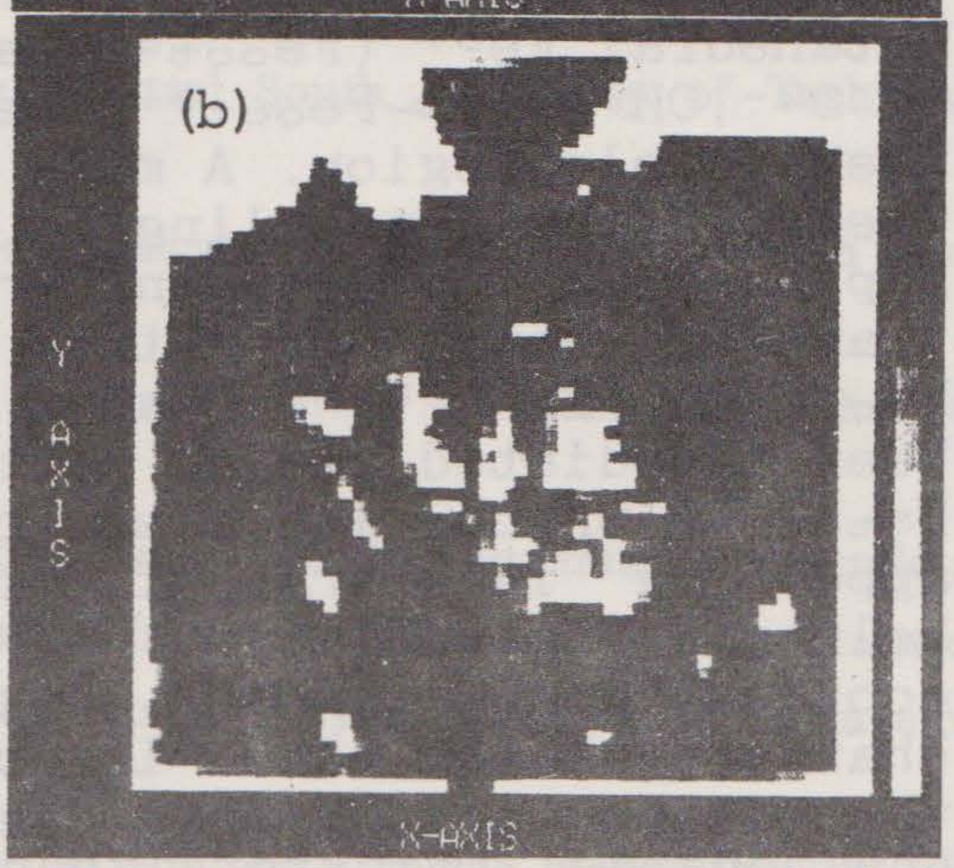

Fig. 2. Distribution of (a) Fe^{2+} and (b)Fe^{3+} in pyrite/goethite. analyzed points 47x59, beam size ca. 0.2x0.2mm2, 0.2mm step, and 2sec/point.

COLOUR CHANGES IN PREHNITE

P 6.8.

G.S.Nazarova, B.A.Ostashenko ,O.Yu.Shilova. Institute of Geology of Komi Science Centre of Ural Department of Academy of Sciences,Syktyvkar,; V.Ya.Mitrofanov. Metallurgy Institute of Ural Department,Academy of Sciences,Sverdlovsk; L.D.Zaripova.Kazan State University,USSR.

Prehnite ($Ca_2Al_2Si_3O_{10}(OH)_2$) of some deposits and the North Timan in particular acquires more saturated green colour after radioactive irradiation and annealling /1/. Moreover the ennobling mineral capacity permits to increase jewellery raw materials yield from 3 to 60 per cent. Therefore it is important to solve the problem of profitability of some deposits in the case of more qualitative ennobled raw materials receipt. At the present time the expansion problem of methods series on unstandart natural raw materials ennobling becomes more actual in connection with the considerable decrease of natural semi-precious stones reserves. To solve the problem, we have investigated the colour nature of prehnite by the complex of spectroscopic methods (infra-red spectroscopy, electron paramagnetic resonance, Mossbauer spectroscopy, differental thermal analysis) and suggested the model /2/ allowing to describe all colour range diversity of prehnite of various deposits.

The natural light-green colour is caused by weak exchange interaction Fe^{2+} in canal (Fe_{can}^{2+}) and octahedral Fe^{3+} (Fe_{oct}^{3+}) and by the border of $O^{2-}, OH^- \longrightarrow Fe_{oct}^{3+}$ the transfer band getting into the visible region. A more saturated green colour in the course of ennobling is obtained at the expense of gap contraction between $O^{2-}, OH^- \longrightarrow Fe_{oct}^{3+}$ the charge transfer band and the band which is caused by $Fe_{can}^{2+} - Fe_{oct}^{3+}$ exchange interraction. After having been irradiated some part of Fe_{can}^{2+} converts to Fe_{tetr}^{3+} which is also confirmed by 745 nm band appearing in X-ray fluorescence spectra at 77 K belonging to radiation of ion Fe^{3+} in tetrahedral coordination. In the result $O^{2-} \longrightarrow Fe_{tetr}^{3+}$ the charge transfer band is put on $O^{2-}, OH^- \rightarrow Fe_{oct}^{3+}$ band, that leads to long-wave displacement of $O^{2-} \rightarrow Fe_{oct}^{3+}$ the charge transfer band border. The band , caused by exchange, shifts to short-wave region still stronger at increasing irradiation dose.

It testifies to the fact that Fe_{can}^{2+} Fe_{tetr}^{3+} the part of ions is increasing as the irradiation dose rises.

Therefore, at irradiation

$$Fe_{can}^{2+} + h\nu \longrightarrow Fe_{tetr}^{3+} + O^-.$$

(O^- axial symmetry centre with parameters $g_{\parallel} = 2.0196^{+}\text{-}0.0018$, $g_{\perp} = 2.0050^{+}\text{-}0.0018$ is found in EPR spectra).

At subsequent annealing

$$Fe_{oct}^{3+} \longrightarrow Fe_{oct}^{2+}; \quad Fe_{tetr}^{3+} + O^- \longrightarrow Fe_{tetr}^{+} + O^{2-} + h\nu_{flu}.$$

The colour model permits to devise the quality prognostication signs of ennobled colour from initial characteristics of natural raw materials. As it is

shown in /3/ the signs permit us to judge about perspective of some deposits as regards to receive ennobled raw materials by the method /1/.

Reference.

1. Nazarova G.S.,Ostashenko B.A.The colour change method of minerals.Author´s certificate 1117344 USSR: MKI⁴ C 30B33/00,29,1984.(Russian).
2. Nazarova G.S., Ostashenko B.A., Mitrofanov V.Ya., Shilova O.Yu., Zaripova L.D. The receipt method of jewellery prehnite colour.Preprint. Geology Institute of Komi Science Centre of Ural Department of Academy of Sciences Syktyvkar,USSR, 1988.(Russian).
3. Nazarova G.S., Ostashenko B.A., Mironova N.A., Shilova O.Yu., Mitrofpnov V.Ya. Author´s certificate 1517536 USSR. MKI⁴4G01N24/10. The determination method of prehnite quality used in jewellery industry.(Russian).

POLARIZED RAMAN SPECTRA OF BERYL AND THE STRUCTURAL STATES OF HYDROGEN IN THE BERYL

Peng Minsheng, Department of Geology, Central South University of Technology, Changsha, Hunan, 410083, China

H.K. Mao, R. Hemley, T. Hoering, Geophysical Laboratory, 2801 Upton Street, Washington D.C., USA

Li Dien, Department of Geology, Central South University of Technology, Changsha, Hunan, 410083, China

Polarized Raman spectra of different color beryls including aquamarine, emerald and chrysoberyl have been presented in this paper. In combination with Fourer Transform Near Infrared spectra (FT–NIR), the structural states of hydrogen in the beryls have been studied.

The spece group of beryl is $P6/mcc–D_{6h}$ with $Z=2$, which means that its factor group is D_{6h}. The site groups of Be, Al, Si and O are C_6, D_2, C_2 and C_1 respectively. The factor group and site group analyses indicate that there should be 22 infrared active modes and 24 Raman active modes which can be seen in the vibrational spectra of beryl.

Polarized Raman spectra of the beryls have been recorded at room temperature. The results show six prominent peaks at 1068(vs), 688(s), 393, 354, 318 and 221cm^{-1} in the Ne direction and at 1073, 1009, 683(vs), 397, 317 and 212cm^{-1} in the No direction. The two stronger peaks at 1086 and 688cm^{-1} are attributable to the Si–O stretching vibration and (Si_6O_{18}) ring symmetrical stretching vibration respectively, whose vibrational modes are A_{1g}. In addition, a sharp single peak at 3608cm^{-1} can be seen in the polarized Raman spectra of all beryl samples. The frequency of the peak in the Ne direction are almost the same as that in the No direction. This peak should belong to the stretching vibration of O–H group.

FT–NIR spectra of the beryls indicate the existence of two types of water in beryls, whose wide and strong peaks are in 3670–3400cm^{-1}and weak peaks split into three components lie in 5446–5083cm^{-1}. The first overtone of the water can be seen in 7494–6800cm^{-1}. Besides, the sharp stretching vibration peak of O–H group can be seen at 3225–3216cm^{-1}, whose combination frequency band is in 4800–4600cm^{-1}. These results indicate the substitution of $Al^{3+}OH^{-} = Si^{4+}O^{2-}$in the Si–O tetrahedra so that the electric charge can be balanced. That is to say, there are two forms of four– and six–coordinated Al^{3+}in the beryl and the O–H group occurs in the Si–O tetrahedra. Therefore, the Raman peak of O–H stretching vibration at 3608cm^{-1}do not change with the orientation of the beryl.

A STUDY OF IR AND RAMAN SPECTRA OF CHRYSOTILE

Peng Tongjiang, Wan Pu, Sichuan Institute of Building Materials, Mianyang, Sichuan 621002; Zhu Zizun, Xi'an, Shaanxi 710054, People's Republic of China

Eight samples of chrysotile, from Xiaobabao Mine, Shuangchagou Mine and Xiaoheicigou Mine, Qilian County, Qinghai Province, have been studied with infrared and Raman spectroscopy.

According to the work of Farmer et al, the tetrahedral sheet and the octahedral sheet in the structure unit layer of serpentine can be considered as mutually independent entities. In this study, we have carried out the factor group analysis for the vibration spectra of these two kinds of sheets in serpentine.

In ideal conditions, the symmetry of the tetrahedral sheet is C_{6v}, and that of the octahedral sheet is C_{3v}. The tetrahedral sheet and the octahedral sheet are divided into Bravais primitive unit cells with composition of $[Si_2O_5]$ and $[Mg_3(OH)_4]$ respec-

Table 1. Normal Mode Distribution and Selection Rules for the Tetrahedral Sheet $[Si_2O_5]$

Symmetry species	A1	A2	B1	B2	E1	E2
Total modes	3	0	3	1	4	3
Acoustic modes	1	0	0	0	1	0
Translational modes	2	0	3	1	3	3
Selection rules	IR & Raman				IR & Raman	Raman

tively.

The results of the factor group analysis are shown in table 1 and 2.

Table 2. Normal Mode Distribution and Selection Rules for the Octahedral Sheet [$Mg_3(OH)_4$]

Symmetry species	A1	A2	E
Total modes	8	3	11
Acoustic modes	1	0	1
Translational modes	4	2	6
Rotational modes	1	1	3
Internal modes (OH)	2	0	1
Selection rules	IR & Raman		IR & Raman

Sixteen absorption bands (or shoulders) of chrysotile were determined in the IR spectra from 4000cm^{-1} to 200cm^{-1}, and eighteen absorption bands of chrysotile were determined in the Raman spectra from 4000cm^{-1} to 85cm^{-1}, which basically coincide with the results of the factor group analysis.

The absorption bands of the IR and Raman spectra of chrysotile were assigned according to the results of the former studies and our factor group analysis.

The IR and Raman absorption band intensity ratios of outer and inner hydroxyl groups are respectively 3.16--4.03 and 3.8--5.7. These values are bigger than the ideal value 3, which is probably due to the formation of the hydrogen bond between the structure unit layers.

The studies show that the frequencies of the absorption bands E (1080cm^{-1} ±), F (1020cm^{-1} ±) and G (959cm^{-1} ±) in the IR spectra are obviously related with the isomorphous substitution ions.

With the increasing of the number of Al^{3+} and Fe^{3+} ions, the frequencies of the E and F bands decrease, but the frequency of the G band increases. These changes influence the resolution of the F and G bands.

A STUDY ON THE INFRARED SPECTRUM OF BAIYUNEBOITE-(Ce)

PENG Wenshi and LIU Gaokui, Institute of Geochemistry, Academia Sinica, Guiyang, Guizhou 550002, People's Republic of China

A new mineral-fluor-carbonate-baiyuneboite-(Ce)

occurs in Fe-Nb-REE ores in Baiyun-obo, Neimenggu. Its chemical formula is $NaBaCe_2[F/(CO_3)_4]$ and the space group belongs to D_{6h}^4-$P6_3/mmc$, Z=2. In the structure, eight CO_3^{2-} ions are divided into two unequivalent sets with different lattice environments and different C-O bond lengthes but the same site symmetry, C_{3v}.

Free CO_3^{2-} ion has D_{3h} molecular symmetry. It has four normal vibrational modes, two of which are non-degeneration modes (ν_1 and ν_2) and the rest are double degeneration modes (ν_3 and ν_4). Of these modes, only ν_1, ν_3 and ν_4 are IR active. The correlation analyses for CO_3^{2-} ions in baiyuneboite-(Ce) indicate that under the C_{3v} symmetry the site group splitting doesn't occur but ν_1 mode becomes IR active, and that although there are more equal CO_3^{2-} ions in the primitive cell the factor group splitting can not exhibit either, bacause the symmetry center divides it into two group-IR active and Raman active. However, two unequivalent sets of CO_3^{2-} ions make all normal modes appear in the form of double bands. It is evident that theoretical results are in good coincidence with the measured spectrum (Fig. 1).

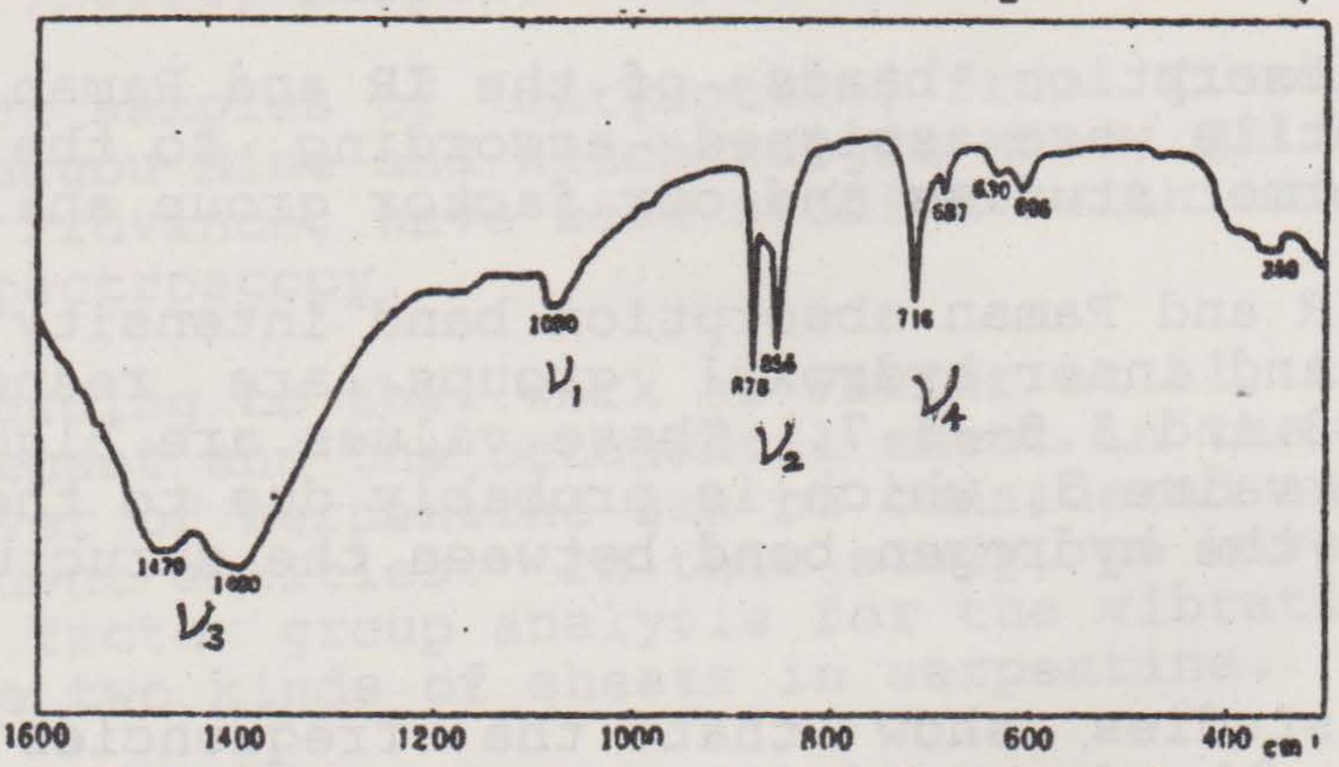

Fig. 1. Infrared spectrum of baiyuneboite-(Ce)

The normal coordinate analysis has been carried out with the GF matrix method presented by Wilson[1]. For the vibrational mode of E Class of CO_3^{2-} ion, the elements of the G matrix and F matrix (U-B simplified force field[1]) are given as follows:

$$G_{33}=\mu_o+\frac{3}{2}\mu_c,\quad G_{34}=G_{43}=\frac{1}{r}\frac{3\sqrt{3}}{2}\mu_c,\quad G_{44}=\frac{1}{r^2}(3\mu_o+\frac{9}{2}\mu_c);$$

$$F_{33}=K+0.625F,\quad F_{34}=F_{43}=-0.225\sqrt{3}rF,\quad F_{44}=r^2(H+0.325F).$$

After fitting calculations, we can obtain the following force constants and calculated frequencies:

	force constants(md/Å)			calculated frequencies(cm^{-1})	
	K	H	F	ν_3	ν_4
CO_3^{2-}(1)	5.22	0.40	1.62	1401	685
CO_3^{2-}(2)	5.80	0.39	1.90	1469	718

Potential energy distribution can provide an objec-

tive judgement for the band assignments. Under the normal coordinate, the normalized potential energy distribution can be expressed as $V_{ia}=F_{ii}L_{ia}^2/\lambda_a$. Here is the potentail energy distribution of CO_3^{2-} ion of baiyuneboite-(Ce):

CO_3^{2-}(1)	ν_3	ν_4	CO_3^{2-}(2)	ν_3	ν_4
S_3	0.80	0.07	S_3	0.81	0.06
S_4	0.20	0.93	S_4	0.19	0.94

Because S_3 comes from the operation of the projection operator on bond length and S_4 results from the operation on bond angle, the assignements of ν_3 and ν_4 to the stretching vibration and bend vibration are approximately reasonable.

Reference

1. Woodward, L.A., Introduction to the theory of molecular vibrations and vibrational spectroscopy, 1972, Oxford University Press, London, pp. 71-225.

HYDROXYL AS IR-PROBE IN MICAS: VACANCIES IN OCTAHEDRA AND DISTRIBUTION OF ALUMINIUM IN TETRAHEDRA.

P6.9

Ponomaryov B.G., Lapides I.L, Geochemistry Institute, Academy of Sciences of USSR, Siberian Branch, Irkutsk, 664033, USSR.

The fine structure of hydroxyl IR-spectra of micas is affected by short range cations. It is the cation substitutions in nearest three octahedra and six tetrahedra of pseudohexagonal ring that make a main contribution to variations of the features of hydroxyl ion vibrational motion . This fact gives a chance, in principle, to investigate the silicium substitutions in tetrahedral sheet and cation site occupancy in octahedral sheet,in particular, to obtain the data about "molar fraction" of octahedral vacancies. Vedder's model is improved to solve these problems. To resolve the observed spectra into "individual components" the spectrum-oriented curve-fitting procedure UPEAK [Zlokazov,1977] was selected and arranged for IR-spectrum processing.

I. A ratio k_V/k_N, where k_i (i=N,I,V) - absorption coefficient of N-, I- and V-peaks, has been estimated as 10±2. This fact in combination with k_I/k_N=1.8 [Rousseaux,1973] gives possibility to obtain the molar fractions of octahedral vacancies of micas. IR-spectra of 19 biotites of varying chemical compositions were recorded in the OH-stretching region (4000-3000 cm^{-1}) and processed in correspondence with this model. The results are compared with those derived from the chemical analysis.

II. A model for resolving of phlogopite OH-stretching spectra is justified. According to it each N-peak arisen from the $OH\text{-}R^{2+}R^{2+}R^{2+}$ groupings would be represented by *triplet* with $\Delta\nu_{1,2}\simeq 8$ cm^{-1} due

to the amount of possible patterns of tetrahedral environment. IR-spectra of 13 phlogopites $\left(R^{3+}_{VI}=0 \; ; \; 0.7 \leq \frac{Mg}{Mg + Fe^{2+}} \leq 0.9 \right)$ were processed. Our results shows that:

a) processing of spectra with new model is better as for all the parameters of comparison.

b) no short range ordering of octahedral cations has been detected (within the magnesiality range studied)

c) relative fractions of tetrahedral rings with one Al_{IV} and those with two Al_{IV} regularly depend on both the type of the corresponding octahedral cation triad and molar fraction of Fe^{2+}_{VI}.

Po 6.10.

THE TRANSFORMATION OF THE SOLID SOLUTION OF THE GREAT CAUCASUS METAMORPHIC AMPHIBOLES

Poporadze N.G., Department of Geology, Georgian Polytechnic Institute, 77 Lenin Street, 380075 Tbilisi, USSR

Nowadays great attention is paid to disintegration of solid solutions of rock-forming minerals. There are many cases when the mineral phase homogeneous under a set of conditions, got into another one, disintegrates into the parts of different composition.

By means of the profile micro X-ray spectral analysis and the electron microscope are revealed the plane isolations-lamellae, being the product of the solid solution disintegration in the separate grains of the great Caucasus metamorphic amphiboles. The homogeneous amphibole, i.e. a one-phase is crystalized at the initial stages of the metamorphism process and it undergoes a phase transformation at the temperatures below that of solvus in the course of further cooling.

We have studied the chemical composition and structure of the solid solution disintegration of hornblende-cummingtonite, hornblende-actinolite hornblende, hornblende-actinolite and anthophilite-actinolite in the great Caucasus metamorphites in the connection with the process of their formation.

The solid solution disintegration of anthophilite-actinolite, hornblende-cummingtonite occurs by means of heterogeneous germ during the uneven transformation, hornblende-actinolite hornblende by homogeneous germ, but hornblende-actinolite occurs by the spinodal mecha nism with the gradual transformation.

The processes of the solid solution disintegration hornblende-cummingtonite, besides the free energy reduction occur by the changing of the cation sizes into the position N4 between the parts rich and poor in calcium. When the temperature lowers Fe, Mg give the

position M4(Ca placa) a noticeable preference and make a little part in the positions M1,M2 and M3. During the solid solution disintegration hornblende-actinolite, hornblende-actinolite hornblende the replacement of Fe, Mg by Al in the positions M2 and Si by Al in the tetrahedral positions take place.

THERMOELASTIC MARTENSITIC TRANSFORMATION BETWEEN HIGH-LOW CLINOPYROXOENES

P3.6.11.

Norimasa Shimobayashi and Masao Kitamura, Department of Geology and Mineralogy, Faculty of Science, Kyoto University, Kyoto, 606, Japan

Ca-poor clinopyroxenes in the common pyroxene quadrilateral have a $P2_1/c$ structure at low temperature. On heating, they undergo a rapid displacive transition to a $C2/c$ structure, which cannot be quenched. *In situ* experiments by use of high temperature X-ray techniques have been carried out mainly on the crystal chemisry of the pyroxenes. However, the nature of the transition has not been well understood. Recently, a new heating stage was constructed for high temperature transmission electron microscopy (HTTEM)[1]. A furnace of the heating stage for a 200kV TEM (HITACHI H-700) was attached to a double-tilting side-entry specimen holder. The temperature is controlled by the wattage of the coil heater, and the maximum temperature of a specimen position is about 1300°C. In the present study, the $P2_1/c$-$C2/c$ transition was studied to elucidate its nature using the HTTEM.

The following three kinds of specimens (single crystals) were prepared for the HTTEM observation; (1) synthetic clinoenstatite (En_{100}): (2) natural clinoenstatite ($En_{91}Fs_8Wo_1$) from Muko-Jima, the Bonin Islands, Japan: (3) natural pigeonite ($En_{58}Fs_{39}Wo_3$) from Hakone-path, Hakone Volcano, Japan. The changes in microstructures and/or microtextures during the heating of these pyroxenes under the HTTEM were observed on a TV monitor and recorded on video tapes by a fiber-optically coupled TV system (GATAN 622).

During the heating experiments of both clinoenstatite and pigeonite, the coexistence of the $P2_1/c$ and $C2/c$ phases was observed in some temperature ranges. At the coexistent stage, the transition did not proceed with the lapse of time at the constant temperature. The coexistence of two phases with coherent interfaces and time-independent reactions suggested that the $P2_1/c$-$C2/c$ transition is of a

first-order and occurs athermal-martensitically. Furthermore, the $P2_1/c$–$C2/c$ transition was revealed to be a thermoelastic type of the martensitic transformation based on the unusual thermal hysteresis (superposing of the transition ranges between the heating and cooling) as shown in Figure 1. This type of the transition was first found on rock-forming minerals.

Antiphase structure is a typical resulting microstructure of the $C2/c$-to-$P2_1/c$ transition on cooling. Antiphase boundaries (APB's) in pigeonite are classified into two types: L APB's parallel to the c axis and H APB's cutting the c axis [2]. In the present study, the formation process of the APB's in pigeonite was *in situ* observed during the transition using the HTTEM. It is shown that the L types form at the earlier stage, and that the H types form as the trace of the interfaces between two phases at the final stage of the $C2/c$-to-$P2_1/c$ transition, respectively. The fact that the L APB's are commonly observed in the rapidly cooled pigeonite while the H APB's tend to be in majority in the slowly cooled pigeonite, can be interpretated by the difference in the formation process between these two types of APB's.

[1] Morimoto *et al.* (1989)
Mineral. J., 14, 246-254.
[2] Carpenter (1978)
Phys. Chem. Minerals, 2, 237-251.

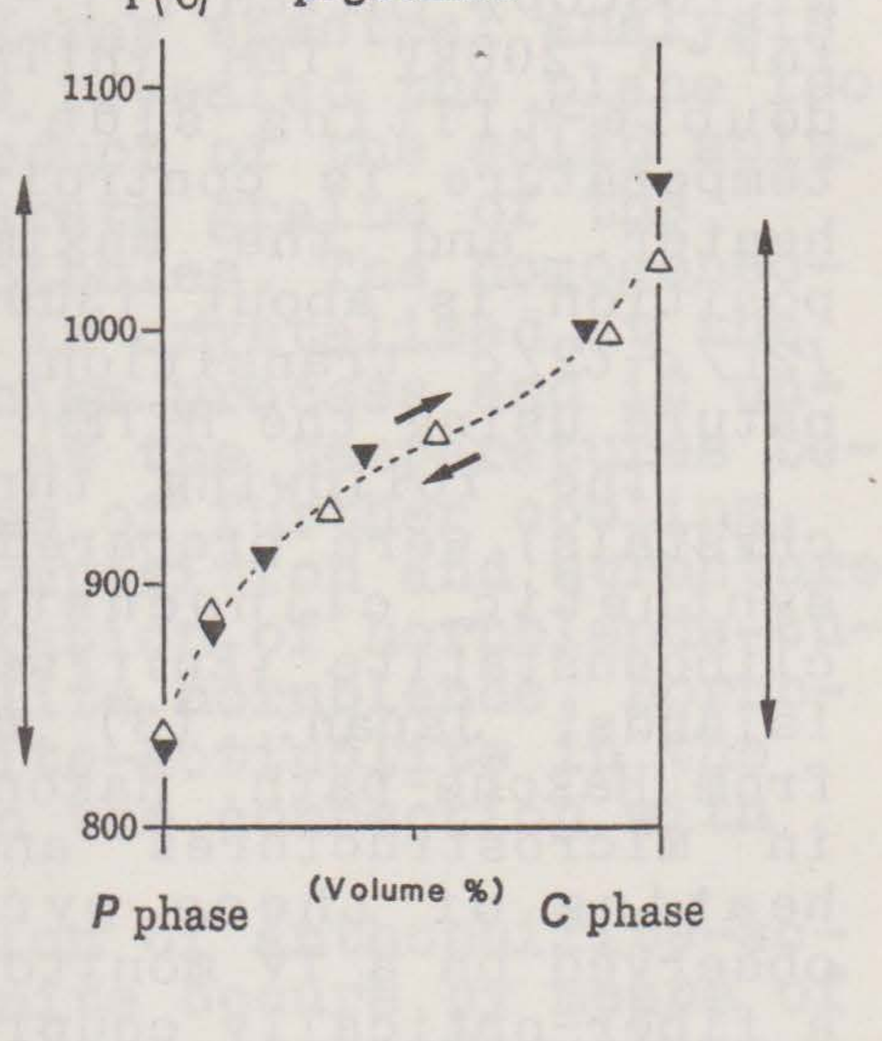

Figure 1. Percent-transformation curve in the second heat treatment of pigeonite. The percentages are shown by the volume ratio transformed (open triangles: during the heating; solid triangles: during the cooling). The transition range during the heating superposes on that during the cooling.

Po6.12

IN-SITU OBSERVATION OF THE FORMATION OF DAUPHINE TWIN IN QUARTZ UNDER A HIGH TEMPERATURE TRANSMISSION ELECTRON MICROSCOPE

Keiji SHINODA*, Norimasa SHIMOBAYASHI and Masao KITAMURA
Department of Geology & Mineralogy, Faculty of Science, Kyoto University, Sakyo, Kyoto 606, Japan.

* Present address : Department of Geosciences, Osaka City University, Sumiyoshi, Osaka 558, Japan.

Dauphine twin in quartz is formed by the phase transformation from high-temperature (β) to low-temperature (α) phases. It has been suggested that the density of Dauphine twin domains is controlled by several factors such as lattice defects and cooling rates. In the present study, the formation process of Dauphine twin and the effect of lattice defects to the domain density were studied using a high temperature transmission electron microscope (HTTEM).

In-situ observations of the transformation of synthetic and natural specimens of quartz were carried out under a 200kV HTTEM (Morimoto, et al., 1989). Under the HTTEM, an incommensurate (INC) phase were confirmed as a stable phase surviving for about 1.8K between α and β phases (Van Tendeloo, et al., 1976). Therefore, the HTTEM study on the formation of Dauphine twin was concentrated on the transformation from INC to α phases.

INC phase has a modulated structure where two kinds of triangular micro-domains of α phase in Dauphine twin relationship are regularly arranged. On the other hand, two individuals in Dauphine twin relationship in α phase are much larger than the micro-domains and not in a regular arrangement. Therefore, as cooled the specimen, the transformation from INC to α phases appeared as coarsening of the micro-domains and loosing their regular arrangement. However, the sizes of two types of the triangular domains did not change equally, resulting in that large domain of one type includes several small triangular domains of the another type in it. This type of the large domain including small triangular domains are called "predominant domain" (P-domain). Though small triangular domains in P-domain survive just below the transformation temperature, they are assimilated to P-domain with decreasing the temperature. At last, the small domain does not survive as Dauphine twin individual on an optical microscopic scale. Consequently, the domain density of Dauphine twin is controlled by the formation of P-domains. The formation of P-domain must be characteristic in a first order transformation between α and INC phases.

In the HTTEM study of natural quartz with dislocations, it was confirmed that some dislocations affect to the formation of P-domain as (1) nucleation or (2) trapping sites of P-domain. This behavior of the dislocations during the transformation process is that expected in a first order transformation.

The effect of cooling rate to the formation of

Dauphine twin could not be studied by the HTTEM, because of its limitation. Therefore, the relation between the density of Dauphine twin domains with cooling rate was examined by the etching method on both natural and synthetic specimens of α quartz. The domain densities in several natural igneous quartz were confirmed to decrease as the cooling rate estimated from their occurrences decreases. This type of the relation is also confirmed on the synthetic specimen which was heated and cooled with different cooling rates. Therefore, the domain density is affected by the cooling rate. However, the domain densities of natural specimens were much higher than those of the synthetic quartz even in a similar range of the cooling rate. This difference in the domain densities can be explained by the strong interaction between some dislocations and P-domains revealed by the present HTTEM study, because natural quartz has higher dislocation density by one order than synthetic quartz.

Morimoto et. al.,(1989) Mineral. Jour. **14**, 246.
Van Tendeloo et.al.,(1976) Phys. Stat. Sol. (a)**33**, 723.

Po 6.13

RADIATIVE EPR SPECTROSCOPIC STUDY OF QUARTZ

M.J.Stcherbakova, Institute of Geology and Geophysics, Siberian Branch of the USSR Academy of Sciences, Universitetskij pr.3, Novosibirsk, 630090, USSR.

By paramagnetic centres possibility of establishing structural forms of impure aluminium in the quartz irradiated by electrons is discussed.

For quartzes - granulated I, hydrothermal II, from rare metal granite pegmatites III, from granites IV, irradiated by electrons (2 Mev, 0,5-7500 Mrad) dependences of the intensities of paramagnetic Al, E', O_2^--centres on the irradiation dose were studied. EPR spectra were studied at a frequency of 9800 MHz, at temperatures of 77 and 300K. It is found, that the intensities of Al and O_2^--centres increase in sequence in samples I,II,IV,III and of E'-centre - in I,III,II,IV. In the region of 500-1000 Mrad the intensities of E'-centres for quartzes II,III,IV, which did not undergo secondary radiative, dynamic influences or recrystallization, acquire close values. For $\sim$ 200 quartzes, irradiated by electrons with 500 Mrad dose, the intensities of Al, E' and O_2^--centres (in per-unit) were measured. Their typical values are given in the table.

	I	II					III					IV				
		1	2	3	4	5	1	2	3	4	5	1	2	3	4	5
$I_{E'}$	4,8	32	30	26	20	9	32	22	16	22	22	32	27	27	24	10
I_{Al}	1,0	23	6,0	7,3	5,1	3,2	35	48	150	19	7,2	20	24	14	7,0	1,0
$I_{O_2^-}$	0,5	37	3,8	3,5	3,2	2,5	24	32	118	8,1	5,3	8,8	7,6	6,4	3,8	1,0

In crystalline quartz stabilization of E′-centre - defect, containing oxygen vacancy, is determined mainly by a low valency impurity cation, i.e. $Al^{3+} \rightarrow Si^{4+}$ [1, 2] The efficiency of arising of this centre may also depend on the type of monovalent cations balancing the deficit of Al, as well as on other point and stretching structural defects. At the given regime of irradiation, the efficiency of stabilizing E′-centre is weakly dependent on the composition of compensator cations. Hence, the intensities of radiatively-induced paramagnetic centres reflect the following relations with structural impurities: E′-centre with $Al^{3+} \rightarrow Si^{4+}$, Al-centre with $[AlO_4/M]^\circ$ and O_2^- - with interstitial impurities of Al and M-alkaline cations. In the frame of this scheme, all quartzes, except I, II 5, III 3, IV 5 are characterized by close values of E′-centre intensity, but by substantially different intensities of Al-centre. Thus, natural quartzes, independently of their genetic type, with almost the same content of substituting Al are distinguished by the composition of compensator cations and, consequently, by the relation of $[AlO_4/M]^\circ$ and $[AlO_4/H]^\circ$. For quartzes III 3, crystallized from substantially oversaturated solutions, the content of interstitial ions of Al, M and $[AlO_4/M]^\circ$ increases and the efficiency of vacancy E′-centre formation decreases. In recrystallized quartzes I, II 5, IV 5 due to the reduction of $Al \rightarrow Si$ in the structure, the intensities of all centres decrease. Peculiarities of structural forms of impure aluminium in quartzes of various genetic origin are discussed.

1. K.L.Brower. Electron paramagnetic resonance of Al, E′-centres in vitreous silica. Phys.Rev. 1979, 20, N 5, p.1799-1811
2. M.G.Jani, R.B.Bossoli, L.E.Halliburton. Father characterization of the E′ centre in crystalline SiO_2. Phys.Rev. B 1983, 27, N 4, p.2285-2293.

6.4.11

A SIMS STUDY ON THE DIFFUSION OF ELEMENTS IN MgO

Shigeho Sueno[1],Hisayoshi Yurimoto[2],Hironori Yamamoto[1] and Isao Sakaguchi[3]:
[1]Institute of Geoscience, University of Tsukuba, Tsukuba, 305 Japan. [2]Institute for the Study of Mineral Deposits, South Dakota School of Mines and Technology, Rapid City, South Dakota, USA. On leave from Inst. of Geoscience, Univ. of Tsukuba. [3]Yamaha Engineering Company, Iwata, Shizuoka, 438 Japan.

Secondary ion mass spectrometry (SIMS) has the several capabilities, such as chemical and isotopic analysis of major and trace elements (% to ppm region) and depth analysis (resolution 50Å) are suitable for studying the diffusion of elements in minerals with slow diffusion speed, such as in oxides or silicates. Although the study of the diffusion coefficients and the activation energies are important to clarify the principle characters of minerals, those reported by previous workers

Table 1

	Lattice		Dislocation		measurement
	Do (m^2/sec)	Q (kJ/mol)	Do (m^2/sec)	Q (kJ/mol)	temp. (K)
Li^+	8.36×10^{-3}	408.61	1.98×10^{2}	384.69	973-1473
Na^+	2.31×10^{-5}	461.48	1.02	452.34	1293-1743
Mg^{2+}	1.85×10^{-5}	331.12	2.82×10^{6}	472.52	973-1573
Al^{3+}	1.29×10^{-11}	163.27	9.33×10^{-7}	137.24	1173-1573
Si^{4+}	2.11×10^{-12}	233.58	2.21×10^{-4}	322.25	1293-1743
P^{5+}	1.65×10^{-16}	120.16	3.39×10^{-4}	327.97	1293-1693
Ca^{2+}	7.56×10^{-13}	231.15	4.49×10^{-5}	318.84	1293-1743
Sc^{3+}	1.70×10^{-5}	295.47			1173-1373
Cr^{3+}	2.04×10^{-13}	118.89	7.46×10^{-9}	99.94	973-1473
Mn^{2+}	2.95×10^{-12}	135.43	2.31×10^{-3}	212.60	773-1473
Fe^{2+}	2.74×10^{-11}	151.06	1.12×10^{-4}	188.28	873-1373
Co^{2+}	1.59×10^{-10}	166.66	6.46×10^{-8}	128.50	873-1473
Ni^{2+}	2.66×10^{-8}	222.30	3.24×10^{-3}	245.17	973-1373
Sr^{2+}	2.62×10^{-11}	268.23	2.81×10^{7}	673.67	1473-1843
Y^{3+}	1.10×10^{-11}	241.98	1.96×10^{-1}	376.25	1273-1673
Zr^{4+}	8.85×10^{-15}	96.30	2.57×10^{-5}	193.91	1173-1573
Tb^{3+}	4.12×10^{-13}	192.02	5.48×10^{-3}	304.98	1273-1673

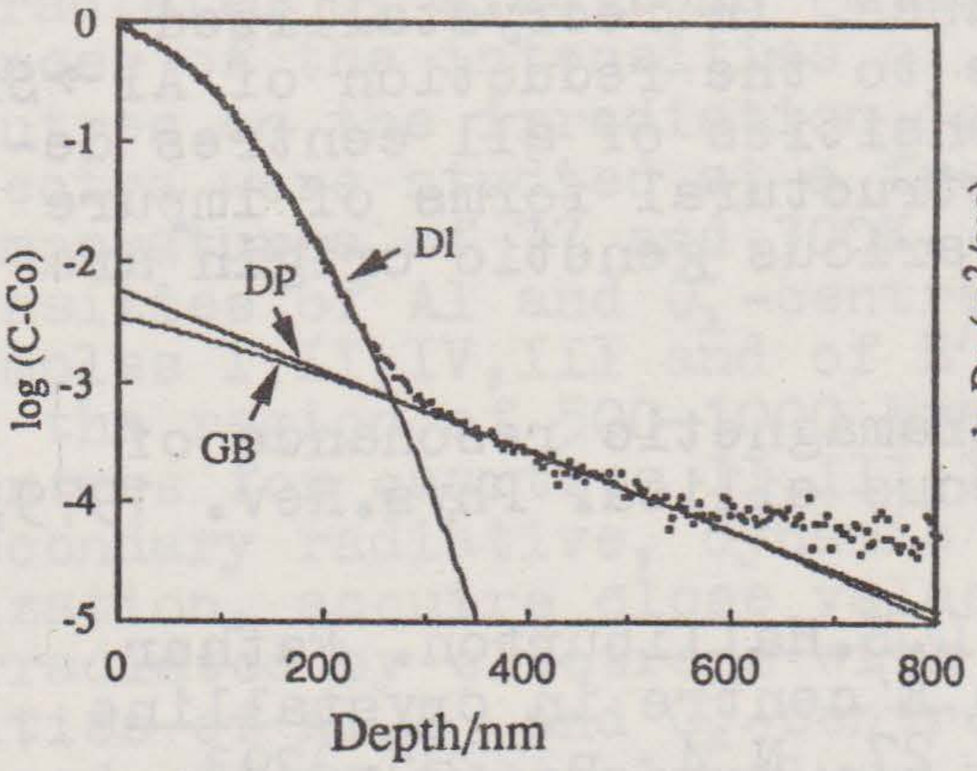

Fig. 1:L- and D-diffusion.

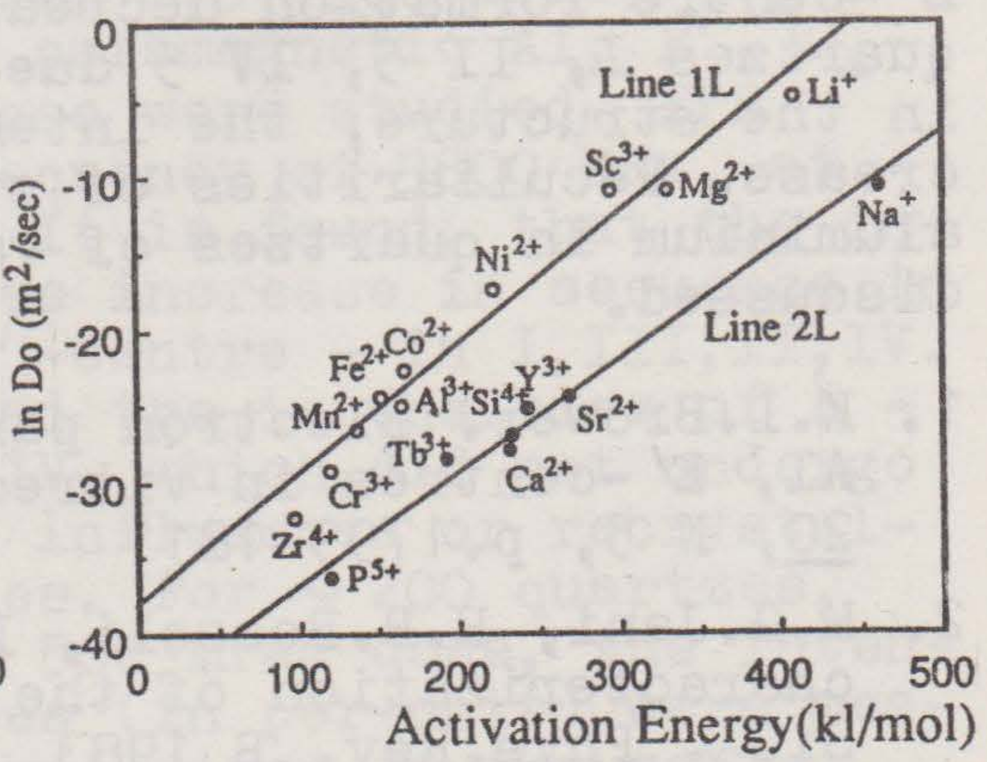

Fig. 2: Compensation diagram of L-diffusion in MgO

are largely fluctuated because of the difficulty for separating the lattice- (L-diffusion) and the dislocaton-diffusion (D-diffusion). However, if the diffusion annealing duration is well designed, it is possible to obtaining in-depth diffusion profile consistent with curved and linear regions (tail) as shown in Fig.1. These two region are corresponding to the L- and D-diffusion, respectively.

We have studied the diffusion coefficients for several diffusant elements in synthetic MgO single crystals. The specimens were annealed in a furnace at several temperatures (500 - 1500°C) for diffusing the elements which are supplied as gas phase. The annealing duration was selected from 1 minutes to several tens of hours depending on the elements to produce a concentration gradient on the order of 1 mm in-depth profiling with SIMS. The annealed specimens were examined using depth analysis method by SIMS. We have successively analyzed the two types of diffusion coefficients (L- and D-diffusion) separately from the depth profiles obtained for various diffusant elements at several different temperatures. The diffusants so far studied in MgO are listed in Table 1. The diffusion coefficients for both L- and D-diffusions measured at several temperatures were analyzed from the depth profiles, and were plotted on the Arrhenius diagrams and calculated their pre-exponencial factor (D_0) and the activation energies (Q) as shown in Table 1. It was found that the D-diffusion coefficients (D_d) among the various diffusants are 10^4-10^5 times larger than those of L-diffusion(D_l), but the activation energies (Q) were almost the same among all.

All of the D_0 and Q values were plotted on D_0/Q diagram to examine the compensation law, in which it was empirically believed that all of the data points to be aligned in one line. However, we found that the data points were approximately aligned on two separated lines not on one line, as shown in Fig.2. Elements such as Cr, Mn, Fe, Co, Li, Sc, Ni and Mg are on the line 1, and those of P, Ca, Si, Y, Sr and Na are on the line 2. The elements belong to the line 1 have similar ionic radii with Mg ion (from 50 to 85 pm) and those belong to the line 2 have larger or smaller ionic radii than those belong to the line 1 group. It is conceivable that the ions in these two groups may be diffused by the different diffuse mechanisms.

THERMAL CONDUCTIVITY MEASUREMENT OF ISOTROPIC AND ANISOTROPIC MINERALS UNDER HIGH PRESSURE

6.8K

J. Susaki, *K. Horai, and T. Yagi, Institute for Solid State Physics, Univ. Tokyo, Roppongi, Minato-ku, Tokyo, Japan 106,
*Meteorological Research Institute, Tsukuba, Ibaraki, Japan 305

A new method of measuring thermal conductivity of rocks under high pressure up to 50 kbar was developed and was applied to the measurement of isotropic and anisotropic crystals. Quasi-hydrostatic high pressure was generated by a wedge type cubic anvil apparatus with pyrophyllite pressure medium. Samples were shaped into cylinders 12 mm long and 8 mm in diameter. A chromel wire was embedded along the cylinder axis as a heater, and the temperature at the center of the cylinder was monitored by a chromel-alumel thermocouple. Thermal conductivity was determined by the transient hot wire method. The temperature(T) was measured as a function of the time(t) elapsed since the onset of the heating. Then the gradient of the T versus ln(t) gives

the thermal conductivity. The assembled sample was placed in a 21 mm-edge-long cubic of pyrophyllite. The pressure was increased up to 50 kbar in increments of 5 kbar. Thermal conductivity was determined at each increment. The accuracy of the determination was confirmed by comparing the result from

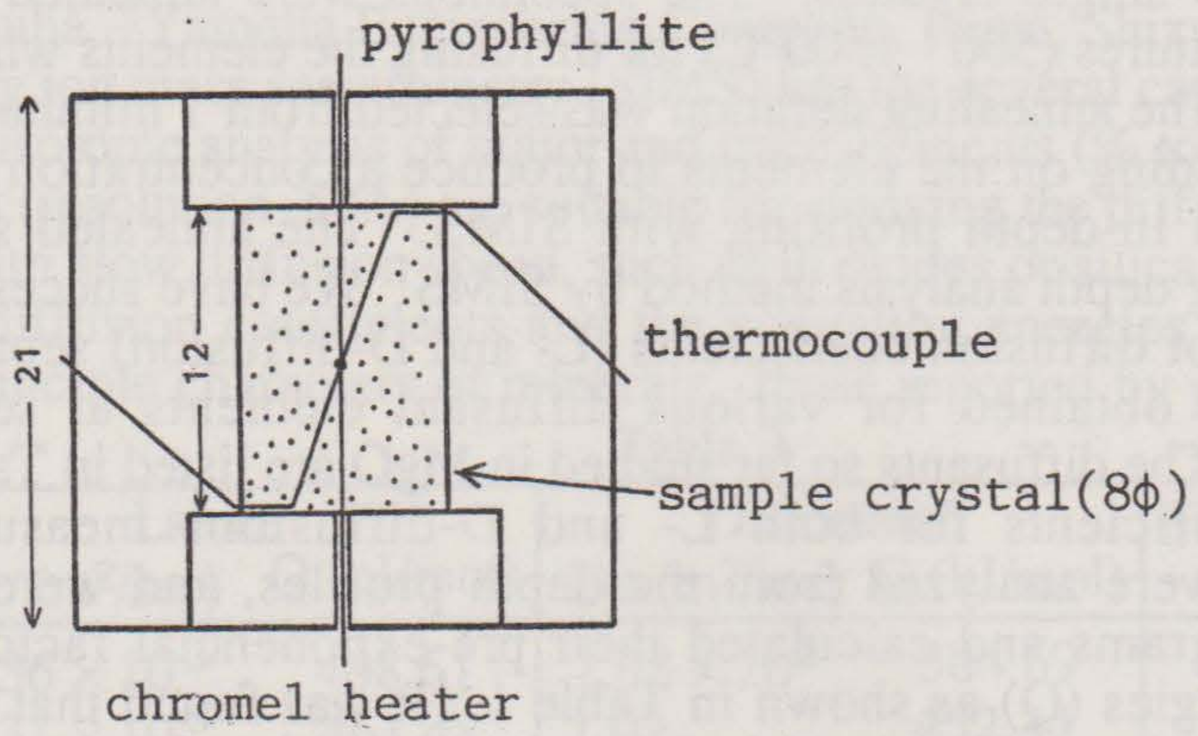

Fig.1 Sample assemblage of the transient hot wire method.

fused quartz at ambient pressure with the standard value from the literature. An advantage of the present method is that sample deformation, which seems inevitable in any high pressure experiment, has no effect on the measurement procedure.

Strontium titanate ($SrTiO_3$) was selected as a crystalline sample, because it has isotropic physical properties like most natural rock samples. The conductivity at the ambient pressure was 6.8±0.3 W/mK, compatible with the literature value. A linear increase of the conductivity of 0.064 W/mK/kbar, was observed between 5 and 35 kbar. No obvious increase of the conductivity was observed above 40 kbar.

The transient hot wire method could be applied to anisotropic crystals of axial symmetry, because measurement by the transient hot wire method yields thermal conductivity in the direction perpendicular to the heating wire. The thermal conductivity of a factory-made quartz crystal was measured. The thermal conductivity(K_a) of quartz to the direction of the crystallographic a axis was easily measured by choosing the crystal's c axis as the direction of the heating wire. For the heating wire stretched in the direction of a axis, the measured thermal conductivity was approximately $\sqrt{K_a K_c}$ According to the mathematical theory of thermal conduction (Takegoshi et al. 1982). Thus both thermal conductivities, K_a and K_c, could be obtained from the measurements in two perpendicular directions. The observed K_a at ambient pressure was 6.6 W/mK and the calculated K_c was 8.3 W/mK. The pressure derivatives of thermal conductivities are calculated to be 0.070 W/mK/kbar and 0.057 W/mK/kbar for K_a and K_c respectively in the range between 10 and 40 kbar. The averaged thermal conductivity ($\sqrt[3]{K_a^2 K_c}$) varies with pressure at 0.061 W/mK/kbar. This change (0.8%/kbar) was lower than the thermal diffusivity change (1.9%/kbar) reported by Yukutake (1974).

OPTICAL ABSORPTION SPECTRA OF SYNTHETIC TOURMALINES

M.N.Taran, A.S.Lebedev, Institute of Geochemistry & Physics of Minerals of the Ukrainian Academy of Sciences 252280, Kiev-142; Institute of Geology & Geophysics, Siberian Branch of the Academy of Sciences of the USSR, 630090, Novosibirsk-90, USSR.

Tourmalines (T)- $Na_{1-0}Al_3Al_6B_3Si_6O_{27}(O,OH,F)_4$ with the impurities Fe(a-c);Fe,Ti(d);Cr(e);Ni(f);Cu(g); Co(h);Mn (i) in the Al-octahedral sites (see Fig.a-i below) have been synthesized in hydrothermal solutions $0.05Na(F,Cl)-0.05H_3BO_3-0.9H_2O$ at 650°C, P=1.5kbar and fo_2 that cor-

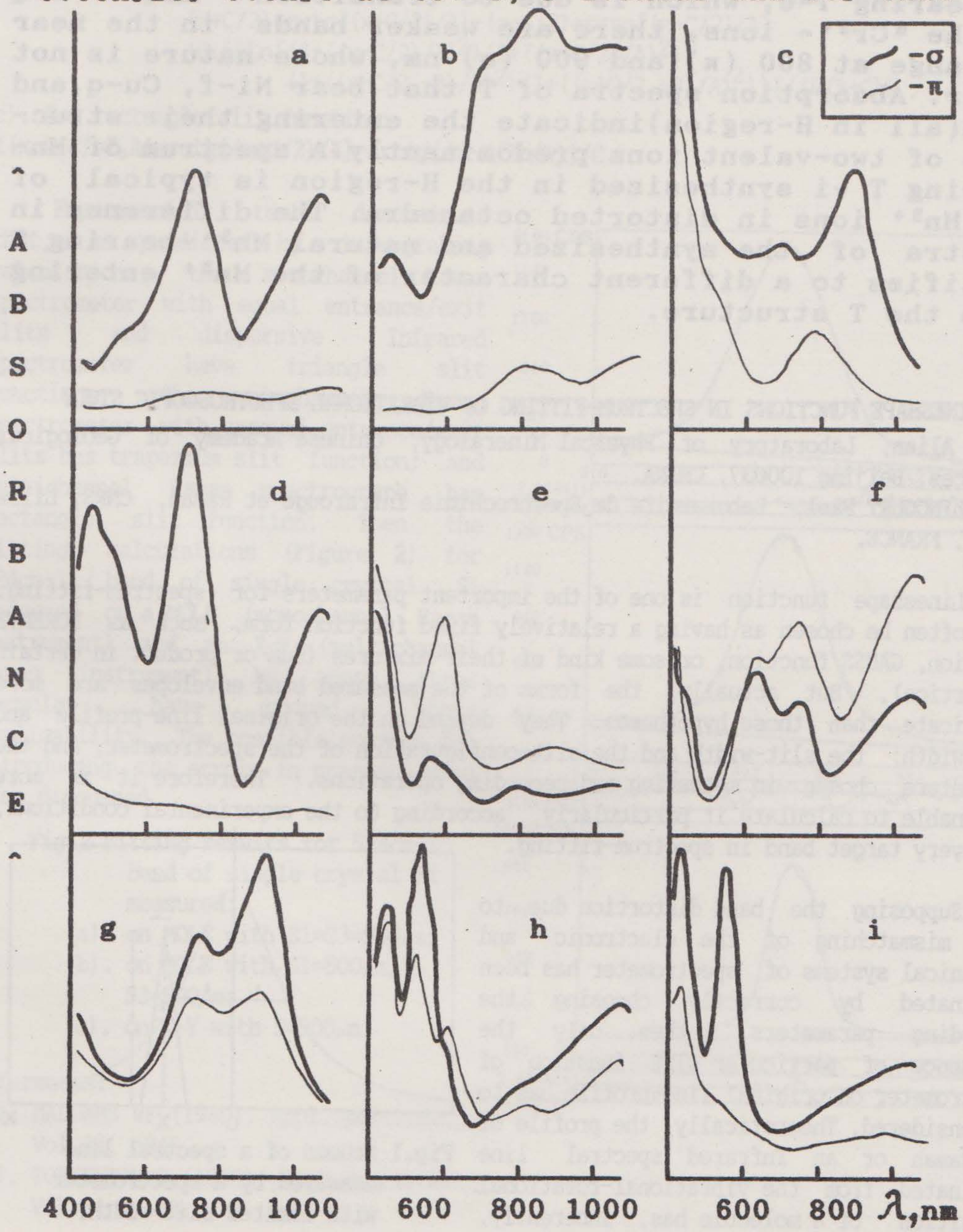

respond to the stability field of magnetite (M) or hematite (H). The ferriferous T display absorption bands of exchange-coupled ions Fe^{2+}-Fe^{3+} -a (M-region) at 710 and 1100 ($\sigma>>\pi$) nm,or Fe^{3+}-Fe^{3+} -c(H-region) at 530,780 (π) and 720,900(σ)nm. The Mössbauer studies showed that 90-100% Fe(0.6-1.0 f.u.-formula units) in tourmaline of H-type are present by Fe^{3+} ions with the most part being in $^{6}Al_{6}$ -octahedrons. In spectra of Fe,Ti-bearing T-d, besides the absorption bands of the exchange-coupled ions Fe^{2+}-Fe^{3+}, a broad intensive band is revealed at 425 nm(σ) probably due to the charge transfer $Fe^{2+}+Ti^{4+}$ -$Fe^{3+}+Ti^{3+}$. Besides the 590 ($\pi>\sigma$) nm band in spectra of Cr-bearing T-e, which is due to transition $^{4}A2q-->^{4}T2q$ in the $^{6}Cr^{3+}$- ions, there are weaker bands in the near IR-range at 800 (π) and 900 (σ) nm, whose nature is not clear. Absorption spectra of T that bear Ni-f, Cu-q,and Co-h(all in H-region)indicate the entering their structure of two-valent ions predominantly.A spectrum of Mn-bearing T -i synthesized in the H-region is typical of the Mn^{3+} ions in distorted octahedra. The difference in spectra of the synthesized and natural Mn^{3+}-bearing T testifies to a different character of the Mn^{3+} entering into the T structure.

R6.14.

THE LINESHAPE FUNCTIONS IN SPECTRUM-FITTING OF VIBRATIONAL SPECTROSCOPIC STUDY

WANG Alian, Laboratory of Physical Mineralogy, Chinese Academy of Geological Sciences, Beijing 100037, CHINA.
DHAMELINCOURT Paul, Laboratoire de Spectrochimie Infrarouge et Raman, CNRS, Lille 59655, FRANCE.

Lineshape function is one of the important parameters for spectrum-fitting, and often be chosen as having a relatively fixed function form, such as LORENTZ function, GAUSS function, or some kind of their mixtures (sum or product in certain proportion). But actually, the forms of the measured band envelopes are more complicate than those hypotheses. They depend on the original line-profile and line-width; the slit-width and the slit-configuration of the spectrometer, and the parameters chosen in measuring and recording operations. Therefore it is more reasonable to calculate it particularly, according to the experimental conditions, for every target band in spectrum-fitting.

Supposing the band distortion due to the mismatching of the electronic and mechanical systems of spectrometer has been eliminated by correctly choosing the recording parameters, then only the influence of particular slit function of spectrometer on original line-profile has to be considered. Theoretically, the profile of a Raman or an Infrared spectral line originated from the vibrational-rotational transition of a molecule has, inherently,

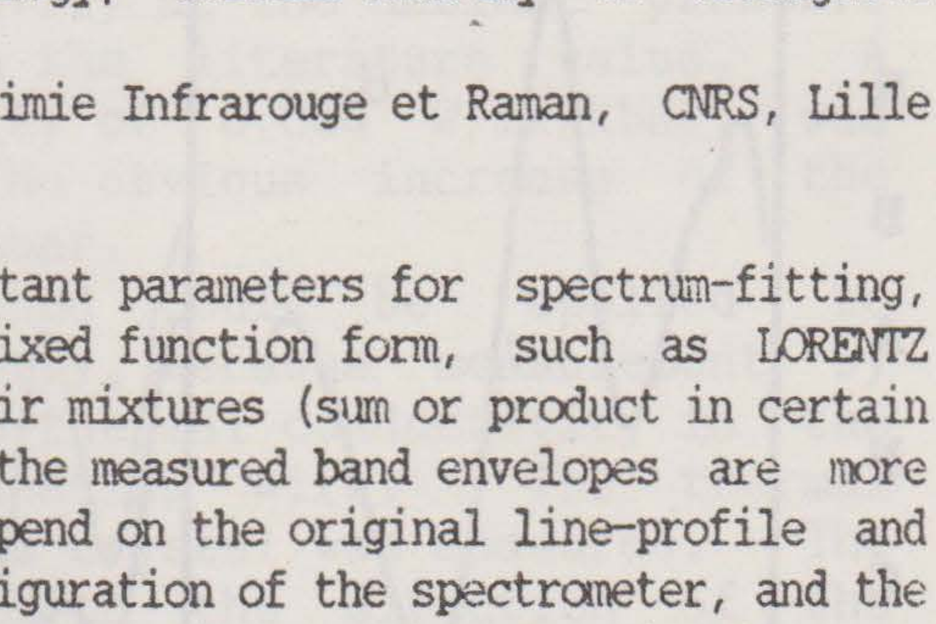

Fig.1 Scheme of a spectral line measured by a spectrometer with limited slit-width.

LORENTZ function form decided by three basic physical processes — radiation damping, Doppler broadening and collision broadening. While in fact, the band envelope measured by a spectrometer is the redistributed radiations, as the function of wavelength, of every partial components of that band which could pass through the slit system of a spectrometer at one wavelength position (Figure 1). Based on this idea, the formulas for calculating the band envelope under three different slit functions were deduced. They are :

a). for triangle slit function:

$$I(x,A,B)=I_oA\{(x+B)\mathrm{arctg}[(x+B)/A]+(x-B)\mathrm{arctg}[(x-B)/A]-2\mathrm{arctg}[x/A] -0.5A\mathrm{Ln}[(1+((x+B)/A)^2)(1+((x-B)/A)^2)/(1+(x/A)^2)^2]\}/B ;$$

b). for trapezium slit function:

$$I(x,A,B,C)=I_oA\{(x+C/2+B)\mathrm{arctg}[(x+C/2+B)/A]+(x-C/2-B)\mathrm{arctg}[(x-C/2-B)/A] -(x+C/2)\mathrm{arctg}[(x+C/2)/A]-(x-C/2)\mathrm{arctg}[(x-C/2)/A] +0.5A\mathrm{Ln}[(1+((x-C/2)/A)^2)(1+((x+C/2)/A)^2)/(1+((x-C/2-B)/A)^2)(1+((x+C/2+B)/A)^2)]\}/(B(B+C)) ;$$

c). for rectangle slit function:

$$I(x,A,C)=I_oA\{\mathrm{arctg}[(x+C/2)/A]-\mathrm{arctg}[(x-C/2)/A]\}/C ;$$

Experimental tests demonstrate that, as predicted by intergrating calculations, the monochannel Raman spectrometer with equal entrance/exit slits and dispersive Infrared spectrometer have triangle slit functions; the monochannel Raman spectrometer with unequal entrance/exit slits has trapezium slit function; and multichannel Raman spectrograph has rectangle slit function. Then the fitting calculations (Figure 2) for 524cm-1 band of single crystal Si measured on a MOLE (monochannel Raman instrument) and an X-Y (multichannel Raman instrument) by those three formulas have proved their applicability. The possible sources for introducing the errors in practice were also discussed.

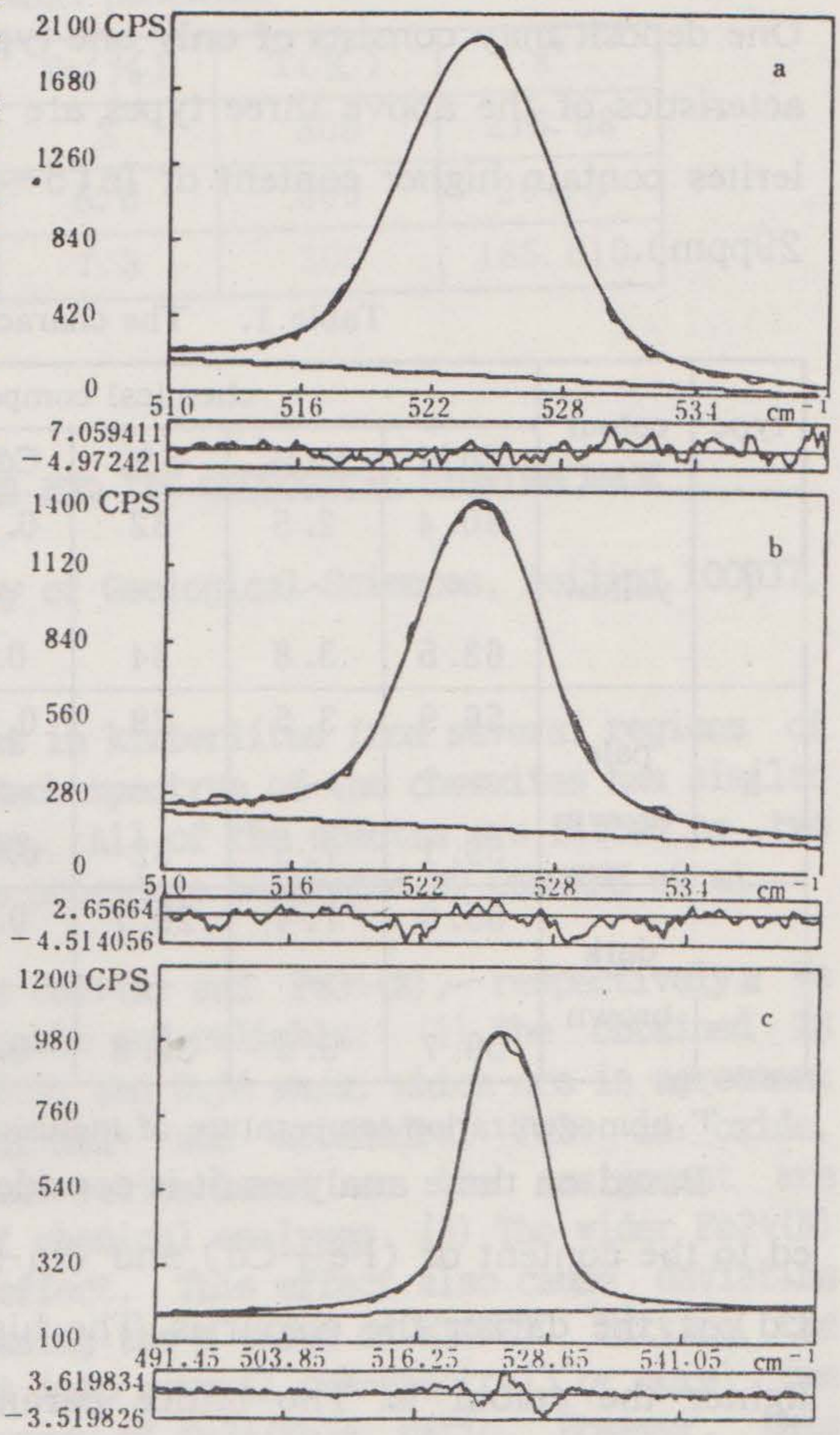

Fig.2 Fitting results for 524cm-1 band of single crystal Si measured:
(a). on MOLE with S1=S3=900μm;
(b). on MOLE with S1=500μm, S3=900μm;
(c). on X-Y with S=900μm.

References:

[1]. MADDAMS WF (1980), Appl.Spectrosc., Vol.34, p245.
[2]. TORKINTON P (1980), Appl.Spectrosc., Vol.34, p189.

P.6.15

THE STUDY ON SPHALERITE IN PB-ZN DEPOSITS AT THE EASTERN PART OF LIAONING PROVINCE

Wang Ende, Shenyang Institute of Gold Technology, Guan Guangyue, Department of Applied Geology, The Northeast University of Technology, Shenyang, Liaoning 110006, People's Republic of China

A lot of Pb-Zn deposits were found at the Eastern Liaoning Province. These deposits distributed on the trend east-west folded zone of metamorphic rocks of Liaohe Group. Sphalerite is one of the main ore minerals in these deposits, and may be divided into three types. Ⅰ). Light yellow to yellowish brown sphalerite occurred in layered ore. Ⅱ). Light brown to brown sphalerite occurred in quartz vein. Ⅲ). Dark brown and black sphalerite occurred in the ores of fault zones. One deposit may consists of only one type or two types or three types. The characteristics of the above three types are listed in Table 1. In addition, the sphalerites contain higher content of In(5～110ppm), Ga(16～108ppm), Ge(1～29ppm).

Table 1. The characteristics of sphalerites

type	colour	chemical composition						$\delta^{34}S$	T (℃)	a_0 (Å)
		Zn%	Fe%	S%	Cd%	Mn ppm	Ag ppm			
Ⅰ	yellow	60.4 ～ 63.5	2.5 ～ 3.8	32 ～ 34	0.38 ～ 0.6	110 ～ 150	100 ～ 120	+6.4 ～ +7.1	136 ～ 196	5.412 ～ 5.415
Ⅱ	pale brown	56.9 ～ 59.1	3.5 ～ 7.5	29 ～ 32	0.63 ～ 0.68	142 ～ 260	135 ～ 185	+6.9 ～ +7.9	284 ～ 364	5.414 ～ 5.417
Ⅲ	dark brown	55.8 ～ 59.7	7.4 ～ 9.6	29.7 ～ 30.8	0.7 ～ 0.9	230 ～ 240	12 ～ 105	+6.8 ～ +7.3	280 ～ 360	5.416 ～ 5.421

T: homogenization temperature of inclusion. a_0: lattice parameter.

Based on these analyses, it is considered that the colour of sphalerite is related to the content of (Fe+Cd) and (In+Ga). The higher the content of (Fe+Cd) is, the darker the colour is. The higher the content of (In+Ga) is , the lighter the colour is. The lattice parameter is influenced by the content of (FeS%) in sphalerite. According to our analyses, as the content of FeS(%) varies from 3% to 15%, the lattice parameter obeys the equation: $a_0=5.406+0.0005X$, and when FeS(%)$>$15-26, $a_0=5.406+0.0005X+0.000004X^2$.

The homogenization temperature of inclusion of sphalerites shows that the lattice enlarged with the increasing of temperature.

The Mossbauer spectrascopy study of sphalerite shows different characteristics among these types of sphalerites. The pattern is an asymmetry two-humped curves. The isomer shift(δ) and quadrupole splitting(Δ) are listed in Table 2. The isomer shift(δ) is controlled by the distance between atom Fe and S. The difference of isomer shift displays the varying of Fe-S distance. The higher the Fe content in sphalerite, the higher the increasing of isomer shift and the larger the Fe-S distance. Thus, along with the increasing of iron content in sphalerite, this may affect its chemical bond, the covalent bond may be weakened, and the ionic bond will be strengthened, which may change the colour of sphalerite. This study shows that the FeS content plays an importance role in the changing of colour and lattice parameter of sphalerite.

Table 2. Mossbauer parameter

type	δ mm/s	Δ mm/s	Fe(%)	T(K)	x^2
I	0.44	0.57	3	300	215.58
II	0.76	0.59	5.6	300	204.0
III	0.79	0.63	7.3	300	165.610

x^2: Fitting factor

MOSSBAUER STUDY OF CHROMITES IN KIMBERLITES AND ITS GEOLOGICAL SIGNIFACANCE

WU Gongbao & DONG Zhenxin, Chinese Academy of Geological Sciences, Beijing 100037, People's Republic of China.

1. Mossbauer spectra of 15 chromites in kimberlites from several regions of China were measured at room temperature. Each spectrum of the chromites has similar features and exibites 3 or 4 resolved peaks. All of the spectra are fitted to two quadrupole doublets(NS=2) according to the procedure suggested by OSBORNE et al.

2. The two doublets are assigned to Fe2+(A) and Fe3+(B), respectively. We consider that this assignment is reasonable and reliable: (1) The obtained IS values of Fe2+(A) and Fe3+(B) are around 0.91 and 0.34 mm/s, which are in agreement with the typical values of tetrahedral Fe2+ and octahedral Fe3+ in oxide, respectively. (2) The obtained Fe3+/Fe2+ ratios based on the assignment are essentially consistent with the results of chemical analyses. (3) The wider Fe2+(A) peak (0.70 mm/s) is caused by N-N-N effect. This effect also cause deviating the peak shape from Lorentzian and increasing the M value of MISFIT. Fitting the Fe2+(A) component spectrum by dividing it into several sub-spectra(3 or more) can improve the fitting quality and the accuracy of Fe3+/Fe2+ ratio. However, this procedure is artificial and each sub-spectrum has no definite physical meaning because of the complexity of factors affecting N-N-N effect. The following discussion will base on NS=2 fitting results.

3. Having studied the relationship between Mossbauer parameters and chemical compositions of the chromites, we found that the QS values of Fe2+(A) and the QS,IS values of Fe3+(B) are closely related with Cr/(Cr+Fe3+ +Al) ratios (Fig.1), whereas there are no obvious correlation between the parameters and Fe3+/Fe2+ or Fe2+/(Mg2+ +Fe2+) etc.

4. The negative correlation between QS[Fe3+(B)] and Cr/(Cr+Fe3+ +Al) shows that with the increaseing substitution of Cr, Fe3+ for Al at B site, the distortion of octahedron of B site become smaller. The negative correlation between QS[Fe2+(A)] and Cr/(Cr+Fe3+ +Al) shows that with the increasing of above substitution, the distortion of tetrahedron of A site become larger. The positive correlation between IS[Fe3+(B)] and Cr/(Cr+Fe3+ +Al) reveals that with the increasing of above substitution, the coordination octahedron become larger and the Fe3+ at B site exibites greater ionicity.

5. The kimberlites from which the chromite samples were collected contain different quantities of diamond ore. They could be divided into three ore-bearing states: I. rather rich (sample No.6-15), II. poor (No.4,5), III. very poor (No.1-3). We discover that the values of IS[Fe3+(B)], QS[Fe3+(B)] or QS[Fe2+(A)] of the measured samples can be also divided into three groups corresponding to the ore-bearing states. Especially, there is a clear bound between the I and II groups (Fig.1). On the basis of this work, it is possible to judge the ore-bearing state of kimberlite. The preliminary criterions determined by us are as follows: if the Mossbauer parameters of chromite at RT satisfy IS[Fe3+(B)]>0.340, QS[Fe3+(B)]<0.540 and QS[Fe2+(A)]<1.05 mm/s, the kimberlite most probably contains rather rich diamond ore.

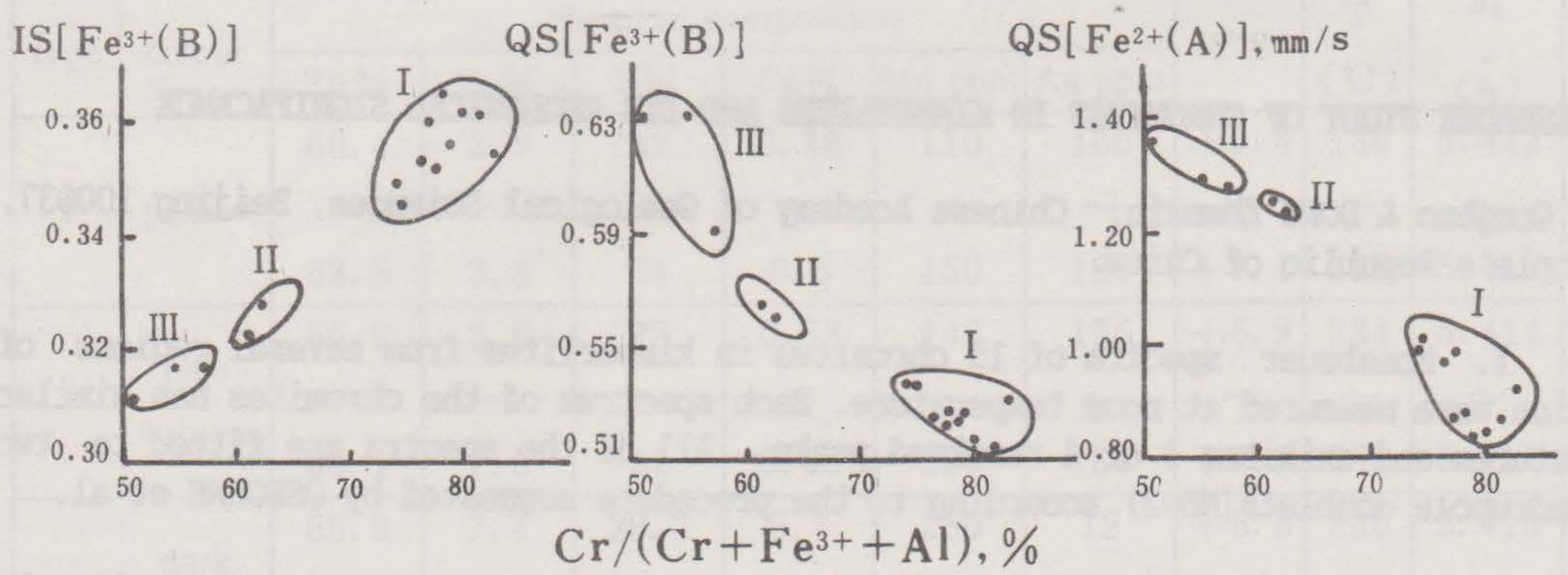

Fig.1 Relationship between Mossbauer parameters and Cr/(Cr+Fe3+ +Al) in chromites

It is known that the chromite of kimberlite which is relatively rich in diamond ore exhibits the feature of high-Cr and low-Al (i.e. has greater substitution of Cr for Al at B site), and it corresponds to the genetic conditions of high pressure (e.g. 40-55kb) and not too high temperature (e.g.950-1050 C). On the other hand, the relevant Mossbauer parameters of chromite have shown a intrisic connection with this Cr-Al substitution (see #4). So it is concluded that the Mossbauer parameters of chromite are sensitive to the changes of genetic conditions of kimberlite, namely they have the typomorphic significance.

6. In the spectra of this study, Fe2+ at B site, Fe3+ at A site and electron delocalization were not observed. Based on the results of chemical and Mossbauer

analyses, the complete crystal chemical formulas of chromites have been given. Our study shows that there are only Fe2+ and Mg2+ at A sites of chromites and the B sites are occupied by Fe3+, Al3+, Cr3+, Mn2+, Ti4+ and the residual Mg2+ after filling A sites. It is concluded that the chromites belong to normal spinel type minerals.

Reference OSBORNE MD,FLEET ME,BANCROFT GM (1981) Contrib Mineral Petrol 77:251-255

RAMAN LASER MICROPROBE STUDY OF GLASS INCLUSIONS IN CHROME SPINEL OF ULTRABASIC ROCKS IN NORTH-WEST CHINA

Po G.16

XU Peicang, WEI Wenzong, LI Rubi, WANG Yongqing. Xian Institute of Geology and Mineral Resources, Xian, Shaanxi, 710054, People's Republic of China

In this paper, the compositions and molecular structures of glass inclusions in chrome spinel are investigated by means of Raman Microprobe. Some new cognitions are obtained.

The samples were taken from Saertuhai ultrabasic rocks zone in Xin Jiang of north-west China. (depth:240m-280m). The ore body is taxitic chromite. It's country rocks are dunite and arsoite. The glass inclusions are seldom seen in the chrome spinel. They exhibit ellipitical shape (diameter:10μm-15μm).

First, the compositions of glass inclusions are measured by Electron probe (Japan Jcxa-733) and Raman probe (France RAMANOR U1000). The results are listed in table 1.

Table 1.

Samples number	Compositions of Glass Inclusion (wt%)									
	Electron Probe Analysis									
	SiO_2	Al_2O_3	Cr_2O_3	FeO	MgO	CaO	Na_2O	K_2O	Cl	S
Uc-1	22.88	20.98	3.81	1.10	32.70	0.57	0.16	0.06	0.08	0.28
Uc-2	25.24	22.02	4.12	0.98	30.47		0.03			
Chlorite	26.66	28.73		5.27	31.34					

Samples number	Raman Probe Analysis								
	CO_2	CO	CH_4	O_2	H_2	SO_2	H_2S	$H_2O(G+L)+OH$	Total*
Uc-1	6.4	1.4	0.2		0.01	1.3		3.5	95.43
Uc-2	6.1		0.5	0.8	0.01	0.8	0.4	3.1	94.57
Chlorite								8.0	100.00

* The "TOTAL" means sum total of measurement data by Electron Probe and Raman Probe.

It can be seen that the glass phase mainly consists of SiO2,Al2O3 and MgO. Its composition tallies with that of chlorite.

The dissolution of H2O in that glass phase is in the form of OH groups which associated with Si^{4+}, and probably with Mg^{2+} or Ca^{2+}. CO_2 associated with one or more network modifying cations (Ca^{2+} or Mg^{2+}).

Studied second, the Si-O molecular group structures of glass phase is by Raman spectroscopy. the feature of that structure all depends on the composition, temperature, pressure and viscosity of the glass phase. Different Si-O structures could be divided into five types which have different characteristical Raman frequency.(Onb/T shows a ratio of nonbridging oxygen to tetrahedral cation. see Tab.2).

Based on table 2 and Fig.1, the molecular structure of sample No.Uc-1 mainly consists of chain and sheet units. It is the glass phase approaching to chlorite. The Raman spectral pattern of crystal chlorite at 705-710cm^{-1} shows a sharp peak which we have measured.

The existences formation of H20 and C02 is related with the increments of the proportions of chain and sheet units in the molecular structure of glass phase.

Table 2.

Name	Sign	Structure Unit	O_{nb}/T	Raman Characteristical Peaks (cm^{-1})	
				$Si-O_{nb}$	$Si-O_{br}-Si$
Monomer	Mo	(SiO_4)	4	840-890	
Dimer	Di	(Si_2O_7)	3	900-950	720-760
Chain	Ch	(Si_2O_6)	2	960-1030	630-680
Sheet	Sh	(Si_2O_5)	1	1050-1100	670-730
Network	Ne	(SiO_2)	0	1060-1190	450-520

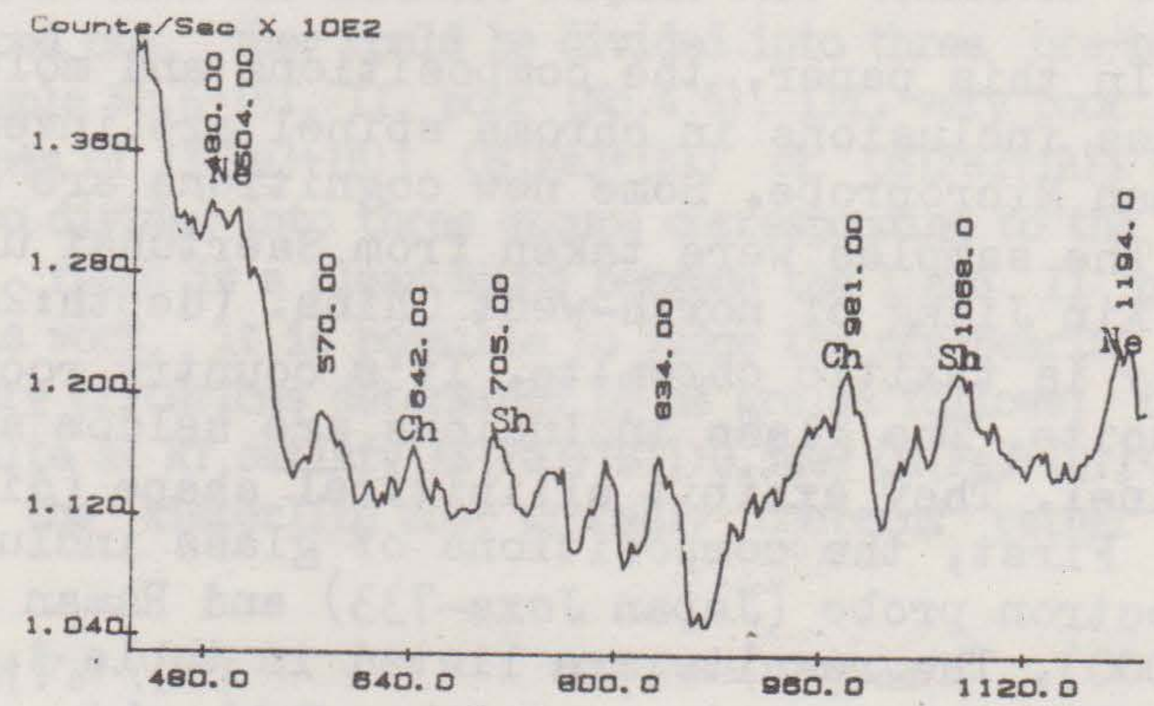

Fig.1. Raman spectrum of glass approaching to chlorite. Sample No.Uc-1.

References
1. Mysen B.O. and Virgo D.(1980) Amer. Miner. Vol.65 Pag. 1176-1184.
2. Dowty E.(1987) Physics and Chemistry of Minerals 14:407-412.

A RIVEIW OF MOSSBAUER SPECTRA OF Fe-Ti GARNET

Ying Yupu,Institute of Geology,Academia Sinica, Beijing,100011,People's Republic of China

Some papers on Mossbauer effect of natural Fe-Ti garnets have been published[1-6].The mentioned authors researched valence state and distributions of Fe and Ti cations,and change of Mossbauer parameters with sample temperature.Up to now about 30 samples of na-

tural Fe-Ti garnets(TiO_2 wt% is from 0.45 to 16) were researched by means of Mossbauer effect at temperature from 15K to 773K.

Three samples of natural schorlomite are researched in this paper.A riveiw of Mossbauer spectra of Fe-Ti garnets is given here.From present study some significant conclusions can be drawn.

1. Different types of Mossbauer spectra can be distinguished for Fe-Ti garnets and the association patterns of the Mossbauer doublets are induced.Most published Mossbauer spectra of the natural schorlomite have five doublets (Fe^{3+}_{tet},Fe^{3+}_{oct},Fe^{2+}_{dod},Fe^{2+}_{oct} and mixed valence absorption). As Fe^{3+}_{tet},Fe^{3+}_{oct},Fe^{2+}_{dod} and Fe^{2+}_{oct} coexist in Fe-Ti garnet,the doublet due to mixed valence absorption is always apparent.

2. It is better that the doublet assingned to "Fe^{2+}_{tet}" are reffered to the mixed valence absorption.

3.The line-width of the mixed valence absorption is always large,which can be fitted into 2 doublets in some Mossbauer spectra of schorlomites.

4.The mixed valence absorption relates not only to electron proccese between Fe^{2+} and Fe^{3+} at sevaral crystallographic sites but also to the effect of Ti cation in Fe-Ti garnet.

5.The variances of Mossbauer parameters of Fe-Ti garnet with sample temperature are apparent.In general there is a inverse temperature-dependence.The doublets due to mixed valence have the largist rate of variance from 300K to 5K.As sample temperature is lower than 30K,the variance rate of Mossbauer parameters becomes more apparent.

6.Tetrahedral preference site order in Fe-Ti garnet is $Fe^{3+} > Ti^{4+} > Al^{3+}$.

References

1. Amthauer, G., Annersten, H. and Hafner, S.S. (1977), Phys. Chem. Minerals, 1, 399-413.
2. Dowty, E. (1971), American Mineralogist, 56, 1983-2009.
3. Huggins, F.E., Virgo, D. and Huchenholz, H.G. (1977), American Mineralogist, 62, 475-490.
4. ——, ——, —— (1977), American Mineralogist, 62, 646-665.
5. Schwartz, K.B., Nolet, D.A. and Burns, R.G. (1980) American Mineralogist, 65, 142-153.
6. Ying Yupu and Cai Ruiying (1985), Science Sinica (series B), 28, 202-209.

6.6H

Site Occupancy and Local Properties of Fe^{2+}, Fe^{3+} in Titanium bearing Andradites

Ying Yupu[a], Lin Chuanyi[b], and S. S. Hafner
Institute of Mineralogy, University of Marburg, 3550 Marburg, West Germany

[a,b] permanent address: Academia Sinica, China, [a]Institute of Geology, Beijing; [b]Institute of Geochemistry, Guangzhou Branch

Titanium bearing andradites are well known for their complex cation distribution over the 8-, 6-, and 4-coordinated positions X, Y, and Z, respectively. For example, Fe^{2+} may occur at X, Y, and possibly Z, while Fe^{3+} may be located at Y and Z. The Fe^{2+} and Fe^{3+} occupancies are derived usually from Mossbauer spectra of ^{57}Fe combined with chemical analyses using e.g. the electron microprobe. Cation distribution may be calculated (i) on the basis of 24 negative charges, neglecting hydroxyl ions substituted for O^{2-}, or (ii) on the basis of 8 cations, assuming that all X, Y, and Z sites are occupied, neglecting H_4^{4+} molecular ions substituted for Si^{4+} at Z and/or vacancies at X, Y, and Z. Both assumptions, (i) and (ii), are not entirely correct as several studies show (e g 1,2). Additional difficulties are the generally unknown oxidation states of Ti and Mn, i.e. the Ti^{3+}/Ti^{4+} and Mn^{2+}/Mn^{3+} ratios.

Moreover, it has been assumed from Mossbauer spectra that some electron delocalization (ED) may be possible between Fe at X, Y, and Z, at least at high temperatures (3-6). Final conclusions could not be made, however, mainly because of incomplete knowledge of the temperature dependence of the ^{57}Fe hyperfine splittings and improper resolution of the spectra.

The ^{57}Fe spectrum consists of at least five partially overlapping doublets, at least at temperatures above 20 K. In this work, the observed QS of the Fe^{2+} doublets were interpreted in terms of crystal field theoy. It was found that their dependences on temperature can be accounted for reasonably. Because of spin-orbit coupling, the QS of Fe^{2+}(Y) is expected to decrease somewhat

with decreasing temperature at temperatures below about 78 K since its ground state is T_{2g}. This should not be observed for the QS of Fe^{2+}(X) and Fe^{2+}(Z) because there are no non-vanishing spin-orbit coupling matrix elements between the states belonging to the ground state E_g of tetrahedral or dodecahedral Fe^{2+}.

It is concluded that ED between Y and Z is unlikely to occur because of the lack of shared edges between these two sites. Although a short distance (3.015 A) exsists between cations at the edge-sharing sites X and Z, ED is not likely either below about 240 K since no significant change in line width of the respective doublets was observed in this region (5). At higher temperatures, however, ED between X and Z may possibly occur, as indicated by the line broadening at 300 K (5,6) compared to the low temperature spectra (3,4).

---

(1) R.D.Aines and G.R.Rossman, Am. Mineral. **69** (1984) 1116-1126. (2) R. Basso, F. Cimmino, and L. Zefiro, Neues Jahrbuch fur Mineralogie, Abhandlungen **148** (1984) 248-258. (3) G. Amthauer, H. Annersten, and S.S. Hafner, Phys. Chem. Minerals, **1** (1977) 399-413. (4) F. E. Huggins, D. Virgo, and H.G. Huckenholz, Am. Mineral., **62** (1977) 475-490; 646-665. (5) K.B. Schwartz, D.A. Nolet, and R.G. Burns, Am. Mineral.,**65** (1980) 142-153. (6) Wu Gongbao and Mu Baolei, Phys. Chem. Minerals, **13** (1986) 198-205.

HAMILTONIAN MATRIX ELEMENTS OF $d^4(d^6)$ ELECTRON CONFIGURATION WITH C_{2v} SYMMETRY AND THEIR APPLICATION TO MINERAL

PO 6.17.

YUAN Yunmei & QUI Xianlun, Physices Group, Guizhou Institute of Technology, Guiyang, Guizhou, People's Republic of China

Because there were no complete crystal field matrices including Trees correction of $d^4(d^6)$ configuration with C_{2v} symmetry and so the involved absorption spectra can not be assigned acoording to its real symmetry untill now. The C_{2v} matrices of $d^4(d^6)$ are derived by an elaborate mathematical procedure on the basis of weak-field scheme. The results have been used to deal with the optical absorption spectra of Fe^{2+} at site M(1) in diopside (Yuan, Y.M., ect. 1985). The results calculated are in good agreement with the experiments.

Acoording to the point-charge model, the crystal field potential with C_{2v} symmetry can be written as

$$V = \sum_i V(\vec{r}) = \sum_i \{[\gamma_{20} Z_{20}(\theta_i, \varphi_i) + \gamma^c_{22} Z^c_{22}(\theta_i, \varphi_i)] r_i^2 + [\gamma_{40} Z_{40}(\theta_i, \varphi_i) + \gamma^c_{42} Z^c_{42}(\theta_i, \varphi_i) + \gamma^c_{44} Z^c_{44}(\theta_i, \varphi_i)] r_i^4\}$$

with $$\gamma^{(a)}_{KM} = \frac{4\pi e q}{2K+1} \sum_\tau \frac{1}{R_\tau^{K+1}} Z^{(a)}_{KM}(\Theta_\tau, \Phi_\tau)$$

By using the basis functions of C symmetry, we have derived the Hamiltonian matrix elements of quintet states, $^5A_1$(2x2 matrix) (Table 1), $^5A_2$, $^5B_1$, $^5B_2$; and of triplet states, $^3A_1$(9x9 matrix), $^3A_2$(12x12 matrix), $^3B_1$(12x12 matrix) and $^3B_2$(12x12 matrix). They could be used in the calculations of absorption spectra of $d^4(d^6)$ ions for all crystals which possessing C_{2v} symmetry. In our calcu-

lation, the crystal field parameters are defined as follows:

$$b_1=-\frac{1}{70\sqrt{5\pi}}\gamma_{20}\langle r^2\rangle,\quad b_2=\frac{1}{70\sqrt{\pi}}\gamma_{40}\langle r^4\rangle,\quad b_3=\frac{5}{4\sqrt{35\pi}}\gamma_{44}^{c}\langle r^4\rangle,$$

$$b_4=\frac{1}{14\sqrt{15\pi}}\gamma_{22}^{c}\langle r^2\rangle,\quad b_5=-\frac{1}{28\sqrt{5\pi}}\gamma_{42}^{c}\langle r^4\rangle.$$

Acoording to d-orbit theory (Zhao, M.G. & DU,M.L. 1983) of Fe^{2+}, the expected values of $\langle r^2\rangle$ and $\langle r^4\rangle$ are $\langle r^2\rangle$=2.2949 a.u., $\langle r^4\rangle$ = 14 a.u., and the Rach parameters are B=947 cm^{-1}, C=3375 cm^{-1}. Trees correction, α is equal to 85 cm^{-1}. Then using the structure data (Warren,B.E. & Bragg,W.L., 1929), we get the absorption spectra.

Table 1

$^5A_1$	^5D	$^5D'$
	$-10b_1-5b_2-2b_3$	$10\sqrt{3}(b_4+b_5)$
	$+6A-21B+6\alpha$	
		$10b_1-30b_2$
		$+6A-21B+6\delta$

Table 9

Transitions	Calc.	obsd.
$^5B_1(1),^5B_2(1)$---		
$^5A_1(1)$	864	
$^5A_1(2)$	9302	8333
		9615
$^5A_2(1)$	11555	10309
$^3B_1(1),^3B_2(1)$	8193	
$^3A_2(1)$	11278	11800
$^3A_2(2)$	13861	13700
$^3B_1(2),^3B_2(2)$	15645	14930
		16700
$^3B_1(3),^3B_2(3)$	18836	18000
$^3A_2(3)$	19092	19800
$^3A_1(4),^3B_2(4)$	21455	20740
$^3A_2(4)$	22200	21000
$^3B_1(5),^3B_2(5)$	22389	
$^3A_2(5)$	22503	
$^3A_1(1)$	22729	23040
$^3A_1(2)$	23776	23360
$^3B_1(6),^3B_2(6)$	26441	
$^3A_2(6)$	26875	
$^3A_1(3)$	27737	27890
$^3B_1(7),^3B_2(7)$	29912	28920
		29680
$^3A_1(4)$	30265	
$^3A_2(7)$	31554	
$^3A_1(5)$	31982	31880
$^3A_2(8)$	32554	32450
$^3B_1(8),^3B_2(8)$	33167	
$^3A_1(6)$	33492	33720
$^3B_1(9),^3B_2(9)$	36081	
$^3A_2(9)$	37041	36730
$^3A_1(7)$	37896	
$^3A_1(8)$	38272	
$^3B_1(10),^3B_2(10)$	43162	
$^3A_1(9)$	51335	
$^3A_2(10)$	52709	
$^3B_1(11),^3B_2(11)$	53936	
$^3B_1(12),^3B_2(12)$	55128	
$^3A_1(11)$	55183	
$^3A_2(12)$	57028	
^5E--^4T(M(2) site)	4250*	4201

*: Estimated value by using cubic approximation(Yuan, Y.M.).

The observed and calculated spin-allowed and spinforbidden transitions of Fe^{2+} at site M(1) in diopside are listed in Table 9. It should be pointed out that there exists accidental degeneracy in the levels B_1 and B_2, which originates from the special structure of diopside. In our calculation, no fitting parameters were used.

The authors thank Professor Zhao Min-Guang for the helpful discussion.

Bonding State of Tellurium in Tellurium Minerals

Zhang Li, S.S. Hafner, G. Moh[1]
Institute of Mineralogy, University of Marburg,
3550 Marburg, West Germany

Tellurium minerals are mainly found in hydrothermal environments of hypogene or supergene mineral deposits. Generally, they occur as tellurides, tellurates, and, more rarely, as oxides, sulfosalts or native tellurium. Tellurium in minerals may be anion or cation with nomimal valence states between -2 to +6. While the crystal structures of those minerals are often of considerable complexity, the valence and bonding states of tellurium are not well known.

The bonding state of tellurium may be studied using Mossbauer

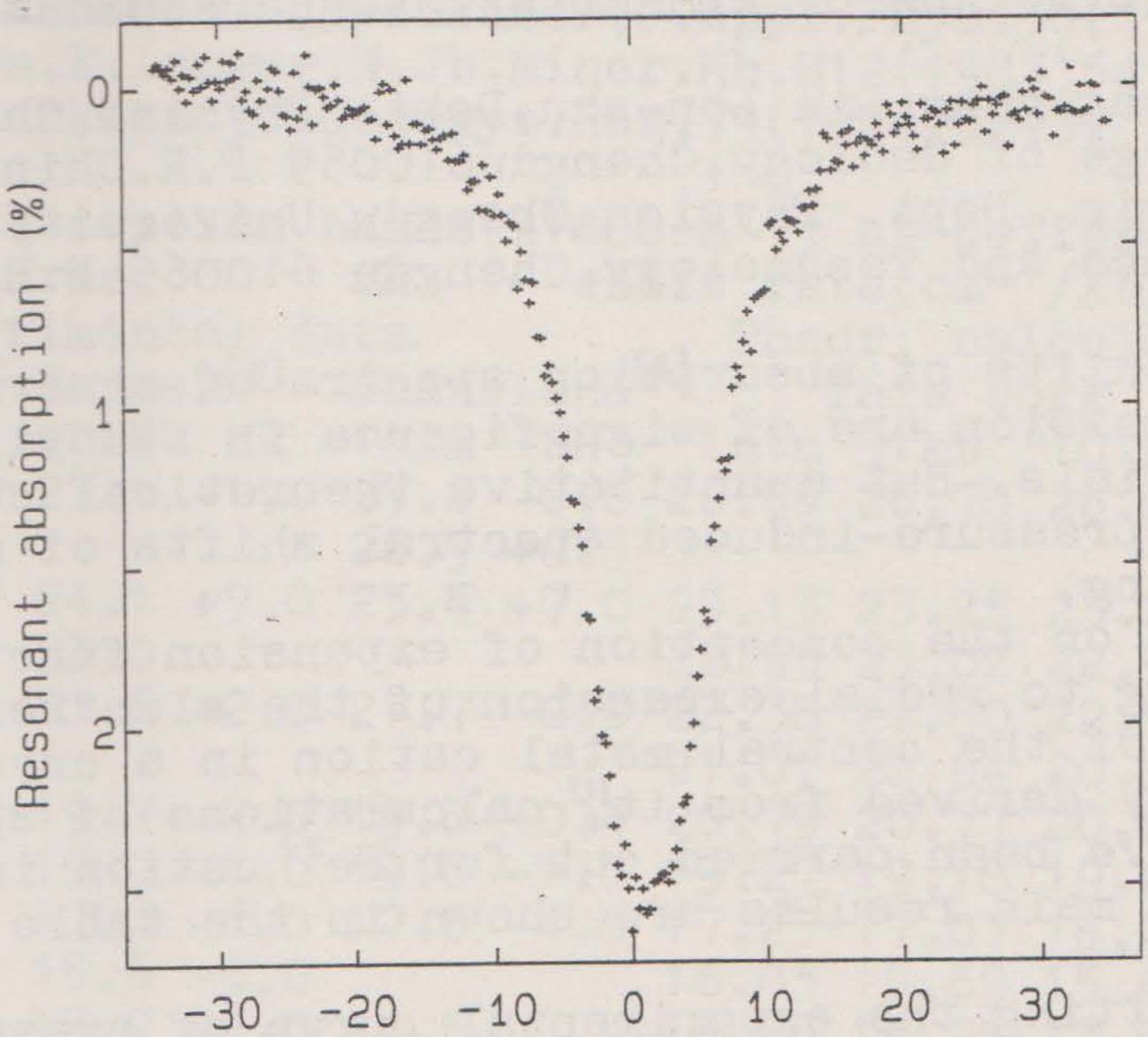

^{125}Te spectrum of $FeTe_2$; the spectrum consists of a doublet due to Te_2^{2-} in a pyrite type structure. From the isomer shift and nuclear quadrupole splitting, an electronic state of $5s^{1.83}5p^{5.67}$ is determined for Te of the Te_2^{2-} molecular ion (Bynczicka et al., 1990).

spectroscopy of ^{125}Te. In the past few years, that technique has been significantly improved by synthesis of a ^{125m}Te source in Mg_3TeO_6 which allows the study of resonant absorption between 4 and 300 K. That source may be held at room temperature, yielding a high recoil-free fraction (Binczycka et al, 1988, 1989).

We have studied Mossbauer spectra of ^{125}Te between 5 and 77 K in a series of natural and synthetic compounds, including tellurides, tellurates and tellurium oxides. The spectra allow determination of Te-coordination numbers, nominal valence states and details on electronic configuration (Binczycka et al, 1988, 1989), cf Figure below. Systematic trends of isomer shifts and nuclear quadrupole splittings may now be tabled.

H. Binczycka, S.S. Hafner, J. Stanek, M. Trömel (1988) Physics Letters A, 131, 135-137.
H. Binczycka, S.S. Hafner, G. Moh, J. Stanek (1990) Physics Letters A (accepted for publication).

---

1. Permanent address: Mineralogisch-Petrographisches Institut der Universität Heidelberg, 6900 Heidelberg, West Germany.

THEORETICAL CALCULATIONS OF THE SHIFTS OF OPTICAL ABSORPTION SPECTRUM OF ALMANDINE UNDER PRESSURE **

Zhang Zheng-gang,Lin Lon-shu,Dept. Physics,Chengdu College of Geology,Chengdu610059 P.R.China
Ma Dong-pin, Dept. Physics,Chengdu University of Science and Technology,Chengdu 610065 P.R.China

The shifts of absorption spectra of minerals under compression are of significance in studying mantle materials. But quantitative theoretical calculations of pressure-induced spectral shifts of minerals are lacking.

Based on the conception of expansion function corresponding to radial expansion of the electron wave function of the central metal cation in a crystal, and the theory derived from it[1], calculations of spectral shifts have been carried out for Fe^{2+} cation in Almandine. The main results are shown in the table and figure.

By fitting the experimental curve of pressure-induced shifts of one of the spin-allowed bands[2], the blue shifts as well as the red shifts of all the spin-allowed and spin-forbidden transitions(in total 40 bands) have been calculated in a unified way. The results were compared with experiments. The Dq and Cp

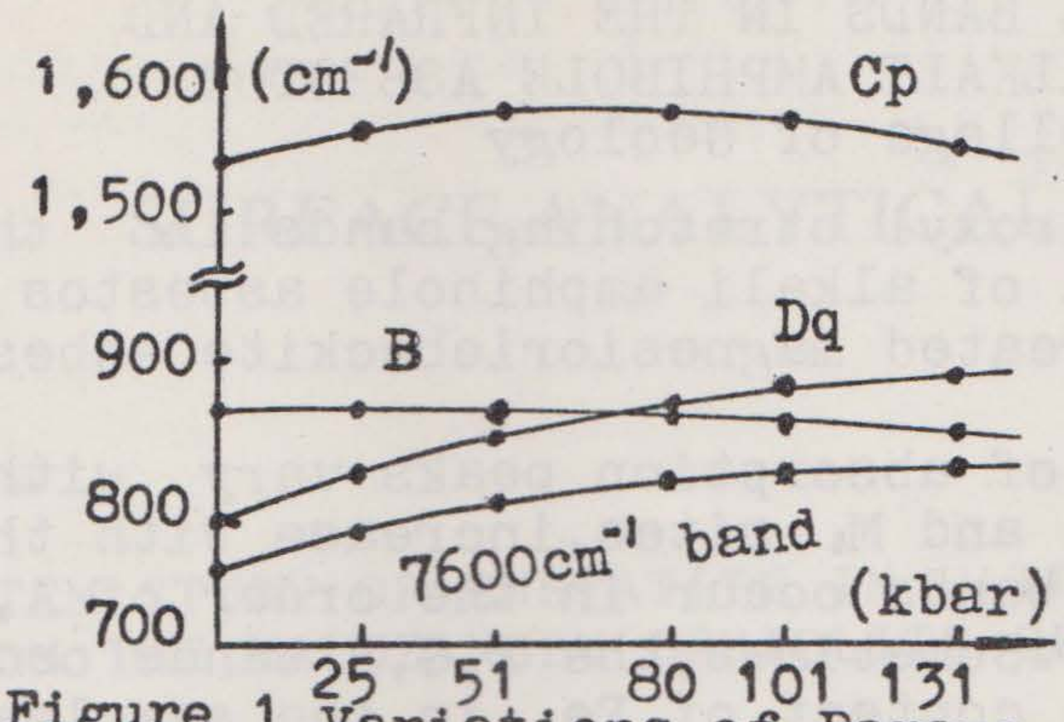

Figure 1 Variations of Parameters and band under pressure

are crystal splitting parameters of cubic and D_2 symmetries respectively.

It is found some bandsshow blue shifts at first and then turn to red shifts. This is related to different behaviors of Dq, Cp and Racah parameters B and C(C=4B) under pressure. A correct relation between Dq and compression ratio κ (=R/R$_0$) was given as:

$$Dq = Dq_0 \cdot \kappa^{-5} \cdot \varphi^{-4}(\kappa) \cdot e^*/e^*_0$$

where Dq_0 is crystal splitting parameter at normal pressure, $\varphi(\kappa)$ is the expansion function, e^*/e^*_0 —— the ratio of effective charges of ligands at normal pressure and under compression, which is also a function of κ.

References

[1] D.P.Ma et al.,Phys.Lett.A126(1988)377,
[2] A.S.Balchan,H.G.Drickamer,J.Appl.Phys.30(1959)1446,
[3] G.Smith,K.Langer,N.Jb.Miner.Mh.H12(1983)541,
[4] T.J.Shankland,J.Geophys.Res.79(1974)3273.

Table 1 Absorption bands(x1000cm^{-1}) at defferent pressures. SR shift rate(cm^{-1}/kbar)

Experimental data						Theor. calculations			
Smith & Langer[3]				Shankland[4]		This work			
1atm	51kb	101kb	SR	1atm	SR	1atm	51kb	101kb	SR
27.2	27.2	27.1	-1.0	27.2	0.0	26.55	26.78	26.85	+29.1
				26.9	+0.5				
23.2	23.7	24.1	+9.0	23.4	+7.0	23.13	23.25	23.27	+1.43
	22.8	23.0				22.93	23.02	22.99	+0.69
21.8	21.8	21.6	-2.0	21.7	0.0	22.38	22.50	22.52	+1.29
	21.0					21.01	20.94	20.82	-1.91
19.9	19.8	19.7	-2.0	19.8	+0.4	20.79	20.77	20.68	-1.05
19.1	19.0	19.0	-1.0	19.0	-1.0	19.27	19.18	19.04	-2.27
17.6	17.3	17.0	-6.0	17.6	-4.8	17.25	17.07	16.95	-2.87
16.2	15.8	15.6	-6.0			16.03	15.69	15.42	-6.01
14.4	14.1	13.9	-5.0	14.5		14.56	14.21	13.95	-6.05
7.60	7.80	8.20	+6.0	7.73	+5.0	7.600	7.979	8.176	+5.70
5.80	6.10	6.70	+9.0			5.800	6.113	6.273	+4.68
						4.400	4.697	4.877	+4.72
						1.100	1.150	1.160	+0.59

** Work partly supported by the National Natural Science Foundation of China.

P.6.8

STUDIES OF HYDROXYL BANDS IN THE INFRARED AND RAMAN SPECTRA OF ALKALI AMPHIBOLE ASBESTOS

Zhu Zizun Xi'an College of Geology

This paper deals with hydroxyl stretching bands in the infrared and raman spectra of alkali amphibole asbestos and one sample of heat-treated magnesioriebeckite asbestos.

The number and intensity of absorption peaks vary with the ratio of $Fe^{2+}/Fe^{2+}+Mg^{2+}$ in M_1 and M_3 sites, increase with the ratio of $Fe^{2+}/Fe^{2+}+Mg^{2+}$, the bands occur in the order of A, B, C, and D peaks respectively. Sometimes, the F, G, H bands occur in raman spectra, when the content of Fe in the samples is higher.

The calculated result of Fe^{2+} and Mg^{2+} in M_1 and M_3 sites shows that the degree of ordering of Fe is higher than that of Mg^{2+}. Various alkali amphibole asbestos show different degrees of ordering Fe^{2+}. Those whose content of Fe^{2+} are low show higher degree of ordering and vice versa.

With the increase of ratio of $Ca^{2+}/Ca^{2+}+Na^{+}$ in M_4 site, the frequency of the band shifts to higher frequency. The presence of Ca at M_4 will produce a band about 7cm above peak A.

The 1-3 absorption bands occur above peak A, when A site is occupied by cation, and the frequency of the band is related to the cation in A site.

With increasing temperatures, the hydroxyl bands of heat-treated magnesioriebeckite asbestos disappear in the order of D, B, C and A peaks. The process of hydroxylation is accompanied by the decrease of ordering degree of cations, the transfer of parts of Na^{+} ions from M_4 site to A site and a broad band occurs peak A.

The results of the Factor Group analysis of vibration modes of alkali amphibole asbestos fit in very nicely with the measured spectra.

SURFACE ANALYTICAL METHODS

HRTEM STUDY OF ENSTATITE IN ULTRAMAFIC TECTONITE FROM THE YALUZANGBU OPHIOLITE BELT, TIBET, CHINA

FU Pingqiu, MEI Houjun, HUANG Bojun (Institute of Geochemistry, Academia Sinica, Guiyang, 550002) and YANG Dayu (Institute of Physics, Academia Sinica, Beijing, _____ People's Republic of China)

The Yaluzangbu Ophiolite Belt starts from Jindong Langxian County in the east and extends to the south of Mana Pass of Zanda County in the west with a total length of about 1400km. According to the distribution of the rockbodies, the ophiolite belt can be divided into three sections: the west section comprising the Langa? ultrabasic rockbody and others, the middle section where the ophiolite suite is developed most completely, and the east section in the east of Dazhuka rockbody including Luobusha and some other rockbodies.

Microscopic observations show significant different textures for the rockbodies in different sections. The rocks in west section have hypidiomorphic granular texture. The large tabular crystals of orthopyroxene are common and contain a great number of lamellae of clinoenstatite(CLEN) which is characteristic for igneous rocks. The bastitized tabular crystals of orthopyroxene are usually orientated. The exsolution lamellae in pyroxene are less common. The contorted structure and the mosaic texture can be seen frequently. The rocks in east section are strongly compressed and show evident texture of metamorphic rocks. Consequently, the rocks in west and east ends of Yaluzangbu Ophiolite belt have suffered from different stress.

The enstatite which occurs in all three sections has been studied using HRTEM. It can be seen from the [010] structural image that the CLEN domains? appear in all orthoenstatites (OREN). The width of domains is 9A (a or b axes of clinoenstatite unit cell) multiplied by 2, 6, 10 or other even numbers. It indicates that

they were probably transformed from orthoenstatite(a-axis of unit cell is 18A)as a result of shearing.? However, the frequencies of CLEN domains in OREN from different sections are various. It is much higher in the east section than that in the west section and they are quite similar in middle and west sections. This suggests that pyroxene in the east section has suffered from stronger stress than those in middle and west sections have. The lattice of pyroxene in east section is obviously deformed and dislocated probably resulting from strong shearing, compression and impaction.

Evidently, the results of HRTEM study are coincident with the field observation and microscopic examination. It leads us to believe the previous speculation in geology. The reason causing different stress in east and west section of the ophiolite belt can be probably described as following. The northward projecting corner of Kashmir in Western Indian Plate has firstly collided with the Eurasian Ancient Continent and played a sustaining role. It prevented the rocks in west section which located in the east of projecting corner of Kashmir, from being strongly compressed. Consequently, it resulted in keeping exsolution texture characteristic for igneous rocks. Meanwhile, the rocks in east section are just located in the place of collision between the Indian Plate and the Eurasian Ancient Continent. They suffered from strong post-orogenic compression. It led to sufficient adjustment in solid rocks, disappearance of exsolution texture and forming the texture of metamorphic rocks which is common in mantle-derived peridotite.

High-energy PIXE of heavy elements in geological materials.

Halden, N.M., Department of Geological Sciences, University of Manitoba, Winnipeg, Manitoba, Canada, R3T 2N2.

High-energy protons (Ep=40 MeV) will efficiently ionize K shells of rare earth and heavy elements. K X-ray spectra have been obtained from Au-bearing minerals in a sulfide ore, a quartz vein ore and Platinum Group Elements (PGE's) in sperrylite and rutheniridosmine. For samples in which Au is the only heavy element present, all four K X-ray lines are well-resolved and would allow quantitative relative intensities to be derived. It is also possible to resolve all four component K X-ray lines for the PGE's. In cases where there is more than one PGE present K X-ray lines may overlap. For example

Ir $K\alpha_1$ would overlap Pt $K\alpha_2$ if both Ir and Pt were present in a sample. In such an instance Pt $K\alpha_1$ would still be available for analysis.

It has been argued that high-energy PIXE spectra would suffer from high bremsstrahlung resulting in poor sensitivity and from interferences in the form of low-energy gamma rays occurring in X-ray spectra (c.f. Folkmann et al., 1974). These problems would be particularly prevalant in chemically complex specimens. Recent work done on rare-earth elements by Durocher et al., (1988) has shown that high bremsstrahlung and gamma-ray interference are not necessary features of high-energy PIXE analysis.

Some low-energy gamma-rays will however interfere with K X-ray lines for heavy elements. Gamma-rays observed in this study are the result of proton bombardment of the sample. A discrete gamma-ray interference (at 67 KeV) was observed during the analysis of electrum from Trout Lake Manitoba. The mineralogy and geochemistry of the sample precluded a simple single stage nuclear reaction as being responsible for the generation of the gamma-ray and constrained the gamma-ray to being the product of a multistage reaction $^{64}Zn(p,\alpha)^{61}Cu^{*}\ ^{61}Cu_{gs}+\gamma$. The Zn was present in sphalerite in the sample.

Proton-charged particle and (p,xn) nuclear reactions also occurred during the bombardment of a ruthenirídosmine sample. These reactions created excited isotopes of Ir, Os and Au. These isotopes decayed to ground state through electron capture and internal transitions accompanied by the emission of K X-rays. The X-rays produced by these processes were observed after proton bombardment and the various isotopes decayed with half-lives of the order of a few hours. These X-rays may also be used to provide quantitative analytical data with knowledge of the nuclear cross-sections for the various reactions.

Durocher, J.J.G., Halden, N.M., Hawthorne, F.C. and Mckee, J.S.C. (1988) PIXE and micro-PIXE analysis of minerals at Ep=40 MeV. Nuclear Instruments and Methods, B30, 470-473.

Folkmann, F.,Gaarde,C., Huus, T., and Kemp, K. (1974) Proton Induced X-ray emission as a tool for trace-element analysis. Nuclear Instruments and Methods, 116. 487-499.

TEM STUDY ON DIABANTITE FROM SHENGSHUIYU, CHINA

LUO Gufeng, WANG Yuhua, Department of Earth Sciences
HU Meisheng, ZHANG Fusheng, Center of Material Analysis

Nanjing University, Nanjing 210008, China

The diabantite studied with chemical formula $(K_{0.01}Na_{0.01}Ca_{0.02}Mn_{0.01}Cr_{0.04}Ti_{0.01}Mg_{2.61}Fe_{1.82}Al_{1.30})_{5.83}(Si_{3.12}Al_{0.88})_{4.00}O_{10}(OH)_8$, as an alteration product of magnesio-hornblende in the diorite from Shengshuiyu, Sishui County, Shandong Province, China, occurs along the cleavage and margin of the parent mineral.

The lattice fringe image of the diabantite cut normal to [100] was observed on the TEM JEM-200CX. The spacing between the adjacent lattice fringes of the chlorite is about 14.2Å. A few talc-like layer with 9.5Å spacing and the lenticular interlayer gaps can be seen in the image. In certain area, however, the diabantite layer and talc-like layer are regularly alternating with each other and constitute the kulkeite lattice, a 1:1 regular interstratification of trioctahedral chlorite and talc layers with repeat spacing of 23.7Å. Authors have also observed that the brucite-like layer within chlorite lattice extends along the b-axis into kulkeite lattice and becomes the talc-like layer, or terminates at the boundary. It intimates that the transformation from kulkeite to chlorite has taken place as a result of either the replacement of talc-like layer by brucite-like one or the insertion of an extra brucite-like layer in the interlayer of kulkeite lattice. Consequently, the untransformed kulkeite is related to the chlorite as a topotaxic intergrowth, and the kulkeite occurs as a intermediate product in the process of transformation from hornblende to chlorite.

Three sets of diffraction spots have been found in the electron diffraction pattern of the same projection of the diabantite as that for lattice fringe image. As a result of indexing, it is revealed that all 0$\underline{k}\underline{l}$ spots with $\underline{k}=3n$ for three sets are fully coincident with each other, but those with $\underline{k}\neq 3n$ are separated from one another. Moreover, the spots of one of these three sets with $\underline{d}_{001}=14.2$Å and $\alpha^*=90°$, are basically not elongate and streaky. It is corresponding to the monoclinic or pseudo-monoclinic regular one-layer polytype. For the lattice of other two sets, the parameters measured are $\underline{d}_{001}=14.2$Å, but $\alpha^*=78°$, because the $0\bar{6}0$ diffraction spots of these two sets just coincide with the 062 and $0\bar{6}2$ ones of the monoclinic polytype respectively. In addition, those spots on 0$\underline{k}\underline{l}$ rows with $\underline{k}\neq 3$ are obviously elongate and streaky, and they are interlinked into the continuous streaks along these row lines. These facts indicates that both of them are triclinic semi-randomly stacking one-layer polytype of

chlorite. They are orientated oppositely and related to each other as a twinning on (001). Meanwhile, the monoclinic polytype is related to the triclinic one as a syntaxic intergrowth.

EPMA STUDY OF ULTRAMICRON GOLD OCCURRENCE IN A "CARLIN TYPE" GOLD DEPOSIT IN CHINA

48.7.3 K

MAO Shuihe
Institute of complex Utilization of Mineral Resources
Emei, Sichuan, 614200, People's Republic of China

The invisible gold (i.e. ultramicron gold) in a "Carlin type" gold deposit in China has been studied. Based on the results of EPMA, SEM study and dissolving test the following conclusions can be drawn:

1. Pyrite is the most important gold bearing mineral. It consists of euhedral crystal core which contains little gold and arsenic, and rims with high gold and arsenic. The average tenor of Au in pyrite is about 257.6 g/t, while it in rims of pyrite increases to 599.8 g/t and it in core is less than 81 g/t.

2. The content of Au in pyrite is closely correlated with that of As. Consequently the distribution of Au in pyrite can be investigated and displayed based on the SEM image and EPMA data of As.

3. The quantitative EPMA data shows that the content of Au in different points of gold rich rim of pyrite is considerably different. As a result of dissolving test of pyrite the gold is not in HNO solution, but in the indissolved residues and will later go into the KI+I gold leaching solution. All of these facts confirm that gold in pyrite occurs in the form of ultramicron native gold inclusions instead of isomorphous substitution.

4. It is proved that more than 60% of gold contained in clay minerals actually occurs in very fine grained pyrite inclusions which are less than 1um in size and difficult to be investigated under optical microscope.

5. The gold tenors in other main minerals, such as arsenopyrite, quartz, calcite, barite etc., are all below the detection limit of EPMA. It can be seen also from the results of assay that these minerals are not gold-bearing ones.

6. The main characteristics of ultramicron gold in the present gold deposit, such as the occurrence, the positive quantitative relationship of simultaneous increasing and decreasing between Au and As, the microstructure of the main gold-bearing minerals, etc., are similar to those in Carlin and Cortez Gold Mines, Nevada, U. S. A.. It indicates that the "Carlin type" gold deposits have their own intrinsic features.

7. The special occurrence of ultramicron gold is favorable to the technological designing for oxidizing-roasting, chloridizing and cyanide-leaching of gold ores. In this case the optimum recovery of gold can be made by sufficient oxidization and leaching of the surface layer of pyrite only. Consequently, it will effectively save time, energy and reagents.

RAMAN MICROPROBING OF STISHOVITE AND LONSDEILITE

M.F.Vigasina, R.Yu.Orlov, Department of Geology,
Moscow State University, Moscow, 119899, USSR

High pressure minerals - stishovite and lonsdeilite are reliable signs of shock metamorphism in astroblems. However a fine size of those minerals (about some microns) make difficult their identification by means of X-ray scattering and IR-spectroscopy. These troubles can be overcame with the help of Raman microprobe thechnique.

We present here some experimental and theoretical vibrational spectra of those minerals. It must be noted that some of published infrared [1,2] and Raman [2,3] spectra contradict one to another and to factor group analysis (Table 1).

Frequencies (in cm^{-1}) Table 1

Symm	Experimental [2]	[1]	[*]	Calc *
B2g	1284		964	966
Eu	950	949		930
A2u	889	885		895
A2g				830
B1u				800
Eu	764	769		764
?		730		
		672		
	634	628		
A1g	1162		751	745
Eg	1056		586	589
Eu	561	560		568
B1u				538
B1g	936		234	230

[*] - this work

We have studied microcrystals of stishovite (30 mcm) synthesied at 1000°C and 9,6 GPa. Our experimental results coincide with [3] and contradict to [2] .Confirmation of these results was received through the vibrational dinamic calculation using general valence force field.

The set of internal coordinates is given Factorgroup analysis show that only 4 mo-

des are active in infrared and 4 modes - in Raman scattering. The force constants (in 10^6 cm^{-2})achived in calculation are next: $K_Q=K_q=3,7$; $K_d=0,04$; $K_\gamma=3,1$; $K_\varphi=2,8$; $K_\delta=3,2$; $h_1=0,58$; $h_2=0,2$; $A=a=0,23$. Here "a" and "A" corresponds to interaction of valence angle with the adjacent bond, h_1 and h_2 are nondiagonal constants of Q-q interaction; K_d describes interaction between oxigen of neigbouring octahedrons. The value $K_{Q,q}$ is in good agreement with correlation K_{Si-O} - R_{Si-O} proposed in [4] for siliates.

Obtained results show that Raman spectra presented in [2] as well as infrared bands 634 cm^{-1} [2],628,672 and 730 cm^{-1} [1] does not pertain to stishovite.

Lonsdeilite was obtained as fine powder by the method of shock synthesis. The experimental Raman spectra received at the first time contains three broad lines (Table 2).

Frequencies Table 2

Symm	Calc.	Exp.
A1g	1335	1335
E1g	1249	1243
E2g	1212	1184
B1g	1215	
B2u	1049	
E2u	439	

Factor-group analysis gives vibrational representation: Γ =A1g+E1g+E2g+B1g+B2u+E2u. Only 3 modes - A1g,E1g and E2g - are active, and only in Raman scattering.

Theoretical vibrational spectra of lonsdeilite was calculated with force constants of diamond.

Thus using received data successful identification of stishovite and lonsdeilite can be achieved by the microraman technique.

1. Lyon R.J.P. Infrared confirmation of 6-fold coordination of silicon in stishovite //Nature,1962,V.196, P.266-267.
2. Von Czarnowski A.,Hübner K. Raman and infrared investigation of stishovite // Phys.Stat.Sol.(b), 1987,V.142, K.91-96.
3. Hemley R.J.,Mao H-K, Bell P.M. Lattice vibrations of high-pressure SiO_2 phases // Physica,1986,V.140B, P.455-457.
4. Лазарев А.Н.,Игнатьев И.С.,Тенишева Т.Ф. Колебания простых молекул со связями Si-O .Ленинград 1980

ELECTRON MICROSCOPICAL STUDY ON AUGITE ALTERATION

WANG Qiming Electron Microscope Laboratory, Physics Building, Peking University, 100871, Beijing, China;
R. A. Eggleton Geology Department, The Australian National Univ. Canberra, ACT 2601, Australia

Electron microscope examinations of augite in mafic monzonite, which sampled at Mt. Dromedary, Narooma, N.S.W. of Australia, have revealed a wide variety of secondary products being formed through augite hydration reactions, both by hydrothermal alteration and weathering. The product phases by hydrothermal alteration were to be amphibole, jimthompsonite, chainwidth disordered pyriboles (mainly 2 and 3 chainwidth mixtures) and chlorite. Uralitization of augite has been observed by multiple mechanisms, either by a bulk transformation along a broad reaction front or by the nucleation and growth of narrow lamellae. A step sequence has also occurred, identified from textural observation, that augite transforms to amphibole, firstly forming a hydrous pyribole zone in which single, double and triple chain lamellae are predominant, then followed by a reordering mechanism by which bulk amphibole replaces the highly hydrated area, with reaction proceeding inward. The amphibole cell dimensions are 1-2% larger than augite's; because of this mismatch of the crystal lattices, the bulk replacement has created many microfractures, arranged in the amphiboles as a pattern of diamond mosaic fragments bound by (110) cleavage.

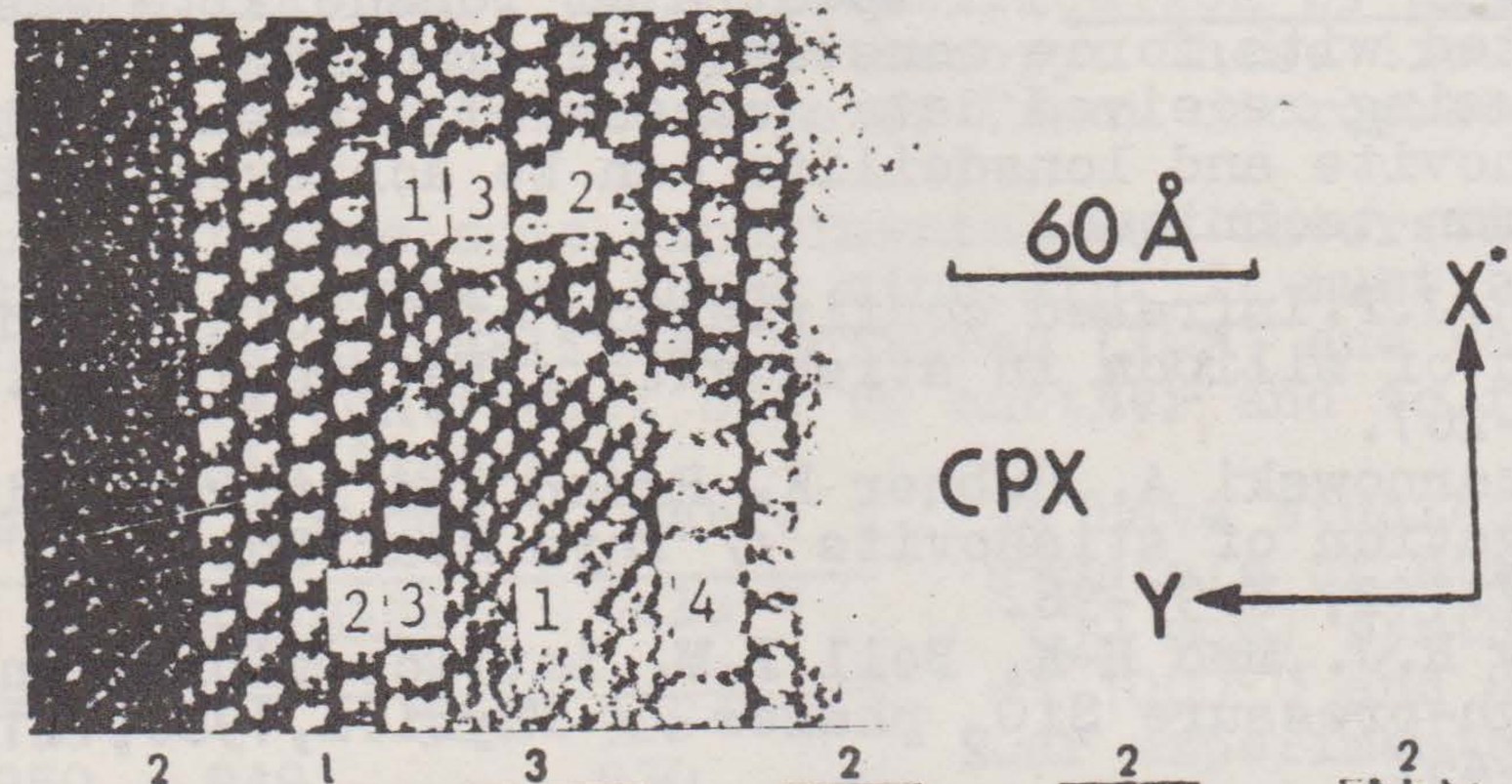

Augite hydrothermally altered to form different chain-width defects.

Superimposed weathering of augite has attacked the crystal at the sites which have excess energy, especially on the outcrops of dislocations, interface boundaries and defects, resulting initially in the formation of 10A layer silicate which is in a topotactic relationship with the augite host. The initial topotactic replacement of 10A layer silicate is disrupted by a stepwise hydration that gradually proceeds to form a mixture of weathering products, noncrystalline and layer-like curved materials (12-15A basal spacings) which bear no regular relationship to augite, then in a final stage giving way to recombine and to enlarge these curved materials into thick, packed, curly smectite (nontronite). Noncrystalline phases contain abnormally high contents of iron, more than can be accommodated in nontronite. The iron was firstly released into solution, then precipitated as a cell-like metastable phase approaching goethite.

ON PREPARING OF STANDARDS FOR ELECTRON PROBE MICROANALYSIS

62.7.6.11

Zhou Jianxiong , Institute of Mineral Deposits , CAGS , 26 Baiwanzhuang Road , Beijing 100037 , China

The electron probe microanalysis has gained acceptance in geoscience as an essential tool in the chemical and microtextual analysis of minerals . Unfortunatly , their are few internationally available sources of standards for electron probe microanalysis of minerals , although a lot of work on data proceeding has been undertek . Nevertheless , there is a general consensus that it is desirable using standards of similar composition to the minerals to be analyzed . That is why we did a considerable amount of work on standards for electron probe microanalysis for about 10 year .

Mineral standards must satisfy rigorous criteria . The main important points are both homogeneous and have an independent chemical analysis , as well as being stable under the electron beam and capable of taking a high degree of polish (Potts , 1983) . Therefore Here we preset a new procedure as a suggestion on technical specifications for preparing standards . The new procedure includes following point : Selection of material , separation and cheeking purity , measurement of homogencity , measurement of stability , chemical analysis , compiling report , packing and preservation .

Specific procedures with regard to the measurement of homogencity are as following : 1. Analyzed grains must be $3\times\sqrt[3]{N}$, three analysis points for each

grain , three counts for each point . That is , when total grains are 1000 , the 30 grains shoud be analyzed , 270 counts are measured . 2. Measurements are performed under following conditions : 10–25 KV accelerating voltages depended on fifferent composition , more than 10 nA beam current , 1 μm diameter beam spot , the total counts more than 10000 . 3. The homogeneit index is determined :

$$HI = S_w^2 / S_b^2$$

$$S_w^2 = \frac{1}{m(n-1)} \sum_{i=1}^{m} \sum_{j=1}^{n} (N_{ij} - \bar{N}_i)^2 = \frac{1}{m} \sum_{i=1}^{m} S_{wi}^2$$

$$S_b^2 = S_t^2 - \frac{1}{n} S_w^2$$

$$S_t = \frac{1}{(m-1)} \sum_{i=1}^{m} (\bar{N}_i - \bar{N})^2$$

$$F = nS_t^2 / S_w^2$$

If HI<2.5 for suphide or <3 for others , the minerals can be used to be standards . F only used to be criteria for homogeneous or not .

Seven groups of standards , including 56 multielement standards , 30 ordinair Bence–Albe oxide–silicate standards , 20 special oxide standards , 15 sulphide standards , 10 light element standards and 30 rare element standards are being prepared and nearly finished .

Reference

1. Boyd , F.R. et al. , 1967 , Carnegie Inst. Wash. Year book , 67 , 210–215 .
2. Jarosewich , J.A. et al. , 1980 , Geostandards Newsletter , 4,43–47 .
3. Potts , P.J. et al. , 1983 , American Mineralogist , 68, 1237–1242 .
4. Zhou Jianxiong , Mao Suihe , 1989 , Electron Probe Microanalysis (book , in Chinese).

ELECTRON MICROSCOPY APPLIED TO MINERALOGY

EXSOLUTION MICROSTRUCTURES OF NATURAL CLINOPYROXENES AS INDICATOR OF THE COOLING HISTORY: A TEM STUDY

PO 6.6.

W.F. Müller[1)], W.Skrotzki[2)], J.Töpel[1)],
1) Institut für Mineralogie, Technische Hochschule, Schnittspahnstr.9, D-6100 Darmstadt, 2) Institut für Geologie, Universität Göttingen, Fed.Rep.Germany

Exsolution phenomena in pyroxenes have been extensively studied by petrographic microscopy, X-ray methods, and by methods of transmission electron microscopy (TEM), including electron diffraction and energy dispersive X-ray microanalysis (EDX). Numerous excellent researchers have contributed to our present knowledge. The stand of the art in the field of TEM until 1980 has been thoroughly reviewed by Buseck et al.(1980). Since then, progress in our understanding was demonstrated by many papers, e.g. Kitamura et al.(1981), Ried and Fuess (1982), Rietmeijer and Champness (1982), Feuer et al.(1989), Livi and Veblen (1989). Clinopyroxenes of intermediate composition within the pyroxene quadrilateral $MgSiO_3$-$FeSiO_3$-$CaFeSi_2O_6$-$CaMgSi_2O_6$ from basaltic rocks commonly display lamellar exsolution into the Ca-poor clinopyroxene pigeonite and the Ca-rich augite. Two different orientation relationships are observed: "001"-lamellae with $a_{aug} \parallel a_{pig}$, $b_{aug} \parallel b_{pig}$, and "100"-lamellae with $c_{aug} \parallel c_{pig}$, $b_{aug} \parallel b_{pig}$.

We studied the variation of the microstructure of clinopyroxenes across a basaltic sill (Whin Sill, N.-England) at localities of different thicknesses (between 2.35 m and 59.20 m). With decreasing cooling rate, the following sequence of types of exsolution microstructures in clinopyroxenes of Ca-rich bulk composition could be established: (1) non-periodic fluctuations; (2) modulated structures on (100) and (001); (3) coarsening of the modulated structures to coherent "001"-pigeonite exsolution lamellae with widths in the 100 Å range; (4) "coarse" "001"-pigeonite lamellae with widths mostly between 200 and 500 Å; (5) two generations of "001"-pigeonite lamellae; generation I:

coarse lamellae like (4), about 0.1 to 0.8 µm distant; in between, separated by a precipitation free zone (PFZ), generation II like (3) with widths from 30 to 150 Å; (6) complex microstructure, similar to (5), in addition with "100"-pigeonite lamellae which formed about at the same time as the "001"-lamellae of generation I. The development of the exsolution microstructure as observed across the sill was plotted into a diagram with different cooling paths. These were calculated using the one-dimensional heat flow model of Carslaw and Jaeger (1959) for different positions within and for different thicknesses of the sill. Thus, a TTT-diagram was obtained which can be used for a rough estimation of the cooling history of suitable volcanic and hypabyssic rocks.

In regions of sufficiently slow cooling rates, the generation II of "001"-lamellae is only observed when the distance between the lamellae I is larger than 0.35 µm. In microstructure type 5, the PFZ widths increase with the widths of lamellae I. Both observations reveal fossil diffusion profiles around the lamellae, which were partially confirmed by EDX.

TEM-analysis of different types of exsolution lamellae in Al-augite websterite dikes of the peridotitic Balmuccia massif (N.Italy) showed the following: There exist two generations of "100" and "001" pigeonite lamellae, generation PI and PII. The PI-lamellae have a width larger than about 0.2 µm. The interphase display misfit dislocations. Generation PII, width < 0.2 µm, are mainly of the "100" type; they nucleated at dislocations. The pigeonite/augite interface orientations and relative lattice rotations (obtained by CBED) have been used as geothermometers (Robinson et al.1979). Exsolution temperatures estimated are about 900 °C for PI and ≤ 500 °C for PII.

Po 6.7

TRANSMISSION ELECTRON MICROSCOPY OF THE HIGH-T_c SUPERCONDUCTORS $YBa_2Cu_3O_{7-x}$ and $Nd_{2-x}Ce_xCu_{4-y}$

W.F. Müller, P. van Aken, Institut für Mineralogie, Technische Hochschule, Schnittspahnstr.9, D-6100 Darmstadt, Federal Republic of Germany

$YBa_2Cu_3O_{7-x}$ has the space group Pmmm and the approximate lattice parameters a = 3.82, b = 3.89, c = 11.68 Å. At temperatures above about 700 to 750 °C, it is tetragonal, P4/mmm. $Nd_{2-x}Ce_xCuO_{4-y}$ belongs to a new family of oxidic superconductors which has found considerable interest, because it shows n-type conductivity above T_c in contrast to the oxidic high-T_c

superconductors known so far. Superconductivity is observed in samples of $Nd_{2-x}Ce_xCuO_{4-y}$ with x between about 0.14 and 0.18. Most crystals of $Nd_{2-x}Ce_xCuO_{4-y}$ in the superconducting samples have the structure of Nd_2CuO_4 with the space group I4/mmm and the lattice parameters a ≈ 3.95 Å and c ≈ 12.16 Å. We used methods of transmission electron microscopy including electron diffraction and energy dispersive X-ray microanalysis in order to characterize superconducting ceramic samples of $YBa_2Cu_3O_{7-x}$ and $Nd_{2-x}Ce_xCuO_{4-y}$.

$YBa_2Cu_3O_{7-x}$. Two ceramic samples were studied. The one, TWO37, was prepared by T.Wolf, KfK Karlsruhe. It displayed a T_c of 93 K and a density of 87 %; its (average) composition was $YBa_2Cu_3O_{6.87}$. The ceramics consist of $YBa_2Cu_3O_{7-x}$ crystals (with a grain size of about 1 to 10 µm) and additional phases which have an amount of about 0.1 %. The dominant crystal defects of $YBa_2Cu_3O_{7-x}$ are twin lamellae on (110) and (1$\bar{1}$0). When they intersect, a kind of chess board pattern is formed wich gives rise to complicated electron diffraction patterns. Free dislocations with the Burgers vector [100] or [010] were occasionally seen. The additional phases found were Y_2BaCuO_5, $Y_2Cu_2O_5$, CuO, $BaCuO_2$ and amorphous $YBa_2Cu_3O_{7-x}$. Y_2BaCuO_5 and $Y_2Cu_2O_5$ occur as intracrystalline inclusions, CuO and $BaCuO_2$ as fillings of triple point junctions. The few grain boundary phases observed were mostly amorphous layers 5 to 15 nm in width.

$Nd_{2-x}Ce_xCuO_{4-y}$. The samples of $Nd_{2-x}Ce_xCuO_{4-y}$ were produced by sintering the appropriate composition of Nd_2O_3, CuO and CeO_2. Three different samples were studied: sample (1) with composition $Nd_{1.88}Ce_{0.12}CuO_{4-y}$, non-superconducting; (2) with composition $Nd_{1.84}Ce_{0.16}CuO_{4-y}$, superconducting below T_c = 21 K; (3) with composition $Nd_{1.86}Ce_{0.14}CuO_{4-y}$ (superconductivity not verified). Tetragonal $Nd_{2-x}Ce_xCuO_{4-y}$ is the dominant phase in all three samples and comprises more than 99 volume percent. Its grain size varies between 1 and 10 µm. Dislocations connected with low angle boundaries as well as free dislocations were observed. Spherical and ellipsoidal inclusions of (Nd,Ce)- oxide are frequently seen. Their size is about 0.1 µm to 1.2 µm, the atomic ratio Nd/Ce between 0.9 to 1.25. In samples (2) and (3) some small crystals of $Nd_{2-x}Ce_xCuO_{4-y}$, about 1 to 3 µm in size, were observed, which obviously have structures different from the bulk material with the tetragonal I4/mmm structure. We found two different structural modifications. The one type of structure may be described as commensurate superstructure of the basic tetragonal I4/mmm structure. Electron diffraction patterns of such crystals display superlattice

reflections of the type h ± 1/4, k ± 1/4, l = 0 (Izumi et al.1989, Van Aken and Müller 1989, Chen et al. 1989). In one case, we observed a crystal with incommensurate superlattice modulations which showed diffuse superstructure reflections and wavy lattice fringes. The other modification is orthorhombic. The original tetragonal cell with a ≈ 3.95 Å is now distorted to an orthorhombic cell with a ≈ 4.14 Å and b ≈ 3.71 Å. Additional reflections demand a doubling of *a* and *c*. All crystals of this structural type display twin lamellae on {110}. The orthorhombic crystals share the orientation of the twin plane and the crystallographic c - axis with {110} and [001] of the tetragonal matrix.

6.2 H

ELECTRON DIFFRACTION AND HIGH RESOLUTION ELECTRON MICROSCOPY APPLIED IN MINERALS

Li Fang-hua, Institute of Physics, Academia Sinica, Beijing, 100080, China

The strong dynamical scattering of electrons makes the electron diffraction more powerful than X-ray diffraction in studying superstructures and incommensurate structures of crystals. The development of high resolution electron microscopy(HREM) affords a new approach to crystal structure determination. HREM is suitable to study minute crystals and crystals with defects. The structure image taken with the high resolution electron microscope mirrors the projected structure intuitively. However, in order to determine the position of atoms by HREM, the work is tedious and the technique remains to be improved. The present paper concerns the study of some minerals by electron diffraction and HREM. It aims at demonstrating both advantage and disadvantage of the techniques.

The electron diffraction patterns(EDPs) of ankangite $(Ba_{0.827}(Ti_{5.827}V_{2.294}Cr_{0.053})O_{16}$ show rather strong satellite spots for each basic spot so that the one-dimensional incommensurate character is recognized straightforward and the modulation wave is determined. The structure model has been proposed and discussed on the basis of both EDPs and images. The samples of antigorite from Xiuyan jade and that from Matterhorn serpentine have the same substructure but different superstructure. High resolution electron microscope images show plenty of defects and the wavy structure. The positions of atoms located at two turning points in the wavy structure has been determined by HREM. Huanghoite($BaCe(CO_3)F$) and cebaite($Ba_3CE_2(CO_3)_5F_2$) are from the same family and have similar substructure. The image contrast change with crystal thickness has been studied for huanghoite of which the structure is known. it is found that under a certain crystal thickness the contribution of light atoms to image is comparable with that of heavy atoms. This implies the possibility to determine the position of light atoms by HREM, which has been confirmed later in the structure determination of cebaite.

EXPERIMENTAL AND COMPUTATIONAL RESULTS ON MANTLE MINERALOGY

MINERAL INCLUSIONS IN THE CHINESE DIAMONDS

Po 1.27.

DENG Chujun, HUANG Yunhui and ZHAO Donggao, Institute of Mineral Deposits, Chinese Academy of Geological Sciences Baiwanzhuang Road 26, Fu Wai, Beijing 100037, P.R.China

The mineral inclusions in the Chinese diamonds examined are olivine, pyrope, enstatite, phlogopite, diamond, chromite, graphite, rutile, zircon, magnetite, hematite and apatite. Most of the inclusions belong to protogenetic or syngenetic inclusions, a small number of them are epigenetic. According to the morphology of the mineral inclusions, they are divisible into three types: 1) minerals possessing well-defined crystal forms; 2) mineral fragments; 3) amorphous substances.

The investigation of a large parcel of the Chinese diamonds show that the abundances and types of mineral inclusions in diamonds vary with the source areas and genetic types of mineral deposits. For instance, in Shandong 36.8% of the diamonds obtained from the No.1 kimberlites zone (including the well-known Victory 1 kimberlite pipes) contain mineral inclusions, and the minerals included commonly have well-defined crystal forms; whereas in the Tancheng diamond alluvial deposits the diamonds with inclusions constitute 75.2% of all the diamonds recovered, and the minerals included are rarely perfect, most of them are graphite or the fragments of other minerals. From this it can be inferred that the Tancheng diamonds didn't come from the No.1 kimberlites zone.

Diamond: One diamond inclusion was obtained and this is octahedral and faintly blue, and wasn't subjected to resorption. A dark carbon film was observed to cover the steplike faces of the included diamond.

Olivine: Olivine inclusions are granular or shortly prismatic, having well-defined crystal forms. Two or more single olivine inclusions are often observed distinctly to occur in one diamond crystal. Sometimes olivine and purplish red pyrope inclusions coexist in one diamond. Occasionally the olivine inclusions occur as

colorless pseudo-tetragonal prisms and resemble zircon. But the Raman spectra can distinguish them.

Table 1. The X-ray diffraction data of the pyroxene inclusion

d (Å)	3.15	2.85	2.70	2.47	2.10	1.96	1.77	1.60	1.51	1.48	1.38	1.30
I/I₀	9	8	1	10	2	1	1	2	1	8	7	6

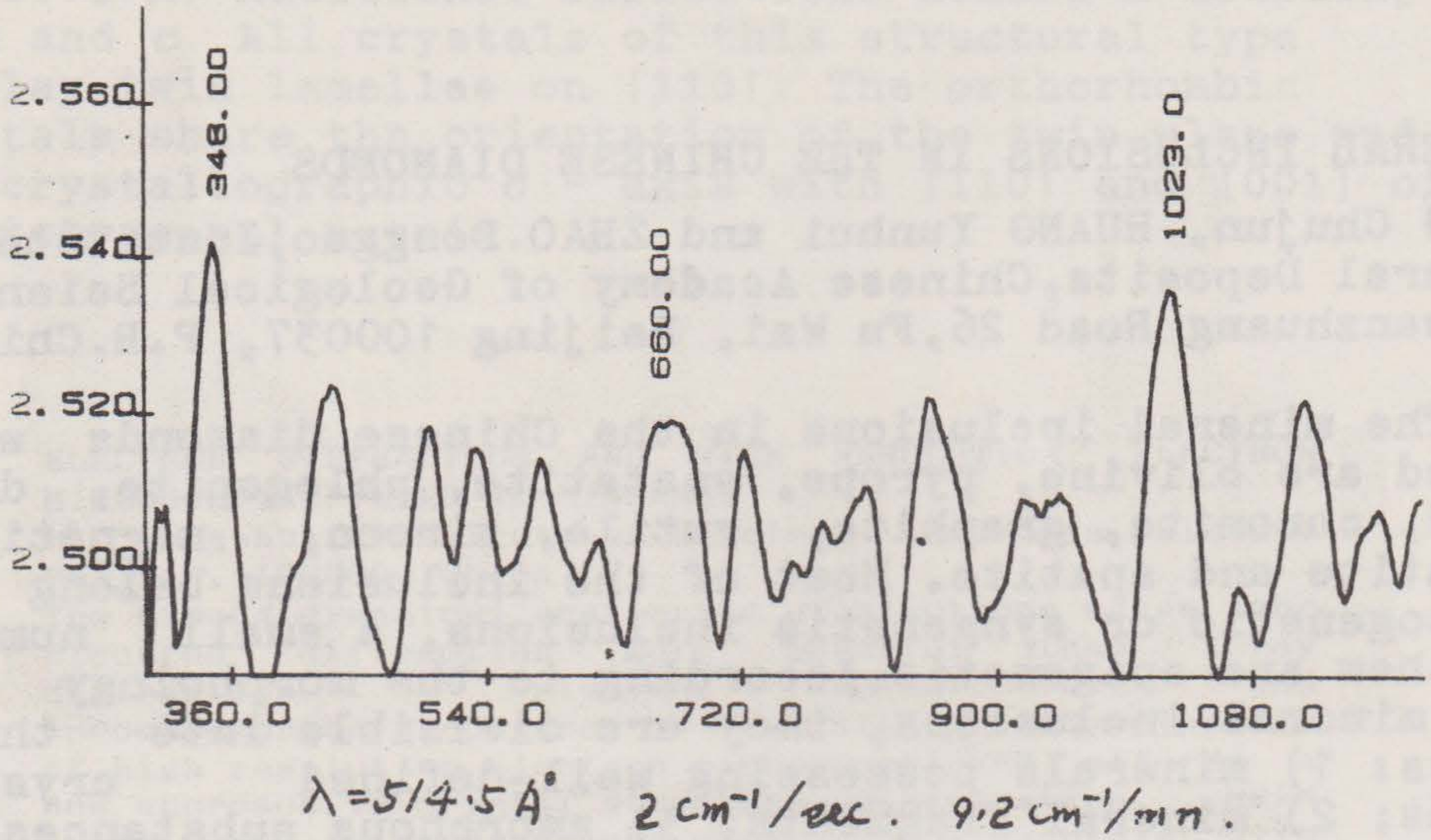

Figure 1. The Raman spectrum of the pyroxene inclusion

Pyroxene: Pyroxene inclusions are shortly prismatic crystals, sometimes elbow crystals, and were subjected to slight resorption. The pyroxenes are colorless, positive in optical character under microscope. A refractive index of 1.689 was measured. The average of the two analyses of electron microprobe of a pyroxene inclusion is SiO_2 58.90%, MgO37.48%, FeO 3.62%. The X-ray diffraction data and the Raman spectrum of the same inclusion are gived in Table 1 and Figure 1 respectively. Apparently the pyroxene is orthopyroxene, i.e. enstatite, and may be assigned to the ultramafic suite inclusions (H.O.A.Meyer, 1985).

Reference

Meyer, H.O.A., 1985, Genesis of diamond: a mantle sapa. American Mineralogist, V.70,p.344-355.

A RARE MANTLE PYROXENE XENOCRYST

Deng Jinfu, Zhou Yongzhang, Zhao Hailing, Luo Zhaohua
China University of geosciences, Beijing, 100083, China

Cenozoic Hannuoba basalts contain abundant peridotite xenoliths, in addition there is a peridotite massive (lherzolite predominately) with size of 330×70 m^2 in Damaping, Wanquan county, Hebei province. The peridotite massive contains about 22% of picritic basalt veins. Zhou Yongzhang and Luo Zhaohua have discovered a green pyroxene xenocryst with size of 16×10×6 cm^3 in one of the picritic basalt veins. The pyroxene xenocryst is composed of Opx and Cpx in banded intergrowth texture, which is believed to be a product of exsolution from primary homogeneous pyroxene solid solution. Both widths of the banded Opx and Cpx are about equal, ranging from 0.05 to 0.5mm. Moreover, the banded Opx has exsolution lamella of Cpx, which is too thin to determine its chemical composition by microprobe, and which may be resulted from the second exsolution event.

The compositions of banded Opx and Cpx are enstatite, $Wo_{2.9}En_{88.5}Fs_{8.6}$, and Cr-bearing (0.37% Cr_2O_3) endiopside, $Wo_{43.5}En_{53.0}Fs_{3.5}$, respectively. The estimated T and P for the formation of banded Opx and Cpx by some geothermobarometries is about 1152℃ and 30.5kb, respectively, which represent the P-T condition of the first exsolution event. The bulk chemical composition of the pyroxene xenocryst, which represent the composition of primary pyroxene before exsolution event, is $Wo_{24.5}En_{68.5}Fs_{7.0}$, and has been plotted in the region of immiscibility gap of $CaSiO_3$-$MgSiO_3$-$FeSiO_3$ triangle. We suggest calling the pyroxene xenocryst as enstatite-diopside. From high pressure melting experiment of KLB-1 lherzolite, Takahashi (1984) indicated that the immiscibility gap of Opx and Opx is narrowed down with increase of pressure. Above the pressure of 30 kb the peridotite KBL-1 at solidus consists of olivine, pigeonitic clinopyroxene without Opx, which is a single pyroxene peridotite. The pigeonitic clinopyroxene have composition of $Wo_{19.3}En_{73.4}Fs_{7.3}$ (30kb), $Wo_{15.1}En_{76.8}Fs_{8.1}$ (50kb), $Wo_{19.9}En_{73.5}Fs_{6.6}$ (140kb). The bulk composition of pyroxene xenocryst is similar to that of Takahashi's pigeonitic clinopyroxene. Takahashi has considered the single pyroxene peridotite to be similar to the protogranular lherzolite by Mercier and Nicolas (1975), and to be a high pressure (50-70 kb) residue in equilibrium with komatiite magma. Therefore, it is suggested that the pyroxene xenocryst in Damaping may be a segment from the single pyroxene peridotite, the

upper mantle residue in equilibrium with komatiite magma, probably in the early stage of earth. Some time after, the single pyroxene peridotite has been moved upward as a diapir to about the 100 km from the depth of 150-200km, and has been became the therzolite because of the formation of Opx and Cpx from the primary homogeneous pyroxene by the exsolution event. It is suggested that the peridotite have a megacryst texture below the depth of 150km.

Based on the chemical compositions of the banded Opx and Cpx, as well as the bulk pyroxene xenocryst, the estimated amount of about 53.2% Cpx and 46.8% Opx from primary pyroxene may be formed during the exsolution event. If there is no melting event during or after diapiric ascending, the upper mantle therzolite above the depth of 150 km in the region has Cpx to be equal or some more than Opx in the amount. The therzolite xenoliths in the Hannouba basalts have 35% Cpx and 65% Opx in proportion in an average of 9 samples, i.e. Cpx < Opx in the amount, which suggests that the therzolite xenoliths in the Hannouba basalts are upper mantle residue after the basaltic melting event at the depth of $\leqslant$100 km.

A STRUCTURE-MINERALOGICAL STUDY OF RINGWOODITE*

Fu Pingqiu, Xie Hongsen and Zhang Liming, Institute of Geochemistry, Academia Sinica, Guiyang, Guizhou 550002, People's Republic of China

As one of the major rock-forming minerals in the crust and upper mantle, the structural evolution of olivine reflects the T-P conditions in the transition zone. In the present work, the structure of ringwoodite (γ-Fe_2SiO_4) was studied by means of X-ray powder diffraction, showing that 27.5% of the Si atoms occupy the octahedral sites. Therefore, ringwoodite belongs to the mixed structure type of the normal and the inversed spinels. This result is conformable with the Mossbauer analysis of the mineral.

Experimental Specimen. At 30 kbar and 1000℃ fayalite was firstly sythesized from the mixture of FeO and SiO_2. After that the black powdered ringwoodite was synthesized in a II-stage anvil high-pressure capsule at about 70 kbar and 900℃. The measured specific gravity D=4.75 g/cm^3. IR and powder XRD analyses provided evidences suggesting that the mineral is of the spinel structure type. Fd3m, Z=8.

Determination of Crystal Structure. Chosing a particle measuring about 0.3mm in size, we took its Debye photograph with a Gandolfi camera. After hkl was worked out from $\sin^2\theta_1/\sin^2\theta_1$, the unit-cell parameters were calculted, a=8.219A, based on the extrapolation of $\cos^2\theta(1/\theta+1/\sin\theta)$ proposed by Taylor et al., with V = 555.2 A^3 and Dc = 4.877 g/cm^3.

Making use of a crystal-intensity scale we measured I, from which $\sqrt{I/MLP}$ could be calculated as |Fo| . In the present paper the Lagrange's interpolation method was used to work out the atomic scattering factors which couldn't be obtained from references. With the simplified formula on the symmetry of the crystal we calculated |Fc| in the following steps, First, on the basis of the structure of spinel (Mg_2SiO_4), whose atomic coordinates are Fe(5/8, 5/8, 5/8), Si(0, 0, 0) and O(x, x, x), after trying a few cycles, we let x equal the value from the series 0.363—0.383 of an equidifference of 0.002. At the same time, we let Oc (Si in octahedra / total Si) equal the value from the series 0—0.475 of an equidifference of 0.025. Correspondingly, |Fc| and R were obtained. As a result, the authors found that when x = 0.379 and Oc = 0.275, R = 0.077 up to the minimum, accoringly the structural formula is

$(Fe_{0.863}Si_{0.137})^{[6]}(Si_{0.725}Fe_{0.275})^{[4]}O_4$, with the bond lengths,

$(Fe,Si)^{[6]}$—O 2.022A and $(Si,Fe)^{[4]}$—O 1.836A.

Discussion. (1) With increasing T and P the atoms in olivine tend to become more closely spaced, with longer Si—O and shorter Fe—O. Hence, its structure turns into the spinel structure type and little difference is shown between Fe—O and Si—O bonds. (2) Because in the specimen used in this work 27.5% of the Si atoms occupy the octahedral sites its structure belongs to the mixed type (72.5% of the normal and 27.5% of the inversed spinels). (3) As far as Fe^{2+} Mossbauer spectrum of ringwoodite are concerned, by comparison with the spectra of relative minerals, the Q.S. of the outer peak is related to the 6-fold coordination and that of the inner peak is related to the 4-fold one. This coincides with the XRD analysis. (4) The amount of the inversed spinel structure type in the crystal structure of ringwoodite is closely related to T and P. More detailed work will be done in this aspect.

* The project supported by the National Natural Science Foundation of China.

A SUMMARY ON THE SERIES OF PYROLYTIC FACES CHANGE OF KAOLINITE IN NATURE

Liu Changling , Tianjin Geological Academy of Ministry of Metallurgical Industry of China , 42 Youyi Road , Tianjin 300061 , China

The author found a series of products from pyrolytic faces change of Kaolinite in nature. Combining relative material with author's new opinion, a long-standing problem that has been debated for a long time bassically is solved. The kind of new type of ore deposits is significant in science and of certain value economically, as well as unprecedented in home and abroad.

1. The present of strong anisotropy and 2V of metakaolinite indicates that it is quasi-crystalline or semicrystalline minerals. It refutes the theory of mixture amorphous and compound homogeneous body or uniaxial crystal. This metakaolin can be found first in nature. Then followed the discovery of new type of pyrometamorphic bauxite deposit with metakaolin-corundum and clay deposits with high Al. Fine grained corundum (formed by dehydration of diaspore with no change in crystal) associated with metakaolinite (formed by dehydration of Kaolinite and retaining crystal form) was formed from widely distributed Mid-Carboniferous bauxite with gentle occurrence and partly exposed at the surface overlying the tertiary and Quaternary basalt, through thermometamorphism heating from top down. ward, at forming temperatures between 450℃ and 850℃.

2. It is first time for finding Si-Al-Spinel in natur. The theory of continuity and succession in composition is definited. The result of comprehensive measurment, especially of identification by infrared ray (showing an asymmetric valley as a duck mouth) agrees with facts. Si-Al-Spinel ore has been found in small scale in Shanxi and Xinjiang, some has been used in refractory industry.

3. As the temperature of second exothermic peak of Kaolinite increasing to av. 1200℃ , the primary mullite and other mullite are formed. Then the new type of mullite deposits can be formed for mining.

Middle zone coarse mullite metatype bauxite deposits occur in a skarn type deposit, Wuan area, Hebei Province. The ores were the metamorphic products through contact between Middle Carboniferous series bauxite and Yanshan Period diorite, consisting of predominantely the coarse columnar form mullite (it was assumed to form at temperatures above 850℃ with slow cooling). Accessory minerials are corundum, sericite, spinel and magnetite, etc. The ores were found only in tow drilling holes and therefore estimated to be small in size.

Epizone acicular mullite type bauxite deposits occurred in a skarn type deposit in Lin country, Henan Province. Fine acicular mullite was formed by contact metamorphism between Yanshan Period dioritic porphyrite and Middle Carboniferors bauxite clay strata in the vicinity of the surface because of rapid cooling (similar to the incrustation of refratory clay in an artifical glass cruscible and

characterized by acicular hairlike mullite feature), but its forming temperature was still above 850℃. These deposits are small in size, and have been mined on a small scale for refractory materials.

GREEN GARNETS FROM LIAONING KIMBERLITE, CHINA

LU Fengxiang, REN Yingxin, ZHENG Jianping, Department of Geology, China University of Geoscience, Wuhan, 430074, People's Republic of China, TAYLOR L.A. Department of Geological Sciences, University of Tennessee, Knoxrille, TN, 37996, U.S.A.

14.13K

Garnet is one of the characteristic minor minerals and widespread in kimberlite. Many researches have been done on color, composition and paragensis of garnet as well as the indicative significance for diamond exploration. Particularly, the lilac–red and orange–yellow garnet series, including lilac, red–purple, red, orange, pink and yellow garnets have been studied in great detail. In this paper, attention is focused on the Ca–rich garnet in Liaoning kimberlite. This kind of garnet has rarely been reported and not abundant in this area. We obtained three types of garnet concentrated from the crushed kimberlite. They are lilac–red, orange–yellow and green series garnet.

Mineral composition were determined by using a fully automated Cameca SX–50 electron microprobe at the University of Tennessee, utilizing ZAF correction procedures and JCXA–733 at China University of Geoscience. The lilac–red and orange–yellow series garnets are compositionally characteristed by Ti–poor, Cr–rich, and Mg–rich, and $TiO_2 > 1\%$, Cr–poor, and Mg–rich respectively. They can be compared with group 9, chrome–pyrope and group 2, high–titanium pyrope which statistical classification were established by Dawson and Stephens in 1975, and can be considered from lherzolites and megacrysts paragenetically. However, the green garnets are Ti–poor Ca–rich, Cr–rich, and Mg medial. Compared with green garnet of other areas in the world, the green garnets in Liaoning are similar compositionally to many previously reported single crystals of green garnet at Kampfersdam, Newlands, and Bultfontein in South African and Yakutia in USSR, although the green garnets in Liaoning are slightly lower in Ca and Cr than that in Newlands and Yakutia. They range to much higher CaO contents approaching those of green garnet from crustal enviroments.

Fig.1 illustrates data for green garnets, lilac–red garnets and orange garnets at Liaoning kimberlite and green garnets in South African and USSR. Those plots show a compositionally trend from low Cr and medial Ca to high Cr and high Ca, even though the range of variation is wide enough.

Clark and Carswell (1977) suggested that the formation of green garnet xenocrysts from the Newlands kimberlite were formed by a disaggregation of garnet wehrlite which themselves had been produced by a fractionating magma at a depth of about 200–250

km (75 kb) and 1900℃ . Schulze (f1988) speculated that green garnets from Kampfersdam, Bultfortein, and Newlands may have originated through subduction and prograde metamorphism of uvarovite–bearing serpentinites. However, Ca–rich garnet wehrlite has never been found and no evidence so far for subduction event exists in Liaoning kimberlite.

Uvarovite can be formed through Si and Ca metasomatism of chromite (Deer, 1982). It is reasonable to envisage that the Ca–rich and Cr–rich green garnet could be formed during serpentinization and dolomitization of kimberlite, and those alterations were widespread in Liaoning kimberlite. The chromium content being derived from Cr–spinel or partly from the rock itself. Such an origin would account for the high Ca and Cr values and easy to explain their considerable variation of Ca and Cr content as well as a rough positive correlation between them.

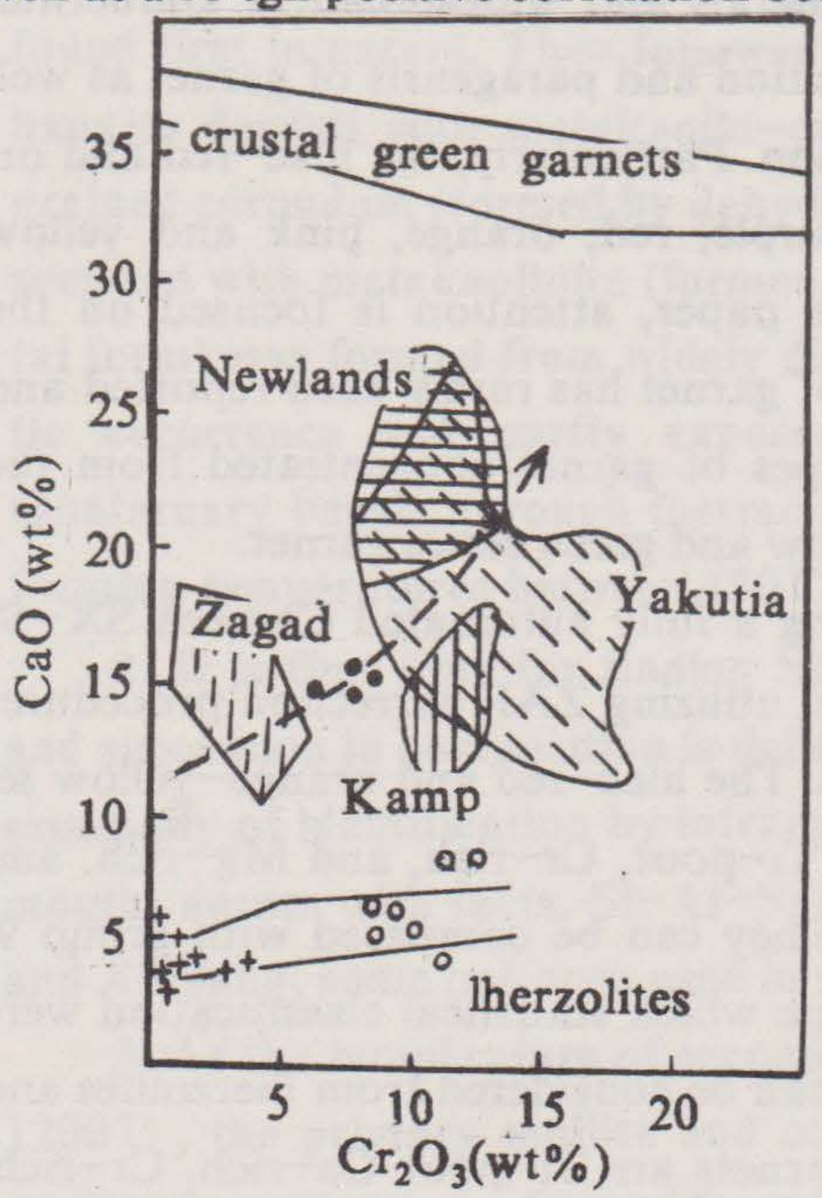

Fig.1 Plot of CaO vs $Cr_2O_3$for selected garnets in Liaoning Kimberlite (this paper); other data sources after Schulze (1988).
chrome–pyrope: open circle,
high–Ti pyrope: cross,
green garnet : solid circle.

references:

Dowson, J, B, & Stephens, W.E. *1975.J. Geol, 83, 589–607.*

Clark, D,B., & Carswell, D.A. *1977. Earth plan. Sci. Lett. 34, 30–38.*

Schulze, L.J., *1988. Kimberlites and Related Rocks, Vol 1.820–826.*

Deer, W.A., et al. *1982. Rock–forming Minerals, Vol. 1A, 642–648.*

Po14.4.

A PRELIMINARY STUDY ON THE REDOX STATE OF THE UPPER MANTLE IN EASTERN CHINA

Mo Xuanxue, Hu Xiangsheng and Chen Wenlin, China University of Geosciences, Beijing 100083, People's Republic of China

A basalt event genetically related to continental rifting took place in the Cenozoic in eastern China. Various types of Cenozoic basaltic lavas, mainly olivine alkaline basalt and basanite, contain abundant mantle-derived peridotite nodules. The rock types of nodules are predominant spinel lherzolite with mineral assemblage of Ol-Opx-Cpx-Sp and much less abundant garnet lherzolite, harzburgite, dunite and pyroxenite. These nodules and their host basalts provide samples for studying the composition and physical state of the upper mantle beneath eastern China. 34 spinel lherzolite nodules, in which mole fraction of ferric iron in spinel is in the range from 0.008 to 0.047, collected from various types of basaltic lavas at different locations in eastern China were employed to calculate the oxygen fugacity in the

upper mantle by using Mattioli & Wood (1988)'s model[1] and two sets of f_{o_2} values were obtained. One set, $\Delta\log f_{o_2}$ (FMQ)= + 1.39 ± 0.62, indicates an oxidized state,i.e., the oxygen fugacity is higher than not only FMQ buffer but also NNO buffer, whereas another set, $\Delta\log f_{o_2}$(FMQ)= + 0.74 ± 0.47,shows a more reduced state being comparable to the oxygen fugacities in the upper mantle beneath western Europe and Autralia, $\Delta\log f_{o_2}$(FMQ)= - 0.89 ± 0.58 and -1.78±0.66 respectively, estimated by O'Neill & Wall (1987)[2]. These two sets of data presumably indicate the redox states in the upper mantle beneath eastern China in different stages. As most of peridotite nodules in the Cenozoic host basalts represent the refractory residue of the upper mantle after subtraction of basaltic melts caused by partial melting and these nodules must have been in equilibrium with basaltic magmas in the source region, it is obvious that most of f_{o_2} values, i.e., the higher values, estimated on the basis of the activities of Mt, Fa and Fs in these ultramafic nodules reflect the redox state in the mantle source region during the generation of basaltic magmas. 34 f_{o_2} values calculated by using Mo et al. (1982)[3]'s method for the Cenozoic primary basaltic magmas in their source regions are also higher than NNO buffer and in the range between NNO and MH buffers, and should also indicate the redox state of the mantle source regions themselves. Thus, the results given by the two above-mentioned independent calculations are consistent with each other when the uncertainties of the calculating methods are taken into account. The first author pointed elsewhere[4] that, in comparison with Ringwood's pyrolite, the upper mantle source of the Cenozoic basaltic magmas and even the refractory residue have higher content of iron and ferric ferous ratio, implying a more oxidized state, which probably attributed to the metasonatism in the upper mantle by relative oxidized Fe-, Ti- and alkali-rich fluids/melts prior to and/or during the basalt event. As to another set of data, lower f_{o_2} values, possibly reflects the redox state in the portion of the upper mantle that was not affected by the Cenozoic basalt event and related mantle metasomatism although further studies are needed. Thus, a preliminary conclusion could be achieved that the oxygen fugacity of the " primative " upper mantle beneath eastern China was likely comparable to that in some other portions of the world such as W.Europe and Australia, i.e., somehow lower than FMQ, and the upper mantle became more oxidized presumably due to the Cenozoic basalt event and the mantle metasomatism taken place prior to and /or during the basalt event.

[1] Mattioli,G.S. & B.J.Wood(1988),Contrib.Mineral.Petrol.,98:148-162.
[2] O'Neill,H.St.C. & V.J.Wall(1987),J.Petrol.,28(6):1169-1191.
[3] Mo.X.,I.S.E.Carmichael,M.Rivers & J.Stebbins(1982),Mineral.Mag.,45:237-245.
[4] Mo,X.: The states of the upper mantle and asthenosphere beneath eastern China during the Cenozoic basalt event. The 1989 GSC Symposium (in press).

THE MICRO-STRUCTURAL VARIANCE IN SOME MINERALS OF THE EARTH'S MANTLE — REVEALED BY MICRO-RAMAN SPECTROSCOPY

13.17K
Bo 13.7.

WANG Alian*, DHAMELINCOURT.Paul**, GUO Lihe*, WANG Wuyi*, ZHANG Andi*

* Laboratory of Physical Mineralogy, Chinese Academy of Geological Sciences, Beijing 100037, CHINA.

** Laboratoire de Spectrochimie Infrarouge et Raman, CNRS, Lille 59655, FRANCE.

In recent years, the investigations about the mantle xenoliths and xenocrysts indicate that various micro-structural variances are commonly existed. Micro-Raman spectroscopy was proved to be a very sensitive probe for studying the problems in this field. By means of Raman technique, the degeneration of long-rang ordering, caused by micro-structural variances, in the lattice of the pyrope crystals of diamondiferous kimberlites has been recognized. It is illustrated in Figure 1 as the obvious difference in the intensity ratios of three main peaks (all have Ag symmetry, corresponding 1, 2 and Rz modes) among the kimberlitic pyropes No.1, No.19 (Victory 1 pipe, Shandong, China) and the nonkimberlitic pyropes No.31(picrite-porphyrite,Gansu,China), No.53 (limburgite, Shaanxi, China). It is also manifested as the enlargement of the bandwidths, the distortion of the bandprofiles, and the appearance of the small shoulders for kimberlitic pyropes.

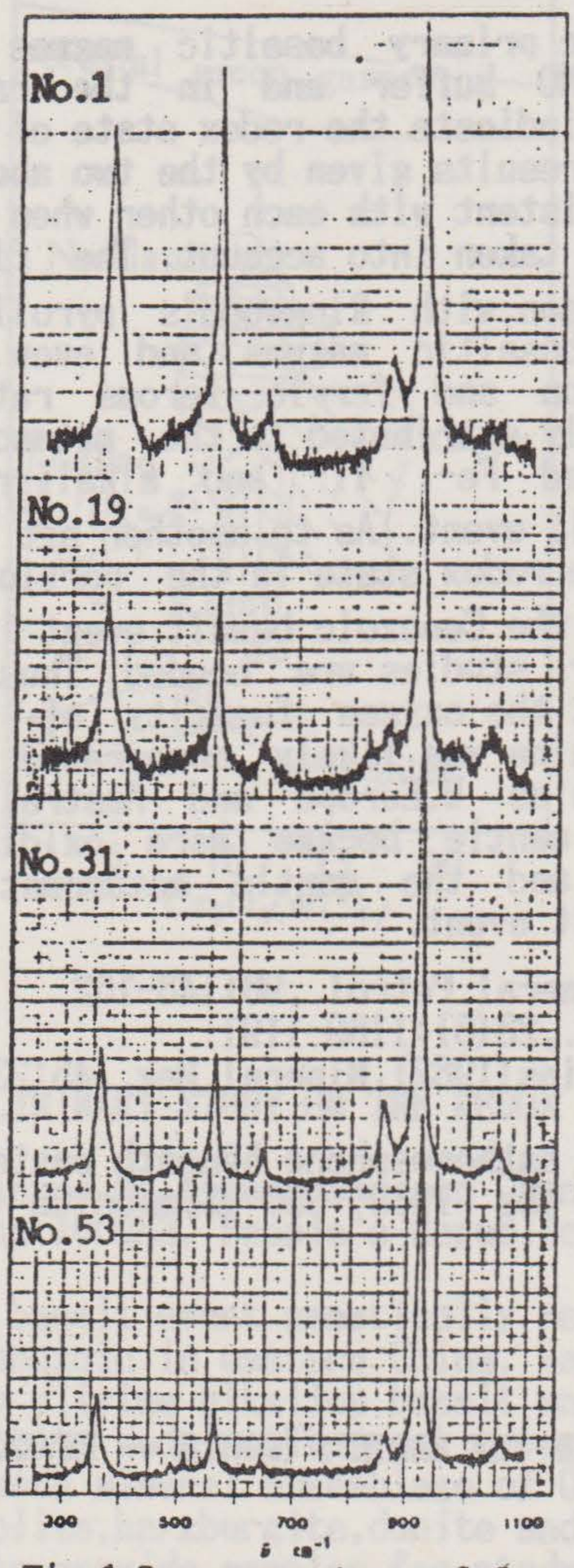

Fig.1 Raman spectra of four pyropes with different occurences.

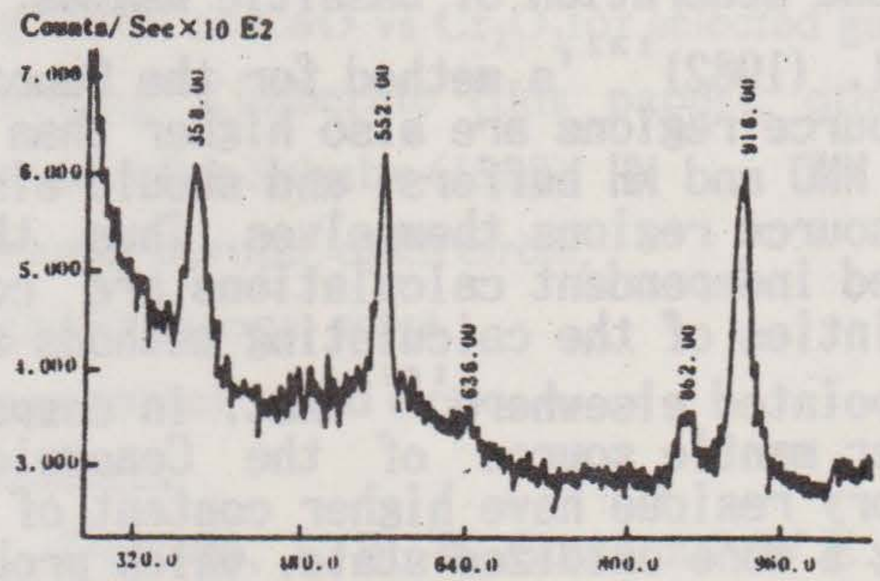

Fig.2 Raman spectrum of a pyrope inclusion in a diamond.

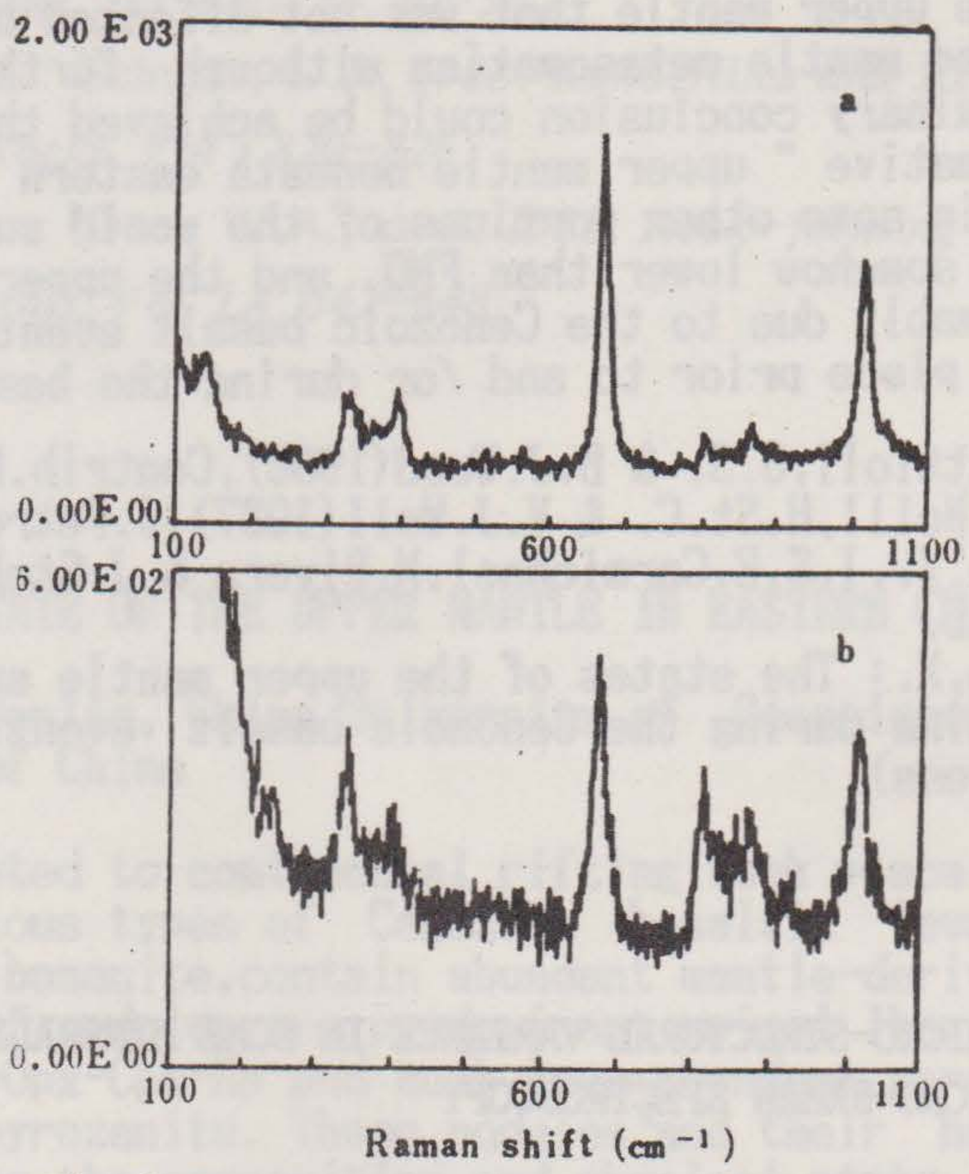

Fig.3 Raman spectra of two diopsides:
a) from nonkimberlitic rock;
b) from kimberlite.

Another Raman experiment (Figure 2) on a pyrope inclusion (100x250 m in size) which was enclosed in a diamond host (No.50 pipe, Liaoning, China) shows the similar spectral features with that of the above kimberlitic pyropes. As we known, the inclusions in diamond are the most ancient, original and unaltered samples of the upper mantle which people could obtained. So this Raman experiment proves that degeneration of long-rang ordering in crystal lattice is really a structural character of deep source pyropes formed under the special physical-chemical conditions of the upper mantle environment.

This conclusion could be extended by further Raman tests on other deep source minerals. As shown in Figure 3, the particular spectral features due to the loss of long-rang ordering in crystal lattice were also recognized in the Raman spectrum of a kimberlitic diopside (No.50 pipe, Liaoning, China). It suggests that this micro-structural variance, distinguished on mantle sourced pyropes, could possibly be a general structural character of many minerals formed in the mantle environment, and could reflect the complex physical-chemical conditions which these minerals underwent. A comprehensive study of TEM is going on.

References:
[1]. BRAWER S (1975) Physical Review B11, pp3173-31194.
[2]. MEYER HOA (1987) Inclusion in diamond in NIXIN PH(ed) Mantle Xenoliths, John Wiley & Sons Ltd.

Po 14.8

A STUDY OF HYDROUS COMPONENT IN PYROPE

Wang Wuyi, Guo Lihe, Wang Alian, Zhang Andi ,Insititute of Mineral Deposits, CAGS, 26 Beiwanzhuang Road, Beijing 100037,China

It was normally considered that there is no hydrous component in pyrope, but recent spectroscopy research revealed that some pyropes do have minor hydrous component in their lattice (Aines RD, Rossman GR,1984). The infrared and Raman spectra of pyropes from Chinese kimberlite pipe, diamond and alkali basalt have been discussed.

Forty pyrope samples had been selected out randomly from the concentrates of kimberlite pipe 50, in Liaoning, China. Representive IR experimental results are shown in Fig.1. About 10% of these samples has a comparatively high content of hydrous component (0.1-0.2 wt%, as estimated). A strong absorption band near 3600cm-1 exists as shown in spectrum C. Hydrous contents in the other samples are comparatively low or beyond the detective limit of the instrument, as spectrum B and spectrum A. Micro-infrared analysis indicated that hydrous component distributed almost homogeneously in the analysised grain. In addition, no relation exists between the content of hydrous component and its chemical composition. All the spectra of six pyrope grains from alkali basalt, in Liaoning, China, are quite flat in the region of 3800-3500cm-1, demonstrating that all the samples analysised have no water at all or are beyond the instrument detective limit. Therefore, the differences in formation and evolution of the two types of rocks are reflected in the fine structure character of their pyropes. All

the experimental results are comparable with the tests of pyropes from Colorado Plateau diatremes, Wesselton kimberlite of South Africa and alkali basalt of Tailand.

Micro-Raman analysis of a syngenetic pyrope inclusion from a type I diamond of Pipe 50 showed that there are three bands (3719cm-1, 3647cm-1, 3575cm-1) in the OH stretching vibration region indicating the existence of hydrous component in the pyrope inclusion(Fig.2). From the experimental results on both macrocrysts and inclusion pyropes, it is concluded that pyropes with various contents of hydrous component were formed under different upper-mantle environments. Hydrous component does exist as deep as the depth where diamond was formed in the upper mantle.

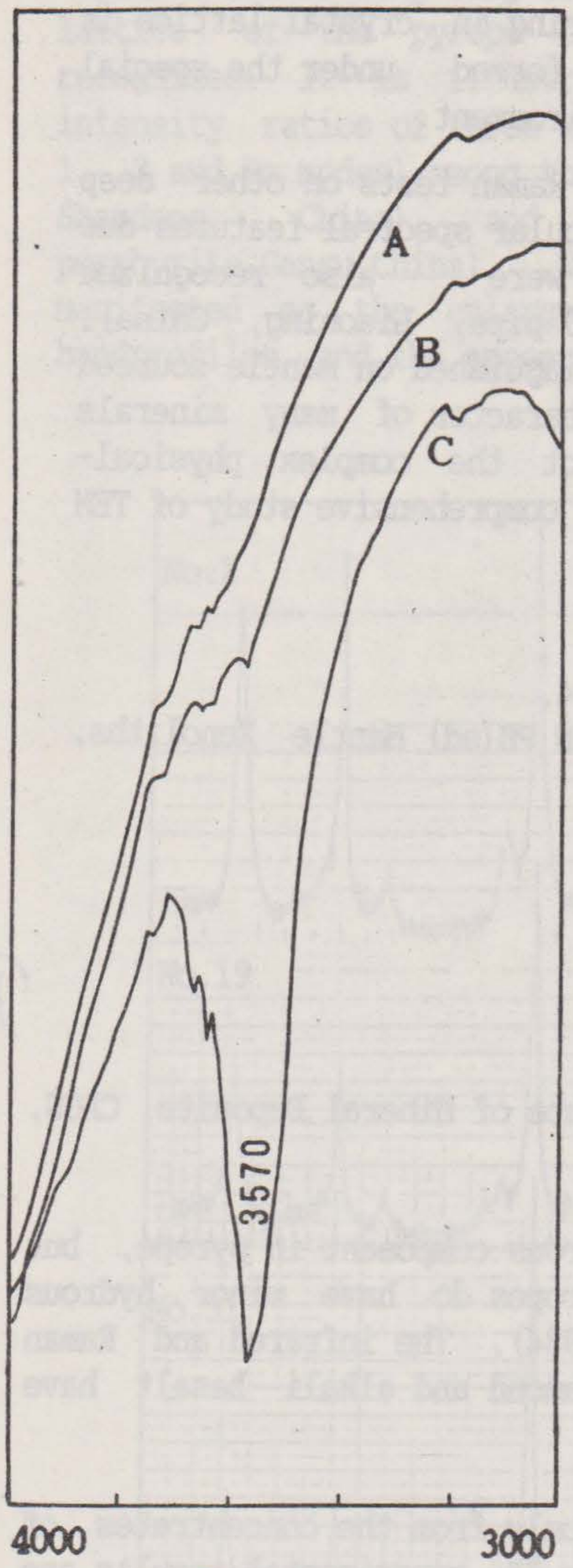

Fig.1 IR spectra of pyropes

It was supposed that the $(SiO4)^{4-}$ tetrahedron is substituted by $(O4H4)^{4-}$ group in S4 site of pyrope lattice (Cohen-Addad C, et al 1967). Based on this model, the 3720cm-1 Raman band belongs to the same symmetric species Ag of the fundamental band near 920cm-1 (V1) of $(SiO4)^{4-}$ group. Group theory analysis indicates that both bands should have same polarization

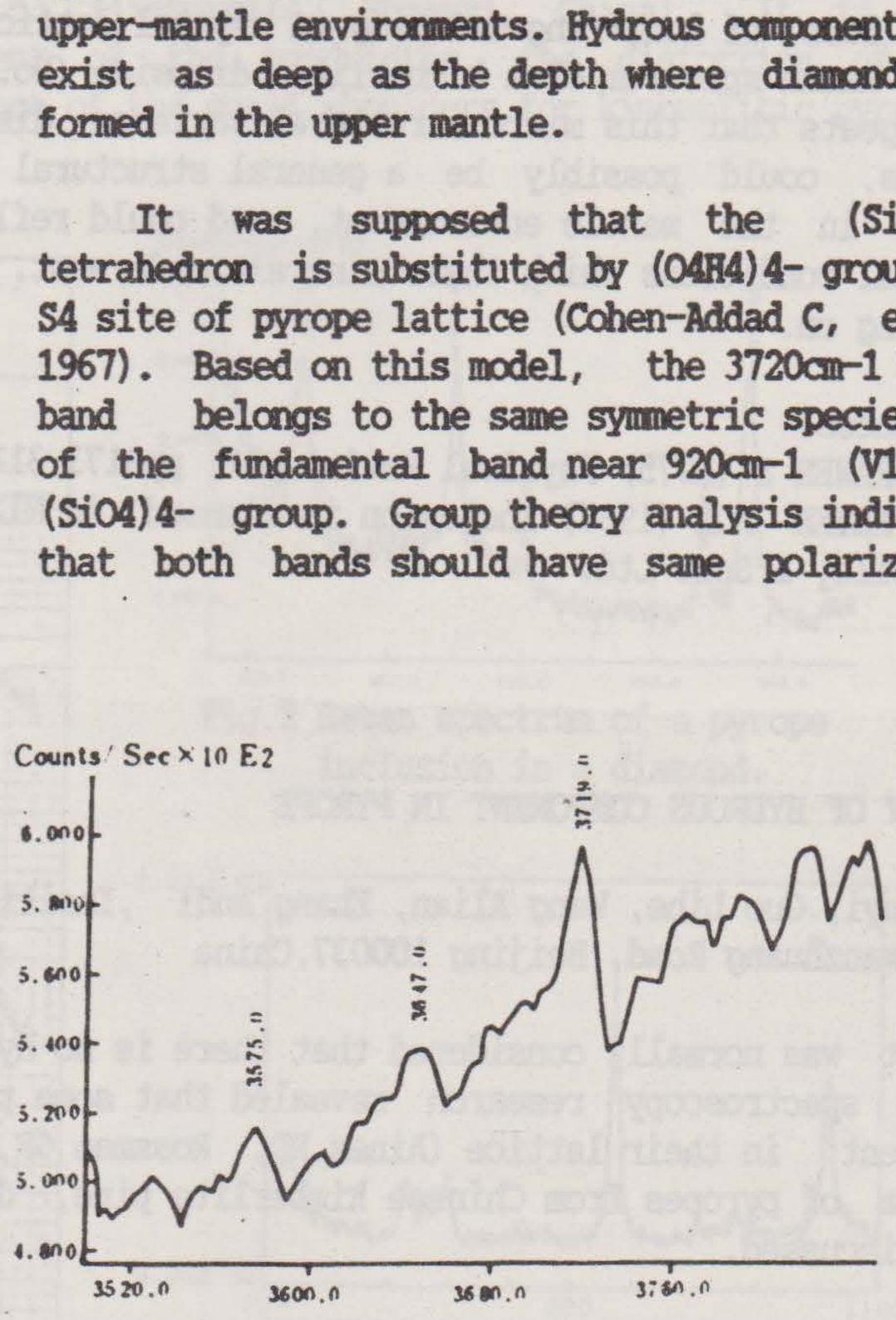

Fig.2 Raman spectrum of pyrope inclusion

behaviour. But the experiment results are in contradiction with this: the 920cm-1 band is in nearly minimum intensity at certain polarization angle where 3720cm-1 band is in maximum. Further study about the model is being carried on.

It is considered that the hydrous component in pyrope resulted from mantle metasomatism. The discovery and study of hydrous component in pyrope, which is an important component of the upper mantle, is significant to the upper mantle research, as well as to the understanding of genesis of kimberlite and diamond.

References

Aines,RD, Rossman GR, 1984, Amer. Miner. 69:1116-1126

Cohen-Added C, et al, 1967, Acta Crystallographica 23:220-230

627.2 H
P0149

MINERALOGY AND GEOLOGICAL IMPLICATION OF THE UPPER MANTLE INCLUSIONS FROM YITONG , JILIN PROVINCE

Wu Dianying , Jilin Research Institute of Mineral Resouces and Geology , China Nonferrous Metal Industry Corporation , Changchun 130012 , P. R. China

The Cenozoic basalt distributed along the Yitong fault zone contains a lot ultranafic inclusions of the upper mantle , which are spacially related to the basalts and have the assemblage of Ol+Opx+Cpx+Sp.

OLIVINES

Olivine , Fo = 89–91 , often shows mortar texture , in which the kink bands are common . In groundmass it occurs as recrystalline microcrystal . The feature of the kink bands indicate that the olivine underwent plastic slip deformation . On the univeral stage , the sliding system with (010) [100] has been determined ; the sliding direction of the olivine which has two groups of kink bands is in [100] for the earlier one and in [010] for the latter one. According to Carter's (1970) flow experiment, the temperature for forming the olivine in this area should be over 1000℃ . The fabric determination shows that the olivine has an obvious selected orientation , reflectibg the general plastic flow in the upper mantle . By measuring the size of the smallest new crystalloblast of olivine and using Mexcier's (1976) experience formula :$\sigma = 40\ d^{-0.81}$ and Gaety's(1975) experience formula :$\sigma = 11\ d^{0.5}$, the value of flow stress for olivine is calculated (about 1.42–2.08Kb) . The dislocation substructures for olivine are developed ..Among which the relatively obvious tyoes are high density unbound dislocations and dislocation tilt walls with (100)(001) . On the basis of Torium's (1979) formula :$d = KGb / \sigma$, from the dislocation wall interval d , the value of flow stress is calculated ($\sigma = 1.65$Kb) . By using the high temperature flow rate formula :$\varepsilon = 10^{8}\ \sigma^{5}\ \exp(-\frac{26.4Tm}{T})$, proposed by Raleigh and Kirby (1970) , the strain rate :$\varepsilon = 1.25 \times 10^{-16}$ / second is obtained .

ORTHORHOMBIC PYROXENE

Orthorpyroxene , En = 89.4–90.3 , often occurs as large cataclast , and the distinct kink bands can be commonly seen .

CLINOPYROXENE

Emerald green . The composition of clinopyroxenes (chrome diopsides) are consistently changing from Wo 34.4 , En 51.2 Fs 5.4 to Wo 44.3 , En 49.3 , Fs 6.3 . Its partial melting texture is well developed . Among the grains , partial melting blebs can often be observed . The stable temperature and pressure for clinopyroxene

are estimated at T = 1034℃ –1102℃ , P = 19.1–23.8Kb .

Mineralogical study of inclusions is of an important significance in revealing the composition of the upper mantle in this region , the dynamic mechanism of lithosphere plate , the origin of basalt and the Cenozoic plate activities in particultar.

Al–RICH AMPHIBOLES IN PRODUCTS OF MELTING–EXPERIMENTS AT HIGH PRESSURES*

Xie Hongsen , Hou Wei , Fang Hong , Zhang Yueming and Xu Huigang , Institute of Geochemistry , Chinese Academy of Sciences , Guiyang 550002 , Guizhou , Peoples Republic of China

In orde to understand the behavior of water in the mantle , we have studied some hydrous mineral phases in products of melting–experiments , taking the silicate phase from Jilin chondrite as a starting material at 30–40 kbar . Some kinds of Al–rich amphibole were discoverd in these experimental products , and the X–Ray power differaction analyses , infrared spectra , DTA and electron microproble analyses of these Al–rich amphiboles have been carried out . The experimental condition and results of electron microprobe analyses are listed in Table 1 . According to the nomenclature and classification of amphiboles provided by CNMMN IMA (1978), These Al–rich amphiboles belong to Mg–gedrite , gedrite and pargasite , respectively . As is shown in Table 1 , the Al–rich amphiboles are formed at 1170℃ to more than 1600℃ at 30–40 kbar and their Na_2O , K_2O , CaO and TiO_2contents increase but MgO content decrease with increasing temperature . The temperature and pressure at which these Al–rich amphiboles are formed have

Table 1. The Experimental Conditions , Mineral Assemblage of Products and Results of Electron Microprobe Analysys of Al–Rich Amphiboles.

No.	Y–71	Y–81	Y–26	Y–27	YF–H1	YF–H2
P(kbar)	35	35	30	30	40	40
T(℃)	1170	1170	1500	1500	>1610	>1610
Assemblage of Product *	Mg–ge Pyx sp cor Py	Mg–ge Pyx sp cor Py	ge sp	ge sp	pa Pyx	Pa Pyx

gone beyond the stable range of other types of amphibole in the mantle . We therefore consider that Al–rich amphibolee may be main hydrous mineral in the upper mantle . The Mg–gedrite and gedrite may be stable at upper levels of the upper mantle and the pargasite at deeper levels of the upper mantles .

Results of Electron Microprobe Analasys of Al–Rich Amphiboles (wt.%)

SiO_2	50.06	49.59	34.11	34.35	41.23	41.02
TiO_2	–	–	0.29	0.12	1.13	1.64
Al_2O_3	10.75	11.03	26.04	21.69	15.23	15.29
Cr_2O_3	0.82	0.78	–	–	–	–
FeO	6.74	8.42	21.71	26.36	19.44	18.33
MnO	0.55	0.45	0.67	0.47	0.58	0.57
MgO	30.54	27.24	12.64	12.12	9.26	9.28
CaO	0.43	0.45	2.98	2.83	6.55	6.69
Na_2O	–	0.13	1.59	2.37	4.46	4.15
K_2O	–	–	0.12	0.13	0.62	0.64
Total	99.89	98.09	100.15	100.44	98.50	97.61

* ge––gedrite pa––pargasite Pyx––pyroxene sp––spinel
fo––fosterite cor––corundum Py––pyrope

* The Project supported by the National Natural Sciences Foundation of China.

A DISCUSSION ABOUT EXISTENCE OF NATURAL γ–SPINEL (SPINEL MODIFICATION OF Mg_2SiO_4) IN MANTLE PERIDOTITE FROM NORTH TIBET

Yang Fengying, Kang Zhiqin, Liu shuchun, Institute of Geology, Chinese Academy of Geological Sciences, Beijing 100037, People's Republic of China

The Mg_2SiO_4 is probably the most important component in the upper mantle. The spinel modification of Mg_2SiO_4 was synthesized at pressure about 170 kbar and 1000℃ (by Ringwood and Major, 1966) and may be a typomorphic mineral probably existing in lower part of the upper mantle. Some foreign scientists have made great contributions in studies on high–pressure phase transition of Mg_2SiO_4, but these studies at present are only confined to experiment and synthesis.

A special pseudomorph of serpentine (lizardite aggregate with spinel form) was discovered in Cr–rich ($Cr_2O_3 > 60\%$) chromite from some diamond bearing peridotites in North Tibet . Optical properties, chemical compositions and x–ray data are similar to that of fibrous serpentine resulted from alteration of general olivine. The octahedral serpentine may transform into octahedral chlorite and

chrom bearing chlorite.

Chemical compositions and optical characteristics of octahedral sepnentine can be summarized as follows:

SiO_2	42.57	MgO	41.55	(FeO)	0.10
Al_2O_3	0.73	Cr_2O_3	0.05	$H_2O \approx$	15

$a_0 = 5.320$ Å $\quad b_0 = 9.198$ Å $\quad c_0 = 7.297$ Å $\quad \beta = 90^\circ 07'$

$N_g \approx N_m = 1.560 \pm 0.003 \quad -2V = 3-5^\circ$

Based on mentioned above materials we can make following discussions and inferences:

1, It is believed that the new octahedral pseudomorph of lisardite, unknown in any literature, occurs only in especial peridotite from the lower part of the upper mantle.

2. The primary mineral of the secondary octahedral pseudomorph of serpentine may be natural γ–spinel in the mantle peridotite, because only γ–spinel has either octahedral form, or composition Mg_2SiO_4 , transforming commonly into serpentine.

3. The perfection of octahedral crystal form in the serpentinization procces may be attributed to the protection by chromite envelops.

4. According to the synthetic pressure of γ–spinel, we suppose peridotite including serpentine with spinel form ought to come from 500km in depth of the upper mantle.

REFERENCES

〔1〕 Suito, K., 1977, High–pressure research application in geophysics, New York, Academic Pr. 255–266.

〔2〕 Yang Fengying et al , 1981, A new octahedral pseudomorph of lizardite and its origin, Acta Mineralogica Sinica, No.1, 53–55.

〔3〕 Lin–gun Liu et al, 1986, Elements, Oxides and Silicates, High–pressure phases with implications for the earth's interior, New York, 215–217.

〔4〕 Yang Fengying et al, 1987, Geological significance of studying pseudomorphous octahedra of serpentine and chlorite in the ultramafic rocks, Acta Petrologica et Mineralogica, No.4, 376–380.

Po1.23

STUDY OF A UNIQUE ECLOGITIC INCLUSION IN THE KIMBERLITE IN SHANDONG, EAST CHINA

YANG Jianjun* and GUO Wenxiang**

* Lithospheric Research Centre, Chinese Academy of Geological Sciences, Beijing 100037, China

** Diamond Mine, Menying, Snandong, China

A bi-mineralic (Gt+Cpx) nodule has been found as the only eclogitic inclusion in the kimberlite of the large breccia pipe at Menying, Shandong province. The largest section of the nodule is 2.8*4.6 cm^2. Rounded red garnet crystals are rimmed by dark glass, which together make up about 40% of the sample. Two kinds of clinopyroxene together making up about 50% of the sample can be recognised. One is represented by large green primary Cpx crystals, the other by irregular secondary Cpx crystals which grew around the edges, or along the intracrystalline fractures of the primary Cpx. Secondary phlogopite, Ti-magnetite, corundum and apatite, together with the penetrated kimberlitic component make up about 10% of the sample.

The garnet is very rich in Mg (Pyr74 Alm17 Gro8 And0.7 Uva0.7) and almost homogeneous in composition. The glass around the garnet has about the same composition in terms of the major elements Al, Fe, Mg, and Ca; apparently it is the partial melting product of the garnet at low pressure (cf. Lappin, 1978). Primary Cpx is Na-augite (Jd8.9 Ac1.3 Es0.6 Di67.4 Hd5.8 En15.0 Fs1.3) and becomes rich in Ca near to its edges and to the intracrystalline fractures where secondary Cpx occurs. The secondary Cpx has very high contents of diopside and Ca-Tschermak molecules (Jd1.1 CaTs6.4 Di78.1 Hd6.2 En7.4 Fs0.6). The compositional features of the two kinds of Cpx and the textural relationships between them indicate that the secondary Cpx is the reaction product of the primary Cpx and the host kimberlite melt at low pressure. Na_2O in the garnet is 0.038 wt%, and K_2O in the primary Cpx is 0.085wt%. This inclusion is thus a group II kimberlite eclogite, according to the criteria proposed by McCandless & Gurney(1986).

Rare earth element contents of Gt and primary Cpx are low (5×chondrite) compared with the kimberlite eclogites from other localities (e.g. Shervais et al, 1986). This indicates that the eclogitic rock described here was not crystalized from the host kimberlite melt. On the other hand, the significant positive Eu anomalies in the REE patterns of Gt and Cpx strongly suggest that the protolith of the Gt+Cpx assemblage was of gabbroic composition, similar to those discussed by Jagoutz et al (1985) and Schultze and Helmstaedt,1988). In addition, the lack of typical magmatic components (e.g. CaTs) in primary Cpx is in accordance with a metamorphic origin of the rock.

The distribution coefficient of the Fe-Mg exchange reaction (KD) between Gt and primary Cpx in the inclusion is 0.902, indicating a very high equilibrium

temperature for the assemblage. The KD line is located below the kimberlite solidus (Eggler & Wendlant, 1979) in the range P≥43 kb and T≥1060 ℃. The cross section of the KD line and the 44 mWm^2 shield geotherm indicates P,T values for the formation of the inclusion 52≥kb and 1110 ℃. These data suggest a mechanism of subduction for the formation of the eclogitic inclusion, which may have been transformed from possible former oceanic crust.

17.19.K
P.14.12

COMPARATIVE STUDY OF INCLUSIONS IN DIAMONDS WITH MACROCRYSTS FROM KIMBERLITES IN NORTH CHINA CRATON

ZHANG Andi, MEYER H.O.A.*, GUO Lihe, ZHOU Jianxiong, XIE Xilin, WANG Alian, XU Dehuan, WANG Wuyi, GAO Honglin
Institute of Mineral Deposits, CAGS, Beijing 100037, China,
*Dept EAS, Purdue University, West Lafayette, IN 47907, U.S.A.

The comparison of mantle macrocrysts with inclusions in diamonds from diamondiferous kimberlites is of importance in the study of the upper mantle and in exploration for diamond. The mineral association, chemistry, IR and Raman spectroscopic features of macrocrysts and inclusions in diamonds from pipe NO. 50 in Liaoning and the Shengli pipe in Shandong in the North China Craton have been investigated.The macrocrysts were gained from the concentrates of 4 and 0.5 cubic meter rocks respectively of the two pipe.About 60 syngenetic inclusions were obtained from 325 posisble inclusion bearing diamonds which themselves were selected from 625 carats of diamond having the size range 1-2mm . On the basis of the mineralogical data obtained,the following conclusions may be drawn:

1. The mineral association of the macrocrysts is limited, mainly comprising of Cr-pyrope and chromite. In addition, almandine-pyrope, ruby and rutile are also present but rare. Fresh xenolith consist predominant of garnet lherzolite and dunite , with minor eclogite.The majority of inclusions studied belong to the ultramafic (peridotitic) suite, only two examples of eclogitic suite inclusions (pyrope-almandine and omphacite) were obtained (Zhang and Meyer, 1989).Macrocrysts from both pipes are mostly of peridotite type with a few examples of eclogitic minerals.The chemical features of low Ca, Cr-bearing garnet and chromite macrocrysts are shown below:

	wt%	macrocrysts	Inclusions
pyrope	Cr_2O_3	1.73-15.3	8.3-14.4
	CaO	1.70-5.2	2.0-7.2
chromite	Cr_2O_3	34.3-66.5	63.8-66.9
	MgO	7.4-15.7	11.9-13.9

2. The macrocrysts are similar in micro-structure to the inclusions. IR and

Raman analysis revealed the presence of hydrous components in both groups, which also exhibit a degeneration of long-range ordering (Wang Alian et al., 1989; Wang wuyi et al., 1989).

Thus, this study supports the concept that the diamond bearing harzburgitic rocks from which they are thought to be derived have disaggregated with great efficiency on sampling by the kimberlite, a process which has been ascribed to decarbonation reactions(proposed by Boyd & Gurney,1986; Wyllie et al 1983; Shimizu and Richardson 1987) or to the presence of an interstitial volatile K, LREE, CO2 enriched melt(Harte et al 1980; Richardson et al; 1984)(Gurney JJ, 1989) , and provides new evidence showing the similarities in both chemistry and microstructure between macrocrysts and inclusions in the diamonds from diamondiferous Kimberlites. It is clear that besides K, LREE, and CO2, the OH as another volatil species has been involved in the disaggregation of harzburgite and sampling by kimberlite. Its involvement extent remains to be studied.

References

(1) GURNEY J.J., 1989, Kimberlites and related rocks, VOl 2, P 955

(2) ZHANG Andi and MEYER H.O.A. 1989, Extented Abstracts on diamonds, 28th Intern. Geol. Cong.

(3) WANG Alian, et al, 1989, The Micro-structural Variance In Some Minerals Of The Earth's Mantle - Revealed By Micro-Roman Spectroscopy. In Same Volume.

(4) WANG Wuyi, et al, 1989, A Study of Hydrous Component in Pyrope. In Same Volume.

Geoscience journals from Springer

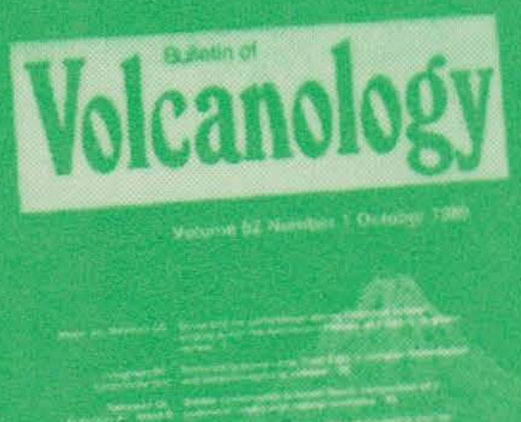

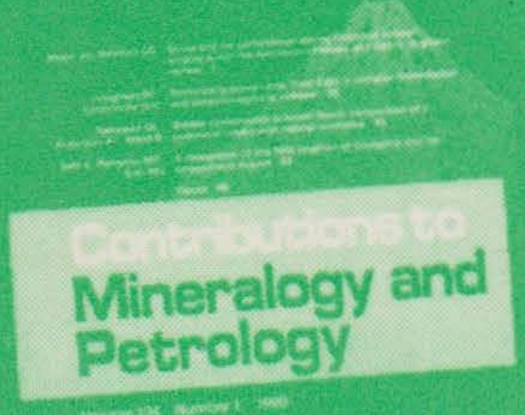

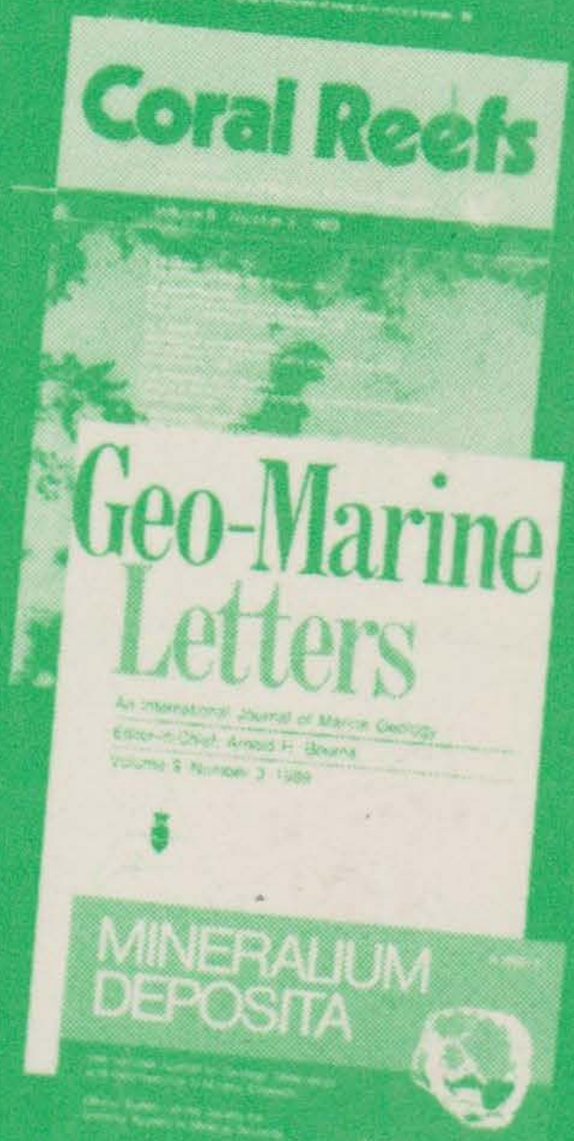

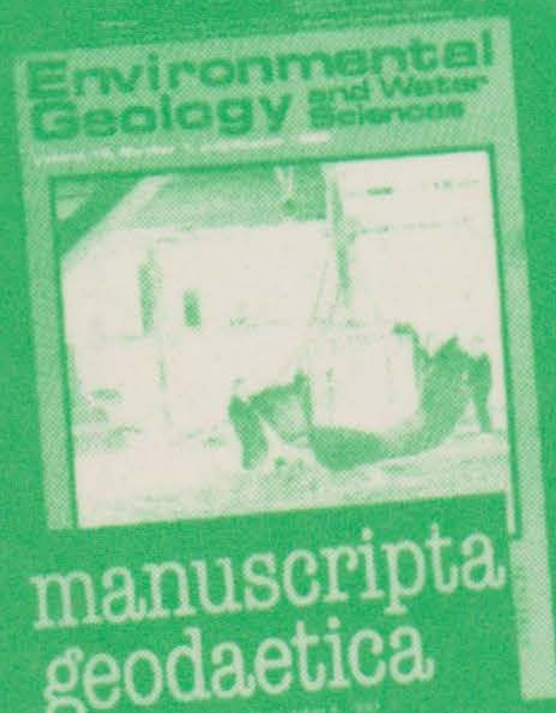

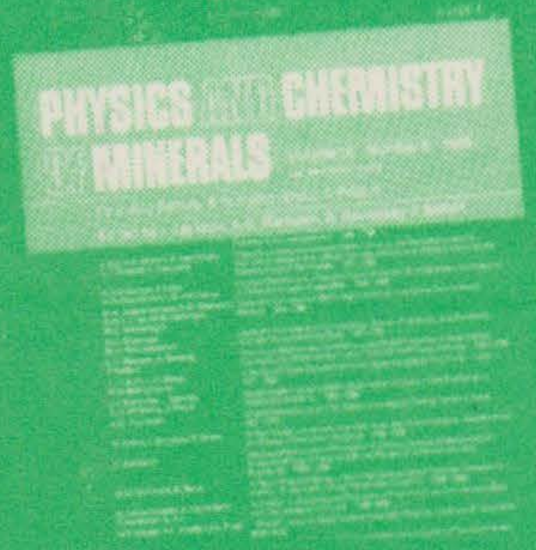

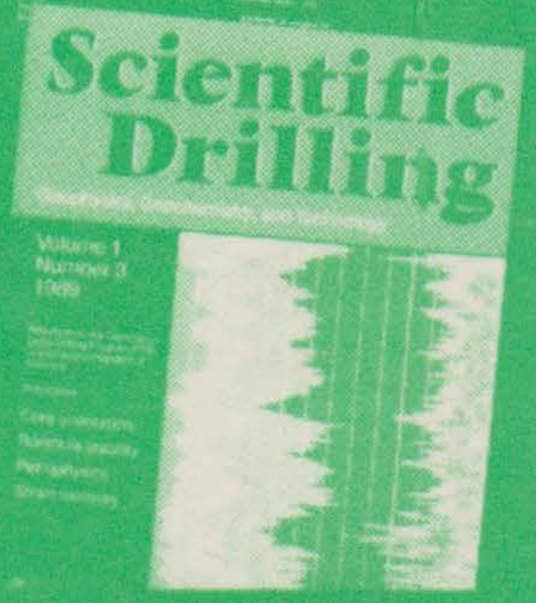

Further information and free sample copies are available on request

Springer-Verlag Berlin Heidelberg New York London Paris Tokyo Hong Kong

Attn. Dr. Nicola Klupsch, Tiergartenstr. 17, D-6900 Heidelberg 1/FRG